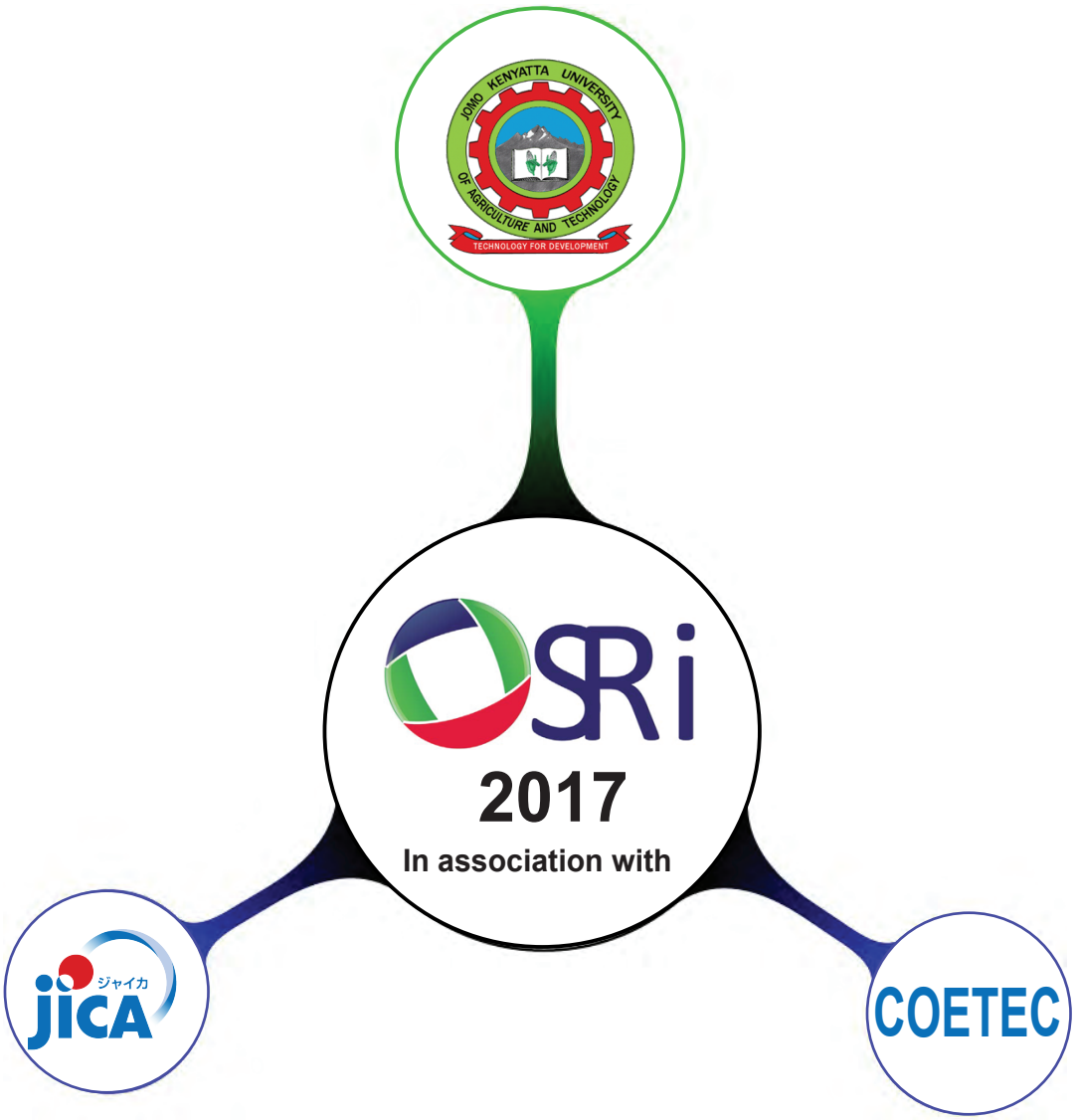


# Proceedings of the 2017 Annual Sustainable Research and Innovation (SRI) Conference

3 - 5 May, 2017

*JKUAT Main Campus*

*Juja, Kenya*

ISSN: 2079-6226

Proceedings of the
2017 Annual Sustainable Research and Innovation Conference
JKUAT Main Campus
Juja, Kenya
3 - 5 May, 2017

The final version of the proceedings will be made available on;
*http://sri.jkuat.ac.ke/ojs/index.php/proceedings/index*

Research, in the 21st century, is dependent on the multi-disciplinary approach for development of new knowledge and products. Industrialized countries spend a significant percentage of their GDP on funding research in universities and other dedicated research institutions and centres. The challenge for developing countries, however, is that of building up capacity in order to ensure that industries remain competitive in the global markets, in addition to offering innovative solutions to the increasing socio-economic problems and developing efficient methods of using the depleting natural resources. The multi-disciplinary approach is a possible method of tackling these challenges. The conference offers a wide selection of topics to give the participants an opportunity to share experiences and link research to the process of industrialization.

The theme for the 2017 Annual Sustainable Research and Innovation Conference is "Engineering Innovations for Industrialization". The conference aims to create a forum for scholars, industry and other stakeholder to interact and exchange ideas on new and existing knowledge in the field of engineering and related subjects. The conference is also a forum for enabling participants to articulate challenges facing the society, and offer viable solutions. In addition, scholars are also able to create networks for multi-disciplinary and industrial based research that will solve national and international challenges. The wide selection of topics listed herein give the participants an opportunity to share experiences and articulate how their activities impact on the process of industrialization in Africa and other developing countries.

The Sustainable Research and Innovation (SRI) Conferences is the successor to the Departmental Annual Seminars which were previously organized by the Department of Mechanical Engineering at JKUAT. The first seminar was held in 1995, under the theme: "The Role of Mechanical Engineering in Changing Industry". Thereafter, seven seminars were held annually until 2001. After a few years' break, the annual seminars resumed in 2006 with the 8th series titled "Sustainable Research and Innovation". In 2010, these Departmental Seminars were scaled to international conferences to run annually organized by the School of Mechanical, Manufacturing and Materials Engineering up to the year 2014 after which the role of organiz - ing this conference was taken up by the college of Engineering. The SRI conferences have offered a platform for researchers and innovators in industry and academia to disseminate their research findings over the years. The conference has growm and gained international profile with submissions and keynote speeches from within and outside the country.

This year's, conference has drawn participation from the academic field and industries in Kenya as well as various countries including Japan, Zimbabwe, South Africa, Botswana and Ghana. The conference has been supported by Jomo Kenyatta University of Agriculture & Technology (JKUAT), and Japan International Cooperation Agency (JICA) through Africa-ai-Japan Project.

The papers presented during ed the 2017 Sustainable Research and Innovation Conference were based on the following topics:

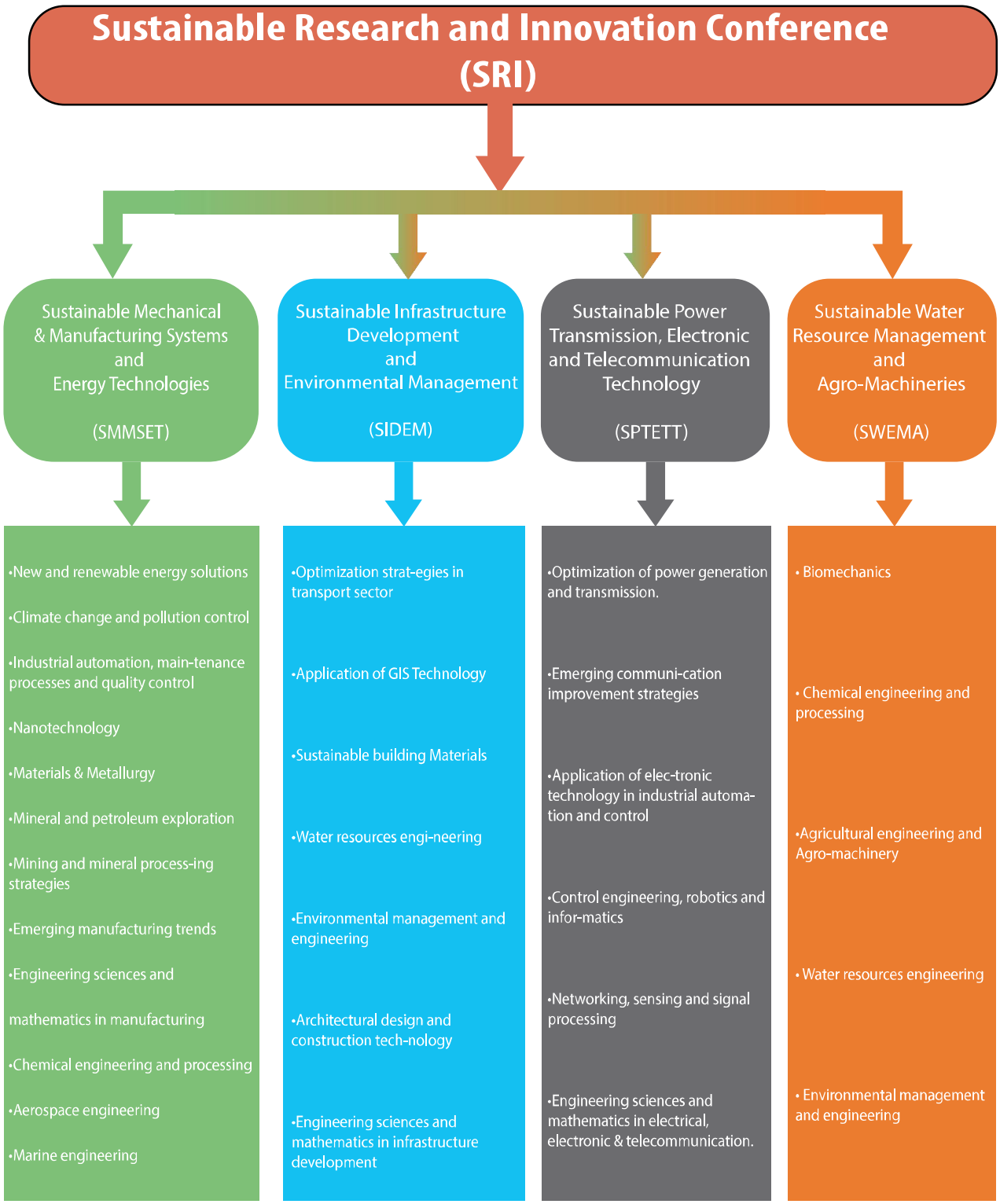

# ACKNOWLEDGEMENTS

The SRI conference seeks support from well-wishers in order to ensure that all the activities in preparation of and during the conference run smoothly. The donors have no influence over the selection or content of the presentations.

In 2017, the conference has received financial support commitment from Jomo Kenyatta University of Agriculture and Technology - JKUAT, and Japan International Cooperation Agency – JICA through the Africa-ai-JAPAN project

Dia mond

Platinum

# THE ADVISORY BOARD

**Prof. Eng. B.W. Ikua**
Jomo Kenyatta University of Agriculture and Technology, Kenya

**Prof. G. Nyakoe**
Jomo Kenyatta University of Agriculture and Technology, Kenya

**Prof. S.M. Maranga**
Jomo Kenyatta University of Agriculture and Technology, Kenya

**Prof. Eng. J.M. Kihiu**
Jomo Kenyatta University of Agriculture and Technology, Kenya

**Prof. Eng. S.P. Ng'ang'a**
Jomo Kenyatta University of Agriculture and Technology, Kenya

**Dr. K. K. Kaberere**
Jomo Kenyatta University of Agriculture and Technology Kenya

**Prof. B. M. Mati**
Jomo Kenyatta University of Agriculture and Technology Kenya

**Prof. P. N. Kioni**
Jomo Kenyatta University of Agriculture and Technology, Kenya

**Dr. Eng. K. Kibicho**
Interior and Coordination of National Government, Kenya

**Prof. F. Gatheri**
Technical University of Kenya

**Prof. G. O. Rading**
University of Nairobi, Kenya

**Prof. E. Sciubba**
University of Roma, Italy

**Prof. E. Tomita**
Okayama University, Japan

**Prof. H. Tanaka**
Tottori University, Japan

**Prof. L. Zuyan**
Harbin Institute of Technology, P.R. China

**Prof. K. Badyda**
Warsaw University of Technology, Poland

**Prof. J. Milewski**
Warsaw University of Technology, Poland

**Prof. A. Beyene**
San Diego State University, USA

## THE CONFERENCE SECRETARIAT

**Prof Bernard Ikua**
**Host**
Principal, College of Engineering and Technology

**Dr. Eng. Hiram Ndiritu**
Dean, School of Mechanical, Mechatronics and Materials Engineering,

**Dr. Urbanus Mutwiwa**
Dean, School of Biosystems and Environmental Engineering

**Prof. Abiero Gariy**
Dean, School of Civil, Environmental and Geomatic Engineering

**Prof. John Nderu**
Dean, School of Electrical, Electronics and Information Engineering

**Dr. Onesmus Muvengei**
Chairman, Mechanical Engineering Department

**Ms. Lina Owino**
Chairman, Mechatronic Engineering Department

**Dr. Julius Weru**
Chairman, Telecommunication and Information Engineering Department

**Prof. Stanley Kamau**
Chairman, Electrical and Electronic Engineering Department

**Eng. Jeremiah Kiptala**
Chairman, Civil Engineering Department

**Dr. Felix Mutua**
Chairman, Geomatics and Geospatial Engineering Department

**Dr. Eng. Gareth Kituu**
Chairman, Agricultural and Bio-Systems Engineering

**Dr. Eng. James Messo**
Chairman, Soil Water and Environmental Engineering Department

**Mr. Mathew Ndeto**
Chair, Secretariat

**Ms. Lucy Kariuki**
Treasurer

**Mr. Elijah Munyao**
Secretary

**Mr. Gilbert Bett**
Communications Liaison

**Mr. Omae Oteri**
Member

**Mr. Linus Aloo**
Member

**Ms. Rehema Ndeda**
Member

**Ms. Esther Wangui**
Member

**Ir. Anthony Muchiri**
Member

**Ms. Irene Fedha**
Member

**Mr. Bonface Kariuki**
Member

**Ms. Dorris Thimba**
Member

# TABLE OF CONTENTS

# Profit Based Unit Commitment in Deregulated Electricity Markets Using A Hybrid Lagrangian Relaxation - Particle Swarm Optimization Approach

Adline K. Bikeri, Christopher M. Maina and Peter K. Kihato

*Abstract*—In deregulated electricity markets, individual generation companies (GENCOs) carry out independent unit commitment based on predicted energy and revenue prices. The GENCOs unit commitment strategies are developed with the aim of maximizing profit based on the cost characteristics of their generators and revenues from predicted prices of energy and reserve subject to all prevailing constraints in what is known as Profit Based Unit Commitment (PBUC). A tool for carrying out PBUC is an important need for the GENCOs. This paper demonstrates the development of a solution methodology for the PBUC optimization problem in deregulated electricity markets. A hybrid of the Lagrangian Relaxation (LR) and Particle Swarm Optimization (PSO) algorithms is used to determine an optimal UC schedule in a day-ahead market using the expected energy and reserve prices taking advantage of the strengths of both algorithms. The PSO algorithm is used to update the Lagrange multipliers giving a better quality solution. An analysis of the PSO algorithm parameters is carried out to determine the parameters that give the best solution. The algorithm is implemented in MATLAB software and tested for a GENCO with 54 thermal units adapted from the standard IEEE 118-bus test system.

*Keywords*—Deregulated Electricity Market, Lagrangian Relaxation, Particle Swarm Optimization, Profit Based Unit Commitment.

## I. INTRODUCTION

Over the last few decades the electric energy sub-sector has been undergoing significant changes. Probably the biggest change has been deregulation of many power systems especially in the developed world; though aspects of deregulation are also beginning to take root in developing nations. Deregulation refers to the unbundling of vertically integrated power systems into Generation Companies (GENCOs), Transmission Companies (TRANSCOs) and Distribution Companies (DISCOs) [1]. The main aim of deregulation is to create competition among GENCOs and hence provide different choices of generation options at lower prices to consumers [1], [2].

Unit Commitment has always been a significant optimization task in power systems [3], [4]. However, the approach in the deregulated environment is significantly different form that in the regulated environment. Here, the GENCO is not the system operator. This means that, unlike the regulated market where the objective of the utility in unit commitment is the minimization of operating cost, in the deregulated environment, the objective of the GENCO is the maximization of profit. This has led to what is now referred to as Profit Based Unit Commitment (PBUC) in deregulated markets [5].

Numerous methodologies for solving both the traditional UC and PBUC problems have been proposed in literature. These methodologies can be classified as classical methods and non-classical methods. Classical methods include Priority Listing, Dynamic Programming, Branch and Bound, Mixed Integer Programming, and Lagrangian Relaxation (LR) [5], [6]. Non-classical methods include Genetic Algorithms, Particle Swarm Optimization, Artificial Bee Colony, Muller method among others [7], [8]. There have also been proposals for hybridization of some of these methods taking advantage of the strengths of two or more methods to provide a more effective solution algorithm [9]–[11]. A comprehensive review of these methods can be found in [3], [4], [12]

Despite the numerous efforts to solve what is a very complex optimization problem over the past few years, a number of research gaps still exist [4]. This paper formulates the PBUC problem incorporating reserve payments and as well as spot market energy prices. A solution methodology for the PBUC optimization problem is then developed. Here, a hybrid of the Lagrangian Relaxation (LR) and Particle Swarm Optimization (PSO) algorithms is used to determine an optimal UC schedule including constraints of having to meet bilaterally agreed energy supply commitments.

Lagrangian Relaxation (LR) is chosen since is currently the most commonly used approach in the solution of the UC problem. However, several methods for updating the Lagrange multipliers have been proposed. The Particle Swarm Optimization (PSO) algorithm is one such method and is implemented in this paper. The biggest challenge with the PSO algorithm lies in the proper selection of the various weighting factors that largely determine the algorithm's performance. Thus, apart from just implementation of the PSO algorithm, parameters selection is also addressed in this paper.

The rest of the paper is organized as follows: Section II introduces the LR and PSO procedures and their application in the solution of optimization problems. Section III outlines the PBUC problem formulation while Section IV explains the proposed solution methodology. In Section V, simulation results on a test IEEE system are presented including section of PSO parameters, analysis of the obtained optimal solution, algorithm convergence performance, and computation time. Finally, paper conclusions are given in Section VI.

A. K. Bikeri, School of Electrical, Electronic, and Information Engineering, JKUAT (phone: +817040882005; e-mail: adlinebikeri@gmail.com).

C. M. Maina, Department of Electrical and Power Engineering, TUK (e-mail: cmainamuriithi@gmail.com).

P. K. Kihato, School of Electrical, Electronic, and Information Engineering, JKUAT (e-mail: pkihato@jkuat.ac.ke).

## II. LAGRANGIAN RELAXATION AND PARTICLE SWARM OPTIMIZATION

The Lagrangian relaxation (LR) method for solving an optimization problem works by incorporating complicated constraints of the problem into the objective function using penalty terms known as Lagrange multipliers [13]. The Lagrange multipliers penalize violations of the corresponding constraints and by systematically updating these penalty factors, an optimal solution of the original problem can be determined. In practice, the modified (relaxed) optimization problem is usually simpler to solve than the original problem hence the application of the method.

The quality of the solution obtained via LR strongly depends on the algorithm used to update the Lagrangian multipliers. Traditionally, gradient based methods have been used but more recently, one or more of the heuristic methods have been applied in an effort to improve the quality of the solution [13], [14].

Particle Swarm Optimization (PSO) is a population based stochastic optimization technique simulating the natural animal's behavior to adapt to the best of the characters among entire populations like bird flocking and fish schooling [15]. Since it's inception in the mid 90's, PSO has been widely applied by researchers in various optimization applications including the solution of the UC problem [7]. In simple terms, a population (swarm) of processing elements called particles, each of which representing a candidate solution forms the basis of computation in the PSO algorithm. A possible solution to the existing optimization problem is represented by each particle in the swarm. A population of random solutions is used to initialize the PSO algorithm and optima are searched by updating the solution in each iteration (epoch).

During a PSO iteration, every particle moves towards its own personal best solution that it achieved so far ($pBest$), as well as towards the global best ($gBest$) solution which is best among the best solutions achieved so far by all particles present in the population. This is done in a random manner ensuring that the algorithm throughly searches the solution space. After a certain pre-set number of iterations (generations), the particle with the global best solution is stored as the optimal solution to the optimization problem.

## III. PBUC PROBLEM FORMULATION

The PBUC problem is formulated as as a maximization of a GENCO's profit by deciding an optimal unit commitment schedule based on expected energy and reserve prices. The GENCO's bilateral contract commitments are also considered. The objective function and the operational constraints are given in the following subsections. The variables in the various equations are shown in Table I.

### A. Objective Function

Profit ($PF$) is defined as the difference between revenue ($RV$) obtained from sale of energy and reserve* and the total operating cost ($TC$) of the GENCO. The objective function of the PBUC problem is then given as:

$$\text{Maximize } PF = RV - TC \tag{1}$$

*1) GENCO Revenue:* $RV$ is given by:

$$RV = \sum_{h=1}^{H} \left( RV_p^h + RV_r^h \right) \tag{2}$$

Revenue from the energy market at a given hour $RV_p^h$ is calculated as:

$$RV_p^h = \alpha_b^h P_b^h + \alpha_s^h \left( \sum_{i=1}^{N} P_i^h - P_b^h \right) + \kappa \left( \alpha_s^h - \alpha_b^h \right) P_b^h \tag{3}$$

The first term in (3) represents revenue from bilateral contracts, the second term represents revenue from the energy sold at the spot market, while the third term represents revenue from contracts of differences.

Contracts of differences (cfds) are usually included in bilateral contracts to compensate suppliers and consumers

TABLE I
NOMENCLATURE

| | |
|---|---|
| $h$ | hour index |
| $i$ | generator index |
| $j$ | PSO particle index |
| $k$ | iteration number index |
| $H$ | number of scheduling hours |
| $J$ | number of PSO particles |
| $K$ | maximum number of PSO algorithm generations |
| $N$ | total number of generators |
| $PF$ | GENCO Profit |
| $RV$ | GENCO Revenue |
| $RV_p^h$ | revenue from energy sales (MWh) at hour $h$ |
| $RV_r^h$ | revenue from reserve sales at hour $h$ |
| $TC$ | GENCO Costs |
| $FC_i^h$ | fuel cost of generator $i$ at hour $h$ |
| $SC_i^h$ | start up cost of generator $i$ at hour $h$ |
| $a_i, b_i, c_i$ | constant for fuel cost curve of generator $i$ |
| $\gamma_i$ | start up cost of generator $i$ |
| $\alpha_s^h$ | unit price for spot market energy sales at hour $h$ |
| $\alpha_b^h$ | unit price for bilateral contracts energy sales at hour $h$ |
| $\alpha_r^h$ | unit price for reserve capacity sales at hour $h$ |
| $P_b^h$ | power supply for bilateral contracts at hour $h$ |
| $P_i^h$ | power output from generator $i$ at hour $h$ |
| $P_i^{min}, P_i^{max}$ | minimum and maximum outputs of generator $i$ respectively |
| $RU_i, RD_i$ | ramp up and ramp down limits of generator $i$ respectively |
| $\kappa$ | factor for contract of differences |
| $U_i^h$ | state of generator $i$ at hour $h$ |
| $\lambda_{j,k}^h$ | Lagrange Multiplier for particle $j$ at hour $h$ for iteration $k$ |
| $\Lambda_{j,k}$ | Set of Lagrange Multipliers for particle $j$ at iteration $k$ |
| $v_{j,k}^h$ | velocity of particle $j$ at hour $h$ for iteration $k$ |
| $V_{j,k}$ | Set of velocities for particle $j$ at iteration $k$ |
| $pBest_j$ | Personal best solution of particle $j$ |
| $gBest$ | Global best solution for all particles |
| $w_1, w_2, w_3$ | weighting factors corresponding to the particle's previous velocity, personal best position and global best position respectively |
| $r_1, r_2$ | random numbers in $[0 \;\; 1]$ |

*Revenue from other ancillary services could be included in a similar manner.

for differences between the bilaterally agreed prices and the prevailing market price. A cfd factor of $\kappa = 0$ would mean that the GENCO sells power in the bilateral market at the bilaterally agreed price even if the market price is higher (no compensation) while a cfd factor of $\kappa = 1$ essentially means that the GENCO sells power in the bilateral market at the prevailing market price (full compensation). A value of $\kappa = 0.5$ is adopted in this paper.

Revenue from sale of reserve at hour $h$ is given by:

$$RV_r^h = \alpha_r^h \sum_{i=1}^{N} \left(P_i^{max} - P_i^h\right) \tag{4}$$

*2) GENCO Costs:* $TC$ is a sum of fuel costs ($FC$) and start up costs ($SC$) for all generators over the entire scheduling period. This is given as:

$$TC = \sum_{h=1}^{H} \sum_{i=1}^{N} \left(FC_i^h + SC_i^h\right) \tag{5}$$

where

$$FC_i^h = a_i + b_i P_i^h + c_i \left(P_i^h\right)^2 \tag{6}$$

$$SC_i^h = \gamma_i \left(1 - U_i^{h-1}\right) U_i^h \tag{7}$$

### B. Operational Constraints

GENCO operational constraints are given as:

(a) Power balance for bilateral contracts

$$\sum_{i=1}^{N} P_i^h \geq P_b^h \qquad \forall h \tag{8}$$

(b) Generation limit constraints

$$U_i^h P_i^{min} \leq U_i^h P_i^h \leq U_i^h P_i^{max} \qquad \forall i, \forall h \tag{9}$$

(c) Ramp up constraints

$$P_i^h - P_i^{h-1} \leq RU_i \qquad \forall i, \forall h \tag{10}$$

(d) Ramp down constraints

$$P_i^{h-1} - P_i^h \leq RD_i \qquad \forall i, \forall h \tag{11}$$

(e) Minimum up time

$$U_i^h = 1 \quad \text{if } U_i^t - U_i^{t-1} = 1, \text{ for } h = t, ..., t + MUT - 1 \tag{12}$$

(f) Minimum down time

$$U_i^h = 0 \quad \text{if } U_i^{t-1} - U_i^t = 1, \text{ for } h = t, ..., t + MDT - 1 \tag{13}$$

Constraints (9)-(13) are similar to the traditional UC formulation [3]. However, constraint (8) indicates that the GENCO's total generation must be greater than its bilateral contracts commitments. This is in contrast with the traditional case where generation must equal total system demand and losses. Unlike the traditional UC formulation, there is no spinning reserve constraint as this is not the GENCO's responsibility. The GENCO only gets payments for supplying part of the reserve. Revenue from reserve sales is therefore added to the objective function.

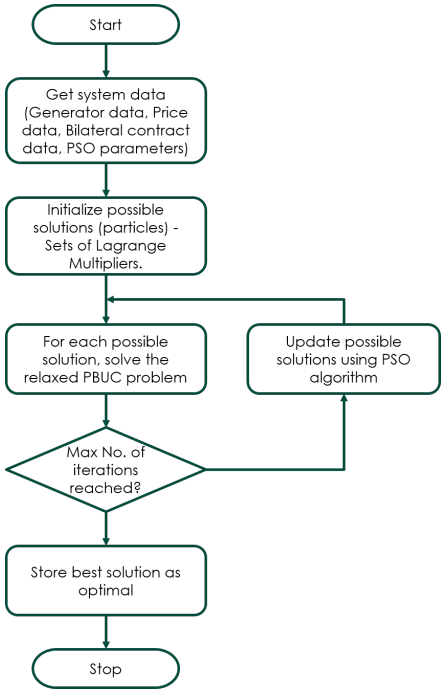


Fig. 1. PBUC solution algorithm using LR-PSO

## IV. SOLUTION METHODOLOGY

### A. PBUC Solution Algorithm

The basic structure of the solution algorithm for solving the PBUC problem using LR and PSO is shown in Fig. 1. Basically, a Lagrangian function is formed by relaxing constraint (8) into the objective function. This is because it is the only constraint that couples the units. Possible solutions to the relaxed problem are then randomly generated and iteratively solved using a two-step process.

The first step involves solving the relaxed problem for each possible solution (sets of Lagrange multipliers). With the relaxation, optimal schedules of individual generation units can be easily determined by breaking down the relaxed function into subproblems for each unit. A 2-state dynamic programming code is implemented to find an optimal UC schedule for each unit given a set of Lagrange multipliers.

The second step involves updating of the possible solutions (particles) using the PSO algorithm. This is done iteratively for a number of pre-set iterations (maximum number of PSO generations). The two steps are outlined in the following subsections.

### B. Solution of the Relaxed Problem

Constraint (8) – the power balance for bilateral contracts – is the only constraint that couples the generating units and is therefore relaxed by being included in the objective function to form the Lagrangian function $L$ as:

$$L = RV - TC - \sum_{h=1}^{H} \lambda^h \left(P_b^h - \sum_{i=1}^{N} P_i^h\right) \tag{14}$$

The relaxed problem is therefore the maximization of $L$ subject to constraints (9) to (13).

To maximize $L$ with respect to $P_i^h$ in (14):

$$\frac{\partial L}{\partial P_i^h} = 0 \quad \forall i, h \tag{15}$$

i.e.

$$\frac{\partial L}{\partial P_i^h} = \left(\alpha_s^h - \alpha_r^h\right) - \left(b_i + 2c_i P_i^h\right) + \lambda^h = 0 \tag{16}$$

hence

$$P_i^h = \frac{\alpha_s^h - \alpha_r^h + \lambda^h - b_i}{2c_i} \tag{17}$$

The following procedure is thus used to solve the relaxed PBUC problem for a set of Lagrange multipliers: $\Lambda = \{\lambda^1, \lambda^2, \ldots, \lambda^H\}$.

**Step 1**: Get input data (generator cost data, hourly price data, Lagrangian multipliers)
**Step 2**: Set $i = 1$
**Step 3**: Set $h = 1$
**Step 4**: calculate $P_i^h$ from (17)
**Step 5**: check for generator limit constraints
if $P_i^h > P_i^{max}$ set $P_i^h = P_i^{max}$
if $P_i^h < P_i^{min}$ set $P_i^h = P_i^{min}$
**Step 6**: check the ramp up and ramp down constraints and change $P_i^h$ accordingly
**Step 7**: check the minimum up time and minimum down time constraints and change $P_i^h$ accordingly
**Step 8**: determine the optimal UC schedule using 2-state dynamic programming
**Step 9**: $h = h + 1$. If $h \leq H$ go to **Step 4**. Else go to **Step 10**
**Step 10**: $i = i + 1$. If $i \leq N$ go to **Step 3**. Else go to **Step 11**
**Step 11**: Calculate total revenue, costs and profits
**Step 12**: Store the results (UC status for all generators, scheduled power, profit)

### C. Lagrange Multipliers Update via Particle Swarm Optimization

The PSO algorithm is used to update the Lagrange Multipliers to determine the set that provides the best results. A particle represents a candidate solution which is a set of Lagrange Multipliers – one for each hour of the scheduling horizon. For a scheduling period of $H$ hours, the $j^{th}$ particle after $k$ iterations $\Lambda_{j,k} = \{\lambda_{j,k}^1, \lambda_{j,k}^2, \lambda_{j,k}^3, \ldots, \lambda_{j,k}^H\}$ represents a position in the $H$-dimension solution space. The particle also has an associated velocity $V_{j,k} = \{v_{j,k}^1, v_{j,k}^2, v_{j,k}^3, \ldots, v_{j,k}^H\}$ which represents a direction in which the particle is moving in the solution space.

The PSO algorithm moves the particles around the solution space after each iteration in a search for the best possible solution. The particle position update follows two "best" positions: $pBest$ and $gBest$. $pBest_j$ is the $j^{th}$ particle's personal best solution found so far while $gBest$ is the entire population's global best solution (the best amongst the various $pBest$s).

At each iteration, the velocity of each particle is updated using†

$$V_{j,k+1} = w_1 V_{j,k} + w_2 r_1 \left(pBest_j - \Lambda_{j,k}\right) + w_3 r_2 \left(gBest - \Lambda_{j,k}\right) \tag{18}$$

†see variable definitions on the nomenclature list in Table I.

The position is then updated using the move equation:

$$\Lambda_{j,k+1} = \Lambda_{j,k} + V_{j,k+1} \tag{19}$$

The following procedure is used to solve the PBUC problem updating candidate solutions (sets of Lagrange Multipliers) using the PSO algorithm:

**Step 1**: Randomly initialize $J$ particles (candidate solutions)
**Step 2**: set $k = 1$
**Step 3**: set $j = 1$
**Step 4**: Solve the relaxed PBUC problem for the $j^{th}$ particle and determine the corresponding GENCO profit $PF_{j,k}$
**Step 5**: If $k = 1$, set $pBest_j = PF_{j,k}$
else if $PF_{j,k} > pBest_j$; set $pBest_j = PF_{j,k}$
**Step 6**: $j = j + 1$.
If $j < J$ go to step 4. Else go to step 7
**Step 7**: Determine $gBest$ as:
$gbest = \max\{pBest_1, pBest_2, \ldots, pBest_J\}$
**Step 8**: set $j = 1$
**Step 9**: Update the velocity of particle $j$ using (18)
**Step 10**: Update the position of particle $j$ using (19)
**Step 11**: $j = j + 1$.
If $j < J$ go to **Step 9**. Else go to **Step 12**
**Step 12**: $k = k + 1$
If $k \leq K$ go to **Step 3**. Else STOP

## V. SIMULATION RESULTS

### A. Test System

The algorithm is tested for a GENCO with 54 thermal units. The generator data is adapted from the IEEE 118-bus test system and obtained from http://motor.ece.iit.edu/data/PBUCData.pdf. The GENCO's own load (bilateral market commitment) is assumed to be constant at 3,500 MW with PEAK and OFF-PEAK prices as shown in Table II.

### B. Selection of PSO Parameters

The quality of the solution obtained from the PSO algorithm is largely dependent on the values of the parameters used. Parameter selection is done in this paper by trying various combinations of the weighting factors $w_1$, $w_2$, and $w_3$ in (18). $w_1$ was varied from 0.25 to 1.0 in steps of 0.25 while $w_2$ was varied from 1.0 to 3.0 in steps of 0.5. $w_3$ was set using the formula: $w_2 + w_3 = 4$ as suggested in literature [15]. These settings give 20 different combinations of the PSO parameters

TABLE II
PRICE DATA

| Hour | Energy Price | Reserve Price | Bilateral Price | Hour | Energy Price | Reserve Price | Bilateral Price |
|---|---|---|---|---|---|---|---|
| 1 | 29.23 | 2.00 | 30.00 | 13 | 57.01 | 2.77 | 56.00 |
| 2 | 26.40 | 1.70 | 30.00 | 14 | 54.42 | 2.87 | 56.00 |
| 3 | 22.47 | 1.27 | 30.00 | 15 | 63.12 | 2.92 | 56.00 |
| 4 | 21.07 | 1.12 | 30.00 | 16 | 65.59 | 3.32 | 56.00 |
| 5 | 23.16 | 1.35 | 30.00 | 17 | 67.24 | 3.23 | 56.00 |
| 6 | 30.86 | 2.18 | 30.00 | 18 | 63.87 | 2.97 | 56.00 |
| 7 | 31.56 | 2.17 | 30.00 | 19 | 55.61 | 2.96 | 56.00 |
| 8 | 47.39 | 2.34 | 56.00 | 20 | 52.55 | 2.73 | 56.00 |
| 9 | 49.70 | 2.51 | 56.00 | 21 | 47.55 | 2.35 | 30.00 |
| 10 | 52.10 | 2.69 | 56.00 | 22 | 39.69 | 1.76 | 30.00 |
| 11 | 55.35 | 2.94 | 56.00 | 23 | 37.00 | 1.57 | 30.00 |
| 12 | 55.50 | 2.95 | 56.00 | 24 | 30.51 | 1.16 | 30.00 |

as shown in table III. In each case, the number of particles was set to $J = 20$ and the number of PSO iterations was set to $K = 500$. The Lagrange multipliers were initialized to take random values ranging from 0 to 50. The velocity was however not restricted so that the final value of the Lagrange multipliers could be any positive real number. For each combination of PSO parameters, 10 different trials of the PSO algorithm were run and the solutions analyzed.

The maximum profit, average profit, and minimum profit from each combination of PSO parameters was determined and the results are shown in Fig. 2. From Fig. 2, it is seen that the $12^{\text{th}}$ combination of PSO parameters ($w_1 = 0.75$; $w_2 = 1.5$; and $w_3 = 2.5$) provides the best results. Hence, for the simulations in this paper these values are chosen as the PSO parameters.

### C. Optimal Solution

*1) Unit Commitment:* The Unit Commitment schedule for the best solution amongst all the trials carried out is shown in Fig. 5. The horizontal axis represents the scheduling hour while the vertical axis refers to the unit number. A single box in the grid therefore indicates whether a unit is ON (shown in red) or OFF (shown in white). The results show that some of the units e.g. 27 and 45 are ON throughout the day while others such as 33 and 46 are OFF throughout the day. Most of the units are ON or OFF depending on the market price at a given hour.

*2) Optimal Power Schedule:* Fig. 3 shows the total committed generation for the 24 hours and the GENCO's own load from the UC schedule of Fig. 5. It also indicates the day's total profit as \$2,355,259. From Fig. 3, the total scheduled power from the LR-PSO algorithm is always greater than the GENCO's load. There is no deficiency in meeting the bilateral contract agreements hence the value of the Energy Not Served ($ENS$) is indicated as zero. Should there be a deficiency in meeting the total committed schedule, the value of $ENS$ will be greater than zero. The value of $ENS = 0$ is ensured by penalizing a result in which $ENS > 0$ when determining the $pBest$ and $gBest$ value in the PSO algorithm.

*3) Optimal Values of Lagrange Multipliers:* Fig. 4 shows the resulting values of the Lagrange Multipliers corresponding to the schedule shown in Fig. 5. It is observed that the LMs are larger for durations of low market price (hrs 0 to 8) and when the market price is lower than the bilateral contract price (hr 14, 20, 21). In these cases, it is relatively expensive to participate in the spot market but it is necessary to generate power to meet bilateral contract commitments. During the periods of relatively high spot market price and when the spot market price is higher than the bilaterally agreed price, constraint (8) is met and there is no need to add a penalty factor hence the value $LM = 0$.

*4) Solution Convergence and Computation Time Analysis:* Fig. 6 shows the evolution of the best solution (value of $gBest$) as well as the computation time against the algorithm iteration number. It is seen that after about 300 iterations, the optimal solution does not change much hence it is sufficient to say that 500 iterations are enough for the current problem size. The solution time increases linearly with the number of iterations hence increasing the number of iterations would only increase the computation time without significantly improving the best solution.

## VI. CONCLUSION

A solution methodology that combines the Lagrangian relaxation technique with the heuristic particle swarm optimization techniques to solve the profit based unity commitment problem for GENCOs in deregulated markets has been

TABLE III
PSO PARAMETER SETS

| Set No. | $w_1$ | $w_2$ | $w_3$ | Set No. | $w_1$ | $w_2$ | $w_3$ |
|---|---|---|---|---|---|---|---|
| 1 | 0.25 | 1.00 | 3.00 | 11 | 0.75 | 1.00 | 3.00 |
| 2 | 0.25 | 1.50 | 2.50 | 12 | 0.75 | 1.50 | 2.50 |
| 3 | 0.25 | 2.00 | 2.00 | 13 | 0.75 | 2.00 | 2.00 |
| 4 | 0.25 | 2.50 | 1.50 | 14 | 0.75 | 2.50 | 1.50 |
| 5 | 0.25 | 3.00 | 1.00 | 15 | 0.75 | 3.00 | 1.00 |
| 6 | 0.50 | 1.00 | 3.00 | 16 | 1.00 | 1.00 | 3.00 |
| 7 | 0.50 | 1.50 | 2.50 | 17 | 1.00 | 1.50 | 2.50 |
| 8 | 0.50 | 2.00 | 2.00 | 18 | 1.00 | 2.00 | 2.00 |
| 9 | 0.50 | 2.50 | 1.50 | 19 | 1.00 | 2.50 | 1.50 |
| 10 | 0.50 | 3.00 | 1.00 | 20 | 1.00 | 3.00 | 1.00 |

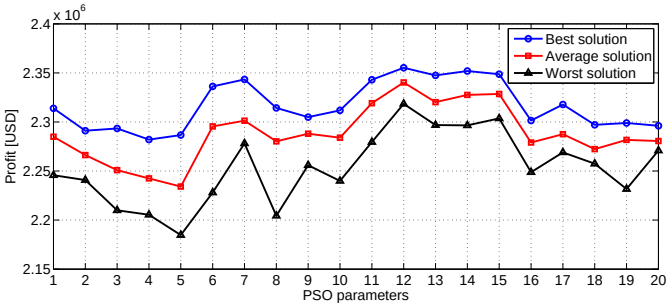


Fig. 2. PSO Parameter Sets Performance

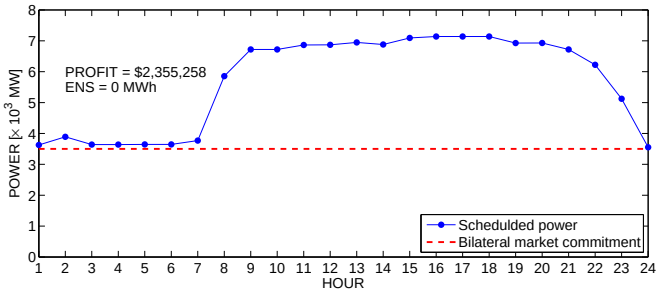


Fig. 3. Optimal GENCO Total Power Generation Schedule

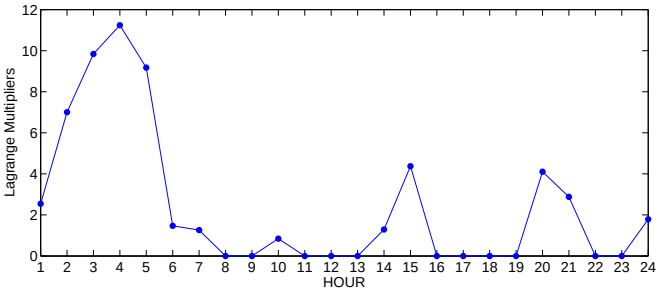


Fig. 4. Lagrange Multipliers Corresponding to the Optimal Solution

| Gen No. | HOUR | | | | | | | | | | | | | | | | | | | | | | | |
|---|---|---|---|---|---|---|---|---|---|---|---|---|---|---|---|---|---|---|---|---|---|---|---|---|
| | 1 | 2 | 3 | 4 | 5 | 6 | 7 | 8 | 9 | 10 | 11 | 12 | 13 | 14 | 15 | 16 | 17 | 18 | 19 | 20 | 21 | 22 | 23 | 24 |
| 1 | 0 | 0 | 0 | 0 | 0 | 0 | 0 | 0 | 0 | 0 | 1 | 1 | 1 | 1 | 1 | 1 | 1 | 1 | 1 | 1 | 0 | 0 | 0 | 0 |
| 2 | 0 | 0 | 0 | 0 | 0 | 0 | 0 | 0 | 0 | 0 | 1 | 1 | 1 | 1 | 1 | 1 | 1 | 1 | 1 | 1 | 0 | 0 | 0 | 0 |
| 3 | 0 | 0 | 0 | 0 | 0 | 0 | 0 | 0 | 0 | 0 | 1 | 1 | 1 | 1 | 1 | 1 | 1 | 1 | 1 | 1 | 0 | 0 | 0 | 0 |
| 4 | 1 | 1 | 1 | 1 | 1 | 1 | 1 | 1 | 1 | 1 | 1 | 1 | 1 | 1 | 1 | 1 | 1 | 1 | 1 | 1 | 1 | 1 | 1 | 1 |
| 5 | 1 | 1 | 1 | 1 | 1 | 1 | 1 | 1 | 1 | 1 | 1 | 1 | 1 | 1 | 1 | 1 | 1 | 1 | 1 | 1 | 1 | 1 | 1 | 1 |
| 6 | 0 | 0 | 0 | 0 | 0 | 0 | 0 | 0 | 0 | 0 | 1 | 1 | 1 | 1 | 1 | 1 | 1 | 1 | 1 | 1 | 0 | 0 | 0 | 0 |
| 7 | 1 | 0 | 0 | 0 | 0 | 0 | 0 | 1 | 1 | 1 | 1 | 1 | 1 | 1 | 1 | 1 | 1 | 1 | 1 | 1 | 1 | 1 | 1 | 0 |
| 8 | 0 | 0 | 0 | 0 | 0 | 0 | 0 | 0 | 0 | 0 | 1 | 1 | 1 | 1 | 1 | 1 | 1 | 1 | 1 | 1 | 0 | 0 | 0 | 0 |
| 9 | 0 | 0 | 0 | 0 | 0 | 0 | 0 | 0 | 0 | 0 | 1 | 1 | 1 | 1 | 1 | 1 | 1 | 1 | 1 | 1 | 0 | 0 | 0 | 0 |
| 10 | 1 | 1 | 1 | 1 | 1 | 1 | 1 | 1 | 1 | 1 | 1 | 1 | 1 | 1 | 1 | 1 | 1 | 1 | 1 | 1 | 1 | 1 | 1 | 1 |
| 11 | 1 | 1 | 1 | 1 | 1 | 1 | 1 | 1 | 1 | 1 | 1 | 1 | 1 | 1 | 1 | 1 | 1 | 1 | 1 | 1 | 1 | 1 | 1 | 1 |
| 12 | 0 | 0 | 0 | 0 | 0 | 0 | 0 | 0 | 0 | 0 | 1 | 1 | 1 | 1 | 1 | 1 | 1 | 1 | 1 | 1 | 0 | 0 | 0 | 0 |
| 13 | 0 | 0 | 0 | 0 | 0 | 0 | 0 | 0 | 0 | 0 | 1 | 1 | 1 | 1 | 1 | 1 | 1 | 1 | 1 | 1 | 0 | 0 | 0 | 0 |
| 14 | 1 | 0 | 0 | 0 | 0 | 0 | 0 | 1 | 1 | 1 | 1 | 1 | 1 | 1 | 1 | 1 | 1 | 1 | 1 | 1 | 1 | 1 | 1 | 0 |
| 15 | 0 | 0 | 0 | 0 | 0 | 0 | 0 | 0 | 0 | 0 | 1 | 1 | 1 | 1 | 1 | 1 | 1 | 1 | 1 | 1 | 0 | 0 | 0 | 0 |
| 16 | 0 | 0 | 0 | 0 | 0 | 0 | 0 | 1 | 1 | 1 | 1 | 1 | 1 | 1 | 1 | 1 | 1 | 1 | 1 | 1 | 1 | 1 | 1 | 0 |
| 17 | 0 | 0 | 0 | 0 | 0 | 0 | 0 | 0 | 0 | 0 | 1 | 1 | 1 | 1 | 1 | 1 | 1 | 1 | 1 | 1 | 0 | 0 | 0 | 0 |
| 18 | 0 | 0 | 0 | 0 | 0 | 0 | 0 | 0 | 0 | 0 | 1 | 1 | 1 | 1 | 1 | 1 | 1 | 1 | 1 | 1 | 0 | 0 | 0 | 0 |
| 19 | 1 | 0 | 0 | 0 | 0 | 0 | 0 | 1 | 1 | 1 | 1 | 1 | 1 | 1 | 1 | 1 | 1 | 1 | 1 | 1 | 1 | 1 | 1 | 0 |
| 20 | 1 | 1 | 1 | 1 | 1 | 1 | 1 | 1 | 1 | 1 | 1 | 1 | 1 | 1 | 1 | 1 | 1 | 1 | 1 | 1 | 1 | 1 | 1 | 1 |
| 21 | 1 | 1 | 1 | 1 | 1 | 1 | 1 | 1 | 1 | 1 | 1 | 1 | 1 | 1 | 1 | 1 | 1 | 1 | 1 | 1 | 1 | 1 | 1 | 1 |
| 22 | 1 | 0 | 0 | 0 | 0 | 0 | 0 | 1 | 1 | 1 | 1 | 1 | 1 | 1 | 1 | 1 | 1 | 1 | 1 | 1 | 1 | 1 | 1 | 0 |
| 23 | 1 | 0 | 0 | 0 | 0 | 0 | 0 | 1 | 1 | 1 | 1 | 1 | 1 | 1 | 1 | 1 | 1 | 1 | 1 | 1 | 1 | 1 | 1 | 0 |
| 24 | 1 | 1 | 1 | 1 | 1 | 1 | 1 | 1 | 1 | 1 | 1 | 1 | 1 | 1 | 1 | 1 | 1 | 1 | 1 | 1 | 1 | 1 | 1 | 1 |
| 25 | 1 | 1 | 1 | 1 | 1 | 1 | 1 | 1 | 1 | 1 | 1 | 1 | 1 | 1 | 1 | 1 | 1 | 1 | 1 | 1 | 1 | 1 | 1 | 1 |
| 26 | 1 | 0 | 0 | 0 | 0 | 0 | 0 | 1 | 1 | 1 | 1 | 1 | 1 | 1 | 1 | 1 | 1 | 1 | 1 | 1 | 1 | 1 | 1 | 0 |
| 27 | 1 | 1 | 1 | 1 | 1 | 1 | 1 | 1 | 1 | 1 | 1 | 1 | 1 | 1 | 1 | 1 | 1 | 1 | 1 | 1 | 1 | 1 | 1 | 1 |
| 28 | 1 | 1 | 1 | 1 | 1 | 1 | 1 | 1 | 1 | 1 | 1 | 1 | 1 | 1 | 1 | 1 | 1 | 1 | 1 | 1 | 1 | 1 | 1 | 1 |
| 29 | 1 | 1 | 1 | 1 | 1 | 1 | 1 | 1 | 1 | 1 | 1 | 1 | 1 | 1 | 1 | 1 | 1 | 1 | 1 | 1 | 1 | 1 | 1 | 1 |
| 30 | 0 | 0 | 0 | 0 | 0 | 0 | 0 | 1 | 1 | 1 | 1 | 1 | 1 | 1 | 1 | 1 | 1 | 1 | 1 | 1 | 1 | 1 | 1 | 0 |
| 31 | 0 | 0 | 0 | 0 | 0 | 0 | 0 | 0 | 0 | 0 | 1 | 1 | 1 | 1 | 1 | 1 | 1 | 1 | 1 | 1 | 0 | 0 | 0 | 0 |
| 32 | 0 | 0 | 0 | 0 | 0 | 0 | 0 | 0 | 0 | 0 | 1 | 1 | 1 | 1 | 1 | 1 | 1 | 1 | 1 | 1 | 0 | 0 | 0 | 0 |
| 33 | 0 | 0 | 0 | 0 | 0 | 0 | 0 | 0 | 0 | 0 | 0 | 0 | 0 | 0 | 0 | 0 | 0 | 0 | 0 | 0 | 0 | 0 | 0 | 0 |
| 34 | 0 | 0 | 0 | 0 | 0 | 0 | 0 | 1 | 1 | 1 | 1 | 1 | 1 | 1 | 1 | 1 | 1 | 1 | 1 | 1 | 1 | 1 | 1 | 0 |
| 35 | 0 | 0 | 0 | 0 | 0 | 0 | 0 | 1 | 1 | 1 | 1 | 1 | 1 | 1 | 1 | 1 | 1 | 1 | 1 | 1 | 1 | 1 | 1 | 0 |
| 36 | 0 | 1 | 1 | 1 | 1 | 1 | 1 | 1 | 1 | 1 | 1 | 1 | 1 | 1 | 1 | 1 | 1 | 1 | 1 | 1 | 1 | 1 | 1 | 1 |
| 37 | 1 | 0 | 0 | 0 | 0 | 0 | 0 | 1 | 1 | 1 | 1 | 1 | 1 | 1 | 1 | 1 | 1 | 1 | 1 | 1 | 1 | 1 | 1 | 0 |
| 38 | 0 | 0 | 0 | 0 | 0 | 0 | 0 | 0 | 0 | 0 | 1 | 1 | 1 | 1 | 1 | 1 | 1 | 1 | 1 | 1 | 0 | 0 | 0 | 0 |
| 39 | 1 | 1 | 1 | 1 | 1 | 1 | 1 | 1 | 1 | 1 | 1 | 1 | 1 | 1 | 1 | 1 | 1 | 1 | 1 | 1 | 1 | 1 | 1 | 1 |
| 40 | 1 | 1 | 1 | 1 | 1 | 1 | 1 | 1 | 1 | 1 | 1 | 1 | 1 | 1 | 1 | 1 | 1 | 1 | 1 | 1 | 1 | 1 | 1 | 1 |
| 41 | 0 | 0 | 0 | 0 | 0 | 0 | 0 | 0 | 0 | 0 | 0 | 0 | 0 | 0 | 0 | 0 | 0 | 0 | 0 | 0 | 0 | 0 | 0 | 0 |
| 42 | 0 | 0 | 0 | 0 | 0 | 0 | 0 | 1 | 1 | 1 | 1 | 1 | 1 | 1 | 1 | 1 | 1 | 1 | 1 | 1 | 1 | 0 | 0 | 0 |
| 43 | 1 | 1 | 1 | 1 | 1 | 1 | 1 | 1 | 1 | 1 | 1 | 1 | 1 | 1 | 1 | 1 | 1 | 1 | 1 | 1 | 1 | 1 | 1 | 1 |
| 44 | 1 | 1 | 1 | 1 | 1 | 1 | 1 | 1 | 1 | 1 | 1 | 1 | 1 | 1 | 1 | 1 | 1 | 1 | 1 | 1 | 1 | 1 | 1 | 1 |
| 45 | 1 | 1 | 1 | 1 | 1 | 1 | 1 | 1 | 1 | 1 | 1 | 1 | 1 | 1 | 1 | 1 | 1 | 1 | 1 | 1 | 1 | 1 | 1 | 1 |
| 46 | 0 | 0 | 0 | 0 | 0 | 0 | 0 | 0 | 0 | 0 | 0 | 0 | 0 | 0 | 0 | 0 | 0 | 0 | 0 | 0 | 0 | 0 | 0 | 0 |
| 47 | 0 | 0 | 0 | 0 | 0 | 0 | 0 | 1 | 1 | 1 | 1 | 1 | 1 | 1 | 1 | 1 | 1 | 1 | 1 | 1 | 1 | 1 | 1 | 0 |
| 48 | 0 | 0 | 0 | 0 | 0 | 0 | 0 | 1 | 1 | 1 | 1 | 1 | 1 | 1 | 1 | 1 | 1 | 1 | 1 | 1 | 1 | 1 | 1 | 0 |
| 49 | 0 | 0 | 0 | 0 | 0 | 0 | 0 | 0 | 0 | 0 | 0 | 0 | 0 | 0 | 0 | 0 | 0 | 0 | 0 | 0 | 0 | 0 | 0 | 0 |
| 50 | 0 | 0 | 0 | 0 | 0 | 0 | 0 | 1 | 1 | 1 | 1 | 1 | 1 | 1 | 1 | 1 | 1 | 1 | 1 | 1 | 1 | 0 | 0 | 0 |
| 51 | 0 | 0 | 0 | 0 | 0 | 0 | 0 | 1 | 1 | 1 | 1 | 1 | 1 | 1 | 1 | 1 | 1 | 1 | 1 | 1 | 1 | 1 | 1 | 0 |
| 52 | 0 | 0 | 0 | 0 | 0 | 0 | 0 | 1 | 1 | 1 | 1 | 1 | 1 | 1 | 1 | 1 | 1 | 1 | 1 | 1 | 1 | 1 | 1 | 0 |
| 53 | 0 | 0 | 0 | 0 | 0 | 0 | 0 | 1 | 1 | 1 | 1 | 1 | 1 | 1 | 1 | 1 | 1 | 1 | 1 | 1 | 1 | 1 | 1 | 0 |
| 54 | 0 | 0 | 0 | 0 | 0 | 0 | 0 | 1 | 1 | 1 | 1 | 1 | 1 | 1 | 1 | 1 | 1 | 1 | 1 | 1 | 1 | 0 | 0 | 0 |

Fig. 5. Unit Commitment Schedule Corresponding to the Optimal Solution

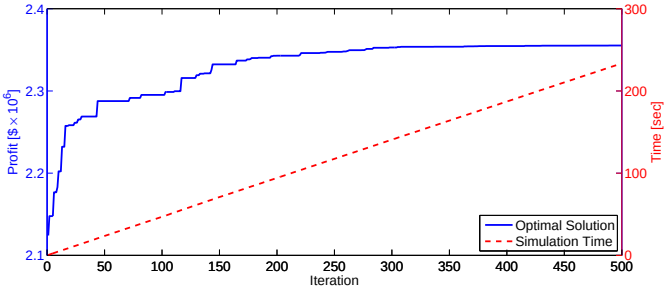


Fig. 6. Analysis of solution convergence and computation time

proposed in this paper. The problem has been formulated including a constraint setting the minimum GENCO output at a given hour as the bilaterally committed generation for the hour. The parameters $w_1 = 0.75, w_2 = 1.5$, and $w_3 = 0.25$ have been chosen based on an assessment of the performance of various combinations of PSO parameters in the solution of the PBUC problem. An implementation for a GENCO with 54 thermal units shows the effectiveness of the proposed methodology.

## REFERENCES

[1] M. Shahidehpour and M. Alomoush, *Restructured Electrical Power Systems, Operation, Trading, and Volatility*. New York: Marcel Decker, 1st ed., 2000.

[2] L. Philipson and H. L. Willis, *Understanding Electric Utilities and De-Regulation*. Florida, USA: Taylor & Francis Group, 2nd ed., 2006.

[3] B. Saravanan, S. Das, S. Sikri, and D. P. Kothari, "A solution to the unit commitment problem — a review," *Frontiers in Energy*, vol. 7, no. 2, pp. 223–236, 2013.

[4] A. K. Bikeri, C. M. Muriithi, and P. K. Kihato, "A review of unit commitment in deregulated electricity markets," in *Scientific Research and Innovation (SRI) Conference, 2015*, pp. 1–5, May 2015.

[5] T. Li and M. Shahidehpour, "Price-based unit commitment: a case of Lagrangian relaxation versus mixed integer programming," *Power Systems, IEEE Transactions on*, vol. 20, pp. 2015–2025, Nov 2005.

[6] A. Rajan, C. Christober, P. Sundarajan, V. Jamuna, R. Madhusubash, and B. Udayakumar, "Multi-area unit commitment in deregulated electricity market using DP approach," *Inter. Journal on Recent Trends in Engineering and Technology*, vol. 3, pp. 210–213, May 2010.

[7] J. Raglend, C. Raghuveer, G. R. Avinash, N. Padhy, and D. Kothari, "Solution to profit based unit commitment problem using particle swarm optimization," *Applied Soft Computing*, vol. 10, no. 4, pp. 1247–1256, Sept. 2010.

[8] H. S. Madraswala and A. S. Deshpande, "Genetic algorithm solution to unit commitment problem," in *2016 IEEE 1st International Conference on Power Electronics, Intelligent Control and Energy Systems (ICPE-ICES)*, pp. 1–6, July 2016.

[9] S. Selvi, M. Moses, and C. Rajan, "LR-EP approach for solving profit based unit commitment problem with losses in deregulated markets," *Przeglad Elektrotechniczny*, vol. 11, pp. 210–213, 2013.

[10] K. Lakshmi and S. Vasantharathna, "Hybrid artificial immune system approach for profit based unit commitment problem," *J. Electrical Eng. Technology*, vol. 8, no. 1, pp. 742–751, March 2013.

[11] A. Sudhakar, C. Karri, and A. J. Laxmi, "Profit based unit commitment for {GENCOs} using lagrange relaxationdifferential evolution," *Engineering Science and Technology, an International Journal*, pp. –, 2016.

[12] N. Padhy, "Unit commitment problem under deregulated environment - A review," in *Power Engineering Society General Meeting, 2003, IEEE*, vol. 2, pp. 11088–1094, July 2003.

[13] C. Lemarechal, *Computational Combinatorial Optimization - Optimal or Provably Near-Optimal Solutions*, ch. Lagrangian relaxation, pp. 112–156. Berlin: Springer-Verlag, 2001.

[14] S. Gao, *Bio-Inspired Computational Algorithms and Their Applications*. InTech, 2012.

[15] J. Kennedy and R. Eberhart, "Particle swarm optimization," in *Neural Networks, 1995. Proceedings., IEEE International Conference on*, vol. 4, pp. 1942–1948 vol.4, Nov 1995.

# Development and Analysis of a Gas Turbine to Run on Syngas from a Mui-Basin Coal Gasifier Using CFD: A Review

Agatha Mbeni Muinde and Eng. Dr. Hiram Ndiritu and Dr. Benson Gathitu

*Abstract*—The global energy demand has been increasing over the years and is still expected to increase by 25% from 2014 to 2040. The rise is demand is being accelerated by economic growth and industrialization of developing countries in Africa and also due to the projected global population growth from 7.2 billion in 2014 to 9 billion in 2040. Fossil fuels have been the major source of global energy, by the end of the $20^{th}$ century they accounted for 85% of the total energy consumed. Combustion of the fossil fuels to produce energy leads to the production of greenhouse gases. Hence there is a need for clean, cheap and reliable source of energy to meet the rise in demand.

Coal is a cheap yet dirty source of energy and it is being used to generate 41.5% of the world electricity and to meet 26.5% of global primary energy needs. Technologies have been developed to reduce emissions from coal power plants such as flue gas clean up technologies, clean coal technologies, and the use of alternative fuel like natural gas. Clean coal technologies include; pressurized fluidized bed combustion, carbon capture and storage and Integrated Gasification Combined Cycle (IGCC).

This review paper deals with the ways being used to increase the performance and efficiency of a syngas turbine for power generation. Increasing the thermal efficiency is one of the ways of increasing the gas turbine performance while loss reduction is also essential.

*Keywords*—Efficiency, Gas turbine, Syngas, TTT

## I. INTRODUCTION

THE global energy demand has been on a steady rise and is expected to be more rapid as economic growth peaks in countries of Africa. The energy demand is expected to rise by 25% from 2014 to 2040. This is due to the projected global population growth from 7.2 billion in 2014 to 9 billions in 2040 [1] and due to the expected growth in GDP.

The energy demand in Kenya can be shown clearly by the electricity demand. As at 2013 the electricity demand was at 1,191 MW and it was projected to increase to 15,000 MW by 2030 [2]. The rise in demand will be caused by; iron ore smelting, standard gauge and light rail, ICT parks that are being constructed, the LAPSET project, rural electrification programs, school computer programs [3]. The government in preparation for the rise in demand started the 5000+ MW 40 months generation program to meet the expected rise in demand. The program is expected to lower the cost electricity from US$ cents 19.78 to 10.43 for domestic and from US$ cents 14.14 to 9.00 for industrial/commercial, to increase electricity supply, access, reliability and safety of services, to reduce lower system losses pass-over cost to customers and to spur economic production, employment, investments and social development [4].

Fossil fuels are a major source of global energy and at the end of the $20^{th}$ they accounted for 85% of the total energy consumed [5]. Coal accounts for one third of the energy used in electric power generation. Gas turbines are being preferred for power generation because of their low level of $CO_2$ and $NO_x$ emissions, small installation time and space and high cycle efficiency [6]. Gas turbines can operate on both liquid and gaseous fuels. The solid fuels such as coal, petroleum coke, biomass, municipal waste and other carbonaceous materials can also be gasified and cleaned then used in a gas turbine as synthetic gas(syngas).

The gas turbines are continuously being improved to increase their power output, efficiency, reduce their emissions, reduce fuel consumption, reduce their size and increase the life cycle. Gas turbine thermal efficiency has been increasing over the years. The increase is attributed to increase in turbine inlet temperature (TIT), which is currently $1200-1500^0$C and research is still being done to raise it higher. In the case of aircrafts, the power can be doubled by increasing the TIT from 1500 to $2000^0$C [7]. The increase in TIT requires the turbine inlet blades to be made with a material that can withstand the extreme inlet temperatures, high pressure, high rotation speed, vibration and small circulation that are experienced at the first stage of a gas turbine [8]. More advanced turbine blade cooling techniques are being developed since the TIT for advanced gas turbines is higher than the melting point of blade material [9].

Blade cooling technologies are needed to ensure turbine operates safely since the current TIT is more than 500K higher than turbine blade materials melting points. Blade cooling was first used in gas turbine in Conway in 1962 and continue being improved [10]. Turbine blade design is being advanced to allow internal cooling channels and to withstand the thermal and rotational stresses. Research is still being

Agatha Mbeni Muinde, Department of Mechanical Engineering, JKUAT, phone: +254713103341; e-mail: amuinde@jkuat.ac.ke
Eng. Dr. Hiram Ndiritu, Department of Mechanical Engineering, JKUAT, e-mail:hndiritu@eng.jkuat.ac.ke
Dr. Benson Gathitu, JKUAT, phone: +254723118800 e-mail:bbg@eng.jkuat.ac.ke

done to determine the optimum shape and size of the blade holes for effective film cooling. Research is being done on effects of rotation on cooling and flow in the casing. Research needs to be done on the effect of velocity, temperature and turbulence profiles exiting the combustion chamber on film cooling of surface and end-walls of the first high pressure gas turbine blade.

Blade tip clearance - the space between the blade and the casing - is responsible for leakage mass flow across the blade tip from the pressure side to the suction side. The leakage causes reduced turbine efficiency by decreasing net work output of each rotor [11]. Further, the aerodynamic losses experienced in a stage are caused by tip leakage loss. Research is till ongoing on different ways to reduce it. This paper will be a review of the effects of blade tip loss and what is being done to reduce it.

## II. REVIEW

### A. Gas turbine

A gas turbines is used to convert the thermal energy into mechanical energy. Gas turbines are light, compact and have a high power to weight ratio [7]. Fig1 shows a schematic diagram of the actual gas turbine engine. It consists of compressor, combustor and turbine. The compressor is used to compress air from the atmosphere to the desired pressure, the combustor is used to burn fuel and the compressed air raising the gas temperature and the turbine converts the gas energy into power work and is coupled to the load which can be a generator for power generation or used to drive other systems.

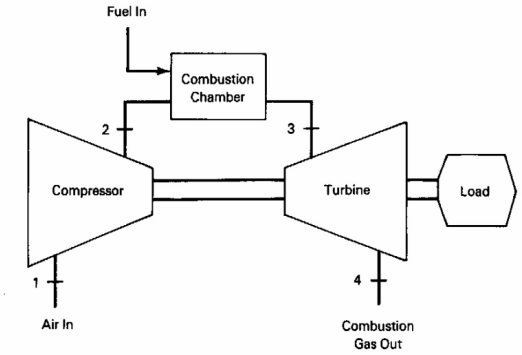


Fig. 1. Schematic diagram of a gas turbine engine

### B. Turbine cooling

Blade cooling technologies are needed to ensure turbine operates safely since the current turbine entry temperature is more than $500^{o}$C higher than turbine blade materials melting points [7]. Blade cooling was first used in gas turbine in Conway in 1962 and continue being improved [10]. Fig2 shows some of the blade cooling techniques used.

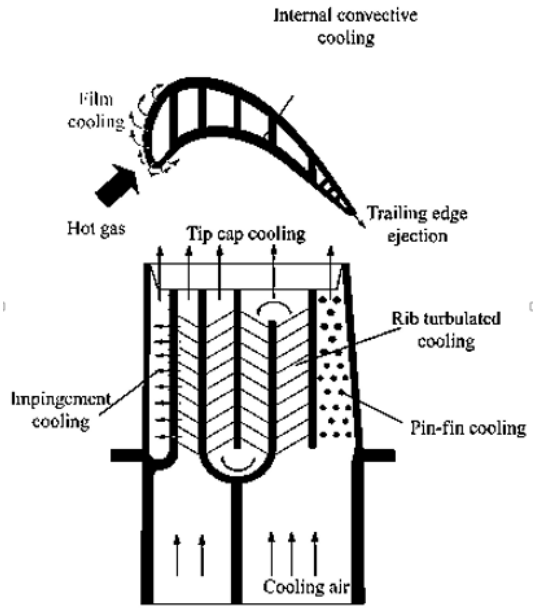


Fig. 2. Blade cooling techniques

Cooling techniques are being improved to cater for the increasing turbine inlet temperature. Trailing edge cooling is one of the techniques being explored. The blade needs to be thin so as not to cause aerodynamic losses. Horbach et al [12] did an experimental study on the performance of external film cooling of the pressure side cutback configuration. The experiment was done using different blade geometry and shapes. The highest cooling effectiveness was achieved in the thinnest ejection lip configuration though it is difficult to manufacture that design. The rounded shape of the tip caused increase in discharge coefficient and it also caused an increase in film cooling effectiveness at high blowing ratios which is a result of changed flow separation.

### C. Film cooling

Film cooling is one of the blade cooling techniques. Cold air is injected from the inside of the blade to the outside surface forming a protective layer between the blade surface and the hot air surrounding the blades [13]. Film cooing effectiveness is affected by rotation speed, blowing ratio, pressure distribution and vortices around the leading-edge region of the gas turbine. The average film cooling effectiveness in the leading edge increases with blowing ratio. The film cooling effectiveness is higher at the suction while on the pressure side the film cooling effectiveness on the blade surface is lower due to presence of upstream wakes.

Film cooling effectiveness is affected by rotation and blade configuration [14]. The objective of the paper was to investigated the effect of tip ejection on film cooling effectiveness on a rotating turbine with four different tip blade configurations: plane tip with tip hole cooling, squealer tip with tip hole cooling, plane tip with pressure-side-edge compound angle hole cooling and squealer tip with pressure-side-edge compound angle hole cooling. An experimental

was done using pressure sensitive paint technique. The film cooling efficiency is increased by increasing the Mach number of the flowing fluid across the different blades of shapes. The coolant particles from the cooling jet of the first two cooling holes of a plane tip blade move in the opposite direction of the blade rotation. Film effectiveness for plane tip increases with increase in rotation speed but decreases with increase in rotation speed for the other three blade shapes. In plane tip blade the film effectiveness follows net velocity vector of incident velocity and leakage velocity for different flow speeds. Research on the effects of heat transfer coefficients, cooling flow losses and stage losses on film cooling effectiveness for different blade configuration at different rotation speed needs to be done.

The direction of coolant flow affects the film cooling effectiveness [15]. A study on backward film cooling was done using numerical simulation and validated by tests. The backward injection has higher and more uniform cooling span then forward injection cooling. The film cooling effectiveness remains high at different blowing ratios in the case of backward injection cooling. The experiment done validated that backward injection is better than forward. A study on ways of improving film cooling effectiveness on curved surfaces need to be done.

Coolant density influences the film cooling effectiveness [16]. A study was done Pressure Sensitive Paint technique to determine film-cooling effectiveness at high blowing ratios, coolant density, and freestream turbulence intensity. The results showed that film cooling effectiveness increases with increase in blowing ratio on the pressure side from 1.2 to 1.7 and on the suction side from 1.1 to 1.4. Film cooling peak effectiveness on the pressure side is at momentum index of approximately 1.15 and at 0.75 on the suction side. Film cooling effectiveness increases proportionally to density ratio in the pressure side while a slight increase in effectiveness on the suction side is seen between axial chord points 0.2 and 0.45 and a major increase between axial chord points 0.45 and 0.75. Increase in freestream turbulence intensity decreases the film cooling effectiveness on the pressure side and on the suction side between axial chord 0 and 0.45 but it increases with increase in turbulence intensity after axial chord 0.45. A study needs to be done on ways of improving film cooling efficiency in turbulent.

### *D. Steam-injection cooling*

Steam-injection cooling offers a potential increase in cycle efficiencies and work output at considerable cost for industrial gas turbines. Higher water flow rate is required to prevent boiling in the system, resulting in higher work output and lower cycle efficiency [17].

Steam injection affects performance parameters of gas turbine and nitrogen oxide emissions [18]. A study was done on gas turbine performance and $NO_x$ production for two different ambient pressure with and without steam injection technique using modeling and analysis method. The results showed that steam injection cooling increased the thrust coefficient, thermal efficiency and turbine work output. The steam injected to the burner reduces $NO_x$ production.

### *E. Transpiration gas cooling*

It is used for cooling turbine blades when operating at very high temperature. An insulating film is created on outer airfoil surface by passing a cooling gas through a porous wire mesh skin. In cases where steam is used, the porous skin has to be selected such that the quantity of steam that penetrates meets the constant wall temperature at the local gas steam temperature and pressure conditions [19].

The performance of gas turbine when using steam or air as a coolant in transpiration is different [20]. Computer modeling was used to compare the performance of combined cycle with air and steam cooling. The results showed that the combined cycle efficiency and specific work output varied with TIT and coolant. As the TIT increased from 1600 K to 1800 K the difference in cycle efficiency between steam and air cooled turbine changed from 1.47% to 2%. The specific work output for a steam cooled combined cycle was 63kJ/kg higher than air cooled combined cycle at TIT of 1800 K. A study on the mixing losses caused by using Steam as a coolant needs to be done.

### *F. Internal Cooling Method*

The turbine blades have internal channels where air extracted from the compressor is forced through hence cooling the turbine. Fig.3 shows a turbine blade with cooling channels. Internal cooling provides better cooling hence increasing the blade life. The main disadvantage is the many cooling channels that are complicated to machine [17].

Rotation affects the internal cooling of turbine blades. Han [13] did a study on blade cooling. The findings were that rotation can cause heating on one side of the cooling channel and cooling on the opposite side due to the secondary flow induced by the rotation. RANS method of turbulent flow is used in computing the flow and heat transfer. Rotation reduces the impingement cooling effect due to jet deflection away from the impinged surface.

### *G. Tip leakage*

The clearance between blade tip and the casing causes turbine tip leakage loss. Reducing the turbine leakage loss in high pressure turbine can instantly save cost and increase the engine life [21].
The gas turbine rotation causes blade tip loses due to the vortices formed as the fluid passes between the blades and the casing. Liu et al [22] did a study on the effects of blade

Fig. 3. Turbine blade with cooling Channels

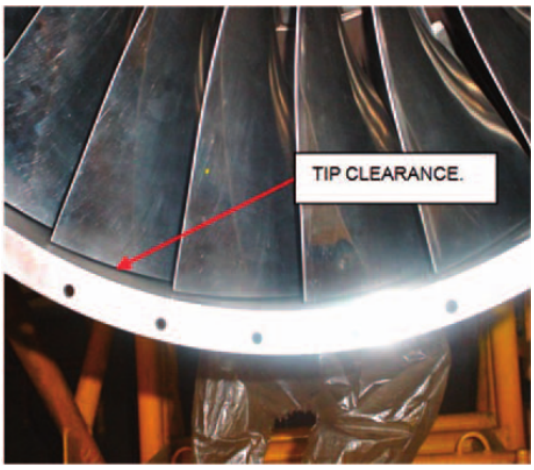


Fig. 4. Tip clearance

rotation on axial turbine tip leakage vortex breakdown and loss. Numerical techniques method was used. The finding were that the tip mixing loss per unit leakage flow reduced with increase in rotation speed. The vortex breakdown is influenced by Coriolis force and the 3D shear flow in the casing endwall region. Tip injection should be used to control vortex breakdown hence reducing tip leakage losses.

Yang [23] did a numerical simulation to study tip leakage flow and heat transfer in rotor blade with flat and squealer tips. A standard k-$\omega$ turbulence model was used to investigate the influence of tip gap height and groove depth on tip leakage flow and heat transfer. Leakage flow is reduced by increasing the tip groove depth up to 3% of the blade span above which any increase tip gap height causes increase in leakage flow. The average heat transfer rate decreases as the groove depth increases while it is increased on the tip surface with increase in tip gap height. When the tip gap height is less than 1% the overall heat transfer coefficient is affected by both vortex structure and leakage velocity but when the tip gap is more than 1% increase in heat transfer coefficient is proportional to increase in tip gap height which can only result from a variety of the leakage velocity.

### *H. Turbine Material*

Material selection is very critical in the design of Gas turbines. Turbine blades operate at high stress conditions, at high temperatures and corrosion conditions. Temperature affects the performance of a gas turbine. As inlet temperature of gas turbine increases, specific fuel and air consumption decreases while the turbine efficiency increases. Nickel base super alloy especially Inconel 718 is used for turbine blade since it has excellent thermal stability, tensile and fatigue strengths, resistance to creep and hot corrosion and micro structural stability [24]. Blade cooling should be done to prevent hot corrosion and creep strain distribution on the trailing edge [25].

### *I. Turbine design*

The gas turbines can be classified according to configuration as radial flow turbines; the flow is along the radius or as axial flow turbines; the flow is along the axis of rotation. The axial turbine can have of one or more stages, each consisting of a stationary nozzle and a rotor. The axial flow turbines are preferred to radial flow turbines because of the following reasons; they can be used for in compressible fluids, they have higher efficiency for high power range above 5MW and they have a high work factor hence a lower fuel consumption and less turbine noise [26]. The area of both the nozzle and the rotor decrease from inlet to the blade to the throat. The fluid enters at an angle tangent to the camber line at the leading edge and leaves at an angle tangent to the camber line at the trailing edge [27]. The first stage of a syngas turbine nozzle area is increased to a performance factor of 1.20 as compared to natural gas turbine nozzle that has a factor of 1.0 which results in a 20% flow area increase [28]. The efficiency of a gas turbine can be increased by increasing the blade area when using syngas in a natural gas turbine [29]. Research is still ongoing to establish an optimum blade area for syngas turbine.

The design specifications of a syngas turbine are; ambient conditions of $15^0$C temperature, 1.013 bar pressure and relative humidity of 60%. Compressor with a pressure ratio of 16.2 and mass flow rate of 17.7 kg/s. Combustor fuel mass flow rate of 47% and pressure drop of 4%. The turbine has inlet temperature of $1314^0$C, rotor inlet temperature of $1267^0$C, exhaust flow rate of 550 kg/s and exhaust temperature of $587^0$C [30]. The blades are 6 in number and the blade size is 100mm in length with tip outer diameter of 10mm and axial chord of 4mm. The flow parameters are; Inlet temperature of $1200^0$C, rotation speed of 8400 RPM mass flow rate of 1 kg per second and discharge temperature of $850^0$C. Fig.5 shows the axial flow turbine nozzle and rotor.

### *J. Syngas*

It is produced through gasification of fuels such as coal, petroleum coke, biomass, municipal waste and other

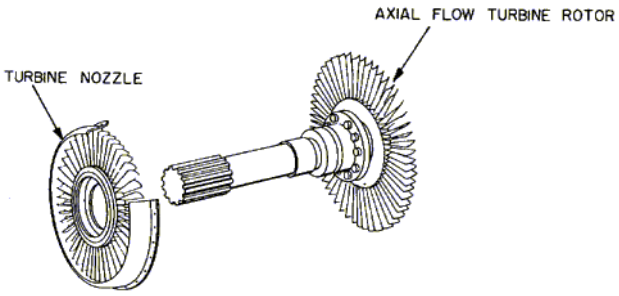


Fig. 5. Axial Flow Turbine Nozzle and Rotor

carbonaceous materials. It is a cleaner and high-value energy source and it is being used to replace natural gas in both power generation and industrial use [31]. Syngas from coal has a low heating value. Most of the existing gas turbines are manufactured specifically to burn standard fuels like natural gas and light diesel fuel. The main challenges facing gasification technologies are in efficient production and processing of quality syngas that is acceptable in gas turbine without reducing the life of turbine components. Since it is difficult to control the quality of the syngas in cases where the coal has high ash and moisture content [32].

A study on the influence of firing medium or low heat value fuel on the safe operation of a gas turbine was done by Xuelei [29]. The syngas flow rate was increased and the firing conditions changed. The compressor surge margin, axial torque and expander metal temperature were considered when changing operating conditions for the safe operation of the turbine. From the study the flow rate was increased by increasing compressor pressure ratio or by closing Inlet Guide Vane angle or by decreasing expander inlet temperature or by extracting air from compressor last stage or by increasing expander flowing area. Increasing the compressor pressure ratio increased the axial torque of the turbine, decreased the compressor surge margin and increased the expander temperature hence it was the worst safe performance strategy.

Oluyede [28] did a study on the fundamental impacts of firing syngas in a gas turbine while maintaining the hot section metal temperature. Syngas has a lower heating value as compared to natural gas, in order to attain the firing temperature and maintain constant energy input to the gas turbine a large fuel flow rate is required. The high hydrogen content in the syngas resulted in high flame temperature and high moisture content hence affecting the hot section of the material hence reducing the life of the turbine. The firing temperature was reduced by reducing the volume of syngas being burned.

### *K. Gaps*

1) Research needs to be done on ways of improving film cooling efficiency in turbulent flow.
2) More research on the detailed and accurate leakage flow and heat and mass transfer characteristics over the blade tip and near-tip region and ways of reducing the leakage.
3) Research is needed on Ways of controlling the moisture content in syngas.
4) Research is still ongoing to establish an optimum blade area for syngas turbine.

## III. Conclusion

There is a need to properly utilize the available sources of energy to meet the ever increasing energy demand. One of the cheap yet dirty source of energy is coal. Gasification of coal to produce syngas has aided in making coal a cheap and clean source of energy. Gas turbines are used to burn the syngas and convert it into ready energy like electricity. The gas turbine performance is still being improved by reducing the tip leakage loss and increasing the thermal efficiency. More research needs to be done to effectively reduce the turbine loss. Materials have been improved to cater for the high turbine inlet temperatures but cooling is still needed to achieve those high temperatures. More research is also needed to reduce the challenges faced when burning syngas in a gas turbine like high moisture content.

## References

[1] U.S Energy Information Administration, *International Energy Outlook 2016 with Projections to 2040*, vol. 0484. 2016.
[2] Institute of Economic Affairs (IEA), "Situational Analysis of Energy Industry , Policy and Strategy for Kenya," p. 77, 2015.
[3] Energy Regulatory Commission, "POWER SECTOR MEDIUM TERM PLAN. Republic of Kenya," vol. 21, no. 21, 2014.
[4] Mobil Exxon, "The 2013 Outlook for Energy: A View to 2040," 2016.
[5] R. Bhargava, M. Bianchi, a. De Pascale, G. Negri di Montenegro, and a. Peretto, "Gas Turbine Based Power Cycles - A State-of-the-Art Review," *Power Eng. Conf.*, p. 11, 2007.
[6] M. Yuri, K. Tsukagoshi, S. Hada, J. Masada, and E. Ito, "Development of 1600 C-Class High-efficiency Gas Turbine for Power Generation Applying J-Type Technology," *Mitsubishi Heavy Ind. Tech. Rev.*, vol. 50, no. 3, pp. 1–10, 2013.
[7] B. Sunden and G. Xie, "Gas Turbine Blade Tip Heat Transfer and Cooling: A Literature Survey," *Heat Transf. Eng.*, vol. 31, no. 7, pp. 527–554, 2010.
[8] C. a. Estrada, "New Technology Used in Gas Turbine Blade Materials .," *Sci. Tech. Año XIII*, no. 36, pp. 297–301, 2007.
[9] D. Dongre, T. Vikas, and R. Vishal, "DESIGN AND ANALYSIS FOR INTERNAL COOLING OF GAS TURBINE BLADE," *Int. J. Eng. Appl. Technol.*
[10] L. Xu, S. Bo, Y. Hongde, and W. Lei, "Evolution of Rolls-royce Air-cooled Turbine Blades and Feature Analysis," *Procedia Eng.*, vol. 99, pp. 1482–1491, 2015.
[11] M. R. Shirzadi and H. Saeidi, "The Effects of Tip Clearance on Performance of a Heavy Duty Multi Stages Axial Turbine," *Proc. ASME Turbo Expo*, no. June 11-15, pp. 1–11, 2012.
[12] T. Horbach, A. Schulz, and H. Bauer, "TRAILING EDGE FILM COOLING OF GAS TURBINE AIRFOILS EXTERNAL COOLING PERFORMANCE OF VARIOUS INTERNAL PIN FIN CONFIGURATIONS," *Proc. ASME Turbo Expo 2010 Power Land, Sea Air Proc.*, no. mm, pp. 1–12, 2010.
[13] J.-c. Han, "Recent Studies in Turbine Blade Cooling ," *Int. J. Rotating Mach.*, vol. 10, no. 6, pp. 443–457, 2004.
[14] M. T. Schobeiri, M. Rezasoltani, K. Lu, and J. C. Han, "A Combined Experimental and Numerical Study of the Turbine Blade Tip Film Cooling Effectiveness under Rotation Condition," in *Turbine Tech. Conf. Expo.*, 2014.
[15] X. C. Li, G. Subbuswamy, and J. Zhou, "Performance of Gas Turbine Film Cooling with Backward Injection," *Energy Power Eng.*, vol. 2013, no. July, pp. 132–137, 2013.

[16] D. P. Narzary, K.-c. Liu, A. P. Rallabandi, and J.-c. Han, "INFLUENCE OF COOLANT DENSITY ON TURBINE BLADE FILM-COOLING USING PRESSURE SENSITIVE PAINT TECHNIQUE," in *Power Land, Sea Air*, pp. 1–12, 2010.
[17] N. Nandakumar and N. S. Moorthi, "Performance Analysis of Gas Turbine Blade Cooling by CFD," vol. 1, no. 4, pp. 3–9, 2015.
[18] R. Tirgar, A. M. Sarmazdeh, M. M. Nezhad, and M. Tahani, "Modelling of Steam Injection Effects on Performance Parameters and NOx Emissions of a Gas Turbine," *J. Appl. Sci. Res.*, vol. 10, no. May, pp. 331–336, 2014.
[19] M. P. Boyce, *GasTurbine Engineering Handbook*. gulfProfrssional Publishing, 2 ed., 2002.
[20] S. Kumar and O. Singh, "Enhancement of combined cycle performance using transpiration cooling of gas turbine blades with steam," *J. Mech. Sci. Technol.*, vol. 28, no. 6, pp. 2429–2437, 2014.
[21] L. Qi and Y. Zhou, "Turbine blade tip leakage flow control by unsteady periodic wakes of upstream blade row," *Procedia Eng.*, vol. 80, pp. 202–205, 2014.
[22] J. Gao, Q. Zheng, Y. Liu, and P. Dong, "Effects of blade rotation on axial turbine tip leakage vortex breakdown and loss," *Proc. Inst. Mech. Eng. Part G J. Aerosp. Eng.*, vol. 0, no. 0, pp. 1–16, 2016.
[23] D. Yang and Z. Feng, "TIP LEAKAGE FLOW AND HEAT TRANSFER PREDICTIONS FOR TURBINE BLADES," *Power Land, Sea Air*, no. May 14-17, pp. 1–8, 2007.
[24] R. J. E. Glenny, J. E. Northwood, and a. B. Smith, "Materials for Gas Turbines," *Int. Mater. Rev.*, vol. 20, no. 1, pp. 1–28, 2013.
[25] T. V, U. P. S, P. G. Reddy, C. J. Manjunath, and A. Professor, "Design and Analysis of Gas Turbine Blade," *Int. J. Innov. Res. Sci. Eng. Technol. (An ISO Certif. Organ.*, vol. 3297, no. 6, pp. 13533–13539, 2007.
[26] N. Binder, X. Carbonneau, and P. Chassaing, "Off-Design Considerations through the Properties of Some Pressure-Ratio Line of Radial Inflow Turbines," *Int. J. RotatingMachinery*, vol. 2008, 2008.
[27] W. Bathie, *Fundamentals of Gas Turbines*. John Wiley & Sons, Inc., 2 ed., 1996.
[28] E. O. Oluyede and J. N. Phillips, "FUNDAMENTAL IMPACT OF FIRING SYNGAS IN GAS TURBINES," *ASME Turbo Expo 2007 Power Land, Sea Air*, pp. 1–8, 2007.
[29] Z. Xuelei, W. Songling, C. Haiping, and Z. Lanxin, "The Influence of Firing Medium or Low Heat Value Fuel on the Safe Operation of Gas Turbine," no. 93102802, pp. 1–3, 2010.
[30] D. W. Kang, C. M. Kim, J. H. Lee, T. S. Kim, and J. L. Sohn, "Performance maximization of IGCC plant considering operating limitations of a gas turbine and ambient temperature," *J. Mech. Sci. Technol.*, vol. 30, no. 5, pp. 2397–2408, 2016.
[31] P. J. Roach and C. B. Ponton, "Aqueous electrophoretic deposition as a method for producing an investment casting shell mould ceramic face-coat. Part 1: Formation of a carbon-filled investment casting wax electrode material," *J. Mater. Sci.*, vol. 48, no. 21, pp. 7476–7492, 2013.
[32] M. S. Bhatt, "Hybrid clean energy technologies for power generation from sub-bituminous coals: a case of 250 MW unit," *Int. J. Sustain. Energy*, vol. 6451, no. March, pp. 1–14, 2012.

# Treatment of manganese-containing mine water: adsorption onto metal oxide decorated bentonite

AM. Muliwa, MS. Onyango, A. Maity and A. Ochieng

***Abstract-*** Water pollution by toxic metals from mining industries is a serious threat to living organisms and the environment. Therefore, it is important to effectively remove metal contaminants from water using appropriate treatment technologies. In this study, bentonite manganese oxide (BMnO) composite was prepared, characterized and evaluated for $Mn^{2+}$ ions adsorption from aqueous solutions. Batch experiments were conducted to explore the effect of different experimental conditions on adsorption efficiency. The adsorption of Mn was reasonably fast and the kinetic data fitted well with the pseudo-second-order model. Equilibrium results showed that increasing the solution pH and adsorbent dose, and temperature increased the adsorption efficiency while it was opposite with the initial concentration. Langmuir isotherm model described equilibrium data better compared to Freundlich isotherm model. The removal of $Mn^{2+}$ ions proceeded by ion-exchange and adsorption. Metal oxide decorated bentonite can effectively reduce $Mn^{2+}$ ions in polluted waters.

***Keywords*—**Adsorption, bentonite, manganese, metal oxide

## 1. Introduction

Manganese is one of the toxic and non-degradable metallic species mainly discharged by industrial effluents from coal and oil burning, dry battery cells, ceramics and electrical coil manufacturing. It can exist in a range of oxidation states, +2, +3, +4, +6 and +7. Amongst these, the divalent form ($Mn^{2+}$) is the predominant species in most waters at pH 4-7, while highly oxidized forms occur at alkaline pH values (pH>7) or may result from microbial oxidation [1, 2]. Although small traces of manganese are essential nutrients for human body, exposure to high amounts can cause irreversible damages to the nervous system and other pathologies [3]. Concentrations in excess of drinking water standards can result in formation of oxide deposits in pipeline, discoloration of water and laundry, and impart an unpleasant metallic taste [4]. Therefore, reduction of manganese concentration in public and industrial water to acceptable levels is an important undertaking from human health and environmental point of view.

The chemistry of manganese in aqueous solution is quite complex, thus making it a difficult contaminant to remove. Many technologies, including precipitation, coagulation-flocculation , sedimentation, oxidation/reduction, solvent extraction, ion-exchange, evaporation and adsorption are available for control and minimization of water pollution by metals [5, 6]. However, most of these processes are characterized by shortcomings such as high operational and maintenance cost, low removal efficiency, and inapplicability to a wide range of toxic pollutants in low concentrations, and generation of toxic sludge [7]. Comparatively, adsorption process is considered a better alternative for decontamination of heavy metal ions polluted water because it requires low capital cost, it is flexible, simple in design, easy to operate, insensitive to toxic pollutants, and the availability of different adsorbents [8]. Moreover, it does not result in the formation of harmful substances. The performance of any adsorption system depends highly on the adsorbent's characteristics such as surface area and chemistry, and the selectivity [9].

Recently, there has been increased focus on application of natural materials such as clays as adsorbents for decontamination of metal polluted water. Clays are abundant, inexpensive, non-toxic, and modifiable [10]. Moreover, clays have layered structure, and they also exhibit high ion-exchange and swelling characteristics, as well as good cation exchange capacity, which make them potential candidates for metal ions removal [11]. However, clays are sticky when wet and they produce low capacity for metal ions. Thus, to enhance adsorption capacity, surface modifications using appropriate organic or inorganic components is required [12, 13]. Metal oxides (MO) nanoparticles are known to have high affinity for metal ions, but cannot be used alone in an adsorption system. This is because their small sizes creates high pressure drops in fixed-bed applications, and that they are not economically attractive [14]. Thus, if MO can be combined with inexpensive materials, like clays, can result to an adsorbent material with improved synergistic effects for metal ions removal.

In this study, bentonite clay was decorated by direct redox precipitations of manganese oxide (MnO) nanoparticles onto its surface, and was examined for adsorption of $Mn^{2+}$ ions from aqueous solution. Equilibrium experiments were performed in batch mode to explore the influence of different process conditions on $Mn^{2+}$ removal. The equilibrium data was fitted with the appropriate adsorption models to extract important adsorber design parameters.

A.M. Muliwa, MS Onyango, Department of Chemical, Metallurgical and Materials Engineering, Tshwane University of Technology (corresponding author phone: +27818445644; fax: +27123823550; e-mail: amuliwa@yahoo.com).

A. Maity, DST/CSIR National Centre for Nanostructured Materials, Council for Scientific and Industrial Research, Pretoria.

A. Ochieng, Centre for Renewable Energy and Water, Vaal University of Technology, South Africa

## 2. Materials and methods

### *2.1. Chemicals and adsorbent preparation*

All chemicals were reagent grade and were purchased from Merck (Pty) Ltd-South Africa. Double distilled water was used for all rinsing and dilutions. A stock solution of 1000 mg$Mn^{2+}$/L was prepared by dissolving an appropriate amount of Mn $(NO3)_2.4H_2O$ salt in 1000 mL distilled water.

Bentonite powder was obtained from ECCA (Pty) Ltd, South Africa. It was washed repeatedly with water to remove impurities, then it was dried at 100°C for 24h. A given mass of the dried bentonite was added into a $KMnO_4$ solution, and the mixture was stirred magnetically for 30min. To this mixture, HCl was added, and thereafter, heated and maintained at 90°C for 1h. The brown mixture was then allowed to cool to room temperature after which it was vacuum filtered and rinsed with water until the filtrate pH was neutral. Finally the solids were vacuum-dried overnight and stored waiting further use. The morphology was observed using scanning electron microscope (SEM, JEOL JSM-6610-LV), operated at an accelerating voltage 15 kV and beam current 20 mA.

### *2.2. Adsorption equilibrium experiments*

In all batch equilibrium experiments, 50mL solutions in 100mL plastic sample bottles, and a thermostatic bath shaker, operated at 160 rpm were used, unless otherwise stated. The effect pH (2-10), adsorbent mass (0.025-0.225 g), temperature (298-318K), and concentration (50-200 mg/L) on Mn removal were explored. For each experiment, one parameter was varied while others were kept constant. Samples were agitated for 24h, filtered and analyzed for residual $Mn^{2+}$ ions using ICP-AES. The removal efficiency and uptake were determined by mass balance expressions as follows:

$$R\% = \left( \frac{C_o - C_e}{C_o} \right) \times 100 \quad (1)$$

$$Q_e = \left( \frac{C_o - C_e}{m} \right) \times V \quad (2)$$

where $C_o$ and $C_e$ are initial and equilibrium concentration (mg/L), $Q_e$ is the uptake (mg/g), m is the mass of adsorbent (g) and $V$ is the solution volume (L).

The effect of contact times was explored by adding a given amount of adsorbent into 1 L $Mn^{2+}$ ions solution, under stirring at 160 rpm. Samples were taken periodically for 3h, and were analyzed and $Mn^{2+}$ ions uptake at any time $t$.

Adsorption experiments were also carried out using real neutral mine water to determine the suitability of CBMnO adsorbent in real wastewater applications. The water samples were obtained from a Gold mining company in Gauteng Province, and the analysis showed that concentration of manganese was 50 mg/L, among other co-ions, and had a pH 6.8; attributable to limestone pretreatment.

## 3. Results and discussion

### *3.1. Material characterization*

Figure 1 shows SEM images of bentonite (a) and BMnO (b). As can be seen, the surface of bentonite was observed to contain discrete spherical particles while the surface of BMnO composite was appeared more dense indicating possible deposition of MnO particles on the surface. Further, the surface of BMnO had a rough morphology which is an important characteristic for adsorption. The presence of MnO onto the bentonite was confirmed by Mn and O peaks in the EDX spectra (not presented).

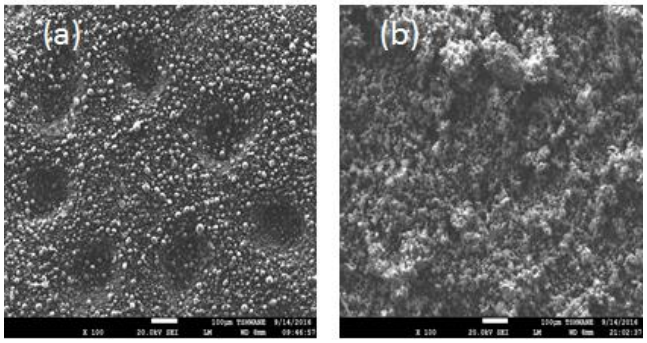


Fig. 1 SEM images of BMnO (a) before and (b) after $Mn^{2+}$ ions adsorption

### *3.2. The effect of solution pH and removal mechanism*

Preliminary experiments showed that the removal efficiency increased with increase in pH. Obviously, this was due to the BMnO surface becoming increasingly negatively charged (deprotonation effects). Literature reports indicate that the charge at the metal (Me) oxide-solution interface occurs as follows:

$$-Me-OH^{o} + H_2O = -Me-O^{-} + H_3O^{+} \quad (3)$$

$$-Me-OH^{o} + H_3O = -Me-OH^{+} + H_2O \quad (4)$$

For the purposes of mimicking the characteristics of real neutral mine water, all experiments were conducted at pH 6. At this pH, also, Mn does not precipitate, hence quantification was exclusively based on adsorptions. Further, the removal mechanism of divalent metal ions by MO surface have been reported to take place *via* ion-exchange and adsorption processes. To validate this, final solutions pHs were measured after each experiment. It was found that all final solutions pHs decreased indicating that protons were released into the solutions.

### *3.3. Effect of sorbent mass*

The amount of an adsorbent used in any given adsorption system is an important factor to consider from the economic point of view and the discharge standards compliance. Figure 2 shows the effect of BMnO mass on the removal efficiency of $Mn^{2+}$ ions. The adsorption efficiency was found to increase from 47.35% to 100% when the mass was increased from 0.025 to 0.225 g. The increment corresponded with a decrease

in adsorption capacity from 73.4 to 22.2 mg/g. The increase in removal with the increase in mass was attributed to increased adsorption sites while the decrease in capacity could be explained by the presence of unsaturated adsorption sites.

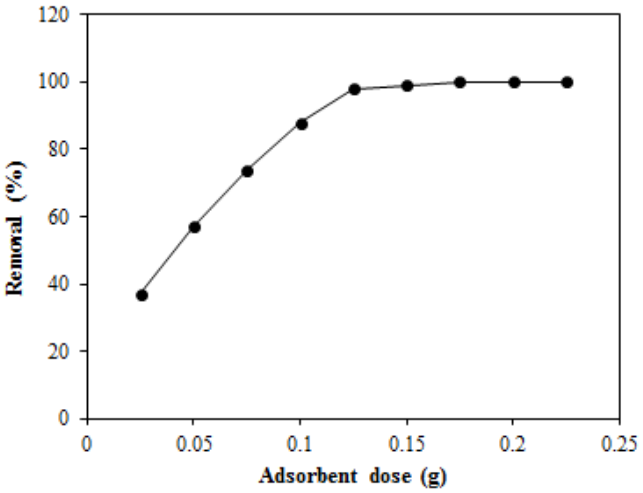


Fig. 2. Effect of adsorbent dose on $Mn^{2+}$ ions removal (pH=6, Vol=50 mL, Temp=298K)

In another set of experiment, results revealed that the removal efficiency decreased with the increase in initial concentration of $Mn^{2+}$ ions. The decline in adsorption efficiency was due to the fact that at lower concentration, there are sufficient adsorption sites available, but at higher concentration, $Mn^{2+}$ ions are greater than the adsorption sites [15].

### *3.4. Adsorption isotherms and thermodynamic studies*

Adsorption isotherms are important in the determination of capacity and selection of a suitable adsorbent. Isotherm models are based on the homogeneity or heterogeneity of the adsorbent's surface. Information on adsorption isotherms is well documented in literature [16]. The experimental data was fitted to Langmuir, Freundlich and Tempkin models. The linear Langmuir isotherm equation is expressed as:

$$\frac{C_e}{Q_e} = \frac{1}{k_L Q_m} + \frac{C_e}{Q_m} \quad (5)$$

where $k_L$ and $Q_m$ are the Langmuir constant (L/g) and monolayer capacity (mg/g), respectively.

The Freundlich isotherm model equation is mathematically expressed as:

$$Q_e = \ln K_F + \frac{1}{n} \ln C_e \quad (6)$$

where $K_F$ and $n$ are the Freundlich parameters representing capacity ($L^n mg^{1/n}/g$) and intensity, respectively.

The linearized Tempkin isotherm model is expressed as:

$$Q_e = \frac{RT}{b_T} \ln A_T + \frac{RT}{b_T} \ln C_e \quad (7)$$

where $b_T$ (kJ/mol) is the Tempkin constant related to heat of adsorption, $A_T$ (L/g) is Tempkin isotherm constant, $R$ (8.314 J/mol.K) is the ideal gas constant, and $T$ (K) is the absolute temperature.

Table 1 presents a summary of isotherm parameters, obtained from the respective linear plots, as per Eqs. (5), (6), and (7). Results showed that Langmuir model gave the highest values of linear regression coefficient, ($R^2$>0.999) than Freundlich and Tempkin models. Further, the monolayer capacity, $Q_m$ increased and $k_L$ decreased with increase in temperature. Moreover, the higher values of $R^2$ suggest that adsorption of $Mn^{2+}$ ions onto BMnO composite is best described by Langmuir model, and occurs by monolayer process.

TABLE I
ISOTHERM PARAMETERS

| Isotherm | Parameter | 298K | 308K | 318K |
|---|---|---|---|---|
| Langmuir | $Q_m$ | 60.98 | 53.76 | 49.02 |
| | $k_L$ | 0.781 | 0.565 | 0.358 |
| | $R^2$ | 0.998 | 0.997 | 0.995 |
| Freundlich | $k_F$ | 31.65 | 27.79 | 23.81 |
| | $n$ | 5.552 | 6.086 | 5.949 |
| | $R_2$ | 0.961 | 0.985 | 0.975 |
| Tempkin | $b_T$ | 0.363 | 0.450 | 0.482 |
| | $A_T$ | 0.144 | 0.169 | 0.079 |
| | $R^2$ | 0.992 | 0.997 | 0.990 |

### *3.5. Effect of contact time and dynamic modelling*

The effect of contact time on $Mn^{2+}$ ions uptake by BMnO composite is shown in Fig. 3. The uptake was rapid initially, and decreased gradually with time. Notably, higher uptakes were observed with high initial concentration, and the equilibrium time for 50, 100 and 150 mg/L were 30, 40 and 80 min, respectively. The rapid $Mn^{2+}$ ions uptake at the commencement of adsorption was attributed to plenty of vacant sites, and as the system approached equilibrium, the vacant sites diminished due to saturation [17].

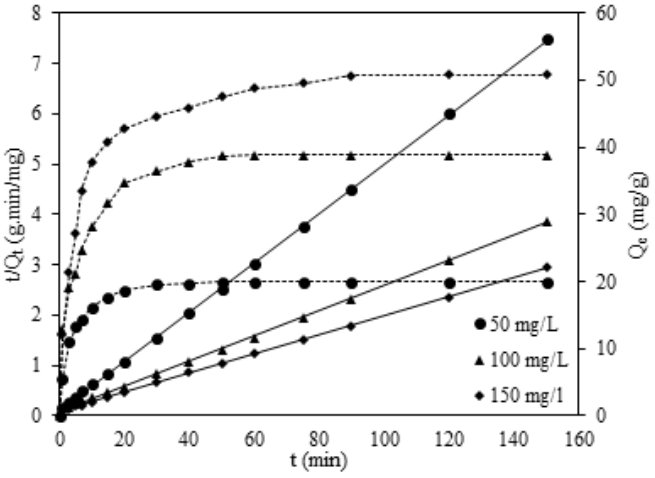


Fig. 3. Effect of contact time and linear kinetic models fits

The experimental data was analyzed using two most

commonly used dynamic models; the pseudo-first order and pseudo-second order models, expressed empirically, by Eqs. (8) and (9), respectively, as:

$$\log\left(Q_e - Q_t\right) = \log Q_e - \frac{k_1}{2.303}t \quad (8)$$

$$\frac{t}{Q_t} = \frac{1}{k_2 Q_e^2} + \frac{t}{Q_e} \quad (9)$$

where $Q_t$ (mg/g), $k_1$ ($min^{-1}$) and $k_2$ (g $mg^{-1}min^{-1}$) are the time depended $Mn^{2+}$ ions uptake, pseudo-first order and pseudo-second order rate constants, respectively. Figure 3 shows a combined plots of kinetic profiles and the linear pseudo-second order kinetic, while Table 2 illustrates all the kinetic parameters of the two models at different $Mn^{2+}$ ions concentration. From Table 2, it was observed that the values of $R^2$ for pseudo second-order model are close to unity than those of pseudo-first order model. Moreover, the theoretic capacity values for pseudo-second order model are in good agreement with those obtained experimentally. The values of $k_2$ decreased with increase in $Mn^{2+}$ ions concentration. These results suggest that pseudo-second order model is more applicable and the adsorption of $Mn^{2+}$ ions onto BMnO composite is inclined towards chemisorption [18].

TABLE 2
KINETIC PARAMETERS

| Model | Parameter | Concentration (mg/L) | | |
|---|---|---|---|---|
| | | 50 | 100 | 150 |
| Pseudo-first order | $Q_e$ | 10.98 | 30.47 | 35.31 |
| | $k_1$ | 0.093 | 0.0.103 | 0.056 |
| | $R^2$ | 0.986 | 0.983 | 0.957 |
| Pseudo-second order | $Q_e$ | 20.40 | 40.00 | 52.63 |
| | $k_2$ | 0.023 | 0.008 | 0.004 |
| | $R^2$ | 0.999 | 0.998 | 0.999 |

Experiments with real mine water samples showed that CBMnO was selective towards $Mn^{2+}$ ions, and complete removal could be achieved with 0.5 g of the adsorbent. However, co-ions were partially removed. This implied that an extra treatment unit, for instance, reverse was required to achieve complete removal.

## 4. CONCLUSIONS

In this study, BMnO composite was prepared, characterized and examined for $Mn^{2+}$ ions adsorption from aqueous solution. SEM characterization showed morphological changes after by MnO particles were precipitated onto bentonite surface. The results obtained from kinetic experiments showed that $Mn^{2+}$ uptake was fast and kinetics followed the pseudo-second order model. The equilibrium capacity depended on process conditions such as mass of adsorbent and initial concentration. The Langmuir isotherm model described the equilibrium data well, and $Mn^{2+}$ ions removal is an endothermic process. The findings of this study suggest that BMnO is an efficient adsorbent of $Mn^{2+}$ ions, and can be applied in the polishing of pre-treated mine water.

## ACKNOWLEDGEMENT

This project was financially supported by the Rand Water, South Africa, through the Rand Water Chair in Water Utilization.

## REFERENCES

[1] M. Anbia, S. Amirmahmoodi, "Removal of Hg (II) and Mn (II) from aqueous solution using nanoporous carbon impregnated with surfactants," *Arab. J. Chem.*, vol. 9, pp. 319-325, 2016.
[2] G.F. Pearson, G.M. Greenway, "Recent developments in manganese speciation," *Trends Analyt. Chem.*, vol. 24, pp. 803-809, 2005
[3] S.C. Homoncik, A.M. MacDonald, K.V. Heal, B.É.Ó. Dochartaigh, B.T. Ngwenya, "Manganese concentrations in Scottish groundwater," *Scie. Total Environ.*, vol. 408, pp. 2467-2473, 2010.
[4] P. Patnaik, *Handbook of Inorganic Chemicals*, McGraw-Hill, New York, 2002.
[5] R.M. Freitas, T.A.G. Perilli, A.C.Q. Ladeira, "Oxidative Precipitation of Manganese from Acid Mine Drainage by Potassium Permanganate," *J. Chem.*, 2013. Available: http://dx.doi.org/10.1155/2013/287257
[6] M.A. Barakat, "New trends in removing heavy metals from industrial wastewater," *Arab. J. Chm.*, pp. 361-377, 2011.
[7] A.F.S. Gomes, L.L. Lopez, A.C.Q. Ladeira, "Characterization and assessment of chemical modifications of metal-bearing sludges arising from unsuitable disposal," *J. Hazard. Mater.*, vol. 199-200, pp. 418-425, 2012.
[8] B. Kebabi, S. Terchi, H. Bougherara, L. Reinert, L. Duclaux, "Removal of manganese (II) by edge site adsorption on raw and milled vermiculites," *Appl. Clay Sci.*, vol. 139, pp. 92-98, 2017.
[9] S.D. Gisi, G. Lofrano, M. Grassi, M. Notarnicola, "Characteristics and adsorption capacities of low-cost sorbents for wastewater treatment: A review," *Sustainable Mater. Technol.*, vol. 9, pp. 10-40, 2016.
[10] I. Ali, M. Asim, T.A. Khan, "Low cost adsorbents for the removal of organic pollutants from wastewater," *J. Environ. Manage.*, vol. 113, pp. 170-183, 2012.
[11] D.S. Patil, S.M. Chavan, K.J.U. Oubagaranadin, "A review of technologies for manganese removal from wastewaters," *J. Environ. Chem. Eng.*, vol. 4, pp. 468-487, 2016.
[12] M.A. Barakat, "New trends in removing heavy metals from industrial wastewater," *Arab. J. Chem.*, vol. 4, pp. 361-377, 2011.
[13] M.K. Uddin, "A review on the adsorption of heavy metals by clay minerals, with special focus on the past decade," *Chem. Eng. J.*, vol. 308, pp. 438-462, 2017.
[14] R. Taman, M.E. Ossman, M.S. Mansour, H.A. Farag, "Metal Oxide Nano-particles as an Adsorbent for Removal of Heavy Metals," *J. Adv. Chem. Eng.*, vol. 5, 2015.
[15] O.E.A. Salam, N.A. Reiad, M.M. ElShafei, "A study of the removal characteristics of heavy metals from wastewater by low-cost adsorbents," *J. Adv. Res.*, vol. 2, pp. 297-303, 2011.
[16] K.Y. Foo, B.H. Hameed, "Insights into the modeling of adsorption isotherm systems," *Chem. Eng. J.*, vol. 156, pp. 2-10, 2016.
[17] D.C. Sicupira, T.T. Silva, V.A. Leão, M.B. Mansur, "Batch Removal Of Manganese from Acid Mine Drainage Using Bone Char," *Brazilian J. Chem. Eng.*, vol. 31, pp. 195-204, 2014.
[18] C.W. Cheung, J.F. Porter, G. McKay, "Sorption kinetics for the removal of copper and zinc from effluents using bone char," *Sep. Purif. Technol.*, vol. 19, pp. 55-64, 2000.

# Microalgae Cultivation Systems for Biodiesel Production

Bonface G. Mukabane[1*], Benson B. Gathitu[2], Urbanus Mutwiwa[2], Paul Njogu[1] and Stephen Ondimu[2]

***Abstract*** - Microalgae represent a sustainable biofuel source because of their high biomass productivity and ability to sequester carbon dioxide from the air and remove water born pollutants. This paper reviews metabolic pathways, the current status of microalgae cultivation systems, including the advantages and disadvantages of both open and closed systems. The key barriers to commercial cultivation of microalgae and the way forward is also discussed.

**Key words**: Biofuel, Current Status, Growth systems, Microalgae

## I. INTRODUCTION

Increased interest in biofuels is mainly driven by; the fluctuating oil prices and recognition of the fact that the global fossil fuel reserves are getting exhausted, concerns about environmental pollution and resultant environmental change due to fossil fuel emissions and the provision of alternative outlets for agricultural producers.

Global biofuel production has been increasing rapidly over the last decade, but the expanding biofuel industry has recently raised pertinent concerns. In particular, the sustainability of many first-generation biofuels; fuels made from food and feed crops and mainly vegetable oil, has been increasingly questioned over concerns such as reported displacement of food crops, effects on the environment and climate change [1]. In general, there is growing consensus that if significant emissions reductions in the transport sector are to be achieved, biofuel technologies must become more efficient in terms of net lifecycle greenhouse gas emission reduction while at the same time be environmentally and socially sustainable. It is increasingly understood that most first-generation biofuels, except sugarcane ethanol, will likely have a limited role in the future transport fuel mix [2].

Biodiesel is a mixture of fatty acid alkyl monoesters (FAMEs) derived from vegetable fats and oils. It can be used as a replacement of petro-diesel because of their structural similarity. Biodiesel is produced using vegetable oil, plant oil, and animal fat. Biodiesel is an alternative fuel for diesel and most diesel engines can use 100% biodiesel [1]. The main feedstock currently used for biodiesel production includes palm oil, sunflower, rapeseed, soybean, and canola seed. A great challenge of using vegetable oils for biodiesel production is the availability of crop land for oil production to produce enough biodiesel that significantly replaces the current fossil fuel consumption [3]. Reference [3] shows that it would take approximately 24% of the existing crop land in the US to grow oil palm that is considered as a high yield oil crop or over three times of the current cropland in the US to grow soybean to produce enough biodiesel that would replace 50% of the transportation fuel in the US. Several studies have been conducted on using alternative oils such as waste oils from restaurants and kitchens and microalgal oils for biodiesel production [1]. Reference [4] shows investigation done with restaurant waste oil as a precursor for sophorolipid and biodiesel production. Reference [5] shows evaluation of the Biodiesel production from waste cooking oil including economic analysis. Reference [6] shows studies on biodiesel production from heterotrophic microalgal oil. A great advantage of using microalgal oil over vegetable oils for biodiesel production is that the production of algal oil does not need cropland and has much higher oil yield per acre of land because the microalgae can be grown in 3 dimensions in photobioreactors [1]. However, a big challenge of biodiesel production using algal oil is that the cost of algal oil production is extremely high [1]. The goal of the present paper is to review recent development in microalgae production systems and identify technological bottlenecks and strategies for further development.

## II. MICROALGE AS A FEEDSTOCK FOR BIODIESEL PRODUCTION

Microalgae are a diverse group of aquatic photosynthetic microorganisms that grow very fast and have the ability to yield large quantities of lipids adequate for biodiesel production [7]-[8]. Algae as a potential source of fuel was initially investigated during the gas scare of the late 1970s [8]. The National Renewable Energy Laboratory (NREL) started its algae feedstock studies in the late 1970s, but their research program was halted in 1996. Recent renewed interest has led the NREL to restart their research in algae [9]. The potential for microalgae to provide biomass for biodiesel production is now widely accepted [10]. Further, microalgae are recognized among the most efficient for this purpose, and some studies, for instance, as in [3], it was asserted that microalgae is the “only source of biodiesel that has the potential to completely displace fossil diesel” (Table I). The superiority of microalgae as a feedstock for biodiesel

**[1]The Institute for Energy and Environmental Technology, Jomo Kenyatta University of Agriculture and Technology (JKUAT), P.O. BOX 62 000-00200. Nairobi-Kenya.**

**[2]Department of Agriculture and Biosystems Engineering JKUAT,**

***Corresponding author: Phone: +254 721 565 335; E-mail: bmukabane@yahoo.com, bmukabane@gmail.com**

production compared with the other conventional oil crops such as soybeans are, as in [11]: (1) microalgae have simple structures, but high photosynthetic efficiency with a growth doubling time as short as 24 h. Moreover, microalgae can be grown all year round. (2) The species abundance and biodiversity of microalgae over a broad spectrum of climates and geographic regions make seasonal and geographical restrictions much less of a concern compared with other lipid feedstocks. Microalgae may be cultivated on fresh water, saltwater lakes with eutrophication, oceans, marginal lands, deserts, etc., hence reducing or eliminating the competition for arable land with conventional agriculture as in [12] and opening economic opportunities in arid or salinity affected regions of the world [13]. (3)Microalgae can effectively remove nutrients such as phosphorus and nitrogen, and heavy metals from wastewaters. (4)Microalgae sequester a large amount of carbon dioxide from the atmosphere via photosynthesis, for example, the $CO_2$ fixation efficiency of *Chlorella vulgaris* was up to 260 $mg.L^{-1}.h^{-1}$ in a membrane photobioreactor [14]. Utilization of $CO_2$ from thermal power plants by large-scale microalgae production facilities can reduce a great deal of the greenhouse gas emissions blamed for global warming [14]. (5)The production and use of microalgae biodiesel contribute near zero net $CO_2$ and sulfur to the atmosphere. (6)Microalgae can produce a number of valuable products, such as proteins, polysaccharides, pigments, animal feeds, fertilizers, and etc. In summary, microalgae are a largely untapped biomass resource for renewable energy production [11].

However, commercialization of microalgae biomass and biofuel production is still facing significant obstacles due to high production costs and poor efficiency. In face of these challenges, researchers are undertaking profound efforts to improve microalgae biomass production and lipid accumulation and lower downstream processing costs [11].

**Table I**
**Comparison of some sources of biodiesel [3].**

| Crop | Oil yield ($L.ha^{-1}$) |
|---|---|
| **Corn** | 172 |
| **Soybean** | 446 |
| **Canola** | 1,190 |
| **Jatropha** | 1,892 |
| **Coconut** | 2,689 |
| **Oil palm** | 5,950 |
| **Microalgae (70% oil in biomass)** | 136,900 |
| **Microalgae (30% oil in biomass)** | 58,700 |

## III. METABOLIC PATHWAYS

Microalgae may use one or more of the three main metabolic pathways depending on carbon conditions and light: photoautotrophy, heterotrophy, and mixotrophy [15]. Most microalgae are capable of photoautotrophic growth. Photoautotrophic cultivation in open ponds is a simple and low-cost method for large-scale production; however the biomass density is low because of contamination by other species or bacteria, limited light transmission and low organic carbon concentration [16]. Some microalgae can make use of organic carbons and oxygen to undergo rapid propagation through heterotrophic pathway. Heterotrophic cultivation has drawn increasing attention and it is regarded as the most practical and promising way to increase the productivity [36]-[38]. Currently, research on heterotrophic cultivation of microalgae is mainly focused on *Chlorella* [11]. Cell densities as high 104.9 $g.L^{-1}$(dry cell weight, *Chlorella pyrenoidosa*) have been reported [20]. Microalgae can adapt to different organic matters such as sucrose, xylan, glycerol and organic acids in slurry after acclimatization [21]. The ability of heterotrophic microalgae to utilize a wide variety of organic carbons provides an opportunity to reduce the overall cost of microalgae biodiesel production since these organic substrates can be found in the waste streams such as municipal and animal wastewaters, effluents from anaerobic digestion, food processing wastes, etc. [11]. On the basis of heterotrophic cultivation, researchers have carried out studies of mixotrophic cultivation which can greatly enhance the growth rate because it realizes the combined effects of photosynthesis and heterotrophy [11]. After examining the biomass and lipid productivities characteristics of fourteen microalgae, as in [22], it was found that lipid and biomass productivities were boosted by mixotrophic cultivation. Reference [23] shows the studied effects of molasses concentration and light levels on mixotrophic growth of *Spirulina platensis*, and it was found that biomass production was stimulated by molasses, which suggested that this industrial by-product could be used as a low-cost supplement for the growth of this species. Reference [24] shows that the mixotrophic growth of *Chlamydomonas globosa*, *Chlorella minutissima* and *Scenedesmus bijuga* resulted in 3-10 times more biomass production compared with that obtained under phototrophic growth conditions. The maximum lipid productivities of *Phaeodactylum tricornutum* in mixotrophic cultures with glucose, acetate and starch in medium were 0.053, 0.023 and 0.020 $g.L^{-1}.day^{-1}$, which were respectively, 4.6-, 2.0-, and 1.7-fold of those obtained in the corresponding photoautotrophic control cultures [25].

## IV. MICROALGAE CULTIVATION SYSTEMS

Annual oil production from high-oil microalgae can be in the range of 58 700 to 136 900 litres per hectare [3]. If this microalgal oil is used for biodiesel production, it would take approximately 1.0 – 2.5% of the current cropland in the US to meet 50% of the US transportation fuel needs, which is much more feasible than the current oil crops [1]. Commercially growing microalgae for value-added products is usually conducted in open ponds (raceways) or closed photobioreactors (PBRs) under autotrophic (making complex organic nutritive compounds from simple inorganic sources by photosynthesis) or heterotrophic (cannot synthesize its own food) conditions at relatively warm temperature (20 – 30 $^0$C) [1]. In autotrophic microalgal cultivation, the microalgae need sunlight (energy source), $CO_2$ (carbon source) and nutrients (P, N and minerals) for their photosynthesis and generate oxygen. The main difference of growing heterotrophic microalgae from autotrophic ones is the carbon

source. The former requires organic carbon source such as glucose to support its growth. Normally autotrophic microalgae are grown for biodiesel production, mainly because they use $CO_2$ as their carbon source for growth [1]. Therefore, the whole cycle of growing microalgae for biodiesel production and combustion of biodiesel as fuel would generate zero net carbon dioxide emission to the atmosphere. However, sometimes heterotrophically grown microalgae can make much more oil than autotrophic ones. Reference [6] shows that heterotrophic growth of *Chlorella protothecoides* resulted in a significant increase of oil content of microalgae from 14.5% under the original autotrophic growth to 55.2% (dry weight).

In a photobioreactor microalgal growth system, pure high-oil microalgae are grown in closed glass or plastic tubular bioreactors. Nutrient water is circulated in the bioreactors for keeping the microalgae from settling and for the growth of the microalgae. Natural sunlight is usually the energy source for microalgal growth [1]. Although artificial illumination to the photobioreactors is viable, it is much more expensive than natural illumination. Pure microalgal culture can be maintained in the photobioreactors. Heat exchanger is usually necessary to maintain an adequate temperature in the photobioreactors. A high concentration of microalgal biomass can be achieved in photobioreactors. In that case high dissolved oxygen may inhibit the microalgal growth, so degassing system is usually necessary to release oxygen from the water [1].

Open (raceway) ponds are similar to oxidation ditches used in wastewater treatment systems. They are large, open basins of shallow depth and a length of at least several times greater than that of the width [26]. Raceway ponds are typically constructed using concrete shell lined with polyvinyl chloride. Dimensions range from 10 to 100 m in length and 1 to 10 m in width with a depth microalgal growth of 10 to 50 cm [26]. Ponds are kept shallow as optical absorption and self-shading by the algal cells limits light penetration through the algal broth [27]. Wastewaters from animal operations and municipalities can be used for growing microalgae. Water recirculation or agitation is necessary to keep the microalgae from settling. Microalgal biomass concentration in the ponds is usually low compared to the photobioreactors. Wild algae and/or bacterial contamination is normally challenging in the open ponds (Table II) [1], [26]. Oswald considered the open pond to be the most viable method of combining algal cultivation and wastewater treatment in the 1950s [28] Photobioreactors (PBRs) are more commonly used for growing algae for high value commodities or for experimental work at a small scale. Recently, however, they have been considered for producing algal biomass on a large scale as they are capable of providing optimal conditions for the growth of the algae [29], [30]. A closed reactor allows species to be protected from bacterial contamination, shallow tubing allows efficient light utilization, bubbling $CO_2$ provides high efficiency carbon uptake and water loss is minimized.

**Table II**

**A comparison of growing microalgae in open ponds and photobioreactors [1],[ 26]**

| | Raceway Pond | Photobioreactor |
|---|---|---|
| **Estimated productivity ($g.m^{-2}.day^{-1}$)** | 11 | 27 |
| **Advantages** | Low energy | Pure algal culture |
| | Simple technology | High volumetric productivity |
| | Inexpensive | High controllability |
| | Well researched | Small area required |
| | | Concentrated biomass |
| **Disadvantages** | Low productivity | High energy |
| | Contamination | Expensive |
| | Large area required | Less researched |
| | High water use | |
| | Dilute biomass | |

PBRs provide very high productivity rates compared with raceway ponds. In their life-cycle assessment (LCA) study, as in [29], volumetric productivity was estimated to be at least eight times higher in flat-plate and tubular PBRs. The reason why PBRs have not become popular is due to the energy and cost intensity of production and operation. PBRs require a far higher surface area for the volume of algal broth compared with alternative infrastructure. Much higher volumes of material are therefore required which in turn requires a higher capital energy input and increases environmental impacts [30]. During operation, algal biomass must be kept in motion to provide adequate mixing and light utilization. These increase productivity but also require additional energy for pumping. So far in comparison to raceway ponds the benefits of PBRs do not outweigh the necessary energy requirements identified in the LCA study published as in [29]. A net energy ratio (*i.e.*, energy produced/energy consumed) of 8.34 has been reported for raceway ponds as compared to a net energy ratio of 4.51 and 0.20 for flat-plate and tubular photobioreactors, respectively [29]. It is likely that ponds will continue to provide the most effective infrastructure for algal cultivation due to their low impact design and low energy input requirement. PBRs will continue to be important however, for laboratory work, developing cultures and producing biomass with high economic value. As research continues it may also be possible to develop infrastructure that will provide the benefits of both PBRs and open ponds together. PBRs are of different configurations including flat plate, column and tubular [31]. In both open and closed microalgae culture systems, light source and light intensity are vital for the performance of phototrophic growth of microalgae. The development of optical trapping system, light delivery and lighting technologies, which improve the distribution and absorption and the advent of some new photobioreactors, will improve the efficiency of photosynthesis [32]. In addition, gas-liquid mass transfer

efficiency is another critical factor affecting $CO_2$ utilization and thus the phototrophic growth [31]. Reference [33] shows a 10 L photobioreactor integrated with a hollow fiber membrane module which increased the gas bubbles retention time from 2 s to more than 20 s, increasing the $CO_2$ fixation rate of *Chlorella vulgaris* from 80 to 260 $mg.L^{-1}.h^{-1}$.

## V. CHALLENGES FOR COMMERCIALIZATION

In principle, producing biodiesel from microalgae has been proven economically viable. The land area required to produce the same amount of oil from microalgae is only a small portion of that for oil crops. Biodiesel production from microalgal biomass or the advanced biodiesel technology has a potential for biofuel production to substitute fossil fuel without serious competition for arable land against food and feed production [1]. However, the prime challenge of the advanced biodiesel production is its high cost. The present microalgae production and the separation of the microalgal biomass from the growing media are too costly. An estimated cost to produce a kilogram of microalgal biomass with a mean oil content of 30% is $2.95 and $3.80 for photobioreactors and open ponds, respectively, assuming that carbon dioxide is available and free [3]. Taking account of 30% oil content in the microalgal biomass and the cost of oil extraction from the microalgae, the cost to produce a kilogram (approximately 1.14 liters) of crude microalgal oil is more than three times of that of producing a kilogram microalgal biomass [1]. This cost is much higher than vegetable oil production, e.g. the market price for crude palm oil which is possibly the cheapest vegetable oil was only $0.52/liter in the US in 2006. It would be more disheartening if compared with petrodiesel production cost (the retail price of petrodiesel including taxes in the US in 2006 was only between $0.66 and $0.97 per liter) [1]. As of late 2008, as in [34], it was indicated that seven US government laboratories, thirty US universities, and around sixty biofuels companies were conducting study in this area. Passionate efforts are also taking place in other parts of the world including (among many others) Australia, Europe, the Middle East, and New Zealand [35].

## VI. FUTURE PERSPECTIVES OF MICROALGAL BIODIESEL PRODUCTION

To improve the economics of microalgal biodiesel production, more research and development are compulsory to reduce the costs of growing microalgae and the separation of microalgal biomass from the growth media, and to competently control culture contamination when grown in open ponds. The research and development efforts probably need to focus on the following areas:

1) Selection and development of high-yield, oil-rich microalgae: Oil-rich microalgal species can be enhanced through cultivation and genetic engineering to increase the oil content in their biomass without compromising the biomass production rate [3].
2) Enhancement of the tolerance oil-rich microalgae to high and/or low temperatures: Most microalgae prefer to grow at the temperatures of 20-30 $^0$C. When the temperature is higher than 30 $^0$C, which happens very frequently during the sunny days in photobioreactors, heat exchangers have to be operated to cool down the microalgal culture to sustain a high microalgae growth. Installation and operation of the heat exchangers significantly add cost to the whole microalgal biomass production. Selection and modification of microalgae to aid them grow fast at high temperatures would probably eradicate the heat exchangers and contribute to the cost reduction of microalgal biomass production [3].
3) Enhancement of the tolerance of oil-rich microalgae to the high concentration of oxygen: When microalgae grow under autotrophic conditions, they produce oxygen that dissolves in water to yield a super saturated dissolved oxygen concentration in the media, sometimes 4-5 times of the air saturation value. A combination of high dissolved oxygen with intense sunlight impedes the growth of the microalgae and destroys the microalgal cells. To prevent the inhibition and damage to the microalgae, a degassing system is necessary to keep the dissolved oxygen at a suitable level in the growth media. Increasing the tolerance of the microalgae to the high dissolved oxygen concentration in the media could also decrease the cost of microalgal biomass production [3].
4) Improvement of the competitiveness of oil-rich microalgae against wild algae and bacteria: In open pond microalgae production, the contamination of wild algae and bacteria is very challenging. If the growth media is contaminated by wild algae and/or bacteria, the wild algae and bacteria will devour the nutrients in the media and significantly diminish the yield of the desired microalgae. Improving the competitiveness of the oil-rich microalgae against the wild algae and bacteria and deterring the wild algal and bacterial activities in the media for growing the microalgae also has a potential to reduce the cost of microalgal biomass production [3].
5) Improvement of the engineering of the microalgae growth systems: Both microalgae growing systems presently used for microalgal biomass production, photobioreactors and open ponds have rooms for improvement. When microalgae grow in tubular photobioreactors, some of them stick on the wall of the tubes, significantly decreasing the penetration of light to the growth media and resulting in a lower yield of the microalgal biomass. Cost-effective materials which inhibit the microalgae from attaching the surface should be explored to maintain a high growth rate of the microalgae. The main drawback of growing microalgae in open ponds is contamination. Greenhouse ponds can be an effective system to avert contamination and to increase the microalgal density in the growth media [3].
6) Development of cost-effective microalgae harvesting systems: Harvesting microalgal biomass contributes markedly to the total costs of the biomass production. Current technologies ordinarily involve coagulation,

filtration and centrifugation, which are costly. Innovative cost-effective harvesting systems need to be explored to significantly reduce the cost of microalgal biomass harvesting [3].

7) Application of the biorefinery model to microalgal biodiesel production system: Microalgal biomass contains lipids (oil), carbohydrates, proteins and other minor components such as minerals and vitamins. Oil is used for biodiesel production. Other constituents can be processed into value-added products. After oil extraction, the residues which are rich in carbohydrates, proteins and minor nutrients can be used to produce animal feed. They can also be utilized for biogas production through anaerobic digestion. Special high-value organic chemicals could be extracted from the residues and should be explored to increase the revenue of the microalgae-to-biodiesel process. All these byproducts have capabilities to improve the economics of the microalgae-to-biodiesel process [3].
8) Combine microalgae cultivation with wastewater treatment. The microalgae could therefore provide a means of improving the water quality of raw or partially treated effluent as well as providing livestock feed and/or biomass for energy generation.

## VII. CONCLUSION

Microalgae are a sustainable energy resource with great potential for $CO_2$ fixation and wastewater purification. For biodiesel production to have a significant impact on renewable fuels, technologies must be developed to enable large scale algae biomass production. Further efforts on microalgae biodiesel production should focus on reducing costs in large-scale algal biomass production systems. Combining microalgae mixotrophic cultivation with sequestration of $CO_2$ from flue gas and wastewater treatment approach to algal biomass conversion will improve the environmental and economic viability.

## ACKNOWLEDGEMENT

The authors are grateful for financial support of the National Council of Science, Technology and Innovation (NACOSTI) of Kenya.

## REFERENCES

[1] J.J. Cheng, **"**Advanced biofuel technologies: Status and Barriers." Development Research Group. The World Bank, September, 2010.
[2] International Energy Agency (IEA) Bioenergy, "From 1st-to 2nd-generation biofuel technologies: An Overview of current Industry and R and D Activities." 2008.
[3] Y. Chisti, **"**Biodiesel from microalgae." *Biotechnology Advances*, vol. 25, pp. 294-306, 2007
**[4]** V. Shar, M. Jurjevic and D. Badia, "Utilization of restaurant waste oil as a precursor for sophorolipid production." *Biotechnology Progress*. vol. 23, no. 2, pp. 512 - 515, 2007.
[5] Y. Zhang, M.A. Dube, D.D. McLean and M. Kates, "Biodiesel production from waste cooking oil: 2. Economic assessment and sensitivity analysis." *Bioresource Technology*, vol. 90, pp. 229 – 240, 2003.
[6] X. Miao and Q. Wu, "Biodiesel production from heterotrophic microalgal oil." *Bioresource Technology*, vol. 97, pp. 841 – 846, 2006.
[7] World Watch Institute (WWI), Biofuels for Transport: "Global Potential and Implications for Sustainable Energy and Agriculture." Eds S. 2007. Hunt. Sterling VA.
[8] Y. Li, M. Horsman, N. Wu, C.Q. Lan and N. Dubois-Calero, "Biofuels from microalgae." *Biotechnology Progress*, vol 24, pp. 815- 820, 2008.
[9] J. Donovan, N Stowe, "Is the future of biofuels in algae?" Renewable EnergyWorld.com/rea/news/article/2009/06/is the-future-of-biofuels-in-algae.
[10] A.C. Miguel, D. Xiaodong and R.T. Govinda, **"**Second – generation biofuels: Economics and Policies. Development Research Group. The World Bank, August 2010.
[11] X. Wu, R. Ruan, Z. Du and Y. Liu, **"**Current status and prospects of biodiesel production from microalgae." *Energies*, vol. 5, pp. 2667 - 2682, 2012.
[12] S.A. Khan, M. Rashmi, Z. Hussain, S. Prasad and U.C. Banergee**,** "Prospects of biodiesel production from microalgae in India." *Renewable and Sustainable Energy Review*. 2009
[13] P.M. Schenk, S.R. Thomas-Hall, E. Stephens, U.C. Marx, J.M Mussgnug, C. Posten, O. Kruse and B. Hankamer, "Second generation biofuels: High-efficiency microalgae for biodiesel production." *Bioenergy Research*, vol. 1, pp. 20 - 43, 2008.
[14] L.H. Cheng, L. Zhang, H.L. Chen and C.J. Gao, "Carbon dioxide removal from air by microalgae cultured in a membrane-photobioreactor." *Sep. Purif. Technol*., vol. 50, pp. 324 - 329, 2006.
[15] K. Chojnacka and A. Noworyta, "Evaluation of *Spirulina sp*. growth in photoautotrophic, heterotrophic and mixotrophic cultures." *Enzyme Microb. Technol*., vol. 34, pp. 461-465, 2004.
[16] H.C. Greenwell, L.M.L. Laurens, R.J. Shields, R.W. Lovitt and K.J. Flynn, "Placing microalgae on the biofuels priority list: A review of the technological challenges." *J. R. Soc. Interface*, vol. 7, pp. 703-726, 2010.
[17] F. Chen**,** "High cell density culture of microalgae in heterotrophic growth." *Trends Biotechnol*., vol. 14, pp. 421- 426, 1996.
[18] X.F**.** Li, H. Xu and Q.Y. Wu, "Large-scale biodiesel production from microalga *Chlorella protothecoides* through heterotrophic cultivation in bioreactors. *Biotechnol. Bioeng., vol. 98*, pp. 764-771, 2007.
[19] J. Doucha and K. Lívansky, "Production of high-density *Chlorella* culture grown in fermenters." *J. Appl. Phycol*., vol. 24, pp. 35 - 43, 2012.
[20] Z.Y. Wu and X.M. Shi, **"**Optimization for high-density cultivation of heterotrophic *Chlorella* based on a hybrid neural network model." *Lett. Appl. Microbiol*., vol. 44, pp. 13-18, 2006.
[21] T. Heredia-Arroyo, W. Wei, R. Ruan and B. Hu, "Mixotrophic cultivation of *Chlorella vulgaris* and its potential application for the oil accumulation from non-sugar materials." *Biomass Bioenergy*, vol. 35, pp. 2245 – 2253, 2011.
[22] K.C. Park *et al*., "Mixotrophic and photoautotrophic cultivation of 14 microalgae isolates from Saskatchewan, Canada: Potential applications for wastewater remediation for biofuel production." *J. Appl. Phycol*., vol. 24, pp. 339-348, 2012.
[23] M.R. Andrade and J.A.V. Costa, **"**Mixotrophic cultivation of microalga *Spirulina platensis* using molasses as organic substrate." *Aquaculture*, vol. 264, pp. 130-134, 2007.
[24] **A.** Bhatnagar, S. Chinnasamy, M. Singh and K.C. Das, "Renewable biomass production by mixotrophic algae in the presence of various carbon sources and wastewaters." *Appl. Energy*, vol. 88, pp. 3425-3431, 2011.
[25] H.Y**.** Wang, R. Fu and G.F. Pei, "A study on lipid production of the mixotrophic microalgae *Phaeodactylum tricornutum* on various carbon sources." *Afr. J. Microbiol. Res.*, vol. 6, pp. 1041- 1047, 2012.
[26] O**.** Jorquera, A. Kiperstok, E.A. Sales, M. Embirucu and M.L. Ghirardi, "Comparative energy lifecycle analyses of micoalgal biomass production in open ponds and photobioreactors." *Bioresour. Technol.*, vol. 101, pp. 1406-1413, 2010.
[27] R. Slade and A. Bauen, "Micro-algae cultivation for biofuels: Cost, energy balance, environmental impacts and future prospects." *Biomass Bioenergy*, vol. 53, pp. 29-38, 2013.
[28] W.J. Oswald, H.B. Gotaas, H.F. Ludwig and V. Lynch, "Algae symbiosis in oxidation ponds. 3. Photosynthetic oxygenation." *Sewage Ind. Wastes*, vol. *25*, pp. 692–705, 1953.
[29] O. Jorquera, A. Kiperstok, E.A. Sales, M. Embirucu and M.L Ghirardi, "Comparative energy lifecycle analyses of microalgal biomass production in open ponds and photobioreactors." *Bioresour. Technol.*, vol. 101, pp. 1406–1413, 2010.
[30] K. Soratana and A.E Landis, "Evaluating industrial symbiosis and algae cultivation from a life cycle perspective." *Bioresour. Technol*., vol. 102, pp. 6892–6901, 2011.

[31] X. Wu, R. Ruan, Z. Du and Y. Liu**,** "Current status and prospects of biodiesel production from microalgae." *Energies*, vol. 5, pp. 2667- 2682, 2012.

[32] J. Masojidek *et al*., "A closed solar photobioreactor for cultivation of microalgae under supra-high irradiance: Basic design and performance." *J. Appl. Phycol*., vol. 15, pp. 239-248, 2003.

[33] L.H. Cheng, L. Zhang, H.L. Chen and C.J. Gao, "Carbon dioxide removal from air by microalgae cultured in a membrane-photobioreactor." *Sep. Purif. Technol*., vol. 50, pp. 324-329, 2006.

[34] A. Darzins, **"**Recent and Current Research & Roadmapping Activities: Overview." National Algal Biofuels Technology Roadmap Workshop, University of Maryland, December 2008.

[35] P.T. Pienkos and A. Darzins**, "**The Promise and Challenges of Microalgal Derived Biofuels." *Biofuels, Bioproducts and Biorefining*, vol. 3, pp. 431-440, 2009.

# Modified Pine Cone for Dye Pollutants Removal from Aqueous solution

Confidence B. Zulu[1*] Maurice S. Onyango[1] Jianwei Ren[2] and Taile Y. Lwesifi[3]

*Abstract*—Water pollution associated with discharge of dye effluents into the natural water resources is a major issue because of the adverse effects on human health and the ecosystem. During the past decade, the use of agricultural by-products as potential adsorbents in environmental remediation has received much attention due to their availability and exceptional properties. In this study, the ability of polyaniline (PANI) coated pine cone as a low-cost adsorbent on the removal of direct orange 26 (DO 26) dye from wastewater was investigated. The physicochemical properties of the adsorbent were studied using various characterization techniques such as Fourier transform infrared (FTIR), Scanning electron microscopy (SEM), X-ray diffraction (XRD) and Brunauer Emmett teller (BET). Batch equilibrium and kinetics adsorption experiments were performed to determine the efficiency of the adsorbents on dye removal and to establish the effect of various operational parameters on the adsorption process. Results showed that the removal of DO 26 dye occurs through the surface of the adsorbent this was confirmed by characterization. It was observed that percentage dye removal decrease with increasing solution pH. The results also indicate that adsorption efficiency increased with increase in temperature which predicts that the adsorption process is endothermic. Maximum percentage dye removal was found to be 99.98% at pH 4.17, adsorbent dosage 0.1g and initial dye concentration 50 mg/L. Kinetic studies revealed that equilibrium was reached within 90, 180 and 240 min of interaction for initial dye concentrations of 50 mg/L, 100 mg/L and 150 mg/L respectively. It can be concluded that PANI coated on pine cones can be used as an effective adsorbent for removal of dye from aqueous solutions.

***Keywords***— Adsorption, Agricultural waste, Dye removal, Equilibrium

## I. INTRODUCTION

Due to rapidly increasing population growth, climate change, industrial activities and agricultural use the availability of fresh water has deteriorated drastically in the whole worldwide. Industrial waste discharges into natural water resources have been identified as a major source of water pollution. of toxic substances in water significantly affects the quality of water and highly contaminates underground water [40].

C.B Zulu, Department of Chemical, Metallurgical and Materials Engineering, Tshwane University of Technology, Pretoria, South Africa(e-mail: bongiwe.zulu@yahoo.com)
M. S. Onyango, Department of Chemical, Metallurgical and Materials Engineering, Tshwane University of Technology, Pretoria, South Africa (e-mail: onyangoms@tut.ac.za)
J. Ren, HySA Infrastructure Centre of Competence, Materials Science and Manufacturing, Council for Scientific and Industrial Research (CSIR), P.O. Box 395, Pretoria 0001, South Africa.
T.Y Leswifi, Department of Chemical, and Metallurgical Engineering, Vaal University of Technology, Pretoria, South Africa.

Moreover, the released of dye-bearing effluents into natural water resources is doing unimaginable harm to the The presence In particular, there has been a growing interest from environmentalists on the presence of dyes in the water/wastewaters originating from industries such as textile, paper, plastic, tannery and paints [6]. environment, threatening the health of people and also increasing the cost of treatment [29]. This is because dyes are of synthetic origin and possess complex aromatic molecular structure, thus which making them more stable and difficult to biodegrade [25].
Dyes are soluble, coloured organic compounds with structures containing aryl ring which have delocalized electron systems [12]. Moreover, dyes have functional groups that are capable of forming covalent bonds between carbon atoms of improves wash- fastness, hence making them very difficult to biodegrade. As a result, they pass through the purification plant without further degradation and are released into the environment [33]. However, wastewater generated from those mentioned industries which contains dyes is being discharged into municipal streamlines and river constitutes the major sources of water pollution [1]. Consequently, the presence of color in water beyond the maximum limits recommended by regulatory bodies greatly affects the water quality [41], inhibits sunlight penetration into the stream and also reduces photosynthetic action [34]. In order to comply with environmental protection laws as well as minimize the aforementioned challenges, there is an urgent need to reduce dyes or completely remove them from wastewater using appropriate and efficient technology in an economical manner [10].

Furthermore, several treatment methods for dyes removal from wastewater have been developed such as coagulation/flocculation [23], reverse osmosis [18], membrane filtration , electrolysis, advanced oxidation, photocatalysis, ion exchange and adsorption [1, 2, 9, 27, 30]. However, some of these processes have been found to have many disadvantages such as high energy demand [11], formation of flocs together with dye stuff, large amount of sludge produced, and uneconomical. In fact, some are not effective at all for dye removal and they also have short half-life [33]. Among these

methods, adsorption process has been identified as the most economical feasible and effective method for removal of dyes due to its wide range of applications, simplicity and low cost of operation [21]. In addition to the mentioned advantages, adsorption is also able to recover adsorbent for reuse and to prevent creation of secondary problems with dye-bearing sludge which is very difficult to dispose [14].

Since the performance of any adsorption process depends on the chemistry of the adsorbent and adsorbate, a variety of adsorption media have been developed and tested in the removal of dyes from aqueous solutions. These include commercially activated carbon (CAC), activated alumina, silica, clays and zeolites [16], to mention a few. However, most of these adsorbents have been linked with many limitations such as low capacity for dyes, slow reaction kinetics, high costs and difficulties in separation from wastewater [17, 18, 36]. Because cost is a very crucial pre-requisite of any adsorption media, lately many researchers have directed their interest in the usage of agricultural wastes such as almond husk, wheat bran, rice husk, pine cone wood and many more as the low cost adsorbents for dye pollutants removal from wastewater [16, 33, 36, 40]. As opposed to the high cost of activated carbon and other adsorbents, agricultural wastes are preferred for the adsorption applications because they are abundant in nature, readily available and environmentally friendly.

Up to date very little information exists in literature on the application of pine cone as a low cost adsorbent for direct orange 26 dye removal. Pine cones are agricultural by-product found in many parts of the world including South Africa. The scales of the mature cone are composed of epidermal and sclerenchyma cells which contain cellulose, hemicelluloses, lignin, rosin and tannins in their cell walls [37]. However, for better utilization of this inexpensive material, chemical modification using conducting polymer has been practiced by many researchers [3]. When chemically modified, the surface properties may be improved due to the anchoring of different functional groups hence improving their adsorption performances [46]. Recently, the use of conducting polymers as modifying agents have been a center of attention to many researchers due to their attractive properties that plays a key role in adsorption of a targeted pollutants [12]. Among the conducting polymers, polyaniline (PANI) has received a great deal of attention in recent years, due to its ease of synthesis, low cost, excellent environmental stability, unique physicochemical behavior towards the targeted contaminants [19].

Therefore, this work aimed at studying the adsorption behavior of modified pine cones for the removal of direct orange 26 (DO 26) dye from aqueous solution. The influence of process variables such as adsorbent dosage, initial pH solution, temperature and initial dye concentration will be explore under batch mode to understand adsorption mechanism modified pine cone in removal of dye pollutants. Kinetic studies were performed to understand adsorption rate and mechanism of the process.

## II. MATERIALS AND METHODS

### A. *Materials*

Raw pine cones were obtained from South Africa-Pretoria. Aniline monomer ($C_6H_5NH_2$), ammonium persulfate [$(NH_4)_2S_2O_8$] for use as an oxidant for initiation of polymerization reaction, hydrochloric acid 32% (HCl) were purchased from Sigma-Aldrich, Germany. Direct orange 26 (DO 26) dye (chemical formula $C_{33}H_{22}N_6Na_2O_9S_2$, double azo class and molecular weight 756.67g/mol) was supplied by Merck chemicals (Pty) Ltd, South Africa and was used as received. All other reagents of analytical reagent (AR) grade used in this work were obtained from Sigma-Aldrich, Germany and were used without any further purification.

### B. *Preparation of synthetic dye wastewater*

The dye stock solution was prepared by dissolving 1000 mg of DO 26 dye powder in 1000 mL of deionized water which makes up to a concentration of 1000 mg/L. All the experimental dye solutions were obtained by diluting the stock solution in accurate proportions as required.

### C. *Preparation of polyaniline coated pine cone*

The synthesis of polyaniline (PANI) coated pine cones used in this work was performed via in-situ chemical oxidative polymerization technique [28]. 10 ml of concentrated hydrochloric acid 32% was added into a 250 ml glass beaker with 80 ml of deionized (DI) water and then it was stirred for 10 minutes using magnetic stirrer at 300 rpm. 2 ml of aniline monomer was injected into the mixture and also allowed to stir for 5 minutes in order to obtain a homogeneous mixture. The collected pine cones were washed, dried and milled using ball mill then 10g of pine cone powder was dispersed into a mixture under continuous stirring. Thereafter, ammonium persulfate (APS) solution was prepared by dissolving 3.064 g of APS into a 10 ml of deionized water then it was added drop wise to the above suspension to properly initiate the polymerization. The whole reaction mixture was further stirred in a magnetic stirrer for a period of 24 hrs to allow polymerization to take place completely. Finally, the suspension was filtered and washed well with acetone to remove the unreacted chemicals. The washed powder was dried in the oven at $60^{O}$C overnight and sieved to achieve a specific particle size. The obtained final product was labeled as PANI-PC.

### D. *Characterization of PANI-PC*

The physico-chemical properties of the modified pine cone adsorbent were studied by conducting the characterization analysis on PANI-PC before and after adsorption process. The evaluation of morphology of the adsorbent was tested using Scanning electron microscopy (SEM) instrument. Meanwhile Fourier transform infared (FTIR) and Brunauer Emmett teller (BET) instruments were used to study the functional groups and surface properties respectively.

*E. Adsorption studies*

Batch equilibrium experiment was carried out to study the effectiveness of polyaniline modified pine cone (PANI-PC) adsorbent on the removal of DO 26 dye and also to investigate the variation of process parameters such as adsorbent mass, initial pH solution, initial dye concentration and temperature towards the adsorption process. A fixed known amount of the adsorbent was placed in contact with dye solution samples of initial DO-26 concentration ranging between (50-400 mg/L), solution pH (3-10) and temperature (25 - 45$^0$C) in a 100 mL plastic bottle. The prepared samples were placed in a thermostatic water bath shaker operated at 160 rpm for 24 hrs. Afterwards, the samples were filtered through a 0.45µm syringe filter in order to analyse dye residual concentration in the filtrate. The amount of dye remaining was analysed using UV-spectrophotometer (Shimadzu UV-1800) at a wavelength of 494 nm. The equilibrium adsorption capacity and efficiency were calculated using equation 1 and 2 respectively:

$$q_e = \frac{C_o - C_e}{m} v \qquad (1)$$

$$\%removal = \frac{C_o - C_e}{C_o} x100 \qquad (2)$$

where, $q_e$ is the adsorption capacity (mg/g), $C_o$ and $C_e$ are the initial and equilibrium concentration (mg/L) of dye, respectively. $V$ is the volume (L) of solution and $M$ is the weight (g) of adsorbent.

Kinetic adsorption study was conducted in a 2L plastic beaker containing 1000 mL of dye solution with 2.0g of PANI-PC adsorbent. The solution with different initial dye concentration (50 mg/L, 100 mg/L and 150 mg/l) was agitated using overhead stirrer at constant speed of 160 rpm under room temperature of 25±1$^0$C. At predetermined time intervals, 5 mL sample was withdrawn from a solution using a syringe, it was filtered and analyzed for remaining dye concentration. The amount of DO 26 dye adsorbed onto modified pine cones at time (t) was evaluated using below equation:

$$q_t = \frac{C_o - C_t}{m} V \qquad (3)$$

where $q_t$ (mg/g) is the time-dependent amount of dye adsorbed per unit mass of adsorbent at time $t$, $C_t$ is the final concentration of dye at any time t (mg/L).

## III. RESULTS AND DISCUSSION

*A. Characterization of PANI-PC adsorbent*

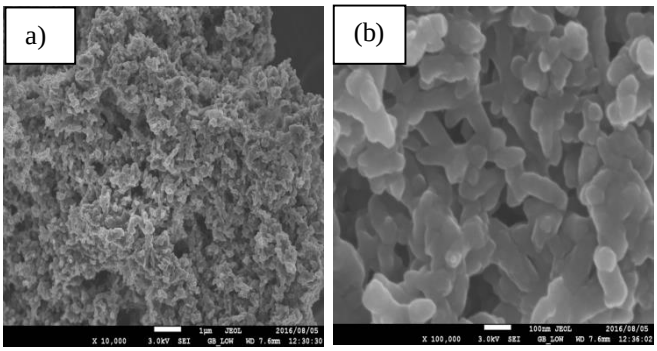


Fig 1: SEM images of PANI-PC (a) before adsorption and (b) after adsorption of DO 26 dye from synthetic water.

Scanning Electron Micrograph (SEM) is the mainly used method to analyze the surface morphology and physical properties of the adsorbent. Fig. 1a) and b) show SEM images of PANI modified pine cone before and after adsorption, respectively. It can be seen in image a) that the availability of pores and internal surface is more clearer than image b) which can be an evidence that adsorption did occur on the surface of adsorbent that is why in the image after adsorption there is a noticeable coverage of pores by the adsorbed DO 26 dye. In addition, EDS analysis (not presented) indicated adsorption of dye by showing high amount of sodium (Na) which is the main constituent of DO 26 DYE.

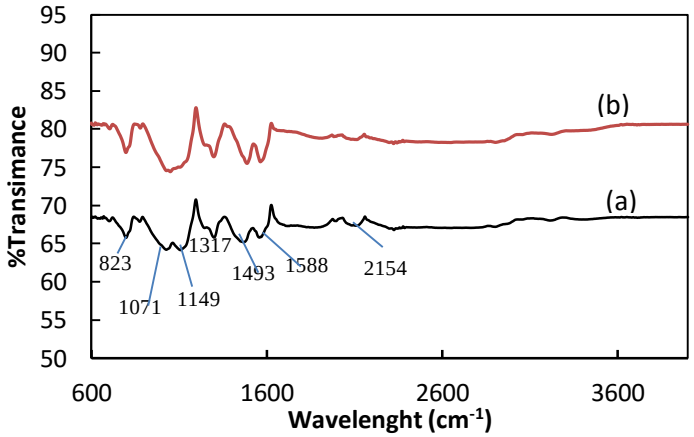


Fig 2: FTIR spectra of PANI-PC (a) before adsorption and (b) after adsorption.

The dye uptake depends upon porosity as well as chemical reactivity of functional groups that are present in the adsorbent. Therefore, a better understanding of functional groups which are involved in the adsorbent and also in dye molecule is necessary. Fig. 2 represents the FTIR spectra of PANI-PC before and after adsorption. The main peaks are observed at 2154 cm$^{-1}$, 1588cm$^{-1}$, 1493 cm$^{-1}$, 1317cm$^{-1}$, 1149 cm$^{-1}$, 1071 cm$^{-1}$ and 823 cm$^{-1}$. These peaks are characteristics peak of both lignocellulose (raw pine cones) and PANI that was coated on the surface of pine cone. The bands at 1588 cm$^{-1}$ and 1493 cm$^{-1}$ representing carbonyl group stretching (amide) and N-H

bonding accordingly. While the bands at 1317 $cm^{-1}$ and 1149 $cm^{-1}$ reflect the C-H bends and C-O stretching, respectively. The peaks between 1071 $cm^{-1}$ and 823$cm^{-1}$ may be a confirmation of –C-C and C-N stretching respectively [23]. It can be seen from spectra of PANI-PC loaded with dye molecule that there is no much change in the peaks except the bands at 1151 $cm^{-1}$ and 1550 $cm^{-1}$ which show high intensity than the peaks before adsorption; this might be due to the dye uptake that occurs on the surface of the adsorbent.

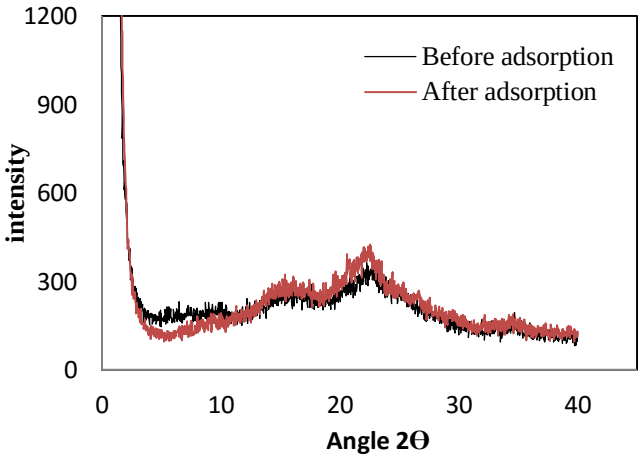


Fig 4: X-ray diffraction (XRD) analysis of PANI-PC before and after DO 26 adsorption.

In order to examine the crystalline structure of PANI-PC before and after adsorption of DO 26 dye, the X-ray diffraction was performed on the samples. The XRD plot is depicted in Fig. 4. It can be observed that diffraction peaks appearing at 2Θ values at 16.9° and 21.29° are attributed to the lignocellulosic structure of pine cones [9]. On the other hand, diffraction peak that normally appear at 25.20° which is the characteristic peak of amorphous PANI is absent, the reason for its disappearance is unknown. In addition, after adsorption there is only a slight change in the peak at 21.29°, which might be a confirmation of dye adsorption on the surface of adsorbent.

*B. Equilibrium Studies*

*1) Effect of solution pH*

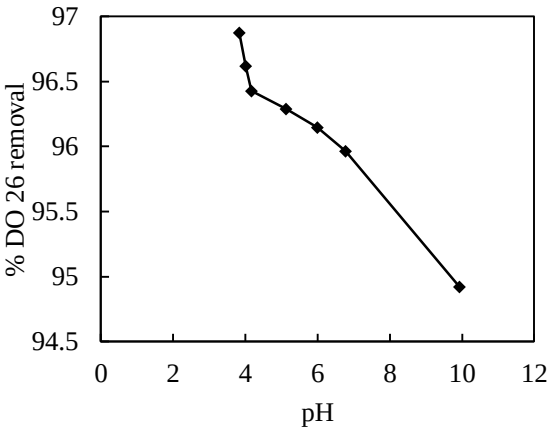


Fig 4: Effect of initial pH on DO 26 adsorption onto polyaniline pine cone. (Initial conc. 50 mg/L, Temp. 298K, adsorbent dose 0.1 g)

The adsorption of dye is highly dependent on the pH of solution as it determines whether dissociation and ionization of the dye molecule will take place through the surface of the adsorbent. Fig 4 displays the effect of pH on the removal of DO 26 onto PANI-PC adsorbent that was varied from pH 3- 10. The results reveal that dye percentage removal gradually decreases with increasing solution pH, this could be attributed by the fact that at lower pH the adsorbent surface is highly positively charged due to the protonated amino groups of PANI which allows electrostatic attraction to develop between positively charged adsorbent and negatively charged sulfonate groups of anionic dye DO 26 [3,9].The results also indicate that more than 97% dye removal was attained at pH = 3.83, therefore the optimal pH for this study was recorded as pH = 3.38.

*2) Adsorbent Dosage*

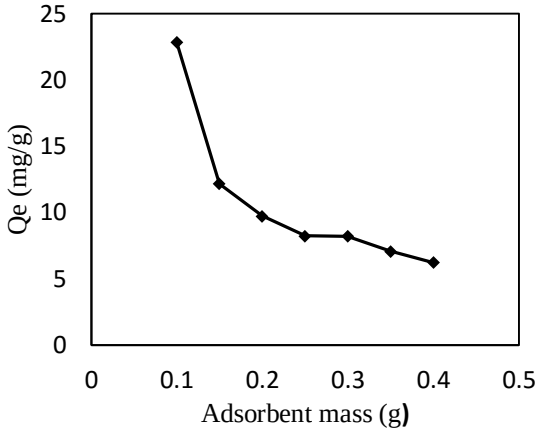


Fig 5: Effect of adsorbent dosage on the removal of DO 26 dye onto PANI-PC adsorbent. (Initial conc. 50 mg/L, Temp. 298K, pH = 3.83)

The influence of adsorbent mass on the remediation efficiency of the direct dye in aqueous solution was investigated under batch mode at 298 K, with sorbent dose between 0.1 - 0.4 g and an initial pH 3.83 as shown in Fig. 5. It is evident that an increase in the sorbent mass from 0.1g to 0.4 g resulted to a decrease in dye uptake from 22.9 mg/g to 6.21 mg/g. However, a reverse trend was observed in the removal efficiency which increases from 91% to 99%. This is due to the fact with large amount of adsorbent dosage there is high number of unsaturated adsorption sites left unoccupied with dye molecule during the adsorption process which causes adsorption capacity to decrease with increasing the dose of the adsorbent [31]. Meanwhile, at high sorbent dosage the number of available sorption site at the adsorbent surface will increase by increasing the adsorbent mass resulting in the increase in dye percentage removal from solution [33]. Similar behavior regarding adsorption of direct orange 26 on rice husk was observed by Safa and Bhatti, (2011b).

*3) Effect of temperature*

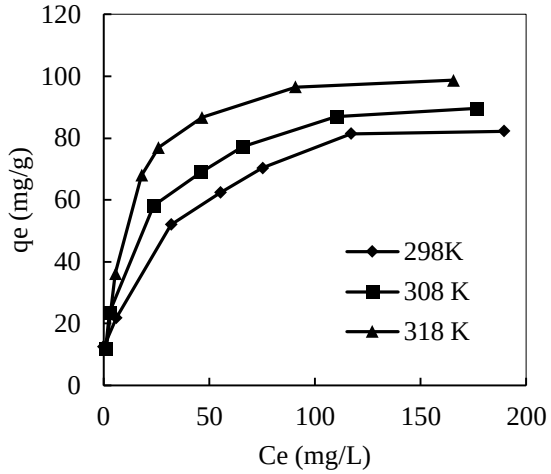


Fig. 6: Effect of temperature on DO26 removal onto PANI-PC adsorbent with solution volume = 50ml, adsorbent mass = 0.1g and initial pH solution = 3.83.

Temperature is an important parameter for any adsorption process as it indicates the nature of the adsorption whether it is an endothermic or exothermic process. The effect of temperature was carried out at different temperature (25, 35 and $45^0$C) as it is illustrated in Fig 6. The results showed that the adsorption capacity of DO 26 dye increase with increasing with system temperature suggesting that the process was endothermic in nature. This increase in dye removal may be attributed to increase in rate of diffusion of the dye molecules across the external boundary layer and into the internal pores of the adsorbent particles [9]. Similar results were reported for various dye adsorptions by other biosorbents [18, 25, 29, 38, and 40].

*C. Adsorption Kinetic Studies*

*1. Effect of contact time*

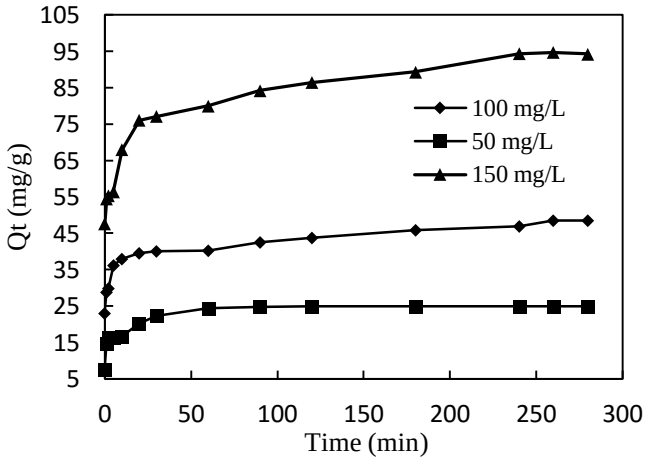


Fig 7: Effects of contact time and initial dye concentration on DO26 adsorption onto PANI-PC (dosage = 2.0g/L, agitation speed = 160 rpm, temp = 298 k and pH = 3.83)

The effect of contact time on the adsorption of DO 26 dye was explored under different initial DO 26 concentrations (50 to 150 mg/L) and results are presented in Fig 7. It was found that the amount of dye adsorbed increased with increasing initial concentration. Further, it was also revealed that equilibrium was attained within 90 min, 120 min and 180 min when concentration was from 50 mg/L, 100 mg/L and 150 mg/L, respectively. This can be explained by the fact that initial concentration provides the driving force to overcome the resistance to the mass transfer [35].

## IV. CONCLUSION

The work revealed that utilization of polyaniline coated pine cones as adsorbent for remediation of anionic DO 26 dye from aqueous solution is viable. Results also revealed that the magnitude of adsorption was primarily dependent on the solution initial pH and the sorbent dosage. In particular, adsorption performance was favored at pH 3.83. This was justified by the fact that at low pH solution the positive charge at the solution-interface will increase allowing the surface of adsorbent to be positively charged which results in an increase in anionic DO 26 dye adsorption. Meanwhile, the maximum adsorption capacity was found to be 22.9 mg/g with 0.1 g, 50 mg/L at $25^0$C. Based on the findings reported in this study, it can be concluded that PANI modified pine cone can be considered as a low-cost adsorbent which is environmentally benign for the effective removal of dyes from wastewater. Although in this work, PANI modified pine cone was tested for removal of dye using only synthetic dye solution. According to the study conducted by other researchers it is proven that modified pine cones can be used as an adsorbent for removal of contaminants from industrial effluents. Therefore, it is assumed that this bio-sorbent can potentially be used for real wastewater containing dyes pollutants. In order to confirm such assumption, similar study on removal of dye contaminants using a real wastewater shall be investigated.

## ACKNOWLEDGEMENT

The authors would like to acknowledge Tshwane University of Technology, National Foundation Research (NRF) for financial support and Council for Scientific and Industrial Research (CSIR) for providing analytical facilities.

## REFERENCES

[1] ADAK, A., BANDYOPADHYAY, M. & PAL, A. 2006. Fixed bed column study for the removal of crystal violet (C. I. Basic Violet 3) dye from aquatic environment by surfactant-modified alumina. Dyes and Pigments, 69:245-251.

[2] AL-JABARI, M. 2016. Kinetic models for adsorption on mineral particles comparison between Langmuir kinetics and mass transfer. Environmental Technology & Innovation, 6, 27-37.

[3] BALLAV, N., DEBNATH, S., PILLAY, K. & MAITY, A. 2015. Efficient removal of Reactive Black from aqueous solution using polyaniline coated ligno-cellulose composite as a potential adsorbent. Journal of Molecular Liquids, 209, 387-396.

[4] Cao, W., Dang, Z., Qiu Zhou, X., Yun Yi, X., Xiao Wu, P., Wu Zhu, N. *et al.* Removal of Sulfate from Aqueous Solution using Modified Rice Straw : Preparation, Characterization and Adsorption Performance. Carbohydrate Polymers BS (2011) 571-577

[5] CHAARI, I., MOUSSI, B. & JAMOUSSI, F. 2015. Interactions of the dye, C.I. direct orange 34 with natural clay. Journal of Alloys and Compounds, 647, 720-727.

[6] CHARUMATHI, D. & DAS, N. 2012. Packed bed column studies for the removal of synthetic dyes from textile wastewater using immobilised dead C. tropicalis. Desalination, 285:22–30.

[7] CHENG, Z., ZHANG, L., GUO, X., JIANG, X. & LI, T. 2015. Adsorption behavior of direct red 80 and congo red onto activated carbon/surfactant: Process optimization, kinetics and equilibrium. Spectrochimica Acta Part A: Molecular and Biomolecular Spectroscopy, 137, 1126-1143.

[8] DALVAND, A., NABIZADEH, R., REZA GANJALI, M., KHOOBI, M., NAZMARA, S. & HOSSEIN MAHVI, A. 2016. Modeling of Reactive Blue 19 azo dye removal from colored textile wastewater using L-arginine-functionalized Fe3O4 nanoparticles: Optimization, reusability, kinetic and equilibrium studies. Journal of Magnetism and Magnetic Materials, 404, 179-189.

[9] DAWOOD, S. & SEN, T. K. 2012. Removal of anionic dye Congo red from aqueous solution by raw pine and acid-treated pine cone powder as adsorbent: Equilibrium, thermodynamic, kinetics, mechanism and process design. Water Research, 46:1933-1 946.

[10] DEBNATH, S., BALLAV, N., MAITY, A. & PILLAY, K. 2015. Development of a polyaniline-lignocellulose composite for optimal adsorption of Congo red. International Journal of Biological Macromolecules, 75:199-209.

[11] EMENIKE, P.P., OMOLE, D.O., NBENE, B.U. & TENEBE, I.T. 2016. Potentiality of agricultural adsorbent for the sequestering of metal ions from wastewater. Global Journal of Environmental Science and Management, 2(4):411-442

[12] ETIM, U. J., UMOREN, S. A. & EDUOK, U.M. 2012. Coconut coir dust as a low cost adsorbent for the removal of cationic dye from aqueous solution. Journal of Saudi Chemical Society, 143:1945-2105.

[13] FALIL, F., ALLAM, F., GOURICH, B., VIAL, C. & AUDONNET, F. 2016. Adsorption of Astrazon Orange G onto natural Moroccan phosphate rock: A mechanistic study. Journal of Environmental Chemical Engineering, 4, 2556-2564.

[14] FERNANDEZ, M.E., NUNELL, G. V., BONELLI, P. R. & CUKIERMAN, A. L. 2010. Effectiveness of Cupressus sempervirens cones as biosorbent for the removal of basic dyes from aqueous solutions in batch and dynamic modes. Bioresource Technology, 101:9500-9507.

[15] FOO, K. Y. & HAMEED, B. H. 2012. Preparation, characterization and evaluation of adsorptive properties of orange peel based activated carbon via microwave induced K2CO3 activation. Bioresource Technology, 104, 679-686.

[16] FUNGARO, D. A., YAMAURA M. & CARVALHO, T. E. M. 2011. Adsorption of anionic dyes from aqueous solution on zeolite from fly ash-iron oxide magnetic nanocomposite. Journal of Atomic and Molecular Sciences, 2:305-316.

[17] GAUTAM, R. K., MUDHOO, A., LOFRANO, G. & CHATTOPADHYAYA, M. C. 2014. Biomass-derived biosorbents for metal ions sequestration: Adsorbent modification and activation methods and adsorbent regeneration. Journal of Environmental Chemical Engineering, 2:239–259.

[18] GUPTA, V. K. & SUHAS. 2009. Application of low-cost adsorbents for dye removal – A review. Journal of Environmental Management 90:2313–2342.

[19] GUSAIN, D., DUBEY, S., UPADHYAY, S. N., WENG, C. H. & SHARMA, Y. C. 2016. Studies on optimization of removal of orange G from aqueous solutions by a novel nano adsorbent, nano zirconia. Journal of Industrial and Engineering Chemistry, 33, 42-50.

[20] INYINBOR, A. A., ADEKOLA, F. A. & OLATUNJI, G. A. 2016. Kinetics, isotherms and thermodynamic modeling of liquid phase adsorption of Rhodamine B dye onto Raphia hookerie fruit epicarp. Water Resources and Industry, 15, 14-27.

[21] JANAKI, V., OH, B.-T., SHANTHI, K., LEE, K.-J., RAMASAMY, A. K. & KAMALA-KANNAN, S. 2012. Polyaniline/chitosan composite: An eco-friendly polymer for enhanced removal of dyes from aqueous solution. Synthetic Metals, 162, 974-980.

[22] LOFRANO, G., MERIÇ, S., ZENGIN, G. E. & ORHON, D. 2013. Chemical and biological treatment technologies for leather tannery chemicals and wastewaters: A review. Science of The Total Environment, 461–462, 265-281.

[23] MAHMOODI, N. M., HAYAT, B., ARAMI, M. & LAN, C. 2011. Adsorption of textile dyes on Pine Cone from colored wastewater: Kinetic, equilibrium and thermodynamic studies. Desalination, 268:117–125.

[24] MAHMOUD, M. E., NABIL, G. M., EL-MALLAH, N. M., BASSIOUNY, H. I., KUMAR, S. & ABDEL-FATTAH, T. M. 2016. Kinetics, isotherm, and thermodynamic studies of the adsorption of reactive red 195 A dye from water by modified Switchgrass Biochar adsorbent. Journal of Industrial and Engineering Chemistry, 37, 156-167.

[25] MOHAMMED, M. A., SHITU, A. & IBRAHIM, A. 2014. Removal of Methylene Blue Using Low Cost Adsorbent: A Review. Research Journal of Chemical Sciences, 4:91-102. J.A., Maree, J.P. and Adlem, C.J.L. 1991 Removal of sulfate from mine water. In: Proceedings of the ARD in Pyrite Environments, Lisbon, Portugal, 16-19 September 1990. 211-221.

[26] MOUSSAVI, G. & KHOSRAVI, R. 2011. The removal of cationic dyes from aqueous solutions by adsorption onto pistachio hull waste. Chemical Engineering Research and Design, 89, 2182-2189.

[27] MUNAGAPATI, V. S. & KIM, D.-S. 2016. Adsorption of anionic azo dye Congo Red from aqueous solution by Cationic Modified Orange Peel Powder. Journal of Molecular Liquids, 220, 540-548.

[28] PAHOVNIK, D., ŽAGAR, E., KOGEJ, K., VOHLÍDAL, J. & ŽIGON, M. 2013. Polyaniline nanostructures prepared in acidic aqueous solutions of ionic liquids acting as soft templates. European Polymer Journal, 49, 1381-1390.

[29] PAVAN, F. A., MAZZOCATO, A. C. & GUSHIKEM, Y. 2008. Removal of methylene blue dye from aqueous solutions by adsorption using yellow passion fruit peel as adsorbent. Bioresource Technology, 99:3162–3165.

[30] PIRKARAMI, A., OLYA, M.E. & YOUSEFI LIMAEE, N. 2013. Decolorization of azo dyes by photo electro adsorption process using polyaniline coated electrode. Progress in Organic Coatings, 76(4):682-688.

[31] RAGHUNATH, S., ANAND, K., GENGAN, R. M., NAYUNIGARI, M. K. & MAITY, A. 2016. Sorption isotherms, kinetic and optimization process of amino acid proline based polymer nanocomposite for the removal of selected textile dyes from industrial wastewater. Journal of Photochemistry and Photobiology B: Biology, 165, 189-201.

[32] RANGABHASHIYAM, S., ANU, N. & SELVARAJU, N. 2013. Sequestration of dye from textile industry wastewater using agricultural waste products as adsorbents. Journal of Environmental Chemical Engineering, 1, 629-641.

[33] RAO, K. S. P., RAO, M. V. & BANGARAIAH, P. 2013. Removal of methylene blue from aqueous solution using grewia orbiculata rottl: Equilibrium, Kinetic and Thermodynamic studies. International Journal of Engineering Research and Science & Technology, 2:2319-5991

[34] SAFA, Y. & BHATTI, H. N. 2011a. Biosorption of Direct Red-31 and Direct Orange-26 dyes by rice husk: Application of factorial design analysis. Chemical Engineering Research and Design, 89, 2566-2574.

[35] SAFA, Y. & BHATTI, H. N. 2011b. Kinetic and thermodynamic modeling for the removal of Direct Red-31 and Direct Orange-26 dyes from aqueous solutions by rice husk. Desalination, 272, 313-322.

[36] SALLEH, M. A. M., MAHMOUD, D. K., KARIM, W. A. W. A. & IDRIS, A. 2011. Cationic and anionic dye adsorption by agricultural solid wastes: A comprehensive review. Desalination, 280, 1-13.

[37] SEN, T. K. 2012. Agricultural by-product biomass for removal of pollutants from aqueous solution by adsorption. Journal of Environmental Research and Development, 6-3.

[38] SEN, T. K., AFROZE, S. & ANG, H.M. 2011. Equilibrium, Kinetics and Mechanism of Removal of Methylene Blue from Aqueous Solution by Adsorption onto Pine Cone Biomass of Pinus radiata. Water Air Soil Pollution, 218:499–515

[39] SINGH, H., CHAUHAN, G., JAIN, A. K. & SHARMA, S. K. 2017. Adsorptive potential of agricultural wastes for removal of dyes from aqueous solutions. Journal of Environmental Chemical Engineering, 5, 122-135.

[40] SINGH, U. & KAUSHAL, R. K. 2013. Treatment of wastewater with low cost adsorbent-A Review. International Journal of Technical & Non-Technical Research, 4:2319-2216.

[41] SIVRI, N., TUFEKCI, N. & TOROZ, I. 2007. Pollutants of Textile Industry Wastewater and Assessment of its Discharge Limits by Water Quality Standards. Turkish Journal of Fisheries and Aquatic Science, 7:97-103.

[42] SUBBAIAH, M. V. & KIM, D.-S. 2016. Adsorption of methyl orange from aqueous solution by aminated pumpkin seed powder: Kinetics, isotherms, and thermodynamic studies. Ecotoxicology and Environmental Safety, 128, 109-117.

[43] TAN, B. H., TENG, T. T. & OMAR, A. K. M. 2000. Removal of dyes and industrial dye wastes by magnesium chloride. Water Research, 34, 597-601.

[44] WAKSAKAL, O. & UCUN, H. 2010. Equilibrium, kinetic and thermodynamic studies of the biosorption of textile dye (Reactive Red 195) onto Pinus sylvestris L. Journal of Hazardous Materials, 181, 666-672.

[45] YAGUB, M. T., SEN, T. K., AFROZE, S. & ANG, H. M. 2014. Dye and its removal from aqueous solution by adsorption: A review. Advances in Colloid and Interface Science, 209, 172-184.

[46] YANEVA, Z. L. & GEORGIEVA, N. V. 2012. Insights into Congo red Adsorption on Agro-Industrial Materials -Spectral, Equilibrium, Kinetic, Thermodynamic, Dynamic and Desorption Studies: A Review. International Review of Chemical Engineering, 4:2035-1755.

# On-Shore Power Supply Stability Analysis on 132 Kv Mombasa Power Distribution Network

C. N.Karue, D. K. Murage, C. M. Muriithi

*Abstract* - As an international best practice, docked ships are required to switch off their generators and use utility power for their activities once in the harbour port as one way to reduce emissions. This paper seeks to analysis the 132kV Kenya power supply from Juja to Mombasa in an effort to assess its capacity and stability with various categories of 22 docked ships connected at Port of Mombasa. The Coast Region power distribution network will be modelled using PSAT. Specific critical buses will be studied with an aim of proposing possible mitigations that can be taken if they are likely to experience voltage drops/ collapse. The loading limits on each of the buses will be determined using continuation power flow. The results will be used to assess the capability of connecting existing ships loads and as a planning tool for future proposed port expansion for cruise and larger container vessels at berth No. 1 and second container terminal phase 2 respectively.

***Keywords*** **-** On- shore power, Emissions, PSAT, Continuation power flow

## I. INTRODUCTION

erthed ships can either generate their own electricity using Bclean fuel, or connect to utility power sockets at the port [1], [2]. Research so far done has shown on –shore power supply is the most sustainable solution in every way [3], [4]. Further studies have revealed the following benefits from on-shore power;
Shore power has the following benefits:

(i) Reduced port fees – Where relevant legislation exists such as in the EU, port fees can vary depending on the environmental rating of a ship. Created by WPCI, the Environment Ship Index (ESI) measures the quantities of NOx, SOx, PM and CO2 emissions from a ship and assigns a grade to each ship. As shore connection is a green technology, ships equipped with the solution receive a higher grade. Greener ships can enjoy fees rebate up to 10% on Port fees.
(ii) Cutting emissions - Electricity generated on land by power plants has a smaller eco-footprint than that produced by ship engines. Use of shore-side electricity cuts CO2 emissions by an average of 50%.
(iii) Elimination of noise and vibrations - Use of auxiliary diesel engines on ships causes noise up to 120dB near the engines and associated vibrations are unpleasant for crew, passengers, and port personnel.
(iv) Reduced fuel costs: - Global demand for fuel is set to rise significantly and this especially affects low sulphur fuel process. The United States Energy Information Administration forecasts that demand for refined petroleum products will grow by 1.5% per year over the next five years. Current fuel prices make use of shore-side electricity that is partially generated from non-fossil fuel sources financially attractive.

(v) Lower maintenance costs - Motor maintenance costs (estimated at 1.6 Euro/h/motor) fall sharply when shore-side electricity is used. The annual average saving per ship is estimated at Euro 9,600.
(vi) New business for ports - Ports installing shore connections would selling electricity to ships, more revenue will be realized by the utilities.

Largely, the size of a shore-to-ship installation will depend on the power requirements for docking ships with an average rating of vessels ranging from 300kVA for RORO ships, 2MW for container ships to 11MW for cruise ships [5] and [6]. The voltage rating for shore connection are 6.6kV or 11kV in order to cater for the largest ships and reduce the number of cables used in connections as per recommendations by EU standard 2006/339/EC . Other standards applied are the Institution of Electrical and Electronic Engineers (IEEE), International Electrotechnical Commission (IEC) and ISO have developed an international standard (IEC_ISO_IEEE 80005-1 Ed1) which HV voltage, sockets and plug points requirements.

On–shore power supply at Port of Mombasa using the existing Kenya Power 132kV system may result in instability phenomena both short term and long term. An analysis study on the impact of using shore power on berthed ships of the effect of such a connection will allow for prediction of negative effects and formulation of mitigation factors to be incorporated in the installation. In this paper, a working methodology for this study is developed and a PSAT/Matlab model of the coast power network applied. The model will be used for long term voltage stability analysis using continuation power flow. The results are used to assess the effect of additional load on various busses using PV and QV curves.

C.N. Karue1, Department of Electrical Engineering, JKUAT (corresponding author; phone: +254 722 647699; e-mail: knyaguthii@kpa.co.ke).

D. K. Murage, Department of Electrical Engineering, JKUAT (dkmurage25@gmail.com) and C. M. Muriithi, Department of Electrical Engineering, TUK (cmainamuriithi@gmail.com)

Future work would be designing the correct size and type of frequency converters that can be used at the Port of Mombasa.

## II. PREVIOUS WORK

### A. *Load modelling*

In order to study an electrical system, load modelling is done. There are different load models that are suitable for different [6], [7], [8]. Examples of static models are polynomial (ZIP) model, exponential recovery model, voltage dependent load and frequency dependent load with induction motors being represented by a dynamic model with variable torque, power and slip. Where there are many motors, aggregation models are applied to reduce complexity. The equivalent PQ model for power flow has been obtained by initialisation of the power flow as proposed in [8].

### B. *Voltage instability and prediction*

Voltage instability in a power system is as a result of a mismatch between generation and the load [9]. Voltage instability is further divided into short term and long term instability. Short term instability is caused by short term disturbances such as increase in load, a fault in the transmission system or reduction in generation. This type of instability is normally rectified by automatic regulating devices such as over excitation limiters and on load tap changers.

Long term voltage instability occurs when the resources required to match generation to load exceed the capacity of the power system. Long term instability occurs when active load exceeds the transmission capacity or the reactive load exceeds the generation capacity which may lead to a voltage collapse [10].

For a heavily loaded power system, the possibility of voltage collapse can be predicted by measuring the distance between the current operating point and the point of collapse. The point of collapse for a given bus is indicated by the bifurcation point (the 'nose') in the P-V curve at the bus ad shown in figure 1.

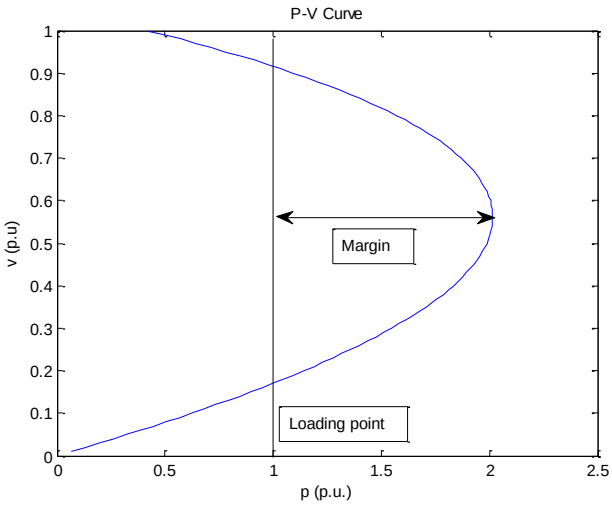


*Figure 1: Loading margin from P-V curve*

This point corresponds to the maximum transmission capacity for active power. Plotting of the P-V curve in the neighbourhood of the bifurcation point is not possible because of the singularity at the point.

### C. *Continuation power flow*

The continuation power flow [11] is a powerful power system tool that can be used to plot the complete P-V curve including the singularity. The continuation power flow is a modification of the standard power flow that is represented by equation (a).

$$p_h = p_G - p_L$$
$$q_h = q_G - q_L \quad \text{(a)}$$

Where
$p_h$ is active power injected at bus *h*,
$p_G$ is active power generated at bus *h*
$p_L$ is load power consumed at bus *h* and

$q_h$, $q_G$ and $q_L$ represent reactive power injected, generated and consumed at bus *h.*

In the continuation power flow model, a loading factor, λ, is used to increment the load in fixed steps from a small value. In order to match power generation with the reduced load, all generator capacities are scaled by a participation factor $k_g$. The expressions for active power generated and load power (active and reactive) therefore become as shown in (b);

$$p_G = (\lambda I_N + k_g I_N) p_{GO}$$
$$p_L = \lambda p_{LO}$$
$$q_L = \lambda q_{LO} \quad \text{(b)}$$

Where
$I_N$ is the identity matrix of size *N*,
*N* is the number of generators in the network and

$p_{GO}$, $p_{LO}$ and $q_{LO}$ are base values for generated power, active load power and reactive load power respectively.

A numerical solution of the continuation power flow is achieved through a series of prediction and correction step as demonstrated in figure 2. This eventually results in a plot of the complete P-V curve, including the bifurcation point and the lower and upper solutions.

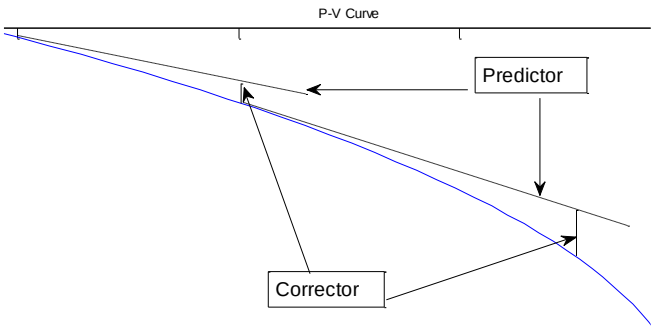


*Figure 2: Predictor and corrector in continuation power flow*

In [12], the method has been applied to a system with induction motor load study. A method proposed in [8], incorporates the limits for reactive power generation in the continuation power flow solution which is achieved by implementing reactive power generation limits in the implementation algorithm.

## III. 132KV COAST NETWORK MODEL

### A. Network description

The coast network is part of the Kenya national grid. It has two connections to the grid [13] and [14] namely,
(i) 132kV single circuit transmission lines from Juja Road Bulk Supply Station (BSP) in Nairobi to the Rabai BSP

(ii) 220kV single circuit transmission line from the Kiambere Power Station on the Tana River to the Rabai BSP.

The main loads include counties of Taita Taveta, Kwale, Mombasa, Kilifi and Tana River using 33kV distribution feeders. Plans are underway to link the system to Lamu County, which is currently supplied by off-grid generation.
The coast network has four generating stations at Rabai, Kipevu I, Kipevu II (Tsavo Power) and Kipevu III whose capacities are listed in Table 1.

*Table 1: Coast Generating Capacity*

| Generating Station | Installed Capacity, MW | Effective Capacity, MW |
|---|---|---|
| Rabai | 90 | 90 |
| Kipevu I | 75 | 51 |
| Kipevu III | 120 | 115 |
| Kipevu II | 74 | 74 |

In addition, the Coast network is also connected to national the grid through a 132kV transmission line from Rabai to Juja Road BSP in Nairobi and a 220kV line from Rabai to the Kiambere power station. The connection to the national grid allows the Coast network to supply excess power to the national grid when local generation exceeds consumption. It also allows the network to draw power from the national grid when local consumption exceeds generation hence the model will assume the connection to the national grid as a slack bus. With Rabai receiving all the generating stations supply power, it acts as the bulk supply point for the coast network where power is then distributed to the coast region through a 132kV network with interconnections as in Table 2.

*Table 2 : 132kV Power distribution interconnections*

| FROM | TO | km | kV | CIRCUITS | CONDUCTOR |
|---|---|---|---|---|---|
| Juja | Mtito | 476 | 132 | Single | 132_LYNX |
| Mtito | Voi | | 132 | Single | 132_LYNX |
| Voi | Maungu | | 132 | Single | 132_LYNX |
| Maungu | Mariakani | | 132 | Single | 132_LYNX |
| Mariakani | Kokotoni | | 132 | Single | 132_LYNX |
| Kokotoni | Rabai | | 132 | Single | 132_LYNX |
| Rabai | Kiambere | 416 | 220 | Single | 220_CANARY |
| Rabai | Galu | 60 | 132 | Single | 132_LYNX |
| Rabai | Kipevu I & III | 17 | 132 | Double | 132_WOLF |
| Rabai | Kipevu I & III | 17 | 132 | Single | 132_LYNX |
| Rabai | Kipevu II | 17 | 132 | Single | 132_LYNX |
| Kipevu | KPA | 1.5 | 132 | Single | 400mm$^2$ Cu U/G |
| Rabai | New Bamburi | 22 | 132 | Single | 132_WOLF |
| New Bamburi | Vipingo | 13 | 132 | Single | 132_WOLF |
| Vipingo | Mombasa Cement | 12.5 | 132 | Single | 132_WOLF |
| Msa Cement | Kilifi | 17.5 | 132 | Single | 132_WOLF |

From BSP Rabai, power is distributed to the using a 132kV network to Galu in South Cost, Kipevu in Mombasa Island and Bamburi, Vipingo and Kilifi on the North Coast. In addition there are two 132kV stations feeding Mombasa Cement on the North Coast and KPA on Mombasa Island with a reactive power compensation 2*15MVAr at the Rabai BSP where each

is served by 132kV/33kV distribution transformers. The total load connected to each station is as shown in Table 3

*Table 3 : Bulk Supply Points load*

| BSP | Active Power, MW | Reactive Power, MVAr | Total MVA |
|---|---|---|---|
| Galu | 14.25 | 6.9 | 15.83 |
| Kilifi | 13.38 | 6.48 | 14.87 |
| Kipevu | 99.86 | 48.37 | 110.95 |
| New Bamburi | 26.47 | 12.82 | 29.4 |
| Rabai | 7.63 | 3.7 | 8.47 |
| MSA Cement | 10.98 | 5.32 | 12.2 |
| KPA | 6.3 | 3.05 | 7 |
| Kokotoni | 3.27 | 7.5 | 7.5 |
| Mariakani | 5.36 | 12.3 | 12.3 |
| Maungu | 1.62 | 3.72 | 3.72 |
| Mtito Andei | 2.05 | 4.69 | 4.69 |
| Voi | 1.69 | 3.87 | 3.87 |

*B. Network model*

The Power network is modelled using PSAT/Matlab platform. A single line diagram of the model is shown in Figure 3 in Appendix A with model parameters Table 4 and Table 5

*Table 4: Line data*

| FROM | TO | r (p.u.) | x (p.u.) | b (p.u.) |
|---|---|---|---|---|
| Rabai BSP | Galu | 0.1962 | 0.4449 | 2.7789E-06 |
| Rabai BSP | Kipevu BSP | 0.0644 | 0.1274 | 7.7858E-07 |
| Rabai BSP | Kipevu BSP | 0.0644 | 0.1274 | 7.7858E-07 |
| Rabai BSP | Kipevu BSP | 0.0556 | 0.1261 | 7.8736E-07 |
| Rabai BSP | Kipevu II | 0.0556 | 0.1261 | 7.8736E-07 |
| Kipevu BSP | KPA | 0.0012 | 0.0058 | 4.1322E-09 |
| Rabai BSP | N. Bamburi | 0.0834 | 0.1649 | 1.0076E-06 |
| N. Bamburi | Vipingo | 0.0493 | 0.0974 | 5.9539E-07 |
| Vipingo | M. Cement | 0.0474 | 0.0937 | 5.7249E-07 |
| M. Cement | Kilifi | 0.0663 | 0.1312 | 8.0148E-07 |
| Grid | Rabai BSP | 0.5479 | 3.1515 | 1.8837E-05 |
| Grid | Mtito | 0.8078 | 1.8315 | 1.1440E-05 |
| Mtito | Voi | 0.2976 | 0.6748 | 4.2147E-06 |
| Voi | Maungu | 0.0981 | 0.2224 | 1.3895E-06 |
| Maungu | Mariakani | 0.2943 | 0.6673 | 4.1684E-06 |

*C. Per unit power line data*

*Table 5: Per Unit Line data*

| BUS NO. | BUS NAME | LOAD | | STATIC VAR (p.u) | BUS TYPE |
|---|---|---|---|---|---|
| | | P (p.u.) | Q (p.u.) | | |
| 1 | Grid | - | - | - | Slack |
| 2 | Rabai BSP | 0.0254 | 0.0123 | 0.1000 | PQ |
| 3 | Galu | 0.0475 | 0.0230 | - | PQ |
| 4 | Kipevu BSP | 0.3329 | 0.1612 | - | PQ |
| 5 | KPA | 0.0210 | 0.0102 | - | PQ |
| 6 | N. Bamburi | 0.0882 | 0.0427 | - | PQ |
| 7 | Vipingo | - | - | - | PQ |
| 8 | M. Cement | 0.0366 | 0.0177 | - | PQ |
| 9 | Kilifi | 0.0446 | 0.0216 | - | PQ |
| 10 | Kipevu II | 0 | 0 | 0 | PV |
| 11 | Mtito | 0.0141 | 0.0068 | - | PQ |
| 12 | Voi | 0.0116 | 0.0056 | - | PQ |
| 13 | Maungu | 0.0112 | 0.0054 | - | PQ |
| 14 | Mariakani | 0.0369 | 0.0179 | - | PQ |
| 15 | Kokotoni | 0.0225 | 0.0109 | - | PQ |

*Table 5: Generation*

| Generating Station | Bus | Power Generated, P (p.u.) |
|---|---|---|
| Rabai | Rabai BSP | 0.3000 |
| Kipevu I | Kipevu BSP | 0.1700 |
| Kipevu III | Kipevu BSP | 0.3833 |
| Tsavo (Kipevu II) | Kipevu II | 0.2467 |

*D. Port Off – shore power demands*

With 22 deep water berths at Port of Mombasa, [15], and a

standard planning of 9 container berths, 9 general cargo, 2 oil tankers and 2 roll-on roll-off vehicle carriers, the power loading can be calculated. Port traffic is estimated as 38% container ship, 20% general cargo, 14% bulk carrier, 14% Ro-Ro and car carriers and 13% oil tankers. The power demand for each category of ship has been estimated by the following process:

a. Data on electrical loads on a ship is collected.
b. The load is modelled as a composite load comprising aggregated induction motor load and constant impedance loads.
c. The steady state PQ load for use in power flow is determined by an initialisation process.

The load aggregation and initialisation method is presented in [16]. A comparison is also done with global data from [1], [17] , which includes data on the actual percentage of total load that is utilised when ships are at berth.

From this analysis, an estimate of the total demand of ships in berth at the port of Mombasa is presented in Table 7.

A shore to ship connection for the port of Mombasa will therefore be expected to carry a load of approximately 22MW.

*Table 6 : Off-shore power demand for Mombasa port*

| Type of Berth | No. | Peak Load (kW) | In Port Demand % | Berth Load (kW) |
|---|---|---|---|---|
| Container | 9 | 4,000 | 20 | 7,200 |
| General Cargo | 9 | 2,800 | 40 | 10,080 |
| Ro-Ro | 2 | 1,800 | 30 | 1,080 |
| Oil Tanker | 2 | 2,500 | 65 | 3,250 |
| Total | 22 | | | 21,610 |

## IV. RESULTS AND DISCUSSIONS

### A. *Power flow results in per unit values*

The results of power flow on the model in Appendix A Figure 3 are presented in Table 8. From the results, buses for Mtito and Voi are seen to have the lowest voltage levels at 0.93 per unit. These are however loads tapped from the transmission line off the grid hence not from the Coast network. Kilifi and Mombasa cement are observed to be from the coast grid and have lowest voltage level. On these buses, further analysis is done using continuation power flow.

*Table 7 : Power flow results*

| BUS | V (p.u.) | phase (rad) | P gen (p.u.) | Q gen (p.u) | P load (p.u.) | Q load (p.u.) |
|---|---|---|---|---|---|---|
| Grid | 1.05 | - | (0.31) | 0.28 | - | - |
| Rabai BSP | 1.00 | 0.73 | 0.30 | 0.49 | 0.03 | 0.11 |
| Galu | 0.98 | 0.71 | - | - | 0.05 | 0.02 |
| Kipevu BSP | 1.00 | 0.74 | 0.55 | 0.08 | 0.33 | 0.16 |
| KPA | 1.00 | 0.74 | - | - | 0.02 | 0.01 |
| New Bamburi | 0.97 | 0.71 | - | - | 0.09 | 0.04 |
| Vipingo | 0.96 | 0.70 | - | - | - | - |
| MSA Cement | 0.95 | 0.69 | - | - | 0.04 | 0.02 |
| Kilifi | 0.95 | 0.69 | - | - | 0.04 | 0.02 |
| Kipevu II | 1.00 | 0.76 | 0.25 | (0.10) | - | - |
| Mtito | 0.93 | 0.34 | - | - | 0.01 | 0.01 |
| Voi | 0.93 | 0.49 | - | - | 0.01 | 0.01 |
| Maungu | 0.94 | 0.54 | - | - | 0.01 | 0.01 |
| Mariakani | 0.98 | 0.69 | - | - | 0.04 | 0.02 |
| Kokotoni | 0.99 | 0.72 | - | - | 0.02 | 0.01 |

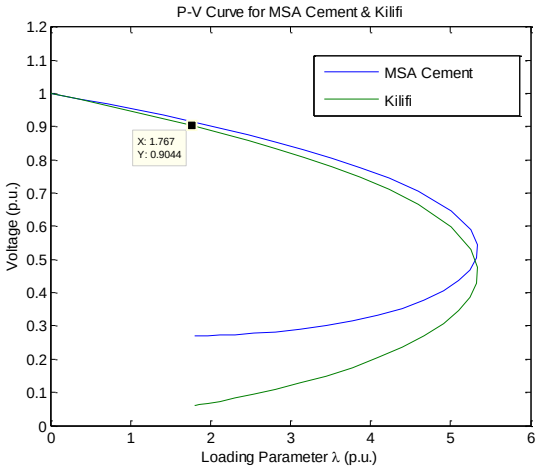


Figure 3: PV Curves for selected buses

### B. *Continuation Power flow results*

A continuation power flow has been carried out with an additional 22MW load connected on bus 5 (KPA) to simulate the shore to ship connection. The resulting P-V curves are presented in Figure 4. It is observed that the point of instability occurs at a loading of more than 5 per unit. This implies that even with the additional load, the network has a large margin of safety against voltage collapse. It is however noted that the voltage level falls below 0.9p.u when the load factor is 1.77p.u. Voltages below this level may lead to motor stalling. This loading value provides a limit for the possible load on the network.

## V. CONCLUSION

This work has demonstrated the application of power flow

and continuation power flow in determining the impact of a shore to ship connection on a regional power network in terms of voltage stability. A complete model of off-shore load at the port of Mombasa has been developed for the stability study. The Coast 132kV power network has also been modelled and a power flow study has been applied to identify the buses with highest likelihood of voltage collapse. Continuation power flow has further been applied to identify the loading limit on the selected buses.

## REFERENCES

[1] P. Ericsson and I. Fazlagic, *Shore-side Power Supply: A feasibility study and technical solution for an on-shore electrical infrastructure to supply vessels with electric power while at port*, Goteborg, Sweden: Chalmers University of Technology / ABB, 2008.

[2] D. Radu, J. P. Sorrel, R. Jeannot and M. Megdiche, "Shore Connection Applications : Main challenges," Schneider Electric (White Paper), Cedex, France, 2013.

[3] D. Bailey and G. Solomon, "Polution prevention at ports: clearing air," *Environmental Impact Assesment Review*, vol. 24, pp. 749 - 774, 2004.

[4] F. Fung, Z. Zhu, R. Becque and B. Finamore, "Prevention and Control of Shipping and Port Air Emissions in China," Natural Resources Defence Council (NRDC), 2014.

[5] "High Voltage Shore Connection (HVSC) Systems - General requirements," IEEE Standard Association , IEC/ISO /IEEE 80005 -1 Ed 1 Cold Ironing Part 1 .

[6] IEEE Task force on load representation for dynamic performance, "Standard load models for power flow and dynamic performance simulation," *IEEE Transactions on Power Systems*, vol. 10, no. 3, pp. 1302 - 1313, 1995.

[7] Reactive Reserve Working Group (RRWG), *Guide to WECC/NERC Planning Standards I.D: Voltage Support and Reactive Power*, Salt Lake City: Western Electricity Coordinating Council, 2006.

[8] F. Milano, Power System Modelling and Scripting, London: Springer-Verlag, 2010.

[9] IEEE PES Power System Stability Subcommittee, *Voltage Stability Assessment: Concepts, Practices and Tools*, IEEE, 2002.

[10] IEEE/CIGRE Joint Task Force on Stability Terms and Definitions, "Definition and classification of power system stability," *IEEE Transactions on Power Systems*, pp. 1 - 15, 2004.

[11] A. V and C. C, " The continuation power flow: a tool for steady state voltage stability analysis," *IEEE Transactions on Power Systems*, vol. 7, no. 1, , pp. 416 - 423, 1992.

[12] L. M. Ngoo, C. M. Muriithi, G. N. Nyakoe and S. N. Njoroge, "A neuro fuzzy model of an induction motor for voltage stability analysis using continuation load flow," *Journal of Electrical and Electronics Engineering Research*, vol. 3, no. 4, pp. 62-70, 2011.

[13] Kenya Power, *Power Sector Medium Term Plan 2015 - 2020*, Nairobi: Kenya Power, 2015.

[14] KPLC, *Kenya Distribution Master Plan*, vol. I, Kenya Power & Lighting Co. Ltd, 2013.

[15] JICA, *Mombasa Port Master Plan including Dongo Kundu*, Japan International Cooperation Agency, 2015.

[16] C. N. Karue, D. K. Murage and C. M. Muriithi, "Shore to Ship Power for Mombasa Port: Possibilities and Challenges," in *Proceedings of the 2016 Annual Conference on Sustainable Research and Innovation*, Nairobi, 2016.

[17] M. Megdiche, D. Radu and R. Jeanot, "Protection plan and safety issues in shore connection," in *22nd International Conference on Electricity Distribution*, Stockholm, 2013.

# APPENDIX A

132kV coast power distribution network model

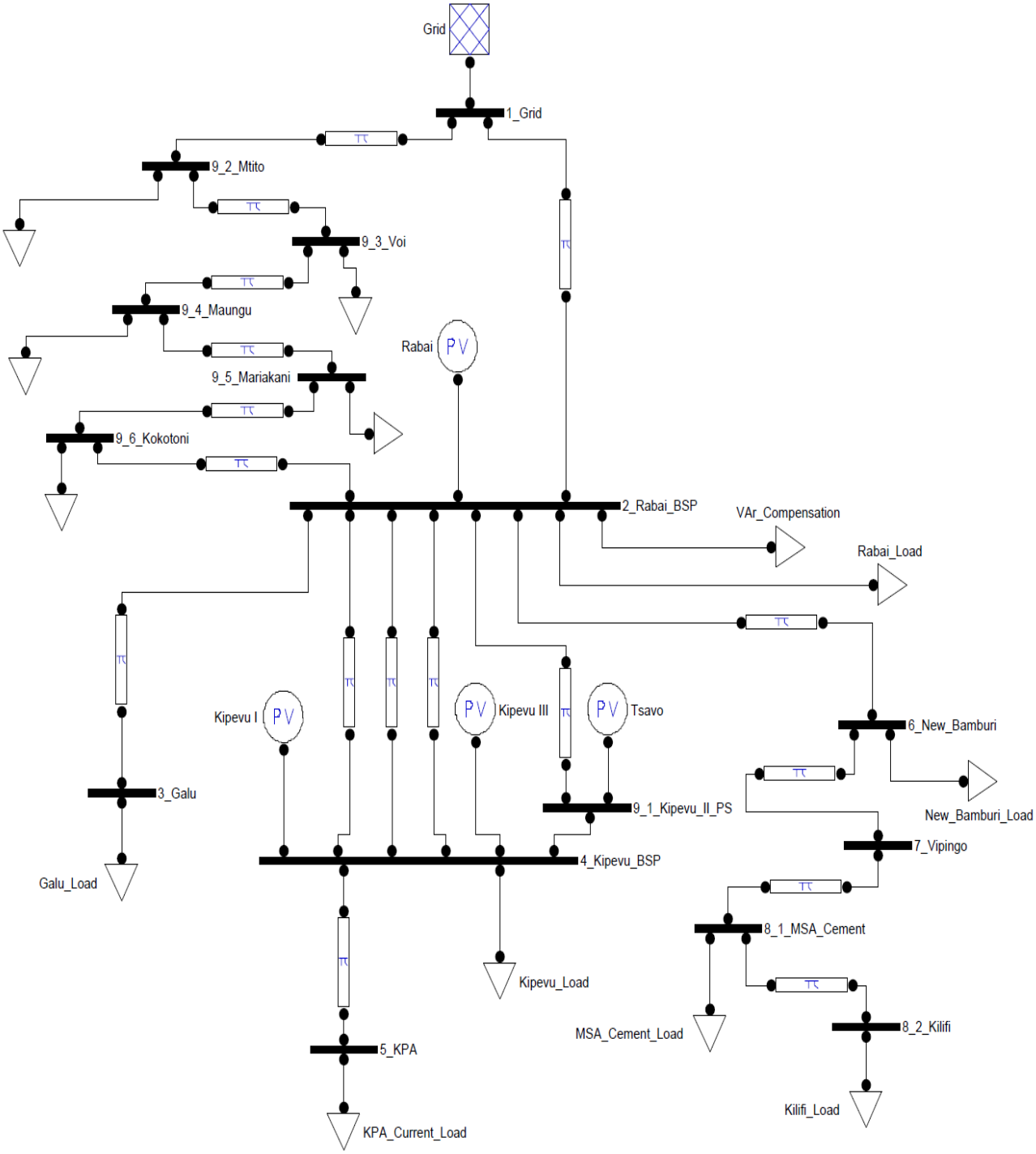


*Figure 3: PSAT/Simulink Coast 132kV network model*

# A Case Study -Reinforcing National Grid Using STATCOM Devices

Charles M. Ndungu and John N. Nderu

***Abstract***— Modern power system is a complex network comprising of numerous distributed generators, transmission lines, switchgears, distribution network and variety of loads. However, the quality of the power supplied to the end users is deteriorating as network expand due to inherent system disturbances such as voltage dips, harmonic distortions and phase angle deviations caused mainly due to low voltage network faults. This has resulted to high level of customers' dissatisfaction and complains. Research has shown that over 60% of system perturbations are caused by natural events such as lightning strikes and system faults. There are various methods power utilities are employing to realize a robust and reliable power transmission system. Such methods include re-conducting of transmission lines, construction of new transmission lines and in recent time installation of Flexible AC transmission system (FACTs) devices. The FACTS are power electronic devices that have ability of controlling the network voltage condition both in steady and transient state of complex power system. The most common power electronic controllers are, Dynamic voltage stabilizer (DVS), Static Synchronous Compensators (STATCOM), shunt compensators and Unified power flow controller (UPFC). The STATCOM devices are the most widely installed power electronic controllers as they provide excellent performance in stabilizing the power system both in steady state and non-steady state (system disturbances) conditions. It is for this reason the author propose installation of STATCOMs to reinforce the Kenya Power national power grid to achieve a robust and resilience system which improves the power quality supplied to the end users.

***Keywords*****:** FACTS, Power quality, Power utility, STATCOM

## I. INTRODUCTION

**A**ny power system has inherent transients that can originate from switching operations (circuit breaker operations, capacitor switching), system faults, lightning strokes, loading of a single large load/ loss of a single large load. The adverse effects of system disturbances are devastating. The major impacts on power system are voltage collapse, voltage dips/ swell or system transients (impulse or oscillatory). A weak system is very vulnerable to system disturbances because line faults usually results to wide spread power outage. This is very rampant occurrences in developing countries. To improve quality of power supplied to the power end users, most power utilities add transmission lines and interconnected them with existing installations. In some solemnly cases, they increase thermal generations at the load center. These mitigation measures are expensive in terms of cost of implementation and time. With advert of power electronic devices such as Thyristors, IGBT, MOS-FET, they have offered a cheaper and faster alternative in stabilizing the power system and making it more reliable and robust both in steady state and transient conditions [1].

The Kenya Power owns and maintains transmission lines and distribution network at the following nominal voltages: (i) Transmission 132kV, 220kV, and 400kV (ii) Sub Transmission- 66kV, (iii) Distribution - 33kV and 11kV and (iv) Low voltage network- 415V and 240V. With the ever increasing of load connected to the existing network as country economy grows, the needs to continually expand and enhance the power system is inevitable in order to meet the additional power demands. With additional 5,000MW expected to be brought on board into the grid by 2018, the existing system and upcoming new transmission lines needs to sustain the power flow with minimum interruptions even in the presence of system perturbations. Due to recently awareness of the customers regarding the requirements of a quality power supplies, it is pertinent for the power utility to meet the laid down statutory power supply requirements. This paper propose installation of STATCOM devices to ensure that the power utility supplies a quality power that is within the statutory requirements as defined by Kenya Bureaus of Standard (KBS) and power regulatory bodies.

The STATCOM is a dynamic shunt compensation device connected to the transmission network to provide dynamic reactive support, balanced as well as unbalanced, to control the voltage to a set point and also provide dynamic support during network contingencies [2]. A STATCOM consist of power electronic converters that damp the changes in transmission system and maintain steady state and transient margins. They are designed to enhance controllability and increase power transfer capability of transmission lines. The STATCOM is one of FACTS family. FACTS devices employ both passive and active elements. Passive element includes inductors and capacitors and on the other hand active elements include IGBT, Thyristors, MOSFET and GTO. The FACTS devices enhance transmission system control and increase line loading up-to the thermal limits without compromising it reliability. Further, it enables the power utility to delay constructing of new transmission facilities and instead maximizes on existing transmission assets [3]-[4]. The FACTS devices can be thyristor switched or static controlled. Thyristor switched employ ON-OFF principle while static controlled employs static elements such as IGBT, MOSFET, or MOS-controlled thyristor (MCT).

The circuit below Fig. 1a depicts elements of STATCOM while Fig. 1b shows a photo of active element (MOSFET).

C. N. Ndung'u Electrical and Electronic Engineering, JKUAT: +254722837236; e-mail: cndungu03@yahoo.com.

J. N. Nderu Electrical and Electronic Engineering, JKUAT (e-mail: adjainderugac@gmail.com.

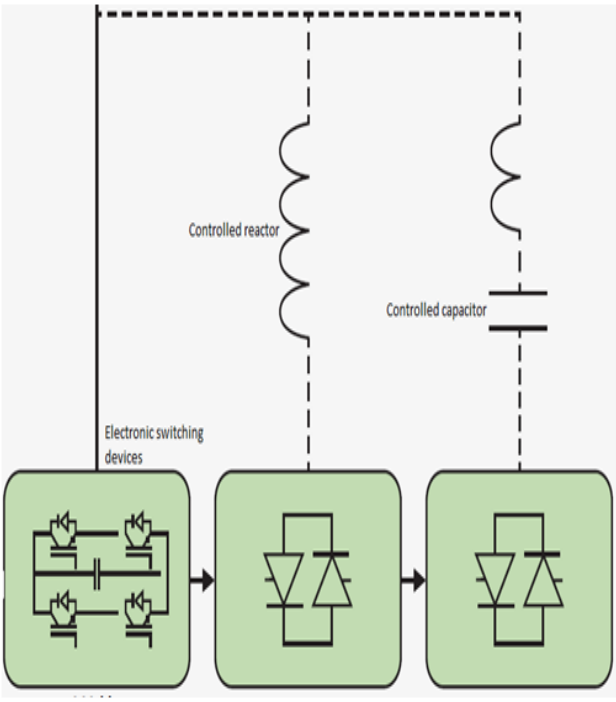


Fig. 1a Elements of the STATCOM
*Source: ABB- An introduction to Facts-2006*

Fig.1b A photo of installed MOS-FET
*Source: ABB- An introduction to Facts- 2006*

1.1. Type of FACTS devices

The table I hereunder presents various types of FACTs devices and their main applications

TABLE 1
FACTS TYPE

| | Load Flow Control | Voltage Control | Transient Stability | Dynamic Stability |
|---|---|---|---|---|
| SVC | | | | |
| STATCOM | | | | |
| TCSC | | | | |
| UPFC | | | | |

*Source: PSD: Power System Dynamics- April, 2016*

Where;

SVC –Static Var compensator, STATCOM- Static Synchronous Compensator, TCSC –Thyristor Controlled Series Compensator, UPFC- Unified Power Flow Compensator

From table 1 above, STATCOM offers a wide range of solutions for perpetual challenges experienced by power system. It is imperative noting that UPFC is not often considered despite giving superior results because of high cost of implementing and maintenance costs. In additional, it requires a robust network which currently the Kenya utility is yet to establish.

## II. MODERN POWER SYSTEM

Continued urbanization, electrification of railway transport and increased use of renewable energy sources such as wind power, place more stringent demands on new and existing infrastructures. It is worth noting in recent time that construction of new transmission lines is becoming difficult and time consuming due to the challenge of acquiring the rights of

way and cost of construction. As result, the existing infrastructures are getting constrained day after day as more loads are added which were not
factored during the design stage. For the power company to meet the statutory regulations of voltage variations limit as stated in IEEE 519-1992 [5], KS 2236-3 [6] and KS 2236-4 [7], two options are proposed;

i. Increase thermal generation at load center
ii. Install STATCOM devices at selected major primary substations

The first option requires ERC approvals and has ripple effects of increasing the price of electricity tariff which can slow down country's economic growth. In contrary, installation of STATCOM enables the power utility to comply with the statutory requirements without impacting negatively on price of the electricity.

*A. The advantages STATCOM device*

The STATCOM has numerous advantages. These include;

i. Control the power flow as system demand
ii. Increase the loading capability of lines to their thermal capacities
iii. Increase the system security through raising the transient stability, limit the short circuit currents and over-load
iv. Prevent cascading of black-outs by damping the system disturbances and oscillation
v. Reduce reactive power hence reducing power losses along transmission lines
vi. Increase utilization of lowest cost generation among the generation mix
vii. Strength a weak system by providing required voltage support during contingencies events thus stabilizes the voltage; eliminates voltage dips/ swell in the network
viii. Reduces frequent transformer tapping for voltage regulation and shunt capacitor frequent switching
ix. Allow system to operate over large range of loading profile without power and voltage oscillations (*as shown in Fig. 2 below*)

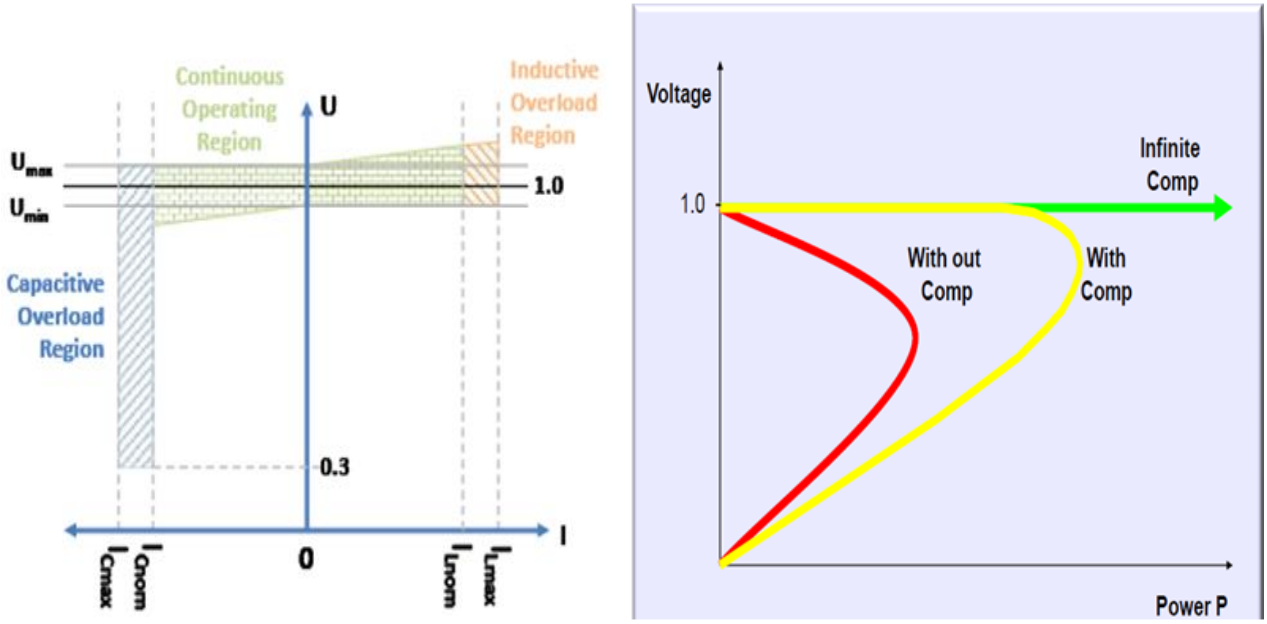


Fig. 2 Operating range of STATCOM
Source: ABB- An introduction to Facts-2006

Where;
Comp implies presence of STATCOM in the system.

It is vivid from fig. 2 that installation of STATCOM improves the voltage profile under system transients and disturbance conditions.

From the above benefits of installing STATCOM in the power system, it is vivid that the STATCOM devices enhances quality of power supplied to the end power users (hence *less complains*).Further it enables the power utility to reduce technical losses and optimizes its existing infrastructures. As observed in one of the large power consumer with issue of poor power quality (*see the voltage profile as captured by the power quality equipment*), installing STATCOM will mitigate the voltage dips which adversely affects the production process of the manufacturing firms by smoothening the voltage profile as shown in Fig. 3 below.

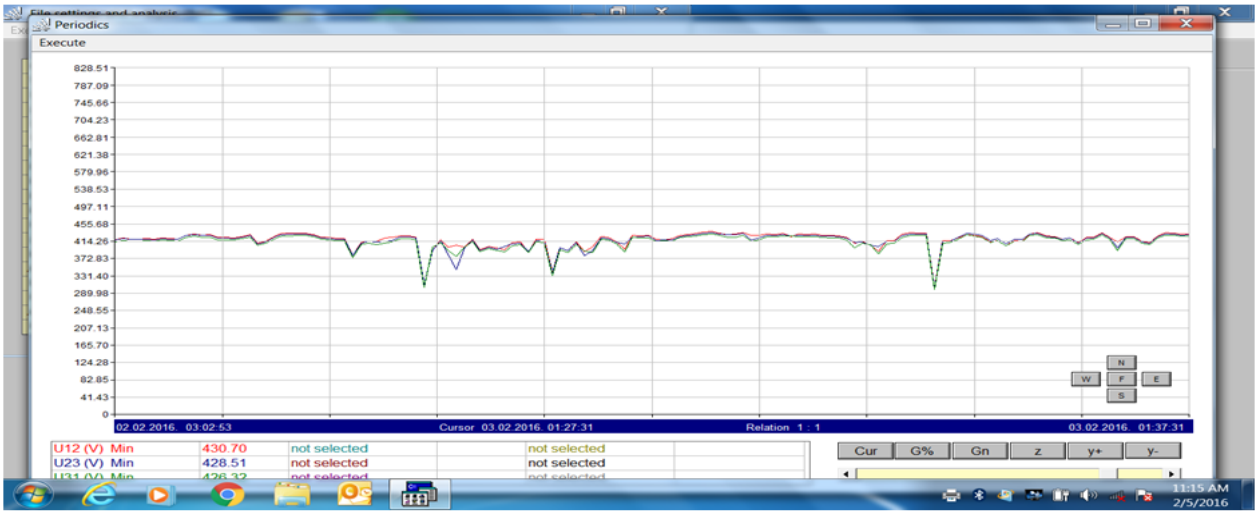


Fig. 3 Power quality at Serana hotel –Mombasa

*Source: Kenya power –power quality data at Serena Hotel on February, 2016*

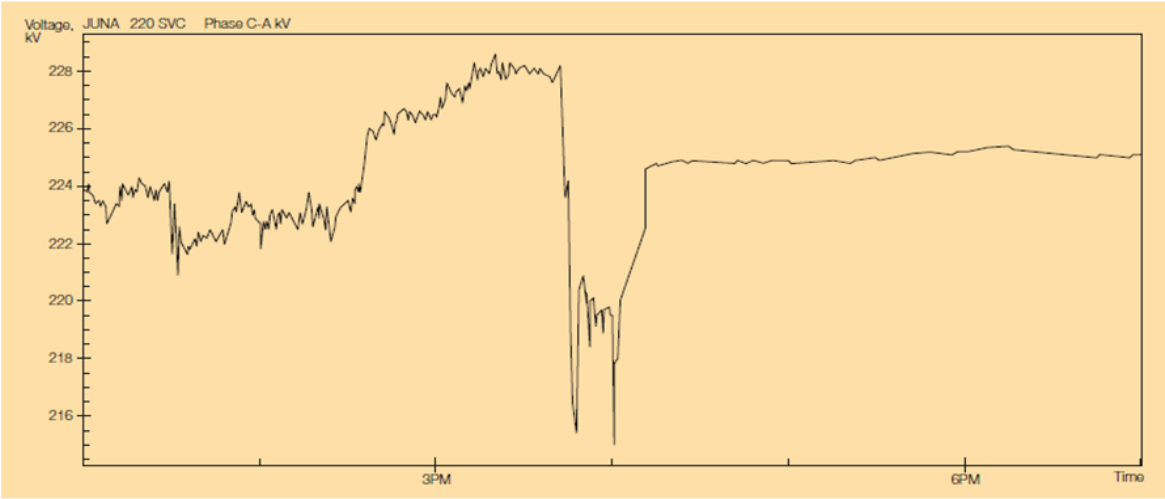


Fig. 4 Voltage waveform before and after installing a compensator [2].

*Source: ABB- SVC for voltage support of 220kV grid feeding mining loads in Western Austria*

It is clear from Fig. 4 that fast response of static compensator improves drastically the voltage profile of power grid and consequently the power quality supplied to the end power users. It can also be deduced that static compensator improve performance of the manufacturing firms by eliminating voltage dips which adversely affect operation of machines with variable speed drives and Switch Mode Power Supplies (SMPS).

## III. KENYA POWER CASE STUDY

In recent time, the power quality supplied to the large power consumers have deteriorated considerably prompting the end power users perpetually keep on complaining to the power utility of poor power quality. This is mainly due to extensive expansion of the network and overloading of existing infrastructures beyond their designed capacity. Expansion of network has increased susceptibility of the system to earth faults and vandalism of the switchgears such as transformers and permanent earthing wire. On the other hand, overload has resulted to frequent operations of overload detecting devices such as auto-reclosers and fuses. Also noted is frequent phase failure due to line jumpers snapping and hotspots at primary and secondary substations. The other main cause of poor quality of power supplied to the end users is location of the generation stations and restriction of energy regulation body on use of the thermal generations which are strategically installed at load center. Geothermal and hydropower generations, which are the main power sources in Kenya, the power has to be transmitted using high voltage transmission lines to the load centers (Nairobi, Mombasa and Kisumu). As result, there is highly ohmic losses which contribute to low voltage at receiving end. It is this reason why regions such as coast region and western Kenya have frequently be experiencing voltage dips and low voltage at end users. It is worth noting that any major or minor perturbations along the transmission lines (*caused by lightning strikes, line fault*) usually results in a wide-spread power outages.

To mitigate susceptibility of power system to voltage collapsing and voltage dips, installation of STATCOM devices will result to a desired system performance even under the

above stated conditions. This is because the STACOM will stabilizes the voltage and increase power transfer capability of transmission line evacuating power from Hydro and geothermal power generations. Moreover, the STATCOM will also improve voltage without necessary adding thermal generation in coast region. Worth noting is that there is 66kV STACOM available which does not need transformer to interface to the power system. This reduces the cost and installation time.
To install the STATCOM, the followings are prerequisite requirements that power utility need to undertake or contract;

*B. Training of the implementing team.*

It is pertinent to build human capacity by comprehensively conducting training on STATCOM specifications, procuring of contractor, system studies, installations, maintenance and servicing.

*C. Harmonic system analysis*

It is paramount to conduct system harmonic analysis on existing power network to establish the dominant harmonic voltage frequencies presents as to achieve desired STATCOM specifications. It is worth noting that STATCOMs inherently generate harmonics and there is need to mitigate voltage series resonance due to magnification of harmonic frequencies with line parameters (*shunt capacitors and series inductors*).

*D. Power system power flow studies*

Carrying-out power flow studies is a prerequisite requirement to enable designer to realizes optimal ratings of the STATCOM and ideal location for installation. This enable the power utility to spend less in initial capital investment and achieve the desired system performance as highlighted above.

## IV. CONCLUSIONS AND RECOMMENDATIONS

### A. Conclusions

The STATCOM is one of family of FACTs that consists of power electronic switches such as IGBT or MOSFET for improving power quality supplied to the end users. The STATCOM has been on the market from 1990s and is already installed globally by many countries. Example of some of countries embraced the STATCOM technologies are South Africa (ESKOM), India, Saudi Arabia (SEC), Mozambique (Edm), USA at Austin Taxas, and Chile at Cerro-Navia. After installation of STATCOM, the power utilities have benefited mainly on the voltage profile stabilization, improvement of utilization of existing transmission equipment and reduction of technical losses.

### B. Recommendations

It has been noted that there is dire need of strengthening the grid network especially at Western, Coast and Nairobi regions. In recent time, power quality has attracted a lot of attention globally due to advent of sensitive equipment which are susceptible to power variations within a narrow bandwidth. In this regard, there is need for Kenya Power to employ the latest technologies to optimize the existing infrastructures and improve the power quality supplied to the end users.

Further, the country is gearing toward transmitting and distributing additional 5000 MW by 2018, hence there is need to establish a robust and resilience power network that can withstand inherent system contingencies. One economical and fast method is to install STATCOM devices, a technology which has already been implemented by other power utilities and has proven to improve power system stability and utilization of existing transmission assets to their thermal limit.

## REFERENCES

[1] V. Chris, "Introduction to dynamic reactive power compensation'', 2nd edn- 2016 pp. 6-18.
[2] B. Sep, *A introduction to SVC and STATCOM*, Journal of research in electrical and electronic engineering (ISTP- JREEE), 2014
[3] M. Thompson and Alex Kuska, *Power quality notes*, Worcester Polytechnic Institute, 2005.
[4] S. Surya, Q*uality requirement for reliable; towards 'perfect' power quality, advanced electricity infrastructure workshop*, Nov-1-2, 2007, Stanford University
[5] *IEEE standard 519-1196*, Recommended practices and requirements of harmonic control in electrical power system, 1996
[6] *KS 2236-3*, Electricity supply quality supply – Part 3 Voltage characteristics capability levels and assessment methods, 2012
[7] *KS 2236-4* Electricity supply- quality of supply part 4 application guidelines for utilities' 2012

# Online Portal Requirements for Computer Science Researchers in Kenya

Stephen Kimani and Daniel Gitahi

***Abstract:*** Computer science research is an expensive undertaking which often requires procurement or availability of expensive state-of-the-art specialized research tools, facilities and forums, which are not readily available in developing countries due to limited financial resources. In addition to this, the available initiatives and portals to address this issue do not provide enough resources and opportunities that are directly relevant to researchers in computer science. They are also not designed with contextual needs and preferences of computer science researchers from developing countries. This research work, therefore, describes a study, in which online portal user requirements of computer science researchers from Kenya, one of the developing countries, are analyzed taking into account their contextual needs and preferences. The study majorly sought the challenges encountered by the aforementioned researchers. In addition, it looked into features and services desirable for Computer Science researchers as well as the most important design characteristics that should be incorporated in an online portal to overcome reported challenges by Kenyan computer science researchers. Building on the findings of this study, we intend to design and develop an online portal that will provide a consolidated or integrated channel to computer science resources and opportunities for active and potential computer science researchers from a developing country, Kenya.

**Keywords:** Online user requirements, online portals, Computer Science, researchers, developing countries.

## I. INTRODUCTION

Research materials meant for computer science researchers such as books and journals, and forums such as conferences and workshops, are normally expensive. This is especially the case for potential computer science researchers from developing countries like Kenya. World Wide Web (WWW) holds a lot of resources offered freely or at nominal prices that can be of great help to researchers. However, these resources are usually scattered all over the WWW making it difficult for the computer science researcher to effectively and efficiently find, manage, and exploit them. Additionally, these researchers face numerous challenges such as limited internet access due to poor internet infrastructure. Other challenges include inconsistency and subscription fees needed in accessing these resources. To address these challenges, it is important to develop an online application or portal that provides a consolidated or integrated channel to all computer science research resources as well as opportunities that are relevant to all researchers including those from developing countries.

This paper describes requirements of an online portal for Computer Science researchers in Kenya. It puts into consideration the challenges they face, design features they would want incorporated in the portal and the specific services and features that the portal should provide.

## II. RELATED WORKS

Over the past few decades, web portals have become gateways through which resources and information found online are accessed. This has risen following the emergence of Web 2.0 technologies and availability of large volume of content found online. As indicated by Arthur[2], a web portal can be seen as an all-in-one website that provide access to other websites and services of guiding and directing users to relevant content, thus shielding users against chaos of the internet. In respect to research- oriented perspective, there exist several initiatives and portals that provide access to career and literature resources. They include: Science Careers (SC) that provides career resources for scientists as well as effective recruiting solutions for employers [6], Online Access to Research in the Environment (OARE) [5] that makes global scientific research in the field of environmental sciences available online to environmental scientists, researchers and policymakers in the developing world for free or at nominal cost, Health InterNetwork Access to Research Initiative (HINARI) [4] that enables developing countries to gain access to biomedical and health literature, Access to Global Online Research in Agriculture (AGORA) [1] that provides free or low cost access to major scientific journals in agriculture and related biological, environmental and social sciences to public institutions in developing countries, and the Global Development Network (GDN) [3] which supports multidisciplinary social science research in order to increase local and policy- relevant knowledge and make it easier for researchers and policymakers to share knowledge, thereby advancing development.

However, none of these portals provide resources and opportunities that are directly relevant to researchers in computer science. In addition to this, the design and structure of these portals do not address contextual needs and preferences of computer science researchers from developing countries.

Efforts, however, have been put by previous works, looking into different aspects related to portal development. In a research conducted by Chen et al. [8] that described the design of a contextual information portal, it is evident that informational portals are useful particularly for groups that experience poor network connectivity or lack internet access. They noted that in developed countries, good network and internet connectivity gives users luxury to use many search queries in a search engine, thus retrieving particular information of interest from the World Wide Web. They contrast this with developing countries and

*Stephen Kimani: School of Computing and Information Technology, JKUAT , Email* stephenkimani@gmail.com

*Daniel Gitahi, School of Computing and Information Technology, JKUAT, Email:* gitahidanwa@gmail.com

note that users in rural areas lack this luxury due to poor network infrastructure and low bandwidth connections. Addressing the same concerns, Chen et al. [8] pointed out that a contextual information portal for developing countries should be low cost as well as scalable, and should be both searchable and browse-able in a fashion that is consistent to the appropriate context.

In a similar work by Sergeant et al. [9] that sought to gather user requirements needed for the development of a portal-based virtual research environment, focusing on Geography and Medicine research staffs, it is evident that users require an easy to use tool that is available even in areas with poor network and internet connectivity. According to the findings of their study, information finding, funding, collaborations, and research outputs are of great concern to users. According to Sergeant et al. [9], ease of information finding in a portal determines the audience gathered by a particular portal. In their study, respondents indicated that researchers need an easy to use tool through which they can search multiple data sets using advanced search mechanisms. The tool should also allow researchers create their own personalized search strategies. Addressing the funding concern, respondents in Sergeant et al. [9] study reported that a portal should additionally give alerts to new funding opportunities, view previously submitted works and should generally simplify grants management. For collaboration as a concern, respondents raised the need of email access via portal alongside working collaboratively on files and documents, and finding out expertise among themselves. Finally regarding research outputs, the study revealed the need for a place to access full-text publications


DOI: http://dx.doi.org/10.1145/12345.67890 and a place to upload their full-text research works.

The findings reported by Sergeant et al. [9] conforms to findings reported by Kimani et al. [7] in a study that entailed online portal requirements for Kenyan female university science &technology students, researchers in developing countries. The challenges echoed in these two studies show that portals are crucial tools in research-oriented groups. According to Kimani et al. [7], female science and technology students lack internet connectivity and adequate web resources to conduct their work. The study also reported user requirements for a portal that would address their concerns. The respondents in this study indicated that a portal that provides information about scholarships, job search, career advice, expert advice, technical support, and contests & awards would suit their needs.

Despite the fact that all these studies revolve around portal-based technology to address the issues pertinent to information needs in developing countries, none of them looked into the contextual needs of computer science researchers in respect to resources they need and challenges they face. For this purpose, this paper presents findings on user requirements for an online portal for Computer Science researchers in Kenya.

## III. STUDY SET UP

The main aim of this study was to determine the requirements for an online portal for Computer Science research resources and opportunities that are relevant to Computer Science researchers in Kenya. As our major primary data collection method, we designed and administered an online questionnaire that was distributed via email targeting computer science researchers in Kenya. The questionnaires were administered between June and September 2016. Out of the contacted target respondents, 63 responded and our analysis is based on the responses of these respondents.The questionnaire had questions on: demographics of computer science researcher respondents, internet access and usage, familiarity with existing portals and challenges faced while using them, and desirable requirements for an online portal for Computer Science research.

## **IV**. INITIAL FINDINGS AND PRELIMINARY USER REQUIREMENTS

The respondents are computer science researchers, majority of who have research interests in Artificial Intelligence, Web Design, Computer Security, Computer networks, Data Mining and Warehousing, Human Computer Interaction, Software Engineering, Database Systems, and Mobile Computing. 34% of these respondents have conducted research in computer science for 1 year or less, 31% for over 1 year to 3 years, 22% for over 3 years to 5 year, while 13% have conducted research for over 5 years. As a majorsource of information in computer science research, 33% use online journals, 24% use conference papers, 22% use e- books, while 21% use web portals.

In order to understand the nature of an integrated and personalized portal that would primarily address the needs of computer science researchers, we sought the main challenges they face while using the existing portals, the design features they would want incorporated in the portal, and the specific services/features relevant to their research work and activities. The findings are as presented below.

### **A.** MAIN CHALLENGES

Computer science researchers face a number of challenges. According to the study, out of the 63 respondents, 44 (70%) indicated that most of the content requires subscription/payment, 36 (57%) lack awareness about the existence of web-based resources for computer science research, 28 (44%) experience slow internet access, 24 (38%) lack web-based resources for computer science research and those available are inadequate, and scattered all over the world wide web. In addition, 23 (37%) respondents highlighted unreliable/intermittent internet access as a challenge while 20 (32%) said they lack internet access. Further, 18 (29%) respondents indicated that content and design of the few available resources is not relevant to the needs of researchers from developing countries while 16 (25%) raised concerns about their online privacy and trust. However, lack of time was not raised as a significant challenge since only 4 (6%) of the respondent lack time to conduct their research activities. These challenges can be seen in Fig. 1.

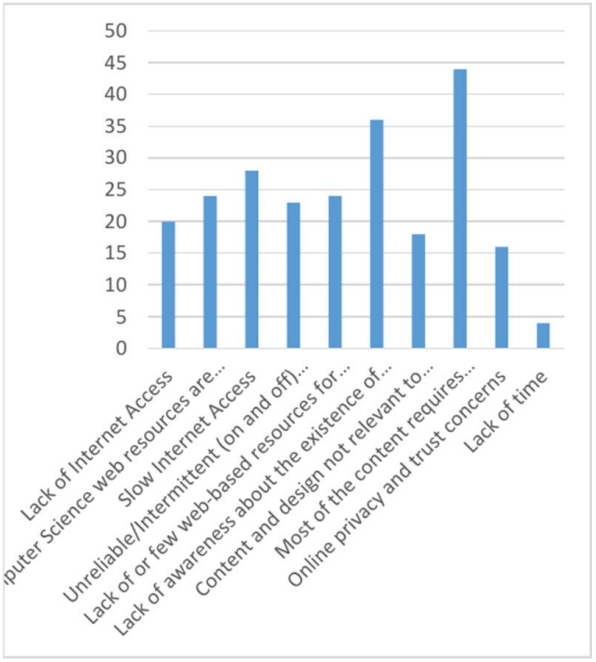


Fig.1. Challenges that Computer Science Researchers experience

### B. Design Features

Computer science researchers also indicated the importance of design features they would want included in an online portal for their research activities. According to the study, 75% of the respondents reported efficiency and protection of user privacy as very important features, and 70% reported that provision of help facilities, response to user instructions and ease of navigation and access to items of interest are very important features to include in the portal. 68% highlighted ability to enable users recognize, diagnose and recover from errors as a very important feature. In addition, 67% reported that easy to reverse or cancel action, and easy to understand and use are very important features while 65% indicated that familiarity and metaphors, provision of error prevention mechanisms and keeping users informed about its current state are very important features too. Consistency and provision of all services/features user wants were also reported as very important features, taking 62% of the respondents. Further, it was reported as very important that the portal be visually appealing, provide more than one way of doing things, and be personalized to the specific needs or profile of users by 56%, 54% and 52 % of the respondents respectively as seen in Fig.2.

### C. Desired specific services/features

In respect to the specific services/features relevant to their research activities, computer science reseachers rated their importance as very improtant, important, slighlty important and not important.

According to the study, accessibility of e-books, information on successful computer science researchers from developing countries, journal publications, research grants, conference proceedings/publications, and research news/events, topped the list of the very imporant specific services/features reported by 84%, 83%, 79%, 78% ,76% and 73% of respondents respectively.

Following closely is accessibility of research jobs with 68% of respondents, and research career advice, academic scholarships & bursaries, research awards & prizes, research fellowships, and support of online discussions & forums each reported by 67% of respondents.

In addition, accessibility of research mentees and research mentors were also reported as very important services by 62% and 63% of the respondents respectively. All the other listed as specific service/feature were reported as very important as. well but by less than 55% of the respondents as expounded by Fig. 3

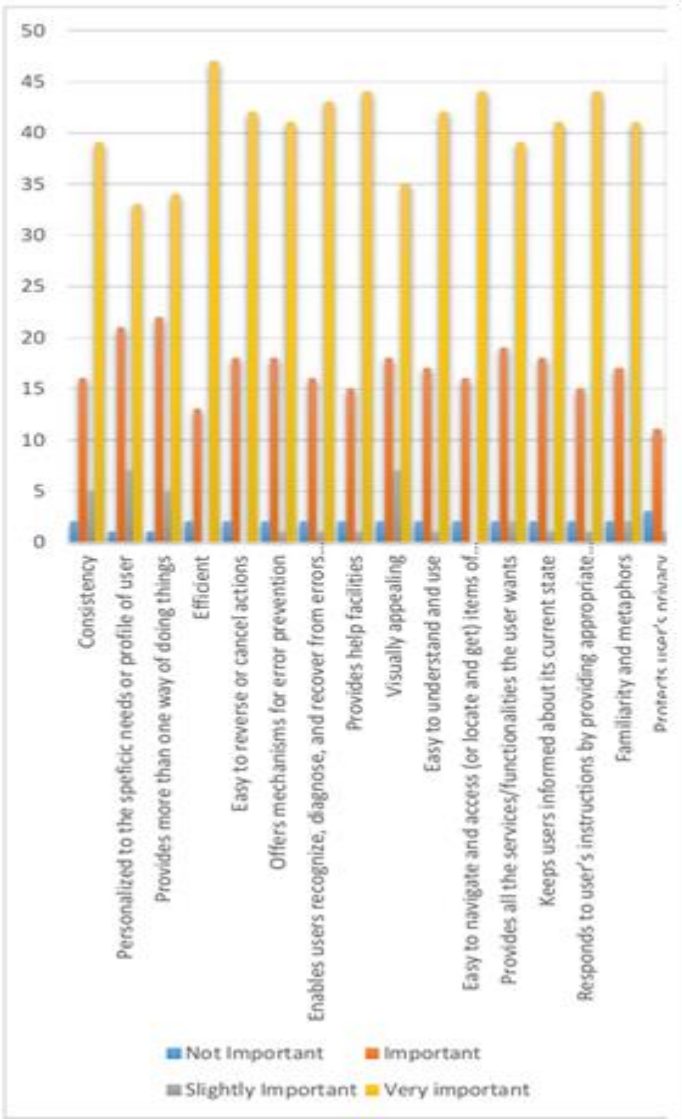


Fig.2. Design features for Computer science researchers' portal and their importance.

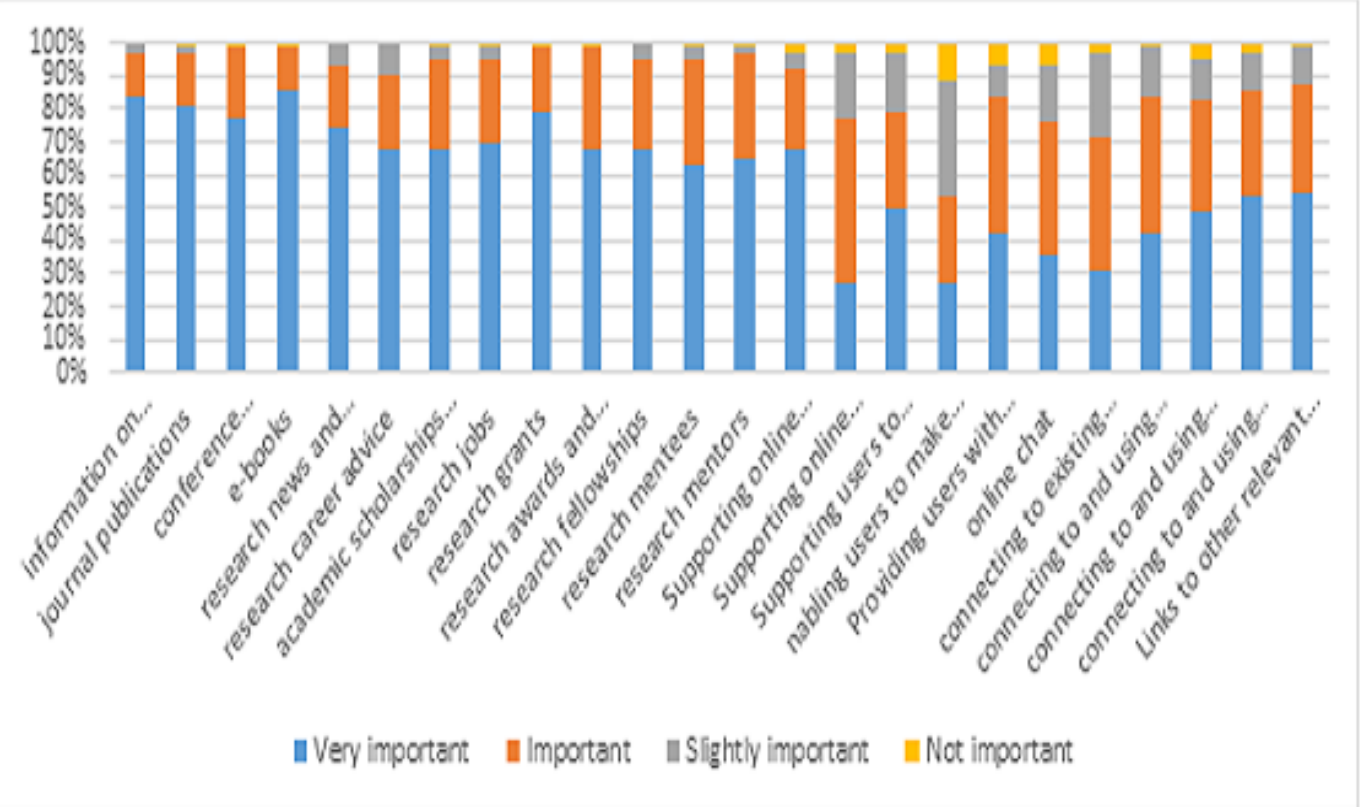


. Fig.3. Desired specific services/features for a computer science research portal and their ratings

## V. DISCUSSION

Among the key outputs of this study are main challenges faced by computer science researchers, design features that would be included in a portal to address the challenges identified and specific services/features relevant to computer science research activities. The main challenges highlighted by this study rhyme with the findings of Chen et al. [8], which recommended a portal with topic extraction, document classification, focused crawling, and information organization. These seek to address the challenge that contents are scattered all over the web. Chen et al. [8] also noted that provision of high bandwidth in developing regions is economically infeasible citing factors such as low demand and high cost of connectivity. This reflects the challenge of lack of internet/intermittent connectivity unveiled in this study, which directly relates to lack of awareness about existence of web resources. On the one hand Sergeant et al. [9] reported the need for information finding, funding, collaboration, and research outputs. This current study on Kenya on the other hand has reported the need for information about scholarships and bursaries, research grants, fellowships, online support for collaboration, and research mentors and mentees as a reflection of sharing expertise.in science research resources and opportunities to active and potential computer science researchers in Kenya.

## ACKNOWLEDGMENTS

We wish to thank Jomo Kenyatta University of Agriculture and Technology (JKUAT) for supporting this research.

## REFERENCES

[1] AGORA (2017). Access to global online research in agriculture (AGORA) Available online at http://www.aginternetwork.org/en (accessed 25th January 2017).

[2] Arthur T. (2005). Web Portals: The new gateways to Internet information and services. USA: Idea Group Publishing. Pp. 3-8.

[3] GDN (2017). The Global Development Network (GDN). Available online at http://www.gdnet.org (accessed 25th January 2017).

[4] HINARI (2017). Health internetwork access to research initiative (HINARI)(http ://www.healthinternetwork. org (accessed 25th January 2017).

[5] OARE (2017). Online access to research in the environment (OARE). Available online at http://www.oaresciences.org (accessed 25th January 2017).

[6] SC (2017). Science careers. Available online at http://sciencecareers.sciencemag.org (accessed 25th January 2017).

[7] Kimani, S. Mwangi E., Mwangi, W. & Njue,J (2013). Online requirements and portal design for female university science & technology students in Kenya.

[8] Chen.J., Karthik, T. & Subrmanian, L. (2010). Contextual Information Portals.

[9] Sergeant, D.M., Andrews, S. & Farquhar, A. (2004). Embedding a VRE in an Institutional Environment (EVIE). Workpackage 2: User requirement analysis.

# Development of an Oxygen Concentrator (Generator) for use in a waste oil burner (gasification process)

Edwin K. Lagat

***Abstract*—**Environmental pollution by industrial combustion and heating processes is a major concern and problem faced by humanity. For future generations, there is an urgent need to conserve our environment to curb carbon dioxide emissions and reduce other harmful pollutants generated during combustion of fossil fuels. This calls for proactive approaches in dealing with combustion of fossil fuels and pollution control as opposed to reactive approaches.

A lot of research is ongoing to avert pollution due to combustion of fossil fuels. A major breakthrough has been combustion in a stream of pure oxygen as opposed to use of air in combustion. One of the key benefits in the elimination of nitrogen from air in combustion is reduction of NOx level produced, and higher flame temperatures can be attained thus extracting as much energy content from the fuel. Existing oxygen generation systems have weaknesses and challenges in that it is expensive and mostly not available on site.

This research involves development of an onsite oxygen generator for use in oxy-fuel and gasification process with capability to produce oxygen with purity of 95 percent. The method to use is adsorption sieve technology to generate oxygen from air at ambient temperature.

It is expected that the designed oxygen generator will be tested to see the effect of its geometry, and test the influence of flow parameters on its performance. This will go a long way in environmental conservation and ensure that fossil fuels re a clean source of fuel for use in power generation and industry.

**Keywords -** Combustion, oxygen generator, pollution.

## I. INTRODUCTION

The use of fossil fuels for energy production and heating is very important for economic growth and for industrial processes and operations. Unfortunately, the use of fossil fuels has contributed a lot in terms of air and environmental pollution and degradation. The combustion of the fuels occurs in presence of air or a stream of air. The air is composed of many elements but oxygen is the only supporter of combustion.

Industrial combustion is key to industrial processes and power generation by converting the energy in fossil fuels to a usable form for driving engines, providing heat requirements and power generation. However, industrial and economic expansion has come at a cost and it is the biggest contributor to air pollution globally. The by-products of combustion in air are the NOx, SOx, carbon monoxide and $CO_2$, which are all pollutants. Pollution has been blamed on environmental degradation, global warming, and chronic respiratory health complications afflicting populations especially in industrially populated areas and its environs.

The best bet on the control of pollutants is pre-combustion control, by carrying out combustion in a stream of air highly enriched in $O_2$ with $N_2$ removed and eventual capture of $CO_2$ in a process known as carbon capture and sequestration (CCS) [17][20][28][36][37]. The capture rate for $CO_2$ is 100% with purity of 95% when combustion takes place in a stream of 95% pure $O_2$ [21] [28].

## II. LITERATURE REVIEW

The three main methods that have been used for pollution control in power plants are pre-combustion control, post combustion control and oxy-fuel combustion.

Oxy-fuel combustion is proving to be the best bet so far. This technology entail carrying out combustion in a stream of oxygen as opposed to air. The oxygen can be gotten in a variety of ways from chemical reaction generation and separation of air into its primary components. Industrially air separation offers better economics and in this regard they are further classified into two methods, cryogenic air separation and non-cryogenic air separation.

### a) CRYOGENIC AIR SEPARATION

Cryogenic air separation technology utilizes cooling and liquification of air, then selectively distilling the components at the various boiling points. The process is good when purity greater than 99.99% are desired, volumes larger than 1000 tons per day are required. Due to the fact that cooling is an essential step, the process is energy intensive and very expensive to set up [20] [21]. For a typical power plant the total set-up cost for a cryogenic ASU (Air Separation Unit) is around 15% of the total power plant cost [8][11][20], with its

F. A. Author, Department of Mechanical Engineering, JKUAT (corresponding author to provide phone: +2540722000000; fax: +2546752711; e-mail: author@eng. jkuat.ac.ke).

S. B. Author, Department of Mechanical Engineering, JKUAT (e-mail: author@eng. jkuat.ac.ke).

energy requirements to operate it being in the range of 10% of the total power produced [8][20]. The energy consumption is substantial and for a modern cryogenic installation, it amounts to about 200kWH/t of oxygen [37], exceeding thermodynamic minimum (53.1kWh/t of oxygen) by almost 4 times. The space requirements are quite sizable [20]. An ASU capacity of 2000 tons per day requires and area of 10,000$M^2$ [21]. However, modern cryogenic air separation units (ASU) use expansion turbines for cooling; the output of the expander helps drive the compressor and efficiency is improved [8] [9] [30] [31].

Pawel Gladyz and Andrzej Ziebik[17] did a system approach to exergy analysis of a conventional coal fired power plant and oxy-fuel power plant with $CO_2$ transport and storage. They looked at the input-output model evaluating direct energy and material consumption, local exergy losses, cumulative exergy consumption and losses, and cumulative exergy efficiency. They observed that in as much as cryogenic air separation is efficient in $CO_2$ capture, transport and storage, the energy and exergy analysis points to a greater need for improvement in the processes for better utility, energy reduction and improved efficiency.

Dowling et al [30], in there research on an advanced equation based flow sheet to optimize a framework of cryogenic air separation design systems for oxy-combustion in power generation, established that cryogenic air separation is an efficient system and good for $CO_2$ capture system, in a fossil fuel power plant, but they did identify that it is a challenge in design because of the very low temperatures and refrigeration cycles involved thus requiring a very tight integration.

### b) NON-CRYOGENIC AIR SEPARATION

There are three main technologies used namely, membrane technology, chemical process and molecular sieving (adsorption) technology.

*1) Membrane Technology*

This technology involves passing air over a membrane filter. The membranes can be nano-porous or polymer, and the gas molecules penetrate according to their size or difusivity. The filter allows fast gases to pass through and the slow gases are retained and they are called retented gases. Oxygen is considered a fast gas, and nitrogen and argon are considered slow gases.

Varying levels of purity, upto 50 percent, can be achieved by varying the time that the gas spends undergoing filtration [13]. Its by-product capability is very low since the by-products still has other contaminants. Membrane technology has quick start-up times and operates at near ambient conditions, with low safety concerns. Capital costs with membrane systems increase linearly with output volume desired. Currently, membrane technologies can satisfy needs of up to 20 tons of oxygen/day. Its running and operation costs are low and
is favored in situations where required oxygen purity is low and the budget is limited. In the recent past there have been technological breakthrough in the membrane technology.

The ion transport membrane (ITM) has been developed by Air Products and Chemicals, in conjunction with the United States Department of Energy and Ceramatec. Reports have shown that this technology can produce greater than 99 percent purity O2 at much lower costs than cryogenic separation[8][11][13]. This technology is still under research and its efficiencies are very low [37].

*2) Chemical Process*

A number of materials have the ability to absorb oxygen at one set of pressure and temperature conditions, and release the oxygen at a different set of conditions. Air Products and Chemicals have investigated into this process and found that molten salt is a good candidate [8] [13].

Air Products and Chemicals operated a small-scale pilot unit that verified 99.9 percent oxygen purity at expected salt loading [13], however, corrosion of the salt/oxygen two-phase areas of the facility was determined to be an economic problem. The set-up cost has shown to be very high, its economic production range is undetermined as the technology is still in the infancy development stages. From the laboratory research, the by-product capability is very poor and the start-up time is very long. So far this technology has not yet been deployed for commercial use.

*3) Molecular Sieving (Adsorption Technology)*

Molecular sieveing or adsorption technology processes are based on the ability of some natural and synthetic materials to preferentially adsorb gases. These materials are called adsorbents. Molecular sieves are used as adsorbents for gases and liquids. Molecules small enough to pass through the pores are adsorbed while larger molecules are not. It is different from a common filter in that it operates on a molecular level and traps the adsorbed substance.

The adsorption processes rely on the fact that under high pressure, gases tend to be attracted to solid surfaces, or "adsorbed". The higher the pressure, the more gas is adsorbed; when the pressure is reduced, the gas is released, or desorbed. Pressure swing adsorption (PSA) processes can be used to separate gases in a mixture because different gases tend to be attracted to different solid surfaces more or less strongly. If a gas mixture such as air, for example, is passed under pressure through a vessel containing an adsorbent bed of zeolite that attracts nitrogen more strongly than it does oxygen, part or all of the nitrogen will stay in the bed, and the gas coming out of the vessel will be enriched in oxygen. When the bed reaches the end of its capacity to adsorb nitrogen, it can be regenerated by reducing the pressure, thereby releasing the adsorbed nitrogen. It is then ready for another cycle of producing oxygen-enriched air. Vacuum pressure swing adsorption (VPSA) lower the pressure in the tank to sub-atmospheric levels, hence improving the regeneration process. On the other hand we have temperature swing adsorbers (TSA) where temperature differential is used to adsorb and desorb the adsorbate.

PSA devices are best suited for processes that do not require extremely high purities of oxygen (less than 95 percent). However, the PSA's can achieve as high as 99.9 percent

purity but at a significant cost as compared to achieving 99.5 percent purity. PSA devices are best suited for small volumes of oxygen production, typically on the order of 200 tons/day.
Since the output of oxygen is largely controlled by the bed size in the PSA systems, costs rise linearly when higher volumes of oxygen are required. PSA devices take a few minutes to start-up, and it has very good safety record. Molecular sieve technologies have shown to have the lowest energy requirements when compared to other air separation technologies [13] [15].
Carlos Grande's [15] research works has shown that PSA in gas separation is a better solution which can be enhanced by having good interaction between material science and process engineering. He too has observed that the biggest challenge is in the development of cyclic strategies that can improve performances of the PSA. In as much as the process is very flexible, its process complexity has been a major issue in the deployment of the technology in various fields [15]. The usability of by-product nitrogen in PSA systems is limited because the nitrogen will have significant levels of oxygen [15]. This technology is semi-mature with room for technology improvements. Advances made in PSA is in technically in two domains, firstly in material sciences for adsorbent development and in engineering through development of new and more efficient ways to regenerate the adsorbent[15].
Research carried out by Liu Meng et all [29] has shown that in packed bed column adsorption the concentration and temperature of feed air strongly influence the equilibrium adsorption. The best fit has to be found for appropriate use with minimal energy cost. An increase in temperature reduces adsorption rate and vice versa. An increase in pressure on the other hand increase adsorption rate and capacity of the adsorbent.
The other drawback seen is the sequential arrangement of valves for adsorption and desorption which in the field has shown to be a problem with break downs being experienced many times. This is through observation and remarks made by the technical team at Laikipia Airbase Department of Defence nitrogen production facility using molecular sieve. Also Mabati Rolling Mills have a molecular sieve nitrogen generator and they experience the same too. Another big drawback of such systems is the production of by-products that are not usable.

## III. Gaps

The major challenge identified by many researchers [25][26][27] in non-cryogenic oxy-gen production is the production of high purity oxygen, cost, number of pumps and compressors, and energy requirements. The major cost component is the number of components required and energy consumption and requirements to run these facilities. Pure oxygen requirements are on the rise and there is need to have this oxygen at a low cost, low maintenance production facility, ease of start and stop operation.

The research works by Jan Mletzko and others [28], the $CO_2$ purity for CCS can be improved by having $O_2$ purity greater than 95 percent. Also, research work by Alexander Dowling et al [30], were able to corellate the purity of $CO_2$ with the purity of $O_2$ fed in, in as much as they had lingering questions on the optimal $O_2$ purity from the air separation unit (ASU), though they concurred anything greater than 95 percent will be best.

Getting the right cyclic strategy is a challenge in that the right matrix has not been well established. This affects the sequential arrangement of valves and getting the right sequence control.

In packed bed column adsorption the concentration and temperature of feed air strongly influence the equilibrium adsorption. The best fit has to be found for appropriate use with minimal energy cost. An increase in temperature reduces adsorption rate and vice versa. An increase in pressure on the other hand increase adsorption rate and capacity of the adsorbent.

The other gap seen affecting the non-cryogenic oxygen concentrator is the usability of the by-products. In all cases the by-products are exhausted back to the atmosphere which is a loss to the optimization of the process.

## IV. Conclusion

From the literature review it is found out that oxy-fuel combustion is the way to go in greenhouse gas emission control mechanism. Therefore the oxygen produced for oxy-fuel combustion or gasification process should overall be cheap and from a process that is not complex and onsite.

## References

[1] Glassman, I., Yetter, R.A., Combustion, Elsevier., 4th edition, 2008.
[2] Beer, J., High Efficiency Electric Power Generation; The Environmental Role, Massachusetts Institute of Technology Cambridge, MA 02139 USA
[3] Emsley, J., "Oxygen". Nature's Building Blocks: An A-Z Guide to the Elements, Oxford University Press, 2001
[4] Cook, Gerhard A.; Lauer, Carol M., The Encyclopedia of the Chemical Elements, New York: Reinhold Book Corporation, 1968.
[5] Prof Ralph Keeling www.scrippso2.ucsd.edu.
[6] Rao, Prakash.; Muller, Michael. Indutrial Oxgen: Its generation and Use, Center for Advanced Energy Systems, Rutgers, the State University of New Jersey, 2007 ACEEE Summer Study on Energy Efficiency in Industry.
[7] KLM Technology Group Air Separation Units - Engineering Design Guidelines, Rev 01, 2013.
[8] Air Products; website www.airproducts.com.
[9] Linde website; www.linde.com.
[10] Ye, Pengcheng.; Sjberg, Erik.; Hedlund, Jonas. Air separation at cryogenic temperature using MFI membranes, Microporous and Mesoporous Materials 192, (2014), 14 - 17..
[11] Air Products Technical Report Air Separation TechnologyIon Transport Membrane.
[12] Alsultanny, Yas A.; Al-Shammari, Nayef N. Oxygen Specifc Power Reduction for Air Separation, ENGINEERING JOURNAL Volume 17 Issue 1, (2013) ISSN 0125-8281 (http://www.engj.org/).
[13] Smith, A.R.; Klosek, J. A Review of Air Separation Technologies and their Integration with Energy Conversion Processes, Fuel Processing Technology 70 (2001) 115 - 134.
[14] Vinson, R.David. Air Separation Control Technology, Computers and Chemical Engineering 30, (2006), 1436 - 1446.
[15] Grande, A.Carlos. Advances in Pressure Swing Adorption for Gas Separation, International Scholarly Research Network ISRN Chemical Engineering Volume 2012, Article ID 982934, 13 pages..

[16] Taniguchi, M.; Asaoka, H.; Ayuhara, T., Energy Saving Air-Separation Plant Based on Exergy Analysis, Technical Paper Shinko Air Water Cryoplant Ltd, Kobelco Technology Review No. 33, Feb 2015..

[17] Gladysz, P.; Zi, A., Complex exergy analysis of an integrated oxy-fuel combustion power plant with C02 transport and storage, Journal of Power Technologies 95(1) 2015, 23 - 31..

[18] Lockwood, T., Developments in Oxy-Fuel Combustion of Coal, IEA Clean Coal Centre, August 2014.

[19] Anheded, M.; Yan, J.; Smedt, G., Denitrogenization (or oxyFuel Concepts), Oil and Gas Science Technology Vol 60 2005, 485 - 495.

[20] Lee, H.; Choi, S., Mun, H., Choi, H., Park, W., Seo, S.; Design considerations for ASU and CPU in 100MWe oxy-coal power generation), 1 Dept. of Mechanical Engineering, Korea Advanced Institute of Science and Technology, Daejeon, Korea, 2 Daesung Industrial Gases Co., Ansan, Korea, 3 Korea Electric Power Research Institute, Daejeon, Korea..

[21] Lee, H.; Choi, S., Proposed Process and Design Considerations for Air Separation and CO2 Purication in a 100 MWe OxyCoal Power-Generation System, Energy Technology,2013.

[22] Al-Abbas, H.A.; Nasser, J., OxyFuel Combustion in the LabScale and LargeScale FuelFired Furnaces for Thermal Power Generations, Thermal Power Plants- Advanced Applications, Chapter 3.

[23] Prax Air; website www.praxair.com.

[24] Carta,M.; Etal,An Efficient Polymer Molecular Sieve for Membrane Gas Separations, Science 339, 303(2013).

[25] Singh, R.; Koros, W. J., Carbon molecular sieve membrane performance tuning by dual temperature secondary oxygen doping (DTSOD), Journal of Membrane Science, 2013.

[26] Mitchell, L. A.; Tovar, T.M.; LeVanM. D., High pressure excess isotherms for adsorption of oxygen and argon in a carbon molecular sieve, Carbon 74, 2014, 120-126.

[27] Ferreira, D.; Boaventura, M.; Barcia, P.; Whitley, R. D.; Mendes, A., Two-Stage Vacuum Pressure Swing Adsorption Using AgLiLSX Zeolite for Producing 99.5+ percent Oxygen from Air, Industrial Engineering Chemistry Research December 2015..

[28] Mletzko, J.; Ehlers, S.; Kather, A., Comparison of Natural Gas Combined Cycle Power Plants with Post Combustion and oxy fuel Technology at Different Capture Rates, Energy Procedia 86 (2016) 2-11.

[29] Meng, L.; Dongsheng, Y.; Liping, P.; Qingni, Y.; Yong, H., Experimental and computational investigation of adsorption performance of TC-5A and PSA-5A for manned spacecraft, Chinese Journal of Aeronautics, (2015), 28(6): 15831592.

[30] Dowling, A.W.; Balwania, C.; Gaoa, Q.; Bieglera, L.T., Equation-Oriented Optimization of Cryogenic Systems for Coal Oxycombustion Power Generation, Energy Procedia 63 (2014 )

[31] Belaissoui, B.; Moullec, Y.;Hagib, H.; Favre, E., Energy Effiency of Oxygen Enriched Air Production Technologies: Cryogeny vs Membranes, Energy Procedia 63 ( 2014 ) 497-503.

[32] Crittenden, B.; Thomas W. J., Adsorption Technology Design, Elseview Science and Technology Books 1998.

[33] Knaebel, K.S. A \How To" Guide for Adsorber Design, Adsorption Research, Inc.Dublin Ohio 43016.

[34] Sircar, S.; Myers A. L., Gas Separation by Zeolites,Marcel Dekker, Inc. 2003

[35] Vaduva, M.; Stanciu, V., Separation of Nitrogen from Air by Selective Adsorption of Carbon Molecular Sieves, U.P.B. Sci. Bull. Series A Vol 68 No. 2 (2006)

[36] Trainer, J.; Dubettier, R.;Perrin,P., Air Separation Unit for Oxy-Coal Combustion Systems, 1st International Oxyfuel Combustion Conference, Cottbus September 9, 2009.

[37] Chorowski, M.; Giziki, W., Technical and Economic Aspects of Oxygen Separation for oxy-Fuel Purposes, Archive of Thermodynamics Vol 36(2015).

[38] Owiti, O. B., Performance of Waste Lubrication Oil Burner for Process Heating in Small to Medium Enterprises, Master's thesis, Jomo Kenyatta University of Agriculture and Technology, Kenya (2015).

# Experimental Investigation of the Thermal Performance of Kenya Defence Forces Mobile Diesel Cooker

Ezra O. Were[1], Augustine B. Makokha[2], Charles Nzila[3]

***Abstract*** - Kenya Defence Forces (KDF) invented a diesel mobile field cooker (DEFKITCH) in the year 2010 capable of serving over two hundred soldiers in military camps and in operation areas (patent number KE 0642 dated 28 April 2014). The cooker was designed with three different sizes of cooking pots made of grade 304 stainless steel: (i)-24 gallon light duty with uniform wall thickness of 3 millimetres (ii)-24 gallon heavy duty with wall thickness of 3 millimetres and bottom thickness of 6 millimetres (iii) - 12 gallon pot with wall thickness of 3 millimetres. The cooker was commercialized in 2012 but since then no experimental assessment had been done to ascertain its performance and emission levels. Therefore this research sought to investigate the thermal performance of the cooker by experimental assessment of the combustion and thermal efficiencies as well as the level of emission of CO and $CO_2$. Thermal efficiency was investigated by conducting Water Boiling Tests (WBT) where parameters like heating time, temperatures and fuel consumption rate were recorded. Average thermal efficiencies computed from the results ranged from 60.37 percent to 65.86 percent using the 24 gallon cooking pots while a lower value of 42.69 percent was obtained using the 12 gallon pot on the same cooker. The average thermal efficiency was found to closely compare with those of other cookers in the open literature – ranging from 58 – 68 percent. Average diesel consumption per burner was found to be 0.8 litres in one hour which was found to be sufficient to prepare a meal for approximately two hundred people. Combustion efficiency of the cooker was determined using TESTO flue gas analyzer and the overall value was determined as 69.0 percent. Emission levels for CO and $CO_2$ were determined as 172.7 ppm and 4.95 percent. These were found to be within the recommended maximum emission level of 400 ppm according to National Comfort and Institute, Incorporation 2008. The cooker was found to be economical in diesel consumption per unit amount of work and a better substitute to using firewood for cooking food for a large group of people especially in remote locations such as military operation areas.

***Keywords*** - Combustion efficiency, Emissions, Kenya Defence Forces, Mobile Field Diesel Cooker, Thermal efficiency.

[1] Ezra O. Were, Department of Mechanical and Production Engineering, Moi University, P.O. Box 3900-30100, Eldoret-Kenya; (phone: +254723452170; e-mail:ezrawere@yahoo.com).

[2] Augustine B. Makokha, Department of Mechanical and Production Engineering, Moi University.

[3] Charles Nzila, Department of Manufacturing, Industrial and Textile Engineering, Moi University.

## I. INTRODUCTION

THE Kenya Ministry of Defence through Kenya Defence Forces (KDF) is committed to responsible energy use and sound environmental management through continuously improving in use of energy in the most efficient, cost effective and in an environmentally sustainable manner in line with the Kenya vision 2030.

The main forms of energy used in the military camps for cooking included Liquefied Petroleum Gas (LPG) and firewood, the latter being the major source of fuel for cooking both in the camps and in operation areas until the year 2010. In one of the energy audits conducted by KDF in the year 2010 in its two barracks, the energy use pattern was found to be as shown in Table 1. From the audit, it was observed that firewood and LPG formed the bulk of energy forms for the Kenyan military.

The use of firewood in large quantities negated the gains achieved by KDF in the Environmental Soldier Program (ESP) because the trees plated in the forests ended up being used as firewood in the camps. It is for this reason that the KDF designed a field cooker branded DEFKITCH that was intended to use diesel. However, no attempt was made to assess the thermal and combustion efficiencies of the cooker as well as the emission levels which formed the basis for the current research.

This study therefore aimed at determining and documenting the thermal and combustion efficiencies of DEFKITCH cooker as is the requirement for all energy utilities [1]. Availability of this performance data would enable manufacturers to modify and adjust design parameters of the cooker during fabrication in order to improve its performance. The data from this study was also aimed at adding to knowledge to earlier studies on various cooker performances. [2]- [4].

*Table I*
*Energy use in KDF (KDF Energy Audit Report 2010)*

| Energy Source | Unit of Measure | Kahawa | Embakasi | Total | Tons of Oil Equivalent/Yr |
|---|---|---|---|---|---|
| **Grid Electricity** | Kwh/Yr | 2,090,618 | 1,287,655 | **3,378,273** | **291** |
| **Diesel** | Ltrs/Yr | 11,733,532 | 3,792,347 | **15,525,879** | **15,215** |
| **LPG** | Tons/Yr | 418,789 | 543,208 | **961,998** | **1,110,337** |
| **Firewood** | Tons/Yr | 6,038,296 | 2,916,804 | **8,955,100** | **2,879,065** |
| | | **TOTAL** | | | **4,004,908** |

## II. DEFKITCH COOKER

The construction of the DEFKITCH cooker is as shown in Figure 1. The main components of the cooker (DEFKITCH) are the fire chambers, burners, fuel pressure cylinder (tank) and fuel pipes. The fuel tank is a seventeen litre pressure cylinder fitted with a pressure relief valve, pressure gauge and a fuel outlet fitting. During operation, fuel is pressurized in the tank to a pressure of between one and maximum of three bars. After the burner has received pressurized diesel from the pressure cylinder, the fuel is then passed through preheating coils before atomization through a nozzle where it is combusted with the aid of natural flow of air from the burner base plate at the bottom of the fire chamber. When gas was used, preheating coils were bypassed and the gas flowed directly to the nozzle for direct ignition. The heat produced from the burner was retained within an insulated fire chamber lagged to reduce heat losses. The cooking pot capacities used were twelve and twenty four gallons depending on the amount of food to be prepared.

*Figure 1: DEFKITCH (a) Two burner cooker*

*(b) Three burner cooker*

## III. EXPERIMENTAL WORK

### A. Equipment

The research was conducted at Kenya Ordnance Factories Corporation (KOFC) in Eldoret where the cookers were being manufactured and the guiding principle for the assessment was the performance of DEFKITCH cooker using Water Boiling Test (WBT) with diesel and flue gas analysis.

The following equipment, tools and materials were used in the study.

(a) DEFKITCH cooker and cooking pots

DEFKITCH cooker complete with stainless steel cooking pots (12 gallon, 24 gallon heavy duty and 12 gallon light duty) was acquired from Production department at KOFC. The DEFKITCH used was a two burner cooker designed to use diesel or LPG and it had fuel cylinder fitted with pressure gauge and a level sight glass. The three different sizes of cooking pots were availed for the tests.

*Fig 2: (a) 12 gallon Pot*

*(b) 24 gallon pots*

(b) Atomic absorption spectrophotometer

The spectrophotometer used was model AA-6300 manufactured by SHIMADZU. The equipment was borrowed from physiochemical laboratory in the Quality Assurance Department at KOFC. The spectrophotometer was used in the study to test the composition of water used in the boiling tests.


*Figure 3: Atomic absorption spectrometer at KOFC physiochemical laboratory*

(c) Thermometer and pH meter

A combined thermometer and pH meter model HI-9025 microcomputer manufactured by HANNA INSTRUMENTS capable of measuring pH and temperature was also obtained from KOFC. It was used to check the pH level of the water and also to measure temperature rise with time during the boiling tests. The boiling time was measured using a stop watch.

(d) Flue gas analyzer

A flue gas analyzer model number 320 manufactured by TESTO was used to analyze flue gas composition, flue gas temperatures and combustion efficiency of the cooker.

*Figure 4: TESTO flue gas analyzer*

(e) Weighing machine

A weighing machine METTLER TOLEDO brand was acquired from production department in KOFC for initial weighing of cooking pots, water and diesel.

B. Materials

(a) Water

The water used in the boiling test was collected from KOFC treated water supply system meant for drinking and use in production processes. The water used in the experiments was found to be fit for drinking [5] and had chemical composition as indicated in the table below.

*Table II*
*Characteristics of water used in the boiling test*

| S/No | Parameter | Recommended limits | Results |
|---|---|---|---|
| 1 | pH | 6.5 -9.2 | 7.8 |
| 2 | Turbidity | $\leq$ 25 FAU | 1 FAU |
| 3 | Temperature | $\leq$ 25 ˚C | 21.7 ˚C |
| 4 | Zinc | 3 mg/l | 0.4 mg/l |
| 5 | Iron | 3 mg/l | 0.05 mg/l |
| 6 | Lead | 0.05 mg/l | 0.001 mg/l |
| 7 | Hardness - (Ca, Mg) | 25 mg/l | 4 mg/l |
| 8 | Chlorine | 0.2 - 0.6 mg/l | 0.4 mg/l |
| 9 | Micro-organisms | Nil | Nil |

| | | | |
|---|---|---|---|
| 10 | Conductivity | ≤ 5 mV | -0.03 mV |

(b) Diesel

The cooker was tested on the automotive diesel. One litre of diesel fuel used in the experiment was weighed and its density determined as 800 kg/m$^3$.

C. Experimental Methods

Water Boiling Test was used to find thermal efficiency and rate of diesel consumption [6]; water was heated to boiling point at standard conditions in 24 gallon light duty, 24 gallon heavy duty and 12 gallon cooking pots using the diesel as fuel. Measurements of burner flame and flue gas temperatures together with composition of flue gases was done for each fuel used in the cooker to determine combustion efficiency. WBT were done in Eldoret where atmospheric pressure is 0.8 bars and room temperature of between 22.1˚C to 22.3˚C. The combusting diesel was pressurized at 2.5 bars.

In the boiling phase, water was heated from an initial average temperature ($T_1$) of 21.7 °C to boiling point of 90.1 °C. During this phase, water in the cooking pot gained energy from fuel with the help of the burner and that value of energy is equivalent to energy required to raise the temperature of that mass of water from $T_1$°C to boiling point. Heating time and temperatures were recorded at intervals of five minutes for the first twenty minutes followed by intervals of three minutes up to boiling point.

In the simmering phase, predetermined weight of water at boiling point was then subjected to boil for 30 minutes and energy gained by this water was calculated by multiplying latent heat of vaporization of water and mass of vaporized water. Fuel consumed during each process was recorded as input energy for these phases. The cooker's thermal efficiency was determined by calculating the heat gained by the water and amount of fuel consumed during this process. Overall thermal efficiency was calculated by dividing output energy by input energy [6]. Three replications of different amounts of water was employed throughout the experiments for different cooking pot sizes and averages of thermal efficiency obtained.

The combustion efficiency test was conducted in Nairobi near Jomo Kenyatta International Airport where atmospheric pressure and ambient temperature were 1.024 bars and 32°C respectively.

## IV. RESULTS AND DISCUSSION

A. *Water boiling tests*

From the results of water boiling tests, it was observed that the temperature of water rose uniformly from an average of 21.7 ˚C to an average boiling point of 90.1 ˚C. After boiling, the temperature remained almost constant at 91 ˚C which is attributed to change of phase of water from liquid to vapour, a process that takes place without increase in temperature [7]. The average flame temperature of the burner while using diesel was 1500˚C.

Results of heating time against water temperature were plotted for the 24 gallon heavy duty, 24 gallon light duty and the 12 gallon cooking pots as shown in Figure 5.

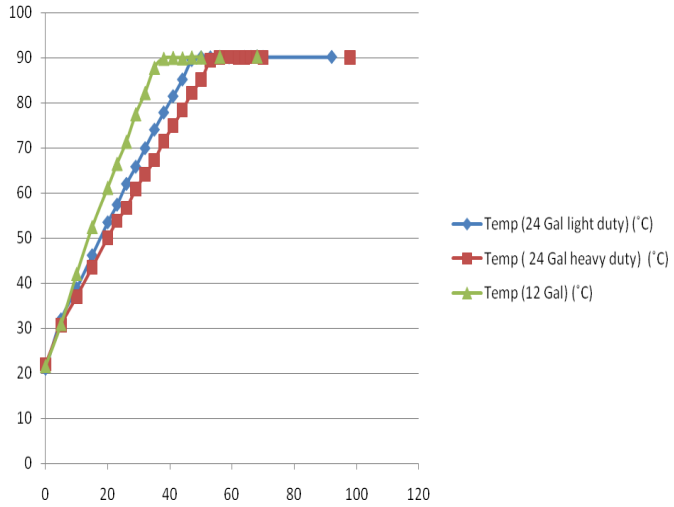


*Figure 5: Heating curves for the 24 gallon light pot, 24 gallon heavy pot and* 12 gallon *pots*

The gradients of the boiling curves varied with the 12 gallon pot being steeper due to the low mass of water of 30 kg and that of the pot of 21.7 kg compared to the 24 gallon pots. This implied less time and energy was needed to raise the temperature of a lesser mass of water to boiling point.

The mass of the 24 gallon heavy duty pot which was the heaviest at 41.8 kg compared to the 24 gallon light duty of 35.1 kg contributed to slower heating rate of water in the heavy duty pot as depicted by the lower gradient of its heating curve.

For comparison, water boiling curve for the ARPA kerosene cooker that was in use in KDF before the development of DEFKITCH cooker is also presented as shown in Figure 6.

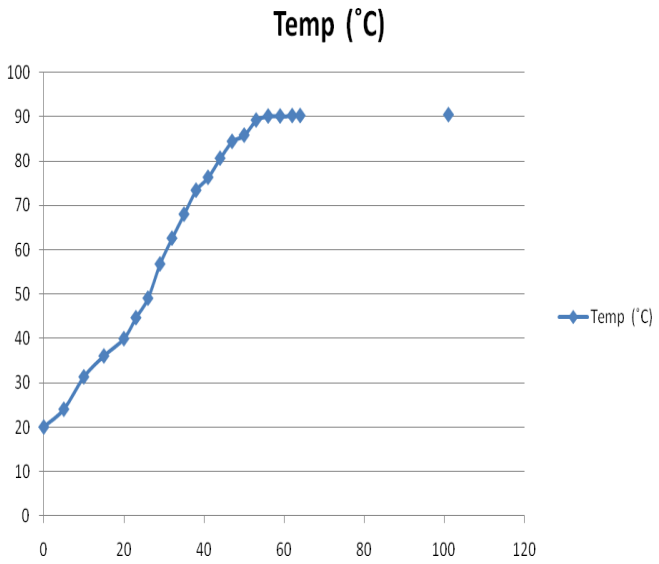


*Figure 6: Heating curve for ARPA cooker*

B. Fuel consumption rate

The average diesel consumption was found to be 0.8 litres in one hour when operating at tank pressure of 2.5 bars for the three types of cooking pots namely 24 gallon light duty, 24 gallon heavy duty and 12 gallon. The consumption of the fuel was found to be lower than in the earlier models like ARPA cooker due to the small size of the nozzles, that is approximately 0.6mm, therefore leading to build up of pressure that result into atomization of the fuel. Thus when the fuel is atomized under pressure its rate of consumption tends to be low since it is released in small quantities of vapour for the burning process and fuel air mixing is sufficient [8].

C. *Thermal efficiency*

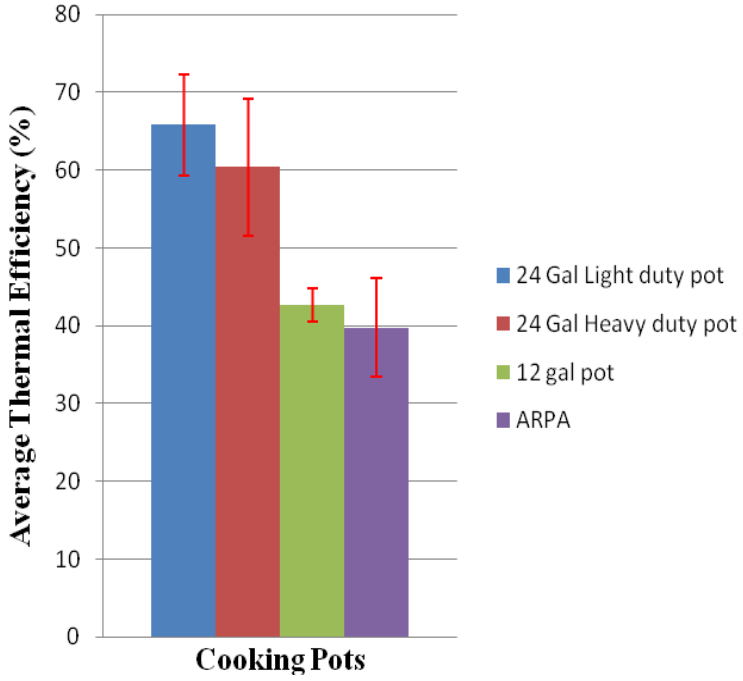


*Figure 7: Comparison of efficiencies on different pots*

Figure 7 above shows the average thermal efficiency of each of the pots and the error bars obtained with four different tests. The thermal efficiency of the cooker using 24 gallon light duty cooking pot was found to be 65.86 percent on average which implies that 34.14 percent of heat energy was being lost through conduction in fire chamber walls and top plate and also through convection to heat the surrounding air. This value dropped to 60.37 percent while using 24 gallon heavy duty cooking pot which was attributed to heat energy lost through conduction by the thick walled bottom of the pot. Thermal efficiency obtained using 12 gallon cooking pot was 42.69 percent. This massive decrease in thermal efficiency was attributed to energy loss through conduction from the cooking pot to the 9.4 kg stainless steel pot adapter used in supporting the pot in the fire chamber. Since the pot diameter is smaller than the fire chamber diameter, the adapter is used to hold the small pot onto the cooker. This therefore makes the 12 gallon pot not energy efficient on the cooker.

The boiling time in the 24 gallon light duty pot was observed to be lower at an average of 46 minutes in the first two experiments as compared with an average of 53 minutes in the 24 gallon heavy duty cooking pot. Despite using the same amount of water in the two cooking pots, the boiling time was longer on the heavy duty pot due to the initial heat energy used to raise the temperature of the double walled bottom of the pot.

D. Flue gas test

From the flue gas analysis conducted on the two burner DEFKITCH cooker with one burner on followed by two burners simultaneously at an ambient temperature of 33.5 degrees Celsius, the composition of the flue gas found was

summarised as shown in the error bar graphs in Figure 8a – 8g below.

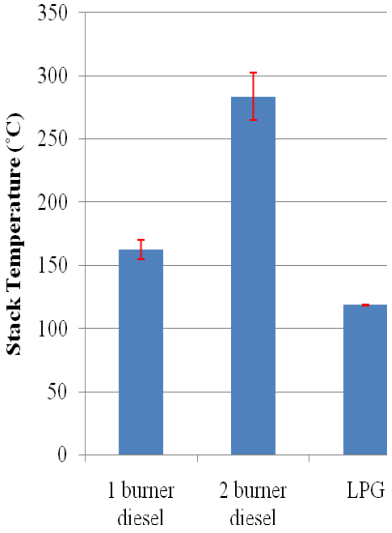


*(a) Stack temperatures*

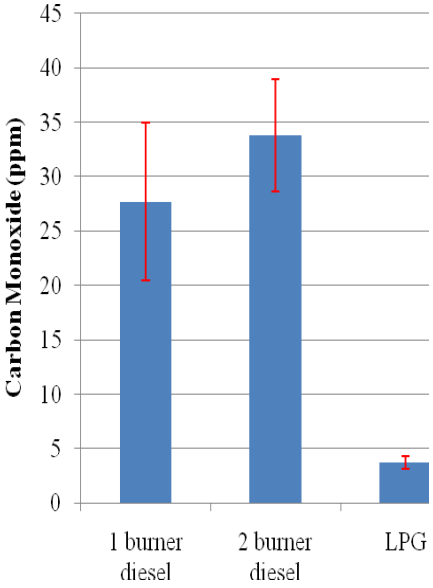


*(b) CO emission*

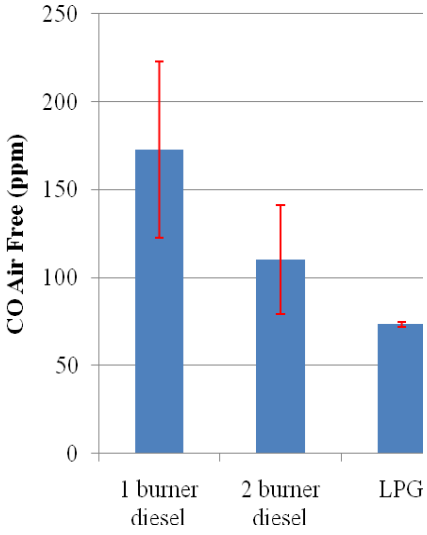


*(c) CO air free in flue gas*

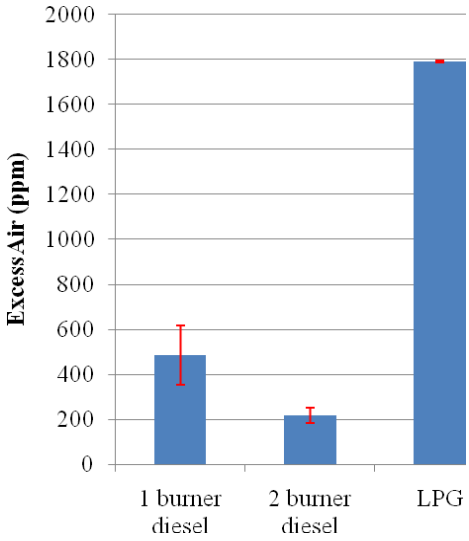


*(d) Excess air in flue gas*

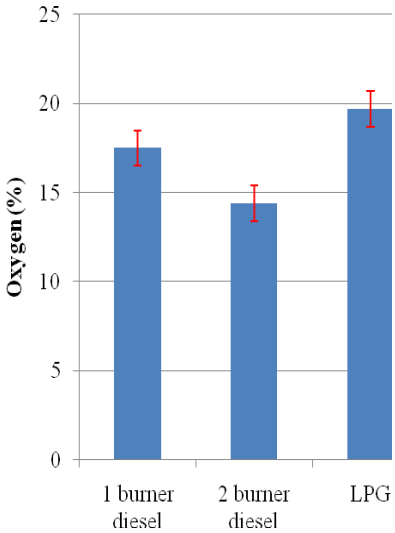


*(e) Oxygen in flue gas*

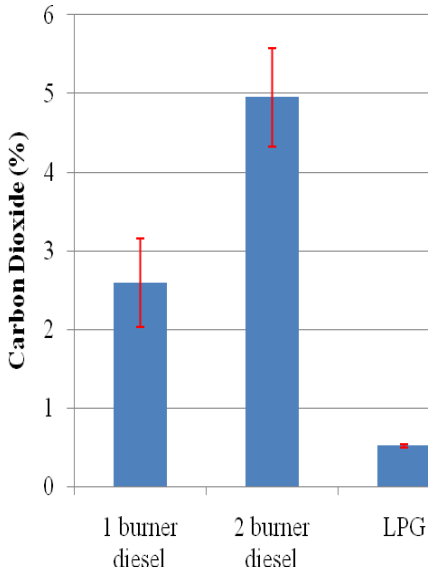


*(f) Carbon dioxide in flue gas*

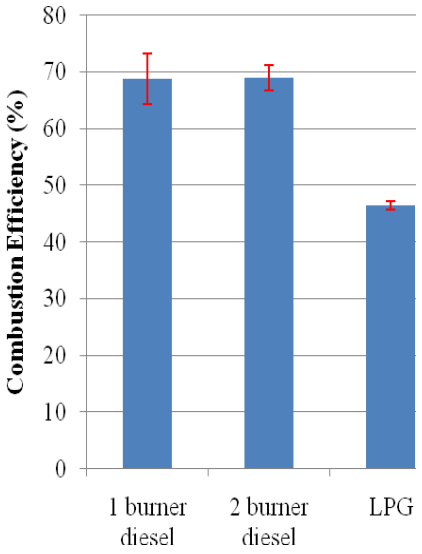


*(g) Combustion efficiencies*

*Figure 8: Error bars from flue gas tests*

The average combustion efficiency of the two burner DEFKITCH cooker was found to be 69 percent while using diesel either on a single burner or on two burners (Fig 8g).

(a) Carbon monoxide

Diluted carbon monoxide level in the flue gas was found to be 27.7 ppm on diesel while the value of CO air free was found to be 172.7 ppm average both for single burner (Fig 8b). The average values of CO air-free for two burners was 110.3 ppm. The CO emission was noted to increase when using two burners due to more fuel injected while maintaining the same amount of the available air for combustion. This trend of CO emitted was observed to be within the recommended maximum limits of 400 ppm air free basis [9].

(b) Carbon dioxide

$CO_2$ increased on using two burners which implied that better combustion of the cooker was achieved using two burners running concurrently as opposed to using a single burner. Complete combustion of any fuel takes place in excess air with production of $CO_2$ and no CO [8].

(c) Oxygen and excess air

The presence of $O_2$ in the flue gas meant that more air (20.9 percent of which is $O_2$) was supplied than was needed for complete combustion to occur therefore some $O_2$ is left over. The value of excess air in the flue gas was observed to reduce from 486.3 ppm using single burner to 217.6 ppm while using two burners (Fig 8d). This was attributed to increased fuel supply due to the introduction of the second burner hence more air was consumed in the combustion process.

(d) Stack temperature

The flue gas temperature of the cooker increased from 162.4 ˚C when using a single burner to 283.4 ˚C when using two burners on diesel (Fig 8a). This increase was attributed to the introduction of the second burner which meant more heat directed to the chimney stack. These temperatures were high enough to prevent water formation in the chimney; however the rise in temperatures obtained on two burners indicated that more heat energy was being lost through exhaust gases and this could be tapped to recover waste heat for higher efficiencies.

(e) Other observations

It was observed that the field kitchen burner produced a lot of noise during operation. This noise may negatively affect cooks and the people nearby the kitchen. This could be minimized by use of noise absorbing materials in the body of the field cooker.

## IV. CONCLUSION

This work is a contribution to the understanding and improvement of thermal and combustion efficiency of the DEFKITCH cooker. The data obtained contributes to the existing database of information on performance of various types of cook stoves and other energy utilities. The equipment was found to be economical in diesel consumption per unit amount of work and a better substitute to using firewood for cooking food for a large group of people especially in remote locations like in military operation areas.

Emission levels for CO and $CO_2$ were obtained, however $NO_x$ and $SO_x$ were not obtained due to the limitation of the flue gas analyser used in the study.

The objectives of this research work of determining DEFKITCH cooker's thermal performance in water boiling

test, analyzing emissions in flue gas test and computing thermal and combustion efficiencies were successfully achieved and suggestion on the future improvements recommended.

## ACKNOWLEDGEMENTS

Authors acknowledge KDF Research and Development Branch, the Managing Director of Kenya Ordnance Factories Corporation (KOFC), Major General L K Tumbo for the support that enabled execution of this research work and to the staff of KOFC Production and Quality Assurance Departments for their support and guidance during the course of experimental work.

## REFERENCES

[1] Wayne C. Turner, Steve Doty,"*Energy management Hand book",* 6th Edition, The Fairmont press Inc 2007, pp 89-116.

[2] N. K. Mishra, P. Muthukumar, Subhash C. Mishra, "Performance Tests on Medium-Scale Porous Radiant Burners for LPG Cooking Applications". *International Journal of Emerging Technology and Advanced Engineering Volume 3, Special Issue 3: ICERTSD 2013,* pp126-130.

[3] Tekle, A. (2014), "Experimental Assessment on Thermal Performance and Efficiency of Pyra-Box Solar Cooker", Journal of Energy Technologies and Policy www.iiste.org ISSN. 2224-3232.

[4] Vishal R. Sardeshpande, D. S, "Thermal performance evaluation of a four pan jaggery processing furnace for improvement in energy utilization", Volume 35, (2010), Issue 12, pp 4740-4747.

[5] Kenya Standards, "Water Quality and Effluent Monitoring Guidelines (Standard)" KS 05 – 459: Para 1: 1996 Schedule 2, pp 26 – 41.

[6] Bureau of Indian Standards, "Oil pressure stoves (Standard)", BIS 1999 and BIS 2002, first and second revision, pp5-10.

[7] A McConkey, T. D Eastop, "*Applied Thermodynamics For Engineering Technologists",* Longman Singapore publishers,1993.

[8] Gordon F. C. Rogers, G. F,"*Engineering Thermodynamics: Work and Heat Transfer : SI Unit",* Longman Scientific & Technical,1992.

[9] www.cloudhvac.com, National Comfort Institute Incorporation, 2008. *Carbon Monoxide levels and Risks*.

# Comparison between Power Line Carrier Communication Based Metering, GSM Based Metering & Keypad-Operated Pre-paid Metering in Kenya

I. W. Maranga, S. I. Kamau and P. M. Musyimi

***Abstract*** – Real time energy monitoring by power utilities is an important energy management practice that is becoming a norm in developing countries. The importance is highlighted by the challenges that follow with improper or no energy monitoring. Examples are revenue losses incurred by utility companies due to vandalism, energy wastage and high electricity bills incurred by electricity consumers. Due to these reasons, utility companies and electricity consumers are employing various energy monitoring techniques. Kenya Power, a power distribution company in Kenya, is currently installing Global System for Mobile Communication (GSM) based smart meters as a pilot program with the aim of energy monitoring. They have also installed Keypad Operated Pre-paid meters to reduce the losses they incur due to vandalism.

In this paper, a low voltage Power Line Communication (PLC) metering system is proposed. Its efficacy as a viable energy monitoring platform is compared to both the Keypad Operated Pre-paid and Global System for Mobile metering systems employed by Kenya Power. In particular, gaps in the established systems are highlighted and their impact presented. This is done through a cost analysis, efficiency analysis and reliability analysis comparison of the three metering techniques. The proposed system is then observed to address these gaps in a significant manner.

***Keywords*** - Energy Metering, Energy Monitoring, Global Service for Mobile Communication (GSM), Keypad Operated Pre-paid metering (KOP), Low Voltage (LV), Power Line Communication (PLC).

## I. Introduction

As Kenya aims on achieving Vision 2030, there has been a significant increase in the number of connected electricity consumers to the grid. Electricity connection rates stand at 23% in Kenya, the highest percentage connection rate in East Africa.

### *A. Statement of the Problem*

Kenya has an average power transmission and distribution loss rate of 16.9%. These are the losses in transmission between sources of supply and points of distribution and in the distribution to customers.

I. W. Maranga, Department of Electrical and Electronic Engineering, JKUAT (Phone: +254721267765; e-mail: ignatiuswaikwa@gmail.com).

S. I. Kamau, Department of Electrical and Electronic Engineering, JKUAT (Phone: +254723423092; email: skamau@eng.jkuat.ac.ke).

P. M. Musyimi, Department of Electrical and Electronic Engineering, JKUAT (e-mail: pclassics@yahoo.com).

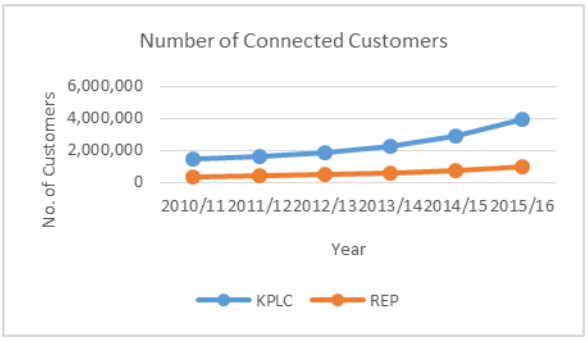


Fig 1 illustrates the increase in number of connected customers which can be attributed to the Government's aim to have full connectivity by 2020.

With an increase in connected customers, the system stands a high chance of power loss. The world's average power transmission and distribution loss rate stands at 8.1%. This shows that Kenya is above the world's average power transmission and distribution loss rate.

Power losses are a result of weak transmission and distribution network. Kenya Power losses stood at 18.1% in 2014 compared to 18.6% in 2013. It is estimated that 1% of power loss is equal to 1 billion shillings lost revenue. From Fig 1, the increase in power loss in the year 2011 can be attributed to the increase in connected customers. 8% of these power losses can be directly attributed to illegal connections and theft. This is a 3.3% increase in total power losses from 2011 to 2016. This loss is estimated to be 8 billion shillings annually. Fig 2 illustrates the trend in percentage power losses in selected African countries.

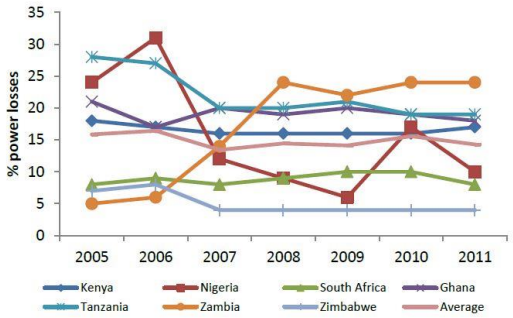


Fig 1: % Power Losses in Selected African Countries.

Blackouts are a major problem facing the country currently. Kenya Power is therefore deemed an unreliable service

provider. Reporting the outages is tedious and the utility company takes a long time working to restore power back to its consumers. It is a problem especially if the fault occurs at distribution level. This is so as it takes a long time to troubleshoot. It is estimated that industries on average lose 5% of the monthly electricity bill in certain sectors and as high as 18% in other sectors. The industries switch to generators when the outages occur increasing their cost of production, hence the continued high prices of commodities. Kenya Power also suffers huge revenue losses during blackouts.

The current distribution network has had no major upgrades since it was first constructed. The network is also outweighed by the rapid electrification the government has embarked on. Having served only 2.2 million households since it was built, the line is now expected to serve 5.5 million households which is about 60% of the country's population.

The network is also expected to distribute an additional 657 MW that has been generated since 2013 as the government targets to hit the 5,000MW power generation goal.

### *B. Existing Solutions to the Problems*

Kenya Power has recently embarked on several projects in a bid solve to the above mentioned challenges. Some include;

- Replacing Electromechanical and Electronic Post-paid meters with Key-pad Operated Pre-paid prepaid meters. Currently there are 160,000 prepaid users in Nairobi North area out of 450,000 Kenya Power customers in the area.
- Network refurbishment and expansion. The Company spent about 11 billion shillings in 2014 on network refurbishment and expansion, which included automation and upgrade of the system, undergrounding of cables, replacement of wooden poles with concrete ones, and creating adequate redundancy in the system. System losses as a percentage of energy purchased have therefore reduced to 18.1% in 2014 from 18.6% in 2013. A 0.5% reduction translating to a 500 million shillings contribution to profits. With the investment in system upgrade, a continued reduction in system losses is expected.
- Installation of GSM Based smart meters to large power consumers. The Company has spent 3.2 billion shillings to connect 4,426 large power consumers, out of 5,600 in the country.

## II. BACKGROUND INFORMATION

### *A. Keypad – Operated Pre-paid Meters*

These are electronic pre-paid energy meters with keypad systems for inputting the credit. The security of keypad payment system is very low. The main reason is that the algorithm that generates the key is stored inside the meter and can easily be hacked.

Key-pad pre-paid energy meters are getting obsolete but they may still be cost-effective for remote areas, where two-way vending may not be feasible. These are the kind of pre – paid meters that are currently being installed by Kenya Power.

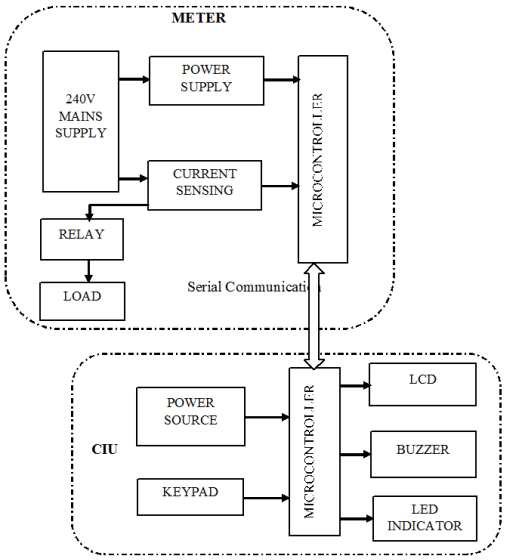


Fig 2: Block Diagram of a Pre – Paid Electronic Meter.

Fig 3: A Pre – Paid Electronic Meter.

### *B. GSM – Based Smart Meters*

GSM Based smart meters digitally send meter readings to the utility company via a GSM network. This ensures more accurate energy bills. These meters also enable monitoring so consumers can better understand their consumption. Kenya Power is installing GSM – Based smart meters for large power consumers as a pilot program. The system is facing challenges as some meters are not able to send data because there is no network coverage. The meters are also bulky, expensive and costly to install.

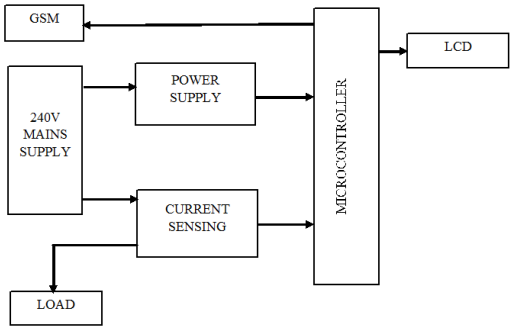


Fig 4: Block Diagram of a GSM – Based post – paid smart meter.

Fig 5: GSM – Based post – paid smart meters being installed.

## III. Power Line Communication Based Smart Meters

A Power Line Communication System is a system whereby communication signals are sent and received from the household to the utility company through a 50Hz current-bearing power line. The concept of PLC is quite old but not brought into use on large scale for commercial purpose. There are several reasons why the technology has not been adopted as the current communication technique, and the main ones are noise, multipath and signal attenuation.

In order to achieve power line communication over low voltage lines (240V), a couple of features need to be taken into consideration - a power line communication modem, a coupling circuit to interface the PLC modem to the power line, source data and message frames, modulation techniques, medium access control (MAC) layers, attenuation and signal to noise ratio.

### *DESIGN CONSIDERATIONS*

#### *Power Line Communication Modem*

Fig 7 describes a power line modem hardware design. Data to be transmitted is modulated onto a high frequency then passed through a coupling circuit for transmission. The received data goes through a coupling circuit where power with low frequency is first filtered out by a low pass filter and the high frequency signal carrying data is then filtered out using a high pass filter. The high frequency signal is demodulated back from the modulated carrier.

#### *Power Line Modem Integrated Circuits*

The use of power line modem integrated circuits simplifies the PLC modem circuit. The modulator, demodulator circuits and interfaces to the microcontroller are now all embedded in single IC. The microcontroller may write data bytes to the communication port of the modem IC using a level converter.

With the use of a power line modem IC, a level converter IC, a power supply circuit, an analog front end, a coupling circuit and an external oscillator circuit are required to design in a power line modem device.

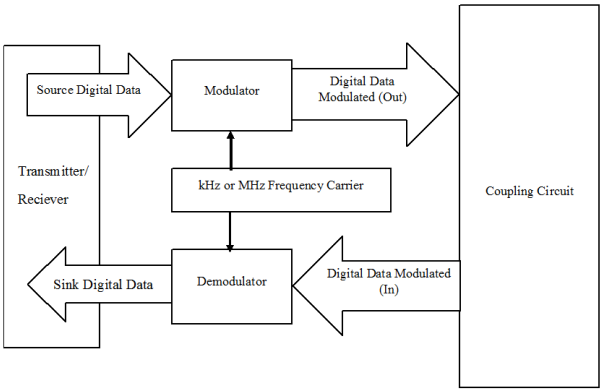


Fig 6: Block Diagram of a Power Line Communication Modem

#### *Coupling Circuit*

The function of a coupling circuit in a power line modem is to create an efficient high-pass filter to remove the 240V AC, 50Hz signal of the mains, without attenuating the incoming high frequency signal. A coupling circuit should be designed to match the modem communication system and power distribution system.

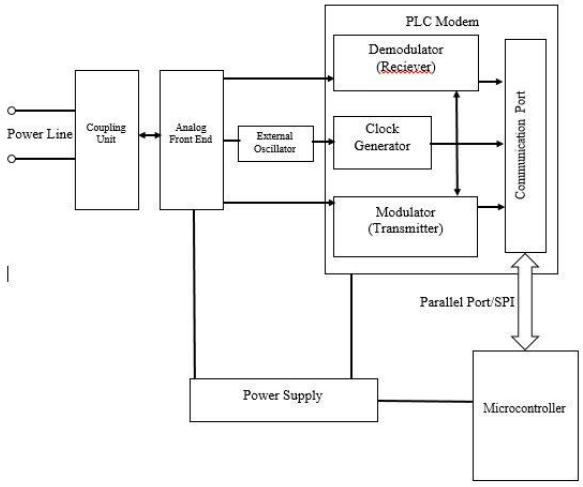


Fig 7: Block Diagram of a Power Line Communication IC

#### *Source Data and Message Frames*

For accurate information to be sent, addresses are given for the PLC meters. When the PLC meter communicates with the receiving device, it will put its address in the address field. Fig 9 below shows an example of a message frame which consists of four fields, preamble, identifying address, data field, and stop bit. The data field in this case will be the meter reading coded in binary form. The message frame will always start with preamble to signify the device that a message is coming

and always ends with a stop bit.

| PREAMBLE | ADDRESS | DATA | STOP BIT |
|---|---|---|---|

Fig 8: Figure showing an example of a message frame.

*Modulation and Demodulation Techniques*

The accuracy of the data coming from the transmitter and receiver is determined by the efficiency of the modulation or demodulation process. The modulation band selected for power line communications must meet the required data rate and must maximize resistance to various noise interferences occurred in Power Lines.

Communicating at the power line communication robust modulation techniques like Frequency Shift Keying (FSK), Code-Division Multiple Access (CDMA) and Orthogonal Frequency Division Multiplexing (OFDM) are demanded.

For low cost, low data rate applications, such as power line protection and tele-metering, FSK is seen as a good solution. For data rates up to 1Mbps, the CDMA technique may provide an effective solution. However, for high data applications beyond that, OFDM is the technology of choice for PLC.

*Medium Access Control (MAC) Layers*

The MAC protocol specifies a resource sharing strategy i.e. the access of multiple users to the network transmission capacity based on a fixed resource sharing protocol. There are various protocols for MAC Layers in power line modems and they are: Polling, Aloha, Token passing schemes and Carrier Sense Multiple Access (CSMA)

*Signal Attenuation and Signal to Noise Ratio*

*Signal Attenuation*

Signal attenuation due to network loading ranges from 40 to 100dB per kilometer. The actual level signal attenuation is the number of loads connected to the main line which determine the main parameter. In power line channel, received signal power can be modelled as a function between transmitter and receiver with a specified distance.

*Signal to Noise Ratio*

Signal-to-noise ratio (SNR) is a key parameter when determine the efficiency or measure the performance in the communications system. The signal-to-noise ratio (SNR) is given as;

$$\frac{S}{N} = 20\ log_{10}\left(\frac{V_s}{V_n}\right)$$

Where;

$\mathbf{V_s}$ is the mean voltage level of the signal.

$\mathbf{V_n}$ is the mean voltage level of the noise.

The result obtained on this parameter is related to the efficiency of a communication system. The higher the SNR, the better is the communication. Select appropriate power communication module with this capability of improving the signal to noise ratio module is essential for each PLC meter.

*DESIGNED METER*

Based on the above mentioned design considerations, a power line communication smart meter was designed. Fig 10 and 11 show the block diagram and simulation of the designed power line communication based real time energy meter.

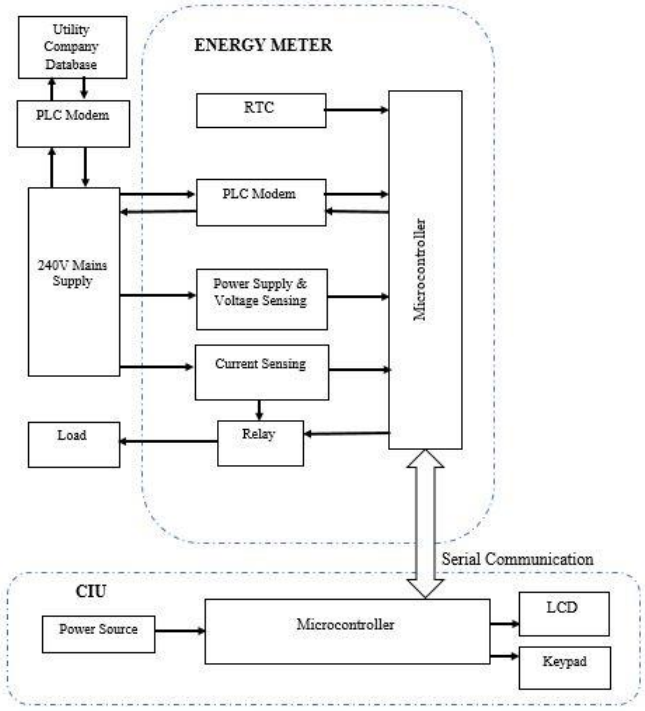


Fig 9: Block Diagram of the Designed PLC Energy Meter.

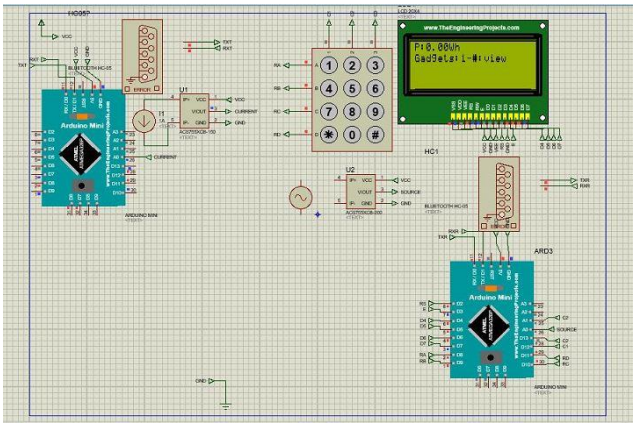

Fig 10: Simulation of the Designed PLC Energy Meter in Proteus Software

## IV. FINDINGS AND DISCUSSIONS

The following is a comparison of the key findings that were identified by the researcher;

TABLE I
COMPARISON OF THE METERING TECHNIQUES

| Key-pad Operated Pre-paid Metering | GSM Based Metering | PLC Based Metering |
|---|---|---|

| | | |
|---|---|---|
| 1. It is accurate.<br>2. The tedious task of paying the bill and waiting for the bill is eliminated.<br>3. Consumer awareness.<br>4. Prone to vandalism.<br>5. It cost Ksh 13 billion to connect 500,000 customers. | 1. Real time energy monitoring.<br>2. Easy detection of power outages.<br>3. Brings an end to estimated billing.<br>4. Hazardous radiation<br>5. Bulky, and unreliable.<br>6. High installation cost.<br>7. It cost Ksh 3.2 billion to connect 4,426 large power consumers. | 1. It is cheap.<br>2. Easy detection of power outages.<br>3. Data from remote areas is accessible.<br>4. Real time energy monitoring.<br>5. Broadband PLC may become a reality.<br>6. Smart home applications.<br>7. Prone to noise.<br>8. It would cost Ksh 11 billion to connect to 500,000 customers based on the cost of developing the prototype. |

## V. CONCLUSION

Kenya's average power transmission and distribution loss rate of 16.9% is above the world's average that stands at 8.1%. It is evident that there is a need for real time energy monitoring in the current systems. The Proposed system addresses these problems at a lower cost compared to other metering techniques. Low-cost broadband may become a reality in areas that cannot get cable or wireless broadband and broadband internet access from every socket in every room will be possible when using power line communication. Adopting the system will also create opportunities in load forecasting, load scheduling and load shaving from the real time data obtained from the meters.

## VI. REFERENCES

[1] *Design of Power-Line Communication System (PLC) Using a PLC Microcontroller,* Q. Al-Zobi1, I. Al-Tawil2, K. Gharaibeh3 and I. S. Al-Kofahi, New York: McGraw Hill, 1997.

[2] *A Course in Electrical and Electronic Measurement and Instrumentation,* K. Sawhney (2007),

[3] 17th Ed., Dhanpat Rai & Co. (p) Ltd, ISBN: 8177000160.

[4] *Digital Electronics, Principles, Devices and Applications,* Anil K. Maini, 2007 John Wiley & Sons, Ltd. ISBN: 978-0-470-03214-5

[5] *TCP-IP Networks and Protocols*

[6] *Kenya Power Company Long – Term Distributing Value, May 2015,* AIB Capital Limited.

[7] Kenya Power Annual Report, 2016.

[8] *Kenya Power Rolls Out Sh 22bn To Tame Outages,* http://www.nation.co.ke/lifestyle/smartcompany/Kenya-Power-rolls-out-Sh22bn-plan-to-tame-outages/1226-3362554-htr038z/. 30th August, Daily Nation.

[9] *Kenya Power Raids Dandora To Curb Power Theft,* http://www.nation.co.ke/business/Kenya-Power-raids-Dandora-to-curb-power-theft/996-2157418-9xa5iqz/. 23rd January, 2014 Daily Nation

[10] *Kenya Power Seeks To Cut Sh 8bn Losses,* http://www.nation.co.ke/business/Kenya-Power-seeks-to-cut-Sh8bn-losses/996-2138188-10620bo/ 7th January, 2014 Daily Nation

[11] *Kenya Power Adopts Outdoor Metering To Boost Revenue Collection,* http://www.kplc.co.ke/content/item/1513/kenya-power-adopts-outdoor-metering-to-boost-revenue-collection Kenya Power Press Releases.

# Solar photodegradation of methyl orange in the presence of cations ($Pb^{2+}$ and $Fe^{2+}$) and anions ($Cl^-$ and $SO_4^{2-}$)

John Akach, Athiambi Davhana, Melody Masilela and Aoyi Ochieng

***Abstract***— The discharge of dyes from textile industries into water bodies is harmful to aquatic life due to the dye color which prevents light from penetrating the water. As a result, it is necessary to decolorize textile water before it is discharged into receiving water bodies. Current decolorization methods such a membrane processes and adsorption are costly due the need to replace the treatment media. Recently, solar photocatalysis has been developed as an alternative and low cost method of treating dyes. Photocatalysis has been observed to be very robust for the degradation of organic chemicals; however, photocatalysis reaction could be inhibited by inorganic chemicals. This is important since textile wastewater usually has dissolved ions. In this work, the effect of cations ($Pb^{2+}$ and $Fe^{2+}$) and anions ($Cl^-$ and $SO_4^{2-}$) on the photocatalysis of methyl orange (MO) was investigated. Nano $TiO_2$ catalysts were employed for MO photocatalysis in glass fluidized bed reactors under solar illumination. The effect of catalyst loading and concentration of $Pb^{2+}$, $Fe^{2+}$, $Cl^-$ and $SO_4^{2-}$ ions between 0.03 and 0.09 mM were investigated. It was found that the optimum catalyst loading was 200 mg/L. The presence of $Pb^{2+}$ ions below a concentration 0.03 mM resulted in a reduction in the removal of MO. However, an increase in MO removal was observed in the presence of $Fe^{2+}$, $Cl^-$ and $SO_4^{2-}$ ions at all concentrations as well as in the presence of $Pb^{2+}$ ions above 0.03 mM. This work showed that the enhancement or inhibition of the photocatalysis reaction depends on the type and concentration of the ion present in solution. As a result, ions which enhance photocatalysis should not be eliminated before photocatalysis while inhibiting ions should be removed from the wastewater before photocatalysis treatment.

***Keywords***— ions, methyl orange, solar photocatalysis, textile wastewater

## I. Introduction

THE growth of textile and dyeing industry has resulted in an increase in the discharge of highly coloured wastewater into the environment. The strong colour of dye wastewater even at very low concentrations results in non-aesthetic pollution [1]. Colour also prevents light from penetrating into the water bodies thus interfering with the growth of aquatic plants which feed fish and other aquatic animals. Furthermore, some dyes are toxic and carcinogenic and can directly poison fish and human beings who use the water in the receiving water body. As a result, there is a need to decolourize dye wastewater prior to its discharge.

In this respect, various methods such as adsorption [2] membrane separation and the advanced oxidation processes such as photo-fenton, ozonation and photocatalysis have been developed. Some of these methods, such as adsorption merely transfer the dye molecules from one phase to another which creates secondary problems of disposal [1]. Membrane separation is costly in terms of the separating medium and high electricity requirements. Therefore, advanced oxidation processes such as photocatalysis have been preferred due to their high activity, low cost and ability to destroy pollutants instead of merely transferring them to another phase [1].

In the photocatalysis reaction, highly reactive holes and electrons are generated on the surface of a semiconductor catalyst, usually $TiO_2$, when irradiated by light of a sufficient quantity. The holes react with water to form hydroxyl radicals which then attack active sites in a dye molecule, such as the azo bond, which breaks and decolourizes the dye molecule [3]. Electrons are trapped by dissolved oxygen to prevent electron-hole recombination. Traditional photocatalysis has been carried out using mercury ultraviolet lamps as the light source. However, due to the high cost of running such lamps, sunlight has been investigated as an alternative energy source for photocatalysis due to its low cost [4].

Textile wastewater normally has ions which are used as fixing agents during the dyeing process. The presence of ions in wastewater is especially important for photocatalysis. Several researchers have found that metal and non-metal ions can increase or decrease the rate of photocatalysis [1]. In order to properly design a photocatalysis treatment system for textile wastewater, the effect of ions on the rate of photocatalysis needs to be investigated. In this work, solar photocatalysis of methyl orange was investigated using the commercial nano-sized catalyst P25 $TiO_2$. The effect of catalyst loading, cations and anions on the rate of methyl orange photocatalysis was evaluated. The aim of the work was to investigate the effect of $Fe^{2+}$, $Pb^{2+}$, $Cl^-$ and $SO_4^{2-}$ ions on the solar photocatalysis of methyl orange.

J. Akach, Centre for Renewable Energy and Water, Vaal University of Technology (phone: +27169506646; fax: +27169509796; e-mail: johna@vut.ac.za).

A. Davhana, Centre for Renewable Energy and Water, Vaal University of Technology (e-mail: d.thiambi@gmail.com).

M. Masilela, Centre for Renewable Energy and Water, Vaal University of Technology (e-mail: mnmmasilela@gmail.com).

A. Ochieng, Centre for Renewable Energy and Water, Vaal University of Technology (e-mail: ochienga@vut.ac.za).

## II. Methodology

### A. Experimental set up

Solar photocatalysis experiments were carried out in a fluidized bed reactor with a diameter of 32 mm and a working volume of 400 mL made of borosilicate glass. The reactor was set up on a roof top with no obstructions to sunlight. Catalyst particles in the reactor were fluidized by air from a compressor set at a flow rate of 40 L/h. The reactor was operated in batch mode for the liquid and catalyst with air being used for fluidization and as a source of oxygen electron acceptor.

### B. Photocatalysis experiments

Solar Photocatalysis experiments were carried out in the reactor in order to determine the effect of catalyst loading and different ions on the rate of methyl orange photocatalysis. First, the mixture of 0.03 mM of methyl orange (Merck) and an ion solution of a specified concentration was mixed with the commercial nano-sized Aeroxide P25 $TiO_2$ catalyst (Evonik) of a specified loading. The mixture of wastewater and catalyst was then added into the reactor followed by air fluidization. During the photocatalysis reaction, sampling was carried out every 10 minutes. The samples were filtered by a 0.45 µm GHP syringe filter (Pall) and then the concentration of methyl orange was analysed using a UV-vis spectrophotometer (PG instruments, T60) at a $\lambda_{max}$ of 465 nm. Solar experiments were carried out between 12.00 and 1.00 pm on sunny days. The salts for preparing the ions were obtained from Merck and used without further purification. Lead, $Fe^{2+}$, $Cl^-$ and $SO_4^{2-}$ ions were obtained from $Pb(NO_3)_2$, $FeCl_2$, NaCl and $Na_2SO_4$ salts, respectively.

## III. Results and Discussion

### A. Effect of catalyst loading

The effect of catalyst loading was investigated in the range of 50 – 400 mg/L. The results (Figure 1) show an increase in the photocatalysis rate constant with an increase in the catalyst loading. For example, an increase in the catalyst loading from 50 to 200 mg/L resulted in an increase in the rate constant from 0.015 to 0.0238 $min^{-1}$. However, a further increase in the catalyst loading to 400 mg/L resulted in a marginal increase in the rate constant to 0.0256 $min^{-1}$. This trend can be attributed to the fact that an increase in the catalyst loading results in an increase in the number of active sites leading to an increase in the rate of reaction [1]. However, an increase in the catalyst loading beyond the optimum loading results in catalyst self-shading; a situation in which some catalysts are not illuminated and do not participate in the photocatalysis reaction [1]. From the results, 200 mg/L was selected as the optimum catalyst loading and used for further studies.

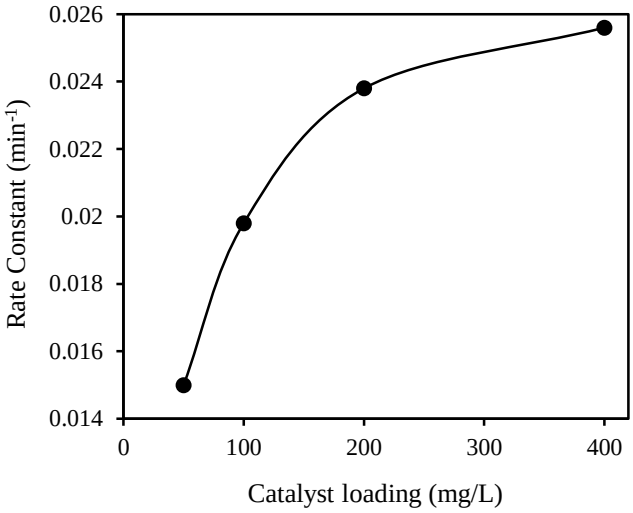


Fig. 1: Effect of catalyst loading on the photocatalysis rate constant. Methyl orange concentration = 0.03 mM

### B. Effect of cations

The effect of $Fe^{2+}$ and $Pb^{2+}$ ions at different concentrations on the rate of photocatalysis was investigated. The results (Figure 2a – b) show an increase in the photocatalysis of methyl orange with an increase in the concentration of $Fe^{2+}$ and $Pb^{2+}$.

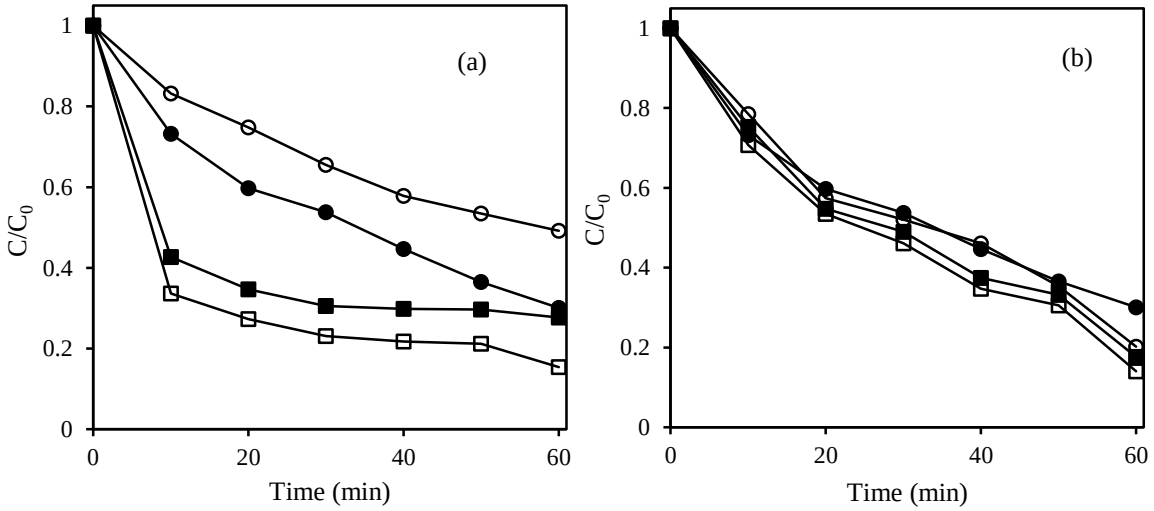


Fig. 2: Effect of different concentrations of (a) $Pb^{2+}$ and (b) $Fe^{2+}$ on methyl orange photocatalysis. 0 mM (●), 0.03 mM (○), 0.06 mM (■), 0.09 mM (□). Catalyst loading = 200 mg/L

However, $Pb^{2+}$ inhibition was observed at a concentration of 0.03 mM. Cations have generally been found to inhibit the rate of photocatalysis [1]. However, Baran and co-workers [5], working with $FeCl_3$ found that $Fe^{3+}$ has a catalytic effect on the photocatalysis of anionic dyes and an inhibitory effect on cationic dyes. This was attributed to the reaction between $Fe^{3+}$ and anionic dyes resulting in the formation of insoluble complexes which resulted in fast decolourization. However, at low concentrations of $Fe^{3+}$, an inhibition in the removal of anionic dyes was observed.

The observations by Baran and co-workers [5] have very striking parallels with the results in this work for methyl orange photocatalysis in the presence of $Pb^{2+}$. The photocatalysis of the anionic methyl orange dye was inhibited at low concentrations of $Pb^{2+}$. However, in the presence of high concentrations of $Pb^{2+}$, methyl orange photocatalysis was found to be very fast. This suggests that the photocatalysis of methyl orange in the presence of $Pb^{2+}$ could be attributed to the reaction between the anions react with hydroxyl radicals thus competing with the target substrate resulting in a reduced rate of photocatalysis [7]. However, at neutral pH, $TiO_2$ exist as $Ti\text{-}O^-$ species which repel anions resulting in a reduced adsorption and competitive reactions with hydroxyl radicals. Thus, at neutral pH, as was the case in this work, anions have been found to have almost no effect on the rate of photocatalysis. However, [7] have found that the presence of sulphate ions can result an increase in the rate of photocatalysis. This was attributed to the reaction between sulphate and hydroxyl radicals resulting in the formation of sulphate radicals:

$$SO_4^{2-} + {}^{\bullet}OH \rightarrow {}^{\bullet}SO_4^{2-} + H_2O \quad (1)$$

The generated sulphate radicals are very strong oxidizing agents and may increase the rate of photocatalysis. A similar mechanism can be attributed to the increase in the photocatalysis of methyl orange in the presence of chloride ions.

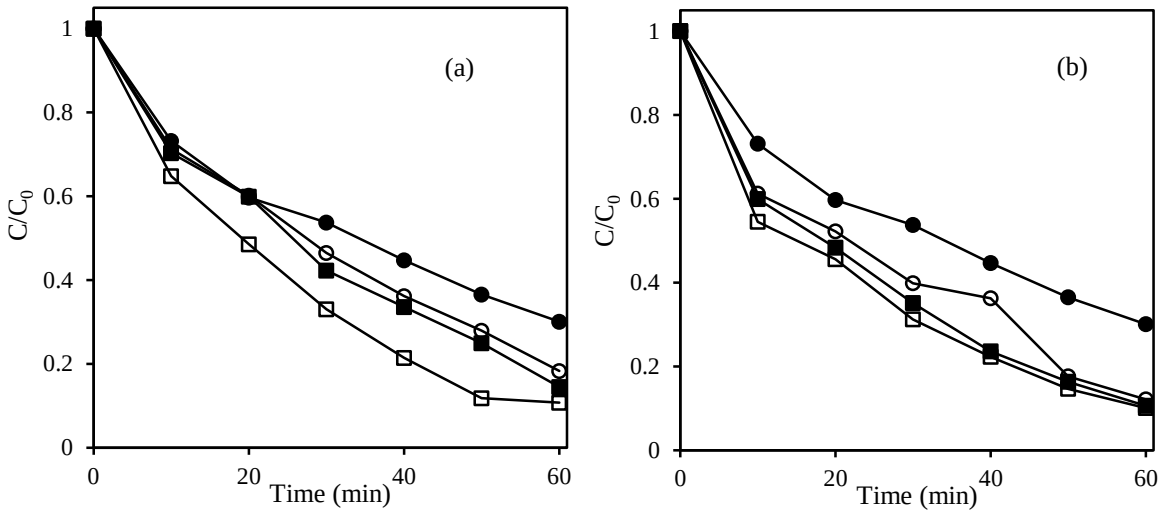


Fig. 3: Effect of different concentrations of (a) $Cl^-$ and (b) $SO_4^{2-}$ on methyl orange photocatalysis. 0 mM (●), 0.03 mM (○), 0.06 mM (■), 0.09 mM (□). Catalyst loading = 200 mg/L

$Pb^{2+}$ and methyl orange.

The presence of $Fe^{2+}$ ions in solution has been associated with an increase in the rate of photocatalysis. During dark adsorption, $Fe^{2+}$ ions are adsorbed on the surface of the catalyst where the ions acts as an electron scavengers thus reducing the electron-hole recombination rate [6]. This process results in an increase in the number of generated holes and hydroxyl radicals leading to an increase in the photocatalysis reaction rate. This explains why the presence of $Fe^{2+}$ ions results in an increase in the removal of methyl orange by photocatalysis.

### *C. Effect of anions*

The effect of different concentrations of $Cl^-$ and $SO_4^{2-}$ ions on the rate of photocatalysis was investigated. The results (Figure 3a – b) show an increase in the photocatalysis of methyl orange with an increase in the concentration of $Cl^-$ and $SO_4^{2+}$ ions. In photocatalysis studies, anions have been observed to inhibit the reaction in acidic pH as they are adsorbed by $TiO_2$ which exist in the form of $Ti\text{-}OH_2^+$ species. After adsorption,

## IV. Conclusion

In this work, the effect of catalyst loading, cation concentration and anion concentration on the rate of methyl orange concentration was investigated. An increase in the catalyst loading resulted in an increase in the photocatalysis rate constant up to an optimum catalyst loading of 200 mg/L. The presence of $Cl^-$, $SO_4^{2+}$, $Fe^{2+}$ and high concentrations of $Pb^{2+}$ ions in the wastewater resulted in an increase in methyl orange removal by photocatalysis. Low concentrations of $Pb^{2+}$ ions were found to inhibit the photocatalysis of methyl orange. This study showed that the influence of ions on photocatalysis depends on the type and concentration of the ion. Thus, in the design of the treatment process, the influence of ions needs to be considered to ensure optimal operation of photocatalysis.

## Acknowledgement

This work was supported by the Water Research Commission of South Africa (Project K5/3288/3).

## REFERENCES

[1] I. K. Konstantinou, and T. A. Albanis, "$TiO_2$-assisted photocatalytic degradation of azo dyes in aqueous solution: kinetic and mechanistic investigations: a review," *Applied Catalysis B: Environmental*, vol. 49, pp.1-14, 2004

[2] V. K. Gupta, "Application of low-cost adsorbents for dye removal–A review," *Journal of Environmental Management*, vol. 90, pp. 2313-2342, 2009

[3] F. Han, V. S. R. Kambala, M. Srinivasan, D. Rajarathnam, and R. Naidu, "Tailored titanium dioxide photocatalysts for the degradation of organic dyes in wastewater treatment: a review," *Applied Catalysis A: General*, vol. 359, pp.25-40, 2009

[4] S. Malato, P. Fernández-Ibáñez, M. I. Maldonado, J. Blanco, and W. Gernjak, "Decontamination and disinfection of water by solar photocatalysis: recent overview and trends," *Catalysis Today*, vol. 147, pp.1-59, 2009

[5] W. Baran, A. Makowski, and W. Wardas, "The influence of $FeCl_3$ on the photocatalytic degradation of dissolved azo dyes in aqueous $TiO_2$ suspensions," *Chemosphere*, vol. 53, pp.87-95, 2003

[6] A. Ortiz-Gomez, B. Serrano-Rosales, and H. De Lasa, "Enhanced effect of $Fe^{3+}$ and $Fe^{2+}$ ions on the photocatalytic oxidation of organic compounds: Reaction mechanism over the $TiO_2$ surface," presented at AIChE Annual Meeting, Salt Lake City, UT, November 4 – 9, 2007.

[7] K. H. Wang, Y. H. Hsieh, C. H. Wu, and C. Y. Chang, "The pH and anion effects on the heterogeneous photocatalytic degradation of o-methylbenzoic acid in $TiO_2$ aqueous suspension," *Chemosphere*, vol. 40, pp.389-394, 2000.

# A Review of Multi-Objective Methods for Optimal Location and Capacity of Distributed Generations in Modern Power Systems

J. M. Karanja[1], L. M. Ngoo[2] and C.M. Muriithi[3]

***Abstract*—**Penetration of distributed generation (DG) units in distribution system has increased rapidly stimulated by reduced network power loss, improved bus voltage profile and better power quality. Appropriate location and capacity of DG play significant role in maximizing beneficial effects. The aim of the optimal DG placement (ODGP) is to provide the best location and capacity of DGs to optimize electrical distribution network operation and planning taking into account DG capacity constraints. Different methods applied to the OPDG problem are reviewed in this paper. Future research trends in this field are also analyzed.

***Keywords*—**Distributed Generation (DG), Optimal Distributed Generation Placement (ODGP), Optimal Site, Optimal Size.

## I. Introduction

THE distributed generation, also termed as embedded generation or dispersed generation or decentralized generation, has been defined as electric power source connected directly to the distribution network or on the customer site of the meter [1]. The emergence of new technological alternatives allows the DG technologies in distribution network to achieve immense technical, economical and environmental benefits. In addition, the governments of the developing and under-development countries are supporting the DG for they can supply the required electrical energy of their increasing customers. Installing DGs at the network buses have a direct impact on the flowing power and the voltage of the network. This impact depends on many different factors and may be positive or negative [2]. The positive impacts of installing DG resources include increasing the power quality, improving the voltage profile, reducing the power loss, decreasing the requirements of installing new transmission lines and deferring the necessity of improving the capacity of substations[3], [4]. On the other hand, the main adverse impact of installing DG is the increase in short circuit level of the network [2]. The studies show that if the capacity and location of DGs are not identified appropriately, not only the network parameters are not improved, but also they are deteriorated [5], [6]. Some of the common distributed technologies are photovoltaic, wind energy, fuel cells, micro turbines and combined heating and power (CHP) generators.

To maximize on the benefits of DG penetration, the optimal location, size, number and type is fundamental. The two of the most important factors of DG plans are identifying the capacity and location of these resources [7]. The place and capacity of DGs can be decided according to the improvement of one or more parameter, in order to increase the efficiency and decrease the adverse effects of installing them.

## II. Types of DGs

DG can be classified into four major types based on their terminal characteristics in terms of real and reactive power delivering capability as follows:

1. Type 1: DG capable of injecting real power, P, only e.g. Photovoltaic, micro turbines, fuel cells, which are integrated to the main grid with the help of converters/inverters
2. Type 2: DG capable of injecting reactive power, Q, only e.g. synchronous compensators such as gas turbines.
3. Type 3: DG capable of injecting both P and Q e.g. DG units that are based on synchronous machine (cogeneration, gas turbine, etc.)
4. Type 4: DG capable of injecting P but consuming Q e.g. squirrel-cage induction generators that are used in wind farms.

## III. Location of DG

The location of a DG is specified by the bus-bars the DG is connected. Effects of location of a DG are determined using load flow analysis. Proper location ensures among others improved voltage profile and minimized power losses.

## IV. Number of DG

Installing and exploiting some DG resources with a small capacity is proven to be more effective than a single DG with a big capacity. On the other hand, increasing the number of installed DGs at the network will cause some extra costs due to the DGs installing and their service costs. Hence, there should be a balance between the imposed costs and the

J. M. Karanja, Department of Electrical and Power Engineering, TUK, (phone: +2540722925214; e-mail: jomaka2012@gmail.com).

L. M. Ngoo, Department of Electrical and Telecommunication, MMU, (e-mail: livingngoo@gmail.com).

C.M. Muriithi, Department of Electrical and Power Engineering, TUK, (e-mail: cmainamuriithi@gmail.com).

improvement of the considered parameters of the network. This balance can be created by deciding the optimal number of DGs.

## V. SIZE OF DG

The size at most should be such that it is consumable within the distribution substation boundary. Any attempt to install high capacity DG with the purpose of exporting power beyond the substation (reverse flow of power though distribution substation), will lead to very high losses. So, the size of distribution system in terms of load (MW) will play important role is selecting the size of DG. The reason for higher losses and high capacity of DG can be explained by the fact that the distribution system was initially designed such that power flows from the sending end (source substation) to the load and conductor sizes are gradually decreased from the substation to consumer point. Thus without reinforcement of the system, the use of high capacity DG will lead to excessive power flow through small sized conductors and hence results in higher losses.[8].

## VI. OBJECTIVES OF DG INSTALLATION

Some examples of objectives of DG installation are; Minimization of the total power loss of the system, Minimization of energy losses, Minimization of system average interruption duration index (SAIDI), Minimization of cost, Minimization of voltage deviations, Maximization of DG capacity, Maximization of profit, Maximization of a benefit/cost ratio and Maximization of system loadability limit.

## VII. OBJECTIVE FUNCTION

The aim of the optimal DG placement (ODGP) is to provide the best location and capacity of DGs to optimize electrical distribution network operation and planning taking into account DG capacity constraints. To achieve this the objective function is formulated and then optimal solution obtained using different optimization techniques.

The objective function can be single-objective or multi-objective. However, sitting and sizing DGs, with the aim of improving a single parameter, enhances the considered parameter significantly, but may have negative impact on other parameters of the network. On the other hand, sitting and sizing DG with the purpose of enhancing some of the parameters of the network will result in improvement of the considered parameters. Hence in this review multi objective ODGP has been considered. This is unique from other review works where single objective ODGP dominated the review [9], [110].

For multi-objective functions we can have:

1. Multi-objective function with weights (also called weighted sum method), where the multi objective formulation is transformed into a single objective function using the weighted sum of individual objectives.
2. Goal Multi objective index, where the multi objective formulation is transformed into a single objective function using the goal programming method.
3. Multi objective formulation considering more than one often contrasting objectives and selecting the best compromise solution in a set of feasible solutions.

## VIII. TAXONOMY

Table I presents taxonomy of the reviewed optimal DG placement works.

## IX. METHODS

In this study the reviewed work is classified based on the three multi objective functions.

### *a. MULTI OBJECTIVE FUNCTION WITH WEIGHTS*

It has been noted in this review that about 2/3 of the researchers have used multi objective functions with weights to transform them into single objective functions. Research has shown that the weighted multi objective index cannot accurately reflect the relationship between the various objectives, and the corresponding weights are difficult to determine due to lack of enough information about the problem.

Invasive weed optimization algorithm is proposed for optimally determining the location and sizing of multiple distributed generations (DG) units in the distribution network with different load models in [11]. In [12], [13], [14], [15], [16], and [17] PSO and its improved version have been used for optimization. Weight-Improved Particle Swarm Optimization Algorithm (WIPSO) for optimal location and size of distribution generation and compensating devices is suggested in [12] to reduce the losses and will also maintain the required voltage profile within limits. A Butterfly-PSO methodology is implemented to optimally allocate multiple DG units to improve voltage profile, increment in the economy, reduction in losses in [13]. DAPSO which is an improved version of PSO is used in [14] for multi objective optimization placement of DG problem for different load levels on distribution systems for reduction of loss, cost and improving voltage profile. PSO is presented in [15] for sizing and sitting of DG in Institute of Electrical and Electronics Engineers (IEEE) 33 bus test system. The proposed objective function is the multi objective function (MOF) that considers active and reactive power losses of the system and the voltage profile in nominal load of system. The study in [16] proposes a multi-objective index-based approach for optimally determining the size and location of multi-distributed generation units in distribution systems with different load models using PSO. In [17] Particle Swarm Optimization approach (PSO) for the placement of Distributed Generators (DG) in the radial distribution systems to reduce the real power losses and to improve the system reliability. Power loss

TABLE I
TAXONOMY OF THE REVIEWED OPTIMAL DG PLACEMENT

| Ref. | year | No. of DGs | Design Variables | Objectives | Optimization Method |
|---|---|---|---|---|---|
| [11] | 2016 | Multiple | Location + Size | Multi objective with weights | Invasive weed optimization Algorithm |
| [12] | 2016 | Single | Location + Size | Multi objective with weights | Weight-Improved Particle Swarm Optimization Algorithm |
| [13] | 2015 | Multiple | Location + Size | Multi-objective function based on the indices | Butterfly- Particle Swarm Optimization Algorithm |
| [14] | 2013 | Multiple | Location + Size | Multi objective with weights | Dynamic Adaptive Particle Swarm Optimization Algorithm |
| [15] | 2013 | Multiple | Location + Size | Multi objective with weights | Particle Swarm Optimization Algorithm |
| [16] | 2011 | Multiple | Location + Size | Multi objective with weights | Particle Swarm Optimization Algorithm |
| [17] | 2011 | Single | Location + Size | Multi objective with weights | Particle Swarm Optimization Algorithm |
| [18] | 2015 | Multiple | Type + Location + Size | Multi objective with weights | Genetic algorithm |
| [19] | 2014 | Multiple | Type + Location + Size | Multi objective with weights | An improved adaptive genetic algorithm |
| [20] | 2014 | Single | Location + Size | Multi objective with weights | Genetic Algorithm |
| [21] | 2011 | Multiple | Number + Location + Size | Multi objective with weights | Genetic Algorithm |
| [22] | 2011 | Multiple | Location + Size | Multi objective with weights | Genetic Algorithm |
| [23] | 2011 | Multiple | Location + Size | Multi objective with weights | Genetic Algorithm |
| [24] | 2011 | Multiple | Type + Location + Size | Multi objective with weights | Genetic Algorithm |
| [25] | 2010 | Single | Location + Size | Multi objective with weights | Genetic Algorithm |
| [26] | 2009 | Single | Location + Size | Multi objective with weights | Genetic Algorithm |
| [27] | 2008 | Single | Location | Multi objective with weights | Hybrid Genetic Algorithm and power flow technique |
| [28] | 2013 | Multiple | Location + Size | Multi objective with weights | Point Estimate Method Embedded Genetic Algorithm |
| [29] | 2016 | Multiple | Location + Size | Multi objective with weights | PSO, GSA, and hybrid PSOGSA algorithms |
| [30] | 2013 | Multiple | Location + Size | Multi-objective index-based approach | Hybrid (PSO & Gravitational Search Algorithm) |
| [31] | 2012 | Multiple | Location + Size | Multi objective with weights | Hybrid (GA &PSO) |
| [32] | 2016 | Multiple | Location + Size | Multi objective with weights | Bat Algorithm |
| [33] | 2015 | Single | Location + Size | Multi objective with weights | Modified Shuffled frog Leaping Algorithm |
| [34] | 2013 | Multiple | Location + Size | Multi objective with weights | Modified Shuffled frog Leaping Algorithm (MSFLA) |
| [35] | 2012 | Multiple | Location + Size | Multi objective with weights | shuffled frog leaping algorithm |
| [36] | 2015 | Single | Location + Size | Multi objective with weights | Supervised Big Bang-Big Crunch method |
| [37] | 2014 | Multiple | Location + Size | Multi objective with weights | Harmony Search Algorithm with Differential Operator |
| [38] | 2012 | Multiple | Location + Size | Multi objective with weights | heuristic iterative method ( clustering techniques and exhaustive search) |
| [39] | 2011 | Multiple | Location + Size | Multi objective with weights | Mixed integer nonlinear programming (MINLP) Technique |
| [40] | 2010 | Single | Location + Size | Multi objective with weights | Heuristic iterative search technique |
| [41] | 2008 | Multiple | Location | Multi objective with weights | Ant Colony Optimization |

TABLE I (CONTINUED)
TAXONOMY OF THE REVIEWED OPTIMAL DG PLACEMENT

| Ref. | year | No. of DGs | Design Variables | Objectives | Optimization Method |
|---|---|---|---|---|---|
| [42] | 2015 | Multiple | Location | Multi objective | NSGA-II Algorithm |
| [43] | 2013 | Multiple | Location + Size | Multi objective | Non-dominated Sorting Genetic Algorithms II |
| [44] | 2008 | Multiple | Location + Size | Multi objective | Genetic Algorithm |
| [45] | 2008 | Multiple | Location | Multi objective | Genetic Algorithm |
| [46] | 2013 | Multiple | Location + Size | Multi objective | Strength Pareto Evolutionary Algorithm |
| [47] | 2011 | Multiple | Location + Size | Multi objective | Strength Pareto Evolutionary Algorithm |
| [48] | 2010 | Single | Location + Size | Multi objective | Strength Pareto Evolutionary Algorithm |
| [49] | 2016 | Multiple | Location + Size | Multi objective | Advanced Pareto Front Non-Dominated Sorting Multi-Objective Particle Swarm Optimization |
| [50] | 2013 | Multiple | Location + Size | Multi-objective | Hybrid (PSO & Evolutionary Programming |
| [51] | 2012 | Multiple | Location + Size | Multi-objective | Hybrid (Binary PSO-based & Fuzzy) |
| [52] | 2011 | Single | Location + Size | Multi objective | GA and an ϵ-constrained method |
| [53] | 2012 | Multiple | Number + Location + Size | Goal Multi objective index | Genetic Algorithm |
| [54] | 2008 | Multiple | Location + Size | Multi objective- goal programming | Genetic Algorithm |

reduction Index and Reliability Improvement Index are used. In [18], [19], [20], [21] [22], [23] [24], [25], [26] and [27] GA and its improved version have been used for optimization. Optimization of distributed generation with voltage step constraint using GA is presented in [18]. An improved adaptive genetic algorithm is suggested in [19] for ODGP of distributed generation considering timing characteristics and environmental benefits. GA methodology for ODGP is proposed in [20] for loss minimization and tail end node voltage improvement during peak load. In [21] GA is proposed to find the optimal place and capacity of DG resources, in order to improve the technical parameters of network, including power losses, voltage profile and short-circuit level. In [22] GA is presented working together with a fuzzy controller which is used to dynamically adjust the crossover and mutation rates to maintain the proper population diversity during GA's operation. A novel methodology that employs fuzzy set theory and the genetic algorithm for formulation and evaluation of a multi-objective function, respectively, for optimal planning of distributed generator units is proposed in [23]. A Monte Carlo simulation embedded GA is suggested to solve an ODGP with uncertainties represented by probability distribution function in [24]. An optimal proposed approach (OPA) to determine the optimal sitting and sizing of DG with multi-system constraints to achieve a single or multi-objectives using genetic algorithm (GA) is presented in [25]. In [26] GA is proposed to study the effects of load models on the optimal location and sizing of DG resources in distribution systems. A hybrid method employing genetic algorithms and optimal power flow is proposed to search a network for the best sites and capacities available to strategically connect a defined number of DGs among a large number of potential combinations in [27]. A probabilistic power flow embedded genetic algorithm based approach is proposed in [28] in order to solve the optimization problem that is modeled mathematically under a chance constrained programming framework.

In [29], [30] and [31] hybrid of PSO, GSA and GA was used for optimization. Combined nature inspired algorithms PSO, GSA, and hybrid PSOGSA algorithms are proposed in [29] for ODGP. PSO & Gravitational Search Algorithm are suggested in [30] for ODGP to improve total real power losses, voltage profile, MVA intake by the grid and greenhouse gases emission. In [31] a novel combined genetic algorithm (GA)/particle swarm optimization (PSO) is presented for optimal location and sizing of DG on distribution systems. In [32] Bat Algorithm (BA) is presented to exploit the benefits of DG by selecting optimal location and size of DGs in the distribution network. The multi-objective function (MOF) considered in this work is to minimize the total real power (Ploss) losses and maximize voltage stability index (VSI), within the range of voltage constraint.

In [33], [34] and [35], Shuffled frog Leaping Algorithm and its modified versions are used. In [33] a comparison is done between modified shuffled frog leaping algorithm (MSFLA) and shuffled frog leaping algorithm (SFLA). The allocation of DGs is done to reduce losses and improve voltage profile in power networks. Modified Shuffled Frog Leaping Algorithm (MSFLA) is proposed in [34] multi objective multiple DGs allocation and sizing to improve Interruption Duration Index (SAIDI) and Average Energy

Not Supplied (AENS) per customer index at the lowest cost. Shuffled frog leaping algorithm (SFLA) is represented in [35] for ODGP to minimize the total real power loss and to improve the voltage profile. In [36] the study presents an efficient multi-objective optimization approach based on the supervised big bang–big crunch method for optimal planning of dispatchable distributed generator. In [37] the study proposes a novel method that employs harmony search algorithm with differential operator to install multiple DG units optimally in distribution system with an objective of minimizing active power loss and improving voltage profile. In [38] a heuristic iterative method (clustering techniques and exhaustive search) is used exploiting information on the time varying voltage magnitude and loss sensitivity factor at each node. Optimal allocation of distributed generation using a two-stage multi-objective mixed-integer-nonlinear programming is proposed in [39]. In [40] a simple conventional iterative search technique along with Newton Raphson method of load flow study is implemented with objective to lower down both cost and loss very effectively. The weighting factors are also optimized. In [41] an ant colony system algorithm is used to derive the optimal recloser and DG placement scheme for radial distribution networks.

### *b. MULTI OBJECTIVE FOR SET OF FEASIBLE SOLUTIONS*

Many studies have come up with set of optimum solutions, each one with its own features, especially for non-commensurable objectives. The choice of optimum solution is dependent on planner's interest.

Weighted sum method can be used to get a set of Pareto-optimal solutions by varying the weights. Unfortunately, this requires multiple runs as many times as the number of desired Pareto-optimal solutions. Furthermore, this method cannot be used to find Pareto-optimal solutions in problems having a non-convex Pareto-optimal front. In addition, there is no rational basis of determining adequate weights and the objective function so formed may lose significance due to combining non-commensurable objectives. To avoid this difficulty, the ε-constraint method for multi-objective optimization has been used. This method is based on optimization of the most preferred objective and considering the other objectives as constraints bounded by some allowable levels. These levels are then altered to generate the entire Pareto-optimal set. The most obvious weaknesses of this approach are that it is time-consuming and tends to find weakly non-dominated solutions. Better approaches, adopted is to Pareto rank candidate solutions, and keep an archive of all non-dominated search. In this way it's possible to explore the entire Pareto front without any a priori knowledge about the problem.

Data Clustering and NSGA-II algorithm are proposed in [42] to investigate optimal placement of wind turbines for reducing losses and improving load ability and voltage profile in distribution networks. In [43] Non-dominated Sorting Genetic Algorithms II (NSGA-II) is proposed is used to obtain the set of Pareto optimal solutions, which form a numerous set of non-dominated solutions and will be employed by the Decision Maker (power system operator) to select the best compromise solution. In [44] true Pareto-optimal solutions are found with a multi-objective genetic algorithm and the final solution is found using a max–min approach. A multi objective programming approach based on the non dominated sorting genetic algorithm (NSGA) is proposed in order to find configurations that maximize the integration of distributed wind power generation (DWPG) while satisfying voltage and thermal limits in [45].

In [46], [47] and [48] Strength Pareto Evolutionary Algorithm is used. A novel Strength Pareto Evolutionary Algorithm (SPEA) is represented in [46] for optimal location and sizing of DG on distribution systems. The objective is minimizing network power losses, better voltage regulation and improves the voltage stability within the security constraints in radial distribution systems. Pareto based Multi-objective Optimization Algorithm (MOA) called Strength Pareto Evolutionary Algorithm (SPEA) is suggested in [47] for Distributed Generation planning in distribution networks considering reliability, cost of energy and power loss. The weighting factors are also optimized. Strength Pareto Multi-Objective Optimization Approach is presented in [48] to generate Pareto front from which a designer can select from.

In [49], [50] and [51] multi objective PSO and its varieties are used. . In [49] Advanced Pareto Front Non-Dominated Sorting Multi-Objective Particle Swarm Optimization is presented to get Pareto front considering power loss reduction and voltage stability improvements with voltage profile and power balance as constraints. A combination of Evolutionary Programming (EP) and PSO methodology is proposed in [50] for distributed generation (DG) placement and sizing using multi-objective optimization concept. A stochastic dynamic multi-objective model for integration of distributed generations in distribution networks is proposed in [51] .The Pareto optimal solutions of the problem are found using a binary particle swarm optimization (PSO) algorithm and finally a fuzzy satisfying method is applied to select the optimal solution considering the desires of the planner.

The ε-constraint method [52] where GA is used for Multi objective ODGP considering voltage rise issue and voltage dependent loads is solved by interactive trade off method.

### *c. GOAL PROGRAMMING METHOD*

Goal attainment or goal programming is becoming a practical method for handling multiple criteria or objectives [7]. In this method, all objectives are assigned target levels for achievement, and these targets are treated as aspirational goals. After the goals have been formed, the deviations of the objective function values from the target values are minimized so as to find an optimal solution.

A novel methodology that employs a goal programming technique and genetic algorithm for formulation and evaluation of a multi-objective function, respectively, is proposed in [53] for optimal planning of distributed generator

units in the distribution system. Multi objective function with fuzzy sets is searched by Genetic Algorithm (GA) to determine optimal size and size of DGs in [54].

## X. FUTURE WORK

A lot of research has been done on optimal location and size of distributed generation to a system for more than one and half a decade. With assumption now that power system networks exists with DGs optimally introduced, it is necessary to carry out research to determine introduction of new DGs to such systems. The research results should show whether there is a trend for introduction of new DGs or the optimization procedure has always to be repeated afresh.
A number of scenarios can be considered as listed below:

1. Introduction of DGs to system which already contains other DGs which had been optimally introduced.
2. Introduction of DGs to system which already contains other DGs which were not optimally introduced.
3. Introduction of a given type of DG of a given capacity to a system which already contains other DGs.
4. Introduction of DGs to a system which already contains other DGs and has also experienced a given percentage of load growth.

## XI. CONCLUSION

This study has presented a critical review of various existing optimization methods applied to the OPDG problem. It has also identified that most common objective is the minimization of the total power loss and improvement of system voltage. Also it is found that multi objective problems are solved mainly by genetic algorithms and particle swarm optimization techniques. Future research areas are in the effects of introduction of new DGs in a network with already existing optimally placed and sized DGs.

## REFERENCES

[1] Mohab, M. Elnashar, R. El Shatshat and M. M.A. Salama, "Optimum siting and sizing of a large distributed generator in a mesh connected system," Electric Power Systems Research, vol. 80, pp. 690-697, 2010.

[2] G.N. Koutroumpezis and A.S. Safigianni, "Optimum allocation of the maximum possible distributed generation penetration in a distribution network", Electric Power Systems Research, vol. 80, pp. 1421-1427, 2010.

[3] T. Gozel and M.H. Hocaoglu, "An analytical method for the sizing and siting of distributed generators in radial systems", Electric Power Systems Research, vol. 79, no. 6, pp. 912-918, Jun. 2009.

[4] J.B.V. Subrahmanyam and C. Radhakrishna, "Distributed generator placement and sizing in unbalanced radial distribution system", International Journal of Electrical and Electronics Engineering, vol. 3, no. 12, 2009.

[5] V.H .Mendez Quezada, J.R. Abbad and T.G. San Roman, "Assessment of energy distribution losses for increasing penetration of distributed generation", IEEE Transactions on Power Systems, vol.21, no. 2, pp. 533-540, May 2006.

[6] N. Acharya, P. Mahat and N. Mithulananthan, 2006. "An analytical approach for DG allocation in primary distribution network", International Journal of Electrical Power and Energy System, vol. 28, no. 10, pp. 669-678, Dec. 2006.

[7] G. P. Liu, J. B. Yang, and J. F. Whidborne, Multiobjective Optimization and Control , Baldock, Hertfordshire, England: Research Studies Press Limited, 2003, pp. 77–78.

[8] S. Kansal, B.B.R. Sai, B. Tyagi and V. Kumar, "Optimal placement of distributed generation in distribution networks," International Journal of Engineering, Science and Technology, vol. 3, no. 3, pp. 47-55, 2011.

[9] P. Georgilakis and N. D. Hatziargyriou, "Optimal Distributed Generation Placement in Power Distribution Networks: Models, Methods and Future Research", IEEE transactions on Power Systems, vol.28, no.3, Aug. 2013.

[10] SD.M. Shareef and T.V. Kumar, "A Review on Models and Methods for Optimal Placement of Distributed Generation in Power Distribution System," International Journal of Education and applied research, vol. 4, issue Spl-1, Jan – Jun. 2014.

[11] D. R. Prabha and T. Jayabarathi, "Optimal placement and sizing of multiple distributed generating units in distribution networks by invasive weed optimization algorithm", Ain Shams Engineering Journal, vol 7, no. 2, pp. 683–694, Jun. 2016.

[12] Mahipa B., G. B. Naik and Ch. N. Kumar, "A Novel Method for Determining Optimal Location and Capacity of DG and Capacitor in Radial Network Using Weight-Improved Particle Swarm Optimization Algorithm (WIPSO)," International Journal of Advanced Research in Electrical, Electronics and Instrumentation Engineering, vol. 5, no. 5, May 2016.

[13] A. K. Bohre, G. Agnihotri and M. Dubey, "The Optimal Distributed Generation Placement and Sizing Using Novel Optimization Technique", Middle-East Journal of Scientific Research, vol. 23, no.6, pp. 1228-1236, 2015.

[14] M. Sadeghi, "Multi Objective Optimization Placement of DG problem for Different Load levels on Distribution Systems with purpose Reduction Loss, Cost and Improving Voltage Profile based on DAPSO Algorithm", Journal of Artificial Intelligence I Electrical Engineering, vol.2, no.5, May 2013.

[15] N. Ghadimi, "A method for placement of distributed generation (DG) units using particle swarm optimization," International Journal for Physical Sciences, vol. 8, no. 27, pp. 1417-1423, Jul. 2013

[16] A. M. ElZonkoly, "Optimal placement of multi-distributed generation units including different load models using particle swarm optimisation," Swarm and Evolutionary Computation, vol. 1, no. 1, pp. 50-59, Mar. 2011.

[17] M. Mohammadi and M. A. Nasab, "PSO Based Multiobjective Approach for Optimal Sizing and Placement of Distributed Generation," Research Journal of Applied Sciences, Engineering and Technology vol. 2, no. 8, pp. 832-837, Aug. 2011.

[18] R. P. Payasi, A. K. Singh, D. Singh, and N. K. Singh, "Multi-objective optimization of distributed generation with voltage step constraint", International Journal of Engineering, Science and Technology, vol. 7, no. 3, pp. 33-41, 2015.

[19] Y. Gao , J. Liu, J. Yang, H. Liang and J. Zhang, "Multi-Objective Planning of Multi-Type Distributed Generation Considering Timing Characteristics and Environmental Benefits", Energies, vol. 7, pp. 6242-6257, Sep. 2014

[20] H. A. M. Prasanna., M. V. L. Kumar, and T. Ananthapadmanabha. "A Novel Approach for Optimal Allocation of a Distributed Generator in a Radial Distribution Feeder for Loss Minimization and Tail End Node Voltage Improvement during Peak Load." International Transaction of Electrical and Computer Engineers System, vol. 2, no. 2, pp. 67-72, Mar. 2014.

[21] S.A. Hossein, M. Karami, S.S. K. Madahi, F. Razavi and A.A.Ghadimi, "Optimal Capacity, Location and Number of Distribution Generation at 20 KV Substations", Australian Journal of Basic and Applied sciences, vol. 5, no. 10, pp 1051-1061, 2011.

[22] M. F. Akorede, H. Hizam, I. Aris, and M. Z. A. Ab Kadir, "Effective method for optimal allocation of distributed generation units in meshed electric power systems," IET Generation, Transmission, & Distribution., vol. 5, no.. 2, pp. 276–287, Feb. 2011.

[23] K.Vinothkumar and M. P. Selvan, "Fuzzy embedded genetic algorithm method for distributed generation planning," Electric Power Components System, vol. 39, no. 4, pp. 346–366, Feb. 2011.

[24] Z. Liu, F. Wen, and G. Ledwich, "Optimal siting and sizing of distributed generators in distribution systems considering uncertainties," IEEE Trans. Power Delivery, vol. 26, no. 4, pp. 2541–2551, Oct. 2011.

[25] A.A.A.El-Ela, S.M. Allam, and M.M. Shatla, "Maximal optimal benefits of distributed generation using genetic algorithms," Electrical Power Systems Research, vol. 80, no. 7, pp. 869–877, Jul. 2010.

[26] D. Singh, D. Singh, and K.S. Verma, "Multiobjective optimization for DG planning with load models," IEEE Transactions on Power System, vol. 24, no. 1, pp. 427–436, Feb. 2009.
[27] G. P. Harrison, A. Piccolo, P. Siano and A. R. Wallace,"Hybrid GA and OPF evaluation of network capacity for distributed generation connections", Electrical Power Systems Research, vol. 78, no. 3, pp. 392–398, Mar. 2008.
[28] V. A. Evangelopoulos, P. S. Georgilakis, "Optimal distributed generation placement under uncertainties based on point estimate method embedded genetic algorithm," IET Generation, Transmission & Distribution, vol. 8, no. 3, pp. 389–400, Mar. 2014
[29] A. Ramamoorthy and R. Ramachandran, "Optimal Siting and Sizing of Multiple DG Units for the Enhancement of Voltage Profile and Loss Minimization in Transmission Systems Using Nature Inspired Algorithms, " The Scientific World Journal, Vol. 2016, 2016.
[30] W. S. Tan, M .Y. Hassan., H.A. Rahman, Md. P. Abdullah and F. Hussin, "Multi-distributed generation planning using hybrid particle swarm optimisation- gravitational search algorithm including voltage rise issue" IET Generation, Transmission & Distribution, vol. 7, no.9, pp. 929 – 942, Sep.2013.
[31] M. H. Moradi and M. Abedini, "A combination of genetic algorithm and particle swarm optimization for optimal DG location and sizing in distribution systems," Electrical Power and Energy System, vol. 34, no. 1, pp. 66–74, Jan. 2012.
[32] R. Prakash and B.C. Sujatha, "Optimal Location and Capacity of Distributed Generation for Multi-objective Function using Bat Algorithm," International Journal of Advanced Research in Electrical, Electronics and Instrumentation Engineering, vol. 5, no. 7, Jul. 2016.
[33] N. D. Mahmoudabadi, B. F. Moghadam and H. kazemipoor , "Optimal Allocation and Sizing of Distributed Generation in Distribution Network Using Modified Shuffled Leaping Algorithm," SAUSSUREA, vol. 5, no.6, pp 75-86, Jan. 2015.
[34] M. Heidari, M. Banejad and A. Hajizadeh, "Using the modified shuffled frog leaping algorithm for optimal sizing and location of distributed generation resources for reliability improvement," Journal of AI and Data Mining vol.1, no.2, pp.103-110, Feb. 2013.
[35] E. Afzalan, M. A. Taghikhani and M. Sedighizadeh, "Optimal Placement and Sizing of DG in Radial Distribution Networks Using SFLA." International Journal of Energy Engineering, vol. 2, no. 3, pp. 73-77, May 2012.
[36] A. Y. Abdelaziz, Y. G. Hegazy, W. El-Khattam and M. M. Othman, "A multi-objective optimization for sizing and placement of voltage-controlled distributed generation using Supervised Big Bang-Big Crunch method" Electric Power Components Systems, vol. 43, no. 1, pp. 105–117, Jan. 2015.
[37] R. Kollu,, S. R. Rayapudi and V. L.N. Sadhu, "A novel method for optimal placement of distributed generation in distribution systems using HSDO," International Transactions on Electrical Energy Systems, vol. 24, no. 4, pp. 547–561, Apr. 2014.
[38] F. Rotaru, G. Chicco, G. Grigoras, and G. Cartina, "Two-stage distributed generation optimal sizing with clustering-based node selection," International Journal of Electrical & Power Energy Syst.ems, vol. 40, no. 1, pp. 120–129, Sep. 2012.
[39] S. Porkar, P. Poure, A. Abbaspour-Tehrani-Fard, and S. Saadate, "Optimal allocation of distributed generation using a two-stage multi-objective mixed-integer-nonlinear programming," European Transactions on Electrical Power, vol. 21, no. 1, pp. 1072–1087, Jan. 2011.
[40] S. Ghosh, S. P. Ghoshal, and S. Ghosh, "Optimal sizing and placement of distributed generation in a network system," International Journal of Electrical & Power Energy Syst.ems, vol. 32, no. 8, pp. 849–856, Oct. 2010.
[41] L. Wang and C. Singh, "Reliability-constrained optimum placement of reclosers and distributed generators in distribution networks using an ant colony system algorithm," IEEE Transactions on Systems, Man, Cybernetics, part C, Applications and Review, vol. 38, no. 6, pp. 757–764, Nov. 2008.
[42] M. Saraninezhad and M. Ramezany, "Optimal Placement of Wind Turbines for Reducing Loss and Improving Loadability and Voltage Profile in Distribution Networks by data Clustering and NSGA-II Algorithm", Turkish Journal of Engineering and Technology , vol.2, no.5, pp 91-99, 2015.
[43] R. D. Mohammedi, A. Hellal, S. Arif and M. Mosbah, "Optimal DG Placement and Sizing in Radial Distribution Systems Using NSGA-II for Power Loss Minimization and Voltage Stability Enhancement," International Review of Electrical Engineering, vol. 8, no.6, pp. 1806-1814, Dec. 2013.
[44] M. R. Haghifam, H. Falaghi, and O. P. Malik, "Risk-based distributed generation placement," IET Generation Transmission and Distribution, vol. 2, no. 2, pp. 252–260, Apr. 2008.
[45] L. F. Ochoa, A. Padilha-Feltrin, and G. P.Harrison, "Time-series-based maximization of distributed wind power generation integration," IEEE Transactions on Energy Conversion, vol. 23, no. 3, pp. 968–974, Sep. 2008.
[46] S. Jalilzadeh, M. Darabian and M. Azari, "Distributed Generation Planning via Strength Pareto Multiobjective Optimization Approach, "International Journal on Technical and Physical Problems of Engineering", vol. 5, no. 2, pp. 1-7, Jun. 2013
[47] H. Yassami1, A. Moeini, S. M. R. Rafiei, A. Darabi and A. Bagheri, "Optimal distributed generation planning considering reliability, cost of energy and power loss", Scientific Research and Essays, vol. 6, no. 9, pp. 1963-1976, May, 2011.
[48] A. Moeini, A. Darabi, H. Yassami and M.H. Sadeghi, "Optimal Dg Allocation in Distribution Network using Strength Pareto Multi-Objective Optimization Approach," International Journal on Technical and Physical Problems of Engineering, vol. 2, no. 1, pp. 50-54, Mar. 2010.
[49] K. Mahesh, P. Nallagownden and I. Elamvazuthi, "Advanced Pareto Front Non-Dominated Sorting Multi-Objective Particle Swarm Optimization for Optimal Placement and Sizing of Distributed Generation, " Energies, Nov. 2016
[50] H. Musa and S. S. Adamu , "Enhanced PSO based multi-objective distributed generation placement and sizing for power loss reduction and voltage stability index improvement" Energytech, IEEE Conference, pages 1-6, May 2013.
[51] A.Soroudi and M.Afrasiab; "Binary PSO-Based Dynamic Multi-Objective Model for Distributed Generation Planning under Uncertainty", IET Renewable Power Generation, vol.6, no. 2, pp. 67 - 78, Mar. 2012.
[52] R. K. Singh and S. K. Goswami, "Multi-objective optimization of distributed generation planning using impact indices and trade-off technique," Electric Power Components and Systems, vol. 39, no. 11, pp. 1175–1190, Aug. 2011.
[53] K. Vinoth kumar and M. P. Selvan, "Distributed generation planning: A new approach based on goal programming," Electric Power Components and Systems, vol. 40, no. 5, pp. 497–512, Feb. 2012.
[54] K.H. Kim, K.B. Song, S.K. Joo, Y.-J. Lee, and J.-O. Kim, "Multiobjective distributed generation placement using fuzzy goal programming with genetic algorithm," European Transaction on Electrical and Power, vol. 18, no. 3, pp. 217–230, Apr. 2008.

# Optimization of KNEC Storage System using Electronic Identification and GSM Communication System

Kelvin Mong'are[1] and P.M. Musyimi[2]

***Abstract*** **-** Examinations provide a standardized criterion for institutions to evaluate whether the set educational objectives are met. However, rising cases of examination cheating for the Kenya Certificate of Primary Education (KCPE) and Kenya Certificate of Secondary Education (KCSE) examinations has been a chronic problem in the country over the recent years. The major challenge faced was the nature of handling of the examination papers, whereby most of the examination papers were in the possession of candidates and other unauthorized persons before the examination commencement date. This has brought insecurities concerning the decay of morals in our various institutions which needs to be addressed with utmost urgency.

This malpractice has necessitated for innovative ways to improve the security of the examination papers. This project intends to come up with an integrated Electronic Identification and Global System for Mobile Communication (GSM) System with access given to the authorized recipient only, and in the process, minimize human contact during storage. This project entails three aspects, the design of a secure unit with anti-tampering technology, programming and design of the communication system that will be used for monitoring.

Through the use of this technology, we aim at laying up the infrastructure that will curb examination cheating incidences.

***Keywords*** **-** Electronic Identification, Global System for Mobile Communication (GSM), Optimization

## I. Introduction

The rate of examination cheating has been on the rise consequently, decreasing the quality of education offered by institutions. It has been a common statement for the Ministry of Education to point out the ever-rising cases of examination cheating in primary and secondary schools every year during the release of examination results. This malpractice has led to the overall decay of morals in the society and loss of integrity of the education system [1]. This ill-mannered behavior spreads to the future life of the candidates and it is no surprise that Kenya is among the leading nations on the corruption index. The World Bank Group (2002) define malpractice in public examinations as a deliberate act of wrongdoing contrary to official examination rules that is designed to place a candidate at an unfair advantage. The social equity of many students has been compromised and many a young people end up depressed and choked by life's frustrations. Their once valued ambitions of achieving their most sought goals quick turn to be pipe dreams. To guarantee social justice, fair evaluation and equity, the education system should be dearth of all malpractice. K.N.E.C. (Kenya National Examination Council) cartels, involving officials, and local university students steal examination papers and marking schemes. The materials are then sold to desperate candidates, subjected to local pressure to attain the highest grade. The rate of examination cheating has increased proportional to the evolving technology. As witnessed in many instances, daring candidates enter examination rooms with their mobile phones to access answers over the internet. The spread of a leaked exam is very fast and is attributed to the presence of social media platforms available to the public. Photos are shared mostly on the WhatsApp platform and university students offer a hand in solving the questions to provide answers thereof. Without overemphasizing on this, it is clear that there is a need to attend to this problem immediately. The major and consistent factor affecting cheating is the ineffectiveness of examination handling and distribution procedures. This project will incorporate recent technology to ensure effective and secure ways to package and store examination papers.

## II. Literature Review

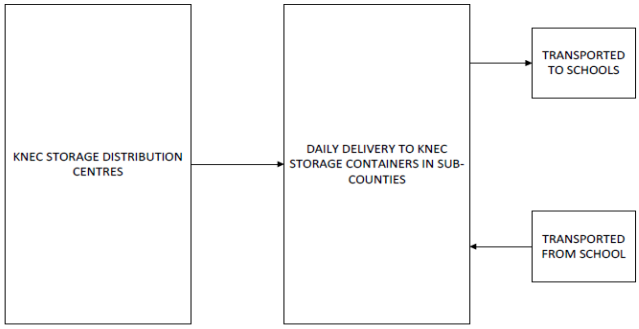


Fig. 1 Current KNEC Storage System

The current storage system comprises of a total of 346 double-lock metal containers whose keys are in the possession of education officials. The metal containers have been distributed across all sub-county offices and county commissioners are

[1] Kelvin Mong'are, Department of Electrical and Electronic Engineering, JKUAT. (Phone: +254721815638; email: mongarekelvin@gmail.com)
[2] P.M. Musyimi, Department of Electrical and Electronic Engineering, JKUAT. (Email: pclassics@yahoo.com )

tasked to ensure 24-hour security. The examination papers arrive from overseas one week to the start of examinations and are temporarily stored in protected regional distribution offices in Nairobi, Mombasa, Eldoret and Wajir. Daily dispatch to sub-county containers take place with some areas requiring airlifting. School heads collect examination papers at 5am in a daily basis from the containers, which are opened jointly by the sub-county education officials and examination official in the presence of a police officer [2]. The school heads and sub-county education officer sign against accountability documents confirming both the container and the exam papers have not been tampered with, and escorted to respective schools by senior officer. County commissioners are the overall managers at the distribution centers. All school heads are required to produce their appointment letters and identification badges for vetting and confirmation of legitimacy by the sub-county officers before receiving the examination papers. The supervisors and invigilators are limited to administration of exams only after which they handover scripts to the school heads. Spare question papers which were present in the older systems have now been removed. Each page of the question papers to be used by candidates will further have specific watermark barcodes that will help in investigations and identification of any copying. Shrink-wrapping has also been introduced on all examination cartons to discourage breakage. After the examination is ended, the examination materials are transported back to the storage facilities. Shrink wrapping is also done to cartons containing examination materials which will act as a visual detector for any tampering [3].


Fig. 2 Manning of Metal Containers

***Advantages***

1. Easier control on release of examination materials

2. Reduction in storage cost

***Disadvantages***

1. Time consuming

2. Vulnerable to human intrusion

3. Many loopholes which facilitate corruption.

4. Inefficient accountability and record-keeping.

5. System is independent on good individuals.

## III. PROPOSED SYSTEM

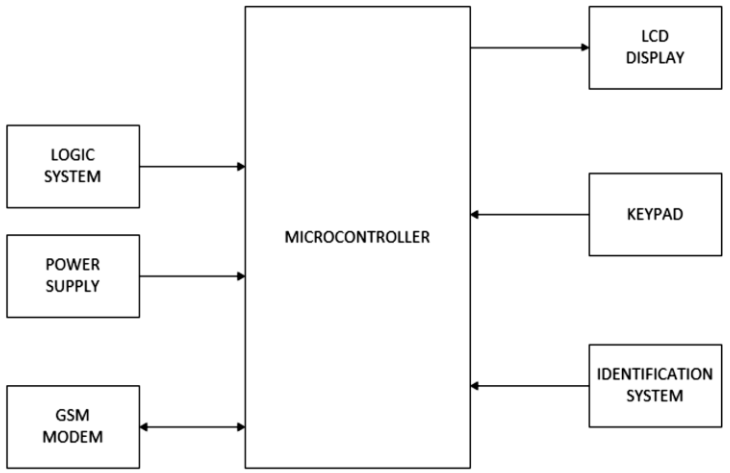


Fig. 3 Proposed System

The proposed system will comprise of the following: A **GSM (Global System for Mobile Communication) Module** which enables communication with the box. Once the box is opened, details of the user opening the box will be sent to the control centre. An implementation of GSM redundancy will enable a more effective communication in different locations. GSM module was chosen because it is readily available in the market. Two identification modules which are RFID (Radio Frequency Identification) Module and Fingerprint scanner. **RFID Module** which will enable an effective and efficient sorting of examination materials. Every school will have their designated box which will contain all the materials assigned to them. RFID form of identification is used because it has superior advantages over the barcode and manual methods of data collection. The identification module will also include a **Fingerprint Scanner** which will be used to securely access the box through user fingerprint. A **Logic System** will ensure that the boxes are only opened at intended times only. During the initial storage, the boxes are fully closed awaiting first delivery. It will also include **Electronic lock** to secure the access to the box. A **Power**

**Supply** will provide the power requirements to the system's circuitry.

The main components of the system include the GSM Module and Identification System

## IV. IDENTIFICATION SYSTEM

### *A. Radio Frequency Identification (RFID)*

RFID system consists of an RFID reader, RFID tag, and information managing host computer. Radio Frequency Identification has emerged as a reliable technology that aims to improve the efficiency of data manipulation. The RFID enables data capture and enable technology which enhances ubiquitous computing and integration of systems seamlessly. Researches has been conducted concerning RFIDs and it has shown that investors using this technology can improve logistics efficiency responsiveness and cut down on labour costs. It is a widely-accepted technology owing to the fact that it is unique and contactless, making it most suitable for security features [4].

A typical RFID system consists of tags, readers, and application software. Tags have a memory embedded and a unique identify code which are either active (with batteries) or passive (without batteries). RFID readers collect data from and write data to compatible RFID tags, pass retrieved data to a server through network and enrich applications, such as inventory control real-time tracking, and business intelligence. The reader contains an RF transceiver module (transmitter and receiver), a signal processor and controller unit, a coupling element(antenna), and a serial data interface (RS232, RS485) to a host system. The tag and reader must work at the same specified working frequency and comply with specific regulations and protocols.

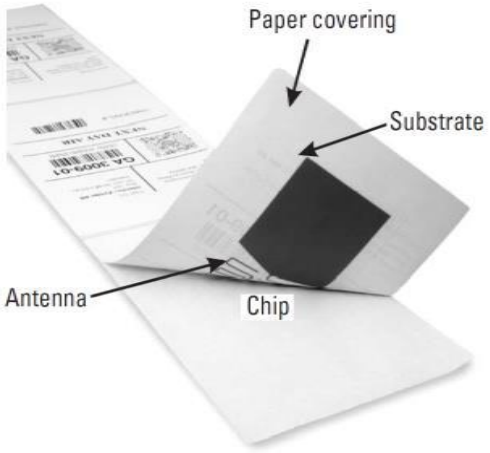


(a)

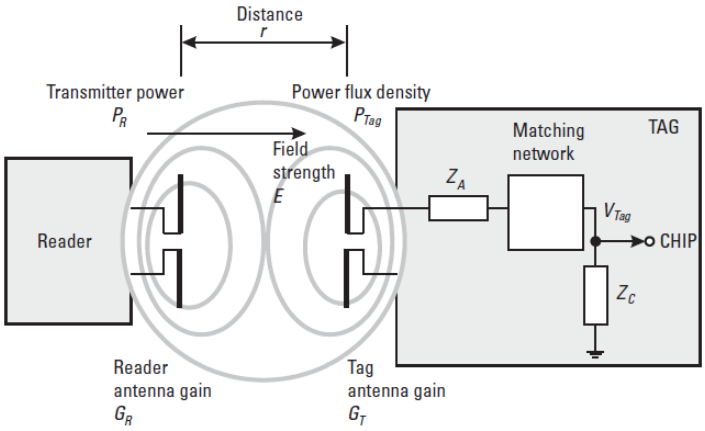


(b)

Fig. 4 RFID System

$$P_{Tag} = \left(\frac{E^2}{120\pi}\right)\left(\frac{\lambda^2}{4\pi}\right)G_T = \frac{{V_{Tag}}^2}{R_c} \qquad (1)$$

$$and \ \frac{E^2}{120\pi} = \frac{P_R G_R}{4\pi r^2}$$

$$P_{Tag} = \left(\frac{P_R G_R}{4\pi r^2}\right)\left(\frac{\lambda^2}{4\pi}\right)G_T = \frac{{V_{Tag}}^2}{R_c} \qquad (2)$$

where

The separation between the antennas is r, which is assumed to be large enough for the tag to be in the far field of the reader. E is the electric field strength of the reader at the tag location. The efficiency of the matching network will be taken as unity and ignored (losses in the network may also be accounted for in the value of $G_T$). Antenna gains $G_R$ and $G_T$ are expressed relative to an isotropic antenna. From considerations of power flux density at the tag, with λ as the wavelength. The typical output power of tag is 500mW. The voltage of the tag can be obtained by:

$$V_{Tag} = \left(\frac{\lambda}{4\pi r}\right)\sqrt{P_R G_R G_T R_C} \qquad (3)$$

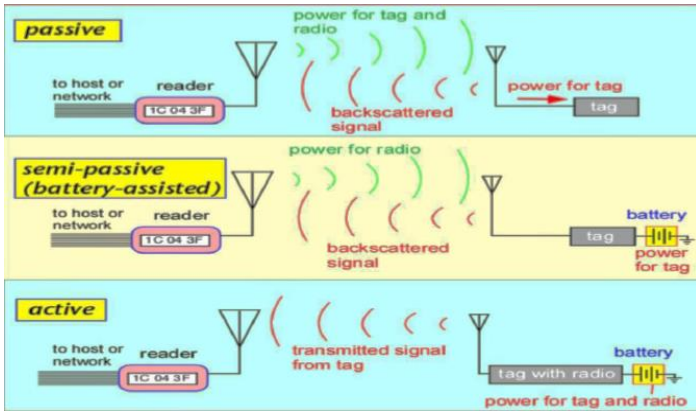


Fig. 5 Types of RFID

From the Fig. 5, the tags can be categorized as:

a. Active Tag

This type of tag contains a battery which supplies power to all functions and a transmitter.

b. Semi-passive Tag

This type of tag contains a battery which us only used to power the tag Integrated Circuit and not for communication.

c. Passive Tag

This tag has no battery integrated to it. This actually makes the tags cheaper and reliable in their use compared to the active tags. They are able to draw power from the reader. The electromagnetic wave received causes a current to be induced in the tag's antenna. The current is then used to power the tag's circuitry.

The quality and reliability of RFID system depends on: tag size, reader/writer antenna size, tag orientation, tag operating time, tag movement velocity, effect of metallic substances on operating range, multiple- tag operating characteristics, and the effect of the number of tags on operating success rate, tag overlapping.

***Advantages***

i. RFID tags are very easy to install/inject inside the body of animals, thus helping to keep a track on them. This is useful in animal husbandry and the poultry industry, wherein the installed tags give information about the age, vaccinations, and health of the animal.

ii. It is more secure than barcodes since it cannot be duplicated easily.

iii. Can store data up to 2KB(Kilobytes) compared to the barcode which contains 10-12 digits. This allows a better encoded identification.

iv. Making updating of stocks, during transportation and logistics of a product more effective.

v. Does not require line of sight.

vi. RFID tags are reusable

***Disadvantages***

i. Difficulty in reading information from tags stored in liquids and metal cases. The radio waves are reflected.

ii. Interference by neighbouring cell towers.

*B. Fingerprint Scanner*

Fingerprint scanning has proved to be more effective and convenient method for biometric systems. The scanners are classified as follows:

**i. Optical Scanners**

This is the oldest method which as the name suggests captures an image of the fingerprint and using an algorithm to detect unique patterns on the surface such as ridges or unique marks. The higher the resolution of the scanner, the higher the accuracy. However, the scanner can be bypassed by prosthetics or images of good quality.

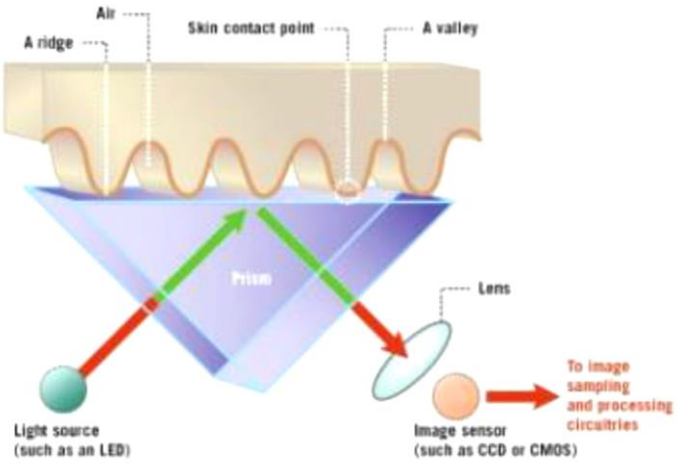


Fig. 6 Optical Scanner

**ii. Capacitive Scanners**

This scanner uses an array of tiny capacitor circuits to collect information about a fingerprint. A plate is connected to charge holding capacitors. When the finger's ridge is placed on the plate, the charge changes slightly while the air gap will leave the charge at the capacitor relatively unchanged. An operational amplifier is incorporated to the circuit to detect these changes and recorded by an analogue-to-digital converter. The information is then stored and distinctive patterns analysed. This method is very secure since it cannot be fooled by an

image. The only loophole is software or hardware hacking. An increase in capacitor components increases the resolution.

$$Capacitance_{Sensor} = Capacitance_{air} + Capacitance_{Oxide}$$

where; $C_x = \frac{\varepsilon_{oA}}{d}$ and $C = \frac{Q}{V}$

$$Q - charge, C - Capacitance, V - Voltage,$$

$$\varepsilon - Permitivity$$

With varying capacitance, the voltage varies and is fed to inverting amplifier.

$$V_{output} = \frac{R_{feedback}}{R_{output}} V_{input}$$

where R – Resistance and V – Voltage.

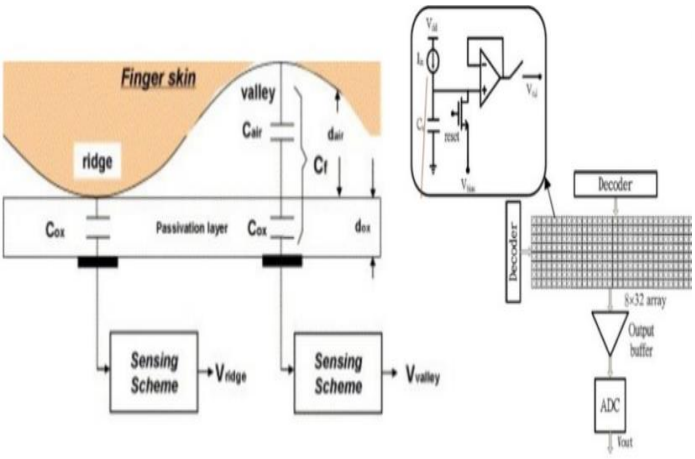


Fig. 7 Capacitive Finger scanner

### iii. Ultrasonic Scanners

This is the latest scanning technology. An ultrasonic transmitter and receiver are used. During the recognition process, an ultrasonic pulse is transmitted against the finger. Some of the pulse is absorbed while others bounce back to the sensor which relies on the pattern of the finger ridge. A sensor is used to detect mechanical stress and calculates the intensity of the returning ultrasonic pulse at different points of the scanner. The longer the scanning the higher the accuracy of the information obtained. This enables the creation of a 3D reproduction making a more secure alternative to the capacitive scanners.

## V. Global System for Mobile Communication (GSM)

This is a cellular technology used for transmitting mobile voice and data services. Initially known as Groupe Spėcial Mobile, it was later renamed to Global System for Mobile Communication to accommodate worldwide usage. This standard was created around 2G networks. It was first deployed in Finland in 1991. It had the following features:

- ✓ Digital, circuit-switched network optimized for full duplex voice telephony.
- ✓ Data communication first by circuit switched transport then by packet data transport through GPRS (General Packet Radio Services) and EDGE (Enhanced Data rates for GSM Evolution)

The system utilizes Time-Division Multiple Access (TDMA) to enable greater capacity. It is the most widespread method of communication in the cell technologies in use in the industry. Through the development of GPS, Short Messaging Service (SMS)was created. The radio spectrum can be shared by various users accessing the same frequency band without obstruction. GSM uses 200kHz radio frequency channels which are time-division multiplexed. Eight concurrent calls on same radio frequency are possible. Multiplexing divides the accessible bandwidth between different channels.

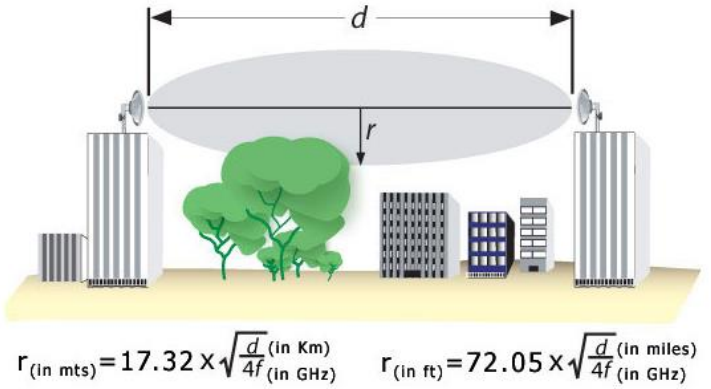


Fig. 8 GSM Coverage

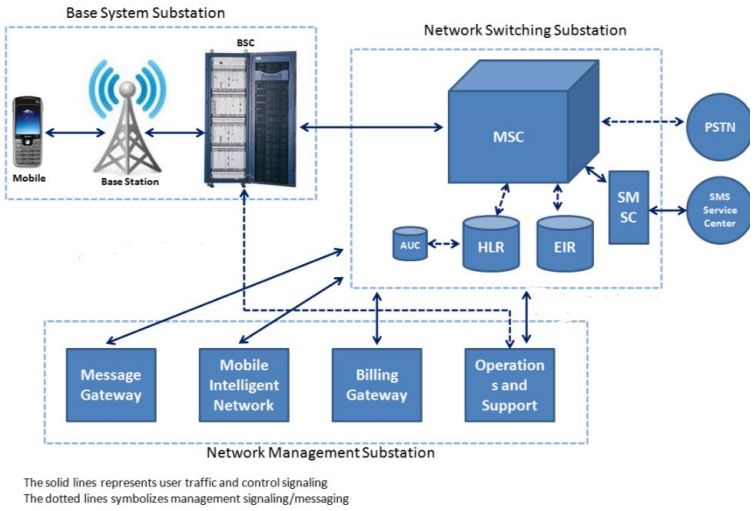


Fig. 9 Network Management

BSC: Base Station Controller

MSC: Mobile Station Controller

SMSC: Short message Service Centre

EIR: Equipment Identity Register

HLR: Home Location Register

AUC: Authentication Centre

PSTN: Public Switched Telephone Network

**Network Structure**

The basic GSM network is divided into:

a. Base Station Subsystem

b. Network and Switching Subsystem

c. GPRS Core Network

d. Operation Support System

GSM system is a cellular network which cell phones connect to the network by searching for cells in the immediate vicinity. The different classes of sizes are:

i. Macro – Base Station Antenna is on a mast or a building above average rooftop.

ii. Micro – Antenna height is under average rooftop and mostly used in urban centers.

iii. Pico – Has a coverage diameter of a few meters and mostly used indoors.

iv. Femto – Used in residential setups or small business to connect to service providers through broadband internet.

v. Umbrella Cells – Cover shadowed regions of smaller cells.

The cell horizontal radius depends on:

a. Antenna height

b. Antenna gain

c. Propagation Conditions (GSM = 35km)

***Advantages***

i. GSM technology has an extensive coverage and contains a harmonized spectrum such that even though countries operate in different frequency bands, users can transfer seamlessly between networks and keep the same number.

ii. GSM technology is supported by many devices

***Disadvantages***

i. When the bandwidth has enough users, the transmission encounters interference.

ii. GSM interferes with other electronic devices such as pace-makers.

## VI. Comparison

TABLE I

| CURRENT SYSTEM | PROPOSED SYSTEM |
|---|---|
| • Vulnerable to human intrusion | • Secure to human intrusion |
| • Time consuming | • Time efficient |
| • Many loopholes to facilitate corruption. | • Does not require human contact |
| • Insufficient accountability and record-keeping. | • Effective automated storage and sorting system. |

## VII. Conclusion

Examination cheating in Kenya has bedeviled the education system. The effects in the society are plain and a solution has to be found immediately. It has been realized that most of the theft occurs at storage points [5] [6]. From my research, it was also noted that both the examination papers and marking schemes were stolen [7] [8].The proposed system addresses this problem by monitoring and controlling access to the examination materials in real time using a computer system. This will enable fair measure of student's performance nationally without compromising on financial constraints of the economy since the components are readily available. The proposed system will also provide a foundation of digital literacy improvement program of the country as per Kenya Vision 2030. Upon full implementation of the proposed system, real-time online examinations would be a reality across the country. More research is to be done concerning examination malpractices to provide better systems.

## VIII. Acknowledgement

Kelvin Mong'are would like to thank God for the strength provided to perform this work.

## REFERENCES

[1] G. B. Nyamoita and K. Otieno, "Effectiveness of Kenya National Examinations Council Measure in Curbing National Examination Malpractices in Public Secondary Schools in Kisii County," *International Journal of scientific research and management (IJSRM),* vol. 4, no. 02, pp. 3882-3907, 2016.

[2] K. Odit, "Record Number of Candidates Sit the 2016 Form Four Exams," 07 November 2016. [Online]. Available: http://allafrica.com/stories/201611070093.html. [Accessed 08 November 2016].

[3] A. Oduor, "New details of how KCSE, KCPE will be conducted," 13 October 2016. [Online]. Available: http://www.standardmedia.co.ke/mobile/article/2000219525/new-details-of-how-kcse-kcpe-will-be-conducted?pageNo=2. [Accessed 28 October 2016].

[4] R. Niranjan, S. Thangapandi, M. Gladwin and G. Thadeus , "A New Approach of RFID and GSM Assisted," *International Journal of Emerging Technology in Computer Science & Electronics (IJETCSE),* vol. 8, no. 1, pp. 0976-1353, 2014.

[5] C. Nyamwange, P. Ondima and P. Onderi, "Factors Influencing Examination Cheating Among Secondary School Students: A Case of Masaba South District of Kisii County, Kenya," *Elixir International Journal,* vol. 56, no. 1, pp. 13519-13524, 2013.

[6] E. K. Njue, G. M. Muthaa and P. K. Muriungi, "Effectiveness of Examination Handling and DIstribution Procedures in Curbing Malpractices in Secondary Schools in Eastern Province, Kenya," *Creative Education,* vol. 5, no. 10, pp. 573-579, 2014.

[7] J. Angote, "A Mandera teacher made Sh1.5 million from selling leaked exam," 29 March 2016. [Online]. Available: http://www.nation.co.ke/news/Revealed-How-police-and-teachers-steal-KCSE-exams/1056-3137164-12f7qm7z/index.html. [Accessed 26 October 2016].

[8] "How KCSE exams are stolen," 14 February 2009. [Online]. Available: http://www.nation.co.ke/news/1056-530526-k7bmstz/index.html. [Accessed 26 Ocotber 2016].

# TV White Spaces Opportunistic Spectrum Access for Wireless Regional Area Networks.

Kenneth Kimani[1*], Kibet Langat[2] and Vitalice Oduol[3]

***Abstract*** **-** Radio spectrum is a finite resource. Demand for access to spectrum is at an all-time high and it is becoming increasingly difficult to find spectrum that can be made available either for new services or to expand existing ones since most of the spectrum has been assigned. The recent migration from analogue transmissions to the spectrally efficient digital television transmissions has however freed up some portions of the spectrum in the Ultra High Frequency (UHF) and Very High Frequency (VHF) bands for reallocation to other licensed uses and also for opportunistic secondary access. These portions of unused spectrum are known as white spaces or spectrum holes in TV transmission bands.

With demand for wireless connectivity increasing, the exploitation of white space is an attractive way of making more efficient use of radio spectrum simply by sharing the spectrum such that if not used in one location or during a given time period by the primary user, then it can be redeployed and used opportunistically by secondary users as long as they will not interfere with the primary users hence making it ripe for deployment of Wireless Regional Area Networks (WRAN). TV white space has immense potential in those parts of the geographical area which are very difficult and expensive to reach by optical fiber techniques and other types of technologies. It's also very applicable to developing countries where the telecommunications infrastructure isn't in place and can potentially be a cost effective way of bridging this telecommunications gap easily.

This paper aims to investigate the suitability of unlicensed use of the TV White Space (TVWS) in a wireless regional area network without causing interference to the incumbent primary users and will also analyze interference if any to the primary users from secondary users in TV White Spaces.

***Keywords*****—**Wireless Regional Area Network (WRAN), Opportunistic Spectrum Access (OSA), TVWS (TV White Space)

## I. INTRODUCTION

TV White Space refers to low-power, unlicensed operation of communications services in unused portions of RF spectrum that fall within frequencies allocated by regulators to television broadcasters and wireless microphones. A TV white space channel is thus an unoccupied or unused TV channel in the Very High Frequency (VHF) and Ultra High Frequency (UHF) where there is no active TV broadcasting on the channel as shown in figure 1.

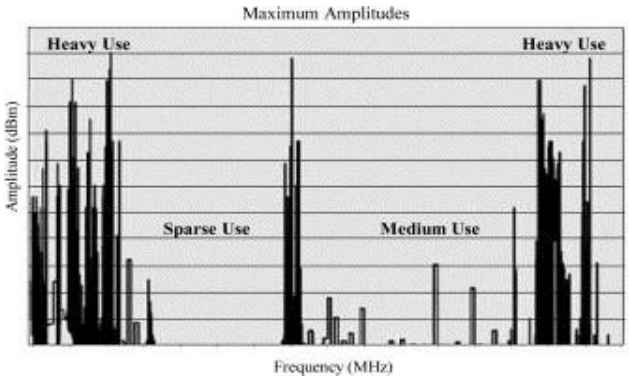


Fig. 1:Usage of spectrum bands showing periods of unoccupancy [1]

The TV white spaces can arise from three main aspects: -

a) Frequency domain - The electromagnetic spectrum is fragmented into sets of frequency bands most of which are licensed to different users or allocated for specific uses. If some band is not allocated to anybody, then that is a white space in frequency domain (often-called Spectrum hole). These spectrum holes have also arisen in TV bands due to analogue to digital migration and includes the guard bands that are left intentionally between two adjacent channels to guard against interference.

b) Time domain - If a user does not use the spectrum allocated to them for a period of time, that spectrum can be utilized by someone else for that idle period. In this case if the TV broadcasters are not using their allocated frequencies for a period of time, it is a TV white space in time domain.

c) Space domain - Any wireless transmission is limited by its range. Whitespaces therefore exist where there is no coverage or where there are holes in the geographical coverage provided by the primary licensee. For example, FM radio stations have a range of around 50 km radius beyond which you can't listen to the FM radio. Thus the same frequency can be used to transmit outside that radius without interfering with that station. This technique is usually applied in GSM, where frequencies are reused in every 7th cell [2].

For purposes of this paper the term TV white space will be used to refer to any or various combinations of the above three domains. Opportunistic Spectrum Access (OSA) enables wireless devices to identify and make use of TVWS at a

Kenneth Kimani, Department of Telecommunications & Information Engineering, JKUAT (phone: +254724012663; e-mail: kuriakimani@yahoo.com).

Kibet Langat, Department of Telecommunications & Information Engineering, JKUAT (e-mail: kibetlp@jkuat.ac.ke).

Vitalice Oduol, Department of Electrical & Information Engineering, UoN (e-mail: vkoduol@uonbi.ac.ke).

particular location and/or at a particular time. OSA therefore enables the borrowing of spectrum from primary users by the secondary users. Primary users (PU) are licensed incumbent users and have the exclusive rights in using certain frequency band for communications while secondary users (SU) are allowed to use the frequency spectra momentarily but only if they do not interfere with the PU. The primary and the secondary users coexist together in the same wireless ecosystem since OSA allows sharing of existing spectrum licensed to primary users to allows the exploitation of unused and under-utilized spectrum by the secondary users. [3]

The rest of the paper is organized as follows: Section II gives a brief description of the digital switchover. Section III introduces the IEEE 802.22 WRAN system. Section IV describes the TV band devices. Section V explores the factors affecting the availability of TV white spaces. Section VI reviews other technologies that could be used to deploy WRAN and how they compare to the IEEE 802.22. Section VII presents interference and describes the main types of interference between the primary and the secondary users. Section VIII describes the interference modelling and simulation. Section IX gives a discussion of the results. Finally, Section X draws the conclusions.

## II. Analogue Switch off

Prior to 17 June 2015, the bands 47 - 68 MHz, 174-230 MHz and 470-806 MHz were allocated to analogue terrestrial television broadcasting service. Analogue signals required more broadcasting spectrum than digital television, were more susceptible to interference and distortion, and hence needed to be spaced far apart to avoid interference. Digital transmissions are more spectrally efficient such that many more fit in the space of the original analogue channel width. [4]

The migration to digital platform of broadcasting has produced what is known as digital dividend. Digital dividend refers to the radio spectrum which is freed up in the process of digital television transition. When television broadcasters switched from analog TV to digital-only platforms, part of the electromagnetic spectrum that had been used for broadcasting was freed-up because digital television needs less spectrum than analog television [5]. One reason is that new digital video compression technology can transmit numerous digital sub-channels using the same amount of spectrum used to transmit one analogue TV channel. Another reason is that digital transmissions require much less of a guard band on either side, since they are not nearly as prone to RF interference from adjacent channels. Because of this, there is no longer any need to leave empty channels to protect stations from each other, in turn allowing stations to be repacked into fewer channels, leaving more contiguous spectrum to be allocated for other wireless services.

The 800MHz frequency (actually consisting of spectrum in 790-862 MHz frequency bands) is referred to as digital dividend 1 (DD1) while the 700MHz frequency (actually consisting of spectrum in the 694-790 MHz frequency bands) is referred to as digital dividend 2 (DD2) [5]. It was agreed by African countries that DD1 be allocated to mobile services after the digital switchover (DSO) whose deadline was June 17, 2015. However most African countries have yet to complete the digital migration process. The amount of spectrum to be released in the switchover depends primarily on national peculiarities such as the geography and topography of a country, the degree of penetration of cable and/or satellite television services, requirements for regional or minority television services, and spectrum usage in neighboring countries. The amount also depends on the digital television technology being implemented to replace analogue services. Therefore, the size of the digital dividend will vary from region to region, and from country to country.

Advancement in technology has led to development of sophisticated digital compression techniques to enable digital transmissions to go beyond the analogue channel bandwidth. The requirement that digital television terrestrial broadcasting should fit in the channels (6, 7 and 8 MHz) intended for analogue television emission in the VHF/UHF bands has led to digital compression systems that allow the transmission of several (up to six, depending on the coding and modulation techniques) standard digital television channels into a single analogue television channel hence reducing the overall use of spectrum [5].

## III. IEEE 802.22 WRAN

IEEE 802.22 is a standard specifying wireless regional area network (WRAN) communication systems operating in TVWS. IEEE 802.22 focuses on constructing wireless regional area networks that utilize UHF/VHF TV bands between 54 and 862MHz (TV channels 2 to 69) with a bandwidth of 6, 7 or 8MHz depending on the country while ensuring that no harmful interference is caused to the incumbent TV broadcasting and low-power licensed devices such as wireless microphones [1]. WRANs are designed to support a point-to-multi-point (P2MP) wireless air interface with one base station (BS) and multiple customer premises equipment (CPE) in an IEEE 802.22 cell. The CPEs will be attached to the BS via a wireless link. The BSs will control the medium access for all the CPEs attached to it and manage the channel allocation amongst CPEs with the and aim of coexistence with the PUs and the neighboring IEEE 802.22 cells. The coverage area of IEEE 802.22 is typically 17-30 km or more in radius (up to 100km) from a base station [6]. One key feature of the WRAN Base Stations is that they are capable of performing cognitive sensing. The CPEs sense the spectrum and then send periodic reports to the BS informing it about what they sense. The BS, with the information gathered, can then evaluate whether a change is necessary in the channel used or if it should stay and continue transmitting and receiving in the same one [1].

The development of the IEEE 802.22 WRAN standard is aimed at using cognitive radio (CR) techniques to allow sharing of geographically unused spectrum allocated to the television broadcast service, on a non-interfering basis, to bring broadband access to hard-to-reach, low population density areas, typical of rural environments, and is therefore timely and has the potential for a wide applicability worldwide. It is the first worldwide effort to define a standardized air interface based on CR techniques for the opportunistic use of TV bands on a non-interfering basis. [7]

## IV. TV Band Devices (TVBDs)

The devices operating in TV band frequencies are referred to as TV band devices (TVBDs). TV band devices are classified into two major classes: fixed and personal or portable. The portable devices are further divided into Mode I (Slave) and Mode II (Master) devices. The fixed devices are allowed to have 4 Watts Effective Instantaneous Radiated Power (EIRP), while the portable devices are allowed to have either 40 or 100 milliwatts (mW) EIRP, depending on the distance between the operating channel and the closest occupied TV channel which has active TV broadcasting [8] [9]. The fixed devices such as base stations are allowed to operate only in the second adjacent white space channels. The portable devices can be allowed to operate in both first and second adjacent channels, with distinction on transmit power. In the first adjacent channels, the transmit power of the portable devices is limited to 40mW and must be separated from the DTV station by a minimum distance called the keep out distance, while in the second adjacent channels, the transmit power of the portable devices is limited to 100mW.A "portable/personal" white space implementation propagates a signal over a smaller area.

There are restrictions on which channels are permissible for use by TVBDs. Fixed devices are permitted in the VHF channels except channels 3-4 and on the UHF channels except channels 36-38. Portable devices are not permitted in the VHF band. Portable devices are permitted on the UHF channels except 14-20 and channel 37. The exclusion for channels 3-4 is to prevent interference with external devices which are often connected to a TV utilizing either channel 3 or 4. Portable devices are not permitted on channels 14-20 since in 13 metropolitan areas some of those channels are used for public safety applications. Finally, Channel 37 is a protected channel, used for radio astronomy measurements.

While being attractive for its desirable propagation characteristics, the biggest hindrance to using white spaces is how to ensure that the TV white space devices (TVBDs) operate only in the unoccupied frequencies or channels and at the same time protecting licensed incumbent TV broadcasters from interference from unlicensed. To prevent this, it is necessary for the TVBDs to:

a) determine the presence of a licensed user (TV signal) by periodic sensing,
b) transmit at a power level that will not cause interference to licensed services (transmit spectral mask).
c) have geolocation capability with access to a TV bands database.

## V. TV White Space Availability

The architecture of a TVWS WRAN is a secondary network is superimposed on a primary network operating in the UHF/VHF spectrum bands and which can transmit and receive data as long as the primary system is not using its assigned frequency and on condition that it does not cause interference to the primary users. The use of available TV channels is usually constrained depending on the device type. Fixed and portable devices have different requirements among which is the separation distance from digital and analog TV protected contours. In particular, fixed devices cannot use every available TV channel since they are not allowed to operate on first adjacent channels to a TV station while portable devices are allowed to operate on first adjacent channels subject to lower maximum transmit power constraints. This causes the number of available TV white space channels to reduce and also translates to different white space availability for fixed and portable devices. TV white space available for fixed devices is mostly available in sparsely populated areas, such as the semi-urban and rural areas, while the densely populated metropolitan areas have few available TVWS channels [10].

The distribution of available TV white spaces in the UHF/VHF spectrum can thus be classified into urban, semi urban, and rural settings. The amount of available TVWS spectrum thus depends on the device physical location setting, the height above average terrain of the transmitter (HAAT), transmitter coordinates (latitude and longitude), effective radiated power (ERP), horizontal transmit antenna pattern (if the antenna is directional) and the channel number and whether fixed or portable operation planned [11].

If the digital dividend is to be utilized by WRANs, a worldwide (or at least region-wide) frequency harmonization is a required condition. Such harmonization would create enormous benefits in terms of social impact and increased productivity. In particular, utility companies and equipment manufacturers would be able to address a large market, leading to economies of scale and preventing high costs for different devices in each region.

The possibility of harmonization depends primarily upon the timing and coordination of the analogue-to digital switchover process; the digital dividend spectrum will be fully available only after analogue switch off. The main challenge to this is that while some countries have made their plans for the analogue switch-off, others are only considering this possibility. Moreover, different analogue standards and different channel rasters are used across different regions. Another constraint is that broadcasting channels are scattered on a non-contiguous basis across the whole UHF band. Though digital terrestrial television services have been introduced in some countries, they are based on different standards (DVB-T, ATSC, ISDB-T, DMB-T), all using a different channel raster. It should also be noted that parts of the UHF band are also allocated to primary terrestrial services other than broadcasting. Protection of other primary services may limit the ability to use the digital dividend in some countries.

## VI. Review of Existing Technology (Wi-Fi/WiMAX)

In [12]it is shown that the performance of TVWS spectral outperforms the 5 GHz and 2.4 GHz for low to medium traffic loadings (around 2 Mb/s per home) at significantly lower energy requirements. In [13], A Comparative Study between Wireless Regional Area Network (IEEE Standard 802.22) and WiMAX (IEEE Standard 802.16e) was done where the change of cell range with respect to transmitter height, modulation schemes was carried out to assist in better coverage planning. 700MHz frequency band was used for TVWS at transmitter and receiver heights of 30m and 5m respectively. The parameters were considered for QPSK ½, QPSK ¾, 16-QAM ½ and 64-QAM ¾ as shown in fig 2 and 3 below.

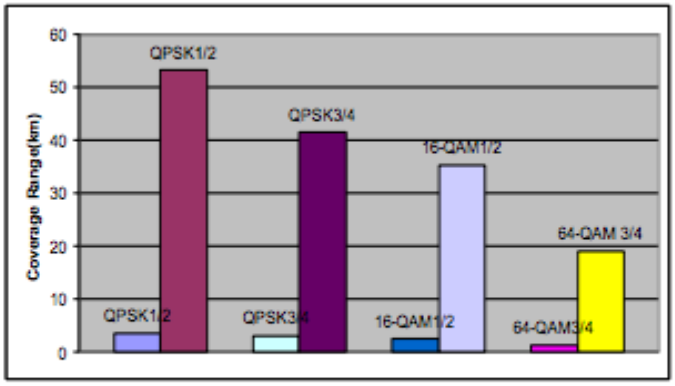


Fig. 2: Downlink coverage range comparison between Wimax and WRAN

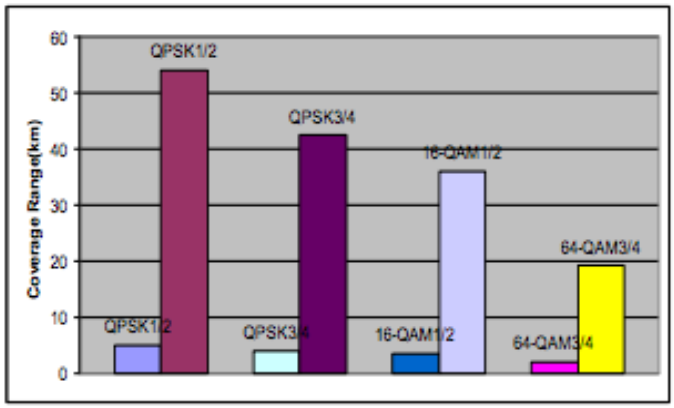


Fig. 3: Uplink coverage range comparison between Wimax and WRAN

One of the differences between WiMAX and WRAN is that WiMAX is based on OFDMA for uplink transmission and OFDM for downlink. TDM is used for creating bidirectional data links. However, on the other hand, WRAN technology uses OFDMA technique for both uplink and downlink transmission [14]. Table I below gives a summary of the major diiferences between the IEEE 802.22 and the IEEE 802.16 standards.

Table I: Comparison between IEEE 802.16e and IEEE 802.22 standards

| Parameter | IEEE 802.16 | IEEE 802.22 |
|---|---|---|
| Coverage Radius | 1 – 5 Km | 33 – 100 Km |
| Air Interference | OFDMA, OFDM, single carrier | OFDMA |
| Multiple Antenna Techniques | Support Multiplexing, space time coding and beam forming | Not Supported |
| Coexistence With Primary Users | Not Supported | Spectrum Sensing, Geolocation, Database Query |
| OFDMA channel profile(MHz) | 28,20,17.5,14, 10,8.75,7,3.5,1.25 | 6,7,8 |
| Self-Coexistence | Master Frame Assignment | Dynamic Spectrum Assignment |

We can see from table I that WRAN offers much better coexistence with existing technologies better than WiMAX and has a much superior range thus providing coverage in a much bigger geographical region. A comparison between the IEEE 802.22 technology relative to other IEEE 802 standards in terms of range, data rate and multipath absorption window is sown below (Figure 4).

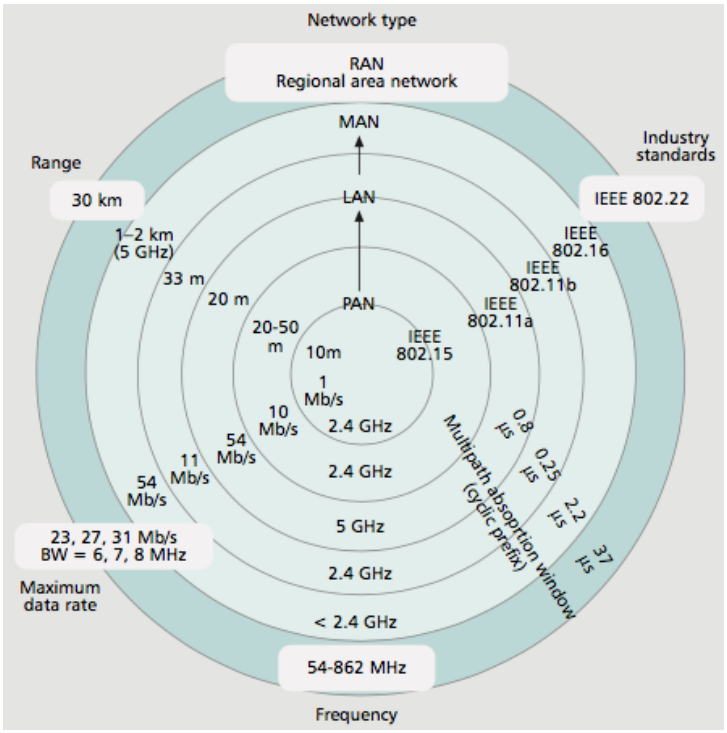


Fig 4**:** Comparison between the IEEE 802.22 standard relative to other IEEE 802 wireless data transmission standards.

Fig 4 shows that IEEE 802.22 is a superior standard and is much better for deployment of WRAN as compared to other IEEE 802 standards. This happens since TV bands are below 1 GHz and have excellent properties for propagation, building and foliage penetration, and non-line of sight connectivity. They offer excellent opportunities to support various applications, including wireless broadband access, Wi-Fi like networks with better coverage and penetration.

By physical law, the coverage of a radio device is proportional to the square of the frequency [15]. Due to this lower frequency spectrum, it costs cheaper to build a wireless network in the TV band frequencies since it allows deployment of fewer antennas operating at lower power levels and hence the number of base stations are lower compared to other higher frequency spectrum. TVWS therefore permits more expansive reach than conventional Wi-Fi networks, which utilize higher frequencies that limit their range. This impressive reach has spawned the nickname “Super Wi-Fi” and “White-Fi” for TVWS networks. [2]

## VII. Interference

One criterion for interference to occur is for the victim receiver to have a carrier to interference ratio (C/I) less than the minimum allowable value (known as the protection ratio). In order to calculate the victim’s C/I it is necessary to establish the

victim's desired Received Signal Strength (dRSS) as well as the interfering Received Signal Strength (iRSS). The position of the victim's wanted signal transmitter is identified and a link budget calculation completed. Having knowledge of both the interfering signal strength and the wanted signal strength allows the victim's C/I ratio to be computed. The main causes of interference between primary users and secondary users are:

**i)** Co-channel Interference

Co-channel interference refers to interference from the transmitter of the secondary system to the receiver of a licensed primary system and usually occurs if the secondary system transmits in an occupied TV channel [16]. This may be due to misdetection where the secondary user detects the primary user as absent due to fading and shadowing and attempts to transmit in the same frequency as the primary user. It can also occur if the spectrum-sensing period is long enough that the secondary user is not able to detect the reappearance of the primary user fast enough in a previously unoccupied channel that it continues to transmit instead of vacating the channel. [17]

**ii)** Adjacent Interference

Adjacent channel interference occurs when the receiver of the licensed primary system is subject to interference in its channel from a secondary system operating in TVWS in an adjacent (neighbouring) channel. This is caused by extraneous power from a signal in an adjacent channel mainly due to different power level employed by the two systems and especially if the secondary system transmits at extremely high power levels beyond those stipulated by the ITU and the regulators [17] [18].

**iii)** Image Channel Interference

Some DVB-T receivers are susceptible to interference from transmissions nine 8 MHz spectrum channels above the intended spectrum channel. This is often referred to as the 'image channel' or the 'n+9 channel' [19]. This means that, for a particular channel, if a transmitter site (for DVB-T or any other service, including TVWS services) were deployed in the n+9 channel, there may be an area around the transmitter site where that DVB-T signal could not be received. [6] [20]

A simulation study in [21] has shown the effect of aggregate interference on the spectrum opportunity of TV white space. The measurement results obtained showed that Adjacent Channel Interference (ACI) is dominant inside the coverage area closer to the primary transmitter while Co-Channel Interference (CCI) is dominant closer to the victim receiver at the boundary region.

## VIII. Interference Modelling And Simulation

In this section we will consider various aspects that are taken to account in modelling the interference between primary and secondary users. The modelling will be carried out using SEAMCAT. SEAMCAT (Spectrum Engineering Advanced Monte Carlo Analysis Tool) is a statistical simulation software tool based on Monte-Carlo analysis [9] and is used for addressing compatibility studies between different radio technologies by assessing the potential interference between different radio communication systems. In order to get the best results, the SEAMCAT simulations were carried out by generation of 20,000 events to ensure the reliability of the probability interference results obtained. The primary and secondary networks were simulated along the parameters shown in table II below. The propagation model employed was the Okumura extended Hata and a spectrum sensing threshold of -110 dBm was considered capable of sensing the digital TV signals. In [21] a review of the application of the extended hata propagation model was carried out and fixed and mobile measurements showed that the extended hata model is appropriate to describe the path loss over in the UHF/VHF frequency bands. We also considered a maximum transmitter power of 33dBm for the victim receiver.

Table II: Simulation modelling parameters

| Simulation Parameters | DVB-T/T2 | Cognitive Radio |
|---|---|---|
| Channel Width | 8 MHz | 8MHz |
| Transmit Power | 72.15 dBm | 33 dBm |
| Receiver Bandwidth | 7.71MHz | 7.71MHz |
| Antenna Height Tx | 100m | 30m |
| Antenna Height Rx | 10m | 1.5m |
| Antenna Gain | 6dBi | 6dBi |
| Receiver Sensitivity | -96dBm | -96dBm |
| Receiver Noise Floor | -110dB | -110dBm |
| Propagation Model | Extended Hata | Extended Hata |
| Receiver Noise Figure | 7dB | 5dB |
| Modulation | 64 QAM | 64 QAM |
| Frequency Band | 594 MHz | 470~698 MHz |

A first adjacent (white space) channel is a white space channel that is right next to an occupied TV channel. A second adjacent (white space) channel is a white space channel that is two channels away from an occupied TV channel. However, for purposes of this simulation, the term second adjacent (white space) channel was used to refer to a white space channel that is not neighboring any occupied TV channel. A WSD transmission commonly occupies most, but not all, of an 8 MHz TV channel, although WSDs with wider and narrower bandwidths are possible. In deriving the protection ratio, the wanted WSD signal power is measured in 8 MHz. We therefore also assumed an 8MHz channel width.

## IX. Results and Discussion

Radio frequency signal-to-interference ratio (C/I) is the ratio of the power of the wanted signal to the total power of interfering signals and noise, evaluated at the receiver input while radio frequency protection ratio (PR) is the minimum value of the signal-to-interference ratio required to obtain a specified reception quality under specified conditions at the receiver input. Usually, PR is specified as a function of the frequency offset between the wanted and interfering signals over a wide frequency range. In this paper we will consider the case where the victim link receiver (VLR) bandwidth and the interfering link transmitter (ILT) reference bandwidth have the same value (i.e. 8 MHz) hence no bandwidth correction factor is to be applied.

Simulation Case 1:

In this case we consider the effects of a secondary user

transmitting at the same frequency as the primary user. The secondary user is transmitting at 594 MHz. There is a high probability of interference at 29.40% as shown in the table below. Fig. 12 compares the dRSS and iRSS values of the secondary user and DVB-T signals. Increasing the power of the cognitive radio to 40dBm raises the probability of interference to 44.80%. The simulation parameters were as shown in table III below.

Table III: Simulation parameters (Same Channel)

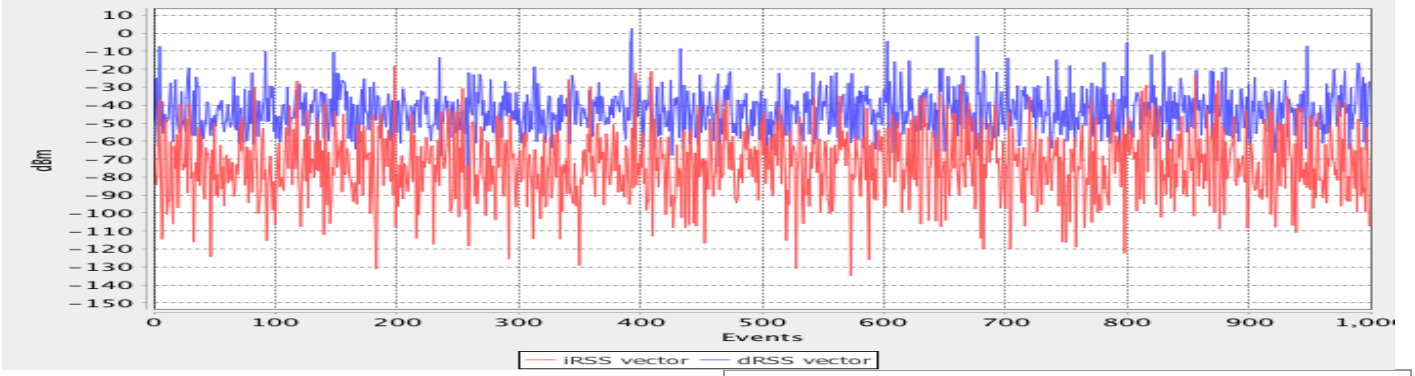


| Simulation Results | |
|---|---|
| **Parameter** | Value |
| **dRSS mean value** | -43.41dBm |
| **iRSS unwanted value** | -73.39dBm |
| **iRSS blocking value** | -102.88dBm |
| **C/I** | 19.0 |
| **Probability of interference** | 29.40% |

Fig. 5: dRSS and iRSS vector values

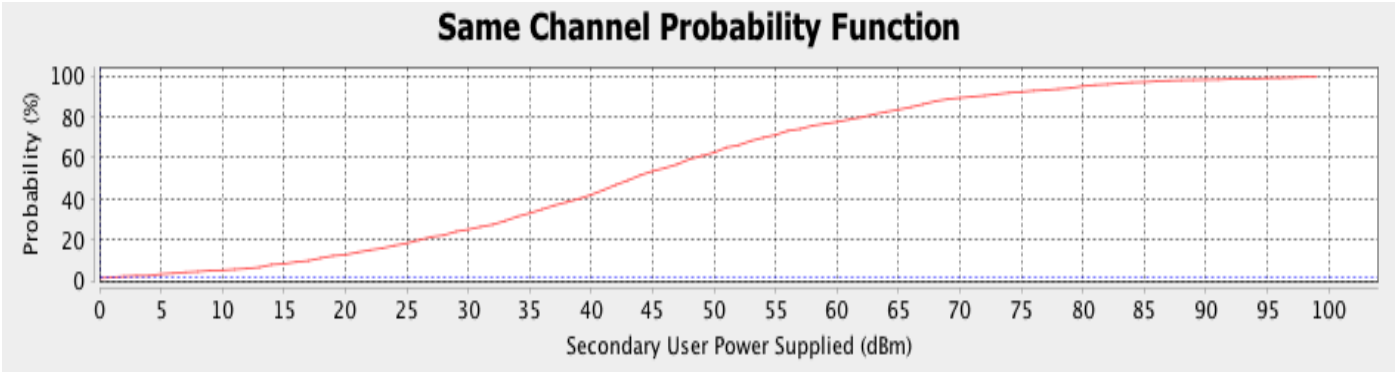


Fig. 6: Probability function of varying power of secondary user

Simulation Case 2:

In this case we consider the effects of a secondary user transmitting in an adjacent channel to the one in use by the primary user. There is a high probability of interference at 19.20% as shown in the table below. Fig. 14 compares the dRSS and iRSS values of the secondary user and DVB-T signals. Increasing the power of the cognitive radio to 40dBm raises the probability of interference to 29.80%. The simulation parameters were as shown in table IV.

Table IV: Simulation parameters (Adjacent Channel)

| Simulation Results | |
|---|---|
| **Parameter** | Value |
| **dRSS mean value** | -44.89dBm |
| **iRSS unwanted value** | -82.87dBm |
| **iRSS blocking value** | -103.42dBm |
| **C/I** | 19.0 |
| **Probability of interference** | 19.20% |

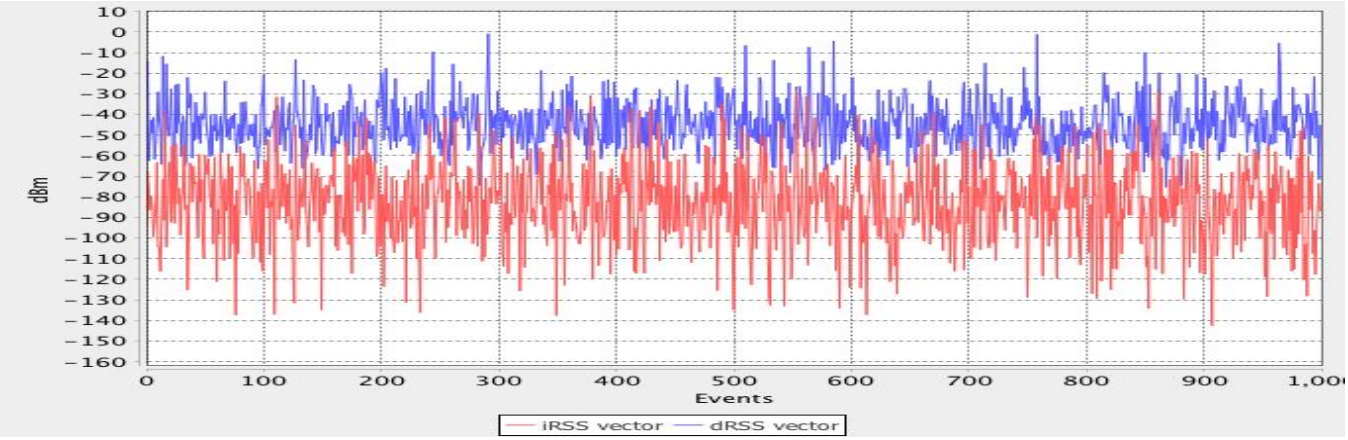


Fig. 7: dRSS and iRSS vector values

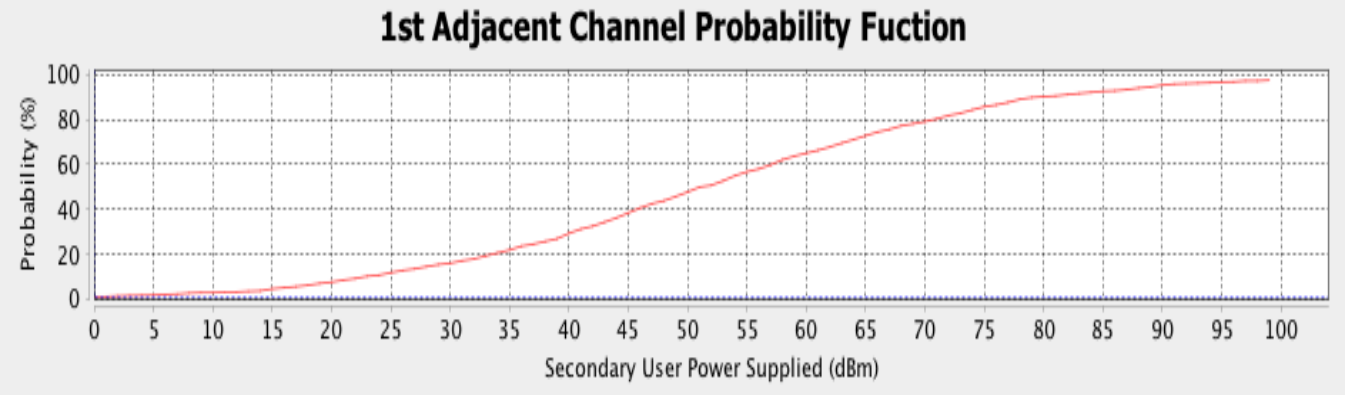


Fig. 8: Probability function of varying power of secondary user

Simulation Case 3:

In this case we consider the effects of a secondary user transmitting in a second adjacent channel to the one in use by the primary user. There is a high probability of interference at 1.80% as shown in the table below. Fig. 16 compares the dRSS and iRSS values of the secondary user and DVB-T signals. Even after Increasing the power of the cognitive radio to 40dBm raises the probability of interference to 3.60%. The simulation parameters were as shown in table V.

Table V: Simulation parameters (2nd Adjacent Channel)

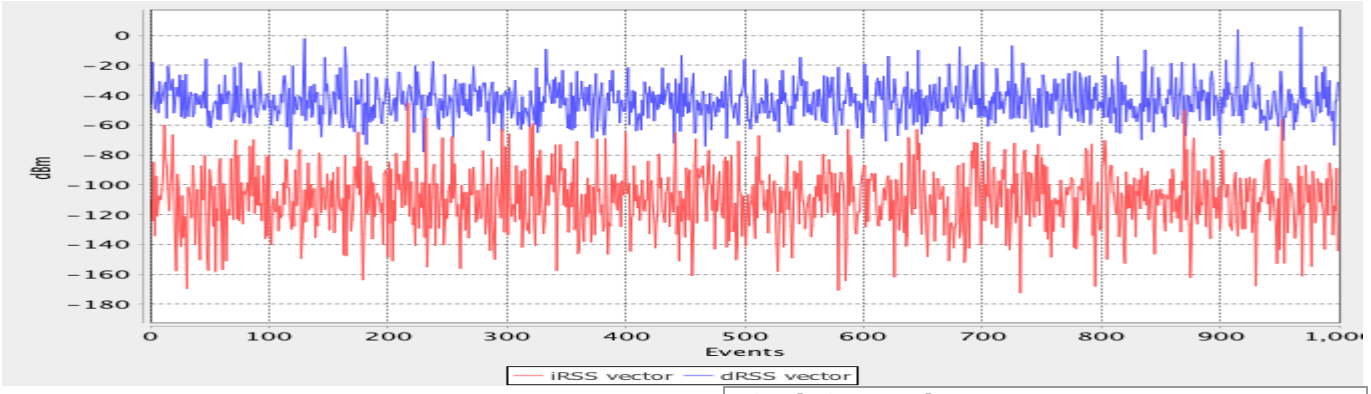


| Simulation Results | |
|---|---|
| **Parameter** | Value |
| **dRSS mean value** | -43.98dBm |

| | |
|---|---|
| **iRSS unwanted value** | -109.88dBm |
| **iRSS blocking value** | -103.36dBm |

| | |
|---|---|
| **C/I** | 19.02 |
| **Probability of interference** | 1.80% |

Fig. 9. dRSS and iRSS vector value

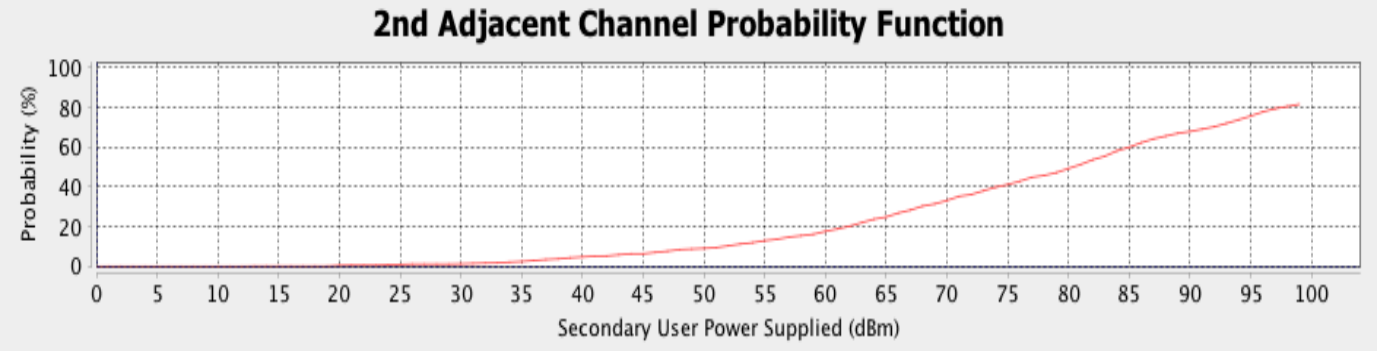


Fig. 10. probability function of varying power of secondary user

One of the most challenging problems of a TVWS WRAN system is the interference which occurs when the SU accesses the spectrum but fails to become aware of the presence of a transmitting primary user in the channel. The interference is thus highest when both the primary user and the secondary user are transmitting on the same channel as can be seen in case 1 where the probability of interference is 32.6% at 4W secondary power. Increasing the power of the secondary user raises the probability of interference to 43.50%. Interference in the same channel may also occur when multiple secondary users select the same TV channel due to an uncoordinated selection process or limited availability or if the spectrum-sensing period is very long such that the secondary user is not able to detect the reappearance of the primary user fast enough in a previously unoccupied channel that it continues to transmit instead of vacating the channel.

It is therefore important for the secondary users to sense not just the primary users but also sense for other secondary users that might be transmitting at the same instance to avoid interference between the secondary users as they try to transmit at the same time. Secondary users transmitting at the adjacent channel to a currently occupied channel also causes interference though not nearly as high as in the same channel interference. This is as demonstrated in case 2. However, we find from figure 14 that the interference can be minimized if the secondary user transmit power is low enough. Mode II portable devices can easily transmit in the adjacent channels since they have low transmit power requirements as low as 40 mW (16.02dBm) compared to the high power fixed TVBDs that require a transmit power of 4W (36.20 db).

Secondary users transmit power control is therefore a very important factor to consider as it is a major factor affecting the interference of primary users by the secondary users. The higher the transmit power supplied to the secondary user, the larger the coverage radius of the secondary cognitive user network, but also the higher the interference on the primary users as can be seen in figures 6, 8 &10. Tradeoff is therefore required when setting up the secondary network to ensure maximum coverage radius at minimum interference to the primary users.

## X. Conclusion

The use of TV white spaces as an alternative to overcome spectrum scarcity is a huge opportunity for new telecommunication systems and services. These frequencies have excellent potential to penetrate buildings and walls, have a superior range and unlicensed access to spectrum. TVWS implementations are well suited to providing connectivity over long distances. This attribute is especially welcome in applications where devices must convey data over geographies whose boundaries are beyond the reach of higher-frequency Wi-Fi networks.

The application of the developing IEEE 802.22 standard in TVWS will allow broadband access to be provided in sparsely populated areas that cannot be economically served by wireline means, or other wireless solutions at higher frequencies, by using cognitive radio techniques to allow operation on a noninterfering basis in the VHF/UHF TV broadcast bands. This will increase the efficiency of utilization of that spectrum, and provide large economic and societal benefits. TV white space would greatly benefit those parts of the geographical areas where it is both difficult and expensive to reach by other types of technologies like fiber and WiMAX and especially in developing countries where the telecommunications infrastructure isn't in place and can be a cost effective way of bridging this telecommunication gap easily. Such areas like in the rural areas might be avoided by telecommunications companies due to low rate of returns but would benefit from deployment of TVWS networks due to its low deployment costs.

However, a WRAN cannot be deployed without accounting for the effect of the interference they could generate. This is to avoid starving the primary users of access to the networks. The WRAN networks are therefore required to coexist with the primary users by limiting their transmission parameters within the acceptable levels. Special attention is thus paid to the issue

of interference and it is shown that limiting the power and transmitting channel of the secondary users ensures that any potential interference that may be impacted on the performance of the primary users is reduced.

## XI. References

[1] D. A. N. Mody, "IEEE 802.22 –Cognitive Radio-based Regional Area and Smart Utility Networks," in ITU Regional Radio-communications Seminar for Arab Countries: Cognitive Radio and TVWS Workshop, 2013.

[2] D. Tse and P. Viswanath, Fundamentals of Wireless Communications, Cambridge University Press, July 11, 2005.

[3] C. Xin and M. Song, "Opportunistic Spectrum Access," in Spectrum Sharing for Wireless Communications, vol. VIII, Springer International Publishing, 2015, p. 66.

[4] S. S. Arato and P. O. Kalecha, "UHF (700 MHz) Spectrum Band Occupancy Measurements, Analysis and Considerations for Deployment of Long Term Evolution (LTE) Deployment in Kenya," International Journal of Scientific & Engineering Research, vol. 4, no. 11, pp. 572-580, 2013.

[5] R. Kennedy, K. George, O. Vitalice and O.-O. W., "TV White Spaces in Africa : Trials and Role in Improving Broadband Access in Africa," in AFRICON, Addis Ababa, 2015.

[6] G. L. S. ¨ber, S. M. Almalfouh and D. S. Stuber, "Interference Analysis of TV-Band Whitespace," Proceedings of the IEEE, vol. 97, no. 4, pp. 741 - 754, 2009.

[7] V. Popescu, M. Fadda and M. Murroni, " Performance analysis of IEEE 802.22 wireless regional area network in the presence of digital video broadcasting – second generation terrestrial broadcasting services," IET Communications , vol. 10, no. 8, pp. 922-928, 19 May 2016.

[8] Federal Communications Commission, "Second Report and Order and Memorandum Opinion and Order FCC 08-260 pg 65," Washington D.C., 2008.

[9] European Communications Office (ECO), SEAMCAT Handbook, vol. 2, European Conference of Postal and Telecommunications Administrations (CEPT) , 2016, p. 413.

[10] A. S. Cacciapuoti and M. Caleffi, "Interference Analysis for Secondary Coexistence in TV White Space," IEEE Communication Letters, vol. 19, no. 3, pp. 383-386, March 2015.

[11] J. P. Choi, H. M. Chang, H. N. Choi and W. C. Lee, "A Study on Interference Analysis Between DVB-T2 Broadcasting Service and TV White Space Device," in Ubiquitous and Future Networks (ICUFN), 2012 Fourth International Conference on , Phuket , 2012.

[12] S. Kawade and M. Nekovee, "Wireless options for high data-rate indoor users: cognitive access to TV white space," in 2009 First UK-India International Workshop on Cognitive Wireless Systems (UKIWCWS), Delhi, 2009 .

[13] S. Rahman, N. Hossain, N. Sayeed and M. Palash, "Comparative Study between Wireless Regional Area Network ( IEEE Standard 802.22) and WiMAX and Coverage Planning of a Wireless Regional Area Network Using Cognitive Radio Technology," International Journal of Recent Technology and Engineering (IJRTE) , vol. 1, no. 6, pp. 161-163, January 2013.

[14] C. R. Stevenson, G. Chouinard, Z. Lei, W. Hu, S. J. Shellhammer and W. Caldwell, "IEEE 802.22: The first cognitive radio wireless regional area network standard," IEEE Communications Magazine, vol. 47, no. 1, pp. 130 - 138, 2009.

[15] C. Xin and M. Song, Spectrum Sharing for Wireless Communications, Springer, 2015.

[16] R. D. Vieira, E. B. Souza, A.´. M. Cavalcante, R. Pirhonen, P. Kafle, A. Malkov and Z. Li, "Interference Analysis of Coexistence Scenarios in TV White Spaces," Nokia, Manaus, Brazil, 2010.

[17] J. P. Choi, H. M. Chang, H. N. Choi and W. C. Lee, "A Study on Interference Analysis Between DVB-T2 Broadcasting Service and TV White Space Device," in 2012 Fourth International Conference on Ubiquitous and Future Networks (ICUFN), Phuket, 2012.

[18] R. Dionisio, P. Marques and J. Rodriguez, "Interference study between wireless microphone systems and TV White Space devices," in 2012 IEEE International Conference on Communications (ICC), 2012.

[19] S. Puri, "Analysis of Interference from Secondary System in TV White Space," Radio Communication Systems Group, KTH, Stockholm, 2012.

[20] S. Agrawal, R. Bhatia and M. S. Bhadoria, "Interference Mapping for Spectrum Sensing in Cognitive Radio," International Journal of Innovations in Engineering and Technology (IJIET), vol. 6, no. 4, pp. 696-702, 2016.

[21] O. Holland, H. Bogucka and A. Medeisis, "Validating the Extended Hata Model for use in UHFs," in Opportunistic Spectrum Sharing and White Space Access: The Practical Reality, John Wiley & Sons, 2015, 2015, p. 736.

[22] V. Popescu, M. Fadda, M. Murroni, J. Morgade and P. Angueira, "Co-Channel and Adjacent Channel Interference and Protection Issues for DVB-T2 and IEEE 802.22 WRAN Operation," IEEE Transactions on Broadcasting, vol. 60, no. 4, pp. 693-700, December 2014.

# *A Technical Report on*
# Design of a transistor based pulse generation circuit for Electrical Discharge machine

Kipkosgei Patrick[1], Kabini Karanja[2], Ikua Bernard[3]

*Abstract*—A Pulse generation circuit is a key component of an Electrical Discharge Machine (EDM) as it regulates and controls the machining process. Machining parameters such as frequency, duty cycle, machining time, voltage and their execution instructions are set through the Graphics User Interface (GUI) and executed by the pulse generator. Coupled to the pulse generation circuit is the motor driver circuit which controls the vertical motion of the tool based on the prevailing machining conditions, normally measured by a voltage sensor connected between the tool electrode and the workpiece.
This paper presents a new approach in the development of a pulse generation and affiliated circuits for EDM machine developed at JKUAT. The current pulse generation circuit is based on resistor capacitor technology.

*Keywords*—Electrical discharge machining, pulse generation circuit, machining.

## I. INTRODUCTION

Electrical discharge machining (EDM) is a non traditional machining process with no cutting forces between the die and the workpiece but uses thermal energy generated by a spark to remove material from an electrically conductive material [1] [2]. The main components of EDM are; power supply, servo system and pulse generation circuit.
The power supply for the pulse generation circuit uses DC voltage which is obtained from a rectified and stepped down AC voltage from the mains. The servo system controls the vertical movement of the tool electrode. The movement of the tool is retraction in case of a short circuit and advancement in case of an open circuit.
There are two types of pulse generation circuits used in EDM namely; Resistor Capacitor (RC) type and transistor type. RC-type generation circuits generates a pulse when the capacitor and resistor are charged and discharged through the workpiece. Transistor-type generation circuits employ transistors to deliver the pulsed energy to the workpiece by switching on/off the DC power. RC-type generation are mostly used in conventional micro EDM although transistor-type is preferred because of its high machining removal rate (MRR) [3]. The other advantage of a transistor-type pulse generation circuit is that the duty cycle and frequency can be set independently unlike the RC-type [4].
In RC-type, the ON and OFF times cannot be independently adjusted and any adjustment causes changes in the duty cycle and frequency. This is because all these parameters are set using a range of capacitances.
The developed pulse generation circuit uses ATMEL ATMEGA328P micro-controller to generate a pulse width modulated (PWM) signal where the duty cycle and frequency can be controlled independently. The PWM signal controls a MOSFET through an opto-isolator which delivers the electrical machining power. A newly developed motor driver circuit and graphics user interface are also presented.

1 Corresponding author: School of Mechanical, Manufacturing and Materials Engineering, JKUAT, P.O. Box 62000-00200, Nairobi (phone: +254715770881; e-mail: patrick.kipkosgei@jkuat.ac.ke).
2,3 School of Mechanical, Manufacturing and Materials Engineering, JKUAT, P.O. Box 62000-00200, Nairobi.

## II. EXPLANATION OF THE DESIGN

A variable transformer rated at 2 kVA is used to step down the voltage and also regulate machining voltage. A rectifier circuit is used to convert the power from AC to DC. The DC voltage is then passed through capacitors to remove ripples and get a smooth DC voltage. The pulse generation circuit and motor driver circuit are coupled to the GUI. Among the inputs fed through the GUI are; frequency, duty cycle, speed of the motor and machining time.
Two potentiometers are provided for entering the frequency and duty cycle. The potentiometers are connected to the micro-controller's analog input of the GUI (for display purposes) and pulse generation circuit. The analog inputs have an in built 10 bit analog to digital converter that outputs a number between 0 and 1023 to represent the minimum and the maximum position of the potentiometers. For the frequency potentiometer, the micro-controller converts this number to between 5000 and 50 microseconds which represents the period of the frequency between 200Hz and 20kHz. The duty cycle ranges between 5 and 95 percent. The micro-controller in the pulse generation circuit uses two values to generate the desired square, one from the set period and the other from the set percentage.
The speed of the stepper motor is set to an optimal value of 18 rpm through the micro-controller in the motor driver circuit. The drive is provided by a stepper motor that has a 1.8 degree per step resolution.
The machining time, entered through a keypad is counted down by the GUI's micro-controller, and when it reaches zero, the power to the pulse generation circuit is switched off. At this point, the motor driver circuit will retract the die

for 30 seconds to provide enough space for the workpiece to be unclamped. During machining, the GUI displays the machining frequency, duty cycle, machining voltage and time remaining to the end machining. The circuit developed for the pulse generation circuit is shown in Figure 1.

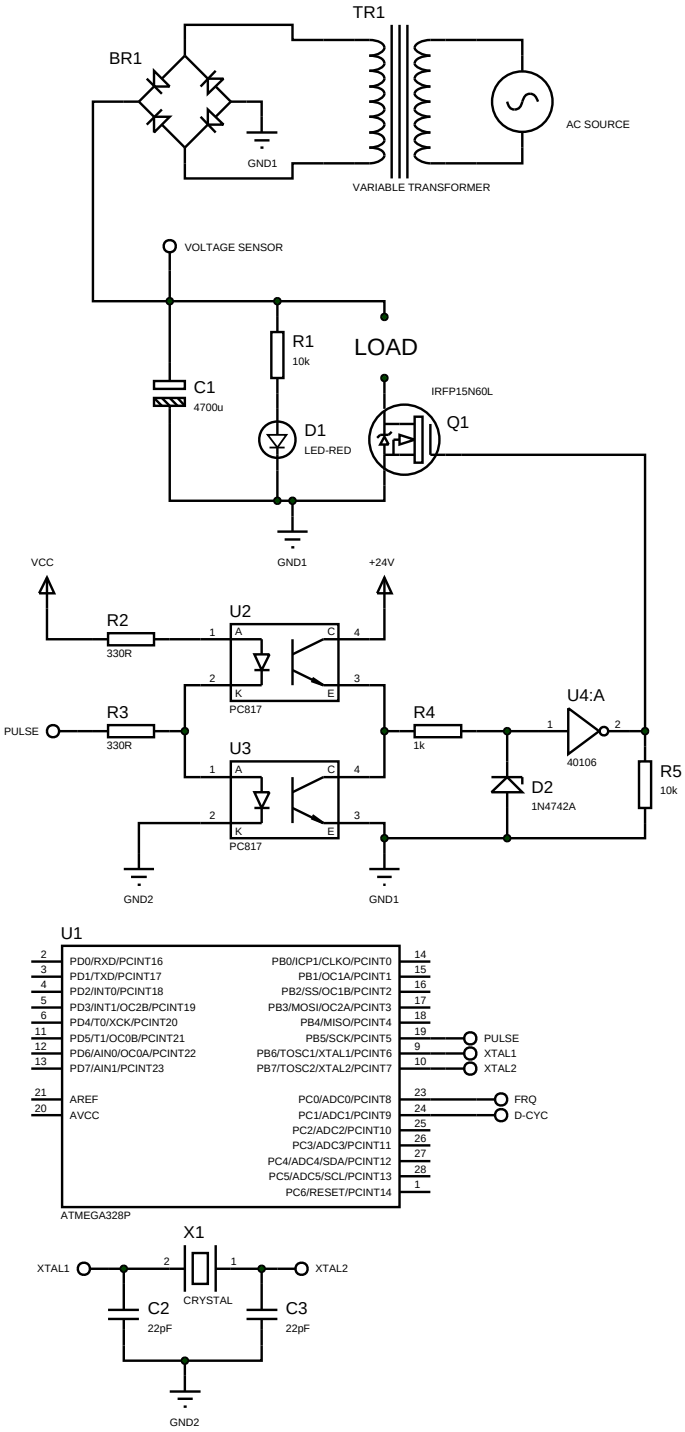


Fig. 1. Schematic of pulse generation circuit

## III. RESULTS

The circuits that were developed for pulse generation, motor drive and graphic user interface were installed in a panel box with the 2 kVA variable transformer supplying the required stepped down power. Figure 2 shows a sample pulsed square waveform generated by the pulse generator, captured using an oscilloscope. Figure 3 shows a discharge signal captured during machining. The discharge signal shows a healthy machining process free of open and short circuit occurrences. In case of short circuit, the discharge voltage signal goes to zero while in case of open circuit the discharge voltage remains at the maximum value.

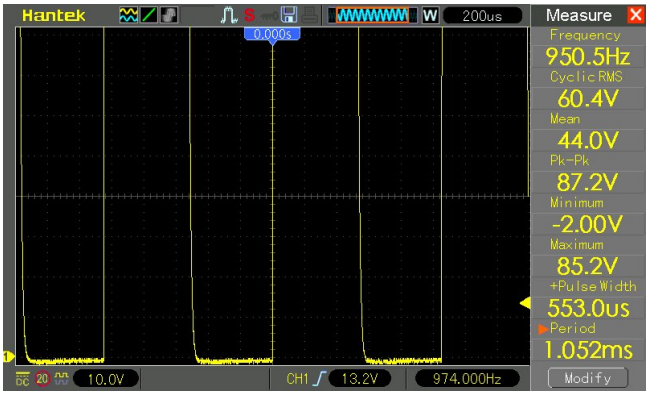


Fig. 2. Generated pulse at 85.4 V and 950.5 Hz

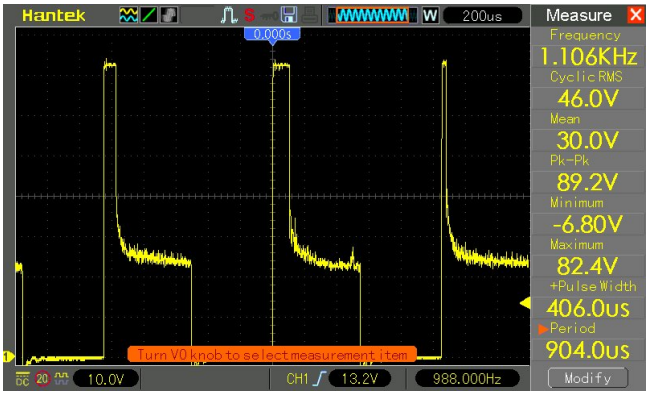


Fig. 3. Machining pulse at 82.4 V and 1.106 kHz

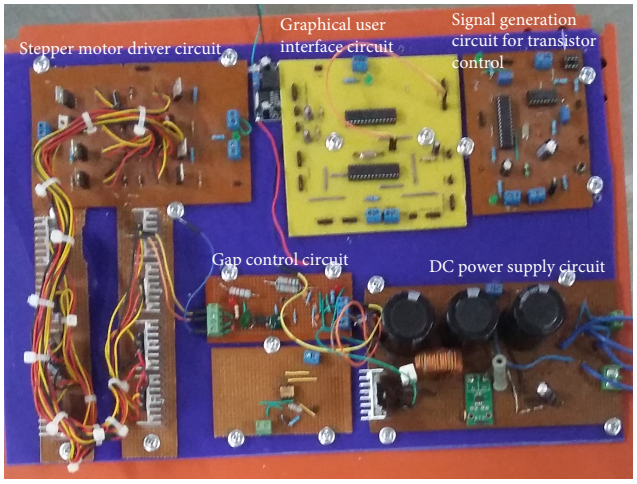


Fig. 4. A photograph of the developed EDM control and pulse generation circuit based on Arduino Atmega 328P microprocessor

## IV. CONCLUSIONS

The pulse generation and other affiliated circuits that were developed for the electrical discharge machine generated the necessary machining pulsed signals as was intended and are currently being tested on the machine. The circuits also provided independent and smooth control of the machining parameters.

## ACKNOWLEDGEMENT

This work was supported by Jomo Kenyatta university of Agriculture and Technology (JKUAT) and the Japan International Co-operation Agency (JICA).

## REFERENCES

[1] S. K. Choudhary and R.S. Jadoun, "Current Advanced Research Development of Electric Discharge Machining (EDM): A Review," *International Journal of Research in Advent Technology*, vol. 2, pp. 273–297, March 2014.

[2] Q.H. Zhang, R. Du, J. H. Zhang and Q. B. Zhang, "An Investigation of Ultrasonic-Assisted Electrical Discharge Machining in Gas," *International Journal of Machine Tools and Manufacture*, vol. 46, pp. 1582–1588, 2016.

[3] U. K. Vishwakarma, "Modelling of Micro Electro Discharge Dachining in Aerospace Material," Master's thesis, National Institute of Technology Rourkela, 2011.

[4] S. K. Kabini, S. K. Bojer, B. W. Ikua, J. M. Kihiu, G. N. Nyakoe and J. W. Wamai, "The Performance of a Resistance-Capacitance Type Pulse Generation Circuit in Electrical Discharge Machining," *Journal of Sustainable Research in Engineering*, vol. 2, no. 4, pp. 158–162, 2015.

# Design and Simulation of Performance of a Gas Turbine Compressor Running on Coal Syngas

Liz Wangui M., Dr. Eng. H. Ndiritu, Dr. B. Gathitu

**Abstract**

There is an increase in demand for electricity. Kenya relies heavily on hydropower as the main source of electricity. The cost of electricity in Kenya is high, it is 15 US cents per kWh as compared to South Africa which is 4 US cents per kWh. The frequency of power outages in Kenya is 33% compared to China which is 1%. Kenya imported 158 million kWh of electricity from Uganda and Tanzania in 2014. With the unveiling of laptop project for primary schools that is currently going on in Kenya, rural areas that did not have access to electricity will be connected to the national grid. This will increase the demand for electricity. In order to achieve vision 2030, more power has to be generated and at a lower cost. The electricity has to be from clean energy or renewable energy sources to reduce carbon emissions to the environment.

The government has invested in geothermal energy for power generation and this has reduced the use of gas turbines that run on fossil fuels. As of 2014, 558 MW of geothermal power had been installed. Renewable energy such as micro wind turbines, solar PV and solar water heaters are being used domestically to reduce the cost of electricity. The installation costs for these sources of renewable energy are costly and there are no proper ways of disposing them once they breakdown or they reach their life limit.

In this research a compressor will be designed and its performance simulated so as to study its effectiveness in generation of power from a syngas turbine. Syngas is obtained when organic wastes or coal is burnt in limited supply of oxygen. The design will entail blade sizing and profile development for the purpose of optimizing pressure ratio and efficiency. The performance will be simulated and optimized in ANSYS Fluent based on flow and geometric conditions. Simulation will involve solving the transport equations of flow and energy based on suitable modelling techniques to study what happens within the designed compressor.

It is expected that an optimized gas turbine compressor will be developed, and inlet conditions of pressure and flowrate will influence compressor efficiency and performance. The simulation results are expected to give an insight to designers of gas turbine devices used for power generation.

**Keywords** ANSYS (American Computer-aided Engineering Software) Fluent, Syngas, TPM (Tiny Particulate Matter), PM (Particulate Matter)

*Liz Wangui, Department of Mechanical Engineering Jomo Kenyatta University of Agriculture and Technology P.O.BOX 6200-00200 Nairobi, Kenya.E-mail: lizmaina78@gmail.com*

*Eng. Dr. Hiram Ndiritu, Department of Mechanical Engineering, JKUAT, e-mail: hndiritu@eng.jkuat.ac.ke*

*Dr. Benson Gathitu, JKUAT, phone: +254723118800 email: bbg@eng.jkuat.ac.ke*

## I. Introduction

### A. Background

Energy demand has grown rapidly because of countries developing and the improvement of living standards. Electricity is the world's fastest-growing form of end-use energy consumption (1). Due to this demand, electricity production has also risen by 76% for the past 20 years (2). Most gas turbines that generate electricity run on fossil fuels such as kerosene and natural gas. The prices of these fossil fuels are volatile since they are determined by players in the country of origin thus the cost of electricity generated is high (2). High prices of natural gas and emission concerns about natural gases has led to a focus shift in replacing these gases with gas derived from coal to run gas turbines (3). Kenya still relies on hydropower as the main source of electricity generation (4). The fluctuation of the hydro power is due to fluctuating river flow (Tana River which is the source of the 7-Folk dam), extreme evaporation rates, and sedimentation and siltation in the dams (5). The graph below shows hydro as the highest source of electricity generated in Kenya.


The government has tried to shift focus from hydropower through exploitation of geothermal energy and setting up of wind power plants. Off grid solar, micro hydro and other renewable energy systems are also being exploited.

A promising direction in coal conversion is coal gasification. With the discovery and subsequent mining of coal from Mui basin in Kenya, it is expected that electricity will soon be generated from coal. This supply can be used to boost the electricity generation that is currently being used.

### B. Syngas Utilization in Power Generation

The use of syngas energy is a new way to generate clean energy. Syngas fuels are obtained from coal, biomass or solid waste gasification processes. Gasification involves burning materials that have carbon in limited supply of oxygen (6). Gas turbine systems are more compact than internal combustion engines,

their mechanical efficiency is higher, and they can be started and stopped more quickly than internal combustion engines (7).

### C. Problem Statement

The energy demand has been on the rise due to economic development of countries, improved living standards, and industrialization. Figure below shows the annual rise in demand for energy with the most consumed being petroleum (1).

**Figure ES-2. Total world energy consumption by energy source, 1990–2040 (quadrillion Btu)**

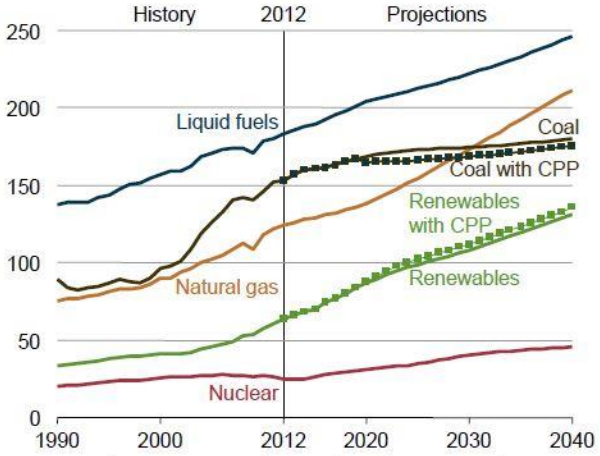


Note: Dotted lines for coal and renewables show projected effects of the U.S. Clean Power Plan.

In Kenya, the need for energy has been on the increase for the past years. Due to over-reliance on hydroelectricity, the frequency of power outages is high (33% compared with the average for Mexico, China and South Africa, which stands at 1%). Production lost due to these outages is approximately 9.3% (compared with the average for Mexico, China and South Africa, which stands at 1.8 per cent). It takes approximately 66 days to obtain electricity connection in Kenya (compared with an average of 18 days in Mexico, China and South Africa (4). The graph below shows the growing demand for energy from both domestic and industries, with industries recording the higher demand than domestic.

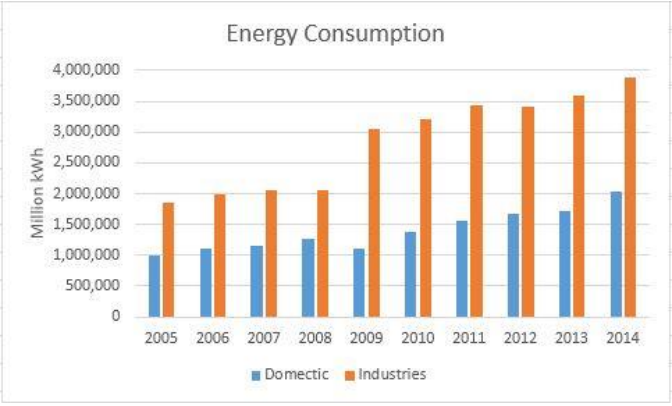


In Kenya, the rate of electricity is still high. The energy cost is 15 US cents per kWh while in South Africa it is 4 US cents per kWh. In China, it is 7 US cents per kWh while in Mexico it is 7.5 US cents per kWh. One of the goals of vision 2030 is to provide a utility sector (water, sewerage and electricity) that is modern, customer oriented and technologically-enabled to provide efficient, cost-effective, quality services to all citizens (8). This can only be achieved by ensuring that electricity production is efficient and affordable, and the source of energy is easily obtained.

The emission of carbon dioxide from existing coal based power plants is however considered one of the main factors responsible for climate change, commonly referred as greenhouse effect (9). Carbon dioxide, Sulphur and TPM produced while burning coal has led to build up of smog, haze, and acid rain in China.

### D. Objectives

The main objective is to develop and simulate performance of syngas compressor for running a gas power plant. This will be done using ANSYS Fluent. The specific objectives are development of a model compressor that would operate on syngas. The performance of the compressor will be simulated using ANSYS to test influence of mass flow rate, inlet temperature, and pressure ratio. Finally, the compressor will be fabricated and resized for testing.

### E. Justification

The use of coal in its raw form causes both health and environmental degradation. The conversion of coal to syngas is a clean way of utilizing the energy content of coal. This syngas can be compressed and fed into a turbine for power generation. Therefore, as the need for clean and renewable energy increases, coal gasification in power generation is the way to go. Also, with the discovery of coal in Kenya, this coal can be gasified and used in power generation.

## II. Literature

### A. Overview

As the demand for energy increases globally and locally, more electricity has to be generated. Use of coal in its raw form is hazardous environmentally and health wise as well. Therefore, conversion of coal to syngas is a clean way of utilizing coal. This syngas can be fed to a gas turbine connected to a generator and used in the production of electricity.

Most gas turbines use natural gas in power generation. When natural gas is replaced with syngas, the flowrate through the gas turbine increases due to its lower calorific value (10).

### B. Gas Turbine Concept

Gas turbines are used in airplanes, and in power generation (7). A simple gas turbine comprises of three elements; a compressor, combustor, and a turbine. The compressor is used to increase the pressure of the operating fluid by compressing it. The fluid then moves to the combustor where it is ignited, and then to the turbine where it is expanded and released. In power generation, the turbine-compressor shaft is coupled to a generator to produce electricity (11). Figure below shows this concept.

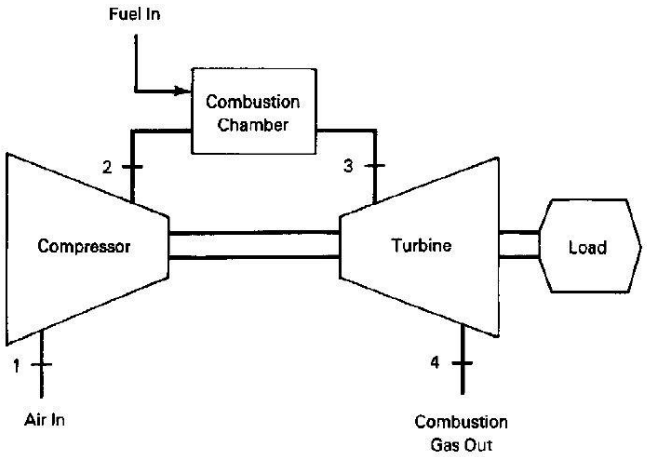


Gas turbines can operate with either axial compressors or centrifugal compressors. Centrifugal compressors can attain higher pressure ratios at one stage than axial compressor (12). Banpurkar et al. (13) recommends use of centrifugal compressor where high speeds are required.

### C. Choke, Stall, and Surge in Compressors

In centrifugal compressors as mass flow is reduced, the pressure rise increases up to a given point at which further reduction of mass flow leads more or less rapidly to more or less severe instabilities like surge and stall (14). In manual transmission vehicles with turbo-chargers, surging occurs during gear change when the throttle is closed thus the air in the system lacks an outlet. The pressure build-up at the outlet becomes more than the inlet pressure thus backflow occurs (15).

Stall occurs when the radial velocity of the gas entering the diffuser, or efficiency of the diffuser, are too low therefore the flow collapses into stall cells as it passes through the diffuser. Stall is more prevalent on low flow impellers and is likely to occur on high pressure low flow applications. It tends to onset as the flow approaches surge.

Choke occurs when the flow is greater than the designed flow resulting in high gas velocities and incidence angles at impeller entry. Operating the machine choke region is usually harmless mechanically, but incurs efficiency losses (16).

The effects of surge are exponential temperature increase, process instability, potential machine trip, process shutdown and machine damage. Surge can be minimized and avoided by use of anti-surge systems. These can either be valves that drain off some of the fluid or programmable units that operate independently. Choke, surge, and stall negatively affect the efficiency of the compressor. When the compressor is operated at high flow rates, chocking occurs. Surge originates in the diffuser and is caused by surface friction that brings about restriction of flow.

Bosman et al. (17) designed an impeller using CAD (Computer Aided Drawing) and used NUMECA AutoGrid to mesh. He used CFD to simulate fluid flow and to analyze the impeller, and mean-line analysis to predict the performance of the designed impeller. He achieved a pressure ratio of 5.34 and an impeller efficiency of 91.6% and found out that the blade shape of the impeller influences its aerodynamic and mechanical performance. He suggested an impeller design with back-sweep at the outlet to avoid choke, improve compressor surge margin and to improve efficiency.

Neshat et al. (18) investigated the effects of blade sweep and lean on the performance of compressor. He did this using numerical solutions and found that an impeller blade with back sweep is less affected by lean, has reduced stall margin, and chocking flow rate reduced by 1.5%. For a blade with forward sweep, the stall margin increases and chocking flow rate increases by 0.18%. He concluded that forward swept blades influence upstream flow while backward swept blades affect the rotor stages downstream.

Wang et al. (16) paper focused on the performance of backward swept impeller on the performance of the centrifugal compressor. During the investigation, a 3D model of the impeller was designed using Vista CCD in ANSYS Workbench and CFD analysis. The results were that backward swept impellers offer better isentropic efficiencies than radial impellers, and that they improve volume flow rate and enhance outlet velocity of the compressor.

### D. Blade Configuration

In compressors, the most crucial element is the impeller. This is because the impeller transfers kinetic energy to the working fluid (13). Blades should be designed in a way that minimizes flow loses. Variables in the impellers that influence efficiency, operating range and blade stress in the compressor are: impeller tip diameter, back-sweep angle, tip/exit depth, inducer inlet angle and rotor eye, blade leading edge shape, curvature of blade shape and, tip clearance.

Blade lead increases the pressure on the pressure surface. Forward swept blades have a better performance and increase compressor efficiency by almost 1% while backward swept blades increase the efficiency by 0.5%. Forward swept blades reduce the interaction between the shockwave and the casing wall boundary layer while the backward swept blades reduce chocking flow rate. Therefore both sweep and lean should be present in a blade design since they improve chocking flow rate and efficiency in various operating ranges of a compressor (18).

### E. Diffuser Influence

Diffusers are located downstream of the impellers in centrifugal compressors. There are vaned and vaneless diffusers.

The diffusers affect the static pressure at the outlet of the compressor. Stall may develop into a surge at diffuser outlet thus it is important to determine what type and design of a diffuser is required (19). Taher et al. (19) aim at conducting his investigation was to compare flow and behavior characteristics near surge conditions in vaneless and vaned diffusers. He used numerical simulations and found that at near surge conditions, static pressure fluctuations at the inlet of the diffusers was higher in vaneless diffusers than in vaned diffusers. He also found out that pressure drop during surge occurs faster in vaneless diffusers than in vaned diffusers. He concluded that compressors with vaneless diffusers are more stable during surge than those with vaned diffusers. In his research, he investigated pressure and velocity in vaned and vaneless diffusers. He did not look at how temperature would fluctuate and be affected by vaned and vaneless diffusers.

Sorokes and Kuzdal et al. (20) in their discussion of the evolution of centrifugal compressors noted that vaneless

diffusers offer wider flow range than vaned diffusers. They also noted that static pressure recovery is higher in vaned diffusers than in vaneless diffusers.

### F. Syngas in Gas Turbine Systems

Gasification is a process that converts low quality fuels to valuable ones. The process can be applied to biomass as well as coal. Gas generated by gasification of coal comprises of $H_2$ and CO and small amounts of $CH_4$ and higher order carbons. Impurities such as Sulphur, alkali species, and small particulate matter are also present but can be eliminated by employing a cleaning process of the syngas (3).

Suhui et al. (21) investigated the behavior of syngas in spark ignition using gas turbine start up conditions, and the effects of the syngas fuel composition and air flow on ignition performance. He discovered that syngas has better ignition performance as compared to natural gas though one of the hindrance of using syngas in gas turbine is its change in composition and heating value.

### G. Gaps Identified in Literature

i. Surge, choke and stall affect flow of diffusers and there is need to reduce their impact on performance of diffusers.

## III. Methodology

### A. Domain Configuration

The passages within the compressor will be designed in 3-Dimensional plane using suitable criteria. For the curves of the impeller, and flow passages. Bezier curves will be formulated using design points. This will ensure that a smooth curve is designed. Figure below shows a design of a centrifugal compressor.

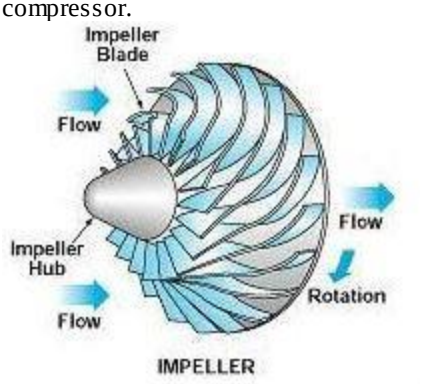

IMPELLER

During the design phase, the compressor hub and shroud profiles will be developed based on appropriate design guidelines.

### B. Governing Equations

Mass conservation equation

$$\nabla V_i = 0$$

Momentum conservation equation

$$\rho(\nabla V_i) = F_i - \nabla . P + \mu \nabla^2 V_i$$

Energy conservation equation

$$\nabla[(\nabla . \rho V_i)(C_p T) - \frac{\lambda}{C_p} \nabla . (C_p T_i)] = \dot{H}$$

Species conservation equation

$$\nabla(\rho V_i) = \nabla . (\rho D \nabla . Y) - \omega$$

These governing equations will be solved using finite volume method for steady-state flows, and RANS for turbulent flows.

### C. Finite Volume Method

Many codes used to solve fluid flow problems use finite volume method. This is because it is convenient for use with unstructured grids, and for its global conservation property. This global conservation property is the principle of conservation produces over the entire domain. Some of the general purpose codes used for fluid ow are CFD programs. Solution of this method starts with the conservation laws in integral form. Finite volume solves the governing equations. These can be structured or unstructured grids (22). There are grid points within each cell. The principle of conservation is reproduced for the entire domain. An equation solved by finite volume method is:

$$\frac{d}{dt}\int_\Omega \Phi \, d\Omega = -\int_s \Phi V . ndS + \int_s X \nabla \Phi . ndS + \int_\Omega Q d\Omega$$

### D. Reynold-Averaged Navier Stokes Equation

Reynold-Averaged Navier Stokes (RANS) equation remains as a primary tool of practical CFD analysis. It is simple, has a broad selection of models, and can be applied to different kinds of turbulent flows (22). The governing equation will be modelled using RANS method. The universally applicable ensemble-averaged field will be:

$$< u > (x,t) = lim_{m \to \infty} \frac{1}{M} \sum_{m=1}^{M} u^{(m)}(x,t)$$

, where $u^{(m)}$ are the realization of flow in M identical experiments.

Using Reynolds-Averaged equation and Newtonian equations, the Reynolds-Averaged Navier Stokes equation for an open system will be written as:

$$\rho \frac{\partial < u_i >}{dt} + \rho \frac{\partial}{\partial x_j}(< u_i >< u_j >) = -\frac{\partial < p >}{\partial x_i} + \mu \nabla^2 < u_i > - \frac{\partial \tau_{ij}}{\partial x_j}, \frac{\partial < u_i >}{\partial x_i}$$

In the two equation model, velocity and length will be determined. The two models to be used are $k - \epsilon$ model and $k - \omega$ model. The $k - \epsilon$ model will use transport equations for turbulent kinetic energy and the rate of viscous dissipation. The k-equation will be given as:

$$\rho \frac{\partial k}{\partial t} + \rho < u_j > \frac{\partial k}{\partial x_j} = 2\mu_t < S_{ij} > \frac{\partial u_i}{\partial x_j} - \rho \epsilon + \frac{\partial}{\partial x_j}[\left(\mu + \frac{\mu_t}{\sigma_k}\right)\frac{\partial k}{\partial x_j}]$$

With boundary conditions set in place, the above equations will be used to solve near-wall treatment turbulent flows. These will be used at boundary walls. Inlet conditions into the compressor will also be solved using $k - \epsilon$ equation.

### E. Recommendations

There exist literature on how surge, stall, and choke affect the compressor performance. Several gaps have been identified in the literature and these will be key areas that will be focused on during the study of centrifugal compressors. Some of these are:

i. Surge, choke and stall affect flow of diffusers and there is need to reduce their impact on performance of diffusers.
ii. It is essential to study the onset of surge in a backward swept impeller, and how the angle of sweep reduces or increases surge occurrence.
iii. How the configuration of diffusers affect the stability. It is therefore necessary to study the use of vaned and vaneless diffusers in a bid to minimize instability, their effects in the centrifugal compressor to determine which diffuser is suitable for which sweep.

## IV. Expected Results

The centrifugal compressor running on syngas will be designed, and simulated using ANSYS Fluent CFD. Its geometry will be investigated to determine how it influences pressure, temperature, and velocity.

a. Design of a compressor for use in gas turbine running on syngas.
b. Simulation results of the performance of the compressor based on pressure, velocity field and temperature across the compressor.
c. Influence of transport properties on the surge, stall, and choke of the compressor
d. A fabricated centrifugal compressor that compressed syngas.

## V. Conclusions

The need for energy globally and in Kenya requires more sources of energy to be utilized. The effects of pollution is now being felt thus those sources have to be clean. Coal from Mui Basin can be a source for power generation in Kenya.

Surge, stall, and choke are common problems that affect the performance of a compressor in a gas turbine running on syngas. Thus, their onset needs to be further studied. Also, the effects of the compressor profile on surge, stall, and choke need to be investigated further so that an optimized and efficient compressor can be used.

## VI. Acknowledgement

I would like to thank my supervisors for their guidance during research, development of the proposal, and ongoing design and analysis. Also, the department of Mechanical Engineering and JKUAT for availing the websites at which research materials can be obtained.

## References

[1] *International Energy Outlook*. May 2016.
[2] Council, W.E. *World Energy Resource Survey*. 2013.
[3] G.Wright, T. B. Gibbons and I. *A review of materials for gas turbines firing syngas fuels*. 2007.
[4] Statistics, Kenya National Bureau of. *Statistical Abstract*. 2015.
[5] *Vulnerability of hydro-electric energy resources in kenya due to climate change effects: The case of the seven folks project*. Bunyasi, M. M. 2012, Journal of Agriculture and Environmental Sciences, pp. 36-49.
[6] *Coal gasification integration with solid oxide fuel cell and chemical looping combustion for high-efficiency power generation with inherent CO2 Capture*. Lior, W. X. Shiyi Chen and Noam. 2015, Elsevier: Applied Energy, pp. 298-312.
[7] *Thermodynamic analysis of a gas turbine power plant modeled with an evaporative cooler*. Kilanko, S. O. Oyedepo and O. 2014, International Journal of Thermodynamics, pp. 14-20.
[8] *Kenya Vision 2030*.
[9] Rubanova, A. *History of Compressors*.
[10] *Performance maximization of IGCC plant considering operating limitations of a gas turbine and ambient temperature*. Do Won Kang, Chang Min Kim, Jae Hong Lee, Tong Seop Kim, and Jeong L. Sohn. s.l. : Journal of Mechanical Science and Technology, 2016, Vol. 30.
[11] P.Spittle. *Gas Turbine Technology*. s.l. : Rolls Royce, 2003.
[12] *A micro gt unit for electric power generation: Design and testing of turbine and compressor*. Varplaetsen, D. R. J. Peirs and F. 2004. 9th International conference on new actuators.
[13] 13. *Review paper on stress distribution over the blade of compresor of micro turbine*. R.D.Banpurkar, P. 2015, International Journal of Advanced Engineering and Global Technology.
[14] *Full-annulus simulation of the surge inception in a transonic centrifugal compressor*. Trbinjac, E. B. I. 2015, Journal of Thermal Science.
[15] http://ksmotorsport.co.za/flutter-compressor-surge/. *Turbo flutter/compressor surge*.
[16] *Back swept angle performance analysis of centrifugal compressor*. Wang, T. 2014, MECHANIKA, pp. 402-406.
[17] 17. Merwe, B. B. van der. *Design of a Centrifugal Compressor Impeller for Micro Gas Turbine Application*. 2012.
[18] 18. *Investigating the effect of blade sweep and lean in one stage of an industrial gas turbine's transonic compressor*. Neshat, M.A. 2015, Propulsion and Power Research, pp. 221-229.
[19] 19. *Numerical investigation of rotating stall in centrifugal compressor with vaned and vaneless diffuser*. Halawa, M. A. Taher. 2015, Journal of thermal science, pp. 323-333.
[20] *Centrifugal compressors evolution*. Sorokes, James M. 2010. Proceedings of the 39th Turbomachinery Symposium.
[21] *Syngas spark ignition behavior at simulated gas turbine startup conditions*. Li, S. 2014, Combustion Science and Technology, pp. 1005-1024.
[22] Zikanov, O. *Essential Computational Fluid Dynamics*. s.l. : John Wiley & Sons, Inc., 2010.

# Sunflower Heavy Metal Phytoextraction on Sewage Sludge

Lynn R. Mutethya

***Abstract:*** Sewage treatment results in two components: the effluent which is usually disposed of at the required regulatory standards; and sludge which is disposed of by utilization in Agriculture, tipping on controlled landfill sites, disposal at sea or by incineration. The application of sewage sludge to land is an effective disposal method. Not only does it provide a solution to the sludge disposal problem, but it is beneficial to agricultural productivity. Typically, large volumes of sludge are produced in sewage treatment plants which is sold to farmers at cheap prices. Despite the perception of sewage sludge being 'dirty fertilizer' it contains useful amounts of plant nutrients such as carbon, nitrogen and phosphorous. When used, less chemical fertilizers are required and the nutrients are released gradually for plant uptake as compared to the more soluble chemical fertilizers. On the other hand, sewage sludge contains toxic heavy metals that may have adverse effects to human life when consumed. Phytoextraction is a process in which certain plants have the ability to absorb, translocate and store toxic contaminants from a soil matrix into their root and shoot tissue. Conventional methods of removing heavy metals are locally inaccessible, phytoextraction is useful technology for local removal of heavy metals in manure sewage sludge. Atomic absorption spectroscopy analysis was used to determine the phytoextraction capability of sunflowers growing in controlled sludge amended soils. Results indicate a significant reduction in heavy metal levels after the phytoextraction process.

***Keywords:*** Hyperaccumulator, phytoextraction, phytoremediation, sewage sludge, sunflower

## INTRODUCTION

The use of sewage sludge as fertilizer can be dated as far back as 1550 in Bunzlau, Germany [11]. In the 1980's American sewage sludge used to be dumped into the Atlantic and Pacific Oceans. Later, scientists discovered that the practice was killing marine life. This led Congress to ban ocean dumping, forcing the country to find an alternative method for disposing of sewage sludge. The result was sewage sludge application to land as fertilizer [2]. Presently, sewage sludge is used as fertilizer in western countries in the form of bio solids, which is sludge that has been conditioned and processed for Agricultural reuse. Locally, sewage sludge has been used by farmers as a result of poverty. The average Kenyan farmer who lacks the ability to purchase commercial chemical fertilizers may opt for sewage sludge which is cheaper and is of good nutrient value.

Heavy metals in sewage are mainly as a result of industrial effluents. The use of sewage sludge as manure therefore may result in soil contamination with heavy metals. These heavy metals which accumulate in the soil when sewage sludge is used as fertilizer, get into the food chain and eventually into human and animal bodies leading to several health effects and even death of human beings and animals [33].

Reference [13] revealed that final effluents from Dandora Wastewater Treatment Plant contained cadmium, manganese and lead levels above the Kenya guideline standards of 0.01, 0.2 and 0.01 mg/L respectively. In his study, cadmium ranged from 0.025 to 0.033 mg/L, manganese concentrations were from 0.085 to 0.748 and lead concentrations were between 0.083 and 0.332 mg/L. A study by Maina David from the University of Nairobi, Kenya, showed that chromium, titanium, nickel, zinc, lead, gallium and rubidium were present in sewage sludge samples from Kariobangi sewage treatment works in excess of safe levels. Reference [20] discovered high levels of lead, mercury and cadmium contamination in soils in Dandora area. Reference [22] determined that extremely high levels of zinc, copper, lead, cadmium and mercury were present in sewage sludge from sewage treatment sites in Kariobangi, Dandora, Kiambu, Limuru, Kiserian and Ngong. However, in all the above studies, options that could be used locally to remove these heavy metals were not investigated.

Recently, several studies have demonstrated the potential of using plants in phytoextraction, a process that uses plants to remove contaminants from soils [9].

Phytoextraction is an accessible and cheap technology that could be used locally to remove heavy metals from sewage sludge.

## PHTYOEXTRACTION AS A METHOD OF HEAVY METAL EXTRACTION

Phytoextraction also known as phytoaccumulation is a process that uses plants to remove contaminants from soil.

Lynn R. Mutethya, Department of Civil Engineering, JKUAT (e-mail: l_mutethya@yahoo.com).

The plants used for this process are called hyperaccumulators, which are plants that absorb unusually large amounts of contaminants in comparison to other plants. During phytoextraction, the plants absorb contaminants through their roots and store them within their roots or transport them into the stems. The plant continues to absorb contaminants from the soil until it is harvested. After harvest the soil contaminant levels are brought down. The harvested plants are usually incinerated with the ash disposed of in a hazardous waste landfill. The process may be repeated as necessary to bring the contaminant levels down to allowable limits.

Reference [3] used a tea herb, *Orthosiphon stamineus* B. for phytoextraction of heavy metals in soils amended with sewage sludge. A decrease in the concentrations of cadmium, chromium, zinc, copper and lead in the amended soils after the phytoextraction process was observed.

Reference [19] used water cabbage, *Pistia stratiotes* to study remediation of waters that had been polluted with heavy metals. The plant was grown in high concentration solutions of lead, nickel and chromium. The plants were grown in these solutions for 21 days before harvesting. Metal analysis was done using atomic absorption spectroscopy. Uptake of the metals 300 times over what is obtainable in normal plants was observed.

Reference [28] used anchored hydrophyte, *Hydrocotyle umbellata* L. for the removal of toxic metals from tannery sludge effluent obtained from a tanneries wastewater treatment plant. *Hydrocotyle umbellata* L. showed a good tolerance for prepared concentrations of wet tannery sludge. The plants were harvested after 30, 60 and 90 days. Accumulation of toxic metals in the plants were observed to have significantly increased, with a higher amount observed in the roots than in the shoots.

Reference [16] used willow, *Salix viminalis* L. in purifying sewage sludge treated soils. In the study, it was realized that willow could accumulate ten times more cadmium than was the concentration in sewage sludge or soil.
For a plant to extract heavy metals from soil the following processes take place:

- The metal is dissolved into a substance that the plant can absorb;
- The plant roots absorb the heavy metal;
- The plant chelates the metal to protect itself and to make the metal more mobile;
- The plant moves the chelated metal to storage;
- The plant adapts to damages caused by the metal's transportation and storage.

With the appropriate plant combination for sewage sludge remediation, nutrient content in the sewage sludge is maintained at favourable levels. Thereby, allowing for good potential in agricultural land application.

## SUNFLOWER AS A PHTYOFILTER

Sunflowers may be used to extract heavy metals from sewage sludge due to their heavy metal uptake capability which is higher than that of other plant species [26], their adaption to soil and climate characteristics and the ease with which they are maintained. Reference [18] reported that the success of phytoextraction depends on the ability of the plant to tolerate large quantities of the toxins without affecting the plant's growth and productivity. All through the study, the sunflowers were observed to grow steadily and productivity was not affected. Reference [31] further reports that the success of phytoextraction depends on the ability of the plant to uptake and translocate toxins to its above ground biomass. Sunflowers used in the study were effective with this regard as a larger concentration of heavy metals was observed in the shoot than in the roots. As illustrated below, cadmium levels were observed to be higher in the shoots than in the roots.

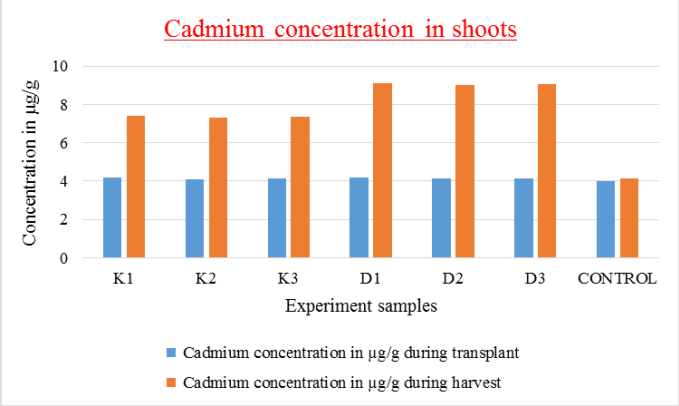


Fig 1 Cadmium concentration in shoots

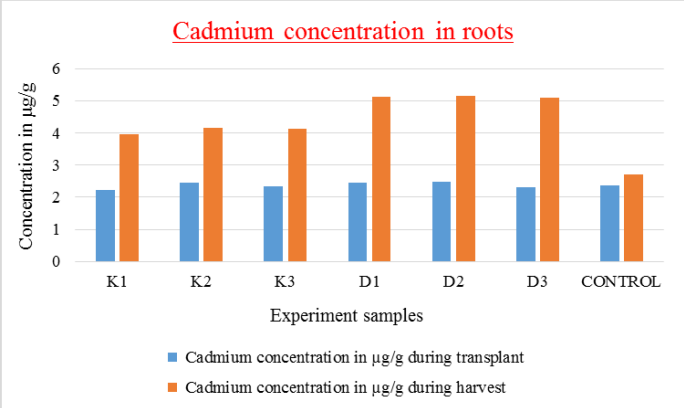


Fig 2 Cadmium concentration in roots

## CONCLUSION

Sewage sludge can be considered as an organic fertilizer for agriculture and forestry because it contains high concentrations of nitrogen and phosphorus which are needed by plants. Sunflower phytoextraction of heavy metals in sewage sludge is a prosperous venture as the sewage sludge is made safe for Agricultural use by the sunflowers' ability to extract and store the heavy metals within their biomass. The overall efficiency was based on analytical findings in the study.

## REFERENCES

[1] Anita N. Azarenko, David R. Sandrock, Timothy L. Righetti (2015). Influence of Plant Age on Nutrient Absorpton for Marigold Seedlings.
[2] Amber Pauline (2007). The Commercialization of Sewage Sludge.
[3] Arifin Abdu, Najihah Aderis, Hazandy Abdul-Hamid, Nik Muhamad Majid, Shamshuddin Jusop, Daljit Singh Karam and Khairulmazmi Ahmad (2010). Using *Orthosiphon stamineus* B. for Phytoremediation of Heavy Metals in Soils Amended with Sewage Sludge.
[4] Bruce Gellerman (2011). Sunflowers Used To Clean Up Radiation.
[5] Chinagate CN (2015). East African Wastewater Treatment and Reusage.
[6] Cornelis E., Guisson R., Elst K., Van Slycken S., Peene A., Dejonghe W. (2011). Combining Bio-energy Production and Phytoextraction: Examination of the Fate of Heavy Metals of Various Conversion Routes.
[7] Dmitri Sobolev and Maria F.T. Begonia (2008). Effects of Heavy Metal Contamination upon Soil Microbes: Lead-induced Changes in General and Denitrifying Microbial Communities as Evidenced by Molecular Markers.
[8] Dr. Ljubinko Jovanovic (2008). Growth and Uranium Uptake in Sunflower, Soybean and Maize Crops.
[9] Dushenkov S. and Kapulnik M. (2000). Phytoremediation: A Novel approach to an Old Problem. Global Environmental Biotechnology.
[10] Earle W Mcmullen and Harry Mccormack (1916). Process for the Manufacture of Paper-Pulp and the Like.
[11] Epstein Eliot (2003). Land Application of Sewage Sludge and Biosolids. CRC Press LLC, United States of America. Pg 7-8.
[12] Eric Dillalogue (2014). Phytoremediation: The Power of Plants to Clean Up the Environment.
[13] Hellen Apondi Sewe (2008). A study on the Efficiency of Dandora Domestic and Industrial Wastewater Treatment Plant in Nairobi.
[14] Hamidreza Rudi, Hossein Kermanian, Hossein Resalati and Rabi Behrooz Eshkiki (2016). Sunflower Stalk Neutral Sulfite Semi-Chemical Pulp: An Alternative Fiber Source for Production of Fluting Paper.
[15] J. Zavertnik (1914). Utilization of Sunflower Stalks in Paper Manufacture.
[16] Jama Anna and Wladyslaw (2012). Willow (Salix viminalis L.) in purifying sewage sludge treated soils.
[17] Lindsey Wolsey (2004). Sunflower – Nature's Perfect Plant.
[18] Muhammad Rizwan, Shafaqat Ali, Hina Rizvi, Jorg Rinklebe, Daniel C. W. Tsang, Erik Meers, Yong Sik Ok, Wajid Ishaque (2016). Phytomanagement of heavy metals in contaminated soils using sunflower: A review
[19] Mohammad Mustapha Abubakar, Mani M. Ahmad, Balarabe U. Getso (2014). Rhizofiltration of Heavy Metals from Eutrophic Water Using *Pistia Stratiotes* in a Controlled Environment.
[20] Mulamu Livingstone Otenyo (2014). Heavy Metal Contamination of Land and Water around Nairobi City Dandora, Kenya.
[21] Muhammad Rizwan, Shafaqat Ali, Hina Rizvi, Jorg Rinklebe, Daniel C. W. Tsang, Erik Meers, Yong Sik Ok and Wajid Ishaque (2016). Phytomanagement of heavy metals in contaminated soils using sunflower: A review
[22] Nduta Jane (1992). Determination of heavy metals in sewage sludge, sewage effluent, garden soils and food crops grown in ordinary and sewage-sludge amended soils.
[23] Nicoletta Rascioa, Flavia Navari-Izzo (2010). Heavy metal hyperaccumulating plants: How and why do they do it? And what makes them so interesting?
[24] Oluoch Japheth Ogola and Fr Daniel Moschetti (2008). Dandora Dumpsite: Struggling for health, security and dignity.
[25] Helena I. Gomes (2012). Phytoremediation for bioenergy: Challenfges and Opportunities.
[26] Prasad, M.N.V. (2007). Sunflower (*Helinathus annuus* L.) - A Potential Crop for Environmental Industry.
[27] Samake M, Wu QT, Mo CH, Morel JL. (2003). Plants grown on sewage sludge in South China and its relevance to sludge stabilization and metal removal.
[28] Sheza Khilji and Firdaus-e-Bareen (2008). Rhizofiltration of heavy metals from the tannery sludge by the anchored hydrophyte, *Hydrocotyle umbellata* L.
[29] The Environmental Management and Co-ordination (Water Quality) Regulations, Kenya (2006). Legal Notice No. 120.
[30] Tiafen Xu, Fangwen Xie, Zebin Wei, Qi-Tang Wu (2014). Phytoremediation of sewage sludge and use of its leachate for crop production.
[31] Turgut C, Pepe MK, Cutright TJ (2004). The effect of EDTA and ciric acid on phytoremediation of Cd, Cr and Ni from soil using *Helianthus annuus*.
[32] United Nations Environmental Programme (2007). Environmental Pollution and Impacts on Public Health; The Impact of the Dandora Dumping Site in Nairobi, Kenya. Pg 12-19.
[33] United States Environmental Protection Agency (1998). Supplemental Environmental Projects Policy Report. Pg 16
[34] United States Environmental Protection Agency (1998). Heavy Metals and Gardens.
[35] W. Dejonghe M., Geurds R., Guisson L., Van Ginneken L., Diels E., Meers N., Witters T., Thewys J.,Vangronsveld J., Kegels B., Defoort E., Beeckman J., Smis S., De Schepper, H. Fastenaekels (2010). Energy Crop Production Combined with Phytoremediation for Heavy Metal Contaminated Soils.
[36] www.ncbi.nlm.nih.gov/m/pubmed/21421358/ : 14-10-2015, 12:15pm

# A femtocell users' resource allocation scheme with fairness control

Macharia Andrew Ruitie[1], Lang'at Philip Kibet[2], Musyoki Stephen[3]

*Abstract*—the availability of adequate resources will always remain to be a concern for mobile network operators. Therefore, for Orthogonal Frequency Division Multiple Access (OFDMA) networks, factors such as Signal to Interference plus Noise Ratio (SINR) and resource capacity continue to be feasible areas of research. A combination resource allocation with fairness control is hereby explored with reference to users' individual requests for resources at a given femtocell being taken into account. In addition, their signal to noise ratios is calculated alongside serialized users' requests per individual. This chooses the users with best SINR values with a given resource allocation to each user.

An example of 3 users is considered with the resource requests and SINR values as follows: user 1 requests for 3 resources and has 5dB, user 2 requests for 2 resources and has 7 Decibels (dB) and user 3 requests for 4 resourcesand has 4dB. The total requests are 9 resources and only 5 are available. When the combination is applied it determines that the best allocation would be as follows: user 1 to be allocated 3 resources and user 2 to be allocated 2 resources. The fairness scheme then allocates a resource to user 3 by deducting one from user 1 to enable him to communicate through the femtocell.

**KEY WORDS**
Femtocell, Orthogonal Frequency Division Multiple Access, Signal to Interference plus Noise Ratio.

## I. INTRODUCTION

Services from mobile service providers will always have a growing demand. This makes it inevitable for higher levels of bandwidth to be incorporated in their mobile capacity development. Increasing demands from users and high levels of bandwidth requirements have made it necessary to develop techniques that seek to take care of factors such as Signal to Interference Noise Ratio (SINR) and resource allocation to all users with varying power, noise and signal to noise levels, among others.

Tackling these factors versus accommodating as many users as possible in the network, have remained a challenge and hence an area of continual research for Communication companiesand institutions. Techniques have been developed to deal with issues such as: users' mobility, users' varying data rates and signal power levels and also combinational techniques to determine the optimum approach to allocate users resources in mobile networks. Some of the algorithms include: Genetic algorithm, Ant colony algorithm, maximum fairness and mobility aware algorithm. These methods have tried to prioritize with regard to their individual aspects in terms of signal power levels, mobility and data rates.[1]

Macharia Andrew Ruitie, (MSC Telecommunications) Department of Telecommunications and Information Engineering, JKUAT.Cell no: +2540725005916; e-mail: armachajnr@gmail.com).

Lang'at Philip Kibet, Department of Telecommunications and Information Engineering, JKUAT. (e-mail: kibetlp@jkuat.ac.ke).

Musyoki Stephen, School of Electrical and Electronic Engineering, Technical University of Kenya. (e-mail: smusyoki@yahoo.com).

## II. LITERATURE REVIEW

The demand for higher bandwidth and faster communication techniques have led to robust development of mobile networks that have evolved from 1G to 4G networks[2].

### a) MOBILE EVOLUTION HISTORY

Mobile networks began with the earliest form of communication which was mainly analog in nature. This was characterized by technologies such as Total Access Communications systems (TACS) and Advanced Mobile Phone System (AMPS)[2]. They had serious challenges of switching and roaming. This was the first generation of mobile phones.

The second generation was characterized by introduction of text messaging and packet switching techniques. Technologies such as Time Division Multiple Access (TDMA) were developed [2].

The third generation technologies brought Wideband Code Division Multiple Access(W-CDMA) and Universal Mobile Telecommunications Service (UMTS). These had very high data rates of up to 10Mbps[3].

The generation that features currently is the fourth generation (4G) networks that utilize technology such as Long Term Evolution Networks (LTE) and Worldwide Interoperability for Microwave Access (WiMAX). This is a purely Internet Protocol (IP) network which has very high data transmission rates that can reach up to 100 Mbps [4].

LTE networks are made up of the following:

i). Mobility Management Entity
ii). Enhanced Node-B
iii). Serving Gateway
iv). Packet Data Network Gateway.

The first gadget is the user equipment. This is what the user owns and is used to avail network facilities to the user. [4]

The second component is called Mobility management Entity (MME). It is useful in providing signaling exchanges between users-core network and base stations-core networks and a unit for data flow between the users and the internet[5]. This is as shown in the figure below.

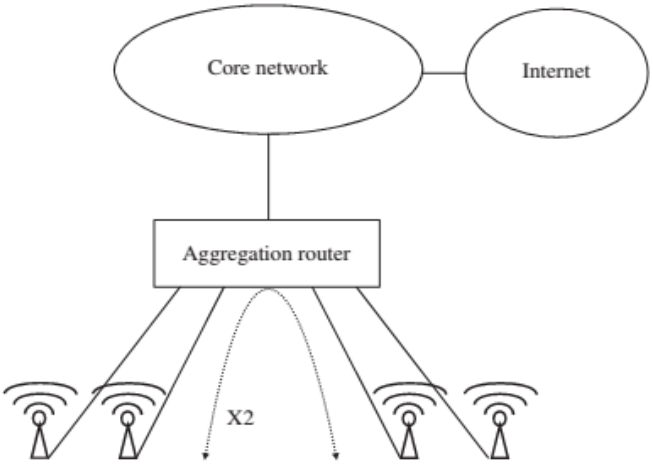


Fig 1: Routing on the MME[5]

This device serves as the termination point for the Non-Access Stratum (NAS) signaling. In addition, it establishes bearers,authenticates, provides SMS support, handover support and handles security key management[5].

Next device is the Packet Data Network Gateway. This device is useful in interconnecting user equipment to the internet and external packet data networks. It also assists with routing and forwarding user data packets plus also storage and management of user equipment contexts[4].

## b) REVIEW OF EXISTING USER RESOURCE ALLOCATION SCHEMES

### 1. Maximum Fairness Algorithm

In this method, user's data rates are scanned. Here, a min-max technique is employed which involves minimizing the power of the users with the highest data rates and SINR values and distributes them to the users with the lowest values [6].

This approach has the problem of improper allocation of resources.This is occasioned by allocating the most resources to the low rate users have low signal to noise ratio. [6].

The problem of this method is deducting SINR values from the high valued users and transferring to the low valued ones. This way, the throughput is reduced and robustness of the system is greatly affected.

### 2. Proportional Rates Algorithm

In this technique, the sum of throughput through the transmission system is maximized.

This is achieved with the use of a predetermined system parameter βk.This parameter isused as a constraint to transmission data rates for all individual users [6]. This is as expressed by the formula below where the data rate for users is given by $R_k$.

$$\frac{R_1}{\beta_1} = \frac{R_2}{\beta_2} = \cdots \ldots \ldots \ldots \ldots \ldots \frac{R_K}{\beta_k} \qquad (1)$$

This method is adequate in terms of handling throughput but in order to improve on it, a dynamic scan for the available resources. Using combination approach is a better placed technique since the best users with best SINR levels to allocate resources are determined[6].

### 3. Mobility Aware Resource Allocation Algorithm

This technique utilizes user position prediction in a given cluster of femtocells to determine allocation of user resources.

It follows the following procedure: First, grouping of users into clusters then one of them is chosen to be the leading femtocell.A group of clusters is formed where in one cluster. The clusters consist of a one user being the cluster head and the others being the cluster members [7].

Furthermore, the method users two major sub-techniques to predict users resource allocation.

Global prediction algorithm: In this technique, the movements of the user form the history of the mobility prediction and thus a sequence is craftedto predict the most probable cell into which the user will move [7].

The global approach is expressed in the formula below.

$$P_e = P\left(\frac{X_{f+1}=Y}{X_f=Y}\right) = \frac{M(X,F_{f+1})}{N(F_{f-1},F_f)} \qquad (2)$$

Where:

Perefers to Transition probability between previous and future femtocells

$F_1, F_2, F_3$……..$F_{f-1}$, $F_f$refers to the mobility history trace of a mobile user [2].

$F_{f-1}F_f$refers to the sequence of the previously visited to the current femtocell

$F_fF_{f+1}$ refer to the sequence of the current femtocell and the future femtocell to be visited.

M and N are sequences of elements of variables outlined in the equations determined by the users' movements in the femtocells[7].

For local prediction, the formula outlined is used.

$$P_m = P\left(\frac{X_{f+1}=Y}{X_f=Y}\right) = \frac{N(F_f,F_{f+1})}{Z(F_f)} \qquad (3)$$

Given that:

$X = F_{f-1}F_f$is the sequence in V of the previously visited femtocell and the current femtocell of the mobile user [2].
$Y = F_fF_{f+1}$is the sequence of the current femtocell and the future femtocell to be visited.
$Z(F_f)$ refers to the number of times the femtocell $F_f$ appears in the mobility trace[7].
This method relies on historical movements to predict movement of a user to a femtocell and secondly, assumes a user will move to either of the adjacent cell in the case of local prediction. A combinational resource allocation technique is better placed in a dynamic environment due to random movement of users.

## 4. Genetic Algorithm

This technique involves a natural process of individuals' selection based on their traits that are carried on from one stage to another[8]. The process entails: Selection, crossover and mutation. In the first process, the chosen users are the ones with the best and moved to the subsequent stages with priority placed on fitness function [8].Next stage is the crossover where good common traits among the ones chosen in the selection stage are moved to the mutation stage. Finally, the mutation stage involves the alteration of traits of the children from the parent users from the crossover stage in order to achieve the best traits[8].
This method is applicable in iterative systems where the next stage depends on the previous one but in a case where resources allocation is instantaneous in terms of SINR valuesamong the users in a femtocell hence the combinational allocation technique is more appropriate.

## 5. Ant Colony Optimization

This technique uses the analogy of ants that move around randomly in search of food from their nest. During their movement, they drop pheromone trails along the paths that they follow [9]. The main aim is to create a trail for other ants to follow later while searching for food hence shorten the time that they need to wander in search for food [9]. These pheromone trails evaporate which means that the trails that remain are fewer for longer distances. This method encourages shorter distances which maintain trails. When applied to systems such as networking and smart grid systems, it becomes usefulfor finding the best routing techniques to improve system throughput.
This method relies on historical data for determining the best paths for routing information. In a dynamic environment, users factors such as SINR are randomly changing and do not rely on historical information. Hence, this becomes a drawback for this approach compared to combinational scheme.

# III. METHODOLOGY

This paper brings forward a combinational technique to allocate users resources in a femtocell.
Combination refers toan arrangement technique in mathematics that finds all possible arrangements of items in a given space. [1]

It is expressed mathematically as shown below

$$\frac{\boldsymbol{n}!}{\boldsymbol{x}!(\boldsymbol{n}-\boldsymbol{x})!} \quad (4)$$

Where:
n! refers to the factorial of n
x! refers to the factorial of x
(n-x)! refers to the factorial of (n-x).

The method seeks to scan for all users who have requested for resources in the femtocell then it arranges them in terms of the groupSINR values. It is after this step that it does the totals of all the SINR groups then allocates the users with the best SINR values [1].

The first step in this method would be to determine the SINR values for the users. This is described in the steps below:

1. Channel bandwidth Calculation.At this stage, the Adaptive Modulation and Coding (AMC) scheme is used from the measurement reports sent from the user equipment[1].

2. Bits per symbol of transmission derivation. This is determined from the AMC scheme and the number of subscribers in the network [1].

3. System throughput calculation.
First, symbol transmission duration is calculated as follows

$$\frac{0.5\ ms}{7} = 71.43\mu S \quad (5)$$

Then, the Throughput is given by =

$$\frac{No\ of\ bits\ transmitted}{symbol\ transmission\ duration\ (71.43\ \mu s)} \quad (6)$$

4. Calculation of the SINR.
Given the expression for a channel capacity as

$$C = Blog_2(1 + SINR) \quad (7)$$

Where:
C = Capacity of the channel or throughput (bps)
B = Bandwidth of the channel (Hz)
SINR = Signal to Interference-Noise Ratio

This makes the expression of the SINR to be

$$SINR = 2^{[C/B]} - 1 \quad (8)$$

Having determined the individual users SINR values, the users are selected through the process described in the flow chart below as described in [1].

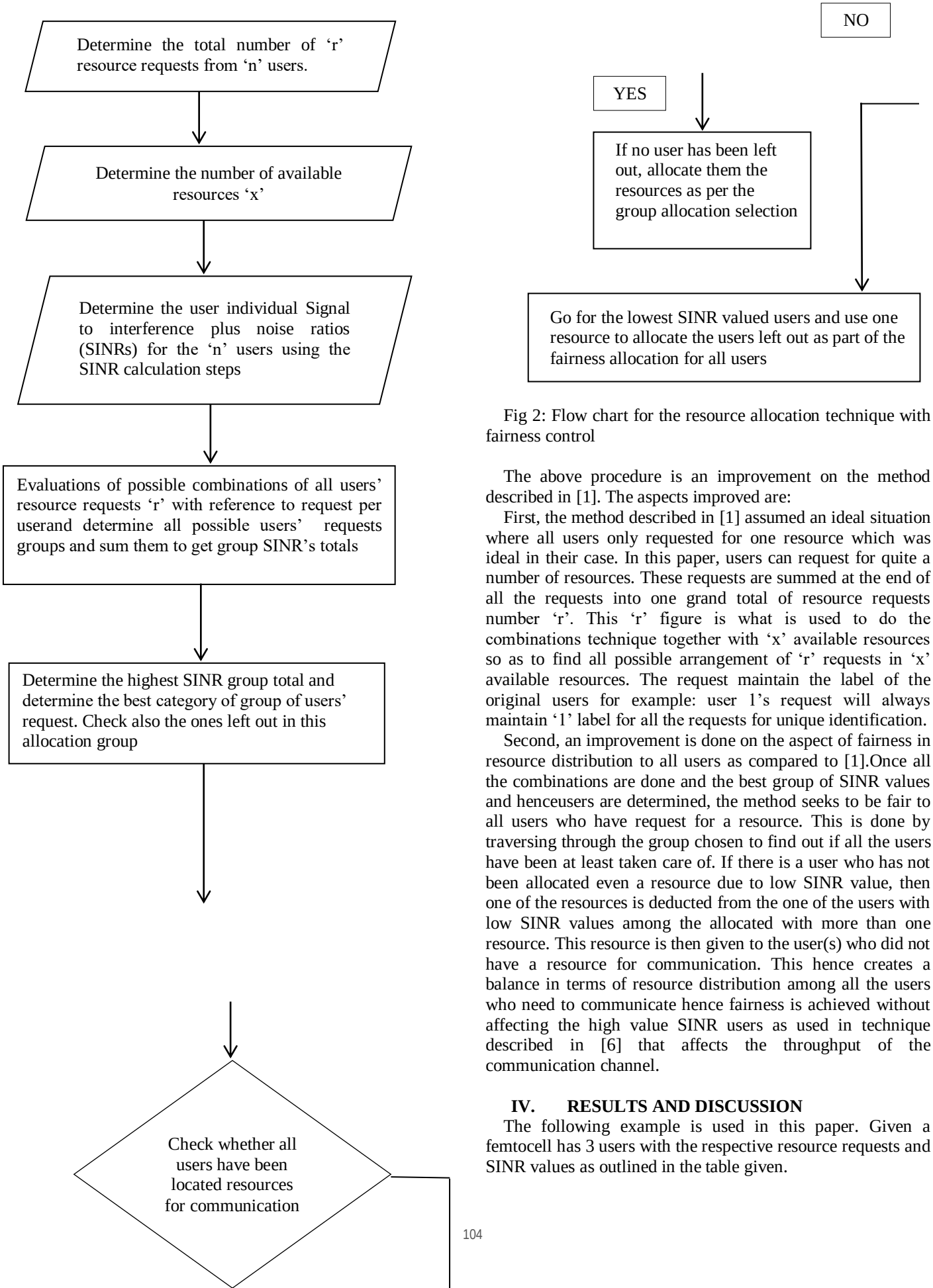


Fig 2: Flow chart for the resource allocation technique with fairness control

The above procedure is an improvement on the method described in [1]. The aspects improved are:

First, the method described in [1] assumed an ideal situation where all users only requested for one resource which was ideal in their case. In this paper, users can request for quite a number of resources. These requests are summed at the end of all the requests into one grand total of resource requests number 'r'. This 'r' figure is what is used to do the combinations technique together with 'x' available resources so as to find all possible arrangement of 'r' requests in 'x' available resources. The request maintain the label of the original users for example: user 1's request will always maintain '1' label for all the requests for unique identification.

Second, an improvement is done on the aspect of fairness in resource distribution to all users as compared to [1].Once all the combinations are done and the best group of SINR values and henceusers are determined, the method seeks to be fair to all users who have request for a resource. This is done by traversing through the group chosen to find out if all the users have been at least taken care of. If there is a user who has not been allocated even a resource due to low SINR value, then one of the resources is deducted from the one of the users with low SINR values among the allocated with more than one resource. This resource is then given to the user(s) who did not have a resource for communication. This hence creates a balance in terms of resource distribution among all the users who need to communicate hence fairness is achieved without affecting the high value SINR users as used in technique described in [6] that affects the throughput of the communication channel.

## IV. RESULTS AND DISCUSSION

The following example is used in this paper. Given a femtocell has 3 users with the respective resource requests and SINR values as outlined in the table given.

Table 1: Users, Resource requests and SINR values

| User | Resource requests | SINR values |
|---|---|---|
| 1 | 3 | 5 dB |
| 2 | 2 | 7 dB |
| 3 | 4 | 4 dB |
| ***Total*** | ***9*** | |

The available resources in the femtocell are 5 and from the above table the total requested is 9.

When combinations is done on the number of arrangement of the 9 requested resources with regard to 5 available ones, a matrix of 126 by 5 is obtained with 126 different ways of arranging the serialized user requests in 5 available resources in the femtocell. These requests are arranged with respect to their corresponding SINR values and the totals done.

From this, the best SINR total value is obtained and the users bearing the SINR values determined to be the following arrangement of requests: *[1 1 1 2 2]*. This corresponds to users 1 and 2 and leaves user 3 out.

Since one of the objectives of this method is to encourage fairness to all users requesting resources, a quick scan shows user 1 has a lower SINR compared to user 2. This user has 3 resources allocated to him and hence one resource can therefore be removed from him and allocated to user 3 to give him a chance to communicate through the system and hence takes care of fairness for all users in the system.

## V. CONCLUSION

The combinational technique with fairness control proves to be effective in terms of use of user SINR values todetermine the best users to allocate resources for communication in a femtocell. This is effective in a dynamic environment where user factors such as SINR often fluctuate due to various aspects in the environment. This makes it appropriate in robust and busy environment due to instantaneous user selection.

## VI. ACKNOWLEDGEMENT

My gratitude goes to my supervisors Dr. Philip KibetLang'at and Professor Stephen Musyoki for their outstanding guidance while conducting my research for documentation and preparation of this paper.

## VII. REFERENCES

[1] Macharia Andrew R., Kibet P. Langat, Stephen Musyoki, "A combinational users selection scheme to enhance efficient resources allocation in a FEMTOCELL," in *Eastern African Multidisciplinary Applied Research Conference, USIU*, Nairobi, 2016.

[2] Vasco Pereira and Tiago Sousa, "Evolution of Mobile Communications: from 1G to 4G," in *Department of Informatics Engineering of the University of Coimbra*, 2004.

[3] Aditi Chakraborty, "A Study on Third Generation Mobile Technology(3G) and Comparison among All Generations of Mobile Communication," *International Journal of Innovative Technology & Adaptive Management (IJITAM) ISSN: 2347-3622*, vol. 1, no. 2, November 2013.

[4] Anritsu, "LTE Resource Giude," 2009.

[5] Martin Sauter, "From GSM to LTE; An Introduction to mobile networks and mobile broadband," *John Wiley and Sons, Ltd, Publication*, 2011.

[6] Dr. J. B. Helonde, Dr. Rajesh Pande Sudhir B. Lande, "Comparison of Resource Allocation Techniques in OFDMA for Wireless communication," *International Journal of Engineering and Innovative Technology (IJEIT), Volume 2, Issue 6*, December 2012.

[7] N. O. Oyie, P. K. Lang'at and S. Musyoki, "Femtocell Cluster-Based Mobility-Aware Resource Allocation Scheme for OFDMA Network," in *Proceedings of 2014 JKUAT International Conference on Sustainable Research and Innovation*, Nairobi, Kenya, 7th-9th, 2014.

[8] Chuan-Kang Ting, "On the Mean Convergence Time of Multi-parent Genetic Algorithms Without Selection," *Advances in Artificial Life*, vol. 403–412. ISBN 978-3-540-28848-0., 2005.

[9] J Zhang, and Y Li X Hu, "Orthogonal methods based ant colony search for solving continuous optimization problems," *Journal of Computer Science and Technology*, vol. 23, no. 1, pp. 2-18, 2008.

# Sustainable Rain-Water Harvesting Strategies: Lessons and Opportunities for Developing Societies Africa

Moses Wandera

***Abstract*** **:**The demand and supply of water in both developed and developing societies has wanting however, the challenges on use and need have tended to be similar. This study sought to explore technologies and sustainable techniques for rain-water harvesting as its main aim. Various societies over time have used their indigenous methods, and this study sought to explore through case surveys as its design in both developed and developing societies on methods both indigenous and modern techniques that have been used. Indigenous systems have been used in Nigeria, Ghana Malta among other countries. In developed societies modern techniques have been used in the United Kingdom over a period of three decades. Further-mention is this study on Livestock Water Productivity in India and how it can be relevant to Sub-Saharan countries mainly in arid and semi-arid regions (ASAL) on rain water harvesting and use. The strategies, lessons and best practices using a sustainable resources theory and its practice as well as analysis have been used. Various lessons have been given for adoption and implementation in sustainable living and learning for developing societies as Kenya.
*Keywords: Developing societies, rain-water harvesting, sustainable techniques*

## I. INTRODUCTION

Kenya is a victim of climate related disasters as 70 per cent of all disasters happening in the country are done to climate change. Globally Kenya ranks 50 in the number of people affected by climate disasters. The frequencies, extent of coverage, timing and severity have change, and seriously eroding people's coping and adaptive capacity. In arid and semi-arid lands (ASALS, droughts are an inherent part of life in the past decade, drought episodes were experience in 2001, 2003, 2006, 2009, 201 and recently in 2016. In addition, major floods occurred in 2006 and 2010 as heavy rains often followed periods of prolonged drought. The prolonged drought of 2008-2011 was one of the worst in Kenya as its impact costed about Ksh 1.2 billion and slowed down GDP growth by an average of 2.8 per cent per year. The UN Office for the coordination of Humanitarian Affairs estimates that the government allocated Ksh. 18 billion to drought response in 2011 alone. The bulk of these funds were used in famine relief (Nyangena, 2014).[1]

*The Cooperative University of Kenya. *[1]Corresponding author: Moses Wandera Email: mosewa2005@yahoo.com*

In Kenya, besides economic loss, drought is responsible for the rising number of climate refugees and migrants, as communities move to less hostile environments and often this exerts pressure on natural resources and results in resource use conflicts or human-human and human wildlife conflicts. In addition, the environmental impacts of drought have included wind erosion, reclining wetlands and poor sanitation. In some areas of the country, drought catalyzes desertification and loss of biodiversity, (ibid).

Access to water in Kenya stands at 53%, however, the target has been 80% from 53% to 100% the conversation that is ongoing in the water sector overtime. Further, 46% of the populations do not have access especially in informal or unplanned settlements. Access to water in Kenya has been strengthened by the constitution 2010 which guarantees the right to water in Article 43. In essence right to water in Article 43. In essence there has been the need for citizens to be informed regularly about the status of the water sector and what plans there are to sustain this important resource called water (Gakubia, 2016).[2]

In 2011 in Kenya, the government recognized the problem of drought and launched a 10-year programme on ending drought emergencies campaign, to consolidate the drought mitigation measures based on experiences acquired over the years through the campaign. It was expected that drought will no longer remain a humanitarian emergency. Further, during the same period, the National Drought Management Authority (NDMA) was established to provide the institution framework to combat drought (Nyangena, 2014). Further, NDMA, just provides the framework for the country to fulfill the international obligations under the Hyogo Framework for Action. The Measures have been important, especially in the ASALS, as they are in line with Article 43 of the constitution which requires the state to take legislative, policy and other measures to achieve the progressive realization of the human rights including the right to freedom from hunger.In Kenya, some agencies established on the same note have included, the National Drought and Disaster contingency fund to finance drought management in livestock, agriculture, water and sanitation, health, education and early warning systems (ibid). The Kenya Food Security Meeting (KFSSM) and its technical

a run, the Kenya Food Security steering Group (KFSSG), the Kenya Red Cross and the National Disaster Operations Centre have all be involved in essence, drought management measures should target the underlying causes of community vulnerability where, there should be innovations to encourage new patterns of responses by increasing participation and social organizations at the local level. Further, traditional social networks used by various communities to survive drought, or as early warning systems should be strengthened as appropriate, since drought is closely associated with water deficit, increasing the country's water storage capacity would greatly ensure rapid expansion of irrigable land and reduce over dependence on rainfed agriculture. It means also that shall-scale dams in pastoral areas should be constructed and be accompanied by other measures such as establishment of disease –free zones, improvement of breeding services and promotion of efficient marketing to increase livestock production. It means also that improving drought assessment capacity and intensifying research on appropriate responses should be an integral part of any drought management agenda (ibid).

Globally, sustainable development goal no. 6 has emphasized on clean water and sanitation, to achieve universal and equitable access to safe and affordable drinking water for all, achieve access to adequate and equitable sanitation and hygiene for all and end open defecation, paying special attention to the needs of women and girls and those in vulnerable situations, improving water quality by reducing pollution, eliminating dumping and minimizing release of hazardous chemicals and materials having the proportion of untreated wastewater substantially increasing recycling and safe reuse globally, substantially increase water-use efficiency across all sectors and ensure sustainable withdrawals and supply of freshwater to address water scarcity and substantially reduce the number of people suffering from water scarcity, implementing integrated water resources management at all levels, including through trans boundary cooperation as appropriate, protect and restore water-related ecosystems, including mountains, forests, wetlands, rivers, acquitters and lakes, expand international cooperation and capacity, building support to development countries in water and sanitation related activities and programmes, including water harvesting, declination, water efficiency, wastewater treatment, recycling and reuse technologies as well as support and strengthen the participation of local communities in improving water and sanitation management (WASREB, 2016).[3]

Measuring sustainability, the challenge has been varied. For instance, some link it to environmental impact based on population, affluence and technology that is;

| | | |
|---|---|---|
| I | = | P x A x T |
| | | Where; |
| I | = | Environmental impact |
| P | = | Population |
| A | = | Affluent |
| T | = | Technology |

(Ehrlich and Holden, 1974 cited in Kerr C, 1990)

Further some link sustainability to health,
Health = Water + sanitation + hygiene education
(Kerr C, 1990) [4]

## II. Problem Definition

In Kenya, according to the National Water Services Strategy (NWSS-2007 to 2015), Kenya's target for water and sewerage services in the urban setting was 80% and 40% respectively, however, only 15% of utilities met this target. In 30% of utilities, more than 50% of the water produced is lost through physical and commercial losses with only 10% (8184) of the utilities meeting the Non- Revenue Water (NRW) country's target of 30% by 2015. On the other hand, only 40% of the utilities are able to cover their operations and management costs.

In Kenya besides, the increased investment for infrastructural expansion and rehabilitation, the real potential in Kenya's urban water sector lies in reducing wastage, improving service quality, maximizing on consumer contribution and improving cash flows to accelerate access to water. It can also leverage on programmes like the Kenya out-put-based Aid (OBA), Aid on Delivery (AOD) programme, or on commercial financing. Also critical is a proper legal and institutional framework, proper sector policies, and incentives for utilities to perform (extend services to the poor, build capacity and network also have financial sustainability. Therefore with the recent enactment of the water act 2015, the sector now has a better instrument to guide its operations.

However, concerns in the Kenya vision 2030, National Development Plan seeks to make water and basic sanitation available to all by 2030. The total cost of investment and rehabilitation needed in water supply is estimated at Ksh 1.7 trillion; national water master plan (NWMP 203). According to the Kenya water master plan, 2030, the available government budget is Ksh 592.4 billion, which leaves a shortfall of Ksh 1.2 trillion. This gap could be plugged partly by increasing sector efficiency, maximizing consumer contributions through tariffs, and encouraging private funding.

In essence, requirements for commercial financing may include; conducive operating and legal environment for bank lending, utilities to continue operating at arm's length as autonomous entities that can borrows, ring fencing of revenue, urban utilities to be managed in business-like manner, tariff setting to allow for funds to leverage more borrowing and not politicized as well as independent regulation (WASREB, 2016).[3]

In essence in Kenya in the last decade, drought episodes were experienced in 2001, 2003, 2006, 2009 and 2011. In addition major floods occurred in 2006 and 2010 as heavy rains often followed periods of prolonged drought. The prolonged drought of 2008-2011 was one of the worst in Kenya's history. Its impact costed about Ksh. 1.2 billion and slowed down GDP

growth by an average of 2.8 per cent per year. The United Nations Office for the coordination of humanitarian Affairs estimates that the government allocated Ksh. 1.8 billion to drought response in 2011 alone. The bulk of these funds were used on famine relief. Further, apart from economic loss, drought is responsible for the rising number of climate refugees and migrants, as communities move to less hostile environments and often this puts pressure on natural resources and results in resource-use conflicts (human- and human wildlife). Environmental impacts of drought have included wind erosion, reclining wetlands and poor sanitation. In some areas of the country, drought catalyzes desertification and low of biodiversity. A recent drought in Turkana County affected 400,000 people and more than 35,000 children were forced to stay out of school due to food insecurity (Nyangena, 2014). Therefore this study seeks to be an eye opener on the techniques for rainwater harvesting based on the above challenges in Kenya and other developing societies.

**Objective of the study**

The main objective of the study was to describe the main sustainable rain water harvest strategies that are applicable in developing societies.

**Theoretical framework**

**Sustainable resource theory**

This theory has been linked to scarce resource theory; unlike for one major point; the concern for the long-term versus short-term agenda. The theory was emphasized by Thurow in 1993, as cited in Swanson 2007),[5] while evaluating organizational performance. Thurow 1993:16 says, "In the future, sustainable advantages will depend on new processes, technologies and less on new product technology. New industries of the future will depend on the brain power. Man-made competitive advantage of Mother Nature (natural – resources endowment or history (capital endowments)". Earlier resource-based view by Barney 1991:10, had emphasized on the same; just like Graut, 1991. This view point is the sustainability link that had been put forward by Bruntland commission and Report in 1987.

## III. Materials and Design

He study adopted survey design involving global regions mainly developing societies with one developed country global regions as its population on strategies adapted in rain water harvesting. Survey design was appropriate because of the research and the ethical concerns that needed to be brought out and its validity, rather than other approaches that may be used (Sapsford, 2004).[6] Further content analysis also consists of scoring specific information that is required. The advantage of this method is on revelation of what was initially considered as descriptive study (Isabel, Luis & Isabel, 2011).[7] This methodology is appropriate for disclosing important information required for benchmarking and it has been employed by (Xiao, Yang and Chow, 2004).[8] Validity and reliability of the study has been based on content, criterion as well as contrust.

## IV. Discussions

**Some Global Sustainable Projects and Strategies**

Among the innovative projects may include:

i) **Rain water harvesting technologies**. This is done in Africa by Amsha Africa as well as in Smart Agriculture, Florida State and Oklahoma in the United States of America. Among the best practices by Amsha Africa include:

a) Runoff rain water harvesting technology is practiced in rural Africa; here cemented rectangle – like hole almost one metre or so deep.

b) Water pans; here a hole or pond dug in the ground, used to collect and store surface run-off from uncultivated grounds, roads, ridges or laggas. It can be square, rectangular or round. Common ones hold 400 to 1000 metres cubed.

c) Plastic- lined underground tank; here runoff water is directed into an underground tank dug into the ground. The advantage of a tank is that it is covered. This stops water from being lost into the air by evaporation. As long as the manhole entrance into the tank is well secured, it is also safer for children. Life span can extend up to 20 years before repair.

Traditional rural African rain water harvesting strategies included from banana stems and leaves, also from backs of trees and leaves also clean utensils placed on roofs of buildings among others.

ii) **Irrigation-related activities**; for instance in the world 144 million of land is cultivated under rice, while Asia produces more than 90% of world's rice. (FAO, 2010). In addition, Israeli-based technologies on customized irrigation in conjunction with the private sector are other techniques, commonly used. Other countries including Uzbekistan, Egypt, Lesotho and Honduras in Lempira are practicing irrigation.

iii) **Livestock projects**

Since grazing land occupies 26% of the earth's ice-free land surface, and 33 percent of cropland is dedicated to the production of feed, similarly fodder crops represent 70% of world's agricultural area. Soils under grasslands, contain 20% of world's carbon stocks, and are at risk from land degradation. In Peru Cajamarca province, milk production increased by 25% and calves reached up to 280 kg in 20 months, instead of 30 months due to good fodder production (FAO, 2010).[9]

iv) **Fishing**

World-wide, 500 million depend directly or indirectly on fisheries and agriculture for their livelihoods. Since fish provides essential nutrition for 3 billion people and at least 50% of animal protection and essential minerals to 400 million people in the poorest countries. However, climate change has affected production as powered fishing vessels consume 41 million tones of fuel. (FAO, 2010)

v) **Other projects**; rooftops gardens in Cairo Egypt as well as national biogas programme in Vietnam and Thailand are worth emulating.

vi) **Wildlife projects**

In Africa there are many wildlife foundations especially for elephants. Among the common ones are, the African Wildlife Foundation (AWF). The David Sheldrick Wildlife Trust, William Holden Wildlife Foundation, African Conservation Foundation.
Other projects include partnership options for resource use innovation(PURI) by USAID; dealing in livestock for livelihoods, Sustainable economic Resources for Africa (SERA), International Elephant Foundation, Amboseli Ecosystem Anti-poaching project, Patty Wagstaff-lindbergh Foundation in east Africa, African Environmental Film Foundation(ARFF), Global Greengrants Funds as Well as Wetlands International, Everglands Foundation from Brazil and Bolivia. The World Conservation Union in Netherland (IUCN) also the World Conservation Union of Eastern African Regional Office (UNCN-EARO) among others.

In the United Kingdom (UK) Rainfall harvest cases have been from the roof of building, otherwise called rainwater harvesting (RWH) (Alan, 2012).[10] This strategy has been of the view of non-potable applications such as water closet (WC) slushing or garden watering. Herrman and Schmida (1999) had identified type of system as indicated below as a remedy. Storage for water supply can be compiled as (Mcmahon, (1978).[11]

$Vt = V_{t-1} + Q_t - D_t$

Subject to $o \leq V_t \leq s$

Where $V_t$; water storage at end of time interval t

$Q_t$ Inflow during time interval t;

$D_t$ demand during time interval t

S Storage capacity

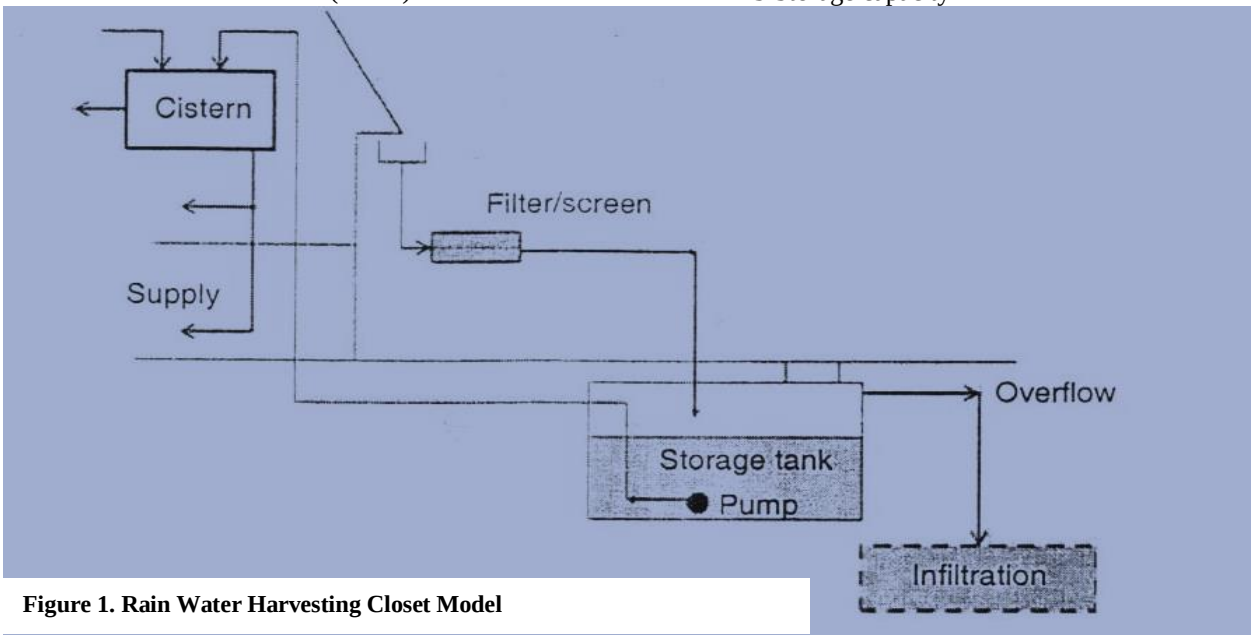


**Figure 1. Rain Water Harvesting Closet Model**

**Source: Herrmanna and Schmida (1999)[12]**

In Malta an Island most rainwater harvesting technologies have been sustainable indigenous technologies on the Maltese Islands whose rain is isolated and spread over a short period of time are have not been adequate. Initially the model of harvesting rain water was that of Munasinghe (2001), [13] that is;

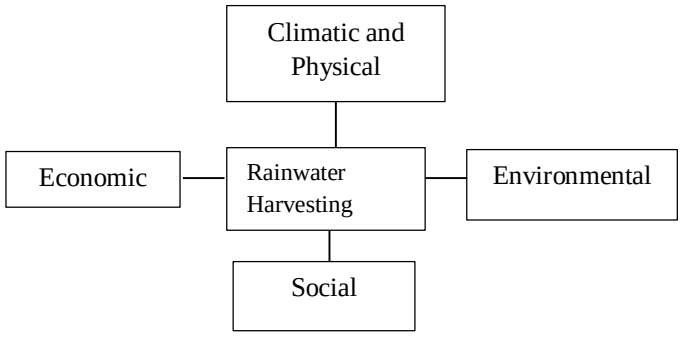


**Figure 2. Rain Water Harvesting structure**

However, the many challenges in all the spheres have provided the interventions by giving alternatives as provide below.

- Semi-permeable surfaces: these would allow for rainwater percolation to be caught in culverts of reservoirs below ground. This would work well in a car-centric community like the Maltese Islands that makes use of large areas for the sake of parking spaces, but seems to lack the imagination to adapt below ground reservoirs to aid the water issue. The benefit of this practice would be that the semi-permeable surfaces allows for filtering of water from large sedimentation, requiring some polishing and making it perfectly viable to be used and apportioned where needed while reducing stress from ground water. Additionally monitoring and combining the capacity and annual collection would also allow the harvesting and retention of water at key areas to be apportioned and used by agriculture during the summer months as needed.
- IKS model: this concept has value for the case of Malta on two fronts. On one hand, the historically adapted practices such as dams, cisterns and aqueducts could hold greater value when coupled with innovative cutting edge technology to maximize efficiency in Rain Water Harvest (RWH) catchment, storage and distribution. On the other hand, the focus of endorsing and pushing of indigenous flora and agriculture could help in enriching a depleting ecological system while also shifting to a demand management frame of mind which is sorely needed when considering the incremental use from the agricultural sector.
- Green roofs: these allow for embellishment through added greenery, and the possibility for minor agricultural uses of large areas. Additionally, they allow a reduction of storm water flowing, enhance rainwater catchment (Fewkes, 2012),[14] recharge ground water and reduce $CO_2$ emissions through plant air filtration (Getter and Rowe, 2006) and improve thermal comfort in buildings (Kohler et al., 2002).[15] The flexibility and implementation of such technology is versatile and offers multiple benefits. It is recommended that plants or vegetation used on Maltese green roofs are endemic or well adapted to the climate to ensure that the water needs of such vegetation is not detrimental to the potential water that could be harvested. (ibid)

These examples, at macro as well as micro level, could be implemented sporadically across the Maltese Islands to allow for an augmented RWH trend, aiding the Maltese Islands to increment water flow recharges as well as ground water stock, while giving rise to new water supplies that could curb a decreasing ground water supply.

The following are some other recommendations that could also play an important role in the initiation of a unified RWH and holistic water management strategy. (Frank and Ians, 2014) [16]

- Enhance enforcement with all stakeholders to a degree that the misuse or abuse of ground water is seen as a criminal act to the extent of fines and or jail time.
- Enhance regulation an policies that actively require follow through and setup incentives for developers to invest cisterns and wells as well as secondary water systems for the occupants, be they homes or apartments. Additionally, incentives for PV panels could be extended to domestic wells. If both programmes are too costly to be run concurrently, then these can be rotated annually or biannually.
- Allowing WSC to charge a small amount for sewage treatment to become more sustainable with regards to its role and operations. Subventions are not a final solution; WSC needs to be given the managerial space to balance its books while fulfilling its social obligation. Additionally, a polluter pay system may be introduced.
- NGO's should try and have a common ground perspective on water issues as such an alignment would aid public consultation processes with the inter-ministerial committee.
- Businesses and industries should also be given incentives to invest in RWH as this may be of advantage to them within their own operations in the long run. Consideration to isolate industrial sewage water from the main sewage affluent, if feasible, to facilitate treatment and reuse of main sewage effluents should be vetted.
- A modular set of campaigns across various social groups to educate residents and awaken a

conservative nature and understanding of water issues, its scarcity and its importance. As the needs and uses are many, the campaigns should be diversified to reflect it and promote a cultural shift.

- Future environmental decision-making processes on problem-oriented matters need to acknowledge community values and to find more effective ways by which the general public is encouraged to participate in consistent, robust and meaningful ways as from the initial stages; such approaches are known to yield better results (Harding, 2005).[17]

In India study on the effects of smallholder farmers access to livelihood capital for instance land, livestock and water on livestock productivity that water management based interventions include; key agricultural activities that enhance sufficient and timely water supply and efficient uptake by the plants especially by rice and wheat crops, which compares with improved feed quality and animal productivity, the study suggested that improvement of water productivity of feed changes with livestock water productivity value significantly as compared to other interventions (Amare, Floriane and Khan, 2011).[18]

In Africa mainly Sub-Sahara Africa including Nigeria institutional capacity challenges on water resources management have included (Sharma, 1996). [19]

- People are unaware that water is a finite resource with supply constraints, that it has a scarcity value, and that there is a cost to using it;
- Lack of understanding of the consequences of deforestation and land degradation on the quantity and quality of water;
- Inadequate capacity building and neglect of traditional knowledge bases as well as gender issues;
- Management of water resources is highly fragmented among sectors and institutions and there is excessive reliance on public sector services; and
- Weal institutional and implementation capacities.

However in Nigeria techniques have involved; water storage techniques including inside drum, jerry can, plastic bowl, buckets, local pots, surface tanks among others. Among the methods commonly preferred were jerry cans at 29.5% and inside drum at 26.2%. (Gbadesign and Olorunfeni, 2011) [20]

Indigenous technologies in Nigeria of water harvesting have included, pit chlorination, solar disinfection, simple sand filters, nylon filters, tagging harvesting of ground water and recharging of ground water among others successful techniques in rainwater harvesting in in Ekpoma state, however, the Nigerian government is yet to assist people fully in terms of materials in harvesting the rain water say the corrugated iron sheets, cement and blocks used in the construction of the reservoirs (Getter and Rowe, 2016). [21]

In Ghana, indigenous agriculture systems mainly, where farmers plans multiple indigenous drought resilient crop varieties and by employing different rounds of seeding or staggering planting between multiple farms. Farmers also apply indigenous forms of organic manure, checking soil erosion through grass strips and stone terracing and adopting paddy farming for improving soil and water conservation towards enhancing plant adaption to drought. These strategies are better applied to reduce vulnerability which is mainly the cause of natural disasters, UNDP, 2004 P11, [22] and Emmanuel (2013).[23]

In Kenya Water Services Trust Fund (WSTF) is the Kenyan State Corporation mandate to finance water and sanitation services for the poor and underserved communities in rural and urban areas. In addition, the water bill 2017. The mandate of the fund has been to provide conditional and unconditional grants to the countries and to assist in financing the development of an management water services in the marginalized and underserved areas; including, community level initiatives for the sustainable management of water resources, development of water services in rural areas considered not to be community viable for provision of water services by licences, and development of water services in the under-served for urban areas. (Shaiye, 2015).[24]

Further, the stakeholders of WSTF have included, county government stakeholders under devolved structures, water resources management authority who assists the authority in developing sub-catchment management plans (SCMPS) and provides oversight for water resources management, water services

boards who in the past have been overseeing the community organizations in rural programmes, and water services providers in the urban programmes, water services providers who implement and provide water and sanitation services in urban and now also rural areas where relevant, community groups (CORUA and CBUS) who participate in implementation of their projects in rural areas as well as other government and private sector institutions for instance in health, education, management organizations (NGO) and others (ibid).

According to FAO (2010), rain-fed agriculture is now 20% in developing countries. Further, if improved water harvesting and retention strategies such as pools, dams, pits, retaining ridges among others and water – use efficiency (irrigation systems), then agriculture land in developing countries can generate 130% more yields than rain fed systems. This will require expansion of efficient management technologies and methods especially those relevant to smallholders, which is fundamentally essential.

In Africa organizations and foundations engaging in wildlife management and conservation are far many than water harvesting strategies yet human – wildlife conflicts have been on the increase. Kenya has 3% of forest cover compared to the recommended 10%. And since forest cover is linked to climate, unfriendly climate conditions in terms of drought and flooding has been evident in Kenya recently than before. In the same way media reports of elephants destroying farm lands is on the increase as the search for water intensifies. It is for this reason that recently Cable Network News (CNN), in its documentary 'Inside Africa', says elephants and livestock battle for water in East Africa. Inside Africa revealed that drought means people and elephants have to use the same water points. Elephants are some of the first of the animals to feel the effects. Similarly,
livestock herders are forced to take their animals to water holds in protected areas;
similarly, elephants are destroying farmers' crops as they search for food, (Wither E. (2011). [25]

In Kenya the overall water masses are only 11,230 square kilometers, for the available population, the use of by animals agriculture, energy and even health and public sector safety besides the basic financing requirement as indicated below which is a major challenge and a source of vulnerability in a bid to achieve sustainable development in Kenya.

**Table i. Status of Kenya; facts and figures**

Water - 11, 230 square kilometers
National parks - 25, 334 square kilometers
Others - 54,082square kilometers
**Total - 582,647 square kilometers**

*Source: Kenya National Bureau of Statistics, 2009* [26]

**Table ii. Vulnerability Assessment in Kenya (ROK, 2013)** [27]

| No | Sector | Vulnerability | Adaptation assessment |
|---|---|---|---|
| 1 | Agriculture | ▪ Poverty among the small scale subsistence farmers.<br>▪ Farming in the marginal rainfall areas.<br>▪ Over-cultivation and land degradation<br>▪ Inadequate technologies to improve production<br>▪ Limited in-economic diversification<br>▪ Weak integration of indigenous knowledge on the use of climate information to maximize agriculture production. | • Adoption of drought resistant/escaping crops.<br>• Soil conservation measures.<br>• Adoption of appropriate agricultural techniques and water conservation technologies.<br>• Crop diversification in subsistence farming.<br>• Alternative means of income generation for subsistence farmers. |

| | | | |
|---|---|---|---|
| | | | • Enhanced public education and awareness raising on effective use of climate information |
| 2. | Water Resources | • Population increase in the marginal areas leading to increased demand for water.<br>• Over-cultivation in slopping areas leading to flash floods and siltation of rivers and reservoirs- Deforestation in the water catchment areas.<br>• Inefficient utilization of available water, e.g. irrigation methods.<br>• Water pollution, especially by industries. | • Enhance water harvesting and conservation methods<br>• Increased afforestation especially in the water catchment areas.<br>• Zoning of environmental significant sites<br>• Exploitation of underground water especially in the marginal rainfall areas.<br>• Adoption of irrigation technologies that lead to water conservation.<br>• Policies and measures that enhance water quality.<br>• Good soil conservation practices in agriculture.<br>• Public education and awareness raising. |
| 3. | Energy Resources | • Deforestation especially in the hydropower dams catchment areas.<br>• Over cultivation resulting in siltation of rivers and dams.<br>• Inefficient utilization of biomass for energy<br>• Poverty leading to over exploitation of biomass. | • Increased afforestation and reforestation.<br>• Good agricultural practices and soil conservation.<br>• Adoption of biomass energy efficient stoves (appropriate energy conservation measures).<br>• Enhance/diversify alternative income generation activities (AIG)<br>• Increasing exploitation of renewable energy resources such as wind, solar and geothermal energy.<br>• Enhance energy efficiency in industrial and commercial operations<br>• Public education and awareness raising. |
| 4. | Health and public safety | • Inadequate health services especially in rural areas.<br>• Increased prevalence of diseases related to climate change<br>• Poverty especially among rural communities. | • Provision of adequate health service in rural areas<br>• Adequate response strategies to the outbreak of climate related diseases. |

| | | | |
|---|---|---|---|
| | | • Lack of alternative means of income especially in marginal rainfall areas.<br>• Traditional ways of life that are not changing with time<br>• Inadequate public awareness of disease risks.<br>• Encroachment of wildlife parks and reserves by farmers and pastoralists. | • Availability and utilization of climate information towards preparedness<br>• Sustainable disease vector control strategies.<br>• Provision of clean and adequate water.<br>• Sustainable community conflicts resolution strategies<br>• Alternatives sources of income for communities in marginal rainfall areas.<br>• Public education and awareness raising<br>The above sectors are only some of the sectors |

**Source: Kenya Meteorological Department Annual Report 2013**

**Table iii. Present and future water demands by sub-sector (before water balance study)**

| **Subsector** | **2010 (MCM/Year)** | **2030 (MCM/Year)** | **2050 (MCM/year)** |
|---|---|---|---|
| Domestic | 1,186 | 2,561 | 3,657 |
| Industrial | 125 | 280 | 613 |
| Irrigation | 1,602 | 18,048 | 18,048 |
| Livestock | 255 | 497 | 710 |
| Wildlife | 8 | 8 | 8 |
| Fisheries | 42 | 74 | 105 |
| **Total** | **3,218** | **21,468** | **23,141** |

**Source: The National Water Master Plan 2030**

**4.3 River flow levels/volumes by basins**

**Table iv. Average Annual Water Availability per Drainage Basin**

| **Drainage Basin** | **Annual Rainfall (MM)** | **Surface Water (MCM)** | **Ground Water (MCM)** | **Total Water (MCM)** |
|---|---|---|---|---|
| Lake Victoria | 1,368 | 1,672 | 116 | 11,788 |
| RiftValley | 562 | 2,784 | 126 | 2,910 |
| Athi River | 739 | 1,152 | 87 | 1,239 |
| Tana River | 697 | 3,744 | 147 | 3,891 |
| Ewaso Ng'iro North | 411 | 339 | 142 | 481 |
| **Total** | **621** | **19,691** | **618** | **20,309** |

**Source: Adapted from (National Water Master Plan, 1992; National Water Master Plan (NWMP)**

*Afterccare, 1998;*

**Ground water levels by potential/volumes**

Annual sustainable yield of groundwater in BCM in comparison to the annual recharge per recharge per catchment area as estimated by National Water Master Plan (NWMP) 2030.

**Table v. Annual sustainable yield of groundwater compared to annual recharge (Unit: BCM).**

| **Catchment** | **2010** | | **2030** | | **2050** | |
|---|---|---|---|---|---|---|
| | **Recharge** | **Safe yield** | **Recharge** | **Safe yield** | **Recharge** | **Safe yield** |
| Lake Victoria North | 1,326 | 116 | 1,251 | 108 | 1,612 | 140 |
| Lake Victoria South | 2,294 | 203 | 2,111 | 188 | 2,126 | 190 |
| Rift Valley | 1,126 | 102 | 1,126 | 102 | 1,209 | 109 |
| Athi | 3,34<br>5 | 305 | 3,303 | 300 | 3,649 | 332 |
| Tana | 7,719 | 675 | 6,520 | 567 | 5,840 | 508 |
| Ewaso Ng'iro North | 1,725 | 526 | 2,536 | 475 | 1,361 | 449 |
| **Total** | **21,462** | **1,927** | **19,407** | **1,740** | **19,287** | **1,728** |

**Source: Adapted From Annual Water Sector Review 2012-2013**

**Table vi. Case of sustainable financing borehole in Mwatate – Kenya**

| | **Ksh.** |
|---|---|
| Licences and legal fees and water analysis | 15,300 |
| Ground water survey | 10,000 |
| Hydrological report | 20,000 |
| Equipment, tools, labour and upkeep for ground workers | 68,400 |
| Pumps, casing, concrete and labour | 400,000 |
| **Total** | **513,700** |

**(Source: Amsha Africa)**

## V. Conclusion

In summary, therefore in Kenya available rainwater harvesting technologies must include those offered by Shabaha engineering on small scale, Amsha Africa, future pump, Brook Sarson among others. These technologies are yet to be fully used in rainwater harvesting initiatives to a large extend. However, much newer technologies are required also in Arid and semi-arid areas (ASALs), to collect and store much rainwater besides clean siltation and use of renewable energy as solar in purifying the water. Hence the study is meant to open upon discussion, as newer technologies are adopted from other countries to reduce vulnerability in Kenya.

Therefore it is recommended that rain water harvesting strategies like those of Amsha Africa, Brook Sarson in San Diego among others be encouraged and adapted so that community and regions to specialize in it and just like using smart farms as it happens in Florida State (USA) in irrigation and rain water harvesting. Further research should be on wildlife foundation especially elephants in Africa on the need to be emphasized on water harvesting strategies as elephants need much water and a major root cause of conflict with humans.

**Acknowledgement**
The author acknowledges The Cooperative University for availing the facilities and resources for the research of this paper.

**REFERENCES**

[1] Nyangena T. (2014). Addressing Drought Occurrences through New Approaches, in Kippra Policy Monitor Issue No. 2 Improving Public Policy Making for Economic Growth and Poverty Reduction Nairobi. Kippra.
[2] Gakubia R. (2016). Chief Executive Officer's Executive Summary, World Water Day 2016. Acqualink News Letter Nairobi. A Publication of the Water Services Regulatory Board [WASREB]
[3] WASREB (2016). Impact: A performance review of Kenya's water services sector 2014-2015 Nairobi Water Service Regulatory Board [WASREB] Issue 9/2016.
[4] Kerr Charles (1990). Community Health and Sanitation. London. Intermediate Technology Publications.
[5] Swanson, R. A. (2007). Analysis for Improving performance: Tools for Diagnosing organizations and Documenting Workplace Expertise. San Francisco. Berrelt – Koehley Publishers. Inc.
[6] Sasford R. (2004). *Survey Research.* London. Sage Publications.
[7] Isabel, G. Luis R & Isabel M.G (2011). Information disclosed online by Spanish. Universities. Content and explanatory factors. Online information review 35 (3) 360-385.
[8] Xiao, J.Z, Yang, H. and Chow, C.W. (2004), "The determinants and characteristics of voluntary internet-based disclosures by listed Chinese companies", Journal of Accounting and Public Policy, Vol. 23 No. 3, pp. 191-225.
[9] FAO (2010). "Climate - smart" Agriculture: Policies, Practices, and Financing for Food Security. Adaptation and Mitigation. Food and Agriculture Organization (FAO) Rome, Italy.
[10] Alan F. (2012). A review of rainwater harvesting in the U.K Structural Survey. Vol. 30 No. 2 pp. 174 -194. Emerald Group Publishing Limited.
[11] Mcmahon, T.A and Main, R.G (1978). Reservoir capacity and yield in Chow V.T (Ed.) Developments in Water Science, Elservier, Amsterdam.
[12] [Herrmann, T and, Schida, V. (1999). Rainwater utilization in Germany; efficiency dimensioning hydraulic and environmental aspects; urban water vol. no. 4 pp. 307-16.
[13] Munasinghe, M (2001). Exploring the linkages between climate change and sustainable development a challenge for trans disciplinary research conservation ecology, vol. 5 No. 1 pp 78-85.
[14] Fewkes, A (2012). A review of rainwater harvesting in the U.K structural survey vol. 30 No. 2 PP. 174-194.
[15] Kohler, M and Tavares, S (2002). Green roofs in temperate climates and in the hot humit tropics for beyond the aesthetic environmental management and health, vol. 13 no. 4 pp 383-391.
[16] [Frank H.B and Ians (2014). Exploring rainwater harvesting opportunities in Malta. Management of Environmental quality. An international journal vol. 27 No. 4 pp. 390-406. Gerald Group Publishing Limited.
[17] Harding R (2005). Environmental decision-making. The roles of scientists, engineers and the Public. Sydney. The Federation Press.
[18] [18] Amare H, Michael B., Floriance C, Saba and Khan M (2011). Adapting livestock water productivity to climate changes. International journal of climate change. Strategies and management vol. 3 no. 2 pp. 156-169; Emerald Group Publishing Limited.
[19] Sharma, N.P, Dambang T, Gilbert-Hurt, E. Grey, D Okaru and Robberg D. (1996). African Water Resources. Challenges and Opportunities for sustainable development. The world bank Washington, DC.
[20] Gbadesign A.S and Olorunfemi FB (2011) Sustainable technological policy options for rural water supply management in selected rural areas of Oyo States, Nigeria. Management of Environmental Quality: An International Journal. Vol. 22. No.4
[21] pp.486-501. Emerald Group Publishing.
[22] Getter, K.L and Rowe D.B (2006). The role of Green roofs in sustainable development. Hortscience, vol. 41 No. 5 pp. 1276-1285.
[23] UNDP (2004). A Global Report, Reducing Disaster Risks a challenge. United Nations Development Programme Bureau for crisis prevention and recovery new york. UNDP.
[24] Emmanuel K.D (2013). Reducing Vulnerability of rain-fed agriculture to drought through indigenous knowledge systems in north Eastern Ghana. International Journal of climate change strategies and management, vol. 5 issues pp. 71-94
[25] Shaiye M. F (2015). Executive Summary of the Chief Executive Office Water Services Trust Fund newsletter. Nairobi water services trust fund.
[26] Wither Emily (2011). Elephants and livestock battle for water in East Africa. Atlanta Cnn.com. September 9, updated 1021 GMT.
[27] KNBS (2009). Kenya Facts and Figures. Nairobi, Kenya National Bureau of Statistics.
[28] Rok (2013). Kenya state of environment report. Nairobi National environment management authority (NEMA).

http://osufacts.okstate.edu
www.awf.org
www.sheldrickwildlifetrust.org
www.amshaafrica.org
www.whwf.org
www.smart.farms.net
www.h20.me.com
www.kenyawetlandsforum.org/index
www.fao.org/ag/ca

# A Review of Quad-rotor UAVs and their Motion Planning

Nelson M. Gachoki, Asaph M. Muhia and Mercy N. Kiio

*Abstract*—This review paper will give an overview of Quad-rotor Unmanned Aerial Vehicle (UAV) systems, their applications and how their motion is planned. It begins with introduction on various UAV types and their uses. It then explains the principles of their operations including flight path planning and finally it demonstrates by use of case studies how UAVs have been used. The case studies expound on the practical experiences of unmanned aerial vehicles in civilian applications. It is anticipated that the findings of this paper will help expedite their use locally and attract wide research, investment and better policy regulation for their application.

*Keywords*—Motion planning, UAVs, UAV applications

## I. INTRODUCTION

UNMANNED Aerial Vehicles (UAVs) refers to aircraft which autonomously fly without a human intervention. They are different from drones and model aircrafts, since drones are not equipped with on-board intelligence but are merely launched into a pre-programmed mission on a pre-programmed course and a return to base [1]. Model aircrafts on the other hand can be radio-controlled within sight of the operator. The operator instructs the aircraft altering its attitude, orientation and position.

UAVs are supported by a system comprising of a set of sub-systems including the unmanned air vehicle (UAV), the control station and communication sub-systems. In this system, the pilot's interfaces and aircraft controls are replaced by an intelligent control system [1]. UAVs have been applied in variety of missions such as continuous surveillance, cargo transport and casualty evacuation in battlefields as well as at sites of natural disaster [2]. For successful completion of such missions there is need for incorporation of properly designed motion plan that in some cases may involve collision avoidance and cooperation. This paper first considers various types of UAVs and then focuses on their motion planning and control.

## II. TYPES OF AERIAL VEHICLES

Aerial vehicles can generally be classified based on their weight relative to air. Under heavier than air we have Non-motorized Glider and motorized planes and rotor-craft. The lighter than air aerial vehicles are balloons and blimp. These are as shown in Figure1 [3].

Under the heavier than air-motorized class, we have the plane type, referring to ordinary fixed wing aircrafts, the bird-like Micro Aerial vehicle (MAV) also known as the flapping wing type and rotor-crafts for Vertical Take-Off and Landing (VTOL) vehicles such as helicopters.

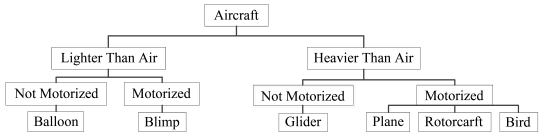


Fig. 1. Aircraft classification

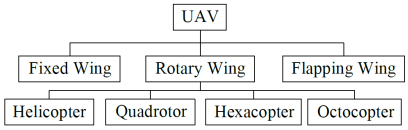


Fig. 2. UAVs classification

### A. Unmanned Aerospace Systems

This is a system comprising of a set of sub-systems including the unmanned air vehicle (UAV), the control station and communication sub-systems. In this system, the pilot's interfaces and aircraft controls are replaced by an intelligent control system [1].

### B. UAV types

UAVs themselves could be classified based on their configurations to have fixed wing models, the flapping wing models, and the rotary wing models (rotor-crafts) as shown in Figure2 [3]. Fixed-wing UAVs find applications in both military and civilian works especially for long-distance missions and research. Flapping-wing UAVs are relatively new in research and do fly like insects and birds and can perform vertical take-off and landing. Rotary wings UAVs, are normally used on missions that require hovering flight due to their high maneuverability, small size, and easy control. Quadrotors have been widely used in security surveillance and research among other applications [4].

## III. UAV FLIGHT PRINCIPLES

The principles applied in flight of UAVs involve dynamics of rigid body motion and aerodynamic forces and moments. The forces are derived from Newton's laws and the moments from the axis system.

N.M Gachoki, Department of Electrical and Electronic Engineering, Kirinyaga University (phone: +2540728073139; e-mail: ngachoki@kyu.ac.ke).
A. M.Muhia, Department of Electrical Engineering, JKUAT
M.N Kiio, Department of Electrical Engineering, JKUAT

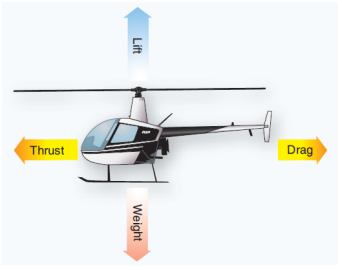


Fig. 3. Four forces acting on a rotor-craft

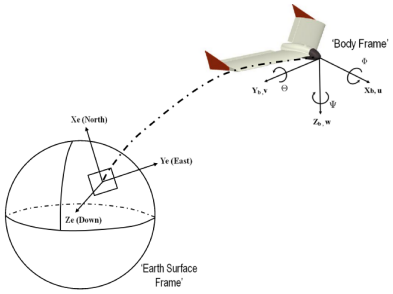


Fig. 4. Earth surface and body reference frames

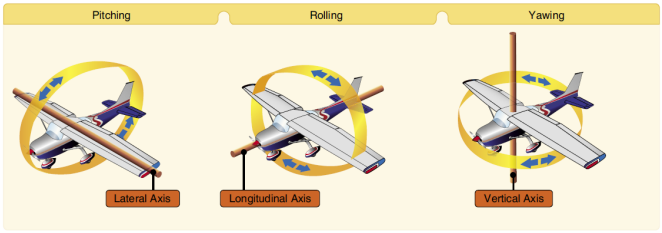


Fig. 5. pitch, roll, and yaw motion of the aircraft along the lateral, longitudinal, and vertical axes [6]

### A. Forces

Four forces act upon an aircraft in relation to straight-and-level, unaccelerated flight. These forces are thrust, lift, weight, and drag [5].Understanding how these forces work and knowing how to control them with the use of power and flight controls are essential to flight. They are defined as follows [6].
**Thrust**. This is the forward force produced by the rotors. It opposes the force of drag and acts parallel to the longitudinal axis.
**Drag**. This is a rearward, retarding force caused by disruption of airflow by the wing, rotor, fuselage, and other protruding objects. It opposes thrust and acts rearward parallel to the relative wind.
**Weight.**The weight force represents the combined load of the aircraft itself, fuel and baggage. It pulls the aircraft downward because of the force of gravity and opposes lift. Weight acts vertically downward throughthe aircraft‘s center of gravity (CoG).
**Lift.** this is the force opposing the downward force of weight. It is produced by the dynamic effect of the air acting on the airfoil, and acts perpendicular to the flightpath through the center of lift. These Forces are illustrated in Figure 3.

### B. Axis System

There are many coordinate systems for representation of UAV motion. Rotation of a rigid body in space can be parameterized using several methods like Euler angles, Quaternions and Tait-Bryan angles. The earth flames are generally described using North-East-Down coordinate system (NED) shown in figure 4 which is comprised of three vectors together forming a right hand orthogonal system. **N** represents the position along the northern axis (Xe), **E** represents position along the east axis (Ye) and **D** represent position along the local gravity vector (Ze). The body axis system is also comprised of three orthogonal vectors. The origin of the body axis frame is located at the CG. Xb points forward towards aircraft's head, Yb points to the right side of the vehicle and Zb points downward [7]. In aerospace engineering the axes are directed as for a craft moving in the positive x direction, with the right side corresponding to the positive y direction, and the vertical underside corresponding to the positive z direction. These three angles are individually called roll, pitch and yaw [8]. Considering a right-hand oriented coordinate system, the three single rotationsare described separately by:

- R(x,$\phi$ ), rotation around x-axis (roll).
- R(y,$\psi$ ), rotation around y-axis(pitch).
- R(z,$\theta$ ), rotation around z-axis(yaw).

They are represented by equations 1:

$$R(x,\phi) = \begin{bmatrix} 1 & 0 & 0 \\ 0 & cos\phi & -sin\phi \\ 0 & sin\phi & cos\phi \end{bmatrix} \tag{1a}$$

$$R(y,\theta) = \begin{bmatrix} cos\theta & 0 & sin\theta \\ 0 & 1 & 0 \\ -sin\theta & 0 & cos\theta \end{bmatrix} \tag{1b}$$

$$R(z,\psi) = \begin{bmatrix} cos\psi & -sin\psi & 0 \\ sin\psi & cos\psi & 0 \\ 0 & 0 & 1 \end{bmatrix} \tag{1c}$$

Equation .1a represents the roll moment while 2.1b is for the pitch and 2.1c is for the yaw. These motions of the aircraft are illustrated in figure 5 The complete rotation matrix is the product of the previous three successive rotations as shown in equation 2.

$$R(\phi,\theta,\psi) = R(x'\psi)R(y,\theta)R(z,\psi) \tag{2}$$

Computing equation 2 results in equation 3.

$$R = \begin{bmatrix} cos\psi cos\theta & cos\psi sin\theta sin\phi - sin\psi cos\phi & cos\psi sin\theta cos\phi + sin\psi si \\ sin\psi cos\theta & sin\psi sin\theta sin\phi + cos\psi cos\phi & sin\psi sin\theta cos\phi - sin\phi co \\ -sin\theta & cos\theta sin\phi & cos\theta cos\phi \end{bmatrix} \tag{3}$$

From the equations, we see that the altitude and orientation of the UAV caan be varied to some extent during flight. in flapping wing type, this is varied by the speed of flaps, while in rotary wing type by variation of speed of one rotor.

## IV. Motion Planning

Motion planning refers to motions of a robot in a 2D or 3D world that contains obstacles. The robot could model an actual robot, or any other collection of moving bodies, such as humans or flexible molecules. A motion plan involves determining what motions are appropriate for the robot so that it reaches a goal state without colliding into obstacles. Planning involves calculation of mechanism to compose and sequence a set of primitives in a way that takes a body from an initial state to a final state while respecting a set of constraints [9]. Path planning in three dimensional (3D) generally involves two steps: First step is environment perception and modeling then path planning algorithm is employed to find the best path according to the cost function. The algorithms convert high-level specifications of tasks from humans into low-level descriptions of how to move [10]. The quadrotor path planning problem is a motion planning problem to compute a path to be followed by quadrotor toward a moving target. [11].

### A. Sampling Based Algorithms

These methods require pre-known information of the workspace, that is, a mathematic representation to describe the workspace. It usually samples the environment as a set of nodes, or cells. Then map the environment or just search randomly to achieve a feasible path. Such a method was applied by [11] to design a collision-free waypoint path for a UAV in urban terrain. The elements of sampling based algorithms include Rapidly-exploring Random Trees (RRT), Waypoint RRT(WRRT) and dynamic RRT (DDRRT). Some researchers such as [12] have shown weaknesses in application of RRT to means to multiple robots hence proposed a graph structure called Rapidly-exploring Random Graphs (RRG) to add quality to RRT.

### B. Node Based Optimal Algorithms

They explore through the decomposed graph. Analyzing from the point of the search mechanism, node based optimal algorithms share the same property that they explore among a set of nodes (cell) in the map, where information sensing and processing procedures are already executed.

### C. Mathematic Model Based Algorithms

These methods model the environment (kinematic constraints) as well as the system (dynamic) and then bound the cost function with all the kinematic and dynamic constraints bounds which are inequalities or equations to achieve an optimal solution. The elements of mathematic model based algorithms include, flatness based method, Mixed-Integer Linear Programming (MILP) Binary Linear Programming (BLP)

### D. Bioinspired Algorithms

Bioinspired algorithms originate from mimicking biological behavior to solve problems. They leave out the process of constructing complex environment models to search a near optimal path based on stochastic approaches; it overcomes the weakness where general mathematic model based algorithms often fail (or drop into local minimum) in solving NP-hard problem with large number of variables and nonlinear objective functions. They are divided into Evolutionary Algorithm (EA) and Neural Network (NN)

### E. Multifusion Based Algorithms

Multifusion based algorithms manage with problems where usually a single approach proposed cannot work to find an optimal path individually. When faced with unknown environments, with whether dynamic threat or static threat, not all traditional single planning approaches can fulfill the task of obtaining cost minimum or fast convergence or computational efficiency. A special requirement in this research however, since the target is moving, planning a path to the current location is not always the best Instead of trying to plan a path to the current location, the algorithm can plan a path to move toward a future predicted target location. With a model for how the target moves, it is possible to predict a future distribution of target locations a method of using a target motion model to make UAV motion decisions [13]. This is a method of planning a path in a directed graph toward a distribution of final states instead of a single goal state.

## V. Case studies

This section gives an outline of UAV research projects at selected Universities.

### A. Pennsylvania State University UAV

They operate a UAV research center which designs and tests research UAVs. They design three subsystems namely, software, electromechanical and electrical. The Software subsystem deals with design and implementation of the autopilot and the associated algorithms for controls. The Aeromechanics subsystem designs and builds the airframe while the electrical subsystem designs and builds RF communication systems, power budget control. The overall tasks include autonomous flight (takeoff, navigation, landing), target recognition and localization [14].

Out of this several research has been published including [15]–[18]. In [15], control methods were presented for an autonomous quadrotor using visual feedback as the primary sensor. Two methods of control were studied one using a series of mode-based, feedback linearizing controllers, and the other using a backstepping-like control law. The research advanced and later [18] developed a small semi-autonomous rotary UAV described below. They used a PIC 8-bit microcontroller to obtain data from sensors and perform control operations.The main advantages of the PIC micro-controller is that its hardware has simple interface of sensors and motors by use of analog to digital converters (ADC), interrupts, timers, and capture/compare/pulse width modulation (CCP) channels. In addition,the micro-controller requires low current (about 12 mA)

This Micro-controller has successfully been applied in other quadrotor designs such as [19]–[22]. In [19], it was interfaced

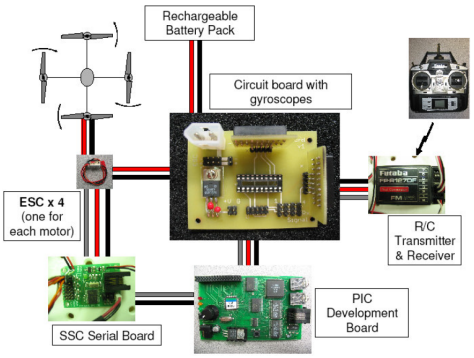


Fig. 6. Hardware connections [18]

with Inertia Measurement Unit (IMU) and Motor Driver Circuit (MDC) both which are key devices in UAV control.The micro-controller is programed using CCS C compiler and Embedded C Language Development Kit.
the small UAV has two MEMS (Micro-Electro-Mechanical Systems) sensors, a gyroscope and an accelerometer, interfaced with the PIC micro-controller. A single chip rate gyro evaluation board used to measure angular velocity [18]. The system was powered by a combination of batteries. The electric motors, and propellers was chosen to meet the desired requirements for flight length, aircraft weight, and thrust production. A flight duration of 15 minutes, a time considered adequate to perform a worthwhile mission.
The overall design is as shown in figure 6

### *B. Brigham Young University Quad-rotor*

The Robotic Vision Lab at Brigham Young University has developed an indoor quad-rotor platform that utilizes a compact FPGA board called Helios. Helios allows researchers to perform on-board vision processing and feature tracking without the aid of a ground station or wireless transmission [23]. The principle of operation is described in [24], [25] and the project was aimed at aimed at stabilization and control using vision sensors.
It uses a reconfigurable board called Helios developed by [26] for On-Board Vision Processing in small UAVs. The board has attractive features for UAV functions such as high speed memory, ability to integrate software execution with custom hardware execution and low power consumption. It also has serial and USB connectionslots of processing power, and using it on the quad-rotor avoids transmission issues such as noise and time delays, allowing it to obtain higher quality images in real time and maintaining controlled flight without a wireless tether. The resulting on-board vision system allows autonomous control algorithms such as drift control and target tracking to be implemented directly on the quad-rotor itself. The entire platform is as shown in figure 7

### *C. Other Universities Quad-rotor Research*

Lot's of other universities are also doing reserch in quad-rotors, for example. The STARMAC project at Stanford University focused on multi-agent control using quad-rotors.

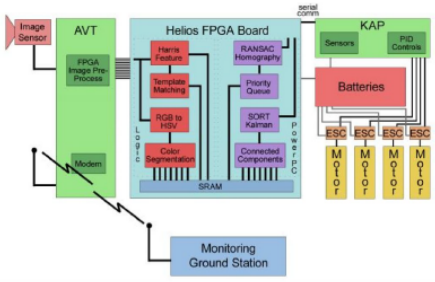


Fig. 7. Communication of the entire platform [27]

Starmac I was a DraganFlyer IV from RC Toys. This platform yielded 1kg of thrust and could maintain hover for up to 10 minutes at full throttle. It used a 3-axis gyro for attitude, sonar for altitude and a GPS receiver for position information. Stanford researchers then developed the Starmac II based on the X-4 yer platform to obtain 4kg of thrust and a much longer ight time. Starmac II used GPS units for location information outdoors and sonar for altitude. when flying indoors an overhead web cam was used for positioning. Collaboration between quad-rotors and ground-station control is done with WiFi [28].

## VI. Conclusion

From this paper we see applications of quad-rotor UAV systems and their motion is planning.The principles of their operations including flight path planning and finally it demonstrates by use of case studies how UAVs have been used. The case studies expound on the practical experiences of unmanned aerial vehicles in civilian applications. From the case studies, it is possible to learn and develop research platforms in our local institutions for advancing research in UAVs.

## References

[1] R. Austin, *Unmanned Aircraft Systems: UAVS Design, Development and Deployment*. Wiley, 2010.
[2] S. Scherer and S. Singh, "Multiple-objective motion planning for unmanned aerial vehicles," in *Intelligent Robots and Systems (IROS), 2011 IEEE/RSJ International Conference on*. IEEE, 2011, pp. 2207–2214.
[3] S. Norouzi Ghazbi, Y. Aghli, M. Alimohammadi, and A. Akbari, "Quadrotors unmanned aerial vehicles: A review." *International Journal on Smart Sensing & Intelligent Systems*, vol. 9, no. 1, 2016.
[4] N. Muchiri and S. Kimathi, "A review of applications and potential applications of uav," in *2016 Annual Conference on Sustainable Research and Innovation(SRI)*, May 2016, pp. 280–283.
[5] F. A. A. F. Staff, U. Transportation, and F. Service, *Pilots Handbook of Aeronautical Knowledge FAA-H-8083-25a*. Books Express Publishing, 2012.
[6] F. A. Administration, *Helicopter Flying Handbook*. Skyhorse Publishing Company, Incorporated, 2013.
[7] S. Bagheri, "Modeling, simulation and control system design for civil unmanned aerial vehicle (uav)," 2014.
[8] S. Bouabdallah, *Design and Control of Quadrotors with Application to Autonomous Flying*. EPFL, 2007.
[9] L. Yang, J. Qi, D. Song, J. Xiao, J. Han, and Y. Xia, "Survey of robot 3d path planning algorithms," *Journal of Control Science and Engineering*, vol. 2016, p. 5, 2016.
[10] S. LaValle, *Planning Algorithms*. Cambridge University Press, 2006. [Online]. Available: https://books.google.co.ke/books?id=-PwLBAAAQBAJ
[11] A. B. Curtis, "Path planning for unmanned air and ground vehicles in urban environments," Ph.D. dissertation, Brigham Young University, 2008.

[12] R. Kala, "Rapidly exploring random graphs: motion planning of multiple mobile robots," *Advanced Robotics*, vol. 27, no. 14, pp. 1113–1122, 2013.
[13] S. M. LaValle, "Rapidly-exploring random trees: A new tool for path planning," 1998.
[14] P. S. University. Penn state uas. [Online]. Available: http://uas.engr.psu.edu/projects.php
[15] E. Altug, J. P. Ostrowski, and R. Mahony, "Control of a quadrotor helicopter using visual feedback," in *Robotics and Automation, 2002. Proceedings. ICRA'02. IEEE International Conference on*, vol. 1. IEEE, 2002, pp. 72–77.
[16] M. Tarhan and E. Altuğ, "Ekf based attitude estimation and stabilization of a quadrotor uav using vanishing points in catadioptric images," *Journal of Intelligent & Robotic Systems*, vol. 62, no. 3, pp. 587–607, 2011.
[17] B. Erginer and E. Altuğ, "Design and implementation of a hybrid fuzzy logic controller for a quadrotor vtol vehicle," *International Journal of Control, Automation and Systems*, vol. 10, no. 1, pp. 61–70, 2012.
[18] S. Hanford, L. Long, and J. Horn, "A small semi-autonomous rotary-wing unmanned air vehicle (uav)," in *Infotech@ Aerospace*, 2005, p. 7077.
[19] C. Patel, S. Rao, and B. Driessen, "A testbed for mini quadrotor unmanned aerial vehicle with protective shroud," in *2nd Annual Symposium on Graduate Research and Scholarly Projects*, 2006.
[20] "Faculty of engineering of the university of porto development of unmanned aerial four-rotor vehicle."
[21] S. A. Raza, "Design and control of a quadrotor unmanned aerial vehicle," Ph.D. dissertation, University of Ottawa (Canada), 2010.
[22] J. Horton, "Low cost quad rotor design and implementation," 2012.
[23] S. G. Fowers, D.-J. Lee, B. J. Tippetts, K. D. Lillywhite, A. W. Dennis, and J. K. Archibald, "Vision aided stabilization and the development of a quad-rotor micro uav," in *Computational Intelligence in Robotics and Automation, 2007. CIRA 2007. International Symposium on*. Ieee, 2007, pp. 143–148.
[24] R. Beard, "Quadrotor dynamics and control rev 0.1," 2008.
[25] B. J. Tippetts, "Real-time implementation of vision algorithm for control, stabilization, and target tracking for a hovering micro-uav," 2008.
[26] W. S. Fife and J. K. Archibald, "Reconfigurable on-board vision processing for small autonomous vehicles," *EURASIP Journal on Embedded Systems*, vol. 2007, no. 1, p. 080141, 2006.
[27] S. G. Fowers, "Stabilization and control of a quad-rotor micro-uav using vision sensors," 2008.
[28] G. Hoffmann, D. G. Rajnarayan, S. L. Waslander, D. Dostal, J. S. Jang, and C. J. Tomlin, "The stanford testbed of autonomous rotorcraft for multi agent control (starmac)," in *Digital Avionics Systems Conference, 2004. DASC 04. The 23rd*, vol. 2. IEEE, 2004, pp. 12–E.

# A Review of Applications of 3D printing technology and potential applications in the plastic thermoforming industry

[a]Nkosilathi Z Nkomo, [b]Nqobizitha R Sibanda, [c]Jephias Gwamuri, [d]Mwasiagi J. Igadwa

***Abstract*** **-** In this review article applications and potential uses of 3D printing in the plastic thermoforming industry are reviewed. 3D printing also known as "Additive manufacturing" has revolutionized the modern manufacturing process and engineering design process. Thermoforming is widely used in plastic manufacturing industries to produce a range of polymer products such products are normally used in the packaging industry. Thermoforming moulds are mostly produced using conventional mould building technologies and are made of steel. These mould are robust but only suitable for mass production and take some time to fabricate. 3D printers are mostly used during the prototyping stage of design. They can be used for proof of concept and also are useful for customer presentations to allow the customer to see and feel exactly what their product will look like. 3D printing can find use in thermoforming industry in creating moulds to thermoform parts this can produce the moulds quickly and economically and prototyping of packaging machine parts as well as fabricating of the packaging material. 3D printing allows ease of production of personalised packaging. With 3D printing the structural design of the package could be customised on request. As more sustainable bioplastic filaments are innovated, the adoption of 3D printing in packaging manufacturing may help save the environment. 3D printing works well with Acrylonitrile Butadiene Styrene (ABS) and polypropylene. This paper looks at the different applications of 3D printing in the plastics thermoforming industry and looks at the viability of the use of this technology as well as the advantages in relation to conventional production technologies and materials.

***Keywords*** - 3D printing, packaging, plastic thermoforming, prototyping

## I. INTRODUCTION

Three dimensional (3D) printing also known as additive manufacturing is a process of making solid objects from a digital file. This creation of the 3D printed object is accomplished by an additive process [1].

[a]Nkosilathi Zinti Nkomo, Department of Fibre and Polymer Materials Engineering, NUST, (e-mail zintinkomo@gmail.com)
[b]Nqobizitha R Sibanda, Department of Fibre and Polymer Materials Engineering, NUST, (e-mail: nqobizitharose.sibanda@gmail.com )
[c]Jephias Gwamuri, Department of Physics. NUST, (e-mail: jephias.gwamuri@nust.ac.zw)
[d]Josphat Mwasiagi, Department of Manufacturing, Industrial & Textile Engineering, Moi University (e-mail: igadwa@gmail.com)

3D printing employs an additive manufacturing process whereby products are built on a layer by layer basis through a series of cross sectional slices [2]. 3D printing enables the low-cost, bottom-up fabrication of objects with complex geometries that are difficult to produce by traditional fabrication methods [3]. The emergence of 3D printing shortens the cycle of design and development for thermoformed products. The application of 3D printing increases the efficiency and promotes product development [4]. Since 1984, when the first 3D printer was designed and realised by Charles W.Hull from 3D Systems Corp [4].

## II. THERMOFORMING

Thermoforming is a reshaping process in which a flat thermoplastic sheet is heated and shaped into moulded parts. The extruded sheet is heated to softening temperature clamped around its edge and formed to the required shape by mechanical stretching and applying pressure against a mould with the desired shape [5]. The softening temperature depends on the thermoplastic material properties.

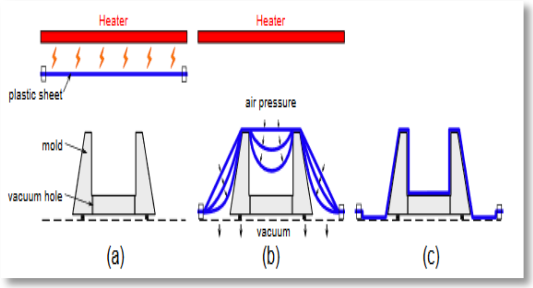


Fig 1.0 Typical vacuum thermoforming process. a) A plastic sheet is heated until soft enough for forming b) then it is loaded to the mould; upon contact with the mould it begins to deform. The air below is vacuumed, the atmospheric pressure forces the plastic sheet to conform to the mould shape c) after cooling down, the plastic is hardened into the new shape [6].

Thermoforming is mainly used in the packaging industry. However it is not limited to small products; hot tubs and refrigerator door panels are two examples of relatively large thermoformed parts [7]. In the thermoforming industry it is necessary to use chillers for cooling the chains transporting the plastic sheet.

## I. CONVECTIONAL MOULD DESIGN FOR THERMOFORMING

The typical thermoforming mould design and manufacturing process used by most manufacturing companies are done manually and rely heavily on craftsmanship. A thermoforming master model is formed first the geometry of the model is often refined region by region since it is difficult to adjust the entire shape of the model manually at one time. From this master model if the customer is satisfied with it then

a metal mould can be made for mass production. The making of the mould has drawbacks in that it relies very much on the skill of the mould maker and the modelling and finishing


Fig 2.0 Vacuum thermoforming machine

processes are laborious and time consuming. This makes this process significantly expensive [8].

The mould used needs to have four basic functional features which are packaging, draw ratio, demoulding and strengthening. The basic function of the thermoforming mould is to hold secure and protect a packed part.

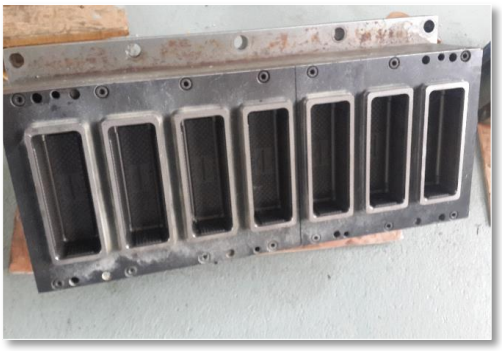

Fig 3.0 Plastic thermoforming mould for biscuits skillets

The drawing process causes an increase of surface area but decrease of sheet thickness [9]. Thermoforming features with low draw ratios are easier to form. This explains why thermoforming mould makes chamfer sharp edges, add fillets to acute corners and fill up deep depressions to avoid the formation of high draw ratio features. The mould used must also allow easy demoulding. This is done by allowing the side walls of the mould to tapper outwards. Fig 4.0 shows the main features of a thermoforming mould.

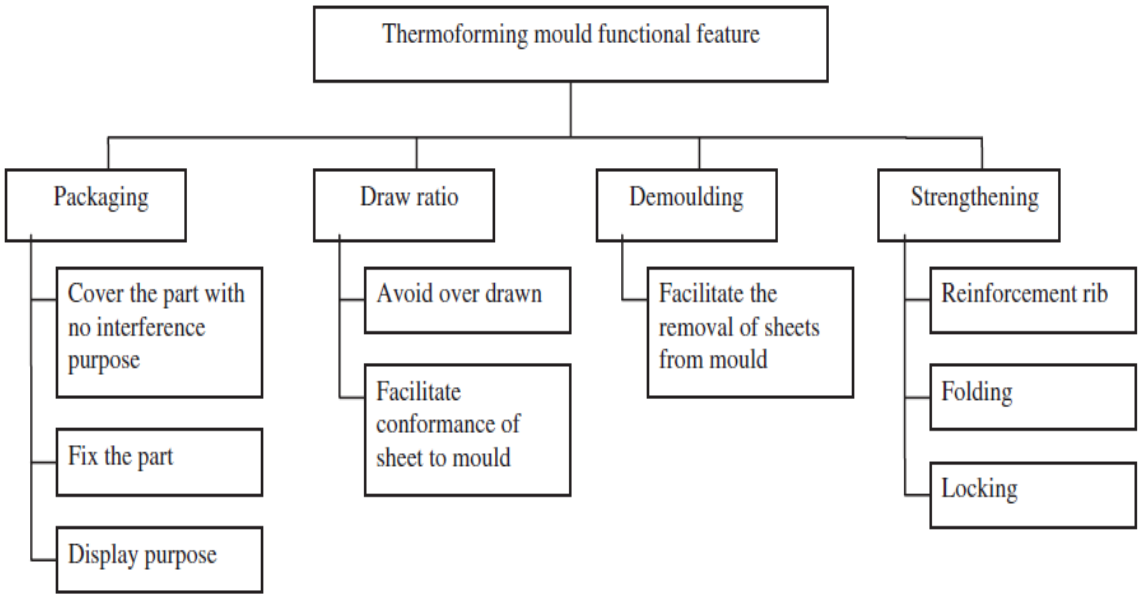


Fig 4.0 Classification of functional feature of thermoforming mould [8]

## II. 3-DIMENSIONAL (3D) PRINTING PROCESS

The 3D printing process consists of two stages:

- The direct transfer from software data to printed structures,
- Repeatedly positioning the print head in all three directions in space in order to print layer by layer [10].

There are three main types of 3D printing which include stereo lithography (SLA), selective laser sintering (SLS) or fused deposition modelling (FDM). The principle of fused deposition modelling (FDM) works by melting a thermoplastic filament in an extruder nozzle and deposition of the thermoplastic in layers on a bed.

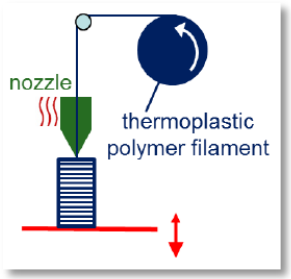


Fig 5.0 Schematic depiction of fused deposition modelling (FDM) technology [11]

Since 2009, the number of low cost 3D printers from both major and start-up companies has greatly increased with many now using the now off-patent FDM technology [12]. An example of such a printer is the Athena 3D printer shown in Fig 6.0 which has been used to prototype some basic packaging products in this study.

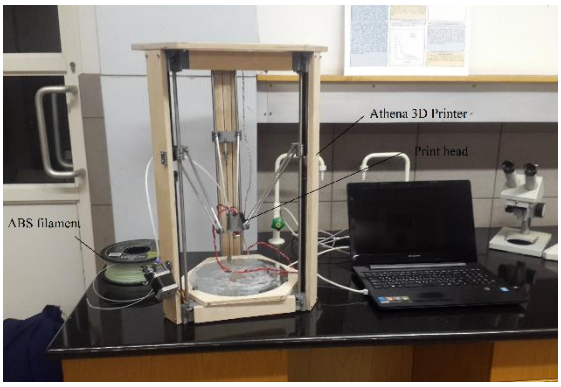


Fig 6.0 Athena 3D printer

The process of 3D printing involves the following key 4 steps:

1. **CAD Model creation:** The objected to be printed is modelled using a Computer-Aided Design (CAD) software package. The designer can use a pre-existing CAD file from various open sources that are available online.
2. **Conversion to STL Format:** the various CAD packages use a number of different algorithms to represent solid objects. To establish consistency, the STL stereo lithography format has been adopted as the standard of the rapid prototyping industry. The second step, therefore is to convert the CAD file into STL, format.
3. **Layer by Layer Construction:** using one of several techniques the 3D printer builds layer by layer the object.
4. **Clean and Finish:** the final step is post processing this involves removing the printed object from the print bed and if necessary carrying out curing on the object. Some objects require minor cleaning and surface treatment.

## III. RAW MATERIALS USED IN 3D PRINTING AND THERMOFORMING INDUSTRY

Similar thermoplastic raw materials are used in the plastic thermoforming industry and in 3D printing. Polylactic Acid (PLA) is one type of thermoplastic filament used which is a biodegradable thermoplastic aliphatic polyester derived from renewable resources such as corn starch, tapioca roots, chips or sugarcane [13]. Fig 7 shows the skeletal formula for PLA.

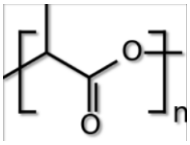


Fig 7.0 Skeletal formula for PLA

Another commonly used filament is ABS which is also commonly in the food packaging industry. ABS is used to make skillets for packaging biscuits as well as plastic cups.

Fig 8.0 Skillets and cups used in food industry

## IV. USE OF 3D PRINTING IN THERMOFORMING INDUSTRY

A major advantage of 3D printing is a firm's ability to quickly and cost effectively supply low demand parts without the risk of carrying unsold finished goods inventory [2]. This can be done without the need for creation of extrusion process to produce the required plastic sheet with the required density and specifications.

Use of 3D printing can create personalised packaging. With 3D printing the structural design could be customised on request without a need for changing the mould or creating another mould.

The packaging of a product can be just as important as the product itself when it comes to accumulating sales this is one of the reasons why prototyping is so important. It helps to create a prototype to show customers as well as to test the product for suitability for use before creating an expensive mould for the product.

Traditional production methods are subtractive production methods which result in huge material losses, which 3D printing is an additive production method [14]. However when using 3D printing technology, only the amount of raw material necessary is used in the fabrication of the intended product. This result in a lesser carbon footprint and has a great positive impact on the environment [15]. Less recycling is needed with 3D printing as it is more exact in the formation of the product.

For lower production volumes, 3D printing can reduce the time and expenses associated with conventional machining processes. It is possible to produce accurate moulds with an automated, unattended process and eliminate the need for setup and operating of CNC machines.

**Advantages of 3D printing in comparison to other technologies include:**

- No need for costly tools, moulds, or punches
- No scrap milling or sanding requirements
- Automated manufacturing
- Use of readily available supplies
- Ability to recycle waste material
- Minimal inventory risk as there is no unsold finished goods inventory
- Improved working capital management as goods are paid before being manufactured
- Ability to easily share designs and outsource manufacturing
- Speed and ease of designing and modifying products

Fused Deposition modelling is the most common 3D technology employed for creating 3D printed moulds for vacuum forming. It allows printing in various fill densities and results in a uniform vacuum to be drawn throughout the tool. In addition FDM 3D printing machines are capable of printing moulds in a variety of durable, heat resistant plastic that prolong the life of the mould [16].

An example of a 3D printed mould is such as the one used in the CREOS encasing which is a PETG plastic shell that was vacuum formed using a 3D printed FDM tool. Fig 9.0 shows the mould that was used. CREOS is a 3D printed action figure with detachable arms and legs. The hat is created in Nylon 12 on an SLS machine and dyed yellow. The callipers were printed in real ABS thermoplastics.

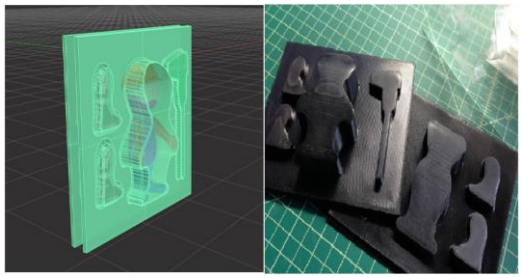

Fig 9.0 Mould used for the encasing of the CREOS action figure [16]


Fig 10.0 CREOS 3D printed action figure in it encasing [16]

## V. CONCLUSION

The use of 3D printing technology plays a role in the plastic thermoforming industry in producing the products as it uses similar thermoplastic materials such as ABS and HIPE which are used in the traditional plastic thermoforming industry. 3D printing has advantage of ease of customisation, minimum wastage during the production of the products as it works by additional manufacturing and only the required material is deposited. However this technology is still limited due to its slow speed compared with vacuum thermoforming. 3D printing is also having growing use in the fabrication of tool used in thermoforming such as the moulds. Fast and efficient mould generation can be done using 3D printing. This technology is growing and in the years ahead it is expected to grow in its capacity usage.

## REFERENCES

[1] S. Mahamood, M. A. Khader and H. Ali, "Applications of 3-D printing in orthodontics: A Review," *International Journal of Scientific Study*, vol. 3, no. 11, p. 267, 2016.

[2] B. Barry and F. G. Zarb, "3-D printing: The new industrial revolution," *Elsevier*, pp. 155-162, 2012.

[3] Y. Jun, Z. Pei and G. M. L. Jennifer, "3D printable antimicrobial composite resins," *Advanced functional materials*, vol. 25, pp. 6756-6767, 2015.

[4] Z. Feixiang, Z. Liyong and K. Xia, "Study of impact of 3D printing technology and development on creative industry," *Journal of social science studies*, vol. 3, no. 2, pp. 57-61, 2016.

[5] M. Moustafa, K. Dotchev, W. Simon, B. Nick and C. James, "Investigating of thermoforming tool design and pocket quality," *Journal of thermal engineering*, vol. 7, no. 2, pp. 670-676, February 2015.

[6] Z. Yizhong and Z. Kun, "Cloring 3D printed surfaces by thermoforming," *IEEE transactions on visualization & computer*, pp. 1-12, 2015.

[7] Stratasys, 2017. [Online]. Available: http://www.stratasys.com/solutions/additive-manufacturing/tooling/thermoforming. [Accessed 13 February 2017].

[8] K. W. Chan and K. W. Tam, "Thermoforming mould design using a reverse engineering approach," *Robots and computer integrated manufacturing*, vol. 23, pp. 305-314, 2007.

[9] G. Gruenwald, "Thermoforming: a plastics processing guide," Lancaster: Technomic ub Co Inc, 1998, pp. 35-60.

[10] S. l. Vanapalli and A. Ramya, "3D printing technologies in various applications," *International Journal of Mechanical Engineering and Technology*, vol. 7, no. 3, pp. 396-409, 2016.

[11] M.Korger, J. Bergschneider, M. Lutz, B. Mahltig, K. Finsterbusch and M. Rabe, "Possible application of 3D printing technology on textile substrates," in *48th Conference of the International Federation of Knitting Technologists (IFKT)*, 2016.

[12] T. Li, J. Aspler, A. Kingsland, L. M. Cormier and Z. Xuejun, "3D printing- a review of technogies, markets, and opportunities for the forest industry," *Journal of Science & Technology for forest products and processes*, vol. 5, no. 2, pp. 30-37, 2016.

[13] S. Vinod and G. Punit, "3D printing process using fused deposition modelling (FDM)," vol. 3, no. 3, 2016.

[14] R. Keskin and I. Gocek, "Production with 3D printers in textiles [review]," *Annals of the university of Oradea fascicle of textiles, leatherwork*, pp. 47-50, 2015.

[15] M. Boubekri and N. Boubekri, "Use of 3D printing echnology in architectural research," *Journal of Engineering and Architecture*, vol. 3, no. 2, pp. 105-113, 2015.

[16] C. Hartman, "Benefits of 3D printing vacuum form molds," *Fathom*, pp. 1-5, 2014.

# Performance prediction of Marine propeller using steady and unsteady flow approaches

OBWOGI Enock Omweri, AMISI Jared Ondieki and SHEN Hai-Long

***Abstract*—** MOST work presented on marine propeller performance prediction using Computational Fluid dynamics is based on suitability of grid density and turbulent models. Finer grids have shown better results as opposed to coarse grids. On the other hand, turbulent models have shown different strengths. In this paper, therefore, simulations are performed by computational fluid dynamics (CFD) code using both steady and unsteady flows. The main aim of this study is to investigate the propeller performance using the steady and unsteady flow state. To study the subject, 5.72 m diameter, right hand skewed propeller was selected. Open water characteristics were then determined for both techniques.

A validation study was carried out where CFD results were compared to extrapolated experimental data. Generally there was good agreement between the CFD results and experimental data. The numerical results demonstrate that the data calculated by unsteady flow approach for Thrust Coefficient and Torque Coefficient is more reliable than that obtained by steady flow approach. However, steady state approach provides better results for open water efficiency. The current study results will be of importance during propeller design and optimization.

*Keywords*— CFD; steady flow; unsteady flow; propeller performance; validation study.

## I. Introduction

PROPELLER open water characteristics are crucial in the early stages of ship design. The conventional way to determine propeller characteristics is by experimental tests carried out at model scale. To obtain corresponding full scale characteristics, extrapolations are carried out. There has been a huge progress in development of Reynolds-Averaged-Navier Stokes (RANS) solvers (for instance Tezdogan et al., demonstrated the application of full-scale unsteady RANS CFD simulations), resulting to higher accuracies and computational capabilities [1]. S. Hai-long et al., in their study on the scale effects, noted that the present CFD simulation technology and method are more sensitive to scale effect than model tests which had been carried out plenteous model scale effect researches [2]. To avoid these scale effects therefore, a full scale propeller model is used.

It is common knowledge that most flow fields in practical marine hydrodynamics are unsteady. Performing simulations for unsteady flows takes longer CPU time. Unsteady flows can therefore be solved as Steady Flows by time averaging the RANS and calculating; resistance in calm water, Steady drift or steady turning or Self-Propulsion with a body force propeller model. According to CD-Adapco, it is possible to apply a moving reference frame (MRF), to a region containing a moving part (propeller in this study) and solve the problem in steady state [3]. However, this approach gives a time-averaged behavior of the flow rather than time-accurate behavior. MRF generates a constant grid flux (calculated based on properties of reference frame rather than local motion of cells), in the appropriate conservation equations. This approach has been widely adopted for the rotation motion of the propeller, [2, 4, 5, 6]. On the other hand, if we want to take into consideration the periodic motion of the propeller, application of the transient Rigid Body Motion in STAR CCM+ could be a convenient way. Although this method is more time-consuming, it is expected to produce more accurate results than steady state approximations, such as in a moving reference frame (MRF), that use frozen-rotor. This method involves actual displacement of mesh vertices of a region during a transient analysis in real time where the simulation is then run using an implicit unsteady solver.

### *A. Propeller Particulars*

The basic geometry of the propeller under study was borrowed from S. Hai-long et al.; the particulars are as shown in Table I [2]. The open water characteristics of the model were obtained from SSSRI[1]. A model scale with $\lambda = 29.197$ was used in the towing tank test, after which full scale data was obtained by extrapolation using the 1978 International

TABLE I
PROPELLER PARTICULARS [2]

| Main Particulars | Symbol | Units | Design Propeller |
|---|---|---|---|
| Diameter | D | m | 5.72 |
| Number of blades | Z | - | 4 |
| Blade area ratio | Ae/Ao | - | 0.51 |
| Rotation | - | - | Right |

[1] Shanghai Shipping Services Research Institute

E. O. Obwogi, Department of Marine and Maritime Operations, JKUAT (corresponding author, phone: +254 (0) 725775365; e-mail: eobwogi@jkuat.ac.ke).

J. O. Amisi, Department of Marine and Maritime Operations, JKUAT (e-mail: jamisi@jkuat.ac.ke).

S. Hai-Long, Science and Technology on Underwater Vehicle Laboratory, Harbin Engineering University, Harbin City, PR China
(e-mail: shenhailong@hrbeu.edu.cn).

Towing tank Conference (ITTC) procedures. The extrapolated full scale data was used for data validation since the simulations are performed at full scale.

### *B. Computational Domain*

THE computational domain adopted in the RANS solver is composed of two cylindrical regions; a rotating region containing the propeller and a static region for the rest of the domain. Fig. 1 presents the main dimensions of the computational domain used in the present study. The propeller rotation motion was imposed on a rotating region around the propeller by means of rotating reference frame and rotating rigid body motion for steady and unsteady simulations respectively. The inlet boundary was treated as a velocity inlet, whereas a pressure outlet condition was adopted for the outlet boundary and a symmetry plane condition for the far field.

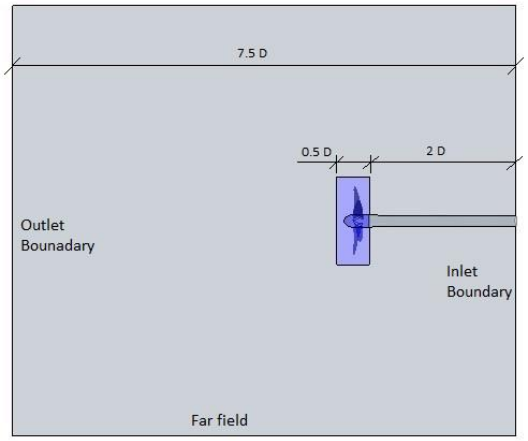


a) Side view

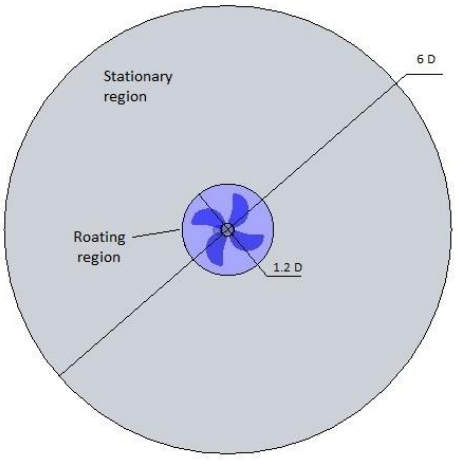


b) Front view

Fig. 1 Computational domain used for the RANS solver. In the figure, D represents the propeller diameter

### *D. Grid Generation*

STAR CCM+ provides an automatic meshing facility, where the Cartesian cut-cell method is applied. Trimmer meshing model was adopted for the generation of the volume mesh. This meshing scheme is not directly influenced by the quality of the starting surface and thus is more likely to generate a good quality mesh in most situations. Trimmed cell mesher employs OCTREE triangulation to produce a volume mesh. Squares containing the boundaries are subdivided recursively until desired resolution is obtained.

The computation mesh was progressively refined with finer mesh in the areas around the propeller and shaft. This was achieved by application of volumetric controls where isotropic refinement technique was adopted. The prism layer mesher was then used to help in resolving flow features near the surface and maintain the first cell height in the required values in terms of y+. To keep the wall y+ values outside the buffer layer, values between 1 and 10 were used. Volume mesh comprising of trimmed cells and prismatic cells were generated as shown in fig. 2. Four (4) prism layers were applied with prism layer thickness of 0.00145m. The total number of cells was 1919924 with 1603090 in the rotating region and 316834 cells in the static region.

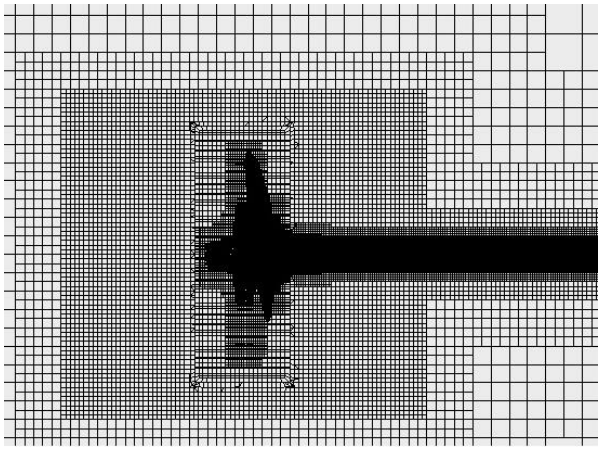

a) Side view

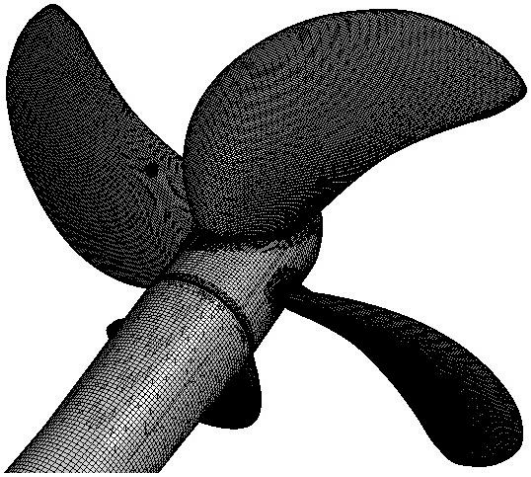

b) Perspective view

Fig. 2 Grid generated for the RANS solver

### *C. Governing Equations*

The present work is based on viscous methods for solving fluid flow motion. In this methods, numerical solution for Navier-Stokes Equations, NSE is applied to the entire computation domain. Equations (1) and (2) presents the

Reynolds-Averaged Navier-Stokes, RANS (obtained by Reynolds decomposition and taking time-average of the transport equations) and the continuity equations respectively [7].

$$\frac{DV}{Dt} = g - \frac{1}{\rho}\nabla p + \frac{\partial}{\partial x_j}\left[\nu\left(\frac{\partial u_i}{\partial x_j} + \frac{\partial u_j}{\partial x_i}\right)\right] \quad (1)$$

$$\nabla \cdot V = 0 \quad (2)$$

In these equations; i=1,2,3 , j=1,2,3 , $V$ is the instantaneous velocity components $u_1$, $u_2$ and $u_3$, p is the pressure, ρ is the density of the fluid, υ is the kinematic viscosity of the fluid and g is the vector acceleration of gravity and t is time. The operator D/Dt is the particle or substantive derivative defined by;

$$\frac{D}{Dt} = \frac{\partial}{\partial t} + (V \cdot \nabla) \quad (3)$$

*E. Numerical Method*

In the present work, commercial CFD code, STAR CCM+ was used to solve RANS equations. This code employs the finite volume method in solving the Navier-Stokes equations where Reynolds decomposition is applied and time-averaging is performed for the continuity and momentum equations. The main goal is to come up with a set of linear algebraic equations, having the total number of unknowns in each equation system corresponding to the number of cells in the grid. The linear equations obtained are then solved with an algebraic multigrid solver [3]. The algebraic multigrid methods (AMG) solve the discrete linear system iteratively. Ideally, obtaining suitable discrete equations on the coarse levels is not always straightforward, hence algebraic multigrid (AMG) algorithm is preferred to geometric multigrid algorithm. Multigrid techniques enable a basic iteration scheme to be greatly accelerated by using SIMPLE.

To obtain the Reynolds-Averaged Navier-Stokes (RANS) equations are obtained by decomposing, the Navier-Stokes equations for the instantaneous velocity and pressure fields into a mean value and a fluctuating component [8]. The averaging process may be thought of as time averaging for steady-state situations and ensemble averaging for repeatable transient situations.

*F. Turbulence model*

RANS solvers have shown great improvement in the recent past. Wei Qiu et al., for instance, used the RANS to compute a steady-state tip vortex flow generated by a marine propeller [9]. In the studies presented, the selection of a turbulence model has proven to greatly influence the accuracy of the numerical simulations. In the present work, the SST k-ω turbulence model was selected. This model has been widely used to study propeller open water characteristics. This choice is based on the findings from various studies carried out in relation to propeller open water performance prediction. Kawamura et al., used the two-layer RNG k-ε, standard k-ω and SST k-ω models on the commercial RANS code FLUENT to investigate the influence of the turbulence model on cavitating and non-cavitating propeller open-water characteristics. They observed that the discrepancy between calculated and measured torque coefficients was smallest for the standard k-ω model [10].

Li et al., also used FLUENT to study the influence of turbulence model on the prediction of model and full-scale propeller open water characteristics and investigate study the scale effects of conventional and highly skewed propellers. They found out that the propeller geometry had an influence turbulence model. The study showed that the SST k-ω model was able to produce the expected distribution of local skin friction at both scales for both propellers. On the other hand, the k- ε models erroneously produced skin friction in both propellers at full scale [11].

Sánchez-Caja et al., used RANS code FINFLO study the scale effects on performance coefficients for a CLT propeller with different endplate geometries. They used SST k-ω as a basic turbulence model for the study. They used a special procedure to generate the computational grids in order to minimize computational errors in the comparison to the other alternative geometries [12].

It should be noted that no one turbulence model can resolve all aspects of propeller flow characteristics. X. Wang and K. Walters, for example, found out that the standard SST k- ω turbulence model indicated excessive dissipation of the vortex core. This is despite the fact that the transition-sensitive turbulence model was able to resolve blade-surface stresses, flow separations, and tip-vortex origin. This was interpreted as improved propeller performance prediction accuracy, especially under high-load conditions [13].

*G. CFD model time step*

The application of the transient Rigid Body Motion in STAR CCM+ uses an implicit unsteady time solver. Sufficient temporal resolution is necessary to ensure proper unsteady simulation. Time step sizes Δt are equivalent to specific rotational displacement. In the present study, Δt used was equal to a $\Delta t = 1^o\omega^{-1}$ (time for one degree equivalent rotation). The time step was selected to reduce the computation time, however a study should be carried out to gain more insight on its influence on simulation accuracy by halving say twice over to get $\Delta t = 0.5^o\omega^{-1}$ and $\Delta t = 0.25^o\omega^{-1}$. Since the performance was examined at 1.867 rps, a time step of 0.0015 sec. (approximately (1/(1.867×360)) was used.

## II. Results and Discussion

Propeller open water simulations are performed to

determine; open water thrust coefficient, $K_T$ , open water torque coefficient, $K_Q$ and open water efficiency, $\eta_0$. These parameters are required in calculating the ship propulsive efficiency, $\eta_D$. These parameters are defined as;

$$K_T = \frac{T}{\rho n^2 D^4} \quad (4a)$$

$$K_Q = \frac{Q}{\rho n^2 D^5} \quad (4b)$$

$$\eta_o = \frac{K_T . J}{2\pi . K_Q} \quad (4c)$$

Where; n is the propeller rps, ρ is the water density, J is the advance coefficient and D is the propeller diameter.

The propeller performance was examined at a range of advance ratios, J =0.1, 0.3, 0.5, 0.6 and 0.7 while the propeller revolution was set to 1.867 rps. The simulations were performed for two scenarios; according to the moving reference frame for steady state case and transient rigid motion for unsteady state case.

*A. Convergence study*

The convergence for steady simulations were controlled by residuals and the values of torque coefficient, $K_Q$ and thrust coefficient $K_T$. The large oscillatations are oberved during the first iterations, after which the results become stable and converge to the final solution with small variations. Fig. 3 & fig. 4 show typical convergence history for steady simulation where J=0.1

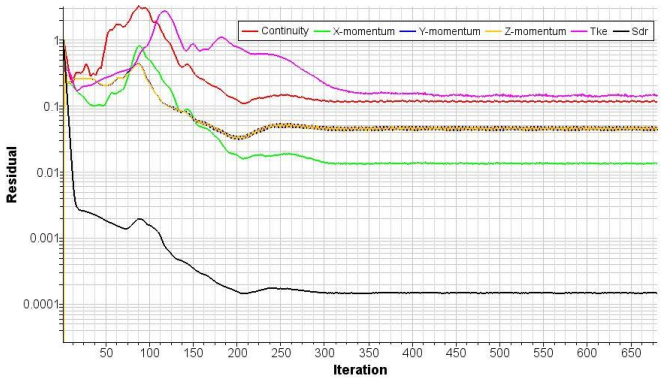


Fig. 3 Residuals for steady simulation for j=0.1

The convergence for unsteady simulations were controlled by the values of torque coefficient, $K_Q$ and thrust coefficient $K_T$. Strong oscillations were observed at the beginning of the simulation. These oscillations leveled out as the simulation progressed. Fig. 5 illustrates typical convergence history for J=0.1 unsteady simulation case. The $K_Q$ and $K_T$ values were obtained by averaging the 3rd propeller revolution data (between time steps of 1.0712 sec to 1.6069 sec).

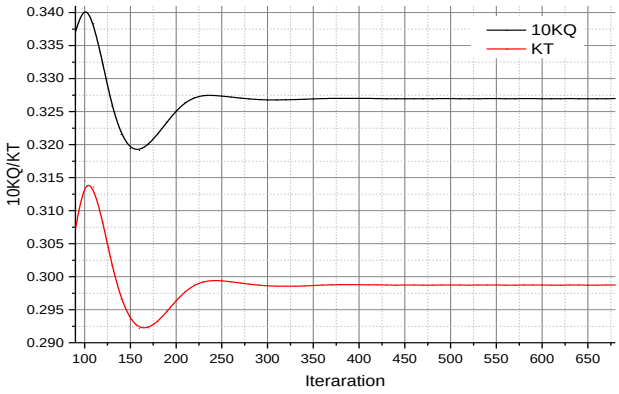


Fig. 4 Plot of 10KQ/KT for steady simulation plots for J=0.1

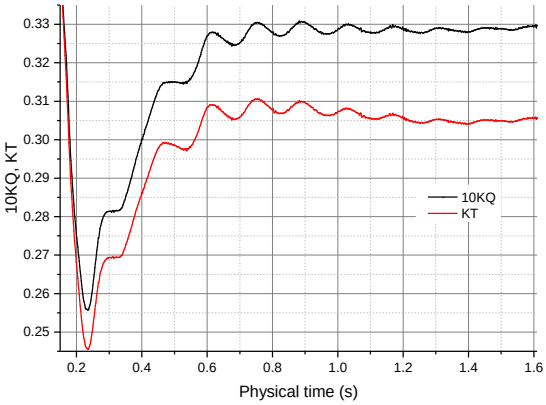


Fig. 5 Convergence study for unsteady simulation with J=0.1

*B. CFD Validation*

Experimental data obtained from SSSRI was used to validate the approach and simulation data obtained. Since the simulations are performed at full scale, the model scale data were extrapolated to full scale according to the ITTC 1978 procedures. The extrapolated data was then used for CFD data validation.

*C. Open water characteristics*

A full-scale propeller model is used for all simulations, to avoid scaling effects. The model was first run in steady state and then run in an unsteady state. The propeller thrust (T) was monitored as a drag force on the propeller blades by integrating pressure and viscous shear over the blades and hub surfaces while the propeller torque (Q) was monitored as a moment resulting from pressure and viscous shear force over the blades and hub surfaces. Equations 4(a, b, c) are used to calculate the thrust coefficient ($K_T$), Torque coefficient ($K_Q$) and open water efficiency respectively ($\eta_0$).

*1) Propeller Open Water Thrust Coefficient*

For the steady state case, $K_T$ was taken from the final value in the simulation. On the other hand, for unsteady case $K_T$ was obtained by averaging the values obtained during the third propeller revolution as illustrated in fig. 6.

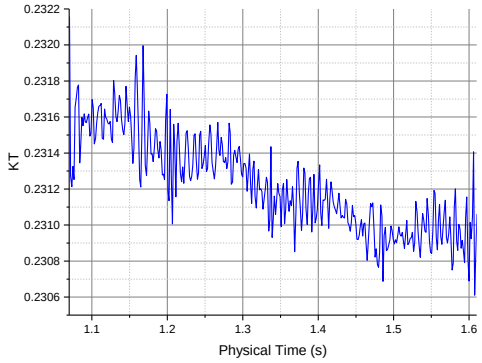


a) J = 0.1

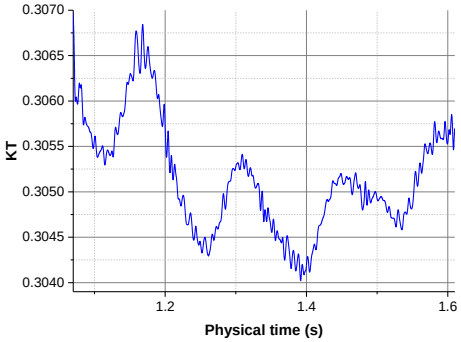


b) J = 0.3

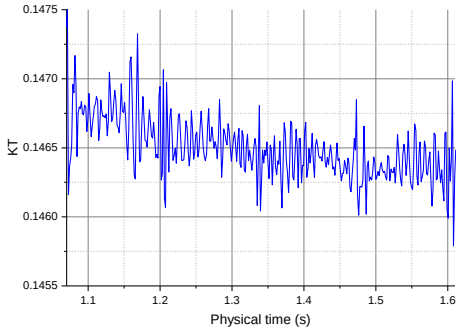


c) J = 0.5

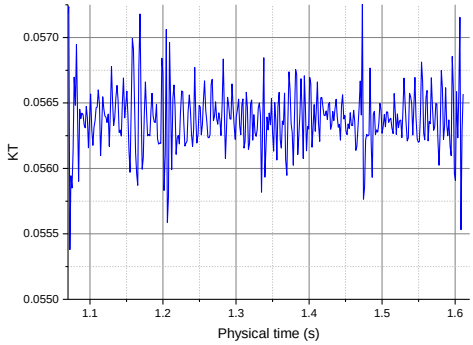


d) J = 0.7

Fig. 6 Plot of the calculated $K_T$ against the time step (s) for unsteady simulation

The thrust coefficient ($K_T$) of the propeller using the steady state and unsteady state approaches for the advance ratios, J =0.1, 0.3, 0.5, 0.6 and 0.7 are tabulated in Table II.

TABLE II
PROPELLER OPEN WATER THRUST COEFFICIENT ($K_T$)

| J | Experimental (extrapolated) | CFD – Steady | Error (%) | CFD – Unsteady | Error (%) |
|---|---|---|---|---|---|
| 0.1 | 0.3108 | 0.2987 | 3.8792 | 0.3052 | 1.8178 |
| 0.3 | 0.2366 | 0.2273 | 3.9513 | 0.2312 | 2.2704 |
| 0.5 | 0.1515 | 0.1449 | 4.3303 | 0.1465 | 3.2997 |
| 0.6 | 0.1051 | 0.1014 | 3.5609 | 0.1023 | 2.6716 |
| 0.7 | 0.0563 | 0.0562 | 0.2646 | 0.0564 | -0.1392 |

Experimental data was extrapolated from model scale to full scale by ITTC 1978 procedures. CFD simulations were the performed in full scale to minimize scale effects

From the presented data, both steady flow and unsteady ow approaches data are in good agreement with the experimental data. However, it is evident that unsteady approach predicts $K_T$ better than the steady approach as expected. The highest error was noted at J=0.5. This could be attributed to the inappropriate assumption that the flow around the propeller is fully turbulent whether in model scale or in full scale. According to Wang and Walters [10], the turbulent transition at the highest load (J=0.5) results to difficulties in numerical simulation.

*2) Propeller Open Water Torque Coefficient*

The torque coefficient ($K_Q$) of the propeller using the steady state and unsteady state approaches for the advance ratios, J =0.1, 0.3, 0.5, 0.6 and 0.7 are tabulated in Table III. From the presented data, both approaches are in good agreement with the experimental data. Similar to $K_T$ prediction, the unsteady approach predicts $K_Q$ better than the steady approach as expected. Unlike in the KT prediction, the error in both approaches increases from the smallest at J=0.1 to the highest error at J=0.7.

TABLE III
PROPELLER OPEN WATER TORQUE COEFFICIENT (10 $K_Q$)

| J | Experimental (extrapolated) | CFD – Steady | Error (%) | CFD – Unsteady | Error (%) |
|---|---|---|---|---|---|
| 0.1 | 0.3398 | 0.3270 | 3.7775 | 0.3286 | 3.2869 |
| 0.3 | 0.2723 | 0.2611 | 4.1129 | 0.2636 | 3.1856 |
| 0.5 | 0.1922 | 0.1841 | 4.2225 | 0.1857 | 3.3837 |
| 0.6 | 0.1464 | 0.1402 | 4.2671 | 0.1412 | 3.5700 |
| 0.7 | 0.0965 | 0.0913 | 5.3859 | 0.0912 | 5.4827 |

Experimental data was extrapolated from model scale to full scale by ITTC 1978 procedures. CFD simulations were the performed in full scale to minimize scale effects

Fig. 7 presents a comparison of $K_T$ and $10K_Q$ for steady and unsteady approaches with experimental data. From the presented data it is noted that the errors in $K_Q$ prediction are generally larger than those obtained in $K_T$ prediction. According to S. H. Rhee and S. Joshi [14], $K_Q$ is seems to be more dependent on the frictional component and sensitive to the viscous stresses exerted on the propeller blades. This could be the reason for the larger error in computed $K_Q$, and

implies that the fully turbulent simulation may not be adequate for propeller flows at high load especially in scenarios where laminar and/or transitional boundary layers are prevalent.

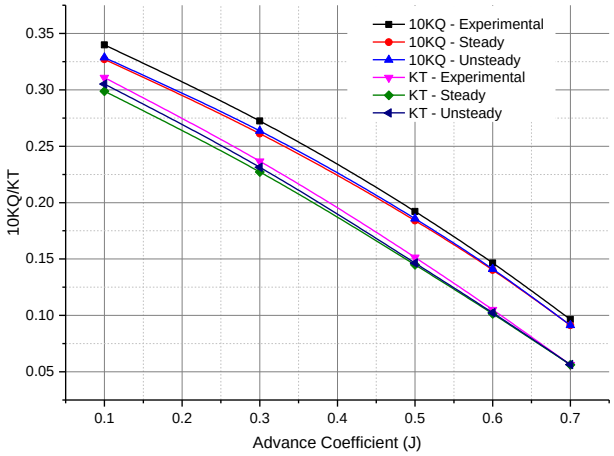


Fig. 7 Plot showing the comparison of KT and KQ for steady and unsteady approaches with experimental data

*3) Propeller Open Water Efficiency*

Table IV presents the tabulated data showing the comparison of open water efficiency, $\eta_0$ obtained from steady ow and unsteady ow approaches against experimental data. Data obtained from both steady ow and unsteady ow approaches are in good agreement with experimental data.

TABLE III
PROPELLER OPEN WATER EFFICIENCY ($H_0$)

| J | Experimental (extrapolated) | CFD – Steady | Error (%) | CFD – Unsteady | Error (%) |
|---|---|---|---|---|---|
| 0.1 | 0.1456 | 0.1454 | 0.1651 | 0.1477 | -1.4587 |
| 0.3 | 0.4147 | 0.4154 | -0.1684 | 0.4186 | -0.9453 |
| 0.5 | 0.6274 | 0.6263 | 0.1746 | 0.6276 | -0.0247 |
| 0.6 | 0.6855 | 0.6903 | -0.7031 | 0.6916 | -0.8969 |
| 0.7 | 0.6497 | 0.6849 | -5.4156 | 0.6884 | -5.9505 |

Experimental data was extrapolated from model scale to full scale by ITTC 1978 procedures. CFD simulations were the performed in full scale to minimize scale effects

From the presented data, steady flow approach has better result for low loads (J = 0.1 and 0.3) whereas for the high load (J=0.5 and 0.6) the unsteady flow approach has better result. In both cases the highest errors are noted at J=0.7 (5.42% and 5.95% for steady and unsteady flows respectively). This increase in error could be attributed to the over-prediction of the torque coefficient. For instance after J=0.5, the error appears to reduce in the case of $K_T$ (at J= 0.6 deviation was 3.56% and 2.67% for steady and unsteady respectively, at J= 0.7 deviation was 0.26% and -0.14% for steady and unsteady respectively) whereas for $K_Q$ case it increases further (for J= 0.6 deviation was 4.27% and 3.57% for steady and unsteady respectively, for J= 0.7 deviation was 5.39% and 5.48% for steady and unsteady respectively). This was translated to over-prediction of the open water efficiency, $\eta_0$.

Fig. 8 comparison of open water efficiency, $\eta_0$ for steady and unsteady flow approaches with experimental data for clear visualization.

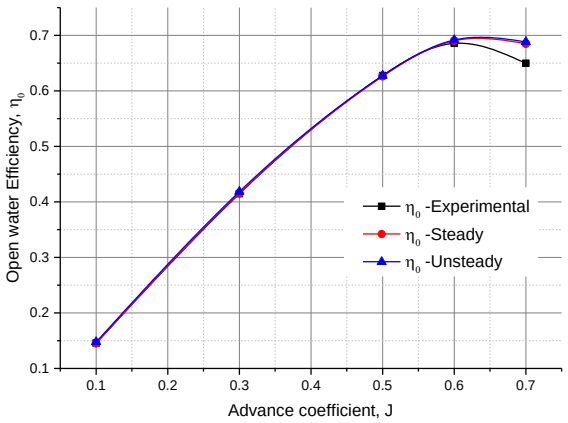


Fig. 8 Plot showing the comparison of open water efficiency, $\eta_0$ for steady and unsteady flow approaches with experimental data

*4) Pressure distribution*

Prediction of pressure distribution is important for analyzing the flow characteristics of a propeller design. The pressure distribution on the propeller and hub surfaces for four (4) advance ratios (0.1, 0.3, 0.5 and 0.7) are presented in fig. 9 and fig. 10 for steady and unsteady flow approaches respectively. The general tendency is well captured by the both numerical methods.

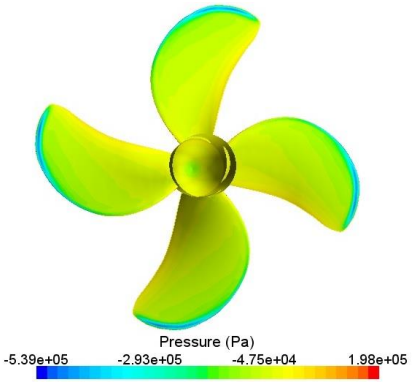


a) J = 0.1

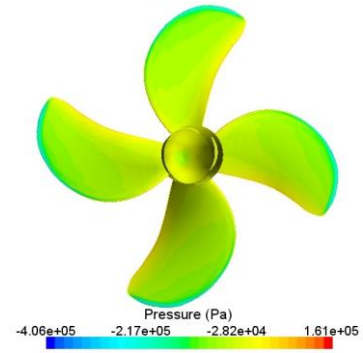


b) J = 0.3

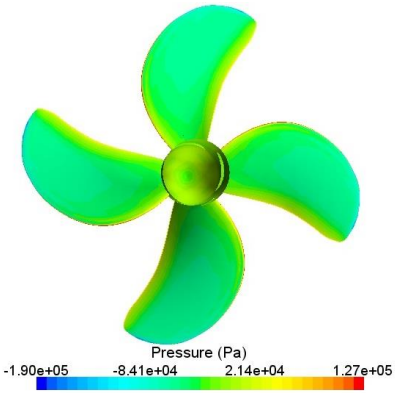


c) J = 0.5

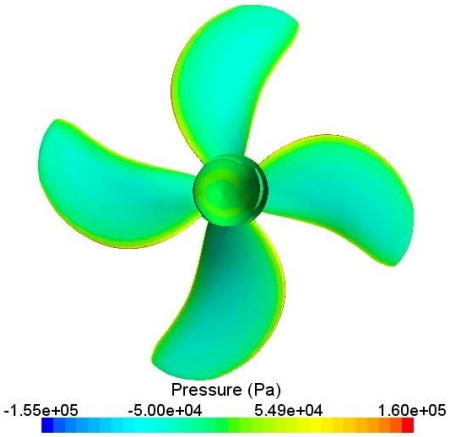


d) J = 0.7

Fig. 9 Pressure distribution on propeller surfaces for steady ow case at advance ratios, J =0.1, 0.3, 0.5, 0.6 and 0.7

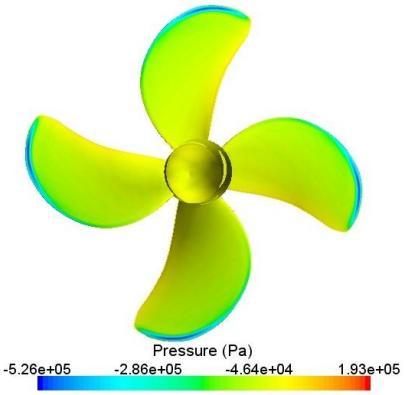


a) J = 0.1

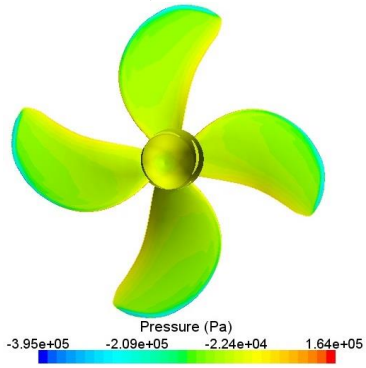


b) J = 0.3

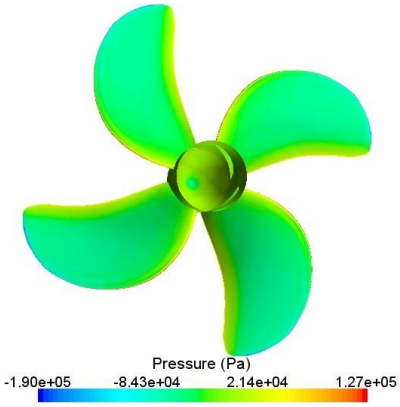


c) J = 0.5

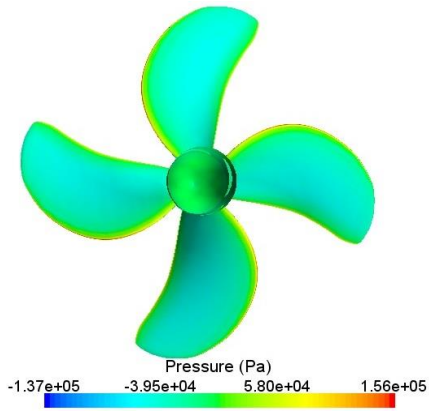


d) J = 0.7

Fig. 10 Pressure distribution on propeller surfaces for steady ow case at advance ratios, J =0.1, 0.3, 0.5, 0.6 and 0.7

## III. Conclusion

Simulations for incompressible flow around marine propeller were performed using a steady flow approach where a moving reference with a frozen rotor was adopted for the rotating region and an unsteady flow approach where a rigid body motion with actual displacement of mesh vertices of the rotating region. Data validation was performed by comparing the obtained data with extrapolated experimental results in accordance with ITTC 1978 procedures. The objectives of this study was to demonstrate the capability of unsteady simulation for turbulent flow around a marine propeller.

It is noted that for all simulations, the errors in $K_Q$ prediction are generally larger than those obtained in $K_T$ prediction. In addition, the error appears to reduce in the case of $K_T$ (for J= 0.6 deviation was 3.56% and 2.67% for steady and unsteady respectively, for J= 0.7 deviation was 0.26% and -0.14% for steady and unsteady respectively) whereas for $K_Q$ case there was a further increase (for J= 0.6 deviation was 4.27% and 3.57% for steady and unsteady respectively, for J= 0.7 deviation was 5.39% and 5.48% for steady and unsteady respectively). This was translated to over-prediction of the open water efficiency, $\eta_0$.

This observation could be attributed to the notion that $K_Q$ could be more dependent on the frictional component and sensitive to the viscous stresses exerted on the propeller blades. This could be the reason for the larger error in computed $K_Q$, and implies that the fully turbulent simulation may not be adequate for propeller flows at high load especially in scenarios where laminar and/or transitional boundary layers are prevalent. In terms of pressure distribution, the general tendency is well captured by the both approaches.

This study shows that CFD data calculated using the unsteady ow approach gives better results than those obtained by steady ow approach. For future applications, it is felt that a study be carried out to gain more insight on the influence of time step on simulation accuracy by halving say twice over to get $\Delta t = 0.5^o\omega^{-1}$ and $\Delta t = 0.25^o\omega^{-1}$.

## References

[1] T. Tezdogan, Y.K. Demirel, P. Kellett, M. Khorasanchi, A. Incecik, and O. Turan, Full-scale un-steady RANS CFD simulations of ship behaviour and performance in head seas due to slow steaming. Ocean. Eng. 97(0), 2015 pp. 186-206. http://dx.doi.org/10.1016/j.oceaneng.2015.01.011.

[2] S. Hai-long, E.O. Obwogi and S. Yu-min, Scale effects for rudder bulb and rudder thrust fin on propulsive efficiency based on computational fluid dynamics. Ocean Eng. 117, 2016 pp, 199–209. http://dx.doi.org/10.1016/j.oceaneng.2016.03.046

[3] CD-Adapco, User Guide STAR CCM+ v9.06 (2016)

[4] F. Çelik and M. Güner, Energy saving device of stator for marine propellers. Ocean Eng. 34(56) 2007, pp, 850-855. http://dx.doi.org/10.1016/j.oceaneng.2006.03.016.

[5] J.E. Choi, K.S. Min, J.H. Kim, S.B. Lee, and H.W. Seo, Resistance and propulsion characteristics of various commercial ships based on CFD results. Ocean Eng. 37(7), 2010, pp, 549-566. http://dx.doi.org/10.1016/j.oceaneng.2010.02.007.

[6] X. Yonghe, W. Guibiao, and W. Wei, Research on hydrodynamic performance of the interaction between ducted propeller and rudder based on CFD. Int. J. Ocean Syst. Eng. 3(4), 2013, pp, 169-174. http://dx.doi.org/10.5574/IJOSE.2013.3.4.169.

[7] J. Blazek, Turbulence modeling, in Computational Fluid Dynamics: Principles and applications, 2nd ed Oxford, UK: Elsevier Ltd., 2005, pp. 225-256.

[8] J.H Ferziger and M. Peric, Computational Methods for Fluid Dynamics, 3rd ed. Germany: Springer-Verlag (2002)

[9] Wei Qiu, H. Peng, S. Ni, L. Liu, S. Mintu, D. Hally, and H. Chao-Tsung, RANS Computation of Propeller Tip Vortex Flow. International Journal of Offshore and Polar Engineering, vol. 23, 2013, pp. 73-79.

[10] T. Kawamura, W. Takayuki, Y. Takekoshi, M. Maeda and H. Yamaguchi, Numerical Simulation of Cavitating Flow around a Propeller. Journal of the Society of Naval Architects of Japan, 2004, pp. 211-219.

[11] Li Da-Qing, N. Berchiche and J. Carl-Erik, Influence of turbulence models on the prediction of full-scale propeller open water characteristics with RANS methods. 26th Symposium on Naval Hydrodynamics, Rome, Italy, (2006)

[12] A. Sánchez-Caja, J. González-Adalid, M. Pérez-Sobrino, and T. Sipilä, Scale effects on tip loaded propeller performance using a RANSE solver. Ocean Engineering, vol. 88, 2014, pp. 607-617.

[13] X. Wang and K. Walters, Computational Analysis of Marine-Propeller Performance Using Transition-Sensitive Turbulence Modeling. Journal of Fluids Engineering, vol. 134, 2012 pp. 071107-071107.

[14] S. H. Rhee, and S. Joshi, Computational Validation for Flow around a Marine Propeller Using Unstructured Mesh Based Navier-Stokes Solver JSME Int. J., Ser. B, 48(3), 2005 pp. 562-570.

# A review on the effect of feed oxygen, water concentration, temperature and pressure on gasification proces

Oyugi George Oyugi, Ndiritu M. Hiram, Gathitu B. Benson

*Abstract*—Much interest is currently being shown on Gasification technology due to its versatility, the various technological arrangements it exhibits and its environmental advantage in converting any biomass or coal into a clean syngas. Many people have conducted studies on gasification processes in the past, but these results are mostly scattered, making it hard to keep track of the findings. This paper presents a comprehensive review of the literature on the effect of various gasification process parameters like feed oxygen, steam concentrations, pressure and temperature on syngas composition, heating value and the efficiency of gasifiers. The review seeks to streamline the information with the objective of determining the optimal gasification process conditions for best quality and quantity of syngas. Reviews of gasification technologies and process classifications are also presented.

*Keywords*—Gasification, Oxidizing agent, Feedstock, Syngas.

## I. INTRODUCTION

THE energy demands today is quite high and meeting these needs is one of the most important challenge of modern world. Despite constant development of new technologies and increase of usage of renewable energy sources, the conventional fossil fuel plays crucial role as an energy sources. One of these fossil fuels is coal. Coal has been used for many decades for production of energy with many developed countries deriving the bulk of their electrical energy from it. But due to strict environmental requirements especially concerning the levels of unwanted emissions permitted, better methods of utilizing coal as an energy source has been necessitated [1]. One such method is gasification process in which the solid fuel is converted to desirable gaseous fuel and the methods of separation and utilization of the environmentally harmful emissions like carbon dioxide, oxides of Sulfur and oxides of Nitrogen can be incorporated. Though gasification is an old technology, the variety of the technological arrangements like fixed-bed, fluidized-bed and entrained-flow reactors and its versatility (production of electricity, syngas, hydrogen) render it a current topic of research.

The traditional technologies for utilizing coal for power generation included grated coal firing plants where the fuel was mechanically distributed onto a moving grate, at the bottom of the firebox, in a partially crushed gravel-like form. Later pulverized coal power plants were introduced where coal was ground into powder. These were broken down into three categories; sub-critical pulverized coal plants which operated below the critical point of water (647.096 K and 22.064 MPa). super-critical pulverized coal plants, and ultra-super-critical pulverized coal plants which operated above the critical point of water. These methods, however, were environmentally unfriendly due to unwanted emissions which included oxides of sulfur, oxides of nitrogen, carbon dioxide and particulates. They also had low plant efficiencies which were at about $\leq 35\%$ for sub-critical plants , about 35-40% for super-critical plants and in the range of 40-45% for ultra-super-critical plants [2]–[4]. In all these, power production involved using coal to heat water and produce steam.

Gasification is a thermo-chemical process taking place at high temperatures typically above $700^oC$ to convert carbonaceous materials including biomass, fossil fuels, plastics, and coal into syngas; which is a mixture of $H_2$, $CH_4$, $CO$, and $CO_2$. Limited amount of oxygen and/or steam is used as the gasifying agent and heat carrier agent.

In the recent years, Integrated coal Gasification Combined Cycle (IGCC) has been used as an alternative to the coal fired plants in which oxidizing agents like steam, oxygen, air, or their combinations are used to change coal into syngas which is then used as fuel for power production giving improved plant efficiencies. In these plants coal reacts with the oxidizing agents to produce a $CO$, $H_2$ and $CH_4$ rich gas which is then taken to gas turbines to produce power and the flue gas taken through steam turbines to produce power. These systems are coupled with $CO_2$ capture and gas purification systems which eliminates harmful emissions to the environment making them environmentally friendly.

## II. GASIFICATION PROCESS OVERVIEW

### A. Stages in a Gasification Process

Coal gasification processes are undertaken in the presence of oxygen, steam, air, carbon dioxide or their combinations in different proportions. A syngas with different composition (with combustible and non-combustible components) and heating value is obtained. The non-combustibles components are removed, using different methods, to produce a clean syngas that can be used as a fuel to generate electricity or steam, as a

O. G. Oyugi, Department of Mechanical Engineering, JKUAT (Corresponding author, Phone: +2540725753700; e-mail: georoys@yahoo.co.uk)
H. M. Ndiritu, Department of Mechanical Engineering, JKUAT (e-mail: hndiritu@eng. jkuat.ac.ke)
B. B. Gathitu, Institute of Energy and Environmental Technology, JKUAT (e-mail: bbgathitu@gmail.com)

basic chemical building block for a large number of uses in the petrochemical and refining industries, and for the production of hydrogen. Thus gasification adds value to coal by converting it to marketable fuels and products [5], [6].

The quality and efficiency of the gasification process, equipment and the products depend on the quality of the feedstock used, the composition, flow rate and the temperature of the oxidizing medium, and the prevailing temperature and pressure in the gasifier [7]. It is also important to consider the way of injection of the oxidizing agent like in a two-stage gasification process, the reactor may be supplied with air in the first stage and with steam in the next stage, or the oxygen may be injected in the two stages or a mixture of the oxygen and steam [8], [9]. All these factors need to be understood for an optimum output from the gasification process.

Generally, the gasification process can be divided into the following stages [10]–[13], [29], which occur consecutively:

*1) Drying:* In this stage, the moisture content of the biomass is reduced. Typically, the moisture content of most biomass vary from 5% to 40%. Drying process take place at between $100^oC - 200^oC$ with a reduction in the moisture content of the biomass to below 2%.

*2) Devolatilization (Pyrolysis):* This is a stage of thermal decomposition of the biomass in the absence of oxygen or air. In this stage, the volatile matter in the biomass is reduced leading to the release of hydrocarbon gases from the biomass. This process reduces the biomass to solid charcoal or char. These hydrocarbon gases can condense at a sufficiently low temperature to generate liquid tars. Factors influencing the devolatization process vary at different stages of the gasification process and depend on the reactor space. These factors include: temperature, pressure, heating rate, reaction atmosphere, particle size and the degree of comminution of coal [10].

*3) Oxidation:* This is a stage of reaction between char and oxygen in the presence of air or oxygen, resulting in formation of $CO_2$. The hydrogen available in the biomass is also oxidized to generate water. A large amount of heat is released with the oxidation of carbon and hydrogen. If the oxygen available is in sub-stoichiometric quantities, then partial oxidation of carbon may occur, resulting in the generation of carbon monoxide hence gasification stage.

*4) Reduction:* This process takes place in the absence or sub-stoichiometric presence of oxygen. At this condition several reduction reactions occur in the $800^oC - 1000^oC$ temperature range. and these reactions are mostly endothermic. The main reactions in this category are the water-gas shift, Boudouard, and methanation.

### *B. The Chemistry of Gasification*

When coal is injected into a high-temperature gasifier, a series of physical and chemical processes occur in the gasifier. The particles are quickly heated, the moisture is evaporated, the volatile matter in the coal is devolatilized and the char is burned or gasified. The gaseous products released from the coal particles will also react with each other according to the surrounding environmental conditions and their intrinsic kinetics mechanism. These reactions in the gasifier are either exothermic or endothermic [15].

Rajul Nayak *et al* [16], in their simulation of gasification process, stated that the heat released by the exothermic reactions of coal and oxygen maintains the reactor at the operating temperature and supports the endothermic gasification reactions occurring inside the gasifier. They further explained that steam can only be used as a sole gasifying agent if an external source of heat that drags the endothermic reactions forward is provided.

One of the main processes is combustion of coal, which is an heterogeneous exothermic reaction between carbon from coal and oxygen to produce carbon dioxide and carbon monoxide as seen in (1) and (2) below [17]. Equation (2) is called Boudouard reaction.

$$C + O_2 \rightarrow CO_2 \quad (-393MJ/kmol) \tag{1}$$

$$C + \frac{1}{2}O_2 \rightarrow CO \quad (-111MJ/kmol) \tag{2}$$

The char-steam in (3) and char-$CO_2$ in (4) gasification reactions are endothermic and rely on the heat from the exothermic combustion reactions.

$$C + H_2O \rightarrow CO + H_2 \quad (+131MJ/kmol) \tag{3}$$

$$C + CO_2 \rightarrow 2CO \quad (+172MJ/kmol) \tag{4}$$

There is an heterogeneous reaction of carbon with hydrogen as shown in (5) which is exothermic and produces methane.

$$C + 2H_2 \rightarrow CH_4 \quad (-75MJ/kmol) \tag{5}$$

Apart from the heterogeneous reactions above, homogeneous reactions among the gases also occur in the reactor as seen below in (6), (7), (8), (9) and (10). Equations (9) and (10) are called methanation reactions

$$CO + \frac{1}{2}O_2 \rightarrow CO_2 \quad (-283MJ/kmol) \tag{6}$$

$$H_2 + \frac{1}{2}O_2 \rightarrow H_2O \quad (-242MJ/kmol) \tag{7}$$

$$CO + H_2O \rightarrow CO_2 + H_2 \quad (-41MJ/kmol) \tag{8}$$

$$CO + 3H_2 \rightarrow CH_4 + H_2O \quad (-206MJ/kmol) \tag{9}$$

$$CO_2 + 4H_2 \rightarrow CH_4 + 2H_2O \quad (-165MJ/kmol) \tag{10}$$

In general, for a constant coal feeding rate, when the $O_2$/coal ratio is increased and then the reaction temperature is high, then the reaction 4 becomes active and consumes the $CO_2$ generated from reaction 1 causing the concentration of $CO_2$ in the product gas to fall. However, high $O_2$/coal ratio leads to increased concentration of $CO_2$ due to excess supply of $O_2$ and the coal is mostly under combustion in the reactor.

### C. Gasification Process Classifications and Technologies

Gasification process can be categorized in several ways [18]: (a) by the gasifying agent, such as air-blown, oxygen blown, or steam gasifiers; (b) by the source of heat, either as auto-thermal (direct ) where heat is supplied by partial combustion of biomass, or allothermal (indirect) gasifiers where heat is supplied by an external source through a heat exchanger or an indirect process like solar or plasma gasification; (c) by the gasifier pressure, as atmospheric or pressurized. (d) by the reactor design and that follows three main subcategories: high temperature entrained flow, fixed bed (sometimes referred to as moving bed), and fluidized bed gasifiers. The most common classification method is the fourth one and thus a brief description of each gasifier type is presented below

*1) Fixed (or Moving) Bed Gasifiers:* Moving bed gasifiers are counter-current flow reactors in which the particle enters at the top of the reactor and air or oxygen enters at the bottom. As the particle slowly moves down through the reactor, it is gasified and the remaining ash drops out of the bottom of the reactor. Because of the counter-current flow arrangement, the heat of reaction from the gasification reactions serves to pre-heat the particle before it enters the gasification reaction zone. Consequently, the temperature of the syngas exiting the gasifier is significantly lower than the temperature needed for complete conversion of the particle. Fixed bed gasifiers are simple to construct and generally operate with high carbon conversion, long feedstock residence time, low gas velocity, and low ash carry-over [19], [20].

*2) Fluidized Bed Gasifiers:* A fluidized bed gasifier is a back-mixed or well-stirred reactor in which there is a consistent mixture of new particle particles mixed in with older, partially gasified and fully gasified particles. The mixing also fosters uniform temperatures throughout the bed. The flow of gas into the reactor (oxidant, steam, recycled syngas) must be sufficient to float the particles within the bed but not so high as to entrain them out of the bed. However, as the particles are gasified, they will become smaller and lighter and will be entrained out of the reactor. It is important that the temperatures within the bed are less than the initial ash fusion temperature of the particle to avoid particle agglomeration. These gasifiers are characterized by short residence time, high temperatures, high pressures, and large capacities [21]

*3) Entrained Flow Gasifiers:* A finely ground particle is injected in concurrent flow with the oxidant. The particle rapidly heats up and reacts with the oxidant. The residence time of an entrained flow gasifier is seconds to several seconds. Because of the short residence time, entrained flow gasifiers must operate at high temperatures to achieve high carbon conversion. Consequently, most entrained flow gasifiers use oxygen rather than air and operate above the slagging temperature of the particle.

## III. The Influence of Process Conditions on Gasification

### A. The Effect of Oxidizing Agent on the Gasification Products

Lee H. *et al* [22] developed a model to analyze chemical reaction processes in a dry-feeding entrained-bed coal gasifier as a function of $O_2$/coal mass ratio, steam/coal mass ratio, and operating pressure. In their study, initially $O_2$/coal ratio was varied from 0.3 to 0.9 with a constant steam/coal ratio of 0.05. Later, steam/coal ratio was varied from 0.01 to 0.2 with an $O_2$/coal ratio of 0.75, the pressure inside the reactor being kept at a constant value of 4.2MPa, They observed that increasing $O_2$ concentration increased carbon conversion rate leading to enhanced syngas yield while decreasing $O_2$ concentration lowered carbon conversion rate. Also increasing $H_2O$ concentration slowly increased carbon conversion efficiency during the initial reaction stages but the rate improved with time. This was because increasing steam concentrations led to decrease in the overall temperature in the reactor and cold gas efficiency. They however did not show the effect of these parameters on gasifier temperature.

Park T. J. *et al* [23] studied the characteristics of entrained-flow coal gasifier. In their research they stated that, the $O_2$/coal ratio is critical to the carbon conversion for a short residence time reactor, since the endothermic gasification reactions are supported by the heat produced from exothermic reactions. They concluded that for such a gasifier $O_2$/coal ratio of between 0.8 and 0.9 is required. this would give better carbon conversion and increased cold gas efficiency. Their study however only involved a slurry-fed entrained-bed gasifier. and thus further study is necessary for a dry-fed gasifier.

Alina Zogala [24] did a thermodynamic equilibrium simulation to determine factors affecting syngas composition from coal gasification. He used coal from four different Polish coal mines: Belchatow (lignite), Bielszowice (sub-bituminous) and Ziemowit and Bobrek (both bituminous). He used three forms of gasifying agents: mixtures of steam-pure oxygen, steam-air and air-pure oxygen. He found out that raising the concentration of $O_2$ in the gasifying agent led to significant rise in molar yield of CO, $H_2$. Carbon dioxide and $H_2O$ yield also grew, though the yield of $CO_2$ exceeded that of $H_2O$ at higher $O_2$ concentrations. Similar trends were seen when using steam in the gasifying agent. Much yield in $H_2$ was realized when $H_2O$ concentrations were increased that when only $O_2$ and air were used. This is shown in his graph presented in Figures 1 and 2. His operating temperatures were however low ($700^oC$) compared to those experienced in fixed bed gasifiers. He also assumed that the process was isothermal in the reactor which is not the case in the actual practice.

Babu B. V. *et al* [25] modeled a biomass gasifier to show the effects of $O_2$/air and steam /air ratio on gasification process. Their results were in agreement with those of Alina Zogala [24]. But they went further and found out that the calorific value of the syngas increased with increasing $O_2$/air ratio but decreased with increasing steam /air ratio and that the reaction temperature also increased for preheated air intake. Their model was however based on wood as the feedstock which is high in volatile matter compared to coal.

Jorge E. Preciado *et al* [26] also did a simulation on gasification of Colombian Coal in a fluidized bed gasifier and got a similar results. In their study they attained a maximum thermal efficiency of 62.6%, that corresponded to a slurry solid concentration of 0.65, a $O_2$/carbon ratio of 0.64, steam to dry gas ratio of 0.59, and low temperature reactor operating

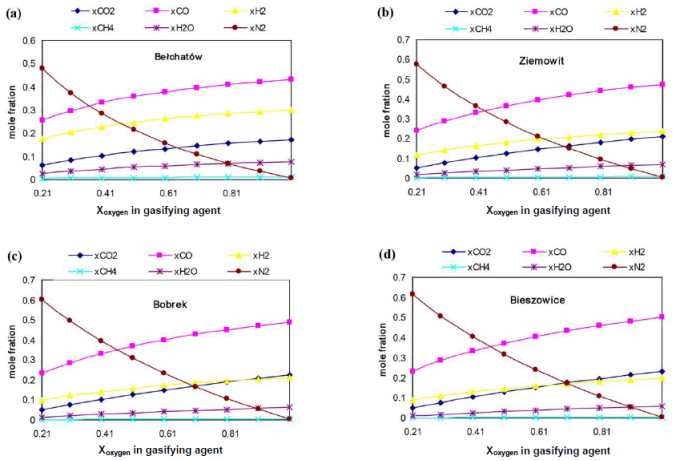


Fig. 1. The effect of oxygen/air ratio on syngas composition (at 700$^o$C) [24]

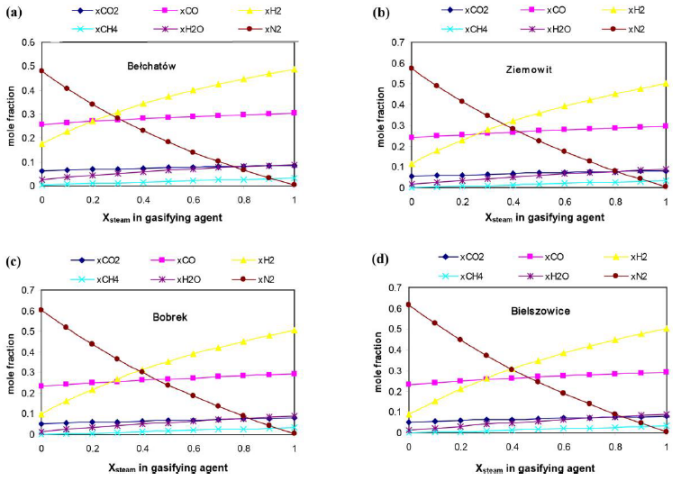


Fig. 2. Effect of steam/air ratio on syngas composition (at 700$^o$C) [24]

temperature of 473 K. They found that thermal efficiency of the process is most sensitive to $O_2$/ carbon ratio and that an excessive increase in the $O_2$ flow rate causes a fall in thermal efficiency. They then concluded that the $O_2$/carbon ratio should not exceed 0.8 for efficient operations. The simulation was however based on low temperature reactor (LTR). These findings are in agreement with those realized by Hao Xie *et al* [27] who simulated coal gasification based on slurry-fed entrained-bed gasifier.

Haibin Li *et al* [28] studied the effect of oxygen flow rate on gasification products and found out that the amount of CO rose gradually as the $O_2$ flow rate approached 20 kg/h beyond which the molar fraction of CO decreased. The amount of $H_2$ decreased gradually as the mass flow rate of $O_2$ rose. They concluded that the optimum LHV of the syngas would be obtained when the $O_2$ flow rate was 20 kg/h and that preheating of the $O_2$could both improve the syngas heating value and the reaction temperature. Their study was however based on pure oxygen and pure carbon dioxide as the gasifying agents which yields a syngas with fairly low heating value due to low hydrogen content. These results also agree with conclusions by Rukayya Ibrahim Muazu *et al* [29] who modeled a fluidized bed gasifier for agricultural biomass gasification based on air as the oxidizing agent. Their air flow rate was 4.5 kg.h

### *B. The Influence of Gasifying Medium on the Reactor Temperature and Pressure*

Biagini E. *et al* [30] modeled a gasifiers for hydrogen production optimization. They varied the $O_2$/coal ratio and the $H_2O$/coal ratio from 0.25-0.50, and 0.0-0.35 respectively. They found out that the higher the $O_2$/coal ratio, the higher the reactor temperature. They did not however identify the optimum values for the oxygen/coal and steam/coal ratios that could give most favorable operating temperature for the efficient production of quality syngas. increasing air flow rate also leads to increased temperature in the reactor as well as temperature of the syngas at outlet [13]

Park T. J. *et al* [23] in their study realized that temperature distribution inside reactor depended upon the feed rate of coal and oxygen unless heat losses were considered. They showed that reactor temperature rose with increase in $O_2$/coal ratio. They concluded that, considering the ash melting temperature and heat losses from the reactor, the desired $O_2$/coal ratio were at least 0.6. They also found out that the $O_2$/coal ratio affects carbon conversion more significantly than the steam/coal ratio. They however did not explore how the heat losses could be minimized to increase the efficiency of the process.

Weihong Yang *et al* [31] analyzed the influence of a preheated feed air on the performance of a fixed-bed biomass gasifier. They found out that when higher air temperature are used, the temperatures of the solid fuels rise from room to peak temperature more quickly compared to when lower air temperature is used, indicating that a fast ignition occurs. They observed from their model that, a feed air of temperature equal to 973 K, the solid peak temperature at the bed top was only 630 K while it was about 900 K for the case of feed air temperature equal to 623 K. This implied that the peak temperatures are lower when higher feed air temperatures are used. This was because the ignition temperature is much lower when high feed gas temperatures are used. Preheating the feed air to this high temperatures is adds to the cost of the gasification system due to specialized materials needed to contain such high temperatures.

H. Lee *et al* [22] in their model explained that the increase in steam/coal ratio lowers the temperature due to the relatively high heat capacity of steam. As a result, the generated syngas concentration is low save for hydrogen due to the high steam concentration. They also noted that increasing the operating pressure improved both carbon conversion and cold gas efficiency because the reactivity of char + $H_2O$ and char + $CO_2$ increased. They observed that during the early stages of combustion and gasification reactions the rate of increase of temperature was higher as pressure increased, but overally the peak temperature was low. This was attributed to the reactivity of endothermic gasification reactions that become active fast after oxygen is consumed because of the combustion of volatiles. They then concluded that the gasifier operating pressure is inversely proportional to the peak

temperature. This model was however not validated due to lack of literature with data on dry-fed gasifiers that could be used to bench mark the same.

### *C. The Effect of Temperature and Pressure on the Gasification Process and Products*

Nearly all the coal gasification reactions are normally reversible and thus the equilibrium point of any of these reactions can be shifted by manipulating the temperature. This therefore illustrates that temperature, as a parameter, has a great influence on the performance of coal gasifiers. The degree of the equilibrium attained by the various coal gasification reactions in the gasifier reactor determine the composition of the volatile matter generated from the gasifier. [32]

Jianxin Mi *et al* [33] compared the char yields, surface area and pore volumes of different coals as a function of gasification temperature in the fluidized-bed reactor at the slow heating rate. They observed that the three parameters above generally decreased with increasing reaction temperature from 700 to 900$^o$C in 15 vol % steam. Yaning Zhang *et al* [34] found out that increase in reactor temperature had a positive impact on syngas energy and exergy. These results were however based on fluidized bed gasifiers, with steam as the gasifying agent. There is thus need for further studies using dry-fed gasifier with inclusion of other gasifying agents like oxygen, air or their mixtures.

Idowu Adeyemi *et al* [35], Leila Emami *et al* [36] in their studies showed that increase in reactor temperature and pressure led to the formation of more CO, $H_2$ and higher calorific value due to improved endothermic reactions between char and steam and carbon dioxide. The heat in this study was however supplied from built-in heating modules which is different from the practical processes where the heat is majorly from the exothermic reaction in the reactor. These conclusions were also in agreement with the study conducted by Shermina Begum *et al* [37] who modeled an integrated fixed-bed gasifier operating on different biomass feed stocks. They further concluded that an average temperature of $700^oC$ provided an ideal condition for their modeled gasifier.

Marek Balas *et al* [38] conducted experiments to investigate the effects of temperature and pressure on the gasification process. After their study they found out that increase in temperature leads to increase $CO$ and $H_2$ yield, an increase in syngas lower calorific value but decline in the yield of $CH_4$ and $CO_2$. They also found out that change in pressure however has a contrary effect.

Neville A. H. Holt [39], in his study of needs and opportunities in coal gasification field, noted that the commercial gasifiers from Global E-Gas and Shell generally operate at higher temperatures and that this accounted for the better carbon conversion rates experienced in these gasifiers with petroleum coke. He observed that increasing the operating temperature would however certainly aggravate the refractory wear, a replacement of which is very expensive and time consuming. This shows the need to control the operating temperatures of the gasifier.

Wadhwani *et al* [40] conducted a 2D CFD simulation to investigate the effects of operating pressure for coal chemical looping combustion. The results obtained showed that the operating pressure had a reverse effect on the gasifier reactor operating temperatures, and the rate of decrease in reactor temperature escalates at higher pressures. Therefore control of reactor pressure is also necessary if optimum temperature is to be achieved.

## IV. Recommendations

From the above studies, the following recommendations are made:

- Almost all the studies above involve entrained and fluidized bed gasifiers. Much research need to be done on fixed bed gasifiers to ascertain their operating conditions.
- There is need for enhanced research on gasifiers for small scale applications like for domestic use so that many house holds can use gasification to generate syngas for cooking
- Most of the studies done involve slurry-fed gasifiers. It is therefore necessary for more studies to be done on dry-fed gasifiers to understand their characteristics and applications.
- Given the importance of temperature and pressure in gasification processes, regulation of gasifier heat is very necessary. More research is necessary on simpler but effective ways of regulating reactor heat for small scale gasifiers like use of water jackets.
- Most of the data available are based on the use of pure oxygen - steam, or air -steam or carbon dioxide-steam as the gasifying agents. More studies should be done on the use of steam - oxygen-enriched air as the oxidizing agents.

## V. Conclusion

It has been shown that feed oxygen and water concentrations have a direct influence on the quality and quantity of syngas produced from a gasifier. It has also been verified that temperature and pressure in the gasifier reactor affects the performance and efficiency of the gasifier.

Increasing oxygen supply to gasifier increases the reactor temperature, cold gas efficiency, and gas calorific value. It also enhances production of carbon monoxide and carbon conversion rate leading to enhanced syngas yield. Increasing steam concentrations in the gasifier reduces gas caloric value, enhances yield in hydrogen and methane but reduces reactor temperature.

Increase in gasifier temperature enhances syngas yield, gas calorific value and cold gas efficiency. But it also increases carbon dioxide and oxides of nitrogen that are not desirable in a gasification process.

## Acknowledgment

We acknowledge the staff and managements of Jomo Kenyatta University of Agriculture and Technology and the Technical University of Mombasa for their support by allowing the authors to use their research facilities and resources to accomplish this review.

## REFERENCES

[1] Sebastian Iwaszenko. *Using Mathematica software for coal gasification simulations - Selected kinetic model application*, Journal of sustainable mining, vol 14, (2015), pp 21 - 29.

[2] Kyle Nicol. *Status of advanced ultra-supercritical pulverised coal technology*, IEA Clean Coal Centre, (December 2013), pp 5

[3] IEA Clean Coal Centre *Coal power database*, London, UK, IEA Clean Coal Centre ,(2012)

[4] Paul Lako. *Coal-Fired Power*, IEA Energy technology systems analysis programme- Technology brief E01, (April 2010), pp 1-6

[5] Chiche D., Diverchy C., Lucquin A. C., Porcheron F., Defoort F. *Synthesis Gas Purification*, Oil and Gas Science and Technology Journal. vol 68 (4), (2013), pp 707-723.

[6] Ronald W. Breault, *Gasification Processes Old and New: A Basic Review of the Major Technologies*, Energies Journal, vol 3, (2010), pp 216-240

[7] Alina Zogaa, Tomasz Janoszek. *CFD simulations of influence of steam in gasification agent on parameters of UCG process*, Journal of Sustainable Mining, vol 14, (2015) , pp 2-11.

[8] Yong Cui, Jie Liang, Zhangqing Wang, Xiaochun Zhang, Chenzi Fan, Xuan Wang. *Experimental forward and reverse in situ combustion gasification of lignite with production of hydrogen-rich syngas*, International Journal of Coal Science and Technology, vol 1 (1), (2014) , pp 70-80.

[9] Ting Wang, Xijia Lu, Heng-Wen Hsu, Cheng-Hsien Shen. *Employment of Two-Stage Oxygen Feeding to Control Temperature in a Downdraft Entrained-Flow Coal Gasifier*, International Journal of Clean Coal and Energy, vol 3, (2014) , pp 29-45.

[10] Beata Urych. *Determination of kinetic parameters of coal pyrolysis to simulate the process of underground coal gasification (UCG).*. Journal of Sustainable Mining vol 13(1), (2014), pp 3- 9.

[11] McKendry, P. *Energy Production from Biomass (Part 3): Gasification Technologies*. Bioresource Technologies, vol 83(1), (2002), pp 55- 63.

[12] Li, X. *Biomass Gasification in Circulating Fluidized Bed*. Doctoral dissertation, University of British Columbia. (2002)

[13] Mandl C., Obernberger I., and Biedermann F. *Modeling of an updraft fixed-bed gasifier operated with softwood pellets*. Fuel, vol 89, (2010), pp 3795 - 3806

[14] Isam Janajreh and Idowu Adeyemi, *Effect of Process Parameters on Gasification: Review*. Proceedings of the IAJC-ISAM International Conference, (2014).

[15] Shabbar Syed. *Thermodynamics Equilibrium Analysis of Gasification*, International Journal of Thermal and Environmental Engineering ,vol 4(1), (2012), pp 47-54.

[16] Rajul Nayak, Raju K Mewada. *Simulation of Coal Gasification Process using ASPEN PLUS*, International Cnference on Current Trends in Technology, (08-10 December 2011) , pp 1-6.

[17] Young-Chan Choi, Tae-Jun Park, Jae-Ho Kim, Jae-Goo Lee, Jae-Chang Hong and Yong-Goo Kim. *Experimental Studies of 1 Ton/Day Coal Slurry Feed Type Oxygen Blown, Entrained Flow Gasifier*, Korean Journal of Chemical Engineering vol 18(4), (2001) , pp 493-498.

[18] Rauch R. *Thermal Gasification of Biomass*, IEA Bioenergy Agreement, Task 33. (2003) Retrieved from http://www.ieabioenergy.com/task/thermal-gasification-ofbiomass

[19] Carlos L. . *High Temperature Air/Steam Gasification of Biomass in an Updraft Fixed Bed Type Gasifier*. Doctoral dissertation, Royal Institute of Technology, Stockholm (2005)

[20] Reed T. B., and Das, A. *Handbook of Biomass Downdraft Gasifier Engine Systems*. Golden, CO: Solar Energy Research Institute. (1988)

[21] Knoef H. A. M. . *Handbook of Biomass Gasification*, Meppel, The Netherlands: BTG Biomass Technology Group B.V. (2005)

[22] H Lee, S Choi, and M. Paek. *A simple process modeling for a dry-feeding entrained bed coal gasifier*, Proc. IMechE vol. 225 Part A: J. Power and Energy (2011) , pp 1-11

[23] Tae-Jun Park, Young-Chan Choi, Jae-Ho Kim, Jae-Goo Lee, Jae-Chang Hong and Yong-Goo Kim. *Experimental Studies on the Characteristics of Entrained Flow Coal Gasifier*, Energy Conversion Research Department, Korea Institute of Energy Research (1998).

[24] Alina Zogaa. *Equilibrium simulations of coal gasification factors affecting syngas composition.*, Journal of Sustainable Mining, vol 13(2), (2014) , pp 30-38

[25] Babu B. V. and Pratik N. Sheth. *Modeling and Simulation of Downdraft Biomass Gasifier: Effect of Oxygen Enrichment and Steam to Air Ratio*, Proceedings of the 57th Indian Chemical Engineering Congress, Chemcon (2004).

[26] Jorge E. Preciado, John J. Ortiz-Martinez, Juan C. Gonzalez-Rivera, Rocio Sierra-Ramirez and Gerardo Gordillo. *Simulation of Synthesis Gas Production from Steam Oxygen Gasification of Colombian Coal Using Aspen Plus*, Energies, vol 5, (2012), pp 4924-4940

[27] Hao Xie, Zhongxiao Zhang, Zhenzhong Li, Yang Wang. *Relations among Main Operating Parameters of Gasifier in IGCC*, Journal on Energy and Power Engineering, vol 5, (2013), pp 552-556.

[28] Haibin Li, Yu Yu, Minfang Han, Ze Lei. *Simulation of coal char gasification using* $O_2/CO_2$, International Journal Coal Science and Technology, vol 1(1), (2014), pp 81-87

[29] Rukayya Ibrahim Muazu, Aiduan Li Borrion, Julia A. Stegemann. *Fluidised Bed Gasification of Multiple Agricultural Biomass Derived Briquettes*, International Journal of Chemical, Molecular, Nuclear, Materials and Metallurgical Engineering vol:9(5), (2015), pp 622 - 628

[30] Biagini E., Masoni L., Pannocchia G. and Tognotti L. *Development of Gasifier Models for Hydrogen Production Optimization*, AIDIC Conference Series, vol 9, (2009), pp 45-52

[31] Weihong Yang, Anna Ponzio, Carlos Lucas, Wlodzimierz Blasiak. *Performance analysis of a fixed-bed biomass gasifier using high-temperature air*, Fuel Processing Technology, vol 87 (2006), pp 235 245

[32] Aly Moustafa Radwan. *An overview on gasification of biomass for production of hydrogen rich gas*, Der Chemica Sinica, vol 3(2), (2012), pp 323-335

[33] Jianxin Mi, Ningbo Wang, Mingfeng Wang, Pengju Huo, Dan Liu. *Investigation on the catalytic effects of AAEM during steam gasification and the resultant char reactivity in oxygen using Shengli lignite at different forms*, International Journal Coal Science and Technology, vol 2(3), (2015), pp 223-231

[34] Yaning Zhang, Zhongbin Fu, Bingxi Li, Hongtao Li, and Bo Zhang. *Energy and Exergy Evaluation of Product Gas from Coal/Biomass Blend Gasification in a Dual Circulating Fluidized Bed Reactor*, Cleaner Combustion and Sustainable World, (2013), pp 599 - 603

[35] Idowu Adeyemi, Thomas Arink, Isam Janajreh. *Numerical Modeling of the Entrained Flow Gasification (EFG) of Kentucky Coal and Biomass*, Energy Procedia, vol 75 ( 2015 ), pp 232 - 239

[36] Leila Emami Taba, Muhammad Faisal Irfan, Wan Ashri Mohd Wan Daud, Mohammed Harun Chakrabarti. *The effect of temperature on various parameters in coal, biomass and CO-gasification: A review*, Renewable and Sustainable Energy Reviews, vol 16, (2012), pp 55845596

[37] Sharmina Begum, Mohammad G. Rasul, Delwar Akbar, and Naveed Ramzan. *Performance Analysis of an Integrated Fixed Bed Gasifier Model for Different Biomass Feedstocks*, Energies, vol 6, (2013), pp 6508-6524

[38] Marek Balas, Martin Lisy and Ota Stecl *The Effect of Temperature on gasification process*, Acta Polytechnica vol. 52(4), (2012), pp 7- 11

[39] Neville A. H. Holt *Coal Gasification Research, Development and Demonstration - Needs and Opportunities*, Gasification Technologies Conference, San Francisco, CA. (10 October 2001),

[40] Rahul Wadhwani, and Bikash Mohanty. *Effects of operating pressure on the key parameters of coal direct chemical looping combustion*, International Journal Coal Science and Technology, vol 3(1), (2016), pp 20- 27

# Use of Waste Materials to Augment Lime's Reactivity towards Flue Gas Desulfurization

Paul Maina

**Abstract:** Four waste materials which are normally disposed off as landfill were recycled and put in good use as additives for improving limes reactivity towards flu gas desulphurization (FGD). Fly ash (coal power plant waste), bottom ash (coal power plant waste), waste activated sludge (waste water treatment plant waste) and iron waste (iron ore refining plant waste) improved limes reactivity by varying amount when tested in pH-stat and fixed bed apparatus which represent wet and dry FGD processes respectively. Increase in surface area of the sorbents produced from the blends of lime and these wastes was thought to be the main reason for improvement of reactivity, a conclusion confirmed by Brunauer, Emmett and Teller (BET) surface area analysis. Iron waste sorbents though, had a different behavior probably because their reactive component was hematite rather than the pozzolanic materials.

***Keywords:*** Land fills, Lime, Reactivity, Surface area, Waste materials.

## I. INTRODUCTION

Land fill is a major cause of land and environmental degradation worldwide. This is caused majorly by industrial processes with solid waste materials. In coal-fired power plant for instance, after the combustion of coal, the flue gas contain particulate matter known as fly ash whereas the coal ash remaining in the furnace is majorly composed of bottom ash. On the other hand, in sewage, municipal and industrial waste water treatment plants, excess sludge known as waste activated sludge (W.A.S) is produced as the bulk waste. Finally in iron ore refining industries, iron waste (or red mud) is produced as the major waste product. These waste products, having no other major economic use, are usually disposed off as land fill thus creating another environmental concern. The same industries i.e. coal fired power plants, municipal waste treatment and metal smelting, are the major cause of emissions of pollutants creating acidic deposition i.e. sulfur dioxide ($SO_2$). Acid deposition is one of the worst environmental pollutants. It deposits acid which changes the chemistry of the environment thus negatively affecting aquatic and terrestrial plants as well as animals, human beings inclued.

Almost all methods of reducing sulfur dioxide in flue gas emissions are categorized into three major groups namely; dry, semi-dry and wet flue gas desulfurization (FGD). FGD processes usually are based on the fact that sulfur dioxide is acidic in nature, therefore, it can be easily removed by reaction with a suitable alkaline sorbent. The most commonly used material for FGD is limestone due to its availability and price. Limestone is mainly made up of calcite ($CaCO_3$) which, although is alkaline in nature, is not reactive enough to remove a desirable amount of sulfur dioxide from flue gases. Therefore, limestone is usually calcined to quicklime (CaO) depending on the carbon dioxide partial pressure. Quick lime reactivity is usually higher than that of limestone. Researchers attributed this increase in reactivity to the increase in surface area and porosity of the calcinations product [1]. To further increase the reactivity, quicklime is usually hydrated to slaked lime ($Ca(OH)_2$).

Slaked lime, although is more reactive than quicklime and limestone, it still is not reactive enough to remove enough sulfur dioxide, and therefore cannot beat the tough regulations imposed on sulfur dioxide emission. This made researchers to look into ways of improving the reactivity of slaked lime. Recently, the most promising result is by reacting it with a pozzolanic material or other metal oxides. In the same way that pozzolans have been found to improve cement properties, it was also found to add the reactivity of slaked lime. Pozzolans, being primarily made of vitreous aluminous-siliceous materials, reacts with slaked lime to form complex calcium alumina-silicates. These complex products have very high surface area and porosity and therefore have very high reactivity. In addition, the products of sulfation reaction with these sorbents are very stable. Fly ash, bottom ash and W.A.S are composed of pozzolanic materials, thus can be used as suitable additives to lime.

Metal oxides have proved to be good sorbents either as a whole or in combination with other materials. One of the most promising metal oxide is hematite ($Fe_2O_3$) due to its high sulfur capacity, reactivity, good regenerability, availability and economy. In 1950's, Appleby-Frodingham Steel Company used sintered iron oxide powder in a fluidized bed and achieved up to 98% desulfurization capacity [2]. The US bureau of mines carried out laboratory testing of different solid sorbents and found out that iron-based sorbents are suitable for bulk desulfurization [3]. $Fe_2O_3$ has the greatest capacity for sulfur removal per gram of sorbent, followed by CaO and $ZnO_2$ [4]. The authors in [5], stated that iron has a catalytic activity in the oxidation process of $SO_2$ to $SO_3$ which reacts more easily. The authors in [3] compared four metal oxides from waste materials of metal processing operations (tin oxides, zinc oxides, iron oxides and a mixed metal oxide with zinc oxide as the predominant mineral). They found out that sorbent based on iron waste were the most reactive and exhibited the highest effective capacities both in reducing and oxidizing atmospheres. The authors in [6] added CaO to $Fe_2O_3$ sorbent to improve its properties for desulfurization. They noted that, depending on the amount of CaO available,

Paul Maina, Department of Mechanical and Production Engineering, Moi University (Phone: +254721812066; e-mail: lypsym@yahoo.com).

complex product between the $Fe_2O_3$ and CaO will be formed owing to its basicity. CaO can stabilize $Fe^{3+}$ by forming $CaFe_2O_4$ (CaO. $Fe_2O_3$) thus making it more effective.

As it has been noted, the solid waste products in the three industries mentioned above can be used to help in reduction of both the pollution of air and landfill. Fly ash and/or bottom ash can be used to pozzolanically improve lime's reactivity towards FGD in coal-fired power plants, W.A.S can be used in the same way in municipal incinerators while iron waste, by the use of hematite in it can be use in iron refining industries. It is the aim of this study therefore to investigate if these waste product will actually improve lime's reactivity towards FGD and thus reduce their landfill menace and at the same time prevent acid deposition.

## II. MATERIALS AND EQUIPMENT

All materials were sourced in South Africa. Natural limestone was mined in the country while fly ash and bottom ash were provided by South Africa electric power producer (ESKOM). W.A.S was provided by the Pretoria sewage treatment plant while iron waste was provided by an iron ore mining and refining industry in South Africa. The raw samples were dried, crushed, ground and sieved to a particle size of utmost 200 μm. The limestone was further calcined in an electric furnace at 900 °C for 4 hours. The chemical analysis of the calcined limestone and the waste materials are shown in table I below.

Table I: chemical analysis of the materials

| Compound | Percentage Present | | | | |
|---|---|---|---|---|---|
| | Quick Lime | Fly Ash | Botto m Ash | W. A.S | Iron Waste |
| Calcite | 5.02 | - | - | 14.2 9 | - |
| Quicklime | 75.54 | 7.36 | 8.34 | - | - |
| Alumina silicates | 9.55 | 79.6 5 | 80.83 | 47.5 6 | 7.08 |
| Hematite | 1.78 | 5.99 | 5.10 | - | 26.77 |
| Others | 8.10 | 6.99 | 5.73 | 38.1 5 | 66.16 |

When strong acids like sulfuric acid or hydrochloric acid are used in the pH-stat, the reaction mechanism is close to that on a wet FGD plant equipped with air oxidation of the bisulfite ion [7]. Recently, ASTM developed a standard test method for the determination of total neutralizing capability of dissolved calcium and magnesium oxides in lime for FGD (ASTM C: 1318-95). This method recommends an acid titration procedure. Both wet and dry FGD processes were used using a pH-stat method and a fixed bed reactor respectively though the dry FGD experiments were conducted on the best sorbents from each additive only. Fig 1 below shows the pH-stat apparatus used. 1.5 g of the sorbent was dissolved into 200 ml of distilled water. The solution was put in a water bath set at 60 °C with a resolution of ±1 °C. The solution was agitated by a stirrer rotating at 225 rev/sec. The pH in the beaker was measured by a pH electrode inserted in the solution and connected to a pH 200 controller supplied by Eutech Instruments with a resolution of ±0.01. A 1 M solution of HCl was titrated accordingly and the reactivity was determined from a recording of the volume of HCl added versus time. Each experiment was done at least twice and the average of the results taken.

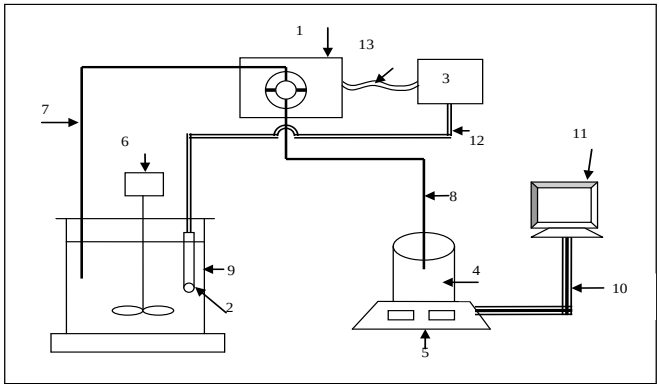


Fig1: A schematic drawing of the experimental set-up. (1) Peristaltic pump, (2) pH electrode, (3) pH controller, (4) Acid solution Beaker, (5) Electronic balance, (6) Stirrer, (7,8) Plastic tubing, (9) Reaction vessel,(10) RS232 Cable, (11) Computer work station, (12) wiring for pH electrode, (13) Connection between pump and controller

Models used to describe the heterogeneous non-catalytic solid-fluid reaction mechanism fall into three main categories[8]:

- Grain models,
- Pore models and
- Deactivation models

The grain model is relatively simple and largely used to describe heterogeneous non-catalytic solid-fluid reaction. This model assumes that the porous solid is made up of small non-porous grains, and each of these grains is converted according to the shrinking unreacted core model. In shrinking unreacted core model, spherical particles making up the grains, are converted at a rate depending on the limiting step on which as derived and explained in [9];

- If the chemical reaction is the rate-limiting step

$$\frac{t}{\tau} = \left[1 - (1-x)^{1/3}\right] \quad (1)$$

Where the reactivity will be given by a plot of [1-(1-x)^(1/3)] versus time .

- If the diffusion through the product layer is the rate-limiting step

$$\frac{t}{\tau} = \left[3 - 3(1-x)^{2/3} - 2x\right] \quad (2)$$

Where the reactivity will be given by a plot of [3-3(1-x)^(2/3)-2x] versus time.

- If the mass transfer through fluid film is the rate limiting step

$$\frac{t}{\tau} = x \quad (3)$$

Where the reactivity will be given by a plot of x versus time.

Due to the nature of the experiments, the product layer will constantly be dislodged from the surface by the agitation therefore there will be minimum resistance due to diffusion through the product layer and thus it won't be the rate limiting step. Similarly, due to the fact that the fluid media is liquid in nature, mass transfer through fluid film will have a minimum effect on the overall reaction, therefore it won't be the rate limiting step. Furthermore, a lot of literature with similar experiments states that this type of reaction is chemically controlled [10]. Hence the reactivity constant was calculated by assuming that these reactions were chemically controlled. Mixtures of operatives affecting reactivity were varied statically to bring out the effect of each operative clearly. In total all the operatives investigated were temperature, lime to diatomite ratio, solid to liquid ratio and stirring speed. Table II below shows the maximum and minimum values of each operative. Design of experiments using design expert software was used in these experiments for regression analysis.

Table II: Range of operatives

| Name of operative | Units | Low | High |
|---|---|---|---|
| Temperature | deg C | 40 | 80 |
| Lime to waste additive ratio (lime mass in 1.5 g sorbent) | g | 0 | 1.5 |
| Solid to liquid ratio (volume of distilled water per 1.5 g sorbent) | ml | 100 | 300 |
| Stirring speed | rev/sec | 100 | 350 |

Response surface methodology (RSM) is a statistical method in design expert that uses quantitative data from appropriate experiments to determine regression model equations and operating conditions. A standard RSM design called the central composite design (CCD) is suitable for investigating linear, quadratic, cubic and cross product effect of the operatives. It also helps to optimize the effective parameters and provide a lot of information with a minimum number of experiments as well as to analyze the interaction between the parameters. In addition, the empirical model that relates the response to the operatives is used to obtain information about the process. CCD comprises a two level full factorial design ($2^4 = 16$), eight axial points and six center points. The center points were used to determine the experimental error and the reproducibility of the data. Alpha (α) value, which is the distance of axial point from the center, was fixed at 2 to make the design rotatable. The experiment sequence was randomized in order to minimize the effects of the uncontrolled factors. Each response of the reactivity was used to develop a mathematical model that correlates the reactivity to the absorbent preparation operatives through first order, second order, third order and interaction terms, according to the following third order polynomial equation:

$$Y = b_0 + \sum_{j=1}^{4} b_j x_j + \sum_{i,j=1}^{4} b_{ij} x_i x_j + \sum_{j=1}^{4} b_{jj} x_j^2 + \sum_{k,i,j=1}^{4} b_{kij} x_k x_i x_j + \sum_{j=1}^{4} b_{jjj} x_j^3 \quad (4)$$

Where Y is the predicted reactivity, $b_0$ is the first (or intercept) term, $b_j$ is the linear effect, $b_{ij}$ is the first order interaction effect, $b_{jj}$ is the squired effect, $b_{kij}$ is the second order interaction effect, $b_{jjj}$ is the cubic effect, $x_i$, $x_j$ and $x_k$ are coded operatives and n, the number of operatives in this case 4. Significance of the second-order model as shown in equation 4, was evaluated by analysis of variance (ANOVA). Insignificant coefficients were eliminated after the f (fisher)-test and the final model was obtained. Additional experiments were carried out to verify the predicted model and the associated optimal conditions.

To further compare the effect of additives on lime, sorption capacity and BET (Brunauer-Emmett-Teller) surface area analysis of sorbents with the highest reactivity from each additive was performed. Prior to sorption capacity and BET surface area analysis, the sorbents underwent a thorough mixing process with respect to the optimum lime to additive ratio. Hydration process then followed, in that, 10 g of the sorbents were mixed with 100 ml of distilled water and placed in a water bath at 60 °C for 4½ hours. The resulting slurry was filtered and dried in an oven at 100 °C for 16 hours to produce a dry solid. It was then ground, milled, and sieved to a particle size of utmost 200 µm.

A laboratory-scale fixed bed reactor was used to simulate dry FGD and calculate sorption capacity. The reaction zone is contained in a 0.009 m inner diameter stainless steel tube fitted in a furnace for isothermal operation. 0.2 g of the sorbent material was packed in the center of the reactor supported by 0.03 g of glass wool. The reactor is heated up to 87 °C. A nitrogen gas ($N_2$) stream was passed through a humidification system consisting of two 750 ml conical flasks immersed in a water bath at a constant temperature to produce 50% humidity ratio depending on the partial pressure of the steam. This humidified stream was allowed through the reactor for 10 minutes to humidify the sorbent. Humidified sorbents are more effective for desulfurization because, $SO_2$ is hydrated by the adsorbed water molecules on the sorbent surface before reacting [11]. After humidification, the nitrogen gas was mixed with a stream of 1500 ppm of sulfur dioxide gas. The total flow rate was set at 300 ml/min. At exit, the flue gas composition was continuously monitored by an IMR 2800P flue gas analyzer with readings taken at an interval of 20 seconds. A blank run was initially tested with glass wool only in the reactor. Afterwards, the sulphation test was run with the hydrated sorbent loaded. The experiment was done at least twice and the average of the results taken. The total sorbent utilization (sorption capacity) was given by [8]:

$$mol\ SO_2 retained \Big/ mol\ sorbent = \left(A_{bl} - A_{\exp}\right) C_0 10^{-6} \frac{\varphi_\upsilon}{23652} \frac{M_{sorbent}}{m_{sorbent}} \quad (5)$$

Where $A_{bl}$ is the area under the blank run, $A_{exp}$ is the area under the reaction curve, $C_0$ is the inlet concentration of $SO_2$ (ppm), $\varphi_v$ is the volumetric flow rate (ml/min$^{-1}$), 23652 is a volumetric constant depending on the operation conditions, $M_{sorbent}$ is the molar mass of the sorbent used and $m_{sorbent}$ is the mass of the sorbent.

Table III: Design of experiments matrix and its response

For the surface area analysis, BJH (Barret, Joyner and Halenda) was applied to obtain the pore-size distribution from nitrogen desorption data. Adsorption measurements were performed on a micrometrics ASAP 2020 Surface Area and Porosity analyzer by the principle of physical adsorption. High purity nitrogen (99.99%) was used.

The pore-size distribution is represented by the derivative $d(V_p)/d(d_p)$ as a function of pore diameter, where, $V_p$ is the pore volume and $d_p$ is the pore diameter. The samples were degassed before being used and characterized using a low temperature (- 196 °C) nitrogen adsorption isotherms measured over a wide range of relative pressures.

| Run | Block | VARIABLES | | | | RESPONSE (Reactivity Constant - Per Sec) | | | |
|---|---|---|---|---|---|---|---|---|---|
| | | A: Temp °C | B: Lime weight g | C: Vol of Water ml | D: Stirring Speed RPM | Fly Ash | Bottom Ash | W.A.S | Iron Waste |
| 1 | Block 1 | 60 | 0.75 | 200 | 225 | 0.000287 | 0.000252 | 0.000302 | 0.000306 |
| 2 | Block 1 | 50 | 1.125 | 250 | 287.5 | 0.000263 | 0.000241 | 0.000289 | 0.000249 |
| 3 | Block 1 | 70 | 1.125 | 150 | 287.5 | 0.000293 | 0.000287 | 0.000321 | 0.000291 |
| 4 | Block 1 | 60 | 0.75 | 200 | 225 | 0.000288 | 0.000254 | 0.000303 | 0.000289 |
| 5 | Block 1 | 50 | 1.125 | 150 | 162.5 | 0.000221 | 0.000209 | 0.000293 | 0.000283 |
| 6 | Block 1 | 70 | 0.375 | 250 | 287.5 | 0.000296 | 0.000280 | 0.000309 | 0.000284 |
| 7 | Block 1 | 50 | 0.375 | 250 | 162.5 | 0.000220 | 0.000218 | 0.000275 | 0.000289 |
| 8 | Block 1 | 70 | 1.125 | 250 | 162.5 | 0.000277 | 0.000277 | 0.000315 | 0.000235 |
| 9 | Block 1 | 50 | 0.375 | 150 | 287.5 | 0.000244 | 0.000235 | 0.000283 | 0.000266 |
| 10 | Block 1 | 70 | 0.375 | 150 | 162.5 | 0.000270 | 0.000258 | 0.000309 | 0.000267 |
| 11 | Block 2 | 70 | 0.375 | 250 | 162.5 | 0.000275 | 0.000270 | 0.000309 | 0.000284 |
| 12 | Block 2 | 50 | 0.375 | 150 | 162.5 | 0.000214 | 0.000206 | 0.000282 | 0.000262 |
| 13 | Block 2 | 70 | 1.125 | 150 | 162.5 | 0.000272 | 0.000269 | 0.000317 | 0.000303 |
| 14 | Block 2 | 50 | 1.125 | 250 | 162.5 | 0.000241 | 0.000223 | 0.000289 | 0.000248 |
| 15 | Block 2 | 70 | 1.125 | 250 | 287.5 | 0.000302 | 0.000291 | 0.000313 | 0.000289 |
| 16 | Block 2 | 60 | 0.75 | 200 | 225 | 0.000287 | 0.000253 | 0.000301 | 0.000285 |
| 17 | Block 2 | 70 | 0.375 | 150 | 287.5 | 0.000292 | 0.000279 | 0.000311 | 0.000235 |
| 18 | Block 2 | 50 | 1.125 | 150 | 287.5 | 0.000258 | 0.000236 | 0.000295 | 0.000291 |
| 19 | Block 2 | 50 | 0.375 | 250 | 287.5 | 0.000251 | 0.000239 | 0.000281 | 0.000280 |
| 20 | Block 2 | 60 | 0.75 | 200 | 225 | 0.000288 | 0.000254 | 0.000304 | 0.000299 |
| 21 | Block 3 | 60 | 0 | 200 | 225 | 0.000248 | 0.000230 | 0.000263 | 0.000249 |
| 22 | Block 3 | 60 | 0.75 | 300 | 225 | 0.000279 | 0.000258 | 0.000293 | 0.000276 |
| 23 | Block 3 | 60 | 0.75 | 200 | 350 | 0.000298 | 0.000287 | 0.000305 | 0.000287 |
| 24 | Block 3 | 60 | 0.75 | 100 | 225 | 0.000268 | 0.000244 | 0.000308 | 0.000285 |
| 25 | Block 3 | 60 | 1.5 | 200 | 225 | 0.000267 | 0.000244 | 0.000273 | 0.000277 |
| 26 | Block 3 | 40 | 0.75 | 200 | 225 | 0.000192 | 0.000193 | 0.000272 | 0.000282 |
| 27 | Block 3 | 60 | 0.75 | 200 | 225 | 0.000287 | 0.000254 | 0.000303 | 0.000288 |
| 28 | Block 3 | 60 | 0.75 | 200 | 225 | 0.000289 | 0.000255 | 0.000305 | 0.000331 |
| 29 | Block 3 | 80 | 0.75 | 200 | 225 | 0.000291 | 0.000296 | 0.000324 | 0.000283 |
| 30 | Block 3 | 60 | 0.75 | 200 | 100 | 0.000251 | 0.000247 | 0.000298 | 0.000259 |

## III. RESULTS AND DISCUSSION

Optimization process of various operatives affecting the reactivity of sorbents was analyzed by design of experiments in design expert software.

Table III shows the experimental design matrix and response of the experiments in terms of the reactivity constant. The maximum reactivity achieved by using the waste products is as shown in table IV. From these results, it is seen that iron waste produced the best sorbents in terms of maximum reactivity, followed by W.A.S, fly ash and finally bottom ash had the worst performance, though it was better when compared with lime without additives.

Table IV also indicates the results from the fixed bed experiments. All the sorbents were tested except for fly ash and bottom ash where the results of Ogenga in [12] were used because he used the same materials and conditions as found in this study. As noted, the results of lime without any additive is also included to prove that all sorbents improved lime's reactivity but by varying capacities. Table IV also presents the BET surface area values of all sorbents plus lime without any additive. In the same way, fly ash and bottom ash results were borrowed from [12]. It will be interesting to note that iron waste had a high sorption rate but very low surface area. From this observation, it was concluded that for iron waste blend sorbents, the metal oxide present in the sorbent were the reactive constituent and not the pozzolanic products as thought before. This conclusion was also supported by the fact that blends of lime to iron waste which had more iron waste than lime were more reactive. The results in table IV though, proves that sorbent made from iron waste are superior, followed by W.A.S, fly ash and finally bottom ash; also sorbents with additives had higher qualities than sorbents without additives. It was also noted that increase in surface area was the cause of increase in reactivity and sorption capacity in all sorbents which depended on pozzolanic reaction for increase in reactivity.

The reason why iron waste had a high performance can be attributed to its content of hematite. Hematite has been found to increase the reactivity of lime and vice versa. The authors in [5, 12] stated that hematite has a catalytic activity which favors the reaction of lime with acidic fluids thus increase in the reactivity whereas the authors in [6] noted that, depending on the amount of CaO available, complex product between the $Fe_2O_3$ and CaO will be formed owing to its basicity, thus making it more effective. Therefore, the actual cause of the performance of this additive is a complex mixture of the pozzolans, lime and the hematite in them, though the hematite played a major role.

The increase in surface area was attributed to the complex calcium alumina silicates products which have superior surface area. The amount and type of alumina silicates available in the additives dictates the amount of the reactive product being formed, therefore, W.A.S superiority might have being caused by the fact that it had more fine, hydrous and amorphous alumina silicates than the other additives. Bottom ash had a higher percentage of alumina silicates than other additives, but as it was seen in [12] that these alumina silicates were in hard agglomerates, partly amorphous-partly crystalline form compared to those in fly ash and W.A.S which are in hydrous and amorphous form and thus more reactive. Iron waste had little amount of alumina silicates thus the low improvement in area. W.A.S and fly ash superiority might have been caused by the fact that their fine structured amorphous alumina silicates are easily accessible by calcium ions in pozzolanic reactions. Therefore, the amount of alumina silicates only is not enough to generate a better additive compared to the type of alumina silicates. All in all, increase in area is the main reason why most sorbents had improved in reactivity (except in iron waste of course).

Table IV: Properties of the sorbent varied by lime to additive ratio

| **Sorbent blend (additive used)** | **Reactivity (X $10^{-4}$/sec)** | **Sorption Capacity (mol $SO_2$/mol Sorbent)** | **Surface Area ($m^2$/g)** |
|---|---|---|---|
| Fly Ash | 3.02 | 0.191 | 21.3 |
| Bottom Ash | 2.96 | 0.183 | 20.4 |
| W.A.S | 3.24 | 0.239 | 26.9 |
| Iron Waste | 3.31 | 0.260 | 19.1 |
| Lime (no additive) | 2.70 | 0.107 | 5.6 |

From statistical point of view, there are three tests required to evaluate the model, these are, significance of factor test, R-squired test and lack of fit test. The significance test was indicated by the Fisher variance ratio (the F-test value) and its associated probability (Prob>F). The model equations were evaluated by F-test ANOVA which revealed that these regressions are statistically significant at 95% confidence level. As a general rule the greater the F-value is from unity, the more certain it is that the empirical model describe the variation in the data about its mean and the estimated significant terms of the adsorbent preparation operatives are real. The values of prob>F which are 0.05 or less indicate significance. Quadratic models were suggested to be the best because their prob>F were less than 0.05 (<0.0001). By using multiple regression analysis, the response (reactivity constants) obtained in table III were correlated with the four operatives studied using the polynomial equations shown in equations (6 to 9) after excluding the insignificant terms identified using Fisher's test method.

Fly Ash: $Y_1 = 2.876 \text{ X } 10^{-4} + 2.341 \text{ X } 10^{-5}A + 4.282 \text{ X } 10^{-6}B + 3.495 \text{ X } 10^{-6}C + 1.276 \text{ X } 10^{-5}D - 1.153 \text{ X } 10^{-5}A^2 - 7.513 \text{ X } 10^{-6}B^2 - 3.413 \text{ X } 10^{-6}C^2 - 3.281 \text{ X } 10^{-6}D^2 - 2.735 \text{ X } 10^{-6}AB - 1.965 \text{ X } 10^{-6}AD$ (6)

Bottom Ash: $Y_2 = 2.536 \times 10^{-4} + 2.542 \times 10^{-5}A + 3.122 \times 10^{-6}B + 3.666 \times 10^{-6}C + 9.883 \times 10^{-5}D - 2.149 \times 10^{-6}A^2 - 4.025 \times 10^{-6}B^2 + 3.676 \times 10^{-6}D^2 - 1.62 \times 10^{-6}AB - 1.928 \times 10^{-6}AD - 1.903 \times 10^{-6}CD$ (7)

W.A.S: $Y_3 = 3.031X10^{-4} + 1.337X10^{-5}A + 3.983X10^{-6}B - 2.628X10^{-6}C - 7.559X10^{-6}B^2$ (8)

Iron Waste: $Y_4 = 2.841 \times 10^{-4} + 1.9 \times 10^{-5}A - 9.425 \times 10^{-6}B + 1.99 \times 10^{-6}C + 3.385 \times 10^{-6}D + 1.686 \times 10^{-6}A^2 - 4.918 \times 10^{-6}B^2 - 2.159 \times 10^{-6}C^2 - 1.622 \times 10^{-6}D^2 + 4.164 \times 10^{-6}AB - 1.993 \times 10^{-6}AD - 2.106 \times 10^{-6}BC$ (9)

Where A, B, C and D are as defined in table III. The coefficient of the full regression model equation and their statistical significance were determined and evaluated using design expert software.

Positive sign before terms indicate synergistic effect, while negative sign indicates antagonistic effect. The coefficients of the operatives in equations (6 to 9) represent the magnitude of the effect the variable have on reactivity. Table V shows the R values for the models. As it can be seen, the R values are very high for the models therefore the variability of the responses could accurately be explained by the mathematical models of equations (6 to 9). On the other hand, the values of $R^2$ for the models as shown in table V implies the percentage of the total variation in the reactivity responses that are attributed to the experimental operatives studied as stipulated by the models. The models are further supported by the low value of their respective standard deviations, the high value of Adequate Precisions (signal to noise ratio) and the closeness between their respective Adjusted R-squired and Predicted R-squired (table V).

Table V: Statistical values of the sorbents varied by lime to additive ratio

| Sorbent (additive used) | R | $R^2$ | Std. Dev. ($X10^{-6}$) | Adeq. Precision | Adj. $R^2$ | Ped. $R^2$ | Quadratic models L.O.F F-values |
|---|---|---|---|---|---|---|---|
| Fly Ash | 0.9982 | 0.9964 | 2.514 | 56.472 | 0.9925 | 0.9722 | 7.86 |
| Bottom Ash | 0.9995 | 0.9991 | 1.153 | 117.187 | 0.9982 | 0.9953 | 4.41 |
| W.A.S | 0.9889 | 0.9780 | 3.387 | 25.481 | 0.9544 | 0.8833 | 7.46 |
| Iron Waste | 0.9961 | 0.9923 | 2.727 | 46.257 | 0.9841 | 0.9558 | 7.38 |

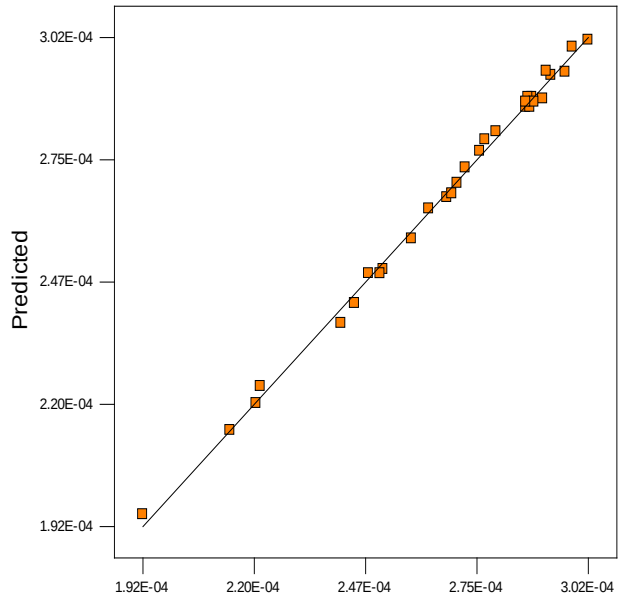

(a)

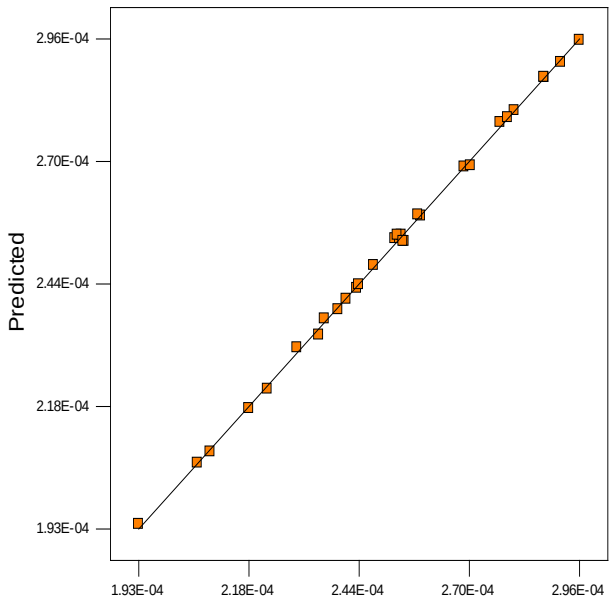

(b)

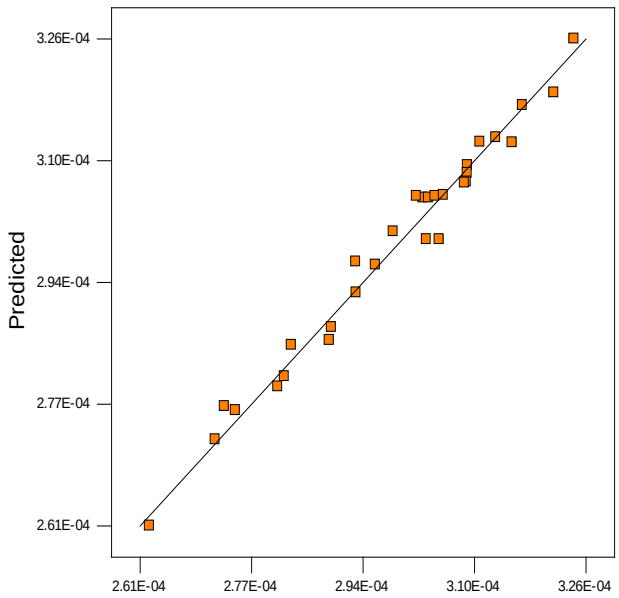


(c)

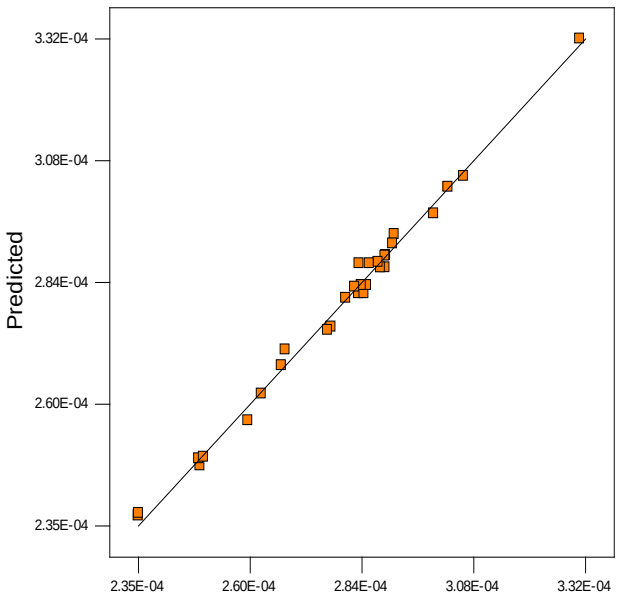


(d)

Fig 2: Model Predicted reactivity responses versus Actual (Experimental) reactivity responses. (a) Fly ash, (b) Bottom ash, (c) W.A.S and (d) Iron waste

The lack of fit (L.O.F) test compares the residual error to the experimental error (pure error) from replicated design points. It is this test which was used to select the quadratic models over the linear models, whereby both of them had model Prob>F values of less than 0.05 (< 0.0001) but the L.O.F test for the linear models were significant whereas the lack of fit test for the quadratic models were insignificant with F-values as shown in table V. This implies that lack of fit is not significant relative to pure errors. Plots of predicted results and actual (experimental) results (fig 2 a, b, c and d) further validates the mathematical model due to their linearity with the line of unit slope (perfect fit with points corresponding to zero error). These plots prove that the models describe the connection between the operatives and output adequately within the range of the operatives being studied. Extra experiments at different operation conditions confirmed the accuracy of these models.

Fig 3 to 6 are 3D plots of interaction between operatives and their effect to reactivity for the blended sorbents respectively. The X and Y-axis values of these figures are the real values. These response surfaces facilitate a straight-forward examination of the effects the operatives exert on the reactivity of the sorbent, especially with respect to the other operatives or in conjunction with them. The interactive effects of these operatives are very important in optimization process. The units of the variables and response are as shown in table II and 3. Part (a) shows the response surface of the reactivity with varying temperature (A) and lime to additive ratio in terms of amount of lime in a 1.5 g of sorbent (B), the other two variables were held constant at their mid-levels. Part (b) shows the response surface of the reactivity with varying solid to liquid ratio presented by volume of distilled water per 1.5 g of sorbent (C) and stirring speed (D), temperature and lime to additive ratio being held at their mid-levels.

The response surfaces have different variation depending on the type of additive and the specific operatives being varied. Temperature had the largest effect on the reactivity of all blends irrespective of the additive as shown in the figures. Large temperature effects were also depicted by the model equations where its linear coefficients were the highest, thus, supporting this conclusion. The behavior of the response (reactivity) depended on the type of additive and the operative being varied. The response were either sinusoidal or mini-max.

Apart from the effect of lime to additive ratio, temperature has been found to increase reaction rates by either increase in activation rate or decrease in diffusion resistance. Increasing the temperature is known to increase the rate of diffusion of molecules across external boundaries and internal pores owing to the decrease in viscosity of solutions. The enhancement of reactivity might be also due to increase in chemical interaction between the reactants, creation of new active sites, increase in mobility of reactants and increase in porosity and total pore volume at higher temperatures. The increase in pore volume and porosity might be due to temperature involvement in release of low-molecular weight reactants from the matrix structure resulting in pore development and porosity which increases the reaction surface area, resulting to higher reactivity [13].

On the other hand, as the solid to liquid ratio reduce, the reactivity appreciates. The increment of reactivity due to the solid to liquid ratio has been reported in literature [14]. A possible explanation is; increase in the amount of solid per unit liquid volume reduces dissolution rates [15]. Finally, agitation caused by stirring enhances convective mass transfer between reactants thus promoting the reaction [16].

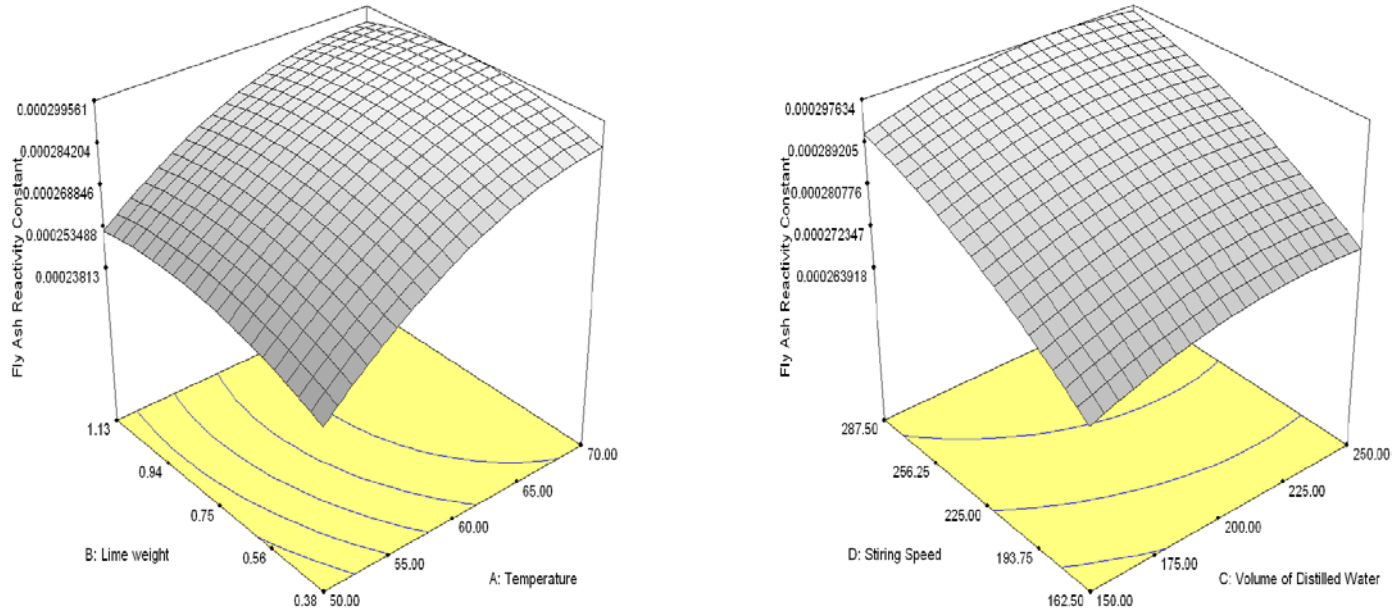


(a) (b)

Fig 3: Interactive effect of fly ash operatives on the reactivity (a) temperature and lime to additive ratio, (b) liquid to solid ratio and stirring speed.

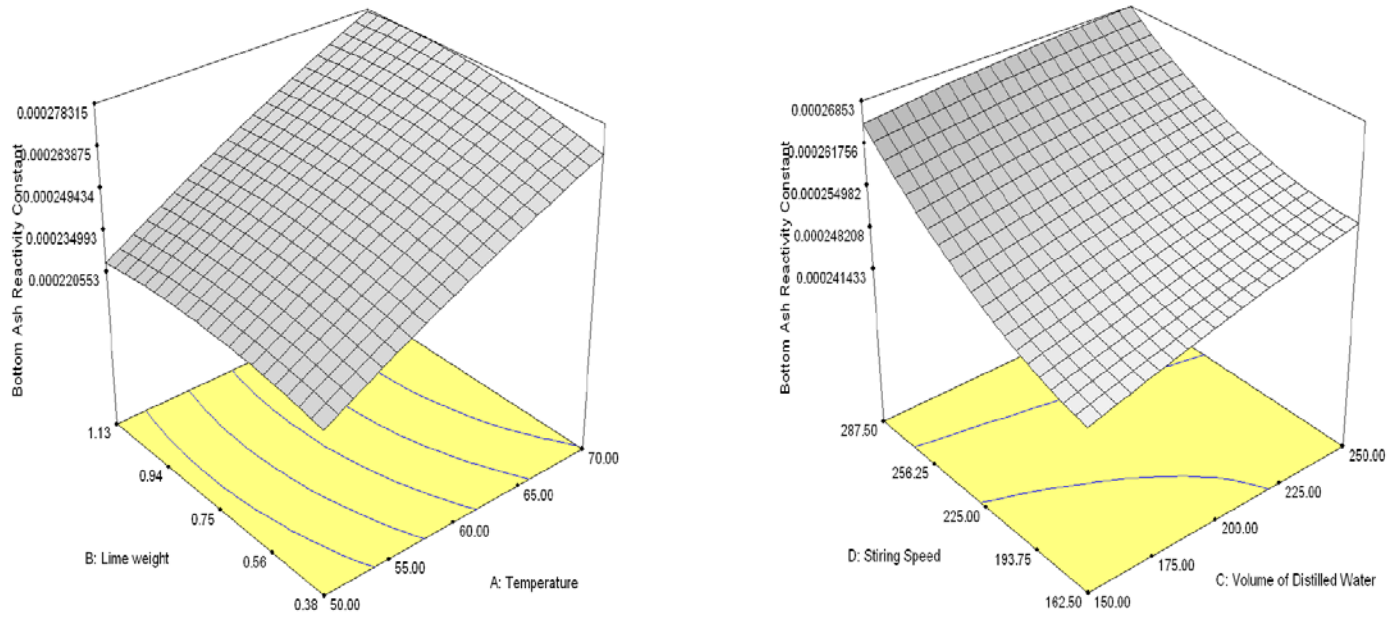


(a) (b)

Fig 4: Interactive effect of bottom ash operatives on the reactivity (a) temperature and lime to additive ratio, (b) liquid to solid ratio and stirring speed.

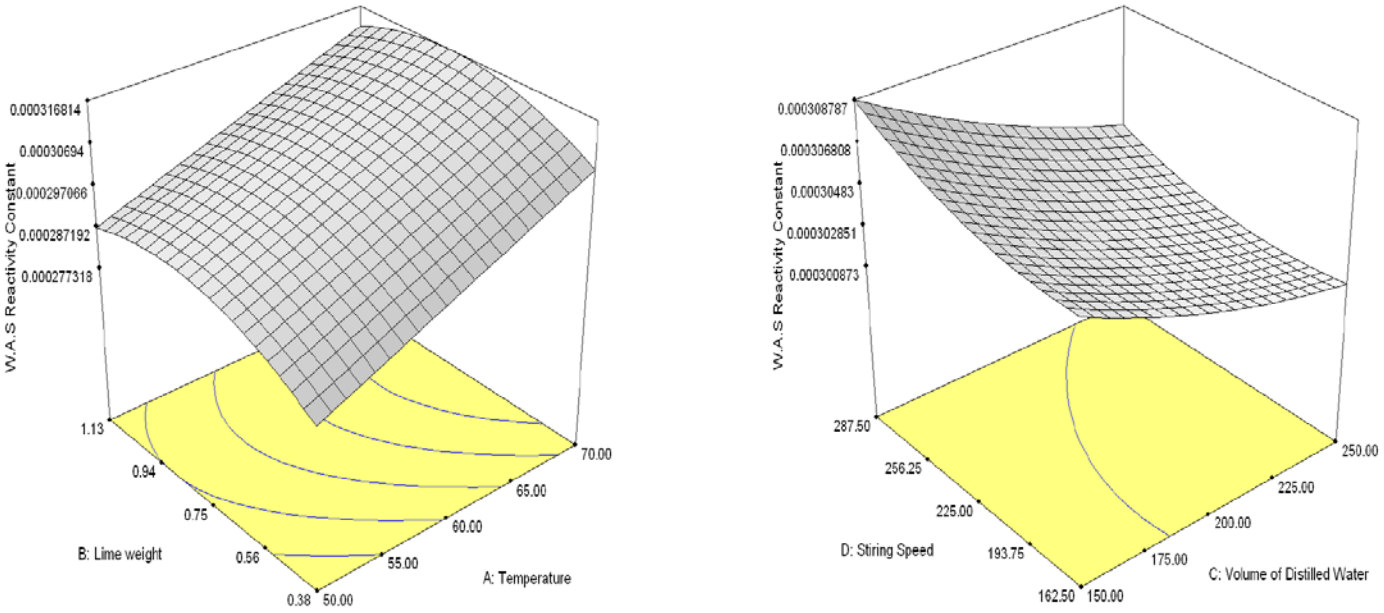


(a) (b)

Fig 5: Interactive effect of W.A.S operatives on the reactivity (a) temperature and lime to additive ratio, (b) liquid to solid ratio and stirring speed.

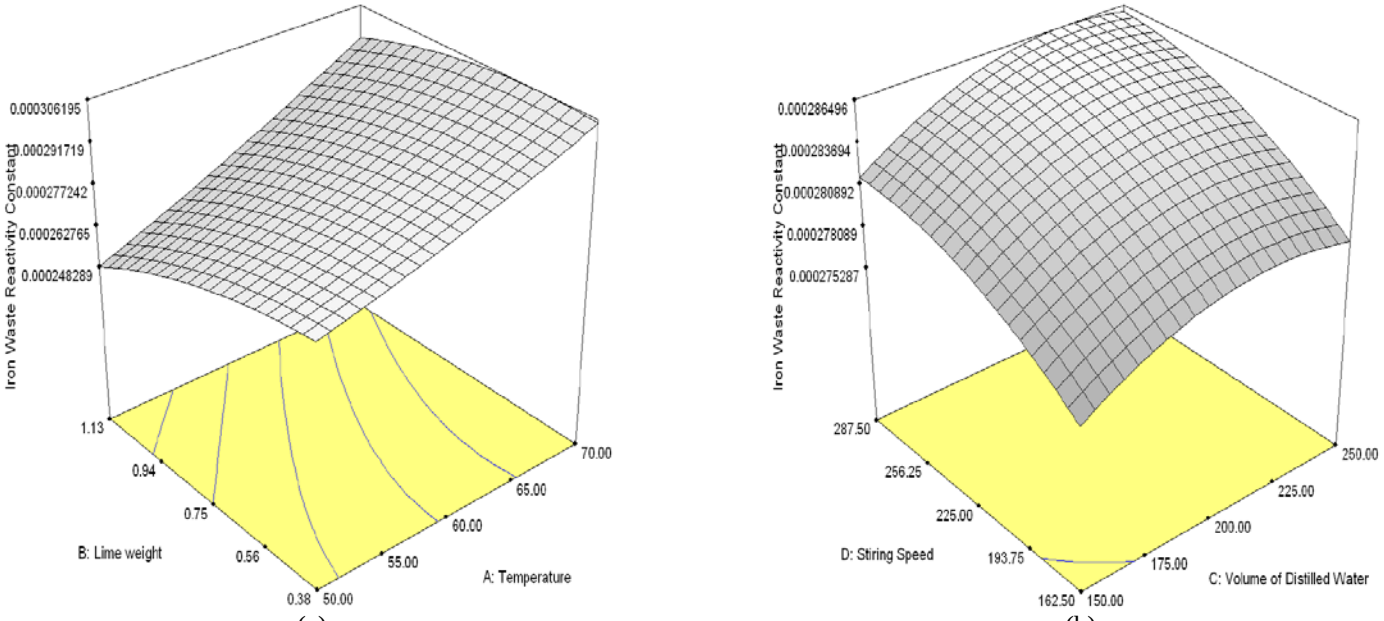


(a) (b)

Fig 6: Interactive effect of iron waste operatives on the reactivity (a) temperature and lime to additive ratio, (b) liquid to solid ratio and stirring speed.

Apart from the effects in the mass transfer, agitation also assists in detaching and removing the product layer therefore greatly reduces resistance due to product layer [17]. At high speeds, the turbulence becomes excessive that it impacts negatively on the reaction. On the other hand, very slow stirring speed do not enhance reactivity due to the inability to keep particles in suspension and sustain a realistically homogenous solution [18], thus an optimum stirring speed is important for maximizing reactivity.

## IV. CONCLUSION

Lime sorption capacity was observed to improve when it was blended with waste products. In a bid to approximate the best reactivity and additive, different ratios of lime to additives were prepared and examined in pH-stat apparatus. Design of experiments using design expert software was used in these experiments for regression analysis. Apart from lime to additive ratio, other operating parameters that affect reactivity were also varied. These are; temperature, solid to liquid ratio

and stirring speed. A laboratory scale fixed bed reactor and BET surface area analysis were used on best sorbents from each waste material in a bid to confirm and explain the results respectively. Iron waste was found to be the best additive, followed by W.A.S, fly ash and finally bottom ash. Iron waste was very reactive by the virtue of the content of hematite in it. The rest of the waste materials depended on the type of pozzolanic materials in them.

## REFERENCES

[1] Lee, K.T., et al., *Optimizing the specific surface area of fly ash-based sorbents for flue gas desulfurization*. Chemosphere, 2006. **62**(1): p. 89-96.

[2] Meng, X., et al., *In bed and downstream hot gas desulphurization during solid fuel gasification: A review*. Fuel Processing Technology, 2010. **In Press, Corrected Proof**.

[3] Slimane, R.B. and J. Abbasian, *Utilization of metal oxide-containing waste materials for hot coal gas desulfurization.* Fuel Processing Technology, 2001. **70**(2): p. 97-113.

[4] Pan, Y.G., et al., *Kinetic behaviour of iron oxide sorbent in hot gas desulfurization.* Fuel, 2005. **84**(9): p. 1105-1109.

[5] Siagi, Z.O., et al., *The effects of limestone type on the sulphur capture of slaked lime.* Fuel, 2007. **86**(17-18): p. 2660-2666.

[6] Fan, H., et al., *Effect of Calcium Oxide Additive on the Performance of Iron Oxide Sorbent for High-Temperature Coal Gas Desulfurization.* Journal of Natural Gas Chemistry, 2007. **16**(4): p. 404-408.

[7] Siagi, Z.O. and M. Mbarawa, *Dissolution rate of South African calcium-based materials at constant pH.* Journal of Hazardous Materials, 2009. **163**(2-3): p. 678-682.

[8] Marta, B.M., *Reactivity of Acid Gas Pollutants with Ca(OH)2 at Low Temperature in the Presence of Water Vapor*, in *Departament d'Enginyeria Química i Metal·lúrgia*. 2005, Universitat de Barcelona: Barcelona. p. 172.

[9] Levenspiel, O., *Chemical reaction engineering*. Third ed. 1999, Oregon: John Wiley and Sons. 668.

[10] Maina, P. and M. Mbarawa, *Use of fly ash, bottom ash and zeolite as additives for enhancing lime reactivity towards flue gas desulfurization.* Environmental Progress & Sustainable Energy, 2011: p. n/a-n/a.

[11] Siagi, O.Z., *Flue Gas Desulphurization Under South African Conditions*, in *Department of Mechanical Engineering*. 2008, Tshwane University of Technology: Pretoria. p. 232.

[12] Ogenga, D.O., *Performance of South African Calcium/Siliceous-Based Materials as Sorbents For SO2 Removal From Flue Gas*, in *Department of Mechanical Engineering*. 2009, Tshwane University of Technology: Pretoria. p. 159.

[13] Sumathi, S., et al., *Optimization of microporous palm shell activated carbon production for flue gas desulphurization: Experimental and statistical studies.* Bioresource Technology, 2009. **100**(4): p. 1614-1621.

[14] Ekmekyapar, A., N. DemirkIran, and A. Künkül, *Dissolution kinetics of ulexite in acetic acid solutions.* Chemical Engineering Research and Design, 2008. **86**(9): p. 1011-1016.

[15] Aphane, M.E., *The Hydration of Magnesium Oxide with Different Reactivities by Water and Magnesium Acetate*, in *Department of Chemistry*. 2007, University of South Africa: Pretoria. p. 160.

[16] Xiang, G., et al., *Dissolution rate of limestone for wet flue gas desulfurization in the presence of sulfite.* Journal of Hazardous Materials, 2009. **168**(2-3): p. 1059-1064.

[17] Xu, B.A., D.E. Giles, and I.M. Ritchie, *Reactions of lime with aluminate-containing solutions.* Hydrometallurgy, 1997. **44**(1-2): p. 231-244.

[18] Aydogan, S., et al., *Dissolution kinetics of celestite (SrSO4) in HCl solution with BaCl2*. Hydrometallurgy, 2006. **84**(3-4): p. 239-246.

# Kinetics of granulated scrap tyre pyrolysis via thermogravimetry

Peter T. Cherop, Sammy L. Kiambi and Paul Musonge

***Abstract*** The global consumption of tyres has increased over the years. However a very small percentage of the total mass of waste tyres can be recycled or reused for other applications. Land-filling has been considered an option to address the problem of scrap tyres. However, large space is required and the reusable resources are wasted. This therefore has led to environmental and economic problem of the disposal of the huge mass of scrap tyres. Scrap tyre pyrolysis, which is basically the thermal decomposition in an oxygen-free atmosphere, can be potentially involved with the recovery of both energy and material. Thermo gravimetric analysis (TGA) and derivative thermogravimetry (DTG) are the techniques commonly used to measure the mass loss kinetics associated with the vaporisation of materials during pyrolysis. Understanding the kinetics of scrap tyre pyrolysis is important in the optimisation design of industrial scale scrap tyre recycling. The purpose of this study was to determine the thermal degradation kinetics of scrap tyres by TGA/DTG, and to compare the apparent activation energy (Ea) and the pre-exponential factor (A) values calculated using Flynn-Wall-Ozawa, Kissinger-Akahira-Sunose and Coats–Redfern and methods. The experiments were conducted under a nitrogen atmosphere and a temperature range of 20°C to 600°C at different heating rates. The thermal decomposition started at an average temperature of about 285°C and was complete at 482°C for the four heating rates. Results indicate that higher heating rates lead to greater mass losses. The average mass loss was 63.59 wt. % while the mean $E_a$ values obtained by the different models used were similar.

**Key words:** activation energy, pyrolysis, scrap tyre, thermogravimetry.

## I. INTRODUCTION

With the increasing population size, the global consumption of tyres has increased over the years in order to meet both personal and commercial transport needs. Approximately 1.5 billion waste tyres are dumped all over the world [1], [2], of which only 15-20% is taken for reuse [3] while the remaining percentage is simply dumped into the earth. As scrap tyres are increasingly dumped, it is necessary that a suitable way of utilising them is explored.

Despite the fact that part of these wastes is recycled, the proportion recycled is small given the continuous accumulation of these scraps [4]. At the same time, owing to the rising concerns of crude oil prices and environmental impacts governments have been forced to focus on developing alternative fuels [5].Therefore, an appropriate means of treating these wastes should be explored, in the context of recovery of energy.Land filling, because of its simplicity, has always been considered an option to address the problem of the ever increasing amount of waste tyres. However, for this to be achieved, large space is required since reduction of the volume of tyres by compaction is not feasible [6], [7].

Due to the high volatile compound content and gross calorific value (GCV) of the scrap tyres (33-35MJ/kg), energy recovery is considered an attractive option for recycling [8]. Pyrolysis can be potentially involved in the recovery of energy from waste tyres. Pyrolysis is a thermal degradation process (in absence of oxygen) ,in which the organic volatile matter in the tyres is decomposed into low molecular weight products, while the inorganic components, majorly from non-volatile carbon black and steel remain as solid residue [9].The main products of pyrolysis are waste tyre pyrolysis oil, the non-condensable gases and char. Before tyres can be used for pyrolysis processes, they must undergo certain preparation stages such as shredding and further size reduction in order to achieve best results.

Tyres contain more than 100 different substances such as steel, rubber, silica gel, carbon black, zinc oxide, sulphur and many other additives .The rubbers commonly used during the manufacture of tyres are natural rubber (NR),styrene-butadiene rubber (SBR) and butadiene rubber (BR) or the blends of these three types. When rubber is subjected to an extended effort or moderate temperatures, polymer chains begin to slide leading to plastic deformation [10].The decomposition of these components occurs at different temperature ranges. Researchers have reported that the thermal decomposition behaviour of scrap tyres depends on the type of rubber and its contents [6], [11], [12].

The common techniques mainly used to measure the mass loss kinetics of materials as a result of valorisation during pyrolysis are thermogravimetric analysis (TGA) and derivative thermogravimetry (DTG) [13],[14]. Understanding the kinetics of scrap tyre pyrolysis is important in the optimization of design of industrial scale scrap tyre recycling.

P. T. Cherop, Department of Chemical Engineering, DUT (phone: +27767223609; e-mail: tumwet2@gmail.com).
S. L. Kiambi, Department of Chemical Engineering, DUT (e-mail: sammyk@dut.ac.za).
P. Musonge, Department of Chemical Engineering, DUT (e-mail: paulm@dut.ac.za).

The purpose of this study therefore was to understand the kinetics of pyrolysis of scrap tyres via TGA/DTG and to determine the activation energy ($E_a$) and pre-exponential factor (A) values using Kissinger-Akahira-Sunose (KAS), Flynn-Wall-Ozawa (FWO) and Coats–Redfern methods.

## II. EXPERIMENTAL

### A. Materials

The rubber crumb used in this study were obtained from Mathe Group,South Africa. The scrap tyre granule size used for the TGA ranged from 841-2000 microns, giving an average particle size of approximately 1400 microns.

### B. Thermal decomposition

The TGA was conducted using a Differential Scanning Calorimeter–Thermo Gravimetric Analyser SDT Q600.The mass of the samples used ranged between 5.68 mg-9.59 mg for different heating rates. To achieve the thermal decomposition, the samples were heated from 20°C to 600°C under nitrogen atmosphere (flow rate 100mLmin$^{-1}$) to prevent oxidation of the samples, which is highly undesirable during pyrolysis. Four heating rates (2°C/min, 5°C/min, 10°C/min, and 20°C/min) were used to examine the pyrolysis behaviour of tyre granules.

### C. Kinetic modelling background

The equation governing the thermal decomposition of solid state matter is expressed as follows:

$$\frac{d\alpha}{dt} = k(T)f(\alpha) \quad (1)$$

where $\alpha$ is the degree of conversion, $\frac{d\alpha}{dt}$ is the rate of conversion over time, while $k(T)$ is the reaction rate constant.The degree of conversion, $\alpha$ can be determined by:

$$\alpha = \frac{m_0 - m_t}{m_0 - m_f} \quad (2)$$

where $m_0$ is the initial mass of the sample, $m_f$ is the final mass of the sample and $m_t$ is the mass of the sample at a given temperature.

$k(T)$ is expressed according to Arrhenius equation as :

$$k(T) = A \exp\left(-\frac{E_a}{RT}\right) \quad (3)$$

where A (min$^{-1}$) is the pre-exponential factor, $E_a$ (J mol$^{-1}$) the activation energy, R (8.314 J mol$^{-1}$ k$^{-1}$) the universal gas constant, and T is the absolute temperature.

Combining eqs. (1) and (3) gives:

$$\frac{d\alpha}{dt} = A \exp\left(-\frac{E_a}{RT}\right) f(\alpha) \quad (4)$$

If there is a temperature increase with a constant heating rate, $\left(\frac{K}{s}\right)$, then $\beta = \frac{dT}{dt} = \frac{dT}{d\alpha} \times \frac{d\alpha}{dt}$ can be introduced to (4) to give (5)

$$\frac{d\alpha}{dt} = \frac{A}{\beta} \exp\left(-\frac{E_a}{RT}\right) f(\alpha) \quad (5)$$

Integration of (5) gives (6), which is the fundamental equation that is the basis of all kinetic methods used in the determination of kinetic parameters during non-isothermal solid state thermal degradation.

$$\int_0^\alpha \frac{d\alpha}{f(\alpha)} = g(\alpha) = \frac{A}{\beta} \int_{T_0}^{T} exp^{\left(-\frac{E_a}{RT}\right)} dT \quad (6)$$

where $g(\alpha)$ is the integral function of conversion and $T_0$ is the initial temperature of the experiment

### D. Flynn-Wall-Ozawa (FWO) Method

The FWO method [15], [16] is an iso-conversional method derived from Doyle's approximation [17] with (6), the rate of reaction in logarithmic can be expressed as:

$$ln(\beta) = ln\left(\frac{AE_a}{R\,g(\alpha)}\right) - 5.331 - 1.052\frac{E_a}{R}\frac{1}{T} \quad (7)$$

Therefore, for a constant $\alpha$ value, the plot $ln(\beta)$ against $\frac{1}{T}$ recorded at different heating rates should give a straight line. The value of $E_a$ can then be determined from the slope.

### E. Kissinger-Akahira-Sunose (KAS) Method

The KAS method [18], [19] is expressed as:

$$ln\left(\frac{\beta}{T^2}\right) = ln\left(\frac{AE_a}{R\,g(\alpha)}\right) - \frac{E_a}{RT} \quad (8)$$

Where, the plot of $ln\left(\frac{\beta}{T^2}\right)$ against $\frac{1}{T}$ gives a straight line. The slope of this plot can then be used to determine the$E_a$.

### F. Coats-Redfern Method

The Coats-Redfern method [20] describes the thermal decomposition mechanism from the mass loss. This method can therefore be used to determine the pre-exponential factor, activation energy, and the apparent reaction order. The method is based on (6) and an asymptotic approximation $\frac{2RT}{E_a} \to 0$ of the equation gives:

$$ln\left(\frac{g(\alpha)}{T^2}\right) = ln\left(\frac{AR}{\beta E}\right) - \frac{E_a}{RT} \quad (9)$$

where, a plot of $ln\left(\frac{g(\alpha)}{T^2}\right)$ against $\frac{1}{T}$ is a straight line. The $E_a$ is determined from the slope, while the pre-exponential factor, A is deduced from the intercept. The Coats-Redfern method is a common integral kinetic method used in the description of the reaction process during pyrolysis. Table I presents the theoretical explanation for the three kinetic mechanisms (first, second and third order reactions) to determine the $g(\alpha)$ values. High regression coefficient values informs the selection of the appropriate mechanism for the thermal decomposition of the solid matter.

## I. RESULTS AND DISCUSSION

### A. Thermal degradation of scrap tyre

The TGA/DTG curves of the scrap tyre samples at heating rates of 2 °C/min, 5 °C/min, 10 °C/min, and 20 °C/min are presented in Fig.1a,b,c and d ,while Fig.2 shows the extent of conversion for the four heating rates. The thermal decomposition (as seen in Fig.1 a, b, c, and d) started at about 275 °C, 284 °C, 287 °C and 293 °C and was complete at about 457 °C, 479 °C, 493 °C and 500 °C for the heating rates of 2 °C/min, 5 °C/min, 10 °C/min, and 20 °C/min respectively. For all the heating rates, there was no further weight loss above the temperature of 500 °C.

TABLE I
THEORETICAL EXPRESSION OF $g(\alpha)$ TO DETERMINE KINETIC VALUES BY COATS-REDFERN METHOD [21]-[23]

| Mechanism | $g(\alpha)$ |
|---|---|
| *Reaction order models* | |
| First-order (F1) | $-\ln(1-\alpha)$ |
| Second-order (F2) | $(1-\alpha)^{-1}-1$ |
| Third-order (F3) | $\left[\frac{(1-\alpha)^{-2}-1}{2}\right]$ |
| *Diffusion models* | |
| One way transport (D1) | $\alpha^2$ |
| Two way transport (D2) | $[(1-\alpha).\ln(1-\alpha)]+\alpha$ |
| Three way transport (D3) | $\left[1-(1-\alpha)^{\frac{1}{3}}\right]^2$ |
| Giustling- Brounshtein (D4) | $1-\left(\frac{2\alpha}{3}\right)-(1-\alpha)^{\frac{2}{3}}$ |
| *Geometrical contraction models* | |
| Contracting area (R2) | $\left[1-(1-\alpha)^{\frac{1}{2}}\right]$ |
| Contracting volume (R3) | $\left[1-(1-\alpha)^{\frac{1}{3}}\right]$ |

The mean peak value ($T_m$ = 367.2 °C) obtained corresponds to that ($T_m$ = 373.1 °C) reported by other

authors [13].The TGA/DTG curves indicate that ,there is a shift to higher temperatures as the heating rate increases during the entire three-stage thermal decomposition process. As it can be seen in the TGA curves, a weight loss of about 1% was achieved at a temperature range of about 130°C – 170 °C.

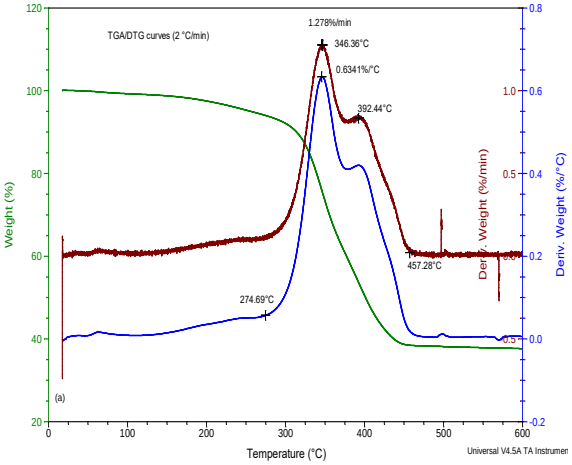


**Fig.1a.** TGA/DTG curves at 2 °C/min

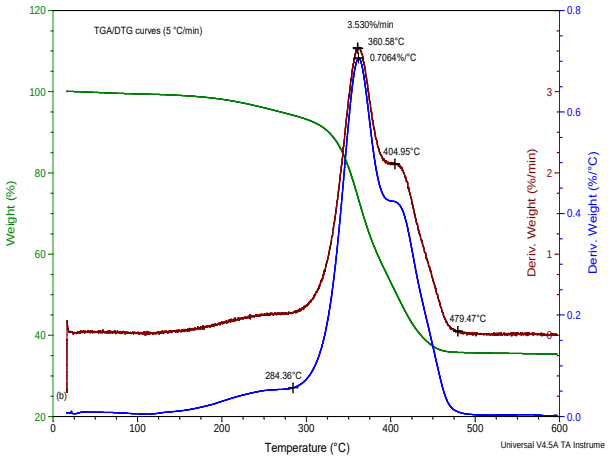


**Fig.1b.** TGA/DTG curves at 5 °C/min

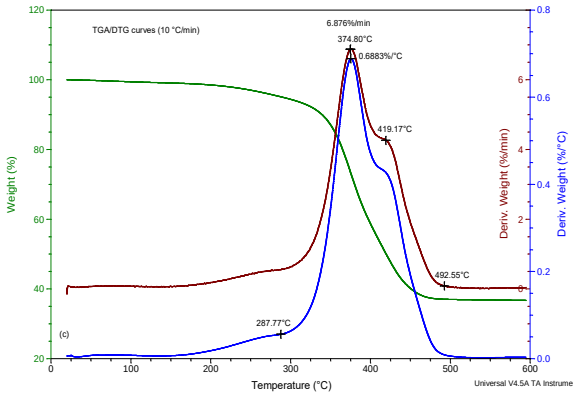


**Fig.1c.** TGA/DTG curves at 10 °C/min

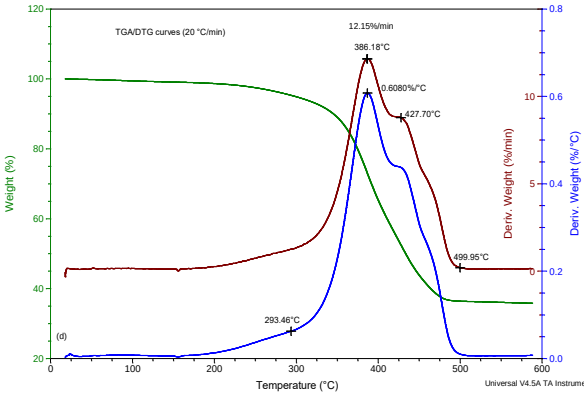


**Fig.1d.** TGA/DTG curves at 20 °C/min

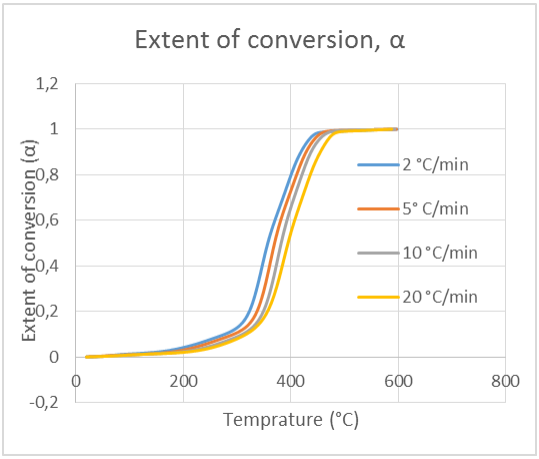


**Fig.2.** Variation of extent of conversion with temperature

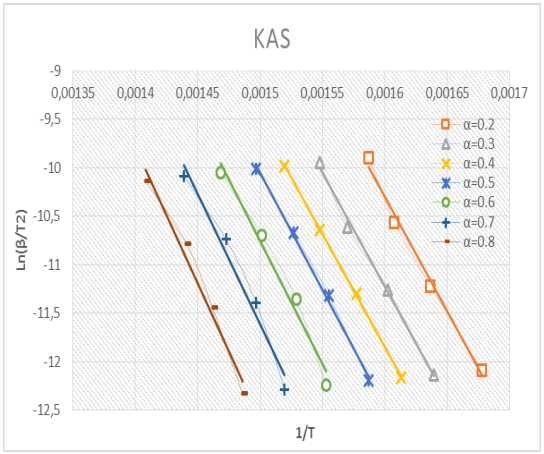


**Fig.3.** KAS plot at various conversion degrees.

*B. Kinetic analysis of tyre pyrolysis*

The iso-conversional KAS and FWO models, and model-free Coats-Redfern method were used to determine the kinetic parameters of tyre pyrolysis. The parameters determined included the activation energy and pre-exponential factor. The iso-conversional models were used to establish the relationship between the extent of conversion and the activation energies. Using KAS model, a plot of $ln\left(\frac{\beta}{T^2}\right)$ versus $\frac{1}{T}$ gave a slope of $-\frac{E_a}{R}$, from which $E_a$ was determined while a plot of $ln(\beta)$ versus $\frac{1}{T}$ using the FWO model gave a slope of $-1.052\frac{E_a}{R}$, from which $E_a$ was determined. Fig. 4 and 5 show the kinetic plots of scrap tyre pyrolysis using the two models.

The conversion degrees considered ranged between 0.2-0.8 (Fig.3 and 4), while those below 0.2 and above 0.8 were not included owing to the low correlation values [24].Table 2 shows the values of activation energies calculated using KAS and FWO methods. The average values of activation energies obtained using KAS and FWO methods were 207.88 kJmol$^{-1}$ and 207.89 kJmol$^{-1}$ respectively. The activation energy values obtained indicate that the two methods were in agreement with a deviation of below 1%,which confirms that KAS and FWO models have a high predictive power [25].High regression coefficient ($R^2$) values, for both methods, were obtained at conversion degrees of between α = 0.3-0.5,while α of 0.7 and 0.8 gave the lowest $R^2$ values.

The kinetic analysis shows that the activation energy highly depends on the extent of conversion, an indication that scrap tyre pyrolysis is a complex process that consists of various reactions that occur at different stages. As seen in Table II, there is a decrease in activation energy values between α = 0.2 and α = 0.3 in both KAS and FWO methods. However, there is an increase in $E_a$ from about 197

kJmol$^{-1}$ at α = 0.3 to about 207 kJmol$^{-1}$ at α = with extent of conversion is as a result of the variation in reaction mechanism. The results indicate that KAS and FWO models gave similar results, where the mean $E_a$ obtained using KAS method was 207.88 kJmol$^{-1}$ while the value obtained using FWO method was 207.89 kJmol$^{-1}$

The pre-exponential factors were determined using Coats-Redfern method by using activation energy values obtained from KAS and FWO models by applying the first-order reaction model (F1) . Table 3 shows the values of calculated pre-exponential factors at heating rates 5 °C/min, 10 °C/min, and 20 °C/min. From Table III, it can be seen that the pre-exponential factor values increase with heating rate 0.8.The change in activation energy values at different conversion degrees (α).The mean pre-exponential factor values were $6.32 \times 10^5$ min$^{-1}$, $1.41 \times 10^7$ min$^{-1}$ and $1.08 \times 10^8$ min$^{-1}$ for heating rates of 5 °C/min, 10 °C/min, and 20 °C/min respectively. This gives an average pre-exponential factor value of $3.62 \times 10^7$ min$^{-1}$.In a study conducted by López, et al. [13] a mean pre-exponential factor value of $2.49 \times 10^{10}$ min$^{-1}$ was obtained. In another study conducted by Uzun and Yaman [7], the values of the mean $E_a$ and pre-exponential factor value obtained were 78.72 kJmol$^{-1}$ and $3.05 \times 10^5$ min$^{-1}$ respectively. The discrepancy in Ea and A (min$^{-1}$) could be due to the variation in proportions of SBR,NR and BR in different tyres.

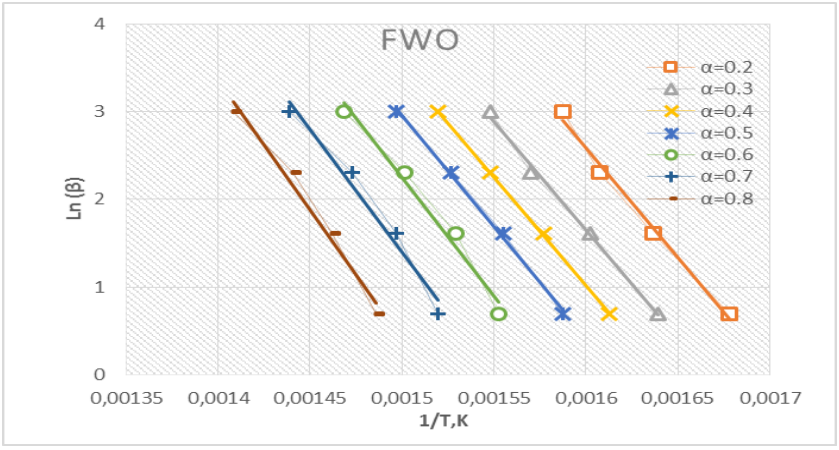


**Fig.4.** FWO plot at various conversion degrees.

TABLE II
ACTIVATION ENERGIES ($E_A$) AND CORRELATION COEFFICIENTS ($R^2$) OBTAINED USING KAS AND FWO METHODS

| Conversion (α) | $E_a$; KAS (kJmol$^{-1}$) | $R^2$ | Ea; FWO (kJmol$^{-1}$) | $R^2$ | % Difference |
|---|---|---|---|---|---|
| 0.20 | 197.27 | 0.9913 | 197.20 | 0.9801 | 0.04 |
| 0.30 | 194.38 | 0.9951 | 194.69 | 0.9956 | -0.16 |
| 0.40 | 194.24 | 0.9997 | 194.73 | 0.9997 | -0.25 |
| 0.50 | 200.53 | 0.9972 | 200.86 | 0.9975 | -0.17 |
| 0.60 | 211.86 | 0.9779 | 211.86 | 0.9801 | 0.00 |
| 0.70 | 221.96 | 0.9724 | 221.68 | 0.9750 | 0.13 |
| 0.80 | 234.90 | 0.9774 | 234.22 | 0.9796 | 0.29 |
| Average | 207.88 | | 207.89 | | -0.01 |

TABLE III
PRE-EXPONENTIAL FACTOR VALUES (A, MIN-1) AS DETERMINED BY COATS-REDFERN METHOD USING EA VALUES FROM KAS AND FWO METHODS.

| Conversion(α) | β = 5 °C/min | | β=10 °C/min | | β=20 °C/min | |
|---|---|---|---|---|---|---|
| | KAS | FWO | KAS | FWO | KAS | FWO |
| 0.2 | 6.00E+05 | 6.00E+05 | 1.34E+07 | 1.34E+07 | 1.03E+08 | 1.03E+08 |
| 0.3 | 5.91E+05 | 5.92E+05 | 1.32E+07 | 1.32E+07 | 1.01E+08 | 1.01E+08 |
| 0.4 | 5.91E+05 | 5.92E+05 | 1.32E+07 | 1.33E+07 | 1.01E+08 | 1.02E+08 |
| 0.5 | 6.10E+05 | 6.11E+05 | 1.36E+07 | 1.37E+07 | 1.05E+08 | 1.05E+08 |
| 0.6 | 6.44E+05 | 6.44E+05 | 1.44E+07 | 1.44E+07 | 1.10E+08 | 1.10E+08 |
| 0.7 | 6.75E+05 | 6.74E+05 | 1.51E+07 | 1.51E+07 | 1.16E+08 | 1.16E+08 |
| 0.8 | 7.14E+05 | 7.12E+05 | 1.60E+07 | 1.59E+07 | 1.22E+08 | 1.22E+08 |
| Average | 6.32E+05 | 6.32E+05 | 1.41E+07 | 1.41E+07 | 1.08E+08 | 1.08E+08 |

## II. CONCLUSION

The motivation behind this study was to understand the kinetics of scrap tyre pyrolysis. TGA was conducted for heating rates of 2°C , 5°C, 10 °C and 20 °C in nitrogen environment. The TGA revealed that pyrolysis of scrap tyres is a three-stage stage process that encompasses removal of oil and lubricants in the scrap tyre, breakdown of NR, and breakdown of SBR and BR.

The data obtained from TGA was applied to both iso-conversional and model free models in order to determine the activation energies and pre-exponential factor values. The mean activation energy value obtained from both KAS and FWO models were similar (207 kJ/mol).This value was then used in the Coats-Redfern model to determine the pre-exponential factor value ($3.62 \times 10^7$ $min^{-1}$). The kinetic data obtained from this study could be used in the design and optimisation of industrial scale scrap tyre pyrolysis units.

## ACKNOWLEDGEMENT

The financial assistance of South Africa's National Research Foundation (NRF) towards this research is hereby acknowledged.

## REFERENCES

[1] Y. Su and B. Zhao, "Pyrolysis of waste tire powder and its comparison with Shenhua coal," in *Energy and Environment Technology, 2009. ICEET'09. International Conference on*, 2009, pp. 262-265.

[2] S. Uçar and S. Karagöz, "Co-pyrolysis of pine nut shells with scrap tires," *Fuel*, vol. 137, pp. 85-93, 2014.

*[3]* [3] Y. Su and W. Deng, "A thermogravimetric study of waste tire powder," in *E-Product E-Service and E-Entertainment (ICEEE), 2010 International Conference on*, 2010, pp. 1-4.

[4] P. Parthasarathy, H. S. Choi, H. C. Park, J. G. Hwang, H. S. Yoo, B.-K. Lee, *et al.*, "Influence of process conditions on product yield of waste tyre pyrolysis-A review," *Korean Journal of Chemical Engineering*, vol. 33, pp. 2268-2286, 2016.

[5] J. Lin, G. Gaustad, and T. A. Trabold, "Profit and policy implications of producing biodiesel–ethanol–diesel fuel blends to specification," *Applied energy*, vol. 104, pp. 936-944, 2013.

[6] M. R. Islam, H. Haniu, and J. Fardoushi, "Pyrolysis kinetics behavior of solid tire wastes available in Bangladesh," *Waste Management*, vol. 29, pp. 668-677, 2// 2009.

[7] B. Uzun and E. Yaman, "Thermogravimetric characteristics and kinetics of scrap tyre and Juglans regia shell co-pyrolysis," *Waste Management & Research*, p. 0734242X14539722, 2014.

[8] F. A. López, T. A. Centeno, F. J. Alguacil, and B. Lobato, "Distillation of granulated scrap tires in a pilot plant," *Journal of Hazardous Materials*, vol. 190, pp. 285-292, 6/15/ 2011.

[9] I. de Marco Rodriguez, M. F. Laresgoiti, M. A. Cabrero, A. Torres, M. J. Chomón, and B. Caballero, "Pyrolysis of scrap tyres," *Fuel Processing Technology*, vol. 72, pp. 9-22, 8// 2001.

[10] A. Nieto-Márquez, E. Atanes, J. Morena, F. Fernández-Martínez, and J. L. Valverde, "Upgrading waste tires by chemical activation for the capture of SO2," *Fuel Processing Technology*, vol. 144, pp. 274-281, 4// 2016.

[11] D. Y. C. Leung and C. L. Wang, "Kinetic study of scrap tyre pyrolysis and combustion," *Journal of Analytical and Applied Pyrolysis*, vol. 45, pp. 153-169, 5// 1998.

[12] S. Seidelt, M. Müller-Hagedorn, and H. Bockhorn, "Description of tire pyrolysis by thermal degradation behaviour of main components," *Journal of Analytical and Applied Pyrolysis*, vol. 75, pp. 11-18, 1// 2006.

[13] F. A. López, A. A. El Hadad, F. J. Alguacil, T. A. Centeno, and B. Lobato, "Kinetics of the Thermal Degradation of Granulated Scrap Tyres: a Model-free Analysis," *Materials Science*, vol. 19, pp. 403-408, 2013.

[14] A. Luyima, L. Zhang, J. Kers, and V. Laurmaa, "Recovery of Metallic Materials from Printed Wiring Boards by Green Pyrolysis Process," *Materials Science*, vol. 18, pp. 238-242, 2012.

[15] T. Ozawa, "A new method of analyzing thermogravimetric data," *Bulletin of the chemical society of Japan*, vol. 38, pp. 1881-1886, 1965.

[16] J. H. Flynn and L. A. Wall, "A quick, direct method for the determination of activation energy from thermogravimetric data," *Journal of Polymer Science Part C: Polymer Letters*, vol. 4, pp. 323-328, 1966.

[17] C. Doyle, "Kinetic analysis of thermogravimetric data," *Journal of applied polymer science*, vol. 5, pp. 285-292, 1961.

[18] H. E. Kissinger, "Reaction kinetics in differential thermal analysis," *Analytical chemistry*, vol. 29, pp. 1702-1706, 1957.

[19] T. Akahira and T. Sunose, "Joint convention of four electrical institutes," *Res Rep Chiba Inst Technol*, vol. 16, pp. 22-31, 1971.

[20] A. W. Coats and J. Redfern, "Kinetic parameters from thermogravimetric data," *Nature*, vol. 201, pp. 68-69, 1964.

[21] J. E. White, W. J. Catallo, and B. L. Legendre, "Biomass pyrolysis kinetics: a comparative critical review with relevant agricultural residue case studies," *Journal of Analytical and Applied Pyrolysis*, vol. 91, pp. 1-33, 2011.

[22] M. A. Islam, M. Asif, and B. H. Hameed, "Pyrolysis kinetics of raw and hydrothermally carbonized Karanj (Pongamia pinnata) fruit hulls via thermogravimetric analysis," *Bioresource Technology*, vol. 179, pp. 227-233, 3// 2015.

[23] M. A. Islam, M. Auta, G. Kabir, and B. H. Hameed, "A thermogravimetric analysis of the combustion kinetics of karanja (Pongamia pinnata) fruit hulls char," *Bioresource Technology*, vol. 200, pp. 335-341, 1// 2016.

[24] T. Damartzis, D. Vamvuka, S. Sfakiotakis, and A. Zabaniotou, "Thermal degradation studies and kinetic modeling of cardoon (Cynara cardunculus) pyrolysis using thermogravimetric analysis (TGA)," *Bioresource Technology*, vol. 102, pp. 6230-6238, 5// 2011.

[25] M. A. Lopez-Velazquez, V. Santes, J. Balmaseda, and E. Torres-Garcia, "Pyrolysis of orange waste: A thermo-kinetic study," *Journal of Analytical and Applied Pyrolysis*, vol. 99, pp. 170-177,1//201

# An analysis of MUSIC, ESPRIT and root-MUSIC Direction of Arrival estimation techniques in Smart Antennas

Mr. Robert Macharia Maina and Dr. Kibet Lang'at and Dr. P. K. Kihato

*Abstract*—Smart Antennas are a core part of modern wireless communication systems owing to the ever increasing demands on network capacity. Smart Antennas are essentially spatial filters encompassing antenna array structures and beamforming techniques aimed at optimizing radiation/ reception in a wireless communication link. A variety of beamforming techniques rely on knowledge of the Directions of Arrival (DoAs) of desired and interfering signals. Methods that have been proposed in literature to keep track of mobile DoAs include MUltiple SIgnal Classification (MUSIC), Estimation of Signal Parameter via Rotational Invariance Technique (ESPRIT) and root-MUSIC. This paper essentially seeks to analyze the performance of the three listed DoA estimation methods from the point of view of varying: Signal to Noise Ratio (SNR), antenna array size and DoA angular separation. MATLAB software environment is used as the main analysis tool.

*Keywords*—Direction of Arrival, ESPRIT, MUSIC, root-MUSIC, Smart Antenna

## I. INTRODUCTION

Smart Antennas (essentially Spatial Division Multiple Access (SDMA) aids) have been adopted as a worthy tool towards increasing wireless communication networks capacity. Among receive beamforming techniques utilized in smart antennas are those that require signal Direction of Arrival (DoA) information such as the null steering technique. DoA information is usually unavailable particularly in mobile communication networks. There are techniques that have been developed to aid in DoA estimation. Such methods include: Bartlett, Capon (Minimum Variance Distortion-less Response (MVDR)), Min-norm, MUltiple SIgnal Classification (MUSIC), root-MUSIC and Estimation of Signal Parameters via Rotational Invariance Techniques (ESPRIT) [1].

MUSIC, root-MUSIC and ESPRIT DoA estimation methods have been widely adopted and are the focus of this paper. Reviews pertaining the three DoA estimation methods are given in the next three Sections followed by pertinent evaluations in situations involving varying: Signal to Noise Ratio (SNR), antenna array size and DoA angular separation.

Fig. 1 depicts a typical DoA estimation problem featuring a 4-element linear antenna array and three signal DoAs that ought to be estimated.

Mr. Robert Macharia Maina, Department of Telecommunication and Information Engineering, JKUAT (e-mail: robertisaacm@gmail.com).

Dr. Kibet Lang'at, Department of Telecommunication and Information Engineering, JKUAT.

Dr. P. K. Kihato, Department of Electrical and Electronic Engineering, JKUAT.

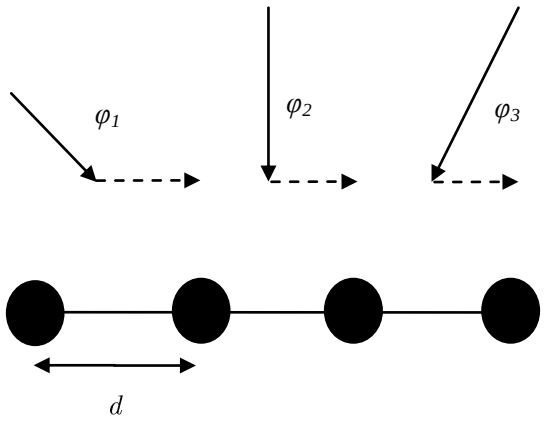


Fig. 1. DoA estimation problem using a linear antenna array

## II. MUSIC DoA ESTIMATION METHOD

Considering a scenario involving $M$ noise corrupted signals incident on a $N$ element linear antenna array, the resultant mathematical model is as per (1) or (2). The components of (2) can be expressed as per (3) and (4).

$$\mathbf{X} = \sum_{m=1}^{M} \alpha_m \mathbf{s}(\phi_m) + \mathbf{n} \tag{1}$$

$$\mathbf{X} = \mathbf{S}\alpha + \mathbf{n} \tag{2}$$

$$\mathbf{S} = [\mathbf{s}(\phi_1), \mathbf{s}(\phi_2)...\mathbf{s}(\phi_m)] \tag{3}$$

$$\alpha = [\alpha_1, \alpha_2...\alpha_m]^T \tag{4}$$

$\mathbf{S}$ is an $N$ by $M$ matrix encompassing some $M$ steering vectors.

The correlation matrix corresponding to $\mathbf{X}$ is as per (5).

$$\mathbf{R} = E[\mathbf{X}\mathbf{X}^H] \tag{5}$$

Substituting $\mathbf{X}$ in (5) with (2) yields (6).

$$\mathbf{R} = E[\mathbf{X}\mathbf{X}^H] = E[\mathbf{S}\alpha\alpha^H\mathbf{S}^H] + E[\mathbf{n}\mathbf{n}^H] \tag{6}$$

In a summarized form, (6) can be framed as (7).

$$\mathbf{R} = \mathbf{S}\mathbf{A}\mathbf{S}^H + \sigma^2\mathbf{I} = \mathbf{R}_s + \sigma^2\mathbf{I} \tag{7}$$

The matrix $\mathbf{A}$ in (7) is equivalent to (8).

$$\mathbf{A} = \begin{bmatrix} E[\alpha_1^2] & 0 & ... & 0 \\ 0 & E[\alpha_2^2] & ... & 0 \\ & & . & \\ & & . & \\ 0 & 0 & ... & E[\alpha_M^2] \end{bmatrix} \tag{8}$$

$\mathbf{R}_s$ (signal covariance matrix) is an $N$ by $N$ matrix of rank $M$. Associated with $\mathbf{R}_s$ are $N$-$M$ eigenvectors ($\mathbf{q}_m$) corresponding to the zero eigenvalue (9).

$$\mathbf{R}_s\mathbf{q}_m = \mathbf{SAS}^H\mathbf{q}_m = 0 \tag{9}$$

Consequently, $\mathbf{q}_m^H\mathbf{SAS}^H\mathbf{q}_m = 0$ and $\mathbf{S}^H\mathbf{q}_m = 0$ since $\mathbf{A}$ is positive definite.

The implication of $\mathbf{S}^H\mathbf{q}_m = 0$ is that all the $N$-$M$ eigenvectors ($\mathbf{q}_m$) corresponding to the zero eigenvalue are orthogonal to all $M$ signal steering vectors, the foundation of MUSIC. The pseudo-spectrum corresponding to MUSIC is as per (10 and 11).

$$P_{MUSIC}(\phi) = \frac{1}{\Sigma_{m=1}^{N-M}|\mathbf{s}^H(\phi)\mathbf{q}_m|^2} \tag{10}$$

$$P_{MUSIC}(\phi) = \frac{1}{\mathbf{s}^H(\phi)\mathbf{Q}_n\mathbf{Q}_n^H\mathbf{s}(\phi)} \tag{11}$$

In (11), $\mathbf{Q}_n$, is the matrix of the eigenvectors.

Owing to the fact that the eigenvectors making up the matrix $\mathbf{Q}_n$ are orthogonal to the signal steering vectors, the denominator corresponding to (11) is zero when $\phi$ is a signal direction. Consequently, estimated signal directions correspond to the highest peaks contained in the pseudo-spectrum. The matrix $\mathbf{R}_s$ is usually estimated from a convenient number of snapshots of received data (12).

$$\mathbf{R} = \frac{1}{K}\Sigma_{k=1}^{K}\mathbf{X}_k\mathbf{X}_k^H \tag{12}$$

Studies utilizing MUSIC DoA estimation method can be found in [2], [3], [4], [5] and [6].

## III. ROOT-MUSIC DoA ESTIMATION METHOD

Shortcomings associated with the MUSIC DoA estimation method are the fact that accuracy is limited by the extent of discretization at which (11) is evaluated and a search algorithm (or human intervention) is a necessity in identifying the peaks of (11). Root-MUSIC gives numeric values corresponding to estimated DoAs.

Defining some parameter $z$ as per (13), and with reference to Fig. 1, a steering vector can be defined as per (14) given that the array in question is uniform and with isotropic elements.

$$z = e^{jkdcos\phi} \tag{13}$$

$$\mathbf{s}(\phi) = \begin{bmatrix} 1 & z & z^2 & . & . & . & z^{N-1} \end{bmatrix}^T \tag{14}$$

Consequently,

$$\mathbf{q}_m^H\mathbf{s} = \sum_{n=0}^{N-1} q_{mn}^* z^n = q_m(z) \tag{15}$$

The product $\mathbf{q}_m^H\mathbf{s}$ is equivalent to a polynomial in z as per (15). The directions ($\phi$) where $\mathbf{q}_m \perp \mathbf{s}(\phi)$ are desired, essentially this translates to looking for the roots of a polynomial going by (15).

The polynomial whose roots are desired is arrived at in (16) to (18).

$$P_{MUSIC}^{-1}(\phi) = \mathbf{s}^H(\phi)\mathbf{Q}_n\mathbf{Q}_n^H\mathbf{s}(\phi) = \mathbf{s}^H(\phi)\mathbf{Cs}(\phi) \tag{16}$$

$$P_{MUSIC}^{-1}(\phi) = \sum_{m=0}^{N-1}\sum_{n=0}^{N-1} z^n C_{mn} z^{-m} \tag{17}$$

$$P_{MUSIC}^{-1}(\phi) = \sum_{m=0}^{N-1}\sum_{n=0}^{N-1} z^{n-m} C_{mn} \tag{18}$$

Setting setting $l = n - m$ yields (19) (a polynomial of degree $(2N-2)$ with $(2N-2)$ zeros $z$).

$$P_{MUSIC}^{-1}(\phi) = \sum_{l=-(N-1)}^{N+1} z^l C_l \tag{19}$$

The DoAs are obtained as per (20).

$$\phi_m = cos^{-1}[\frac{\Im \ln(z_m)}{kd}] \quad m = 1, ...M \tag{20}$$

Studies utilizing root-MUSIC DoA estimation method can be found in [7] and [8].

## IV. ESPRIT DoA ESTIMATION METHOD

ESPRIT DoA estimation method is grounded on the fact that the steering vector features elements with progressive uniform phase shift (14). The matrix of steering vectors can be presented as per (21).

$$\mathbf{S} = \begin{bmatrix} 1 & 1 & ... & 1 \\ z_1 & z_2 & ... & z_M \\ & & . & \\ & & . & \\ z_1^{N-1} & z_2^{N-1} & ... & z_M^{N-1} \end{bmatrix} \tag{21}$$

Based on $\mathbf{S}$ in (21), we define $\mathbf{S}_0$ and $\mathbf{S}_1$ as per (22) and (23).

$$\mathbf{S}_0 = \begin{bmatrix} 1 & 1 & ... & 1 \\ z_1 & z_2 & ... & z_M \\ & & . & \\ & & . & \\ z_1^{N-2} & z_2^{N-2} & ... & z_M^{N-2} \end{bmatrix} \tag{22}$$

$$\mathbf{S}_1 = \begin{bmatrix} z_1 & z_2 & ... & z_M \\ & & . & \\ & & . & \\ & & . & \\ z_1^{N-1} & z_2^{N-1} & ... & z_M^{N-1} \end{bmatrix} \tag{23}$$

It can be noted that $\mathbf{S}_1 = \mathbf{S}_0\Phi$, where $\Phi$ is as per (24).

$$\Phi = \begin{bmatrix} z_1 & 0 & ... & 0 \\ 0 & z_2 & ... & 0 \\ & & . & \\ & & . & \\ 0 & 0 & ... & z_M \end{bmatrix} \tag{24}$$

The diagonal entries of $\Phi$ correspond to element to element phase shift. If $\Phi$ can be estimated, DoAs can be estimated on the basis of (13). But $\mathbf{S}_0$ and $\mathbf{S}_1$ are unknown. The approach towards realizing an ESPRIT solution flows from (25).

$$\mathbf{Q}_s = \mathbf{SC} \tag{25}$$

Where $\mathbf{Q}_s$ is a matrix of signal eigenvectors, and $\mathbf{C}$ is some invertible matrix.

Consequently,

$$\mathbf{Q}_0 = \mathbf{S}_0\mathbf{C} \tag{26}$$

$$\mathbf{Q}_1 = \mathbf{S}_1\mathbf{C} = \mathbf{S}_0\Phi\mathbf{C} \tag{27}$$

Considering (28),

$$\mathbf{Q}_1\mathbf{C}^{-1}\Phi^{-1}\mathbf{C} = \mathbf{S}_0\Phi\mathbf{C}\mathbf{C}^{-1}\Phi^{-1}\mathbf{C} = \mathbf{S}_0\mathbf{C} = \mathbf{Q}_0 \tag{28}$$

Letting

$$\Psi^{-1} = \mathbf{C}^{-1}\Phi^{-1}\mathbf{C} \tag{29}$$

We have

$$\mathbf{Q}_1\Psi^{-1} = \mathbf{Q}_0 \tag{30}$$

and

$$\mathbf{Q}_1 = \mathbf{Q}_0\Psi \tag{31}$$

where

$$\Psi = \mathbf{C}^{-1}\Phi\mathbf{C} \tag{32}$$

Going by (31), $\Phi$ is a diagonal matrix of the eigenvalues of $\Psi$.

The DoAs are obtained as per (20) upon finding the eigenvalues of $\Psi$.

Studies utilizing ESPRIT DoA estimation method can be found in [9], [10] and [11].

## V. METHODOLOGY

This work is modeled on the basis of estimating the DoAs associated with two uncorrelated, equal amplitude signal sources. A uniform linear antenna array framework is utilized (with isotropic elements).

The performance of MUSIC, root-MUSIC and ESPRIT DoA estimation methods is compared graphically via the respective pseudo-spectrum results in a variety of conditions. Initially, SNR is varied in an environment featuring a 15-element linear antenna array. Other cases analyzed involve varying antenna array size and DoA angular separation.

## VI. RESULTS

### A. SNR variation

The figures presented in this section (Fig. 2 to Fig. 10) correspond to DoA estimation results obtained in varying SNR conditions. A 15 size uniform linear antenna array is assumed, with half a wavelength spacing distance. The two expected DoAs are -10 and +10 degrees.

Fig. 2 to Fig. 4 correspond to DoA estimation results obtained in zero noise conditions.

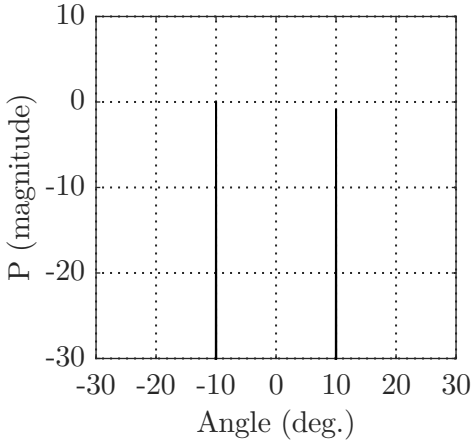


Fig. 2. Zero noise MUSIC result.

The two expected DoAs (-10 and +10 degrees) can be easily deciphered from the MUSIC result in Fig. 2.

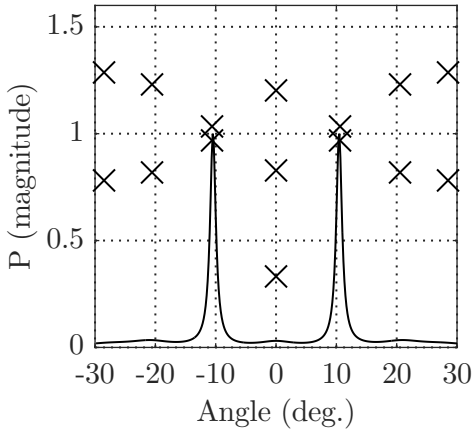


Fig. 3. Zero noise root-MUSIC result.

The two expected DoAs (-10 and +10 degrees) can be easily deciphered from the root-MUSIC result in Fig. 3.

The two expected DoAs (-10 and +10 degrees) can be easily deciphered from the ESPRIT result in Fig. 4.

A comparative observation of the pseudo-spectrums in Fig. 2, Fig. 3 and Fig. 4 (zero noise condition) depict the MUSIC result as the best even though roughly similar results can be obtained graphically from the other two DoA estimation methods.

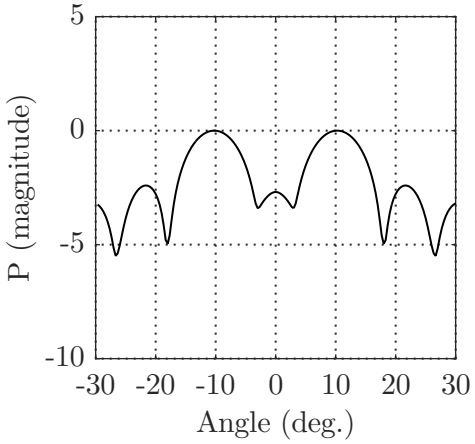


Fig. 4. Zero noise ESPRIT result.

Fig. 5 to Fig. 7 correspond to DoA estimation results obtained in average noise conditions.

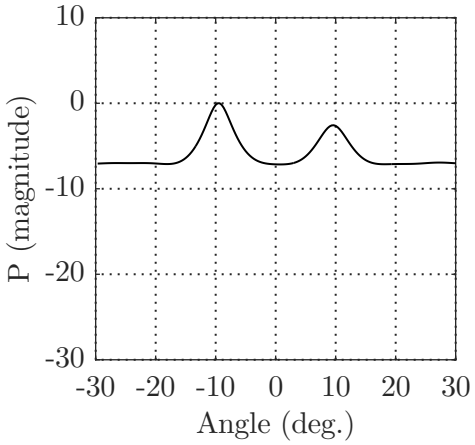


Fig. 5. Average noise MUSIC result.

The two expected DoAs (-10 and +10 degrees) can be somewhat deciphered from the MUSIC result in Fig. 5.

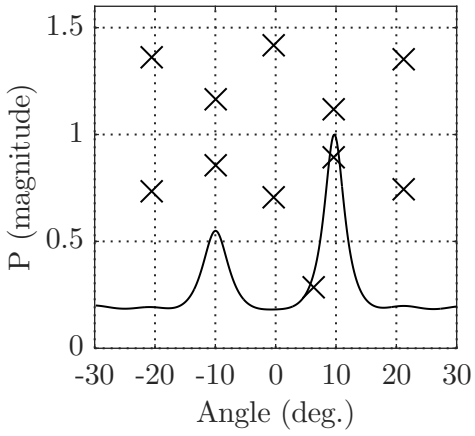


Fig. 6. Average noise root-MUSIC result.

The two expected DoAs (-10 and +10 degrees) can be somewhat deciphered from the root-MUSIC result in Fig. 6.

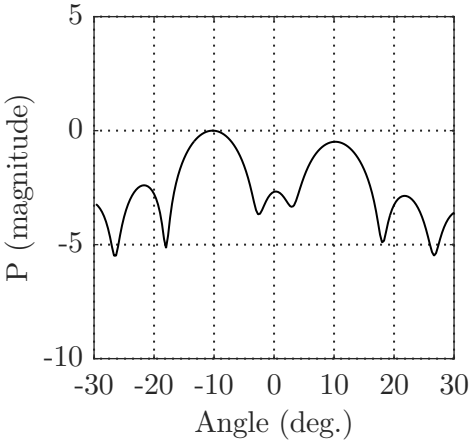


Fig. 7. Average noise ESPRIT result.

The two expected DoAs (-10 and +10 degrees) can be somewhat deciphered from the ESPRIT result in Fig. 7.

A comparative observation of the pseudo-spectrums in Fig. 5, Fig. 6 and Fig. 7 (average noise condition) depict the MUSIC and root-MUSIC results as the best even though roughly similar results can be obtained graphically from the ESPRIT estimation method.

Fig. 8 to Fig. 10 correspond to DoA estimation results obtained in high noise conditions.

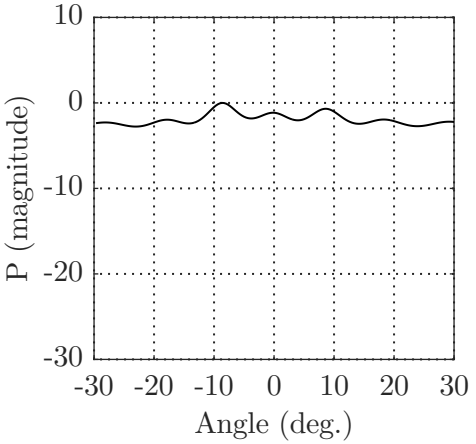


Fig. 8. High noise MUSIC result.

The two expected DoAs (-10 and +10 degrees) are difficult to decipher from the MUSIC result in Fig. 8.

The two expected DoAs (-10 and +10 degrees) can be somewhat deciphered with difficulty from the root-MUSIC result in Fig. 9.

The two expected DoAs (-10 and +10 degrees) can be somewhat deciphered from the ESPRIT result in Fig. 7.

A comparative observation of the pseudo-spectrums in Fig. 8, Fig. 9 and Fig. 10 (high noise condition) depict the ESPRIT result as the best. A roughly good result is obtained with the root-MUSIC method and a poor result with the MUSIC estimation method.

Going by the results obtained with the 3 different methods under various noise conditions, the MUSIC/ root-MUSIC

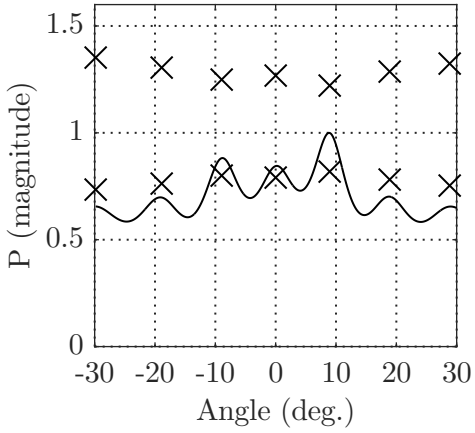


Fig. 9. High noise root-MUSIC result.

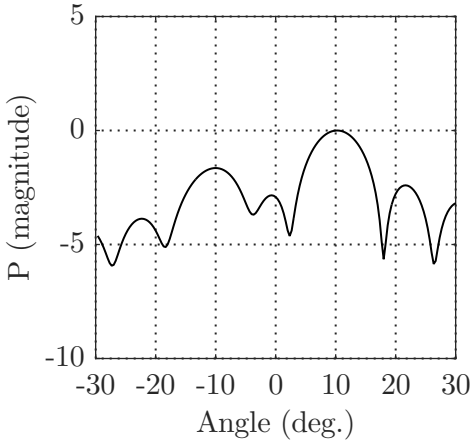


Fig. 10. High noise ESPRIT result.

methods are identified as better options in low noise conditions whereas the ESPRIT method is better suited for application in high noise environments.

### *B. Array size variation*

The figures presented in this section (Fig. 11 to Fig. 19) correspond to DoA estimation results obtained in varying array size scenarios.Half a wavelength array element spacing distance is used. The two expected DoAs are -10 and +10 degrees. Average noise conditions are assumed.

*1) 5 element array:* A comparative observation of the pseudo-spectrums in Fig. 11, Fig. 12 and Fig. 13 (5 element arrays) depict wide pseudo-spectrum lobe widths. The MUSIC result is somewhat the best even though roughly similar results can be obtained graphically from the root-MUSIC method. The wide pseudo-spectrum lobe width in the ESPRIT estimation method result implies poor DoA estimation accuracy.

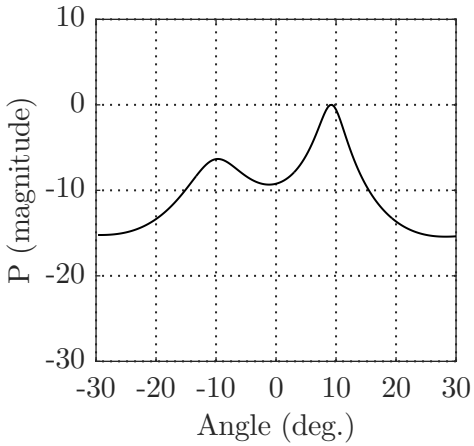


Fig. 11. 5 element array MUSIC result.

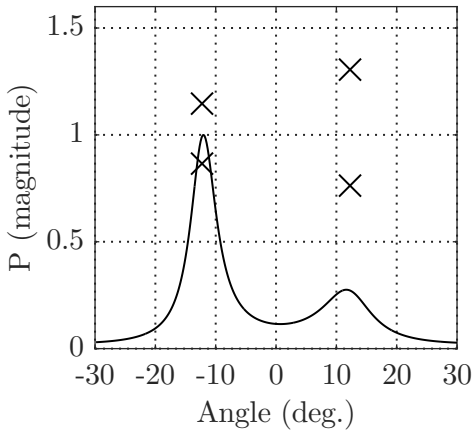


Fig. 12. 5 element array root-MUSIC result.

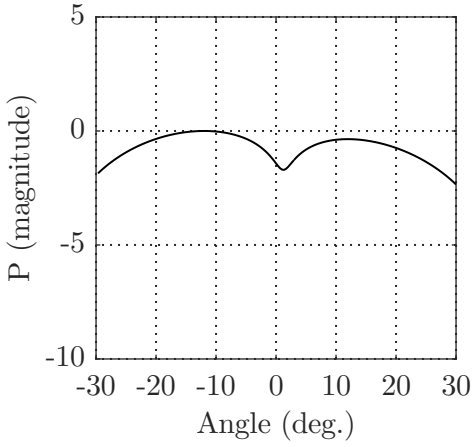


Fig. 13. 5 element array ESPRIT result.

*2) 10 element array:* A comparative observation of the pseudo-spectrums in Fig. 14, Fig. 15 and Fig. 16 (10 element arrays) depict roughly similar DoA estimation results, with narrower pseudo-spectrum lobe widths than in the 5 element array case.

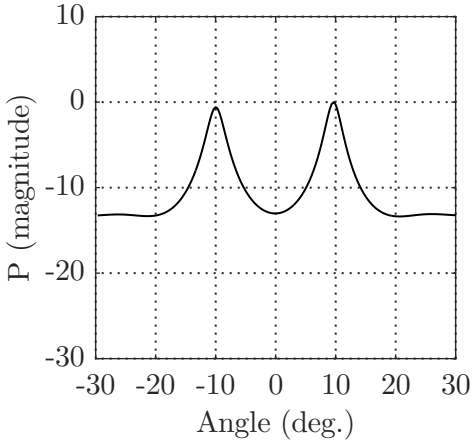


Fig. 14. 10 element array MUSIC result.

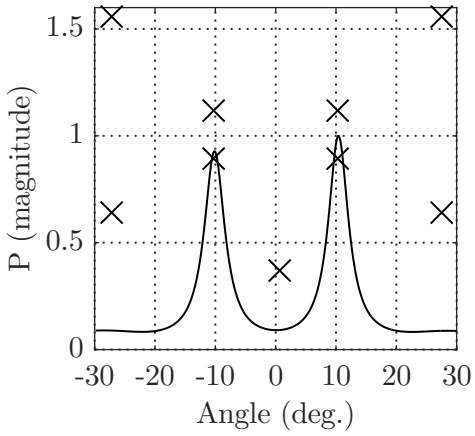


Fig. 15. 10 element array root-MUSIC result.

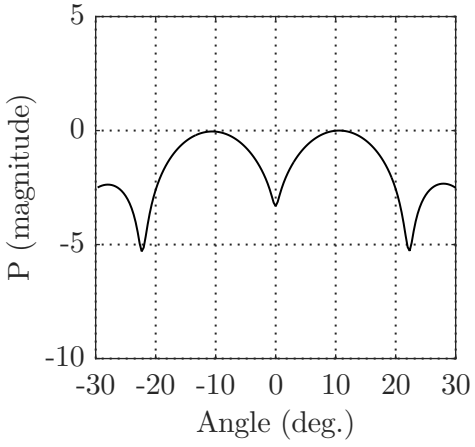


Fig. 16. 10 element array ESPRIT result.

*3) 15 element array:* A comparative observation of the pseudo-spectrums in Fig. 17, Fig. 18 and Fig. 19 (15 element arrays) depict roughly similar DoA estimation results, with narrower pseudo-spectrum lobe widths than in the 5 and 10 element array cases. It is easily deduced that DoA estimation accuracy improves with increase in antenna array size.

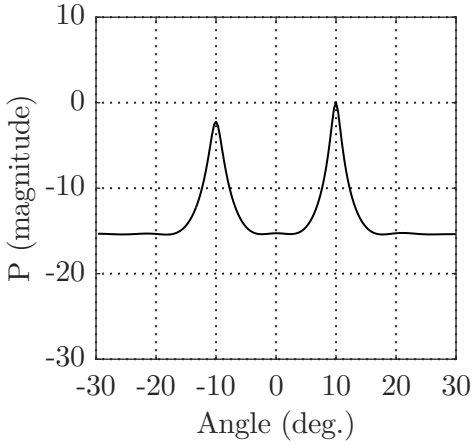


Fig. 17. 15 element array MUSIC result.

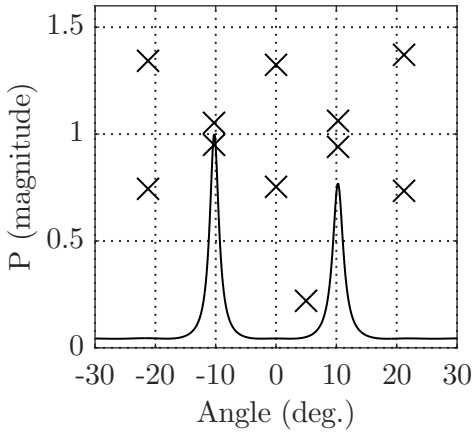


Fig. 18. 15 element array root-MUSIC result.

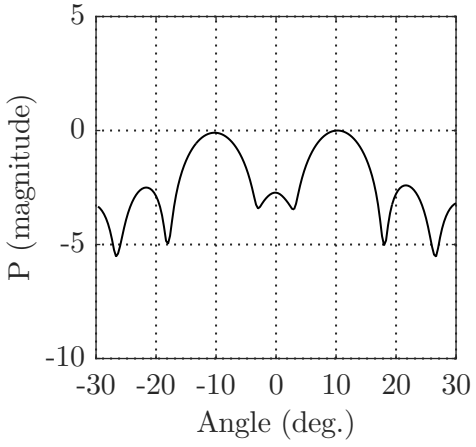


Fig. 19. 15 element array ESPRIT result.

### C. DoA angular separation variation

The figures presented in this section (Fig. 20 to Fig. 37) correspond to DoA estimation results obtained in varying DoA angular separation scenarios. A 10 element array with half a wavelength element spacing distance is considered. Zero noise and average noise conditions are considered.

*1) 20 degrees separation:* Results obtained in a 20 degrees separation scenario (-10 and +10 degrees) in a situation featuring zero noise are depicted in Fig. 20, Fig. 21 and Fig. 22. Good DoA estimation results are obtained in all cases (MUSIC, root-MUSIC and ESPRIT).

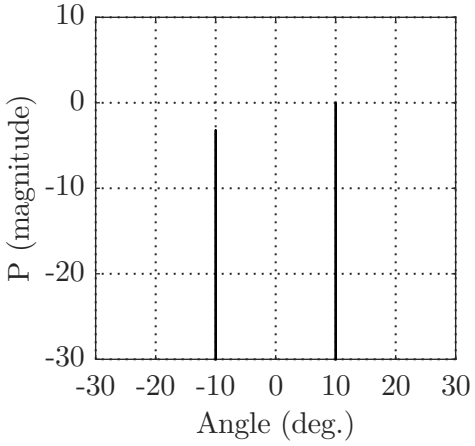


Fig. 20. Zero noise MUSIC result.

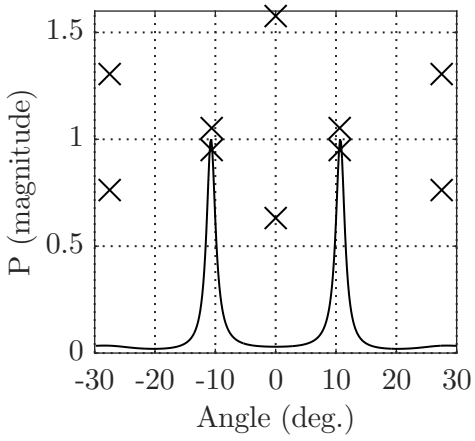


Fig. 21. Zero noise root-MUSIC result.

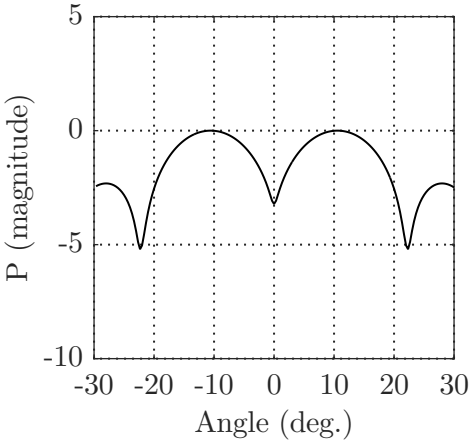


Fig. 22. Zero noise ESPRIT result.

Results obtained in a 20 degrees separation scenario (-10 and +10 degrees) in a situation featuring average noise are depicted in Fig. 23, Fig. 24 and Fig. 25. Fairly good DoA estimation results are obtained in all cases (MUSIC, root-MUSIC and ESPRIT).

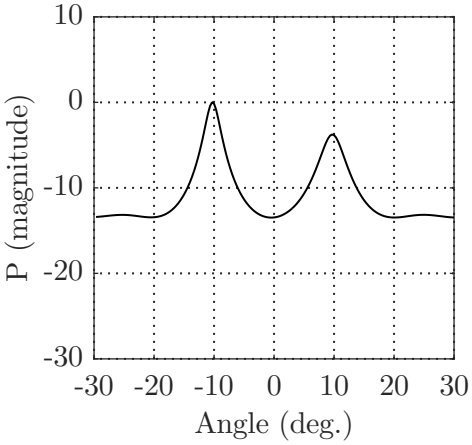


Fig. 23. Average noise MUSIC result.

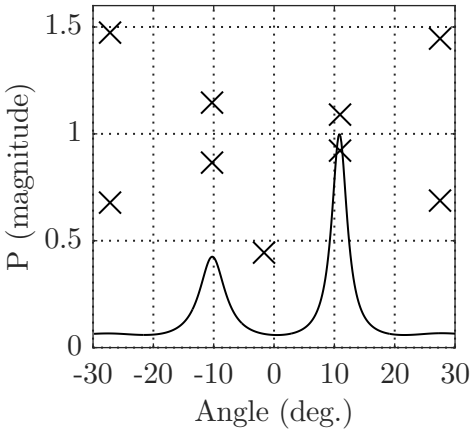


Fig. 24. Average noise root-MUSIC result.

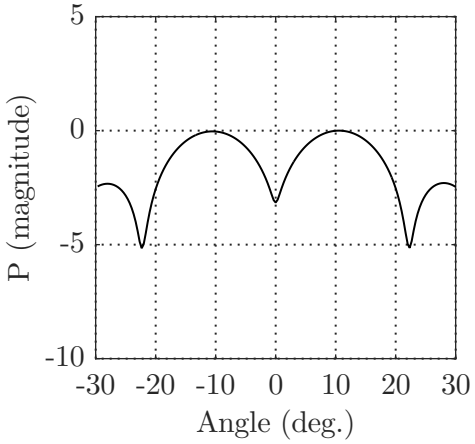


Fig. 25. Average noise ESPRIT result.

*2) 10 degrees separation:* Results obtained in a 10 degrees separation scenario (-5 and +5 degrees) in a situation featuring zero noise are depicted in Fig. 26, Fig. 27 and Fig. 28. Good DoA estimation results are obtained in MUSIC and root-MUSIC cases with average results being observed in the ESPRIT case.

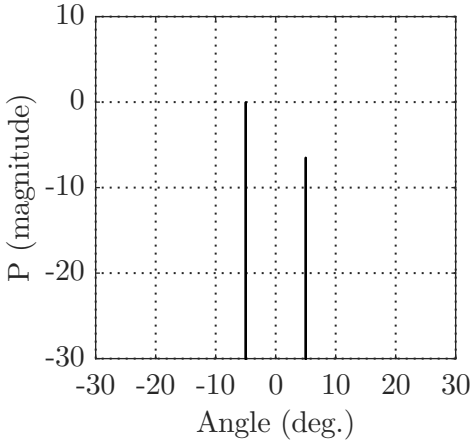


Fig. 26. Zero noise MUSIC result.

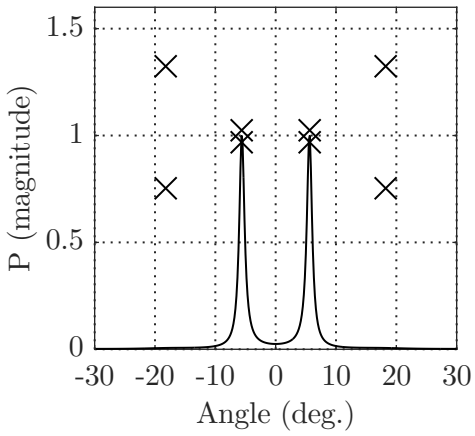


Fig. 27. Zero noise root-MUSIC result.

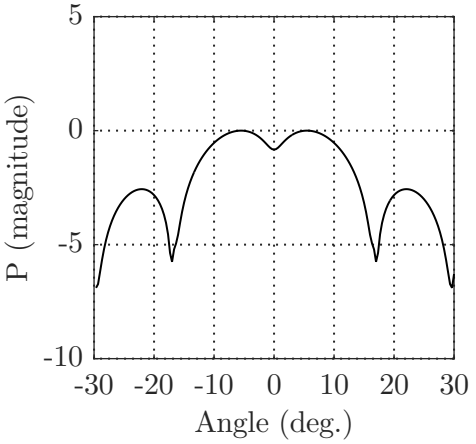


Fig. 28. Zero noise ESPRIT result.

Results obtained in a 10 degrees separation scenario (-5 and +5 degrees) in a situation featuring average noise are depicted in Fig. 29, Fig. 30 and Fig. 31. Fairly good DoA estimation results are obtained in MUSIC and root-MUSIC cases with average results being observed in the ESPRIT case.

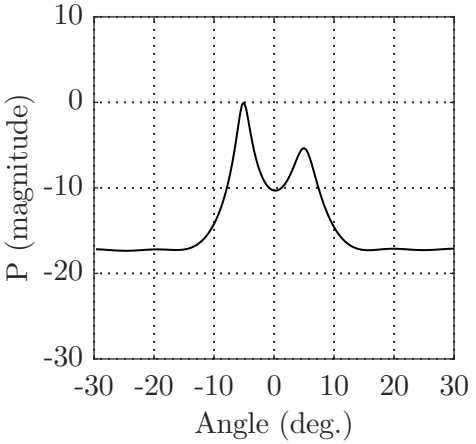


Fig. 29. Average noise MUSIC result.

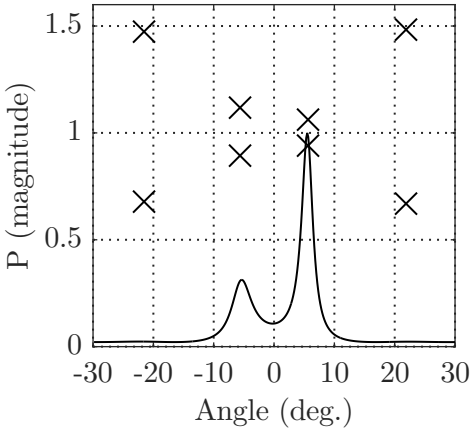


Fig. 30. Average noise root-MUSIC result.

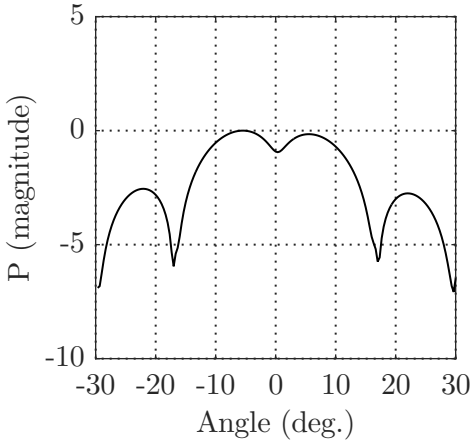


Fig. 31. Average noise ESPRIT result.

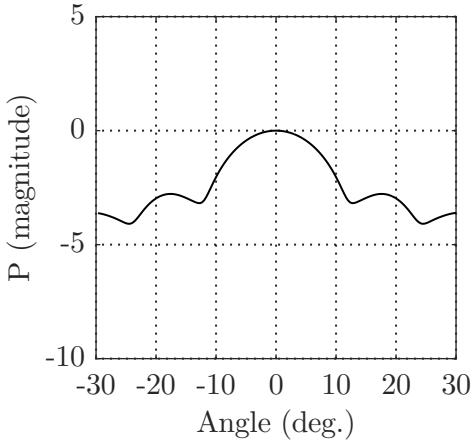


Fig. 34. Zero noise ESPRIT result.

*3) 4 degrees separation:* Results obtained in a 4 degrees separation scenario (-2 and +2 degrees) in a situation featuring zero noise are depicted in Fig. 32, Fig. 33 and Fig. 34. Fairly good DoA estimation results are obtained in MUSIC and root-MUSIC cases with indecipherable results being observed in the ESPRIT case.

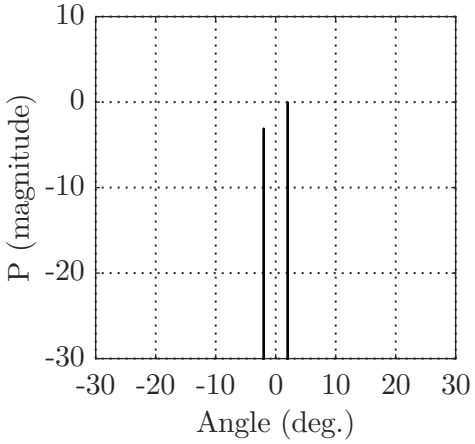


Fig. 32. Zero noise MUSIC result.

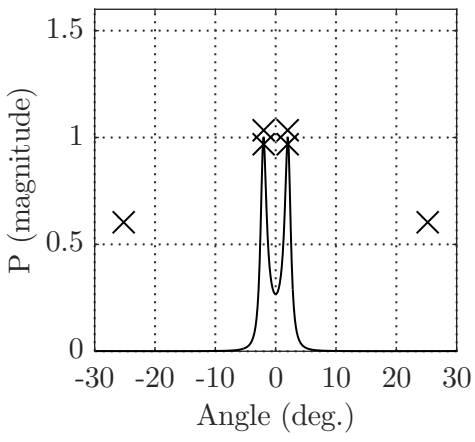


Fig. 33. Zero noise root-MUSIC result.

Results obtained in a 4 degrees separation scenario (-2 and +2 degrees) in a situation featuring average noise are depicted in Fig. 35, Fig. 36 and Fig. 37. Indecipherable DoA estimation results are obtained in all cases (MUSIC, root-MUSIC and ESPRIT).

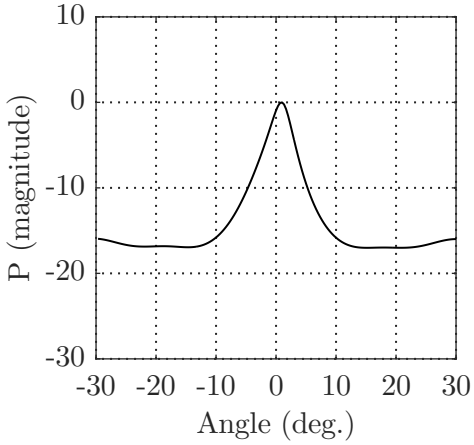


Fig. 35. Average noise MUSIC result.

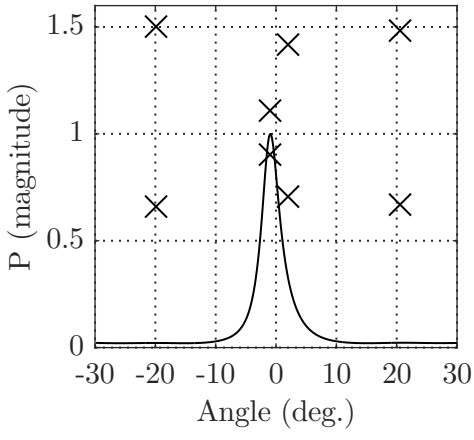


Fig. 36. Average noise root-MUSIC result.

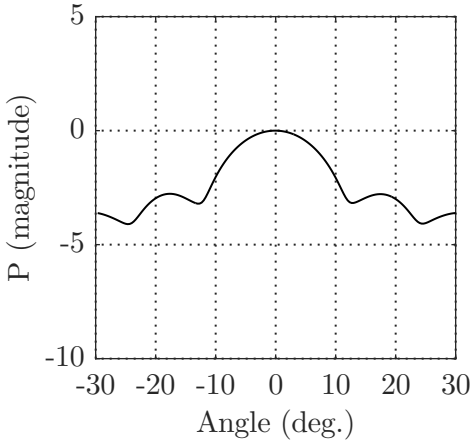


Fig. 37. Average noise ESPRIT result.

## VII. CONCLUSION

The performance of MUSIC, root-MUSIC and ESPRIT DoA estimation methods has been looked into under various conditions.

MUSIC/ root-MUSIC methods are identified as better options in low noise (high SNR) conditions whereas the ESPRIT method is better suited for application in high noise (low SNR) environments.

Antenna array size is noted to be of significance: It is deduced that DoA estimation accuracy improves with increase in antenna array size.

MUSIC/ root-MUSIC methods are identified as better options in estimating DoAs associated with closely spaced sources as opposed to the ESPRIT method.

## REFERENCES

[1] F. B. Gross, *Smart Antennas for Wireless Communications*. McGraw-Hill, 2005.

[2] Y. Gao, X. Jia, J. Xu, T. Long, and X.-G. Xia, "A novel doa estimation method for closely spaced multiple sources with large power differences," *IEEE*, pp. 1276–1279, 2015.

[3] G. Bartoli, R. Fantacci, D. Marabissi, and M. Pucci, "Lte-a femto-cell interference mitigation with music doa estimation and null steering in an actual indoor environment," *IEEE ICC 2013 - Cognitive Radio and Networks Symposium*, pp. 2707–2711, 2013.

[4] M. Jin and X. Qiao, "Low-complexity doa estimation based on compressed music and its performance analysis," *IEEE Transactions on Signal Processing*, vol. 61, pp. 1915–1930, April 2013.

[5] X. Zhang, L. Xu, L. Xu, and D. Xu, "Direction of departure (dod) and direction of arrival (doa) estimation in mimo radar with reduced-dimension music," *IEEE Communications Letters*, vol. 14, pp. 1161–1163, December 2010.

[6] A. Ferreol, P. Larzabal, and M. Viberg, "On the asymptotic performance analysis of subspace doa estimation in the presence of modeling errors: Case of music," *IEEE Transactions on Signal Processing*, vol. 54, pp. 907–920, March 2006.

[7] C. Shu, Y. Liu, Z. Yu, W. Wang, Y. Peng, W. Zhang, and T. Wu, "Research on modified root-music algorithm of doa estimation based on covariance matrix reconstruction," *Sensors and Transducers*, vol. 178, pp. 214–218, September 2014.

[8] C. Qian, L. Huang, and H. C. So, "Improved unitary root-music for doa estimation based on pseudo-noise resampling," *IEEE Transactions on Signal Processing*, vol. 21, pp. 140–144, February 2014.

[9] K. Cui, W. Wu, J. Huang, X. Chen, and N. Yuan, "2-d doa estimation of lfm signals for uca based on time-frequency multiple invariance esprit," *Progress In Electromagnetics Research M*, vol. 53, p. 153165, 2017.

[10] T. Lavate and V. Kokate, "Performance analysis of music and esprit doa estimation algorithms for adaptive array smart antenna in mobile communication," *Second International Conference on Computer and Network Technology*, pp. 308–312, 2010.

[11] Y. Wu, L. Amir, J. R. Jensen, and G. Liao, "Joint pitch and doa estimation using the esprit method," *IEEE/ ACM Transactions on Audio, Speech and Lang Processing*, vol. 23, pp. 32–45, January 2015.

# Application of standard window functions in side-lobe minimization in rectangular antenna array based smart antennas

Mr. Robert Macharia Maina and Dr. Kibet Lang'at and Dr. P. K. Kihato

*Abstract*—Smart antennas are commonly utilized in modern wireless communication systems with an aim of improving network capacity. Smart antennas optimize radiation/ reception in wireless communication links and are composed of antenna array structures and digital beamforming platforms. A typical beamformed radiation/ reception pattern usually features undesired radiation/ reception lobes (side-lobes). This paper seeks to analyze the capability of standard window functions in minimizing such side-lobes on the basis of a rectangular antenna array null steering problem. Particle Swarm Optimization (PSO) algorithm is utilized to solve the null steering problem. Bartlett, Blackman, Hann, Hamming, Tukey and Bohman windows are considered. MATLAB software environment is used as the main analysis tool.

*Keywords*—Null steering, Rectangular antenna array, Side-lobe, Smart Antenna, Window function

## I. INTRODUCTION

The history of antennas dates back to the late $19^{th}$ century, with the advent of practical realization of wireless communication [1]. Initial antennas were simplistic wire based devices. Developments in wireless communication fueled demand and design of various antenna types. A case in point is an antenna array, an arrangement of antenna elements in a particular geometric pattern to aid in improving radiation/ reception patterns. Antenna arrays form a core part of Smart antennas. Smart antennas are utilized in wireless communication networks to ensure optimal signal transmission/ reception through modifying radiation/ reception patterns, an aspect loosely referred to as beamforming. Antenna array radiation/ reception patterns feature undesired minor radiation/ reception directions: side-lobes. Side-lobes can be minimized through application of standard digital filter window functions. This paper focuses on the application of standard window functions in side-lobe minimization in a null steering beamforming problem on the basis of a rectangular antenna array. Reference can be made to [1] and [2] .

## II. STANDARD WINDOW FUNCTIONS

A plethora of window functions have been proposed in literature for instance: Binomial, Triangular, Hamming, Blackman, Bartlett, Hann, Chebyshev, Taylor, Kaiser, Gaussian, Priestley, Tukey, Daniell, Sasaki, Parzen and Bohman windows [2]. Window functions utilized in this paper (Bartlett, Blackman, Hann, Hamming, Tukey and Bohman) are hereby described briefly.

The Bartlett window function is as per (1). The Bartlett window (Fig. 1) is very similar to a triangular window. The Bartlett window has zero first and last samples unlike the case of a triangular window which features nonzero first and last samples.

$$\begin{aligned} w(n) &= \frac{2n}{N} \quad \text{for } 0 \leq n \leq \frac{N}{2} \\ &= 2 - \frac{2n}{N} \quad \text{for } \frac{N}{2} < n \leq N \\ &= 0 \quad \text{otherwise} \end{aligned} \tag{1}$$

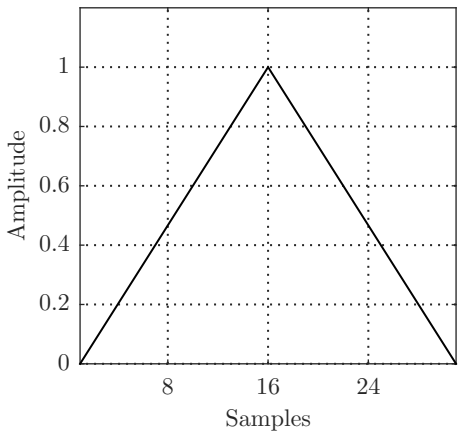


Fig. 1. Bartlett window.

The Blackman window function is as per (2). The window is presented in Fig. 2.

$$\begin{aligned} w(n) &= 0.42 - 0.5\cos(\frac{2\pi n}{N-1}) \\ &\quad +0.08\cos(\frac{4\pi n}{N-1}) \quad \text{for } 0 \leq n \leq N-1 \\ &= 0 \quad \text{otherwise} \end{aligned} \tag{2}$$

The Hann window function is as per (3). The window is presented in Fig. 3.

Mr. Robert Macharia Maina, Department of Telecommunication and Information Engineering, JKUAT (e-mail: robertisaacm@gmail.com).

Dr. Kibet Lang'at, Department of Telecommunication and Information Engineering, JKUAT.

Dr. P. K. Kihato, Department of Electrical and Electronic Engineering, JKUAT.

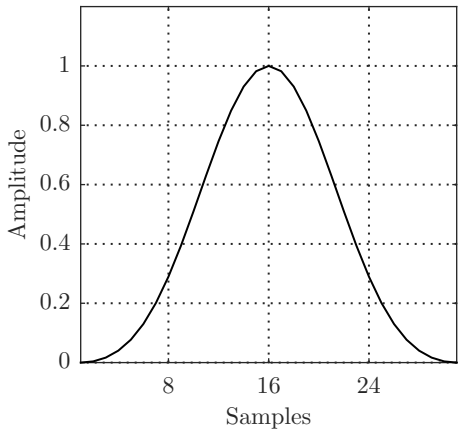


Fig. 2. Blackman window.

$$\begin{aligned} w(n) &= 0.5 - 0.5\cos(\frac{2\pi n}{N-1}) \\ &\quad \text{for } 0 \le n \le N-1 \\ &= 0 \quad \text{otherwise} \end{aligned} \tag{3}$$

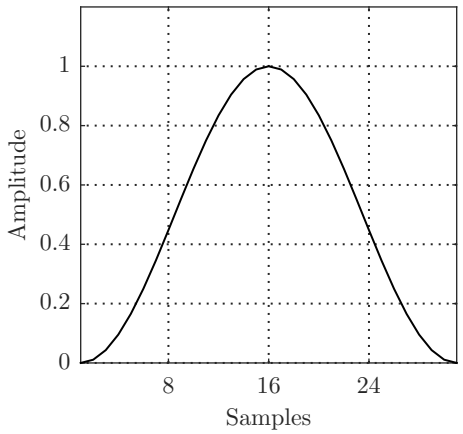


Fig. 3. Hann window.

Hamming window function is as per (4). The window is presented in Fig. 4.

$$\begin{aligned} w(n) &= 0.54 - 0.46\cos(\frac{2\pi n}{N-1}) \\ &\quad \text{for } 0 \le n \le N-1 \\ &= 0 \quad \text{otherwise} \end{aligned} \tag{4}$$

Tukey window function is as per (5). The window is presented in Fig. 5.

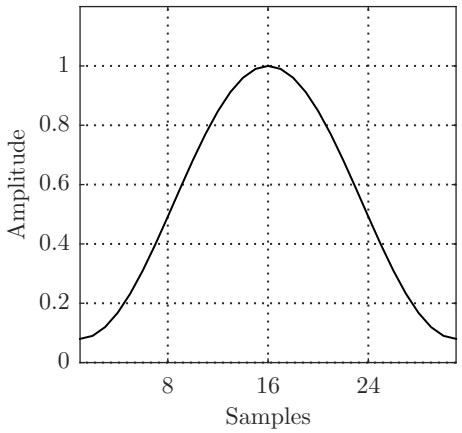


Fig. 4. Hamming window.

$$\begin{aligned} w(n) &= 0.5(1 + \cos(\frac{2\pi}{r}[n - \frac{r}{2}])) \\ &\quad \text{for } 0 \le n \le \frac{r}{2} \\ &= 1 \qquad \text{for } \frac{r}{2} \le n \le 1 - \frac{r}{2} \\ &= 0.5(1 + \cos(\frac{2\pi}{r}[n - 1 + \frac{r}{2}])) \\ &\quad \text{for } 1 - \frac{r}{2} \le n \le 1 \end{aligned} \tag{5}$$

In (5), parameter $r$ ($0 \le r \le 1$) is the ratio of cosine-tapered section length to the entire window length. $r = 0.5$ corresponds to a Tukey window. $r \le 0$ corresponds to an L-point rectangular window. $r \ge 1$ corresponds to an L-point von Hann window.

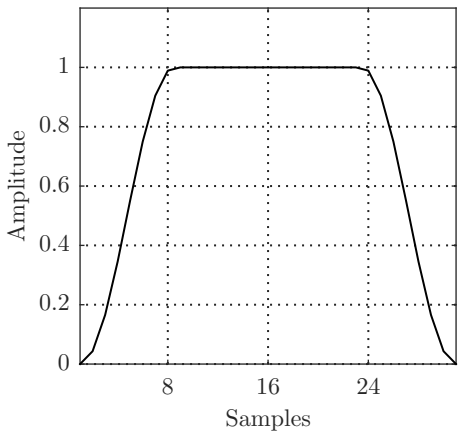


Fig. 5. Tukey window.

The Bohman window function is as per (6). The window is presented in Fig. 6.

$$\begin{aligned} w(n) &= (1 - |n|)\cos(\pi|n|) + \frac{1}{\pi}\sin(\pi|n|) \\ &\quad \text{for } -1 \le n \le 1 \\ &= 0 \quad \text{otherwise} \end{aligned} \tag{6}$$

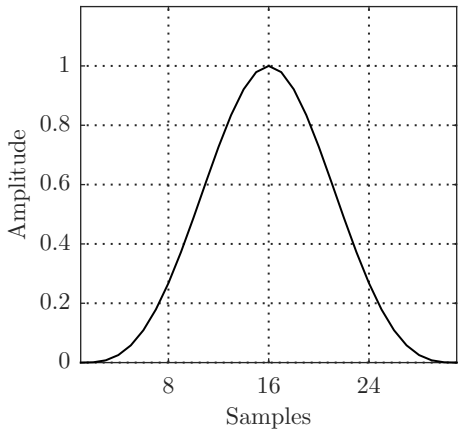


Fig. 6. Bohman window.

A Bohman window can be typically interpreted as the convolution of two half-duration cosine lobes.

Studies involving application of window functions can be found in [3], [4], [5], [6], [7], [8], [9] and [10].

## III. RECTANGULAR ANTENNA ARRAYS

A rectangular antenna array is typically a planar arrangement of antenna elements in a rectangular geometry. A rectangular antenna array holds the premise of beamforming in any desired elevation/ azimuth angle as opposed to one dimension beamforming associated with linear antenna arrays. The radiation/ reception pattern associated with a rectangular array composed of isotropic elements is of the form presented in (7). Reference can be made to [2] and [1].

$$AF = \sum_{m=1}^{M}\sum_{n=1}^{N} e^{j(m-1)(kd_x sin(\theta)cos(\phi)+\delta_x)} + e^{j(n-1)(kd_y sin(\theta)sin(\phi)+\delta_y)} \quad (7)$$

Where:

- $M$ is the number of array elements in the x direction.
- $N$ is the number of array elements in the y direction.
- $d_x$ is the element separation distance in the x direction.
- $d_y$ is the element separation distance in the y direction.
- $k$ denotes wave number.
- $AF$ denotes array factor.

## IV. METHODOLOGY

A null steering reception beamforming problem on the basis of a rectangular antenna array is modeled in MATLAB, with the objective being to maximize reception in a single desired direction and minimize reception in four undesired directions. The directions utilized are as per Table I. An 8x8 element rectangular antenna array is utilized. Particle Swarm Optimization (PSO) algorithm is utilized to optimize the resultant objective function. Windowing operations (in a two-dimension form) are consequently performed on the resultant reception patterns using Bartlett, Blackman, Hann, Hamming, Tukey and Bohman windows.

TABLE I
DIRECTIONS OF ARRIVAL (DOA) UTILIZED IN DEGREES.

| | Elevation | Azimuth |
|---|---|---|
| Desired signal DoA | 45 | 180 |
| Interferer 1 DoA | 20 | 30 |
| Interferer 2 DoA | 20 | 350 |
| Interferer 3 DoA | 80 | 300 |
| Interferer 4 DoA | 70 | 20 |

## V. RESULTS

The results obtained upon application of Bartlett, Blackman, Hann, Hamming, Tukey and Bohman windows in null steered patterns are covered in this section.

Fig. 7 is indicative of the evolution of objective function value with iterations in the null steering beamforming process.

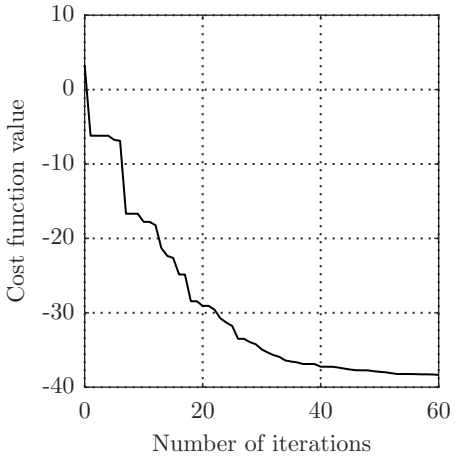


Fig. 7. Evaluation of objective function value with iterations.

Fig. 8 is a three dimension view of the null steering beamforming result before application of a window.

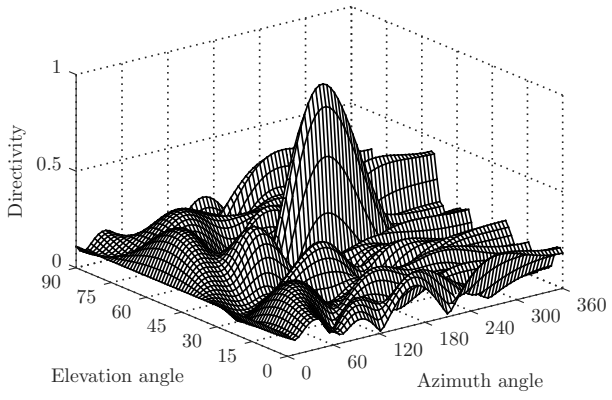


Fig. 8. Three dimension view of the null steering beamforming result without windowing.

The results obtained upon application of the Bartlett window are as per Fig. 9, Fig. 10 and Fig. 11. The results are indicative of lower sidelobes and a somewhat narrower main lobe width.

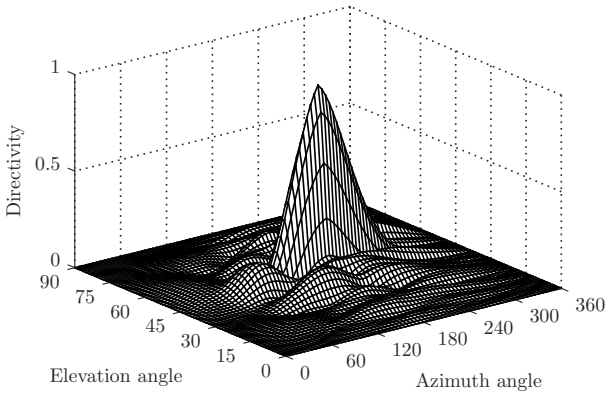


Fig. 9. Bartlett window result: Three dimension view.

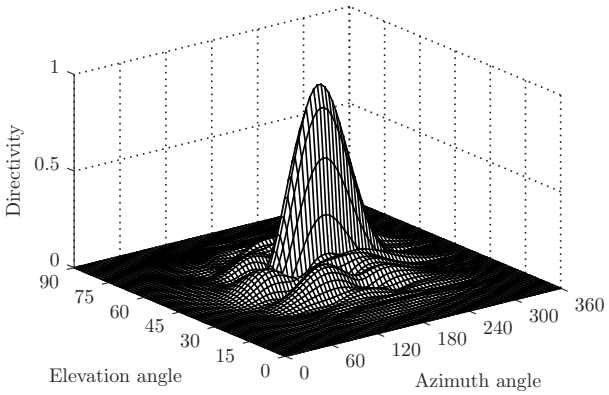


Fig. 12. Blackman window result: Three dimension view.

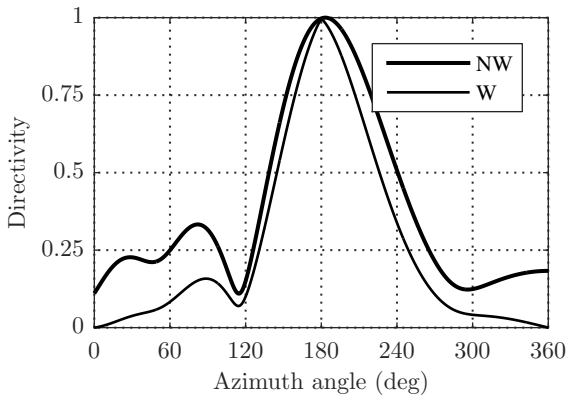


Fig. 10. Bartlett window result: Azimuth plane pattern for Elevation = 45 degrees.

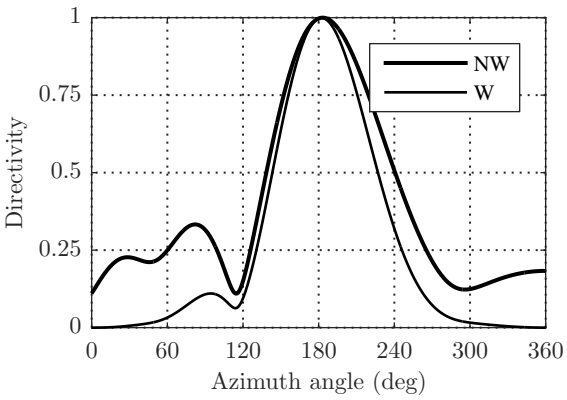


Fig. 13. Blackman window result: Azimuth plane pattern for Elevation = 45 degrees.

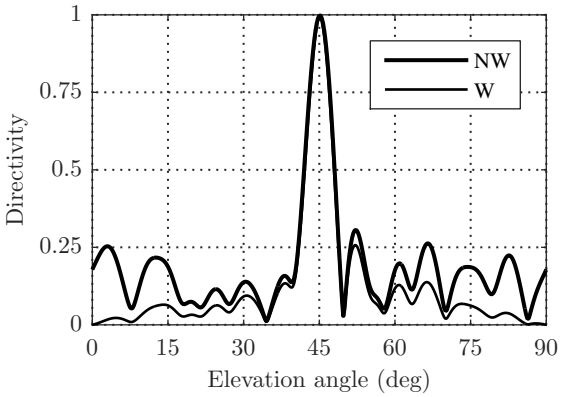


Fig. 11. Bartlett window result: Elevation plane pattern for Azimuth = 180 degrees.

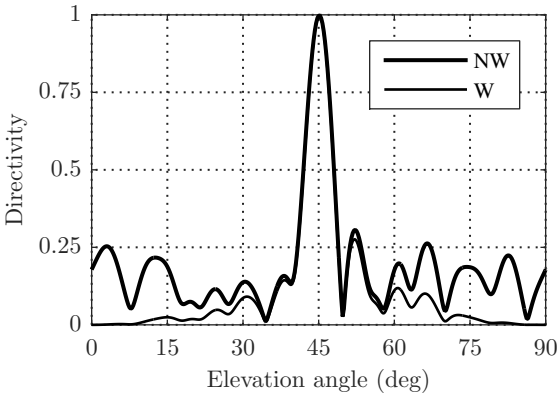


Fig. 14. Blackman window result: Elevation plane pattern for Azimuth = 180 degrees.

The results obtained upon application of the Blackman window are as per Fig. 12, Fig. 13 and Fig. 14. The results are indicative of lower sidelobes and a somewhat narrower main lobe width.

The results obtained upon application of the Hann window are as per Fig. 15, Fig. 16 and Fig. 17. The results are indicative of lower sidelobes and a somewhat narrower main lobe width.

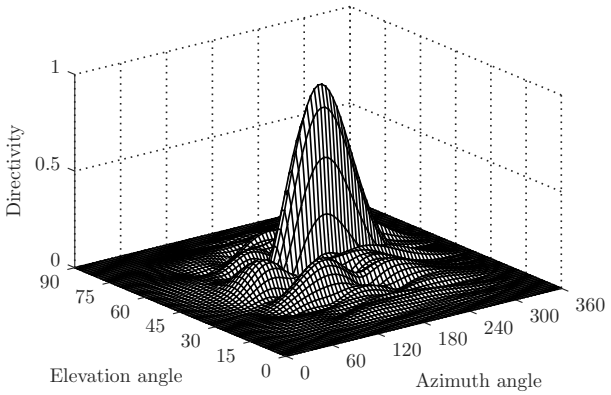


Fig. 15. Hann window result: Three dimension view.

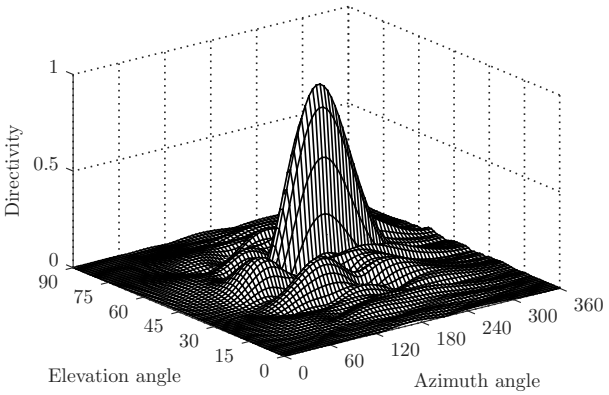


Fig. 18. Hamming window result: Three dimension view.

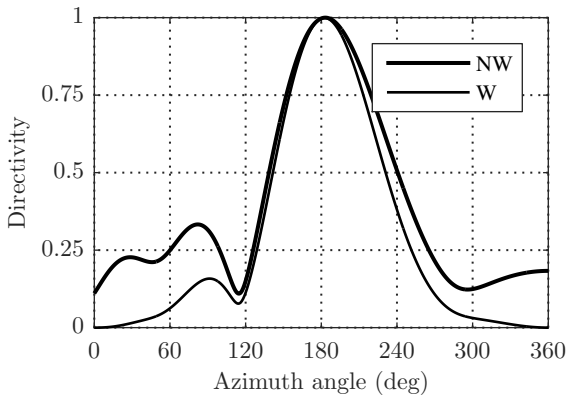


Fig. 16. Hann window result: Azimuth plane pattern for Elevation = 45 degrees.

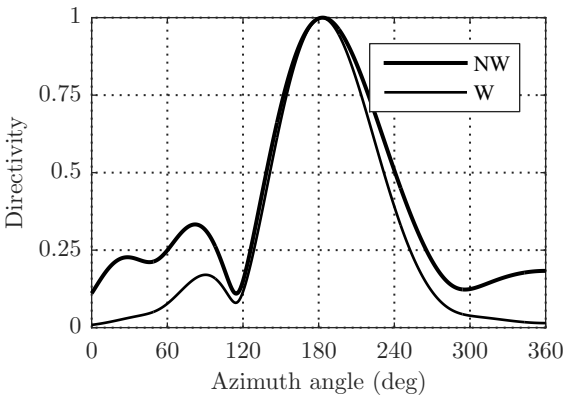


Fig. 19. Hamming window result: Azimuth plane pattern for Elevation = 45 degrees.

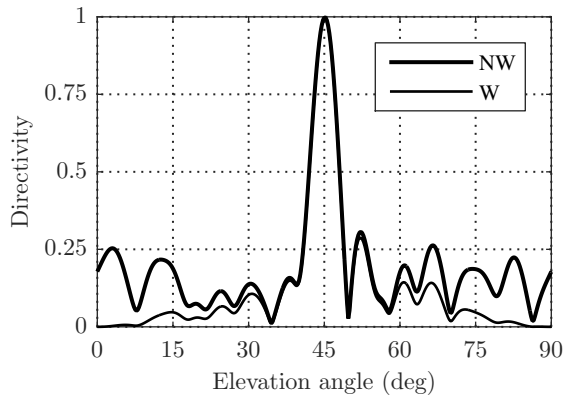


Fig. 17. Hann window result: Elevation plane pattern for Azimuth = 180 degrees.

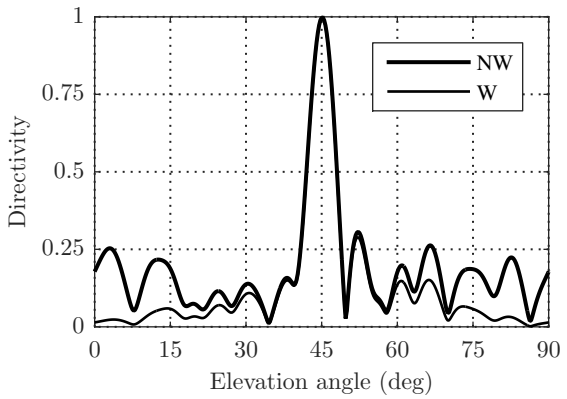


Fig. 20. Hamming window result: Elevation plane pattern for Azimuth = 180 degrees.

The results obtained upon application of the Hamming window are as per Fig. 18, Fig. 19 and Fig. 20. The results are indicative of lower sidelobes and a somewhat narrower main lobe width.

The results obtained upon application of the Tukey window are as per Fig. 21, Fig. 22 and Fig. 23. The results are indicative of lower sidelobes and a somewhat narrower main lobe width.

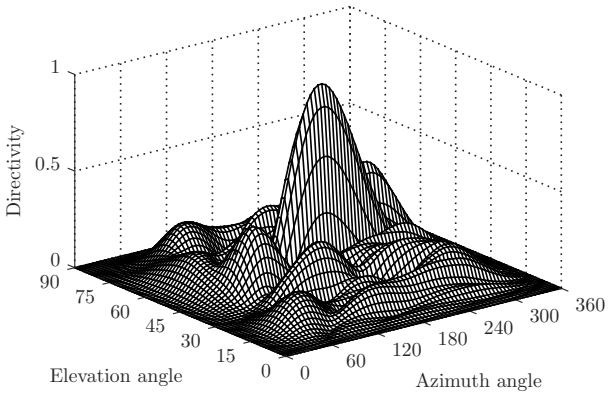


Fig. 21. Tukey window result: Three dimension view.

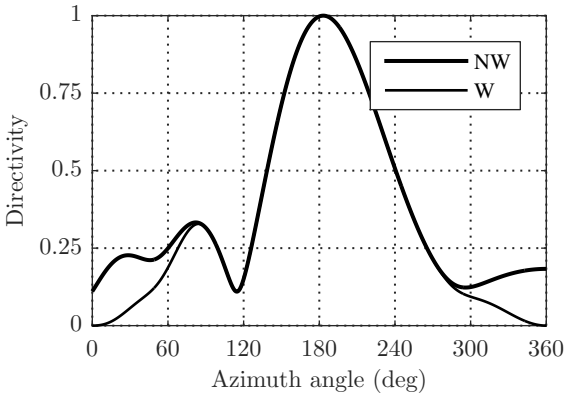


Fig. 22. Tukey window result: Azimuth plane pattern for Elevation = 45 degrees.

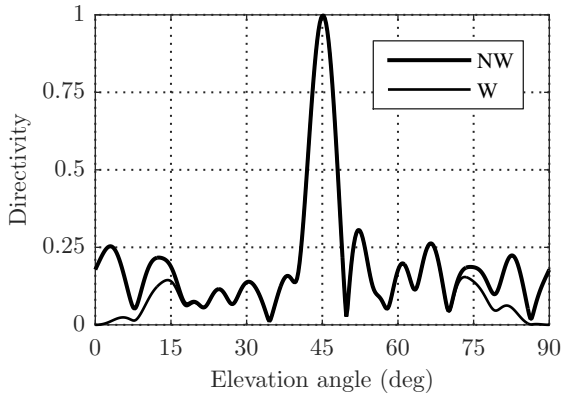


Fig. 23. Tukey window result: Elevation plane pattern for Azimuth = 180 degrees.

The results obtained upon application of the Bohman window are as per Fig. 24, Fig. 25 and Fig. 26. The results are indicative of lower sidelobes and a somewhat narrower main lobe width.

Quantitative results are tabulated in Tables II and III. Improved performance upon window application is noted in all cases going by the lower relative reception strength values associated with the undesired DoAs.

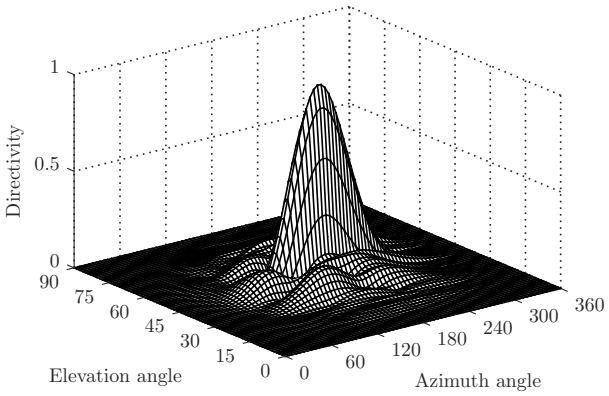


Fig. 24. Bohman window result: Three dimension view.

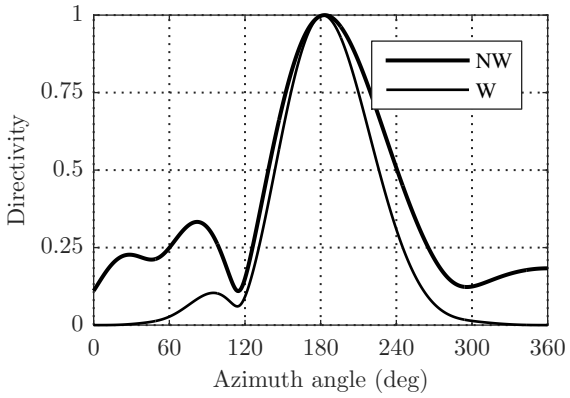


Fig. 25. Bohmanwindow result: Azimuth plane pattern for Elevation = 45 degrees.

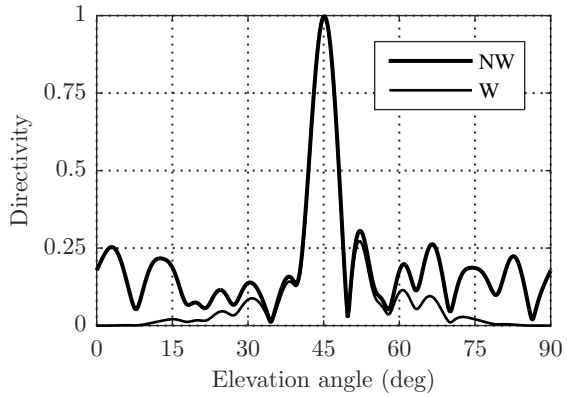


Fig. 26. Bohman window result: Elevation plane pattern for Azimuth = 180 degrees.

TABLE II
RELATIVE RECEPTION STRENGTH IN DECIBELS (DB) IN DESIRED AND UNDESIRED DOAS.

| | No Window | Bartlett | Blackman |
|---|---|---|---|
| Desired signal DoA | -0.11 | -0.1848 | -0.1049 |
| Interferer 1 DoA | -47.4758 | -70.4642 | -91.5073 |
| Interferer 2 DoA | -39.4333 | -70.8417 | -100.9229 |
| Interferer 3 DoA | -39.4412 | -61.6678 | -82.202 |
| Interferer 4 DoA | -39.1291 | -65.5732 | -90.3929 |

TABLE III
RELATIVE RECEPTION STRENGTH IN DECIBELS (DB) IN DESIRED AND UNDESIRED DOAS.

| | Hann | Hamming | Tukey | Bohman |
|---|---|---|---|---|
| Desired signal DoA | -0.1057 | -0.1058 | -0.11 | -0.1044 |
| Interferer 1 DoA | -79.3858 | -71.5862 | -60.3751 | -97.7338 |
| Interferer 2 DoA | -88.0243 | -67.3866 | -68.5314 | -114.7603 |
| Interferer 3 DoA | -69.4438 | -63.7113 | -49.0907 | -86.9408 |
| Interferer 4 DoA | -77.9174 | -65.2892 | -58.8387 | -99.7165 |

## VI. CONCLUSION

Analysis of the results obtained is indicative of the significance of windowing operations in beamforming in rectangular antenna array based smart antennas. Lower side lobe levels are obtained. Somewhat narrower main lobe widths are observed although this positive outcome could be dependant on array size, a subject that can be researched into. Slight differences are observable with utilization of different windowing techniques. The ultimate choice of a windowing technique is highly dependant on location of DoAs, a subject open to further research.

## REFERENCES

[1] C. A. Balanis, *Antenna Theory, Analysis and Design*. John-Wiley and sons, 2016.
[2] F. B. Gross, *Smart Antennas for Wireless Communications*. McGraw-Hill, 2005.
[3] P. Podder, T. Z. Khan, and M. H. Khan, "Comparative performance analysis of hamming, hanning and blackman window," *International Journal of Computer Applications*, vol. 96, June 2014.
[4] S. N. Monteiro and H.G.Virani, "Improved null steering with sidelobe canceller for linear antenna arrays," *International Journal of Advanced Research in Computer and Communication Engineering*, vol. 4, pp. 97–100, March 2015.
[5] A. Bhattacharya, "A window function with modified co-efficients for fir filter design with an improved frequency response and its comparison with the bartlett-hann window," *International Journal of Science, Engineering and Technology Research (IJSETR)*, vol. 2, pp. 1345–1352, June 2013.
[6] J. G. Reddy, T. K. Teja, and B. S. Seshu, "A novel approach for interference suppression using a improved lms based adaptive beam forming algorithm," *International Journal of Research in Science and Technology*, vol. 2, pp. 26–35, April 2015.
[7] T. MVSR, A. Kumar, and C. S. Prasanth, "Comparative analysis of windowing techniques in minimizing side lobes in an antenna array," *International Conference on Communication and Signal Processing, India*, pp. 1380–1383, April 2014.
[8] S. Chakraborty, "Design and realization of digital fir filter using dolph-chebysheb window," *International Journal of Computer Science and Engineering Technology (IJCSET)*, vol. 4, pp. 987–996, July 2013.
[9] L. Sarika, P. Nandini, S. Bharathi, Y. D. Lakshmi, and S. Suresh, "Sidelobe rejection in a uniform linear array antenna using windowing techniques," *International Journal of Research in Engineering and Technology*, vol. 3, pp. 46–50, May 2014.
[10] A. Bhattacharya, "A modified window function for fir filter design with an improved frequency response and its comparison with the hamming window," *International Journal of Science, Engineering and Technology Research (IJSETR)*, vol. 2, pp. 1122–1128, May 2013.

# Mitigating Against Conflicts in the Kenyan Mining Cycle: Identification of Gaps in the Participation and Recourse for Rights Holders (Civil Society & Community)

Seroni Anyona[1], Bernard K. Rop [2]
.

***Abstract***— One of the major obstacles to sustainable development of the mining sector in Africa is conflicts. These conflicts emanate from various sources. However one of the key sources of misunderstanding is lack of communication between the rights holders (community) and duty bearers (government and corporate) and this breakdown of communication is due to poor or nonexistent mechanisms of involvement of affected communities in decision making and ignorance. This study sought to examine the Kenyan Mining cycle and identify procedural and systemic gaps that if not addressed could trigger conflict in the emerging mining sector and suggest ways of mitigating them. Key among the greatest barriers to communal participation is ignorance regarding mining activities and also the language of instruction. Most rural people are uneducated and yet a large number of communications and notices are in English. Poor management of expectations is also a critical source of misunderstanding and leading to conflict. Poor communal organization and lack of some sort of recognized authority gives room for disorder and hence poor channels of communication.

***Keywords*****:** New Mining Act, Mining Cadaster, human rights, rights holders, duty bearers, community participation, mining lincence, prospecting licence, licence requirements, mining cycle

## I. INTRODUCTION

The management of extractive industries is one of the most critical challenges facing many resource-dependent developing countries today. Rather than stimulating broad-based economic development, reliance on resource extraction has tended to concentrate wealth and power in the hands of a few, exacerbate corruption and inequalities, lead to environmental degradation and pollution, while doing little to reduce poverty, economic disparities and generate employment. Worse still, in many countries extractive resources have fuelled violent conflicts.

The recent announcement of oil discovery and other minerals has propelled Kenya as a new player in the global market for hydrocarbons and valued minerals. The International Monetary Fund (IMF) projects that oil production in Kenya is expected to start in two to three years from now, giving the country time to prepare to manage its endowment to achieve its development goals as stipulated in the 2030 Vision.

Kenya is well endowed with bulk mineral resources, some of which are already being exploited by private companies and some are yet to be prospected and exploited.

Minerals found in Kenya include inter alia soda ash, fluorite, diatomite, carbon dioxide, gold, iron ore, lead, vermiculite, Kyanite, manganese, titanium, silica sands, gemstones and precious minerals, gypsum and limestone.

## II. OBJECTIVE OF THE STUDY

The key objective of this study is to examine the Kenyan mining cycle and identify gaps and priority areas for future learning and activities to ensure involvement of affected communities in the decision making process. One of the key aspects in mitigating mining related conflicts is to internalize human rights in the mining cycle. It is important to note that meaningful participation is a core human right principle that is important to minimize negative social and environmental impacts of mining and it is important to note that there can be no participation without communication. In line with this thinking, it is important to examine the legal procedures and identify procedural entitlements of rights holders and corresponding responsibilities of duty bearers along the mining cycle process from a human rights based perspective.

The aim of this study was to contribute to a more user-driven design of the way government agencies interface with people

1. Mr. Seroni Anyona, Mining, Materials & Petroleum Engineering Department Jomo Kenyatta University of Agriculture & Technology, , P.O. Box 62000 – 00200, Nairobi, Kenya (e-mail: sanyona@jkuat.ac.ke ).

2. Prof. B. Rop Jomo Mining, Materials & Petroleum Engineering Department Kenyatta University of Agriculture & Technology, , P.O. Box 62000 – 00200, Nairobi, Kenya (e-mail: drropben@gmail.com ).

and to ensure engagement from a human rights perspective in the public administration of the mining sector.

Procedural rights, including accessibility, right to be heard, participation, transparency, right to appeal and accountability are enshrined in the Constitution of Kenya 2010, as well as in other legal frameworks and public administration guidelines that govern the mining sector in Kenya.

However, current administrative practice often does not take into account these existing legal entitlements or the perceived needs of the end user. Furthermore, rights holders as well as duty bearers are often unfamiliar with procedural rights based on the three pillars of right to information, participation and access to justice. Therefore, there is a need to map, illustrate and communicate procedural rights along the mining cycle in a clear, accessible and transparent way.

An illustration of the entry points for right holders in the Kenyan mining cycle could advise the government on which parts of their administrative processes might benefit from re-engineering for improved adherence to the legal framework and international human rights standards. This holds the potential of improving state-society relations through addressing citizen's expectations for voice and participation towards a more inclusive, transparent, just and responsible management of the mining sector.

The specific task of the study will be to make a "users' journey" – examine the point of contact/interface between duty bearers (government agencies and mining companies) and rights holders (civil society) hereunder the various entry points for participation and recourse throughout the mining cycle; from establishing a mining site, exploration, licensing, engagement of stakeholders to actual mining and the final closure of the mines, within the framework of existing laws regulating the mining cycle in Kenya.

## III. ENACTMENT OF A NEW MINING ACT 2016

Kenya enacted a new law in 2016 to reinvigorate the mining sector. The new Act seeks to provide clear guidance on mining activities in Kenya. It introduces amongst other things legalization of Artisanal Miners and Transparency and Accountability through use of the Online Mining Cadastre portal for licensing and for management of mineral rights and permits. It also introduces Community Development Agreements, mandatory for all holders of large scale mining rights, and sharing of royalties among the national government, the county governments and the local communities.

The Act is intended to streamline the country's mining sector and open the gates for its development as well as ensure environmental conservation and sustainable development in the mining sector. It also seeks to address the key gaps in the Mining Act of 1940, and align the sector to the latest global trends such as value-addition and the use of technology to spur investor interest. The Cabinet Secretary for Mining has termed the Act as one of the most "progressive mining laws in the continent."(Oraro & Co. Advocates)

From a human rights based perspective the new Act introduces major changes in how communities (rights holders) will be engaged in the mining cycle and licensing process.

### A. Community Development Agreement

The Act makes it mandatory for a holder of a large scale mining licence to enter into an agreement with the community where the mining operations will be carried out. This agreement is known as the Community Development Agreement

### B. Employment and Training

The Act seeks to ensure employment opportunities are created for Kenyans, ensure skills transfer and capacity building for the citizens. Section 46 thereof provides that each mineral right holder is required to submit to the Cabinet Secretary, a program detailing how it shall recruit and train Kenyans.

Furthermore, the holder of a mineral right is required to give preference to members of the community and Kenyan citizens when it comes to employment and only engage non-citizen technical experts in accordance with such local standards for registration as may be prescribed in the relevant law.

### C. Local Equity Participation

The Act protects local participation with provisions for equity participation in large mining operations. The Act also provides for the prioritization of local procurement of goods, services and workforce.

### D. Land Use, Water Rights Laws and Pollution

A holder of a mineral right is also required to comply with the prevailing laws on water rights and use the land in accordance with the terms of the permit of licence. In doing so, the holder of the permit or licence will ensure that the land is used in a sustainable manner.

Section 179 of the Act which deals with land use requires the holder of a permit or mining licence to ensure the sustainable use of land through restoration of abandoned mines and quarries; that the seepage of toxic waste into streams, rivers, lakes and wetlands is avoided and that disposal of any toxic waste is done in the approved areas only; that blasting and all works that cause massive vibration are properly carried out and muffled to keep such vibrations and blasts to reasonable and permissible levels in conformity with the Environmental Management and Coordination Act, (Cap. 387); and that upon completion of prospecting or mining, the land in question shall be restored to its original status or to an acceptable and reasonable condition as close as possible to its original state.

### E. Health and Safety

The Act has provisions to ensure the health and safety of persons working at the mines. It provides that the holder of a mineral right will comply with the Occupational Health and Safety Act, 2007 with regards to the safety of workers and mine operations.

### F. Revenue Sharing

The Act makes provision for the sharing of the royalties that are payable under the Act. Section 183(5) provides that the National Government will be entitled to 70%, the County Government 20% and the community where the mining operations occur will be entitled to 10% of the revenue.

This provision has been viewed as being probably one of the most progressive provisions in the Act, if not the environmental provisions. It embodies the spirit of the Constitution that requires equitable distribution of revenue among the national and county governments and inclusion, more so, financial inclusion for the people of Kenya.

### G. Dispute Resolution

Section 154 of the Act provides for dispute resolution. It provides that any dispute arising as a result of a mineral right issued under the Act, may be determined by the Cabinet Secretary, through a mediation or arbitration process as may be agreed upon by the disputing parties or as may be stated in an agreement; or through a court of competent jurisdiction. Section 155 sets out the disputes that may be determined by the Cabinet Secretary.

### H. International Best Practice on Mining

The Act generally prescribes for the carrying out of prospecting and mining activities in accordance with international best practice. Below is a discussion on some of the international best practices on mining.

### I. Sustainable Development in Mining

Sustainable development is at the heart of international best practice on mining. There is no universally adopted definition of sustainability in the mining industry. However, there are five (5) main pillars that embody sustainable mining practices. These are Economy, Safety, Resource efficiency, Environment and Community. A brief description of each dimension follows.

### J. Environmental Management

Environmental assessment is a process that will ensure the mineral right holder considers the potential environmental effects before they can begin the mining process. It is important that the impact to the environment is managed through specialized low impact exploration practices, water management, pollution prevention and control and the rehabilitation of mines after closure.

The Act has several very progressive provisions on environmental management, which include the requirement for a person to obtain an impact assessment licence before being granted a mining licence. The Act also requires the holder of a mineral right to comply with the prevailing laws on water and use the land in a sustainable manner

The Act has enhanced the provisions on the environment, health and safety. Section 176(1) states that a mineral right or other licence or permit granted under the Act shall not exempt a person from complying with any law concerning the protection of the environment. Section 176(2) further provides that a mining licence shall not be granted to a person under this Act unless the person has obtained an Environmental Impact Assessment licence, social heritage assessment and the environmental management plan has been approved.

After completion of the prospecting or mining, the mineral right holder will ensure that the land in question is restored to its original status or to an acceptable or reasonable condition as close as possible to its original state.

## IV. JUSTIFICATION

Despite the fact that the new Mining Act provides for community (rights holders) engagement in decision making on paper, the actual implementation is far from the spirit and letter of the Act. So it is important to review the licensing procedure and identify the existing gaps between the written law and practice. This is will be to:

- Identifying gaps in human rights inclusion in the mining cycle and communal involvement will help reduce potential mining related conflicts
- Enhance human rights in the mining sector that will ensure maximum returns to affected communities
- Identify loopholes in the licensing process with the objective of helping to improve the legislative regimes affecting the mining sector
- Address Human rights issues. One way or another touch on the environment. So improvement of the concerned regulations will lead to better environmental protection
- Manage reputation, operational, legal, and financial risks.
- Engage, retain, and motivate staff.
- Demonstrate leadership and management standards.

## V. METHODOLOGY

The key objective was to analyze existing information; baseline data; mining policies, plans, and processes; and external reports and articles and using international instruments, such as the Aarhus convention, the Bali Guidelines and Principle 10 as reference points evaluate adherence to international best practice.

For conducting a comprehensive and in-depth literature review on policy and legal framework governing large scale mining, licensing process and focusing on community participation provisions issues in the sector, the following methodology was used:

### A. Research, identification and gathering of reference materials. This entailed:

- Identifying relevant sources of information; Legal policy documents related to mining(old and new Acts),Print media articles, Electronic media documentaries submissions from court cases, Academic papers, Books, write-ups, government reports, International journals and UN case studies, Private Sector Assessment Reports, Feasibility Studies for mining Programs
- Collect and collate references materials
- Definition of topic, terms, scope of review as well as intentional exclusions

### B. Information extraction:

This entailed: Reading and analysis of collected materials, Synthesize of content and presentation, Chronological/thematic organization of content, identify key themes, gaps, and opportunities by analysing available secondary data, Identify the context and indicators selected according to the assessment's priority outline an overview of the mining system and key players and evaluate trends in the mining sector

### C. Identified weaknesses/strengths

Using international instruments such as the Aarhus convention, the Bali Guidelines and Principle 10 to establish conformity to international best practice the Kenyan Mining Cycle for conformity.

The three pillars of the Aarhus convention include:

a. Access to information: any citizen should have the right to get a wide and easy access to environmental information. Public authorities must provide all the information required and collect and disseminate them and in a timely and transparent manner.

*Figure 1 ASMs at Mkuku area*

b. Public participation in decision making: the public must be informed over all the relevant projects and it has to have the chance to participate during the decision-making and legislative process. Decision makers can take advantage from people's knowledge and expertise; this contribution is a strong opportunity to improve the quality of the environmental decisions, outcomes and to guarantee procedural legitimacy.

c. Access to justice: the public has the right to judicial or administrative recourse procedures in case a Party violates or fails to adhere to environmental law and the convention's principles.

4. Bali Guidelines

The Bali guidelines consist of fourteen key implementation guiding principles to ensure public access to information. These guidelines state as follows:

Guideline 1 – Public authorities to make information available upon request, Guideline 2 – Standards for environmental information in the public domain, Guideline 3 – Limited grounds for refusal to provide information, Guideline 4 – Public authorities to collect and update various types of environmental information, Guideline 5 – State of the environment reporting, Guideline 6 – Information in emergency situations, Guideline 7 – Provide means for and encourage effective capacity-building, Guideline 8 – Early and effective public participation in decision-making, Guideline 9 – Authorities proactively seek transparent and consultative public participation, Guideline 10 – All information relevant to decision-making to be made available, Guideline 11 – Due account of comments received, Guideline 12 – Updating public participation where information or circumstances change, Guideline 13 – Public participation in preparation of legal norms, policies, plans and programs, Guideline 14 – Capacity-building, education and awareness-raising

### D. Interviewed key persons/players and stakeholders in the mining sector:

Kenya National Commission for Human Rights (KNCHR), National Environmental Management Agency(NEMA), Ministry of Mining, Kenya Chamber of Mines, Ministry of Energy and Petroleum (ME&P)

*Figure 2 Open mine pit at Mkuki area*

## VI. FINDINGS OF THE STUDY

### A. Online Mining Cadastre

Under these regulations, application for Mining licenses and permits shall be done on-line on an "**Online Mining Cadastre"** (OMC). Pursuant to Clauses 191 and 192(3) of the Act the OMC means the online interactive, digital system for administering the provisions of the Act and these regulations in relation to the rights and obligations of licence and permit holders, which is available for public inspection. This shall act as the online repository and information management tool for regulating the licensing and the permitting of mineral rights, dealer's rights, import permits and export permits and shall be implemented by the Registrar.

The government shall maintain a **"cadastral register**". This means a digital as well as a paper-based, spatially integrated database and associated applications used to store and manage all mineral rights' tenures within Kenya, including: reconnaissance licence register, prospecting licence register, retention licence register, mining licence register, reconnaissance permit register, prospecting permit register, mining permit register, artisanal mining permit register,

Mineral Agreements register and any other register established by the Director that is to be used to record information for all mineral rights and related matters, as specified in these regulations;

## B. Mining Cadastre Office (MCO)

The Mining Cadastre Office shall be established under the Ministry of Mining, Directorate of Mines and may be referred to as the "MCO.".The Office shall be headed by the Registrar of mineral rights and dealer's Rights and is referred to as the "Registrar". The Registrar shall be the authorised officer, appointed by the Cabinet Secretary, responsible for administering mineral rights and dealer's rights in Kenya. The Cabinet Secretary may establish County offices as are useful to implement the responsibilities of the MCO.

The Mining Cadastre Office responsibilities include:

a) installation, operation and maintenance of the Online Mining Cadastre;
b) developing, maintaining and updating the cadastral survey map;
c) developing and maintaining registries to ensure up-to-date cataloguing of licence and permit applications and activities;
d) managing licence and permit reporting requirements;
e) harmonising, as required, with other cadastres including land, agriculture, social cadastres;
f) participating, as required, in Ministry activities to ensure responsible implementation of licence and permit requirements; and
g) Any other functions or responsibilities that the Cabinet Secretary may reasonably assign to the MCO.

Based on these new regulations the following is a summary of the Kenyan licensing requirements, procedures and obligations for interested large scale investors.

## C. THE KENYAN MINING LICENSING PROCESS

There are about five licences issued in the Kenyan mining cycle, these include:

1. Reconnaissance Licence
   Reconnaissance Licence (Airborne survey)
2. Prospecting Licence
3. Retention Licence
4. Mining Licence
5. Mineral Dealer's Licence

**Reconnaissance Licence**

For an interested party to acquire a reconnaissance licence the following are the requirements:

**Requirements**

1. Area coordinates, Digital area map and the area in respect of which the licence is issued
2. approved plans for the procurement of Kenyan goods and services and plan for employment and training of Kenyan citizens
3. certified or signed statement or formal letter of intent from a bank or other financial source
4. Resumes of the Project Manager and key staffs committed at least throughout year one for airborne reconnaissance-all transfer camps, temporary installations or installed machinery shall be removed
5. the legally registered name and address
6. a statement of attestation of no mining Act Offence Penal conviction of the applicant using appropriate forms
7. a statement of relevant past work
8. a programme for reconnaissance or prospecting operations or mining operation a special
9. a certified copy of the applicants' audited accounts for the previous three (3) years;

**Procedure**

10. agreement with the Government ( for airborne survey)
11. Within five (5) days of the end of every month of each licence year, monthly reports on mine development and mineral production, using appropriate forms
12. A prospecting or reconnaissance licence holder shall submit a written notice in the form recommended in the regulations
13. within fourteen (14) days of the end of six (6) months of each licence year, the holder shall submit a six (6) monthly progress report on all reconnaissance work carried out over the licence area

**Prospecting Licence**

Most requirements are as in reconnaissance licence above including:

1. a plan describing how, on an ongoing basis, local government, traditional authorities and communities will be informed
2. Identify activities and actions that, as a result of the programme of prospecting operations, may be reasonably expected to result in significant adverse effects on the environment, gender impact and on any monument, cultural heritage, artefacts or relic the rehabilitation programme
3. An agreement signed by all relevant land holders for land use including detailed information on compensation, resettlement or other land use arrangements

4. Submit consents and agreements should be submitted not later than forty-nine (49) days after the original application is made
5. In writing inform any affected land holders in accordance to the regulations before commencement of exploration/prospecting
6. provide a bond or some other form of financial security in this section called an environmental protection bond
7. Undertake an environmental and social impact assessment (ESIA) and submit a report and an environmental licence, providing an environmental and social management plan (ESMP), , accompanied by a mine closure and rehabilitation plan

**Retention Licence**

Most requirements for this licence are the same as those for reconnaissance and prospecting licence above including:

1. Submission of a full study and assessment of the mineral deposit by an independent expert, pursuant to Clause 87 of the Act, sufficient to demonstrate that the deposit is potentially commercially exploitable (retention licence)
2. demarcate and keep demarcated the mining area
3. The holder of a retention licence shall submit quarterly reports, accompanied by appropriate forms

**Mining Licence**

Most requirements for this licence are the same as those for reconnaissance, prospecting and retention licence above including:

1. The holder of a mining licence shall pay the annual area-based charges
2. The holder of a mining licence shall pay royalties, calculated as set out in the regulations
3. The holder shall submit the feasibility study report
4. The holder shall submit Community Development Agreement(s), giving particulars of the applicant's proposals with respect to social responsible investments for the local community
5. The holder shall submit a written notice by using appropriate forms not later than thirty-five (35) days before commencing mine development and shall at the same time inform all affected land holders
6. The holder shall submit a written notice using appropriate forms, at least thirty-five (35) days prior to the commercial production start date, and each time that there is a significant change in capacity
7. The holder shall submit the proposed programme of mining operations and production forecasts over the term of the licence, including plans for mineral processing and beneficiation within and outside of Kenya, mineral transportation, together with details of the type and sourcing of equipment and mining methodologies expected to be used;

**Mineral Dealer's Licence**

1. The holder of a mineral dealer's licence shall keep a register of the mineral dealings & record in the register all the transactions and relevant information
2. The holder shall submit an Articles of Incorporation, place and date of incorporation
3. The holder shall submit the Resumes of the Project Manager and key staffs committed at least throughout year one. The holder shall update this information if at any time during the term of the licence the manager is replaced
4. The holder shall submit the legally registered name and address
5. Submit a statement of attestation of no mining Act Offence Penal conviction of the applicant using appropriate forms
6. The holder shall submit a statement of relevant past work
7. The applicant shall submit a certified copy of the audited accounts for the previous three (3) years;
8. The holder of a mineral dealer's licence shall submit to the Cabinet Secretary a true copy of the register in duplicate for the preceding three months, together with a statutory declaration of the correctness thereof

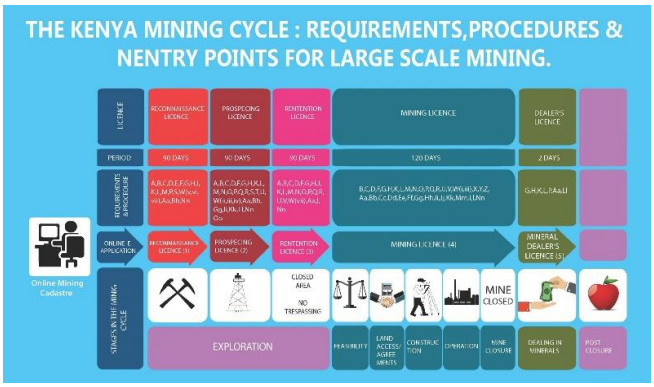


**Licencing Requirements Key for the Poster**

| NO. | LETTER CODE | DESCRIPTION | LICENCE |
|---|---|---|---|
| 1 | A | Area coordinates | 1,2,3,4 |
| 2 | B | Digital area map | 1,2,3,4 |
| 3 | C | approved plans for the procurement of Kenyan goods and services | 1,2,3,4 |

| | | | |
|---|---|---|---|
| 4 | D | approved plan for employment and training of Kenyan citizens | 1,2,3,4 |
| 5 | E | for airborne reconnaissance-all transfer camps, temporary installations or installed machinery shall be removed | 1 |
| 6 | F | certified or signed statement or formal letter of intent from a bank or other financial source | 1,2,3,4 |
| 7 | G | Resumes of the Project Manager and key staffs committed at least throughout year one. The holder shall update this information if at any time during the term of the licence the manager is replaced | 1,2,3,4,5 |
| 8 | H | the legally registered name and address | 1,2,3,4,5 |
| 9 | I | a special agreement with the Government (airborne survey) | 1 |
| 10 | J | Submit a full study and assessment of the mineral deposit by an independent expert, pursuant to Clause 87 of the Act, sufficient to demonstrate that the deposit is potentially commercially exploitable (retention licence) | 3 |
| 11 | K | a statement of attestation of no mining Act Offence Penal conviction of the applicant using appropriate forms | 1,2,3,4,5 |
| 12 | L | a statement of relevant past work | 1,2,3,4,5 |
| 13 | M | a programme for reconnaissance or prospecting operations or mining operation | 1,2,3,4 |
| 14 | N | a plan describing how, on an ongoing basis, local government, traditional authorities and communities will be informed | 2,3,4 |
| 15 | O | Identify activities and actions that, as a result of the programme of prospecting operations, may be reasonably expected to result in significant adverse effects on the environment, gender impact and on any monument, cultural heritage, artefacts or relic the rehabilitation programme | 2,3,4 |
| 16 | P | a certified copy of the applicants' audited accounts for the previous three (3) years; | 1,2,3,4,5 |
| 17 | Q | undertake an environmental and social impact assessment (ESIA) and submit a report and an environmental licence, providing an environmental and social management plan (ESMP), , accompanied by a mine closure and rehabilitation plan | 2,3,4 |
| 18 | R | All consents and agreements should be submitted not later than forty-nine (49) days after the original application is made | 2,3,4 |
| 19 | S | A prospecting or reconnaissance licence holder shall submit a written notice in the form of as recommended in the regulations | 1,2 |
| 20 | T | in writing inform any affected land holders in accordance to the regulations before commencement of exploration/prospecting | 2 |
| 21 | U | An applicant for a prospecting licence, a retention licence or a mining licence shall provide a bond or some other form of financial security in this section called an environmental protection bond within thirty-five (35) days of receiving notice of the amount submit copies of the bond document and other security via the OMC, and within a further seven (7) days shall deliver the original hard copy documents to the Mining Cadastre Office | 2,3,4 |

| | | | |
|---|---|---|---|
| 22 | V | demarcate and keep demarcated the mining area | 3,4 |
| 23 | W | i. Within five (5) days of the end of every month of each licence year, monthly reports on mine development and mineral production, using appropriate forms<br>ii. Within fourteen (14) days of the end of every quarter of each licence year, a quarterly progress report, using appropriate forms<br>iii. An annual ESIA report, using appropriate forms or, where there is an ESMP attached to the licence, a detailed progress report prepared according to guidelines<br>iv. Within thirty-five (35) days of the end of each licence year, a full and detailed annual technical report covering all prospecting activities carried out over the prospecting licence area in compliance with published Ministry guidelines accompanied by appropriate forms not later than thirty-five (35) days following the end of each licence year, a full and detailed annual report, using appropriate forms on all reconnaissance work carried out over the licence area<br>v. within fourteen (14) days of the end of six (6) months of each licence year, a six (6) monthly progress report on all reconnaissance work carried out over the licence area<br>vi. an annual declaration of minimum operational expenditures on reconnaissance activities using appropriate forms to accompany the annual report<br>vii. The holder of a retention licence shall submit quarterly reports, accompanied by appropriate forms | 1,2,3,4 |
| 24 | X | the holder of a mining licence shall pay the annual area-based charges, calculated according to the Second Schedule within thirty-five (35) days of the grant of the licence and annually thereafter at the start date of each licence year | 4 |
| 25 | Y | The holder of a mineral dealer's licence shall keep a register of the mineral dealings & record in the register all the transactions and relevant information | 5 |
| | Z | The holder of a mineral dealer's licence shall submit to the Cabinet Secretary a true copy of the register in duplicate for the preceding three months, together with a statutory declaration of the correctness thereof | 5 |
| 26 | Aa | the name, nationality and address of the licence holder; or names and nationalities of Directors and names and address of all shareholders holding more than ten per cent (10%) of the registered share capital and registered address in Kenya for a company<br>the mineral or minerals in respect of which the mining licence is issued | 1,2,3,4,5 |
| 27 | Bb | The holder shall provide the area in respect of which the licence is issued; | 1,2,3,4 |
| 28 | Cc | the holder of a mining licence shall pay royalties, calculated as set out in the | 4 |

| | | | |
|---|---|---|---|
| | | Third Schedule(not yet generated), within thirty-five (35) days after the commencement of production, and monthly thereafter | |
| 29 | Dd | Submit the feasibility study report | 4 |
| | Ee | the Community Development Agreement(s), giving particulars of the applicant's proposals with respect to social responsible investments for the local community | 4 |
| | Ff | submit a written notice by using appropriate forms not later than thirty-five (35) days before commencing mine development and shall at the same time inform all affected land holders | 4 |
| | Gg | an agreement signed by all relevant land holders for land use including detailed information on compensation, resettlement or other land use arrangements | 2,3,4 |
| | Hh | submit a written notice using appropriate forms, at least thirty-five (35) days prior to the commercial production start date, and each time that there is a significant change in capacity | 4 |
| | Ii | performance bond or escrow account information for the previous three (3) years; | 2,3,4 |
| | Jj | Submit a written notice using appropriate forms not later than ninety-one (91) days before the commercial production start date and shall at the same time inform any affected land holders | 4 |
| | Kk | Community Development Agreement(s), giving particulars of the applicant's proposals with respect to social responsible investments for the local community; | 2,3,4 |
| | Ll | Articles of Incorporation, place and date of incorporation | 2,3,4,5 |
| | Mm | the proposed programme of mining operations and production forecasts over the term of the licence, including plans for mineral processing and beneficiation within and outside of Kenya, mineral transportation, together with details of the type and sourcing of equipment and mining methodologies expected to be used; | 4 |
| | Nn | The holder should submit a detailed statement of relevant past work; | 1,2,3,4 |
| | Oo | Report exploration results using the Australasian Code for Reporting of Mineral Resources and Ore Reserves (The JORC Code); or the Canadian Institute of Mining, Metallurgy and Petroleum (CIM), CIM Standards on Mineral Resources and Reserves; or The South African Code for the Reporting of Exploration Results, Mineral Resources and Mineral Reserves (The SAMREC Code); or The SME Guide for Reporting Exploration | 2 |

**Types of Licenses**

1. Reconnaissance License
2. Prospecting License
3. Retention License
4. Mining License
5. Mineral Dealers License

## VII. THE OUTCOME OF THE ASSESSMENT AND EVALUATION OF PUBLIC INVOLVEMENT AND PARTICIPATION IN THE MINING SECTOR – KENYA

Analysis of the Kenyan mining cycle, based on the above stated international conventions including the Aarhus convention, Bali guidelines and Principle 10 reveals major gaps in the public, information, participation and involvement in the mining cycle. Most of these gaps emanate from the ignorance of the public, poor communication systems and lack of commitment on the part of the duty bearers. Identified gaps include (see appendix 1):

- Public notices inviting citizen participation are published in the print media which are unaffordable and not accessible to most common people
- These notices and publications are written in English language which is not familiar to the larger section of the uneducated population
- Experience shows that the public participation in ESIA's is limited and normally skewed towards duty bearers
- Over centralizing decision making power in the position of the Cabinet secretary delays the process of decision making and may lead to abuse of power.
- Ignorance on the part of the public regarding the mining sector and mining cycle has led to poor public participation, exploitation and conflicts. The most common means of engaging public participation is during the Environmental and Social Impact Assessment. However ESIA and ESMP reports are very technical documents for the uneducated population to comprehend
- Most local people are unskilled in complex negotiations dealing with compensation and resettlement with large multinational companies. This can lead to possible exploitation of unexposed communities
- Lack of understanding regarding the true value of land and dynamics and mining economics could lead to unrealistic expectations on the part of the public that often result in conflicts
- No clear regulations to identify and weed out land speculators
- Not well elaborated dispute resolution system
- The Online Mining Cadastre (OMC) system is unreliable currently due to poor connectivity. The management of the system is not well established yet. This will present a major challenge in the operationalization of the new online licence application system
- Mining Registration Board is not yet constituted and its mode of operation may be a major bottleneck if not handled properly. Checks and balances need to be put in place to curtail its likely susceptibility to corruption.

## VIII. CONCLUSION

After a thorough examination of the Kenyan mining cycle it's revealed that Kenya's mining sector is comparatively young and this presents an opportunity for internalizing and integrating progressive ideas and culture that emulate international best practice at its infant stage. Setting the right foundation will ensure a stable and vibrant mining sector. To achieve this, it is imperative that public participation and involvement in decision making be an integral part of the mining policy. This study has revealed a number of challenges and missing links that hinder effective public participation. To mitigate these challenges it's here suggested that:

- There be developed a long-term public sensitization strategy regarding mining activities and the mining sector in Kenya to help in reducing conflicts and possible exploitation of the communities.
- There is needs to impose a legal requirement to compel government and mineral rights holders(duty bearers) to translate any public notices and communications to Kiswahili at least or to respective native languages
- The government needs to form a consortium of lawyers, mining and economic experts to offer probono services to local communities and individuals when carrying out land negotiations and writing agreements and consents.
- Provide as much information as possible about the exploration program, including its potential brevity, to manage community expectations
- The civil society needs to get involve in sensitizing the public on their rights and obligations regarding mining activities.
- There is need to engage experienced community relations staff at every stage of the way in a mine development to constantly appraise and enhance community participation and confidence
- The environmental protection bond should be paid annually as opposed to the current situation where it is paid once during application for licence. This will ensure that the fluctuation/depreciation of the shilling does not affect the value of the bond over time
- Technical documents such as the ESIA should be translated to local languages and simplified for the common people
- Social and political criteria should be part of a comprehensive feasibility study and collect data for cultural baseline and to identify stakeholders

- Due to the complex socio-cultural dynamics in Kenya the term community can be interpreted in many ways including clan, tribe or religion etc. So there is need to have a clear definition of the term community for the sake of those who will benefit from the loyalties. It may also be prudent to define the benefitting community based on the distance from the mining operation or the degree of impact on a community in relation to resource extraction.
- There are various structures of communal organization in different areas in Kenya. There needs to be a legally recognized communal organization system that will manage the community loyalties independent of government structures
- Allow communal access to monthly, quarterly and annual reports to ensure affected communities are sufficiently and regularly updated.
- Depoliticize the Mining Sector
- Competent staff with appropriate social science or community development training and experience will be needed to build a strong, stable and collaborative relationships and partnerships
- Adequate budget support will be needed to fund impact mitigation and community investment programs
- Design a full program of community investments in a participatory manner with community members and other partners. The program should be sustainable.
- Continuously collect socio-economic data using appropriate forms indicators to monitor mining activity impact

If these identified concerns are addressed there will more effective community participation in decision making in the mining sector in Kenya and this will in turn reduce potential conflicts in the mining sector.

## IX. REFERENCES

[1]. Khalid Salim - MINING ACT, 2014 OF KENYA-AN OVERVIEW

[2]. Evans Khamala Masachi - Implications Of The Old Mining Law Cap. 306 And The Proposed Mining Act 2014 On Artisanal And Small Scale Gemstone & Precious Metal Mining - Presentation December 2014

[3]. Bawa Ibrahim – Minerals Commission , Managing Africa's Resources Sustainably: Challenges of Small Scale Mining in Ghana.

[4]. Bridges, C.R. (1974) Green grossularite garnets (tsavorites) in East Taita Taveta County (TTC). Gems & Gemology, Summer, pp. 290–295. Scale mining and sustainable development within the SADC Region.

[5]. Butler, J., 1990, Gender Trouble: Feminism and the Subversion of Identity, Routledge publ., L.J. Nicholson, ed., 172p.

[6]. Çagatay, N., 2001, Trade, Gender and Poverty, United Nations Development Programme, 45p.

[7]. Dreschler, B. (2001) Small-scale and sustainable development within the SADC.

[8]. Dreschler, B. (2001). Small Scale Mining and Sustainable Development within the SADC Region. Mining, Minerals and Sustainable Development. IIED. London.2002,

[9]. http://commdev.org/files/1798_file_asm_southern_Taita Taveta County (TTC).pdf.

[10]. Gueye, D. (2001) Small Scale Mining in Burkina Faso. Mining, Minerals and Sustainable Development No. 73, http://pubs.iied.org/pdfs/G00717.pdf.

[11]. Hentschel, T., Hruschel, F. and Priester M. (2003) Artisanal and Small Scale Mining: Challenges and Opportunities, International Institute for Environment and Development and WBCD,London, http://afrim.org.ph/IDLS/files/original/94db37ffd394f7786a06f03b5ccf9c69.pdf.

[12]. Hinton, J. (2003) CASM, an integrated Review for Development Planning.

[13]. Hinton, J.J. et al. (2002) Clean artisanal gold mining: a utopian approach? Journal of Cleaner production (2003) 11:99-115.

[14]. Hinton, J.J., Veiga, M.M. and Veiga, A.T.C., 2003, Clean Artisanal Gold Mining: A Utopian Approach?, Journal of Cleaner Production, Vol.11, Issue: 2, March, 2003, pp. 99-115.

[15]. IGF, (2010) A MINING POLICY FRAMEWORK; Mining and Sustainable Development.

[16]. The Mining Act, 2016 : Government of Kenya

[17]. Bawa Ibrahim – Minerals Commission, Managing Africa's Resources Sustainably: Challenges of Small Scale Mining in Ghana.

[18]. Bridges, C.R. (1974) Green grossularite garnets (tsavorites) in East TaitaTaveta County (TTC). *Gems & Gemology*,Summer, pp. 290–295. Scale mining and sustainable development within the SADC Region.

[19]. Butler, J., 1990, Gender Trouble: Feminism and the Subversion of Identity, Routledge publ., L.J. Nicholson, ed., 172p.

[20]. Çagatay, N., 2001, *Trade, Gender and Poverty*, United Nations Development Programme, 45p.

[21]. Dreschler, B. (2001) Small-scale and sustainable development within the SADC.

[22]. Dreschler, B. (2001). Small Scale Mining and Sustainable Development within the SADC Region.Mining, Minerals and Sustainable Development.IIED.London.2002, http://commdev.org/files/1798_file_asm_southern_Taita Taveta County (TTC).pdf.

[23]. Gueye, D. (2001) Small Scale Mining in Burkina Faso. Mining, Minerals and Sustainable Development No. 73, http://pubs.iied.org/pdfs/G00717.pdf.

[24]. Hentschel, T., Hruschel, F. and Priester M. (2003) Artisanal and Small Scale Mining: Challenges and Opportunities, International Institute for Environment and Development and WBCD,London, http://afrim.org.ph/IDLS/files/original/94db37ffd394f7786a06f03b5ccf9c69.pdf.

[25]. *Hinton, J. (2003) CASM, an integrated Review for Development Planning.*

[26]. Hinton, J.J. et al. (2002) Clean artisanal gold mining: a utopian approach? Journal of Cleaner production (2003) 11:99-115.

[27]. Hinton, J.J., Veiga, M.M. and Veiga, A.T.C., 2003, Clean Artisanal Gold Mining: A Utopian Approach?,*Journal of Cleaner Production*, Vol.11, Issue: 2, March, 2003, pp. 99-115.

[28]. IGF, (2010) A MINING POLICY FRAMEWORK; Mining and Sustainable Development.

[29]. International Labour Organization (ILO), 1999, *Social and Labour Issues in Small-scale Mines*. Report for discussion at the Tripartite Meeting on Social and Labour Issues in Small-scale Mines, ILO, Geneva.

[30]. Kenya: Vision 2030. Government of the Republic of Kenya.Ministry of Planning and national Development.Office of the President, Nairobi, 2007.
[31]. Keller, P.C. (1992) Gemstones in East TaitaTaveta County (TTC). Phoenix. Geoscience Press. Nairobi.
[32]. KARI, H.K. (2007) Availability and accessibility of ICT in rural communities in Nigeria.The Electronic Library Vol. 25 No. 3 pp. 363-372, http://dx.doi.org/10.1108/02640470710754869.
[33]. Labonne, B. (1996) Artisanal Mining: An Economic Stepping Stone for Women.
[34]. Mayer Brown, (2013) Mining in Kenya – The start of a new era?
[35]. Taita Taveta Professionals' forum 2010
[36]. Moyi E.D (2003) Networks, information and small enterprises: New technologies and the ambiguity of empowerment IN Information Technology for Development 10 (2003) pp. 221–232 221.
[37]. Mutemeri N., Lahiri-Dutt K., Hinton J., Strongman J., Heller K., Eftimie A. (2012) Gender Dimensions of small scale mining - A Rapid Assessment Toolkit.
[38]. Mutie, B. (2012) Policy Gaps in Mining and Mineral Sector in Kenya
[39]. Mwaipopo, R. Mutagwaba, W. and Nyange, D. (2004) Increasing the contribution of Artisanal and Small Scale Mining to poverty reduction in Tanzania, http://r4d.dfid.gov.uk/pdf/outputs/C393.pdf.
[40]. Nyaberi, M.D. and Rop, B.K. (2014) Petroleum prospects of Lamu Basin, South-Eastern Kenya. Journal of the Geological Society of India, Volume 83, Issue 4, pp. 414-422.
[41]. Priester M., Hruschka F., Hentschel T. (2003) Artisanal and Small-scale mining, London.
[42]. Promotion of Extractive and Mineral Processing Industries in the EAC – Kenya Status
[43]. Pohl W. and Horkel, A (1980) Notes on the Geology and Mineral Resources of the MtitoAndei-Taita Area (Southern Kenya), Kenya Austria Mineral Exploration Project.
[44]. Report on the gemology course for small scale miners in TaitaTaveta County, Department of Mining and Mineral Process Engineering, TaitaTaveta University College, 2011.
[45]. Simonet, C., Okundi, S. and Masai, P. (2001) General setting of coloured gemstone deposits in the Mozambique Belt of Kenya—preliminary considerations.*Proc. 9th Conf. Geol. Soc. Kenya, Nairobi, November 2000*, pp. 123–138.
[46]. The World Bank (2005) The Millennium Development Goals and Small-Scale Mining.
[47]. The World Bank (2008) Communities, Artisanal and Small-Scale Mining (CASM) – Issue Brief.
[48]. UNDESA (2003) Poverty Eradication and Sustainable Livelihoods: Focus on Artisanal Mining Communities. Sssp Project RAF/99/023.
[49]. WWF (2012) Artisanal and Small-Scale Mining in protected areas and critical ecosystems programme(ASM. A Global Solution Study.)
[50]. Mwandawiro Mganga:Mining in Taita Taveta County:Prospects & Problems 2009
[51]. Cohen et al 2007 Research Methods in Education, Sixth Edition - Teacher ...
[52]. Bertini & Santucci, (2006) Enabling automatic clutter reduction in parallel coordinate plots
[53]. UNEP 2012 A New Angle on Sovereign Credit Risk - Global Footprint
[54]. SSM CFC Gender in small scale mining
[55]. Susapu and Crispin, 2001 Women and Artisanal Mining: Gender Roles and the Road Ahead
[56]. Wasserman, 1999 WOMEN IN MINING - ICMM

# Optimal Acid Mine Water Treatment Network Design with Multipurpose Evaporation and Irrigation Regenerator Subnetwork

Timothy T. Rukuni[1*], Maurice S. Onyango[1,2] & Andrei kolesnikov[1]

***Abstract*—** South Africa is a water strained country. It is speculated on good grounds that the demand for water is already equal to or exceeds the supply. The limited water supplies are frequently contaminated by acid mine water discharges which also poses huge environmental, ecological and health risks where water users are frequently exposed to high metal concentrations. In South Africa, like in other countries in the region, mining started over a century ago and most of the acid mine drainage (AMD) discharge is coming from abandoned mines and this leaves the government to carry the burden to avoid further decants and contamination of the scarce surface and underground water resource. The current estimated cost by the Department of Water & Sanitation for AMD neutralisation and desalination is R3.6 million/(ML/day) and R60 million/(ML/day) respectively. These figures are huge taking into consideration that the total flow in Gauteng province alone is 200 ML/day.

By using process integration and its enabling tools, the current study seeks to develop and evaluate a robust integrated acid mine water treatment network with multiple treatment or regeneration units. This allows for selective use of the treated mine water in agriculture, process industries, municipalities for drinking water purposes while simultaneously minimising the environmental impacts and costs. This was achieved by embedding a subnetwork of detailed evaporation and irrigation network linked to a neutralisation, softening and desalination (e.g. reverse osmosis and ion exchange) water treatment network. Based on the network and a fixed flow-rate of 30 ML/day for the Western Basin, a mathematical optimization model will be developed and optimised for optimal flow-rates of acid mine drainage into the treatment units and treated water into the distribution systems (Agriculture, Industry, rivers, environment and municipalities). The results of the preliminary water network development on the neutralisation stage have indicated that the total chemical cost for the neutralisation stage can be reduced from the estimated R3.6 million/(ML/day) to R1.9 million/(ML/day).

Keywords:

***Keywords*—** Acid mine drainage, process integration, desalination, neutralisation.

## I. Introduction

LARGE investments have been made in mine water treatment in South Africa. R2.50 billion was invested for neutralization of the mine water in the Western, Central and Eastern Basins and R2.95 billion for desalination of mine water in Mpumalanga. A further R10 billion needs to be invested, for desalination of the neutralised mine water in the Witwatersrand Western, Central and Eastern Basins. Despite these large investments, the environment is still threatened by the discharge of untreated or partly treated mine water into watercourses. The current cost of desalination, following neutralization, is estimated at R60 million/(ML/d). Despite the large investments made into research and development, construction of full-scale plants and strict legislation forcing industry to desalinate water, even at high cost, the environment is becoming more and more polluted.

The questions addressed in this investigation were:

- Can the projected desalination cost be reduced from R60 million/(ML/d) to less than R10 million/(ML/d)?;
- Is it possible for pollution due to disposal of solid waste and brines be turned into income through recovery of saleable products?
- How can large volumes of surface water be protected from salination by small volumes of un-treated or semi-treated mine water?.

The Conference Secretariat will do the final formatting of your paper.

## II. Cost of Water Treatment

Treatment of acid mine water includes neutralization and desalination. Acid mine water in the Wits, Western, Central and Eastern Basins is, or is shortly to be neutralized [5]. The cost of the three plants is R2.5 billion [6]. The construction cost of the plant in the Central Basin was R319-million and it was operational by August 2012 [7]. The cost of the plant in the Eastern Basin was estimated at R950-million and was projected to be operational by December 2015 [6]. In the Western Basin it was decided to upgrade the existing facilities at Harmony Gold Mine. The Trans-Caledon Tunnel Authority (TCTA) opted to employ proven local technology that uses limestone treatment for neutralisation of free acid, followed by additional lime treatment for removal of iron (II) and other heavy metals [8]. The projects made provision for pumping of mine water to the ECL of 165m, 168 m and 290 m for the Western, Central and Eastern Basins, respectively [7, 9]. Specialized submersible pumps (double suction, 2 400 kW, 6 600 V, 50 Hz) were

Corresponding Author: T.T Rukuni Department of Chemical, Metallurgical & Materials Engineering, Tshwane University of Technology (TUT), Private Bag X680, 0001, Pretoria, South Africa. Telephone phone: +2784 026 1133; e-mail: rukunitt@tut.ac.za

A. Kolesnikov Department of Chemical, Metallurgical & Materials Engineering, TUT. e-mail: kolesnikova@tut.ac.za

M.S. Onyango Rand Water Chair in Water Utilisation, TUT. Email: onyangoMS@tut.ac.za

installed in the three Basins to pump water to the ECL [10]. Two were installed in the Central Basin, three in the Eastern Basin and two in the Western Basin, while two were placed on standby. A tenth smaller pump was initially installed in the Western Basin. The cost of two large pumps amounted to R60-million [7].

After neutralisation mine water has to be desalinated. The gold mines in Gauteng produce 350 ML/d of mine water and the coal mines in Mpumalanga, 200 ML/d. Three mine water desalination plants have been constructed in Mpumalanga: at eMalahleni (50 ML/d at a capital cost of R900 million), Optimum Colliery (15 ML/d at a cost of R800-million) and Middelburg Colliery (25 ML/d at a cost of R1 250-million). The three plants treat 90 ML/d and had a total capital cost of R2 950-million [11, 12, 13, 14, 15, 16, 17]. At a treatment cost of R15/m3, the annual running cost amounts R493-million [11]. A large portion of the 75 ML/d treated at eMalahleni and Optimum is sold as drinking water. The balance is discharged into the Olifants River. As detailed above, three neutralization plants were constructed in Gauteng, or are under construction at an estimated cost of R2-billion [18]. This will be followed by three desalination plants at an expected cost of R10-billion [18]. These figures exclude the cost of sludge and brine disposal. The large, essential investments confirm the need for ongoing research and development to develop more cost-effective mine water treatment processes.

## III. Sludge And Brine Disposal

South Africa's total waste stream amounts to 539 million t/a of which industrial and mining waste amounts to about 487 million t/a (90%) [19]. Mining waste contributes 72.3% to the solid waste stream. The legal definitions of waste are contained in the National Environmental Management: Waste Act, 2008 and the National Water Act, 1998. South Africa supports the waste hierarchy in its approach to waste management, by promoting cleaner production, waste minimization, water reuse, recycling and waste treatment, with disposal seen as a last resort [20]. The Act stipulates that acids should be neutralised to have a pH between 6 and 12 before discharge onto a landfill site. The TDS content of brine or waste with a high salt content should not exceed 50 000 mg/L and the TDS from leachables should not exceed 100 000 mg/L [21].

## IV. Objectives

The purpose of this study was to investigate the changes required to current practices to reduce the negative environmental impacts of mine water. The following specific objectives were set:

- Reduce the cost of desalination from R60-million/(ML/d) to R10-million/(ML/d).
- Identify technologies that will protect large volumes of clean surface water from in-flows of small volumes of partially treated mine water.
- Identify technologies where disposal of waste sludge and brine streams is replaced by the recovery of saleable products.

## V. Results and Discussion

### *A. Treatment*

The capital and running costs are high for mine-water treatment plants, as indicated in Background (above). These high costs should serve as motivation for investigations into reducing the cost of mine water treatment.

Table 1 shows the costs of raw materials used during water treatment by various processes. Table 2 shows the chemical compositions of the raw and treated water, flow-rates and compositions of streams, mass of solid waste and estimated running and capital costs for the various neutralization technologies. Option A is when neutralisation is effected by the use of limestone for the removal of free acidity followed by lime for removal of metals. Option B utilises lime alone for neutralisation. In Option C, soda-ash is used for neutralisation. A combination of limestone and lime neutralisation, when given sufficient residence time, allows for partial sulphate removal through gypsum crystallisation (Table 2; Columns A & B). The cost of neutralization of Western Basin water with $CaCO_3$ and $Ca(OH)_2$ amounts to R2.72/$m^3$ compared to R5.00/$m^3$ when solely lime is used. Gypsum crystallization, results in partial sulphate removal from 3 500 mg/L down to 1802 mg/L. When $Na_2CO_3$ is used for neutralization, the alkali cost amounts to R8.64/$m^3$.

TABLE I
PRICES OF CHEMICALS USED IN THIS INVESTIGATION

| Chemical | Source | Utilization | Purity | Price |
|---|---|---|---|---|
| | | % | % | R/t |
| Ca(OH)2 | Purchase | 90 | 88 | 2 200 |
| Na2CO3 | Purchase | 99 | 98 | 2 947 |
| NaOH | Purchase | 99 | 88 | 3 000 |
| H2SO4 | Purchase | 99 | 98 | 1 800 |
| BaCO3 | Recover | 95 | 98 | 5 000 |
| HNO3 | Purchase | 99 | 65 | 4 000 |
| NH4OH | Purchase | 99 | 90 | 4 000 |
| Al(OH)3 | Recover | 90 | 97 | 5 000 |

TABLE 2
NEUTRALIZATION OF WESTERN BASIN WATER WITH VARIOUS ALKALIS

| Parameter | Units | | Neutralization | | | | | |
|---|---|---|---|---|---|---|---|---|
| Parameter | | | Feed 1 | Option A | | Option B | A & B | Option C |
| | | Eq mass | | CaCO3 | Ca(OH)2 | Ca(OH)2 | Gypsum | Na2CO3 |
| Recovery | % | | | | | | | |
| Salt rejection | % | | | | | | | |
| Flow | m3/h | | 160,00 | 160,00 | 160,00 | 160,00 | 160,00 | 160,00 |
| Flow | m3/d | | 3 840,00 | 3 840,00 | 3 840,00 | 3 840,00 | 3 840,00 | 3 840,00 |
| CaCO3 | mg/l | | | 1 845,34 | | | | |
| Ca(OH)2 | mg/l | 37,00 | | | 434,46 | 1 800,02 | | |
| Na2CO3 | mg/l | 53,00 | | | | | | 2 844,02 |
| NaOH | mg/l | 40,00 | | | | | | |
| H2SO4 | mg/l | 49,00 | | | | | | |
| Coal | | | | | | | | |
| BaCO3 | mg/l | 98,50 | | | | | | |
| HNO3 | mg/l | 63,00 | | | | | | |
| NH4OH | mg/l | 35,00 | | | | | | |
| Al(OH)3 | mg/l | 26,00 | | | | | | |
| Utilization | % | | | 90,00 | 90,00 | 90,00 | | 99,00 |
| Purity | % | | | 88,00 | 88,00 | 88,00 | | 98,00 |
| Dosage | mg/l | | | 2 329,98 | 548,57 | 2 272,75 | | 2 931,38 |
| Price | R/t | | | 650,00 | 2 200,00 | 2 200,00 | | 2 947,00 |
| Usage | t/day | | | 8,95 | 2,11 | 8,73 | | 11,26 |
| Chemical cost | R/m3 | | | 1,51 | 1,21 | 5,00 | | 8,64 |
| Chemical cost | R/m3 | | | 2,72 | | 5,00 | | 8,64 |
| CO2 | mg/l | 22,00 | | | | | | |
| Water | | | Western Basin | | | | | |
| pH | | 5,76 | 2,80 | 9,20 | 9,20 | 9,20 | 9,20 | 8,00 |
| Carbonate | mg CO3/L | 30,00 | 0,00 | 60,00 | 60,00 | 60,00 | 60,00 | 0,00 |
| Sulphate | mg SO4/L | 48,00 | 3 500,00 | 3 500,00 | 3 500,00 | 3 500,00 | 1 801,88 | 3 500,00 |
| Chloride | mg Cl/L | 35,50 | 30,00 | 30,00 | 30,00 | 30,00 | 30,00 | 30,00 |
| H+ | mg H+/L | 1,00 | 13,38 | 1,00 | 0,00 | 0,00 | 0,00 | 13,38 |
| Sodium | mg Na/L | 23,00 | 50,00 | 50,00 | 50,00 | 50,00 | 50,00 | 1 284,20 |
| Magnesium | mg Mg/L | 12,15 | 150,00 | 150,00 | 50,00 | 50,00 | 50,00 | 50,00 |
| Calcium | mg Ca/L | 20,00 | 415,00 | 1 153 | 1 388 | 1 388 | 680 | 5,00 |
| Aluminium | mg Al/L | 9,00 | 50,00 | 0,00 | 0,00 | 0,00 | 0,00 | 1,00 |
| Iron(II) | mg Fe/L | 27,93 | 400,00 | 1,00 | 1,00 | 1,00 | 1,00 | 1,00 |
| Iron(III) | mg Fe/L | 18,62 | 50,00 | 0,00 | 0,00 | 0,00 | 0,00 | 0,00 |
| Manganese | mg Mn/L | 27,47 | 70,00 | 70,00 | 1,00 | 1,00 | 1,00 | 1,00 |
| Barium | mg Ba/L | 68,50 | 0,00 | 0,00 | 0,00 | 0,00 | 0,00 | 0,00 |
| Strontium | mg Sr/L | 43,81 | 0,00 | 0,00 | 0,00 | 0,00 | 0,00 | 0,00 |
| Total Acidity | mg/L | 50,00 | 1 797,13 | 37,23 | 1,29 | 1,29 | 1,29 | 71,89 |
| Anion Sum | | | 73,76 | 75,76 | 75,76 | 75,76 | 40,38 | 73,76 |
| Cation Sum | | | 73,76 | 75,76 | 75,76 | 75,76 | 40,38 | 73,76 |
| Total Dissolved Solids | mg/L | | 4 728 | 5 015 | 5 080 | 5 080 | 2 674 | 4 886 |
| Solids | kg/m3 feed | | | 0,75 | 0,35 | 1,10 | 3,04 | 0,00 |

The following processes were evaluated for the desalination of 160$m^3$/h Western Basin water and evaluation of treated water qualities: HIPRO (reverse osmosis), $BaCO_3$ (chemical precipitation with barium salts), KNEW (ion-exchange), Savmin (chemical precipitation with an aluminium complex) and ROC (reverse osmosis/cooling) (Table 3)

The TDS content of Western Basin water after lime treatment, including gypsum crystallization, is 2 674 mg/L. During desalination with the HiPRO process, the TDS can be reduced to 28 mg/L, with the $BaCO_3$ process, to 604 mg/L, with the KNEW process, to 26 mg/L, and with the Savmin process, to 405 mg/L. The reason for the less efficient TDS removals by the chemical desalination processes ($BaCO_3$ and Savmin) is that sodium sulphate is soluble and cannot be removed with the $BaCO_3$ or Savmin (ettringite) processes. Monovalent ions such as $Na^+$ and $Cl^-$ can be removed by adding ion-exchange as a polishing stage to the chemical desalination processes, as described by Ruto et al. [30].

The chemical costs for the various technologies are, R6.98/$m^3$ for HIPRO (Lime, $H_2SO_4$ and membrane cleaning chemicals); R15.82/$m^3$ for $BaCO_3$ ($BaCO_3$); R26.93/$m^3$ for KNEW ($Na_2CO_3$, $HNO_3$, $NH_4OH$); R12.41/$m^3$ for Savmin (Lime, $Al(OH)_3$ and $H_2SO_4$) and R8.19/$m^3$ for the ROC process (Table 3). The corresponding total running costs (including capital redemption costs) are R19.65 for the HIPRO process, R20.32/$m^3$ for the $BaCO_3$ process, R32.56/$m^3$ for the KNEW process, R18.44/$m^3$ for the Savmin process and R16.59 for the ROC process (Table 3). Table 4 shows the costs of the various technologies when a value was given to the treated water, as a function of its TDS content.

TABLE 3
DESALINATION OF NEUTRALIZED WATER UTILISING THREE DIFFERENT TECHNOLOGIES

| Parameter | Units | | Desalination Technology | | | | | |
|---|---|---|---|---|---|---|---|---|
| | | | Pre-treated | RO | BaCO3 | KNEW | Savmin | RO/ F Desal. |
| Flow | m3/h | | 160,00 | 160,00 | 160,00 | 160,00 | 160,00 | 160,00 |
| Recovery | % | | | 97,30 | | | | 98,80 |
| Salt rejection | % | | | 99,02 | | | | 98,66 |
| | | | Chemical dosage (mg/l) | | | | | |
| Chemical | | | Pre-treated | RO | BaCO3 | KNEW | Savmin | RO/ F Desal. |
| Ca(OH)2 | | | | 449,2 | | | 1 584,8 | |
| Na2CO3 | | | | | | 1 890,2 | | 1 784,7 |
| NaOH | | | | | | | | |
| H2SO4 | | | | 147,0 | | | 1 635,3 | 147,0 |
| Coal | | | | | 876,2 | | | |
| BaCO3 | | | | | 2 876,8 | | | |
| HNO3 | | | | | | 2 402,9 | | |
| NH4OH | | | | | | 1 327,6 | | |
| Al(OH)3 | | | | | | | 867,7 | |
| Chemical cost | R/m3 | | 2,72 | 6,98 | 15,82 | 26,93 | 12,41 | 8,19 |
| Membrane protection chemicals | R/m3 | | | 2,00 | 0,00 | 0,00 | 0,00 | 1,00 |
| Electricity | R/m3 | | 1,20 | 2,40 | 0,80 | 0,80 | 1,20 | 3,20 |
| Labour | R/m3 | | 1,00 | 2,00 | 2,00 | 2,00 | 2,00 | 2,00 |
| Maintenance | R/m3 | | 0,50 | 0,50 | 0,50 | 0,50 | 0,50 | 0,50 |
| Membrane replacement | | | - | 0,60 | 0,00 | 0,00 | 0,00 | 0,30 |
| Admin | R/m3 | | 0,15 | 0,25 | 0,25 | 0,25 | 0,25 | 0,25 |
| Management | | | 0,20 | 0,20 | 0,20 | 0,20 | 0,20 | 0,20 |
| Running cost | R/m3 | | 5,77 | 14,93 | 19,57 | 30,68 | 16,56 | 15,64 |
| Capital redemption cost (10%, 20 y)*[1] | | | 0,57 | 4,71 | 0,75 | 1,89 | 1,89 | 0,94 |
| Running cost (incl Capital Redemption) | | | **6,34** | **19,65** | **20,32** | **32,56** | **18,44** | **16,59** |
| Capital cost (Rm/(Ml/d)) | | | 6,00 | 50,00 | 8,00 | 20,00 | 20,00 | 10,00 |
| Electricity (kWh/m3) | | | 1,50 | 3,00 | 1,00 | 1,00 | 1,50 | 4,00 |
| Interest (%) | | | 12,00 | 12,00 | 12,00 | 12,00 | 12,00 | 12,00 |
| Term | | | 240,00 | 240,00 | 240,00 | 240,00 | 240,00 | 240,00 |
| **Parameter** | | | **Water Quality** | | | | | |
| | **Units** | **Feed** | **Pre-treated** | **RO** | **BaCO3** | **KNEW** | **Savmin** | **RO/ F Desal.** |
| pH | | 2,80 | 7,80 | 7,50 | 7,80 | 8,00 | 8,30 | 7,50 |
| Carbonate | mg/l | 0,00 | 60,00 | 1,16 | 60,00 | 0,00 | 60,00 | 1,68 |
| Sulphate | mg/l | 3 500,00 | 1 801,88 | 17,51 | 400,00 | 15,00 | 200,00 | 43,70 |
| Chloride | mg/l | 30,00 | 30,00 | 0,58 | 30,00 | 5,00 | 30,00 | 0,84 |
| Nitrate | mg/l | 0,00 | 0,00 | 0,00 | 0,00 | 0,00 | 0,00 | 0,00 |
| H+ | mg/l | 13,38 | 0,00 | 0,00 | 0,00 | 0,21 | 0,00 | 0,08 |
| Sodium | mg/l | 50,00 | 50,00 | 0,97 | 50,00 | 5,00 | 50,00 | 17,91 |
| Potassium | mg/l | 0,00 | 0,00 | 0,00 | 0,00 | 0,00 | 0,00 | 0,00 |
| Magnesium | mg/l | 150,00 | 50,00 | 0,02 | 50,00 | 0,50 | 50,00 | 1,40 |
| Calcium | mg/l | 415,00 | 680,43 | 7,50 | 96,32 | 0,50 | 12,98 | 0,20 |
| Aluminium | mg/l | 50,00 | 0,00 | 0,00 | 0,00 | 0,10 | 0,00 | 0,00 |
| Iron(II) | mg/l | 400,00 | 1,00 | 0,02 | 1,00 | 0,00 | 1,00 | 0,03 |
| Iron(III) | mg/l | 50,00 | 0,00 | 0,00 | 0,00 | 0,00 | 0,00 | 0,00 |
| Manganese | mg/l | 70,00 | 1,00 | 0,02 | 1,00 | 0,05 | 1,00 | 0,03 |
| Anion Sum | meq/l | 73,76 | 40,38 | 0,42 | 11,18 | 0,45 | 7,01 | 0,99 |
| Cation Sum | meq/l | 73,76 | 40,38 | 0,42 | 11,18 | 0,51 | 7,01 | 0,99 |
| Total Dissolved Solids | mg/l | 4 728,38 | 2 674,31 | 27,78 | 604,32 | 26,36 | 404,98 | 63,53 |
| Value of water | R/m3 | | 1,09 | 9,91 | 7,99 | 9,91 | 8,65 | 9,79 |
| *[1] - Estimated figures; Correct figures need to be obtained from the suppliers of the various technologies | | | | | | | | |

For zero mg/L TDS the value was taken at R10/$m^3$ and for 1000 mg/L, at R6.67/$m^3$. The cost of the KNEW process was the highest, at R22.65/$m^3$. When the values of its by-products are taken into account the process will be cost-effective. The cost of the ROC process, was the lowest, R6.80/$m^3$. The main reason is its lower capital cost and consequently lower capital redemption cost.

The second observation was that no brine was produced with the chemical desalination processes. The HIPRO process produces 4.32 $m^3$/h brine containing 18 157 mg/L TDS and the KNEW process, 12.96 $m^3$/h ion-exchange regenerant with a TDS of 70 000 mg/L (Table 5). The regenerant from the KNEW process can be processed to recover saleable $Ca(NO_3)_2$ and $(NH_4)2SO_4$. In the case of HIPRO process, the sludge that has to be disposed of amounts to 4.84 kg/($m^3$ feed), 0.49 kg/($m^3$ feed) in the case of $BaCO_3$, 0.18 kg/($m^3$ feed) in the case of KNEW and 3.34 kg/($m^3$ feed) in the case of the Savmin process (Table 5).

### *B. Sludge Disposal versus Recovery Of Saleable Products*

The sludge resulting from mine water treatment systems usually contains elevated levels of contaminants that were

originally contained in the mine water. Proper disposal of these solids with careful environmental considerations must be done to avoid shifting of the original pollutants in the waste-stream to the final disposal site where they may again become free to change its state or properties to facilitate safe disposal. These methods still leave residues which in most cases must be removed from the plant site. Treatment and final disposal of the primary and secondary sludge makes up a significant part of the material and financial resources of the wastewater treatment plant.

Zero waste disposal is a real and necessary aim due to the high costs of disposal of solid wastes and brines. Table 5, shows the costs associated with the disposal of sludge and/or brines that are produced by the various technologies. A cost of R3 100/t, was used as the typical cost for disposal at a toxic waste disposal site. The high costs that were calculated would be unaffordable and therefore, much emphasis should be towards the recovery of saleable products from waste streams.

During neutralization with limestone and/or lime, gypsum-rich sludge and metal hydroxides are produced. Such a mixed sludge has no value and has to be disposed of at a high cost. The gypsum that is produced during desalination with the HiPRO process is essentially pure or only contaminated with $Mg(OH)_2$. This pure gypsum has some value and can be used as building material or for processing into sulphur and $CaCO_3$.

The economic viability of several desalination processes is highly dependent on the feasibility of the recovery of process raw materials. Gypsum is produced as a by-product in the HIPRO process and $CaCO_3$ and sulphur can be recovered from the gypsum. Gypsum can also be sold as a soil conditioner or as a raw material to the cement industry. In the barium process, $BaCO_3$ can be regenerated from $BaSO_4$, or the $BaSO_4$ sold as a drilling mud. Other saleable products that can be recovered from the Barium process sludge are sulphur and $CaCO_3$. In the case of the Savmin process, $Al(OH)_3$ should be recovered from etteringite, $3CaO.3CaSO_4.Al_2O_3$, whilst gypsum and $CaCO_3$ are produced as by-products. In the case of the KNEW process, by-product $NaNO_3$ and $(NH_4)2SO_4$, can be sold to at least partially cover the cost of the ion-exchange elution raw materials, $HNO_3$ and $NH_4OH$.

TABLE 4
TOTAL OF WATER, PRODUCTS AND RUNNING COST

| Parameter | Unit | | | Value | | | | | |
|---|---|---|---|---|---|---|---|---|---|
| | | | | Feed | RO | BaCO3 | KNEW | Savmin | RO/F Des |
| **Values in R/m3** | | | | | | | | | |
| Capital cost (estimate) | Rm/(ML/d) | | | | 50,00 | 8,00 | 20,00 | 20,00 | 10,00 |
| TDS | mg/L | | | 2 674,31 | 27,78 | 604,32 | 26,36 | 404,98 | 63,53 |
| Value of water (Table 5) | R/m3 | | | 1,09 | 9,91 | 7,99 | 9,91 | 8,65 | 9,79 |
| Running cost (Table 5) | R/m3 | | | | -19,65 | -20,32 | -32,56 | -18,44 | -16,59 |
| Total cost | R/m3 | | | | -9,74 | -12,34 | -22,65 | -9,79 | -6,80 |

TABLE 5
SLUDGE AND BRINE DISPOSAL COST

| Brine disposal cost | | Units | | | RO | BaCO3 | KNEW | Savmin | RO/F Des |
|---|---|---|---|---|---|---|---|---|---|
| Total dissolved solids | | mg/l | | | 18 157,24 | | 70 000 | | 53 569 |
| Flow | | m3/h | | | 4,32 | | 12,96 | | 1,92 |
| Flow | | t/month | | | 3 152 | | 9 459 | | 1 401 |
| Disposal cost | | R/t | | | 3 100 | | 3 100 | | 3 100 |
| Disposal cost | | R/month | | | 9 770 803 | | 29 323 609 | | 4 342 579 |
| Disposal cost | | R/m3 feed | | | 83,70 | | 251,20 | | 37,20 |
| **Sludge disposal cost** | | | | | | | | | |
| Solids (dry) | | kg/m3 feed | | | 4,83 | 0,49 | 0,18 | 3,34 | 0,37 |
| Mass (dry) | | kg/h | | | 772,12 | 77,80 | 28,17 | 534,88 | 58,99 |
| Sludge (30% solids) | | t/month | | | 1 878 | 189 | 69 | 1 301 | 143 |
| Disposal cost (R3 100/t) | | R/month | | | 5 821 198 | 586 582 | 212 403 | 4 032 574 | 444 757 |
| Disposal cost | | R/m3 feed | | | 49,87 | 5,02 | 1,82 | 34,54 | 3,81 |
| **Brine + Sludge disposal cost** | | **R/m3 feed** | | | **133,57** | **5,02** | **253,02** | **34,54** | **41,01** |

Table 6 shows the value of saleable products that can be recovered from the various processes. Values between R0.93/($m^3$ feed) and R14.18/($m^3$ feed) were calculated. These costs only include the value of products that can be recovered from the desalination stage. The potential values of metal compounds, namely $CaCO_3$, magnetite and $Na_2SO_4$, which can be recovered during the pre-treatment and cooling stages were not calculated.

TABLE 6
VALUE OF PROCESS BY-PRODUCTS

| By-product | Price (R/t) | | | | Production (mg/l) | | | | |
|---|---|---|---|---|---|---|---|---|---|
| | | | | | RO | BaCO3 | KNEW | Savmin | RO/F Des |
| CaSO4.2H2O | 300 | | | | 3 103 | | | 2 870 | |
| CaCO3 | 1 000 | | | | | 1 460 | | 473 | |
| BaCO3 | 5 000 | | | | | | | | |
| BaSO4 | 1 000 | | | | | 3 402 | | | |
| Sulphur | 1 400 | | | | | 0 | | | |
| Al(OH)3 | 5 000 | | | | | | | 868 | |
| H2SO4 | 1 800 | | | | | | | | |
| NaNO3 | 2 500 | | | | | | 3 215 | | |
| (NH4)2SO4 | 2 500 | | | | | | 2 457 | | |
| Na2CO3 | 2 947 | | | | | | | | |
| Na2SO4 | 2 000 | | | | | | | | 1 354 |
| **Value (R/m3)** | | | | | **0,93** | **4,86** | **14,18** | **5,67** | **2,71** |

*C. Protection of surface water*

*i. Volume of water*

All mine water should be desalinated to protect surface water. It is environmentally futile if only a portion of the neutralized mine water is desalinated at high cost while the remaining neutralized mine water is allowed to be discharged into water courses. Alternative methods have to be considered on how to deal with the non-desalinated mine water, other than to discharge it into the environment.

The volume of AMD discharged in Gauteng amounts to 350 ML/d. This is only 3.4% of the total volume of river water in the region (Table 7). The percentage will be even less if mine water is allowed to rise to higher levels before it is pumped to surface. The individual figures for mine-water that is discharged into the two main rivers, the Vaal and Crocodile Rivers, amounts to 3.0% and 4.6%, respectively. Thus, since mine-water amounts to only 3.4% of the surface water, a cost comparison is needed for desalination of the mine-water versus complete prevention of mine-water discharge into rivers. Methods such as forced evaporation and/or irrigation should be considered in combination with treatment of the residual leachate. In the controlled release of mine-water, good quality water is used to dilute the resultant salinity of river water following mine-water discharge. Up to seven times more good quality water, compared to the mine-water, is used for dilution. It may be more cost-effective to keep surface water free from the salts in mine-water through forced evaporation or irrigation plus treatment of the residual water/leachate, than to desalinate mine-water.

TABLE 7
VOLUME OF MINE-WATER PRODUCED IN GAUTENG

| River | Basin | Flow (Ml/d) | | | Mine water/ River water (%) |
|---|---|---|---|---|---|
| | | Mine water | Mine water | River water | |
| Vaal | | | | 10 800 | |
| | Central | 60 | | | |
| | Eastern | 110 | 320 | | 3,0 |
| | Far Western | 150 | | | |
| Crocodile | | | | 650 | |
| | Western | 30 | 30 | | 4,6 |
| Olifants | | | | 2 728 | |
| | Mpumalanga | 130 | 130 | | 4,8 |
| Total | | | 480 | 14 178 | 3,4 |

*ii. Evaporation*

Pond evaporation is widely used to separate pure water from hazardous waste and this greatly reduces the volume for further treatment or disposal. Reduction of water volumes enables the contaminated water to be easily managed and hence prevent the contamination from spreading to environmental water bodies. Convectional pond evaporation systems are driven by heat-energy and given sufficient energy, water molecules on the surface will evaporate. The quantity of water that will evaporate in the system will be directly proportional to the net heat absorbed from all sources less heat losses.

Pond evaporation is usually slow and often limited by land availability and the limitations of cost of constructing additional evaporation ponds and the added cost of clean-up and re-vegetation [32]. Forced evaporation is currently finding its way into mine water management with evaporation rates beyond the traditional evaporation ponds. Forced evaporation makes use of high pressures to force the water through a nozzle to produce fine droplets that will increase the surface area and hence improved evaporation rates. Most of these evaporators are compact, equipped with fine nozzles, a high-pressure pump and an air-fan to give the water droplets enough residence time in suspension, for evaporation. Suppliers of mechanical evaporators claim 70% evaporation rates and the current units on the South African market are operating at 50% evaporation rates, with each unit evaporating approximately 22.5$m^3$/h.

The two most significant sources of heat in forced

evaporation are solar radiation and the heat extractable from moving air. Figure 1, shows mechanical evaporators installed at a mine closure site in South Africa, for management of mine water balances.

There are several forced evaporation units in operation at several mine sites. One case during this study revealed that, for the evaporation of 2 ML/d of water, a pump and 10 evaporation units would be required. The capital redemption and running costs were calculated at R2.90/$m^3$ as shown in Table 10. This is significantly less than the total running cost of R16/$m^3$ - R32/$m^3$ for the desalination technologies when the value of products is excluded. Forced evaporation therefore deserves to be considered as one of the processes that can be used in mine water treatment/disposal followed by neutralisation and desalination of the concentrated stream.

The major advantage of the mechanical evaporator is improved evaporation rates due to increased surface area. In the past decades, the process efficiencies and economic impacts of mechanical wastewater evaporation were underscored by the environmental impacts of the resultant spray-drift and this led to unwarranted public anxieties. Spray-drift and off-target losses are the inherent problems of conventional, air-assisted, fine droplet, mechanical evaporators. Due to concerns for environmental safety and process efficiency, it is important to maximize the amount of water evaporated and deposited back into the source or target site. Current installations include drift barriers to restrict drift to its source or the target site.

Fig. 1 Mechanical evaporator equipped with a booster pump

The net effect of evaporation is concentration of the wastewater for further treatment with other processes such as RO/Freeze desalination, reverse osmosis, ion- exchange, Savmin or the ABC process.

TABLE 8
COST OF FORCED EVAPORATION

| Parameter | Value |
|---|---|
| Capacity (m3/d) | 2 000 |
| Capacity (m3/h) | 83 |
| Pump (110 kW; 24m3/h) | 135 000 |
| Beast (11 kW; 10 units) | 2 450 000 |
| Mother pipe ( 172 mm) | 65 000 |
| Distribution pipes (50 mm; 2 km; R15/ | 32 000 |
| Nozzles (500; R50/nozzle) | 35 000 |
| Support + Cables | 68 000 |
| Nozzles | |
| Capital cost (R) | 2 785 000 |
| Capital cost (R/Ml/d)) | 1 392 500 |
| Interest (%/a) | 12 |
| Term (Months) | 60 |
| Capital redemption cost (R/m3) | 1,02 |
| Velocity (m/sec) | 1 |
| Pipe ddia (mm) | 172 |
| Electricity (kW) | |
| Pump | 110 |
| Beast | 110 |
| Electricity (kW) | 220 |
| Power (kWh/d) | 5 280 |
| Power (kWh/m3) | 2,64 |
| Electricity cost (R/kWh) | 0,60 |
| Electricity cost (R/m3) | 1,58 |
| Labour (R/m3) | 0,10 |
| Maintenance (R/m3) | 0,10 |
| Admin (R/m3) | 0,05 |
| Management (R/m3) | 0,05 |
| Running cost (R/m3) | 1,88 |
| Total cost (R/m3) | 2,90 |

*iii. Irrigation*

An alternative application of evaporation is when it is used to evaporate neutralised acid mine water through irrigation. The irrigation option is attractive as the relatively small volume of neutralized mine water (for example, 200ML/d from the three basins in Gauteng), is kept away from the far larger volume of surface water which is used for domestic purposes (Rand Water produces 4 000 ML/d and current irrigation in the Gauteng region is roughly estimated at 10 000ML/d). Through irrigation, depending on prevailing weather conditions, cropping system selection and irrigation management, around 80% of the mine water can be beneficially evaporated. This will result in precipitation in the soil of 80% of the soluble gypsum in the neutralised water. At an estimated average irrigation rate of 750 mm/year, an area of around 3.9 km x 3.9 km will be needed for irrigation of 30 ML/d, and 10 km x 10 km for 200ML/d. The areas will depend highly on the cropping system selection.

According to Annandale [33], irrigation with gypsiferous mine water is feasible and worth considering as part of the solution to South Africa's AMD problems. Irrigation provides some flexibility, while cropping systems and irrigation practices can be designed to optimise water use, evaporation rates, area needed for irrigation, gypsum precipitation, profit, or job creation. Makgae et al. estimated the capital cost for neutralization and irrigation at R4.9-million/(ML/d) [34].

The effect of leachate on groundwater can be addressed by careful site selection for irrigated fields and, if necessary, the installation of a drainage system. The collected leachate will have to be treated, where necessary, with RO/Freeze desalination to recover clean water and salt as in other mechanical evaporation processes. Possible scaling of the pivot system will be avoided by diluting the neutralized water with desalinated or fresh water. The volume needed for dilution will not exceed 10% as it is only to ensure that the saturation level of gypsum is not exceeded.

The irrigation application offers the following benefits: (i) Low initial treatment cost of acid water, as neutralization will only cost 46% of that of the current operation; (ii) Irrigation of

mine water will result in job creation and the generation of agricultural products. The big benefit of irrigation is that it can handle large volumes of water, and if carefully designed and well managed, should be able to pay for itself. Even if irrigation is subsidised to a degree through the supply of irrigation and storage infrastructure, the supply of some farming equipment, and the pumping of water, this is likely to be a relatively small cost compared to other treatment options. (iii) There will be no need to contaminate large volumes of clean water with neutralized, saline mine water; (iv) There will be no or minimal waste sludge due to sludge processing into raw materials and saleable by-products; and (v) Limited pollution of groundwater.

The geohydrological setting will determine the approach to be followed to intercept and manage the leachate from the irrigated fields, e.g. minimizing the leachate to treat through

ii. Zero waste disposal requires processing of sludge and brine streams that are generated during neutralization and desalination of mine water. Technologies will have to be selected that allow the recovery of saleable products during mine water treatment. With the ROC process, metal compounds can be recovered selectively, including magnetite, $CaCO_3$ and $Na_2SO_4$.

iii. Surface water must be protected by avoiding discharge of untreated or only neutralized mine water into rivers. Since mine water amounts to only 3.4% of the volume of surface water, alternative methods, such as forced evaporation or irrigation should also be considered

interception and evapotranspiration with trees, freeze desalination or controlled release.

## VI. Conclusions and Recommendations

The following conclusions and recommendations were made:

i. Large investments have been made for mine water treatment. This high cost can be lowered by upgrading the HiPRO process to include improvements of the ROC process or by considering alternative new technologies such as the CSIR ABC process ($BaCO_3$), KNEW process (ion-exchange) or Savmin process (chemical desalination).

## Acknowledgements

Financial support from Rand Water and Tshwane University of Technology is gratefully acknowledged.

## References

[1] M. Muller, "Water: Decide now on Lesotho 2, acid mine drainage projects – Prof," http://www.engineeringnews.co.za/article/water-decide-now-on-lesotho-2-acid-mine-drainage-projects-prof-2015-12-03/rep_id:3182, Pretoria, 2015.

[2] J. Zuma, "State of The Nation Address 2015," 15 February 2015. [Online]. Available: http://www.gov.za/president-jacob-zuma-state-nation-address-2015. [Accessed 15 December 2015].

[3] Expert-team, "Mine water management in the Witwatersrand Goldfields with special emphasis on acid mine drainage. Report to the Inter-Ministerial Committee on AMD," Council for Geoscience, Pretoria, 2010.

[4] J. Maree, M. Mujuru, V. Bologo, N. Daniels and D. Mpholoane, "Neutralisation treatment of AMD at affordable cost," Water SA, vol. 39, no. 2, pp. 245-250, 2013.

[5] T. Creamer, "TCTA again warns of funding shortfall for acid water projects," Mining Weekly, vol. 19 January, 2012.

[6] L. Cornish, "www.miningreview.com," 2014. [Online]. Available: http://spintelligentpublishing.com/Digital/Mining-Review-Africa/issue9-2014/files/40.html. [Accessed 30 July 2015].

[7] C. Hasenjager, "Group Five starts to work on TCTA AMD contract," http://nepadwatercoe.org/tag/craig-hasenjager/, 2013.

[8] A. van Niekerk, Interviewee, Divisional Director – Water Engineering, Golder Associates Africa (Pty) Ltd, PO Box 13776, Hatfield, 0028, South Africa. [Interview]. 5 July 2011.

[9] L. van Vuuren, "Acid Mine Drainage solutions rearing to go," The Water Wheel, p. 16, November/December 2011.

[10] Ritz, "Ritz Pumps SA Africa's leading dewatering submercible pumps supplier," Mining Review Africa, pp. 41-43, September 2014.

[11] M. Koen, Interviewee, Mr. [Interview]. 21 July 2015.

[12] L. Kolver, "Kromdraai water treatment plant follows success of eMalahleni," http://www.miningweekly.com/article/contract-awarded-to-increase-capacity-of-eMalahleni-mine-water-treatment-plant-2012-05-04, 2012.

[13] P. Gunther and W. Mey, "Selection of mine water treatment technologies for the eMalahleni (Witbank) water reclamation project," Sun City, South Africa, 2008.

[14] W. Aveng, "eMalahleni Water Reclamation Plant," http://www.avengwater.co.za/projects/emalahleni-water-reclamation-plant, 2014.

[15] L. Tshwete, P. Gunther, W. Mey and A. van Niekerk, "Emalahleni (Witbank) mine water reclamation project," Durban, 2006.

[16] B. Hutton, I. Kahan, T. Naidu and P. Gunther, "Operating and maintenance experience at the eMalahleni water reclamation plant," http://www.imwa.info/docs/imwa_2009/IMWA2009_Hutton.pdf, 2009.

[17] E. Karakatsanis and V. Cogho, "Drinking Water from Mine Water Using the HiPrO® Process – Optimum coal Mine Water reclamation Plant," http://www.imwa.info/docs/imwa_2010/IMWA2010_Karakatsanis_430.pdf, 2010.

[18] I. Solomons, "War on AMD," Mining Weekly (http://www.miningweekly.com/article/govt-private-sector-working-constructively-to-tackle-acid-mine-drainage-in-wits-basin-2015-07-03-1), 3 July 2015.

[19] DWAF, "Waste disposal on land," 1997. [Online]. Available: https://www.dwa.gov.za/dir_wqm/wqm_wasteDispLand.htm. [Accessed 18 December 2015].

[20] W. M. S. A. Institute, "Waste Management," 2000. [Online]. Available: http://www.enviropaedia.com/topic/default.php?topic_id=239. [Accessed 18 December 2015].

[21] Gazette, Landfill, National norms and standards for disposal of waste to landfill, National Environmental Management: Waste Act 59 of 2008 (Gazette No. 32000, Notice No. 278. Commencement date: 1 July 2009 – save for sections 28(7)(a), sections 35 to 41 and section 46 [Proc. No. 34, Gazette No. 32189]), 2008.

[22] W. S. Mey and A. van Niekerk, "Evolution of mine water management in the Highveld coalfields,," http://www.imwa.info/docs/imwa_2009/IMWA2009_Mey.pdf, 2009.

[23] J. P. Maree, "Mine water – Pump or decant? Internal report," Tshwane University of Technology, Pretoria, 2012.

[24] T. T. Rukuni, J. P. Maree, C. M. Zvinowanda and F. H. H. Carlsson, "The effect of temperature and pressure on the separation of calcium carbonate and barium sulphate from a mixed sludge," Chemical Engineering & Process Technology, vol. 3, no. 3, pp. 1-6, 2012.

[25] V. Akinwekomi, J. P. Maree, A. Strydom and C. Zvinowanda, "Recovery of magnetite from iron-rich mine water," Durban, 2016.

[26] N. Zikalala, J. P. Maree, T. Mtombeni, L. Monyatsi and C. J. S. Fourie, "Sodium sulphate behaviour during freeze desalination," WISA 2016, Durban, 2016.

[27] R. K. Tewo, J. P. Maree, S. Ruto, V. Bologo and A. V. Kolesnikov, "Chemical desalination of mine water with by-product recovery: A feasibility study through modelling," WISA 2016 Biennial Conference, Durban, 2016.

[28] S. Ruto, J. P. Maree, M. de Beer, E. Hardwick, J. Hardwick, A. Kolesnikov, R. K. Tewo, C. J. S. Fourie and A. Steytler, "Chemical/resin desalination of mine water," WISA 2016 Biennial Conference, Durban, 2016.

[29] T. Mtombeni, J. P. Maree, N. Zikalala and F. C. J. S, "Desalination with a combined membrane filtration/freeze desalination process," WISA 2016 Biennial Conference, Durban, 2016.

[30] S. Ruto, J. P. Maree, M. de Beer, E. Hardwick, J. Hardwick, A. Kolesnikov, R. K. Tewo, C. J. S. S Fourie and A. Steytler, "Chemical/resin desalination of mine water," WISA 2016, Durban, 2016.

[31] T. T. Rukuni, J. P. Maree, C. M. Zvinowanda and F. H. H. Carlsson, "Separation of magnesium hydroxide and barium sulphate from a barium sulphate – magnesium hydroxide mixed sludge by carbonation: The effect of temperature.," Journal of Civil and Environmental Engineering, vol. 2, no. 116, pp. 16-28, 2012.

[32] P. Dama-Fakir and A. Toerien, "The effect of salinity on evaporation rates of brines resulting from the treatment of mine water," http://www.ewisa.co.za/literature/files/200_150%20Dama-Fakir.pdf, Midrand, 2010.

[33] J. G. Annandale, Y. G. Beletse, R. J. Stirzaker and K. L. Bristow, "Managing poor quality coal-mine water: Is irrigation part of the solution?," in Observations on Environmental Change in South Africa, L. Zietsman, Ed., Sun Press, 2011, pp. 174-177.

[34] M. Makgae, J. P. Maree and J. Annandale, "Neutralized mine water for irrigation – cost and feasibility study," Denver, Colorado, USA (Publ. 2013.

[35] Newsroom, "Kader Asmal wins Stockholm," 24 March 2000. [Online]. Available: http://www.edie.net/news/0/Kader-Asmal-wins-Stockholm-Water-Prize/2492/. [Accessed 16 December 2015].

# The Status of Kenyan Aluminum Recycling Industry

Daniel N. Wang'ombe, Stephen M. Maranga, Bruno R. Mose and Thomas O. Mbuya

***Abstract*—** Aluminum enters Kenya as imported products, and Scrap is either recycled locally or exported. A survey was conducted in Nairobi, Mombasa and Nakuru to study sources, quantity and composition of the scrap through a material flow analysis. A questionnaire, site visits and interviews were used to collect data for the year 2015 from 34 scrap dealers and 29 foundries. Further, data on aluminum exports and imports was provided by Kenya National Bureau of Statistics (KNBS). Major sources of the scrap were motor vehicle, household and building parts. Scrap dealers sold 7,059.6 Mt of scrap to the foundries; composed of 38, 37, and 25 % of rolled, cast and extruded scrap respectively. However, the surplus cast scrap (68.4 %) was exported. The foundries consumed 11,028 Mt of: end of life scrap, internal scrap and primary aluminium. A net addition of 36,782 Mt indicates that more scrap will be available in future.

***Keywords*—** Aluminum, recycling, scrap, secondary alloy.

## I. Introduction

Aluminum has become a popular engineering material (second to iron) due to its superior properties and recyclability. Properties of aluminum include light weight, high resistance to corrosion, good thermal and electrical conductivity. These superior properties have made aluminum to be widely used in transport (aerospace and automobile), building, household and electrical industry [1]. Aluminum products are usually organised in three main categories: cast, rolled and extruded. Rolling and Extrusion use wrought alloys, which allow less alloying elements than cast alloys, and are then more challenging to recycle.

Aluminum has been recycled without losing its chemical and physical properties. By the year 2006 it was estimated that about 75% of the aluminum ever produced in the world was still in use [2]. This has allowed secondary aluminum processing to be conducted in areas where bauxite is not mined. Secondary processing of aluminum consumes 5 % of the energy used to process a similar quantity during primary processing [3]. Mining and processing of bauxite to produce primary aluminum degrades and pollutes the environment. As a result aluminum recycling is cheaper and conserves the environment.

Kenya does not produce primary aluminum; however it mainly enters the local market as primary aluminum, fabrications and finished products. The primary aluminum is used to dilute scrap during secondary processing of aluminum in the local foundries. Imported semi-fabrications in form of billets, slabs, sheets or extrusions are used to manufacture finished products. Both the imported products and the locally manufactured products enter into use until their end of life. The life spans of different aluminum products have been approximated and found to range between 1 and 30 years [4]. Aluminum scrap collection system in Kenya starts from the village level, and terminates in the major urban centres; whereby the scrap is sold to local foundries or exported. A comprehensive view of the interconnections within the Kenyan aluminum industry can be projected by a material flow analysis.

Material flow analysis (MFA) is defined as the study of physical flows of natural resources and materials through and out of a given system. Dahlström et al [5] conducted an MFA study to provide data on the flows and stocks of iron/steel and aluminum that passed through the United Kingdom (UK) economy. From the study, end of life (EoL) scrap was estimated at 700,000 Mt per year. Another study by Rombach [6] found that the EoL scrap in North America

D.N. Wang'ombe, Department of Mechanical Engineering, JKUAT (+2540722283492; e-mail: wangombedanielngera@tum.ac.ke).
S.M. Maranga, Department of Mechanical Engineering, JKUAT (e-mail: smmaranga@yahoo.com).
B.R. Mose, Department of Mechanical Engineering, JKUAT (e-mail: mbruno@eng.jkuat.ac.ke).
T.O. Mbuya, Department of Mechanical and Manufacturing Engineering, UoN (e-mail: tmbuya@uonbi.ac.ke).

and Europe mainly came from automotive, building and packaging industry. These two studies looked at aluminum scrap in general and were particular to Europe and North America respectively. Billy [4] conducted a study of the flow of extruded aluminum in French buildings. From this study the aluminum extruded scrap generated in French building industry was estimated; a Kenyan study can be modeled along these lines, and widened to also include scrap from rolled and cast products.

Several studies have been carried out on Kenyan aluminum industry. Bruno [7] conducted a survey in the Kenyan aluminum foundries. From the survey it was established that the foundries were not undertaking quality control practices while melting the scrap. Weramwanja [8] did a study on Kenyan aluminum material flow, with an aim of establishing a local aluminum processing plant. This was a general study that covered extensively on use of bauxite and aluminum fabrications. In addition to that little information was gathered on quantities of aluminum scrap. Mbuya et al [9] sorted cast scrap that was collected randomly from Nairobi city scrap dealers, and the resulting castings were found to be closely related in chemical composition to the parent components like pistons, cylinder heads and housings.

Although Kenyan aluminum scrap is collected and either sold to local processors or exported, there is no literature on the sources, quantity and the ranges of composition of this scrap. Such data is important to industrial players; especially when planning on raw materials, and development of new products and alloys. Policies for regulating this industry can be formulated based on this data. Consequently it was found necessary to establish the likely sources, quantities and ranges of composition of the scrap through an industry survey.

## II. PROCEEDURE

The industry survey data that was to be collected was modelled in form of an aluminum material flow as shown in Fig. 1. The model assisted in identifying the institutions that participated in the survey and data acquisition tools. The institutions included Kenya Association of Manufacturers (KAM), scrap dealers, foundries and Kenya National Bureau of Statics (KNBS). The tools used to collect data included a questionnaire, site visits and interviews.

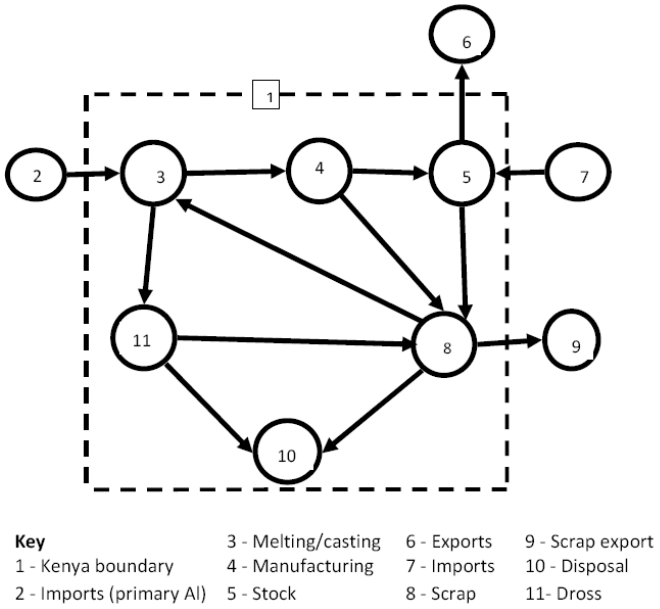


Fig. 1 The Aluminum flows into, out of and within the Kenyan aluminum recycling industry.

An industry survey was conducted in three major towns in Kenya namely: Nairobi, Mombasa and Nakuru. Nairobi is the Kenya's capital city, and Mombasa is the second largest city and the only major sea port. Nakuru is also a major town in the agricultural Rift Valley region. The KAM data base [10] showed that the major aluminum industries and scrap dealers are located in these towns. For the purpose of this research the industries were referred to as foundries. Since not all aluminum industrial players were members of KAM, a preliminary survey was conducted in the towns and their environs to establish additional foundries and scrap dealers. The scrap dealers were the firms dealing with bulky aluminum scrap sourced from small scale dealers located within their home town and other smaller towns. They also bought scrap through tenders from companies and government institutions. The scrap collected was sold to the foundries, and the surplus was exported. A summary of the 34 scrap dealers and 29 foundries that were selected for this survey in the three towns are presented in Table I. A questionnaire of the structure shown in Table II was designed and sent to the various scrap dealers and foundries. The data collected was for the year 2015. Visits were made to different firms. Observations regarding the handling of the scrap were made. Interviews and site visits were conducted to give more information that was not covered by the questionnaire.

TABLE I
SUMMARY OF THE SCRAP DEALERS AND FOUNDRIES THAT PARTICIPATED IN THE SURVEY

| Town | Scrap Dealers | Foundries | | |
|---|---|---|---|---|
| | | Casting | Rolling | Extrusion |
| Nairobi | 20 | 12 | 4 | 3 |
| Mombasa | 8 | 2 | 3 | - |
| Nakuru | 6 | 5 | - | - |
| Total | 34 | 19 | 7 | 3 |

TABLE II
QUESTIONNAIRE STRUCTURE

| Issue | Question focus |
|---|---|
| Cover letter | Introduction from JKUAT |
| Preamble | Introduction, Benefits of the study, confidentiality, contact person |
| General company information | The respondent's identification data<br>Name, address, telephone, contact person |
| End of life (EoL) scrap | Type, Source (local or imports), Quantity, Purpose, destination (local or Export), Re-use |
| New scrap | Source, quantity |
| Primary Al | Source, quantity, value, purpose |
| Melting | Primary Aluminum, EoL scrap, new scrap, Quantity generated, dross generated and destination. |
| Fabrication & manufacturing | Products (Semis or new products) Quantity, destination, quantity of new scrap. |
| New goods | Locally produced, Imports, Exports, Quantity |
| Disposal (Land fill ) | Any amount that is not recycled |
| Research interest | To report the outcome of the survey to the participating groups. |

Additional data on imports and exports of aluminum products was extracted from statistical abstract and economic survey reports prepared by KNBS [11], [12].

## III. RESULTS

The feedback of the questionnaires was collected, and 28 scrap dealers and 22 foundries responded. The data collected is shown in Table III and IV, and KNBS provided data on aluminum imports and exports shown in Table V.

TABLE III
SUMMARY OF ALUMINUM SCRAP IN METRIC TONNES (Mt) HANDLED BY DEALERS IN YEAR 2015

| Town | cast | Extruded | Rolled | Total | cast (export) |
|---|---|---|---|---|---|
| Nairobi | 2375 | 2449.2 | 1569.6 | 6393.6 | 1800 |
| Mombasa | 141.6 | 170.4 | 92.4 | 404.4 | 0 |
| Nakuru | 115.2 | 68.4 | 78 | 261.6 | 0 |
| Total | 2632 | 2688 | 1740 | 7059.6 | 1800 |

TABLE IV
SUMMARY OF ALUMINUM SCRAP IN METRIC TONNES (Mt) HANDLED BY THE FOUNDRIES FOR THE YEAR 2015

| Town | EoL Scrap | | | | Internal scrap | | Import (Primary AL) | Export (Al products) |
|---|---|---|---|---|---|---|---|---|
| | Cast | Rolling | Extrusion | Total | New | Recovery | | |
| Mombasa | 0.0 | 4080.0 | 0.0 | 4080 | 78.0 | 66.0 | 1800.0 | 1734.0 |
| Nairobi | 493.2 | 960.0 | 1920.0 | 3373.2 | 355.1 | 32.2 | 1080.0 | 480.0 |
| Nakuru | 162.0 | 0.0 | 0.0 | 162.0 | 1.8 | 0.0 | 0.0 | 0.0 |
| Total | 655.2 | 5040.0 | 1920.0 | 7615.2 | 434.9 | 98.2 | 2880.0 | 2214.0 |

TABLE V
ALUMINUM IMPORTS AND EXPORTS EXTRACTED FROM KNBS REPORTS

| Commodity (Mt) | 2008 | 2009 | 2010 | 2011 | 2012 | 2013 | 2014 | 2015 |
|---|---|---|---|---|---|---|---|---|
| Aluminum imports | 18,525 | 25,568 | 19,962 | 23,427 | 24,981 | 26,963 | 29,371 | |
| Motor vehicle imports | 9,189 | 9,255 | 10,912 | 9,238 | 10,376 | 12,918 | 14,492 | 15,369 |
| House ware exports | 5,631 | 5,507 | 5,795 | 6,311 | 7,328 | 8,182 | 7,879 | |

The end of life scrap handled by dealers was divided into cast, extruded and rolled. The classification of the scrap was based on the process used to make item from which it was derived from. A total of 7,059.6 metric tons (Mt) were collected in the three towns. Nairobi compared to the other two towns had the highest quantities of scrap in all the three categories as shown in Fig. 2. This scrap was consumed by the casting, extrusion and rolling foundries. However 1800 Mt of surplus cast scrap was exported.

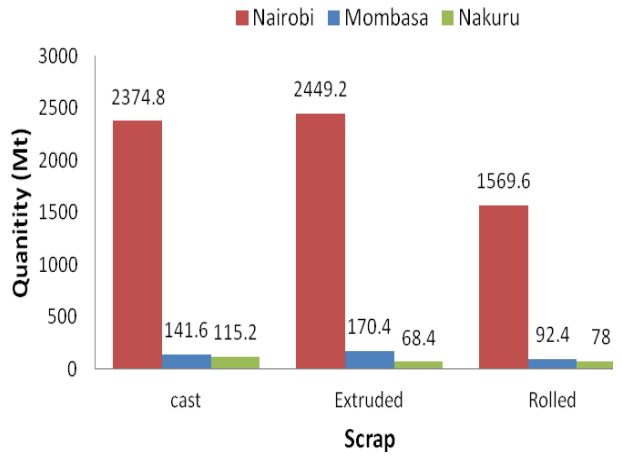


Fig. 2 Categories of the scrap in metric tons (Mt) collected in the three Kenyan towns in year 2015

The foundries used a variety of aluminum including EoL scrap, internal scrap and imported primary aluminum to process products as shown in Table IV. The EoL scrap was supplied by contracted dealers, and its consumption was highest in Mombasa as shown in Fig. 3. New scrap consisted of scrap generated during melting and processing of aluminum. Foundries were recovering aluminum from dross. The rolling and extrusion foundries were exporting primary aluminum to dilute the impurities when melting the scrap. About 2214 Mt of aluminum products were exported; while the rest were consumed locally.

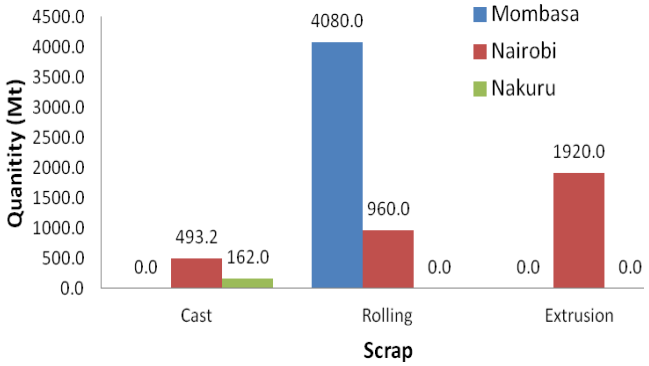


Fig. 3 EoL scrap in metric tons consumed by foundries in the three Kenyan towns in the year 2015

The KNBS reports [11], [12] gave the data on aluminum imports and exports shown in Table V. Aluminum entered the country as billets, rolled sheets and plates, and sections. Imported aluminum in the year 2015 was approximated as 30,000 Mt using linear forecasting shown in Fig. 4. Motor vehicles from Japan, Europe and North America have been reported to contain an average of 140 kg of aluminum [13], [14]. Therefore, the units of imported motor vehicles were multiplied by 140 to obtain 15,369 Mt of aluminum brought into the country in 2015. Aluminum house ware export for the year 2015 was 9000 Mt.

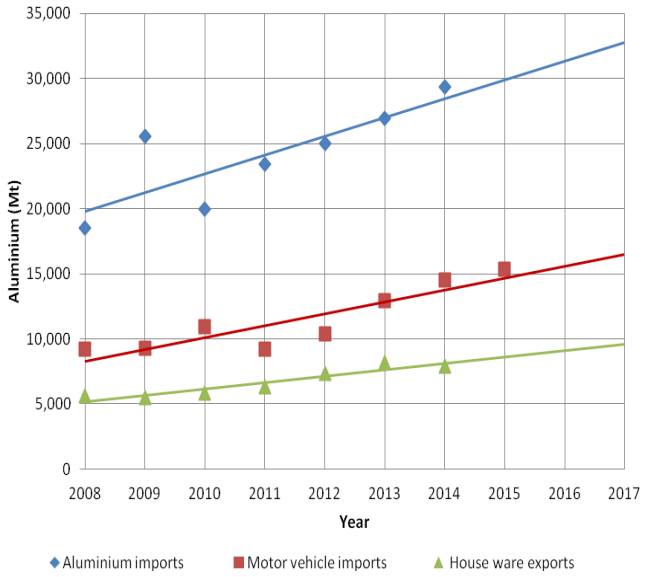


Fig. 4 Kenyan aluminum imports and exports

## IV. DISCUSSION

Scrap dealers responded by 82.4%. The reasons for non response include: that two dealers were out of business and another one had just started the business; another three pulled out without giving reasons. The response from foundries was 75.9%, and reasons were not given for non response.

Dealers in Nairobi collected 90% of the EoL scrap. This was contributed by the fact that 59% of the dealers were based in Nairobi, and had both branches and agents country wide. Nairobi was found to generate a lot of scrap from its numerous industrial activities and large urban population. Further, the city dealers were contracted to supply bulk scrap to Kenyan foundries, and whenever there was surplus the government allowed them to export it. The EoL scrap collected by dealers consisted of cast, rolled and extruded aluminum in the following proportions 37, 38 and 25% respectively.

Cast scrap mostly originated from automotive components like engine blocks, wheels, cylinder heads, pistons and gear box casing. However, a small proportion was found to arise

from industrial machines like motor housings. From the literature review, these components are cast from 3xx.x alloys which are silicon based, and with additions of magnesium and/or copper. Silicon based alloys have been found to be popular because of their excellent castability and superior mechanical properties. Local foundries consumed 31.6% of the cast scrap, and the surplus was exported. The government only allowed export of surplus nonferrous scrap; in order to protect the local market.

Rolled and extruded EoL scrap was made up of aluminum wrought alloys, and particularly 3xxx and 6xxx series alloys respectively. Rolled scrap was found to be composed of house ware (pots, pans and urns), vehicle parts (radiators and panels), used beverage cans, sheets and pipes. Further, structural rolled scrap (structural plates and automotive body panels) was present, and was suspected to be composed of 5xxx series wrought alloys. Extruded scrap originated mainly from automotive and building structures. Extruded motor vehicle structural components included frames (space, seat, door and window), beams, tread plates, hand rails, carriers and general automotive trim. Building and construction structural scrap consisted of frames (door, window and green house), office partitions, door handles and locks. Extruded scrap also consisted of 15.7 Mt of electrical scrap inform of cables and bus connectors. The electrical scrap was handled by 12% of the dealers who were accredited, so as to curb rampant thefts and vandalism. All the wrought scrap was consumed by extrusion and rolling foundries.

The foundries were found to consume 11,028 Mt of aluminum, which was composed of Eol scrap, primary aluminum and internal scrap in the following percentages 69, 26 and 5 respectively. The EoL scrap consumed by the foundries was higher than the amount supplied by dealers by 45%. This is an indication that there were other suppliers outside the towns that were surveyed. The pattern of consumption of the scrap clearly indicated that Kenyan

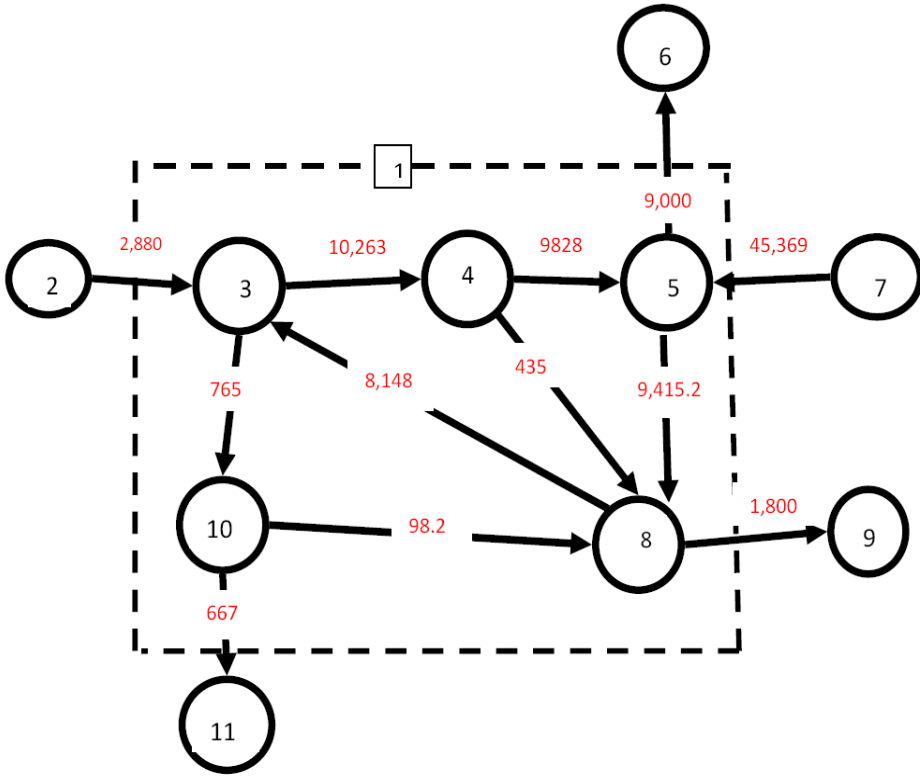


Fig. 5 The Aluminum flows in metric tons (Mt) into, out of and within the Kenyan aluminum recycling industry for the year 2015

foundries can be categorized as casting, rolling and extrusion. The 533 Mt of internal scrap generated by the foundries was used together with the EoL scrap. Casting was performed by small scale informal foundries concentrated in Nairobi and Nakuru. Nakuru foundries were buying cast scrap from Nairobi to cater for the deficiency of 29%. Rolling foundries in Mombasa consumed 81% of the EoL rolled scrap. Imported primary aluminum was added to dilute this scrap. The extrusion foundries were in Nairobi and used the extrusion EoL scrap mixed with the related internal scrap,

and diluted with imported primary aluminum. Internal scrap of 98 Mt was recovered from dross generated by 64% of the foundries.

Dross has been found to contain about 20% aluminum, and most foundries reported a recovery of about 10% aluminum. From these figures the dross generated by the foundries was found to be 765 Mt.

Aluminum was found to enter the country as imported motor vehicles and other goods. The number of imported vehicles continued to increase from year 2008 to 2015 as shown in Figure 4, as a result of sustained economic growth. Consequently the amount of aluminum contained in motor vehicles also increased, and 15,369 Mt were imported in the year 2015. The vehicles were used in the country. Other aluminum imports consisted of primary aluminum for foundries, extruded sections for automotive and construction industries, house wares and many other goods. In the year 2015 the aluminum imports amounted to 30,000 Mt. Exports of 2214 Mt by foundries was lower than the 9000 Mt reported by KNBS. This is an indication that there were other industries that were importing aluminum semi-fabrications, and later exported finished products after value addition.

The data that was collected on the flow of aluminum was summarized as shown in Figure 5. The aluminum products in the market were being increased by imports and local manufacturing, and simultaneously reduced by export and scraping. By applying the law of mass balance, the net addition of aluminum products in the Kenyan market for the year 2015 was 36,782 Mt. This meant that the future aluminum scrap will continue to increase. For the foundries to achieve maximum benefit of this scrap they need to explore on the development of new alloys that will minimize the use of costly primary aluminum. This will make their products competitive both in local and international markets. Further, ways of minimizing loss of aluminum through dross should be sought, and explore opportunities of value addition to cast scrap before exportation.

## V. Conclusions

The status of the Kenyan aluminum recycling industry, based upon year 2015 data has been investigated. The following conclusions can be drawn from work:

i. Percentages of the aluminum scrap collected from Nairobi, Mombasa and Nakuru were 90.6, 5.7 and 3.7 respectively, and the scrap was derived from automotive, construction, house hold and electrical components in the following percentages 44.2, 32.5, 20.6 and 2.7 respectively.

ii. The available scrap was categorized as extruded, cast or rolled, and occurred in the following percentages 38.1, 37.3 and 24.6 respectively.

iii. The Kenyan foundries consumed all the extruded, rolled and their internal (new, recovery and process) scrap, and added 2880 Mt of imported primary aluminum to dilute the scrap; however, only 31.6 % of cast scrap was consumed while the surplus was exported without value addition.

iv. The fact that sum EoL scrap consumed by foundries and the cast scrap exported exceeded the quantity handled by the dealers by 45 %, indicates that there were other dealers (outside the three towns surveyed) supplying scrap to the foundries.

v. The net addition of 36,782 Mt of aluminum in the Kenyan market indicated that in future aluminum scrap would be available for the Kenyan foundries.

## Acknowledgement

The authors wish to thank the JKUAT Research, Production & Extension (RPE) Division, for the financial assistance to the ongoing research on the *"Development of Recycle-friendly Aluminum Alloys for Automotive and Structural Applications''* under grant No JKU/2/4/RP/196.

## References

[1] S. K. Das, and W. Yin, ''The worldwide aluminum economy: the current state of the industry,'' *Journal of Materials*, vol. pp. 57- 63, 2007.

[2] Z. Kamberovic, E. Romhanji, M. Filipovic, and M. Korac, ''The recycling of high magnesium aluminum alloys: estimation of the most reliable procedure,'' *Association of Metallurgical Engineers of Serbia (MJoM)*, vol. 15 (3), pp. 189-200, 2009.

[3] S. K. Das, ''Designing aluminum alloys for a recycle-friendly world,'' *Light Metal Age*, vol. , pp. 26-29, 2006.

[4] R. Billy, ''Material flow analyses of extruded aluminum in french buildings: opportunities and challenges for the implementation of a window-to-window system in France,'' Master's Thesis, Dept., Norwegian University of Science and Technology, 2012.

[5] K. Dahlström, P. Ekins, J. He, J. Davis, and R. Clift, ''Iron, steel and aluminum in the UK: material flows and their economic dimensions,'' Centre for Environmental Strategy, University of Surrey, United Kingdom, 2004.

[6] G. Rombach, ''Future availability of aluminum scrap,'' *Light Metals*, vol. , pp. 1011- 1017, 2002.

[7] R. M. Bruno, ''Effect of minor elements on castability, microstructure and mechanical properties of recycled aluminum alloys,'' Master's thesis, Department of Mechanical Engineering, Jomo Kenyatta University of Agriculture and Technology, 2009.

[8] P. M. Weramwanja, ''Aluminum material flow and value chain analysis in the kenyan industry,'' Master's thesis, Department of Mechanical Engineering, Jomo Kenyatta University of Agriculture and Technology, 2010.

[9] T. O. Mbuya, B. O. Odera, S. P. Ng'ang'a, and F. M. Oduori, ''Effective recycling of cast aluminum alloys for small foundries,'' *Journal of Agriculture, Science and Technology*, vol. 12, pp. 161 – 181, 2010.

[10] Kenya Association of Manufacturers, Kenya Manufacturers and Exports Directory, 2015.

[11] Kenya National Bureau of Statistics, Statistical Abstract 2015, 2015.

[12] Kenya National Bureau of Statistics, Economic Survey 2016, 2016.

[13] S. Bell, B. Davis, A. Javaid, and E. Essadiqi, '' Final report on scrap management, sorting and classification of aluminum,'' Natural Resources, Canada, 2003.

[14] International Aluminum Institute, Global aluminum recycling: a cornerstone of sustainable development, United Kingdom, 2009.

| SNo. | Institution/Country | No. of Papers |
|---|---|---|
| 1 | Jomo Kenyatta University of Agriculture and Technology | 23 |
| 3 | Moi University | 4 |
| 4 | Tshwane University of Technology, Pretoria, South Africa | 3 |
| 5 | National University of Science and Technology, Zimbabwe | 1 |
| 6 | Technical University of Kenya | 1 |
| 7 | The Cooperative University of Kenya | 1 |
| 8 | Vaal University of Technology, South Africa | 1 |
| 9 | Kirinyaga University | 1 |
| 10 | Tshwane University of Technology, Pretoria, South Africa | 3 |
| 11 | Durban University of Technology, South Africa | 1 |
| 12 | Kenya Ports Authority (KPA) | 1 |
| 13 | University of KwaZulu-Natal, Pietermaritzburg, South Africa | 1 |


**JSRE is an international peer reviewed journal that publishes quarterly the original and high quality research papers with properly documented results that have major positive impact in Science and Technology, for the benefit of mankind.**

The journal enjoys a global list of prestigious academic reviewers drawn from leading international universities and the editors are committed to a fair and efficient handling of manuscripts received.

We have an online manuscript management where authors can submit and track their manuscripts editorial process through our portal.

To submit your manuscript, create an account at
http://sri.jkuat.ac.ke/ojs/index.php/sri/index

Jomo Kenyatta University
of
Agriculture & Technology

*Setting treds in higher learning*